

Environmental Science

Joseph L. Awange
John B. Kyalo Kiema

Environmental Geoinformatics

Monitoring and Management

 Springer

Environmental Science and Engineering

Environmental Science

Series Editors

Rod Allan
Ulrich Förstner
Wim Salomons

For further volumes:
<http://www.springer.com/series/3234>

Joseph L. Awange · John B. Kyalo Kiema

Environmental Geoinformatics

Monitoring and Management

 Springer

Joseph L. Awange
Department of Spatial Sciences
Curtin University
Perth, WA
Australia

John B. Kyalo Kiema
Department of Geospatial
and Space Technology
University of Nairobi
Nairobi
Kenya

Karlsruhe Institute of Technology
Karlsruhe
Germany

Institut d'Enseignement Supérieur
(INES) - Ruhengeri
Musanze
Rwanda

Kyoto University
Kyoto
Japan

School of Environment
Maseno University
Kisumu
Kenya

ISSN 1431-6250

ISBN 978-3-642-34084-0

ISBN 978-3-642-34085-7 (eBook)

DOI 10.1007/978-3-642-34085-7

Springer Heidelberg New York Dordrecht London

Library of Congress Control Number: 2013934385

© Springer-Verlag Berlin Heidelberg 2013

This work is subject to copyright. All rights are reserved by the Publisher, whether the whole or part of the material is concerned, specifically the rights of translation, reprinting, reuse of illustrations, recitation, broadcasting, reproduction on microfilms or in any other physical way, and transmission or information storage and retrieval, electronic adaptation, computer software, or by similar or dissimilar methodology now known or hereafter developed. Exempted from this legal reservation are brief excerpts in connection with reviews or scholarly analysis or material supplied specifically for the purpose of being entered and executed on a computer system, for exclusive use by the purchaser of the work. Duplication of this publication or parts thereof is permitted only under the provisions of the Copyright Law of the Publisher's location, in its current version, and permission for use must always be obtained from Springer. Permissions for use may be obtained through RightsLink at the Copyright Clearance Center. Violations are liable to prosecution under the respective Copyright Law. The use of general descriptive names, registered names, trademarks, service marks, etc. in this publication does not imply, even in the absence of a specific statement, that such names are exempt from the relevant protective laws and regulations and therefore free for general use.

While the advice and information in this book are believed to be true and accurate at the date of publication, neither the authors nor the editors nor the publisher can accept any legal responsibility for any errors or omissions that may be made. The publisher makes no warranty, express or implied, with respect to the material contained herein.

Printed on acid-free paper

Springer is part of Springer Science+Business Media (www.springer.com)

Foreword



The title and subtitle of this textbook convey a distinct message. Monitoring—the passive part in the subtitle—refers to *observation* and *data acquisition*, whereas management—the active component—stands for *operation* and *performance*. The topic is our environment, which is intimately related to geoinformatics. The overall message is: all the mentioned elements do interact and must not be separated.

There are still other aspects which must not be separated: *theory* and *practice* of geoinformatics. The book presents an excellent balance of both fields. Technology is introduced from the Geodesist's view including; Reference Systems, Positioning Systems, Remote Sensing, Photogrammetry, and Geographic Information Systems.

Applications range from Climate, Water, and Land Management to Vegetation, Disaster, and Pollution. Today, many textbooks are written by specialists from these particular fields. However, in the applications there are many common technical elements in space and time, like impact from scale, regionalization, time series, data fusion, visualization, etc.—just to mention but a few. An advanced prospect for environmental management requires system-based thinking and interdisciplinary approaches. Furthermore, technology may be a common denominator for better understanding our environment.

Finally, geoinformatics is a modern tool for location-based decision making. Most decisions in public administration and economy are directly or indirectly related to space. Today, advanced models and digital spatial data may make decisions more transparent than ever before. Very often, in geoprojects a lot of money is involved, and the risk of manipulation in decision making inevitably increases. Quantitative analysis and restitution of the results may, however, reduce this risk.

Both authors, Joseph L. Awange and John B. Kyalo Kiema, are experienced researchers and lecturers with a strong international background acquired from different parts of the world. During research fellowships in Germany, they got the picture that “geodesy” is a global concept beyond measuring just the figure of the Earth.

Germany, January 2013

Prof. Dr.-Ing. Dr.h.c.,
Hans-Peter Bähr
Karlsruhe Institute of Technology

Preface

There is no doubt that today, perhaps more than ever before, humanity faces a myriad of complex and demanding challenges. This has been propelled by the ever increasing global population and intense pressure being exerted on the Earth's resources. The resulting consequences are severe changes in land cover (e.g., forests giving way to settlements), diminishing biodiversity and natural habitats, dwindling fresh water supplies, and the degradation in the quality of the little that is available, and changing weather and climatic patterns, especially global warming with its associated predicted catastrophes such as rising sea level and increased numbers of extreme weather events.

These *human-induced* and *natural impacts* on the environment need to be well understood in order to develop *informed policies, decisions, and remedial measures* to mitigate current and future negative impacts. This can be achieved through continuous monitoring of the environment to acquire data that can be soundly and rigorously analyzed to provide information about the current state of the environment and its changing patterns, and to enable predictions of possible future impacts. Environmental monitoring techniques that may provide such information are under scrutiny from an increasingly environmentally conscious society that demands the efficient delivery of such information at a minimal cost. In addition, it is the nature of environmental changes that they vary both spatially and temporally, thereby putting pressure on traditional methods of data acquisition, some of which are very labor intensive, such as tracking animals for conservation purposes. With these challenges, conventional monitoring techniques, particularly those that record spatial changes, call for more sophisticated approaches that deliver the necessary information at an affordable cost.

Developing pragmatic and sustainable solutions to address these and many other similar challenges requires the use of geodata and the application of geoinformatics. Geoinformatics, defined by Ehlers (2003) as “the art, science or technology dealing with the acquisition, storage, processing, production, presentation and dissemination of geoinformation”, is a multidisciplinary field. It has at its core different technologies that support the acquisition, analysis, and visualization of geodata. The geodata is usually acquired from Earth observation sensors as remotely sensed images, analyzed by geographic information systems (GIS), and visualized on paper or on computer screens. Furthermore, it combines

geospatial analysis and modeling, development of geospatial databases, information systems design, human–computer interaction, and both wired and wireless networking technologies. Geoinformatics uses geocomputation and geovisualization for analyzing geoinformation. Typical branches of geoinformatics include: *cartography, geodesy, geographic information systems, global navigation satellite systems (GNSS), photogrammetry, remote sensing, and web mapping.*

For example, a typical application of geoinformatics to environmental monitoring and management is the *GNSS-based radio telemetry*, which is a modern method for observing animal movements. This method moves the burden of making observations from the observer (i.e., researcher) to the observed (i.e., animal), and in so doing alleviates the difficulties associated with personal bias, animal reactions to human presence, and animal habits that make most of them secretive and unseen (Cagnacci et al. 2010). The method provides large, continuous, high-frequency data about animal movement, data which, if complemented by other information dealing with animal behavior, physiology, and the environment itself, contributes significantly to our knowledge of the behavior and ecological effects of animals, allowing the promotion of quantitative and mechanistic analysis (Cagnacci et al. 2010).

This book presents the concepts and applications of geoinformatics in environmental monitoring and management. We depart from the 4D to the 5D data paradigm, which defines geodata accurately, consistently, rapidly, and completely, in order to be useful without any restrictions in space, time, or scale to represent a truly global dimension of the digital Earth. The book also features the state-of-the-art discussion of Web GIS and mapping, an invited chapter written by Prof. Bert Veenendaal of the Department of Spatial Sciences, Curtin University (Australia).

The concepts and applications of geoinformatics presented in this book will be of benefit to decision makers across a wide range of fields, including those working in environmental management agencies, in the emergency services, public health and epidemiology, crime mapping, tourism industry, market analysis and e-commerce, or mineral exploration, among many others.

This is a TIGeR publication No 442.

Perth (Australia), Karlsruhe (Germany)
Nairobi (Kenya), Musanze (Rwanda)

Joseph L. Awange
John B. Kyalo Kiema

References

- Cagnacci F, Boitani L, Powell PA, Boyce MS (eds) (2010) Challenges and opportunities of using GPS-based location data in animal ecology. *Philos Trans R Soc B* 365:2155. doi: [10.1098/rstb.2010.0098](https://doi.org/10.1098/rstb.2010.0098)
- Ehlers M (2003) Geoinformatics and digital earth initiatives: A German perspective. *Int J Digit Earth* 1(1):17–30

Acknowledgments

Several figures in this book have been generously provided by various authors. In this regard, the first author (Joseph) would like to thank D. Rieser (Graz University of Technology), M. Motagh (GFZ), M. Jia (Geoscience Australia), F. Urbano (RICENRA, Edmund Mach Foundation, Italy), and R. Mikosz (Federal University of Pernambuco, Brazil). Some figures and materials also came from the work undertaken jointly with colleagues B. Heck (Karlsruhe Institute of Technology, Germany), W. Featherstone, M. Kuhn, K. Fleming, and I. Anjasmara (Curtin University), M. Sharifi (Tehran University), A. Hunegnaw (University of Edinburgh), O. Baur (Space Research Institute, Austrian Academy of Science), E. Forootan (Bonn University), J. Wickert, T. Schmidt (GFZ, Germany), J. B. K. Kiema (University of Nairobi), and students N. Wallace, Khandu, G. Schloderer, M. Bingham, and T. Opande. To you all, “arigato gozaimasu” (Japanese for thank you very much). To all his Curtin University 3rd year (Satellite and Space Geodesy unit), and 2nd year (Civil Engineering) students who used materials from the draft book and provided feedback, Joseph would like to say “Danke sehr” (German for thank you very much).

Joseph also wishes to express his sincere thanks to Prof. B. Heck of the Department of Physical Geodesy (Karlsruhe Institute of Technology (KIT), Germany) for hosting him during the period of his Alexander von Humboldt Fellowship (2008–2011) when part of this book was written. In particular, his ideas, suggestions, and motivation on [Chaps. 20–22](#) have enriched the book considerably. Joseph is also grateful to Prof. B. Veenendaal (Head of Department, Spatial Sciences, Curtin University, Australia) for the support and motivation that enabled the preparation of this edition. He also wishes to acknowledge the support of *Curtin Research Fellowship*, while his stay at KIT was supported by a *Alexander von Humboldt’s Ludwig Leichhardts Memorial Fellowship*. To all, he says, “ahsante sana” (Swahili for thank you very much). Last, but not least, he wishes to thank his wife Naomi Awange and daughters Lucy and Ruth Awange for their patience and support, especially the hard times they endured when he was away in Germany.

On the other hand, the second author (Kiema) wishes to thank staff and students at the Department of Geospatial and Space Technology, University of Nairobi. In particular, he wishes to acknowledge G. C. Mulaku, R. S. Rostom, J. N. Mwenda,

and S. M. Musyoka for support and motivation, along with D. N. Siriba who graciously proof read this work. He wishes to also express sincere thanks to among others G. Konecny (University of Hannover), S. Murai (University of Tokyo), J. L. Awange (Curtin University), Q. Weng (Indiana State University), E. Nyadimo (Oakar Sevices Ltd., Kenya), B. Kumi-Boateng (University of Mines and Technology, Ghana), G. Eshiamwata (Birdlife International, Kenya), J. M. Mwangi, and M. A. Dangana (University of Nairobi) for material used in the book.

Kiema is also indebted to Prof. H.-P. Bähr of KIT for first, mentorship through the years and secondly, for agreeing to write the foreword for this book. Gratitude is also accorded to the Institut d'Enseignement Supérieur (INES)—Ruhengeri where the second author was stationed for the duration of his sabbatical leave, during which period this monogram was completed. Special regards to Rev. Fr. Dr. F. Hagenimana, Vice Rector Academics at INES for his kind support. Finally, Kiema also wishes to acknowledge his wife Joy and children Abigail and Jayden for their patience and understanding during the long spell when he was away from home.

Contents

Part I Introduction

1	Environmental Monitoring and Management.	3
1.1	Why Monitor the Environment?	3
1.2	Challenges and Practice of Environmental Monitoring	5
1.3	Geoinformatics and Environmental Monitoring.	7
1.4	Geoinformatics and Environmental Management	12
1.5	Objectives and Aims of the Book.	13
	References	14
2	Geodata and Geoinformatics.	17
2.1	Dimensions of Space, Time and Scale.	17
2.2	Geodata	21
2.3	Digital Earth Concept	22
2.4	Fundamentals of Geoinformatics.	24
2.5	Concluding Remarks	25
	References	26

Part II Environmental Geodesy

3	Fundamentals of Surveying and Geodesy.	31
3.1	Environmental Geodesy	31
3.2	Definitions: Plane and Geodetic Surveying	32
3.3	Types of Measurements.	33
3.3.1	Plane Surveying Measurements and Instruments.	34
3.3.2	Geodetic Measuring Techniques	36
3.3.3	Basic Measuring Principles and Error Management.	37

- 3.4 Measuring Techniques 38
 - 3.4.1 Linear Measurements 38
 - 3.4.2 Traversing 39
 - 3.4.3 Very Long Baseline Interferometry (VLBI) 40
 - 3.4.4 Laser Ranging Techniques 41
- 3.5 Concluding Remarks 44
- References 45

- 4 Modernization of GNSS 47**
 - 4.1 Introductory Remarks 47
 - 4.2 The GNSS Family 49
 - 4.3 Future Missions 50
 - 4.4 Environmental Benefits of the Expanded GNSS Family 51
 - 4.5 Concluding Remarks 53
 - References 54

- 5 The Global Positioning System 55**
 - 5.1 Introductory Remarks 55
 - 5.2 GPS Design and Operation 56
 - 5.2.1 Space Segment 56
 - 5.2.2 Control Segment 57
 - 5.2.3 User Segment 58
 - 5.3 GPS Observation Principles 59
 - 5.3.1 GPS Signals 59
 - 5.3.2 Measuring Principle 61
 - 5.4 Errors in GPS Measurements 64
 - 5.4.1 Ephemeris Errors 65
 - 5.4.2 Clock Errors 65
 - 5.4.3 Atmospheric Errors 66
 - 5.4.4 Multipath 69
 - 5.4.5 Satellite Constellation “Geometry” 70
 - 5.4.6 Other Sources of Errors 70
 - 5.5 Concluding Remarks 70
 - References 71

- 6 Environmental Surveying and Surveillance 73**
 - 6.1 Environmental Monitoring Parameters 73
 - 6.2 Design of GNSS Monitoring Survey 74
 - 6.3 Mission Planning and Reconnaissance 75
 - 6.4 GNSS Field Procedures 80
 - 6.4.1 Single Point Positioning 81
 - 6.4.2 Static Relative Positioning 83
 - 6.4.3 Real-Time GNSS (RTGNSS) 85
 - 6.4.4 Differential and Augmented GNSS 86

- 6.4.5 Rapid Positioning Methods 88
- 6.4.6 Real-Time Kinematic (RTK) 91
- 6.5 Environmental Surveillance: CORS Monitoring 93
- 6.6 Coordinate Reference System. 98
 - 6.6.1 Datum 100
 - 6.6.2 Coordinate Systems and Transformations. 102
 - 6.6.3 Map Projection 104
- 6.7 Concluding Remarks 104
- References 106

Part III Remote Sensing and Photogrammetry

- 7 Fundamentals of Remote Sensing 111**
 - 7.1 Basic Concept 111
 - 7.2 Principles of Electromagnetic Radiation 113
 - 7.2.1 Electromagnetic Spectrum 113
 - 7.2.2 Interaction with the Atmosphere and Targets 115
 - 7.3 Passive Versus Active Remote Sensing 117
 - 7.4 Concluding Remarks 117
 - References 118
- 8 Optical Remote Sensing 119**
 - 8.1 Data Acquisition—Sensors and Systems 119
 - 8.2 Characteristics of Optical Remote Sensing Data 121
 - 8.3 High Spatial Resolution Imagery 124
 - 8.3.1 Development and Characteristics of HSRI 124
 - 8.3.2 Potential of HSRI 125
 - 8.4 Light Detection and Ranging 127
 - 8.5 Concluding Remarks 129
 - References 130
- 9 Microwave Remote Sensing 133**
 - 9.1 Principles of Microwave Remote Sensing 133
 - 9.1.1 Basic Concept 133
 - 9.1.2 Radar Backscattering. 135
 - 9.1.3 Attenuation of Microwave Signals 136
 - 9.2 Structure of Microwave Systems. 137
 - 9.2.1 Microwave Antenna 137
 - 9.2.2 Microwave Sensors 138
 - 9.3 Radar Imaging and Geometry of SAR. 139
 - 9.4 Image Reconstruction of SAR Data. 140
 - 9.5 Interferometric SAR 141

- 9.6 SAR Polarimetry 142
- 9.7 Concluding Remarks 143
- References 143

- 10 Image Interpretation and Analysis 145**
 - 10.1 Introductory Remarks 145
 - 10.2 Visual Image Interpretation 146
 - 10.3 Digital Image Processing 148
 - 10.3.1 Image Reconstruction/Correction 149
 - 10.3.2 Image Transformation/Conversion. 151
 - 10.3.3 Image Classification 152
 - 10.4 Concluding Remarks 154
 - References 154

- 11 Fundamentals of Photogrammetry 157**
 - 11.1 Definition and Scope. 157
 - 11.2 Geometry of Aerial Photography 159
 - 11.2.1 Central Perspective Projection 159
 - 11.2.2 Photographic Scale 160
 - 11.2.3 Classification of Aerial Photographs 160
 - 11.3 Photogrammetric Procedures 162
 - 11.3.1 Data Acquisition. 162
 - 11.3.2 Photogrammetric Restitution 167
 - 11.3.3 Photogrammetric Output 172
 - 11.4 Concluding Remarks 173
 - References 174

- 12 Digital Photogrammetry 175**
 - 12.1 Introduction 175
 - 12.2 Sensor Models 176
 - 12.3 Digital Photogrammetric Workstations 177
 - 12.3.1 Basic Hardware Requirements 177
 - 12.3.2 Basic Software Requirements 178
 - 12.4 Image Matching 179
 - 12.5 Automated Photogrammetric Mapping. 181
 - 12.5.1 Interior Orientation 181
 - 12.5.2 Relative Orientation 182
 - 12.5.3 Aerial Triangulation 183
 - 12.6 Generating DEMs and Orthoimages 184
 - 12.6.1 Automated Generation of DEMs. 184
 - 12.6.2 Automated Orthoimage Generation 184
 - 12.7 Automated Feature Extraction 185
 - 12.8 Concluding Remarks 185
 - References 186

Part IV Geographic Information Systems

- 13 Fundamentals of GIS** 191
 - 13.1 Basic Concept 191
 - 13.2 Key Components 193
 - 13.3 Basic Functions and Applications 195
 - 13.4 Reasons for Success or Failure 197
 - 13.5 Concluding Remarks 199
 - References 200

- 14 Data Models and Structure** 201
 - 14.1 Introductory Remarks 201
 - 14.2 Vector and Raster Models 202
 - 14.3 GIS Topology 203
 - 14.4 Concluding Remarks 204
 - References 205

- 15 Input of GIS Data** 207
 - 15.1 Data Sources for GIS 207
 - 15.2 Data Capture and Editing 208
 - 15.2.1 Vector Data Input 210
 - 15.2.2 Raster Data Input 211
 - 15.3 Rasterization and Vectorization 212
 - 15.4 Concluding Remarks 213
 - References 213

- 16 GIS Database** 215
 - 16.1 Basic Concept 215
 - 16.2 Design Considerations 216
 - 16.3 Database Management System 216
 - 16.4 Design Procedure 221
 - 16.5 Concluding Remarks 222
 - References 223

- 17 Spatial Analysis** 225
 - 17.1 Introductory Remarks 225
 - 17.2 Methods and Techniques 226
 - 17.2.1 Spatial Exploration 226
 - 17.2.2 Measurements 226
 - 17.2.3 Reclassification 227
 - 17.2.4 Coverage Rebuilding 227
 - 17.2.5 Overlay 228
 - 17.2.6 Connectivity Analysis 229

17.3 Concluding Remarks 235

References 235

18 Web GIS and Mapping. 237

18.1 The Web and its Influence. 237

18.2 Concept and Applications of Web GIS 238

18.3 The Development of Web Mapping 240

18.4 Web Services 242

18.5 Mobile and cloud-based GIS 245

18.6 Concluding Remarks 248

References 249

Part V Applications to Environmental Monitoring and Management

19 Maps in Environmental Monitoring 253

19.1 Introductory Remarks 253

19.2 Types of Maps 254

 19.2.1 Thematic Maps 255

 19.2.2 Topographic Maps 255

19.3 Maps and their Environmental Applications 255

 19.3.1 GNSS-Derived Topographic Maps 257

19.4 Concluding Remarks 264

References 266

20 Satellite Environmental Sensing 269

20.1 Introductory Remarks 269

20.2 Sensing the Atmosphere Using GNSS 270

 20.2.1 Background to GNSS Meteorology 271

 20.2.2 GNSS-Derived Atmospheric Parameters 273

 20.2.3 GNSS Remote Sensing Techniques 280

20.3 Remote Sensing of Gravity Variations 289

 20.3.1 Mass Variation and Gravity 290

 20.3.2 High and Low Earth Orbiting Satellites 291

 20.3.3 Gravity Recovery and Climate Experiment 292

20.4 Satellite Altimetry 296

 20.4.1 Environmental Sensing Using Satellite Altimetry 296

 20.4.2 Satellite Altimetry Missions 296

20.5 Sensing Using GNSS Reflected Signals 298

20.6 Concluding Remarks 300

References 300

21	Weather, Climate and Global Warming	305
21.1	Introductory Remarks	305
21.2	Impacts of Weather and the Changing Climate.	307
	21.2.1 Weather Related Impacts	307
	21.2.2 Climate Related Impacts	308
21.3	Water Vapour.	310
	21.3.1 Significance	310
	21.3.2 Numerical Weather Prediction	311
21.4	Carbon Sequestration and Estimation of Vegetation Carbon Stocks	314
21.5	Environmental Monitoring Applications.	316
	21.5.1 Weather Monitoring Applications	316
	21.5.2 Climate Change Monitoring Applications	318
	21.5.3 Monitoring of Global Warming	321
	21.5.4 Sensing Cryospheric Changes.	326
	21.5.5 Geoinformatics Support of International Environmental Agreements	328
21.6	Concluding Remarks	333
	References	334
22	Water Resources	341
22.1	Status and Impact of Diminishing Fresh Water Resources	341
22.2	Monitoring Variation in Fresh Water Resources	343
22.3	Gravity Field and Changes in Stored Water	346
	22.3.1 Gravity Field Changes and the Hydrological Processes	346
	22.3.2 Sensing Changes in Stored Water Using Temporal Gravity Field	346
22.4	Examples of Geoinformatics-Based Monitoring of Changes in Stored Water	349
	22.4.1 The Nile Basin	349
	22.4.2 Understanding the Decline of Lake Naivasha, Kenya.	362
	22.4.3 Water, a Critical Dwindling Australian Resource	368
22.5	Concluding Remarks	374
	References	375
23	Land Management	381
23.1	Introductory Remarks	381
23.2	Reconnaissance and Validation.	381
23.3	Monitoring of Land Conditions	383
	23.3.1 Soil Landscape Mapping	383
	23.3.2 Provision of Point Data	383
	23.3.3 Provision of Polygon Data	384

- 23.4 Monitoring of Land Degradation. 385
 - 23.4.1 Soil Erosion Monitoring 385
 - 23.4.2 Salinity Monitoring: The Catchment Approach. 386
- 23.5 Role of Geoinformatics in Precision Farming. 391
 - 23.5.1 Precise Farming 391
 - 23.5.2 Farm Topographic Maps 392
- 23.6 Concluding Remarks 395
- References 395

- 24 Marine and Coastal Resources 397**
 - 24.1 Marine Habitat 397
 - 24.1.1 Background 397
 - 24.1.2 Geoinformatics-Based Monitoring
of Marine Habitats 398
 - 24.2 Shoreline Monitoring and Prediction 400
 - 24.2.1 Definition and Scope. 400
 - 24.2.2 Monitoring 403
 - 24.2.3 Prediction 404
 - 24.3 Concluding Remarks 410
 - References 412

- 25 Protection and Conservation of Animals and Vegetation 415**
 - 25.1 Introductory Remarks 415
 - 25.2 GNSS Animal Telemetry. 416
 - 25.2.1 Background and Benefits. 416
 - 25.2.2 Observation and Data Management Techniques 419
 - 25.2.3 Applications. 420
 - 25.3 Vegetation 427
 - 25.3.1 Forests. 427
 - 25.3.2 Wetlands 429
 - 25.4 Concluding Remarks 432
 - References 433

- 26 Disaster Monitoring and Management. 437**
 - 26.1 Introductory Remarks 437
 - 26.2 Definition and Scope. 438
 - 26.3 Geosensor Networks in Disaster Monitoring. 440
 - 26.4 Floods 444
 - 26.4.1 Flood Risk Zone Mapping 445
 - 26.4.2 Flood Monitoring and Forecasting 445
 - 26.4.3 Flood Response and Mitigation 446
 - 26.4.4 Geoinformatics Support of Flood Management. 447
 - 26.4.5 Monitoring of ENSO and IOD 450

26.5	Droughts	452
26.5.1	Early Warning of Drought	454
26.5.2	Drought Monitoring and Assessment.	454
26.5.3	Combating Drought.	455
26.6	Vector-Borne Diseases and Outbreak	456
26.7	Earthquakes	458
26.8	Changing Sea Levels.	465
26.8.1	Impacts of Rise in Sea Level	466
26.8.2	Tide Gauge Monitoring	467
26.8.3	GNSS Monitoring	468
26.9	Tsunami Early Warning System	470
26.10	Land Subsidence and Landslides.	473
26.11	Concluding Remarks	476
	References	477
27	Environmental Pollution	483
27.1	Concept of Pollution and Role of Geoinformatics.	483
27.2	Water Pollution	484
27.2.1	Point and Non-point Sources	484
27.2.2	Eutrophication of Lakes.	486
27.3	Air Pollution	488
27.3.1	Background	488
27.3.2	Pollution from Transportation Sector.	489
27.4	Land Pollution	491
27.4.1	Solid Waste Collection and Management.	491
27.4.2	Role of Geoinformatics in Solid Waste Management.	492
27.4.3	Solid Waste from Transportation Sector	494
27.4.4	Acid Mine Deposit Sites	497
27.5	Concluding Remarks	498
	References	498
28	Environmental Impact Assessment	501
28.1	Role of Geoinformatics in EIA, SEA, and SA	501
28.1.1	Impact Assessments and the Need for Monitoring.	501
28.1.2	Applications of Geoinformatics	502
28.2	Impact Monitoring to Detect Change.	504
28.3	Project EIA	505
28.3.1	Geoinformatics in Support of EIA Process.	505
28.3.2	Geoinformatics and Multi-Criteria Analysis (MCA).	508
28.3.3	Example of Gngara Mound Groundwater Resources	515

28.4	Strategic Environmental Assessment	523
28.4.1	Geoinformatics and Cumulative Impacts Assessments	524
28.4.2	Example of Marillana Creek (Yandi) Mine	525
28.5	Sustainability Assessment	527
28.6	Concluding Remarks	528
	References	528
Index	533

Part I
Introduction

Chapter 1

Environmental Monitoring and Management

“If environmental monitoring is not carried out in a deep and exacting scientific manner, then it is likely that no action will be taken when needed for lack of firm evidence.”

Frank Burden (2002)

1.1 Why Monitor the Environment?

A natural way to begin this monogram is by posing several pertinent questions. Firstly, what exactly does the term “*monitoring*” mean. Furthermore, is monitoring synonymous to measuring or observing? And more specifically, what does it mean within an environmental perspective? *Monitoring* has been defined by James et al. (2003) as observing, detecting, or recording the operation of a system; watching closely for purposes of control; surveillance; keeping track of; checking continually; detecting change. They state that since monitoring implies change, and change implies time, monitoring then means *measuring those things that change in a system over time and space*. It is a process based on *surveying* and *surveillance*, but assumes that there is a specific reason for the collection of data (Spellerberg 2005). A similar definition is provided by Study of Critical Environmental Problems (1970) who states that *monitoring is a systematic observation of parameters related to a specific problem, designed to provide information on the characteristics of the problem and their changes with time*.

Developing the above argument further, surveying entails the *collection of quantitative and qualitative data* within a specified time frame without having a preconceived idea of what the results would be. Surveillance introduces the concept of time to surveying, leading to the systematic observation of variables and processes, with the aim of producing time series. Monitoring, therefore, is an extension of surveillance, but with a specific purpose in mind. It is thus a systematic observation

of variables and processes for a specific purpose, such as ascertaining whether a given project is being undertaken according to predefined environmental standards (Finlayson 1996; Spellerberg 2005).

Consequently, the observation and study of the environment is defined as environmental monitoring. This entails objective observations that produce sound data, which in turn produce valuable information that is useful, e.g., in the protection of public water supplies, hazardous, non-hazardous and radioactive waste management, natural resource protection and management, weather forecasting, and global climate change studies (Artiola et al. 2004).

There are various different ways of categorizing monitoring. In one example, Spellerberg (2005) cites the Department of Conservation in New Zealand who recognizes three types of monitoring (*results monitoring*, *outcome monitoring* and *surveillance monitoring*). In yet another example, Spellerberg (2005) outlines four different categories of environmental monitoring based on Vaughan et al. (2001):

- (1) *Simple monitoring* records the value of a single variable at one point over time.
- (2) *Survey monitoring* examines the current state of environmental conditions in both affected and non-affected areas.
- (3) *Surrogate or proxy monitoring* which compensates for the lack of previous monitoring by using surrogate information to infer changes.
- (4) *Integrated monitoring* using detailed sets of ecological information.

On the other hand, Downes et al. (2002) classify monitoring into four categories that clarify the objectives of monitoring prior to a specific design. These include the following:

- *Environmental monitoring*. This takes on many forms for many objectives, e.g., those undertaking environmental monitoring might be interested in gaining some indication of the state, as opposed to assessing human impacts upon the environment, of a particular place.
- *Long term monitoring* and *reference site monitoring*. These are forms of environmental state monitoring that are useful in providing a background measure for the long term dynamics of natural systems that may be used to indicate systematic, monotonic, or cyclical changes in the environment at large scales over long time periods. They are relevant in providing frameworks upon which shorter term or localized changes such as those arising from anthropogenic impacts could be measured against.
- *Compliance monitoring*. This seeks to ensure that a stipulated regulation is being followed, e.g., measuring the pollution level of effluent at a given location without bothering with neighboring locations outside of the area of interest. The objective in compliance monitoring is usually to assess whether the level of particular compounds are below critical levels stipulated under some regulatory framework. Compliance monitoring could also be viewed as quality control measures.
- *Impact monitoring*. This is undertaken to assess the human impact upon the natural environment, with the objective of taking remedial measures to prevent or minimize such impacts. This type of monitoring is useful in compliance and impact assessment monitoring.

Within all the above categorization, a framework for designing a monitoring program is essential. As an example, Finlayson (1996) presents a framework that consists of the identification of issues or problems, definition of objectives, formulation of hypothesis, choosing the desired methods and variables to observe, assessment of feasibility and cost effectiveness, conducting pilot studies, collecting samples, analyzing the collected samples, interpreting data and reporting the results, and implementing management actions. A similar model is presented by Maher and Batley as reported in Burden et al. (2002), who point out that good monitoring programs obtain information and are not just data collection exercise and as such should be cost effective, yet provide information and knowledge to inform those commissioning the data collection.

Spellerberg (2005) summarizes the relevance of environmental monitoring as *adaptive management*, which provides a basis for managing data and provides a learning experience from outcomes of operational programs, *environmental planning* as a basis for the better use of land, *monitoring the state of the environment* using organism to monitor pollution and indicate the quality of the environment, *ecological sciences* monitoring as a way of advancing knowledge about the dynamics of the ecosystem, *pest and diseases* monitoring for agriculture and forestry in order to establish effective means of controlling these, and *climate change* to monitor, for example, the effect of global warming.

1.2 Challenges and Practice of Environmental Monitoring

With increasing development and technological advancement in the world and the rapidly changing state of environmental management, the task of monitoring the environment continues to become more important, as noted, e.g., by Burden et al. (2002), who elucidates the role and practice of environmental monitoring. Burden et al. (2002), in realizing the importance that underpins environmental monitoring, present a handbook that guides environmental monitoring of water, soil and sediments, and the atmosphere. Their work also considers chemical, physical and biological monitoring, all aimed at enhancing environmental management. An attempt to address environmental monitoring in an integrated manner is presented, e.g., in Wiersma (2004), while Goldsmith (1991) and Downes et al. (2002) provide thorough overviews of ecological monitoring and conservation.

In most countries, environmental management requires development projects to undertake an Environmental Impact Assessment (EIA) (see Chap. 28), which brings with it the need for baseline survey data that are useful in assisting the prediction of the environmental impacts of a proposed project. The collection of baseline survey data therefore requires some form of monitoring. Downes et al. (2002) put forward the Before-After-Control-Impact (BACI) model, which helps to assess whether a given activity has impacted upon the environment at a given location.

Owing to the increase in human population and the pressure it exerts on the Earth's resources, the planet's environment has been changing at an alarming rate

which necessitates monitoring measures to be put in place (Mackenzie 2003). In summary, therefore, environmental monitoring serves *to assess the effectiveness of an environmental legislation or policy, to monitor and assess compliance with regulatory statutes established to protect the environment, e.g., monitoring that the effluence from a given factory draining into a given river must be treated to a given standard, and for environmental change detection, e.g., vegetation change for the purpose of early warning.*

An example of change monitoring of agricultural land is shown in the photograph in Fig. 1.1, taken at Mt. Kokeby, Australia. In this figure, the vegetation (except salt tolerant fodders) are dying due to the effect of secondary salinity caused by vegetation clearing for farming purposes. The salinity is caused by increased water recharge, which seeped into the ground and caused an upsurge of groundwater (rising to within 1 m of the top soil (i.e., root zone)), dissolving the salt trapped inside the soil and thereby causing the vegetation to die. Monitoring the extent of salinity in this case enables comparisons to be made between the current state (Fig. 1.1) and the baseline data before the salinity effect had a noticeable impact. This can be done by comparing the spatial extent covered by the dying vegetation to that occupied by undisturbed vegetation (baseline data). Geoinformatics provides technologies useful in mapping the spatial boundaries and is thus essential for monitoring changes in agricultural areas thereby assisting in environmental issues.

In 1997, the premier and legally binding protocol on climate change by the United Nation's framework convention on climate change—the Kyoto protocol—was signed (see Sect. 21.5.5). Within its many articles, this protocol outlined measures that were to be taken by signatory countries to reduce the greenhouse gas emissions that are contributing to climate change, e.g., *global warming*. Although political will seems to be wanning in the post Kyoto era, with some of the key players even renegading on their earlier promises, while others have opted out of the framework altogether, global



Fig. 1.1 Effect of secondary salinity at Mt. Kokeby, Australia

warming still remains one of the daunting challenges facing our environment and as a consequence, human society, today. Similarly, the rapid increase in *desertification* on the one hand, and *flooding* on the other, are environmental issues that are of increasing concern globally.

For instance, the damage arising from the torrential rains that caused havoc and destroyed properties in the USA in 1993 is estimated to have been US\$15 billion, with 50 people killed and thousands of people evacuated, some for several months (Larson 1996). Today, the threat from torrential rains and flooding still remains real, as was seen in the 1997 El Niño-Southern Oscillation (ENSO) rains that swept away roads and bridges in Kenya, the 2000 Mozambique floods, the 2002 Germany floods, Hurricane Isabel in the US coast in 2003, the flooding in Pakistan in 2010 that displaced millions of people, the 2011 eastern Australian floods that displaced thousand of people and destroyed property estimated at billions of Australian dollars, the Brazilian flash floods that killed more than 500 people, and the 2012 floods in the USA caused by hurricane Candy. Meanwhile, the melting of polar ice and the resulting raising sea level raises concerns for the submersion of beaches and many coastal cities including those already below sea level.

To be able to predict and model these occurrences so as to minimize the negative consequences, such as those indicated by Larson (1996), atmospheric studies must be undertaken with the aim of improving current methods for providing *accurate*, *reliable* and *timely* data. These data are useful in Numerical Weather Prediction (NWP) models for weather forecasting, and climatic models for monitoring climatic changes. In addition, *accurate*, *reliable* and *timely information* on weather is essential for other applications, such as flight navigation, precision agriculture etc.

In practice, data for NWP and climatic models are normally collected using balloon-borne radiosondes, satellites (polar and geostationary) and other sources, e.g., flight data from airplanes. Whereas Mackenzie (2003, p. 94) points out that about 9,500 land-based stations and 7,000 merchant ships at any one time send up weather balloons, Wickert (2002) noted that most of these data cover the northern hemisphere, with the southern hemisphere (especially Africa and South America) lacking adequate data due to financial constraints. The lack of radiosonde data is also noted in the oceanic areas, hence leading to inadequate data for NWP and climatic models.

1.3 Geoinformatics and Environmental Monitoring

To effectively address the diverse challenges typical in environmental monitoring, as outlined in Sect. 1.2, calls for the integration of various multi-disciplinary technologies. In this section, the role of geoinformatics in environmental monitoring is articulated. However, details of various geoinformation technologies are espoused in subsequent chapters. Within the monitoring framework proposed by Finlayson (1996) (see Sect. 1.1), geoinformatics could play a key role by providing efficient

methods for measuring and documenting *spatial environmental changes* at local, regional and global scales and over varying temporal scales.

Satellite remote sensing has been extensively applied in monitoring the environment, see e.g., Spitzer (1986), Leimgruber et al. (2005), Dymond (2001) etc. According to Lein (2012), satellite data enjoys a comparative advantage over other methodologies in several ways:

- Large areal coverage;
- Describes a recent historical record dating from the 1970s to present;
- Offers convenient digital storage and retrieval;
- Facilitates objective assessment of environmental conditions; and
- Provides a consistent basis for measurement that permits the analysis of change.

The ability to map and detect environmental changes is key to the successful application of satellite remote sensing in environmental monitoring. Either a *top-down* or *bottom-up* approach can be employed to integrate remote sensing into a monitoring program. Whereas a top-down approach is suitable with low spatial resolution imagery, and is therefore appropriate for monitoring areas of large geographic extent, the bottom-up approach, on the other hand, focuses on regional to local environmental scenarios and relies heavily on input from local stakeholders and/or governmental agencies. To be able to detect changes in remotely sensed imagery, different change detection algorithms ranging from algebraic to classification-based techniques have been developed.

Integrating satellite remote sensing and global navigation satellite systems (GNSS) satellites could be useful in conducting rapid pilot studies such as providing quick and accurate spatial coverage and in recording the locations of the collected samples. These space-based techniques could also play a vital role in implementing management actions and in auditing environmental plans. As an example, for coastal management plans, these technologies could be used to locate areas prone to erosion caused by variations in shoreline position, thereby leading to preventive actions being taken (see, e.g., Goncalves (2010), Goncalves et al. (2012)). For auditing purposes, for example, they could be used to indicate the locations of effluent from a given factory. Such spatial information can then be used to study the ecosystem at that particular location.

To enhance global weather and climatic predictions, current systems have to be complemented by a system that will provide global coverage, and whose signals will be able to penetrate clouds and dust to remote sense the atmosphere. Such a system, already proposed as early as 1965 by Fischbach (1965), and which is currently an active area of research, is the new field of *GNSS-Meteorology*. This involves the use of global positioning system (GPS) satellites to obtain atmospheric profiles of *temperature, pressure and water vapour/humidity*.

GPS was developed by the US for its military purposes. It is an all weather tool capable of providing three-dimensional positions at any time (Hofman-Wellenhof et al. 2001). At the time of its conception, fewer civilian applications were envisaged. In recent years, however, its use has widened to include, e.g., meteorological and environmental applications such as monitoring of sea level and variation in stored

fresh water (Awange et al. 2007; Awange 2012). This wide increase in GPS usage has led to the establishment of other equivalent systems by various nations/group of nations to meet their security and scientific needs.

For example, the European Union (EU) is launching the Galileo satellites, expected to be operational by 2014 or 2015, the Chinese are developing COMPASS (also known as Beidou-2, BD2) that is expected to have 35 satellites, and the Russians are improving upon their GLONASS system by having smaller and more manageable satellites that have now achieved the 24 satellites needed to reach a full operational capability. These constellations of satellites, collectively termed Global Navigation Satellite Systems (GNSS), will provide very useful tools for monitoring the environment. In Chap. 4 a brief overview of the GNSS systems and their future will be presented.

On the other hand, remote sensing is a rapidly advancing field of study that aims at the gathering of environmental data using a wide range of satellite and air-borne platforms. When combined with location-based GNSS data, remote sensing contributes enormously to spatio-temporal Earth surface monitoring with a spatial resolution approaching GPS data precision (Urbano et al. 2010). Various forms of remote sensing approaches, e.g., optical (passive), thermal (passive), photogrammetry (passive), LiDAR (Light Detection And Ranging) (active) and microwave (active), see e.g., Lillesand et al. (2010), Richards (1994), Jensen (2005) are available for environmental monitoring.

The importance of remote sensing for environmental applications has been demonstrated through NASA's launch of the Earth Observation Satellites (EOS) 'Terra' and 'Aqua' in 1999 and 2002, respectively, among many others. The objective of the EOS program was to develop the ability to monitor and predict environmental changes that occur both naturally and as a result of human activities through measurements of global and seasonally distributed Earth surface and atmospheric parameters such as land use, land cover, surface wetness, snow and ice cover, surface temperature, clouds, aerosols, fire occurrence, volcanic effects and trace gases (Huete 2004).

The inadequacy in the coverage of radiosonde data, as pointed out at the end of Sect. 1.2, is partly compensated for by the availability of polar and geostationary remote sensing satellite data. Polar orbiting satellites include the US-owned National Ocean and Atmospheric Administration NOAA-14 and NOAA-15 spacecrafts, while examples of geostationary satellites include the US-based Geostationary Operational Environmental Satellite (GEOS) and the European-owned METEORological SATellite (METEOSAT).

Polar and geostationary satellites, such as the above, provide temperature and water vapour profile measurements. However, they have their own limitations. For high altitude winter conditions, for instance, the use of passive Infra Red (IR) is difficult due to *very cold temperatures, common near-surface thermal inversion*, and a *high percentage of ice cloud* coverage that play a role in limiting IR soundings (Melbourne et al. 1994). In volcanic areas, remote sensing satellite measurements are also affected by the presence of dust and aerosol. Large-scale volcanic eruptions normally inject large amounts of aerosols into the lower stratosphere, thus limiting the IR observation of the stratosphere and lower regions.

Coupled with the above technologies for geodata acquisition is geographic information system (GIS). This is a spatial decision support tool comprised of hardware, software, data (which forms the primary component of GIS), human resource, and end users (clients). Until recently, GIS and related technologies such as GPS and remote sensing were largely the domain of a few researchers. Things, however, are changing with the exploitation of these systems for environmental monitoring. For instance, GIS is finding use in environmental applications because (Macarthur 2004):

- Environmental issues are subject to widespread interest and heated debate;
- GIS can handle a large amount of different kinds of data and organize these data into topics or themes that represent the multiple aspect of complex environmental issues; and
- GIS serves as a collaborative tool that promotes interaction.

The important feature of GIS that sets it apart from other information systems, e.g., those used in the financial world that need not or cannot make use of spatial or location-based attributes of the dataset, is its capability to make use of its databases to reference spatial features to locations (longitude, latitude, and altitude), relate these spatial attributes to maps of the region, and to offer spatial integration with other pertinent databases for the region (Taylor et al. 2000). It is in providing these cost effective location-based data for creating and updating GIS databases that GNSS plays a major role. GNSS also provides ground control points for remote sensing techniques that supply geodata to GIS, and the provision of a field mapping tool that enables attributes or features to be directly captured together with positions (see Fig. 2.2, p. 25).

In most text books, e.g., Spellerberg (2005), the most common satellite technique mentioned in environmental monitoring is remote sensing. Several applications have, however, directly reported the direct combination of GIS and GNSS for environmental monitoring, see e.g., Steede-Terry (2000). As an example of the integration of GNSS and GIS, Taylor et al. (2000) discuss the case of monitoring traffic congestion, which has the environmental impact of emitting CO₂ into the atmosphere thus contributing to global warming and increasing fuel consumption. They demonstrate how a GIS-GNSS system can be integrated to provide useful monitoring information, where GNSS provides locations for both static and dynamic recordings of vehicles' positions over time on the one hand. GIS on the other hand plays the role of database integrator by super-positioning separate map layers of the data base, e.g., maps of topography and land use, transport networks, infrastructure, socio-economic and demographic data, traffic flow data, pollution, and environmental impact data (Taylor et al. 2000). However, for such a system to be operationalized, remote sensing would still be required to provide updated map data as shown in Fig. 2.2 (p. 25).

Uriel (1998) discusses the relevance of spatial tools and landscape ecology to emerging infectious diseases and to studies of global change effects on vector-borne diseases, while Bonner et al. (2003) consider the combination of GNSS and GIS geocoding in epidemiological research. Barbari et al. (2006) examined the potential of combining GNSS and GIS to support studies on livestock behaviour in

pastures. They illustrated the potential to acquire information useful for cases such as breeding and good environmental management. In another animal behavioural study, Hebblewhite and Haydon (2010) found that the populations of most wide-ranging species move over areas in orders of magnitude larger in scope than could be revealed by traditional methods such as very high frequency (VHF) radio telemetry, and that the advent of GNSS-based radio telemetry offered the possibility of conservation benefits such as harvest management, habitat and movement corridor protection, and trans-boundary collaboration. They present the example of the Serengeti where simple GNSS-based locations over different jurisdictions with different levels of protection highlighted the precarious state of one of the wonders of the world—the Serengeti-Mara wildebeest migration (Hebblewhite and Haydon 2010; Thirgood et al. 2004).

A combination of GNSS and Argos collars have been used by Durner et al. (2009) to contribute to understanding the impact of climate change on polar bears. This is achieved, thanks to GNSS’ all-weather continuous observations that permitted year-round observations, revealing the circumpolar nature of polar bear movements, and the details of how sea ice thickness and structure influences polar bear success in hunting their main prey, seals (Hebblewhite and Haydon 2010). In Janssen (2012) an indirect tracking of drop bears using GNSS is presented. The possibility of integrating GNSS spatial data with other data, e.g., from remote sensing satellites, and socio-

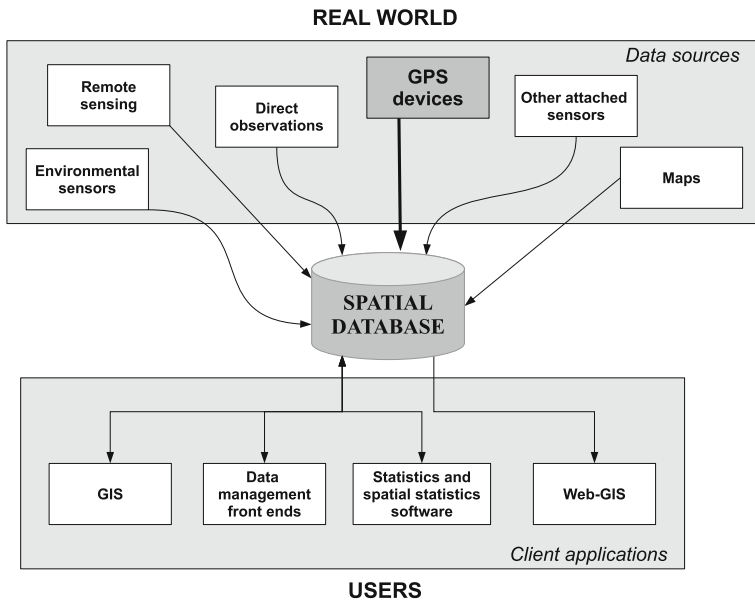


Fig. 1.2 Schema of a possible client/server software system that combines information from several data sources, including core GNSS data, into the central spatial database where it is accessed, locally or remotely, by client applications for manipulation, visualization and analysis. Outputs are stored back in the database. *Source* Urbano et al. (2010)

economic studies could potentially create a spatial database (see Fig. 1.2), which is of valuable use to environmental monitoring and management.

1.4 Geoinformatics and Environmental Management

Conacher (1978) start by distinguishing between resource and environmental management. On the one hand, *resource management* is defined as the set of technical, economic and managerial practices by which stocks are converted to resources for the purpose of satisfying man's utilitarian needs and wants under prevailing socio-economic and technological conditions. *Environmental management* on the other hand is defined as those activities that enhance beneficial links and minimize adverse links between resource systems and their environments, and which seek to attain desirable environmental system states in response to community perceptions and desires under prevailing socio-economic conditions. In this definitions, resource systems incorporate all the technical, economic, and managerial activities associated with the conversion of stocks to resources and resource management.

Whereas resource management is specific in focus and operates within set limits often with single purpose goals, environmental management is connected with adaptability of complex environments to future uncertainties and are invariably multi-purpose (Conacher 1978). The multi-purpose goals of environmental management comes about due to the fact that community desires and values form the bedrock of any environmental management and achieving unanimity of these desires and values are always impossible hence the use of multi-criteria analysis discussed in Chap. 28. Environmental management is therefore undertaken by first identifying the values that are to be protected, identifying management objectives to protect these values, setting out means to achieve the management objectives, and finally implementing the approaches. The whole procedure can be reviewed and improved as new data become available or new lessons are learnt. In general, environmental management can be undertaken for proprietors individual reasons, e.g., to fulfill legal requirement, fear of negative publicity or for cost-effectiveness purposes. Environmental management can also be undertaken for sustainability purposes.

Environmental management has seen a rapid evolution in its state from conservation in the early twentieth Century, preservation in the early-mid twentieth Century, protection in mid-late twentieth Century to Sustainability in the twenty-first century. The drivers to these rapid changes could be attributed partly to increased awareness that now sees environmental management being undertaken at both local and international levels. For instance, increase international awareness contributed to increased international agreements such as the Kyoto protocol (see Sect. 21.5.5). From implementation perspective, changes are now being seen is self motivation approach from industries, where they take a leading role of managing the environment rather than wait for the command and control approach from the government. This is partly due to image preservation and/or inducements in terms of tax rebate in some countries.

As stated in Sect. 1.1, environment, unlike resources that are measured in economic terms, are usually measured in terms of quality with respect to given benchmarks

(standards). Conacher (1978) notes that more useful and functional approaches are those that measure linkages between resource systems and their environments, e.g., statistical approaches, environmental impact assessment, and population interviews. In all these approaches, geoinformatics techniques discussed in this book comes in handy. For example, in undertaking environmental impact assessment, communities are nowadays well informed and the use of GIS to generate graphical environmental impact statements (EIS) for visualization is revolutionizing the procedures as we shall see later in Chap. 28. Further, since environmental management and planning are closely linked, use of geoinformatic techniques in planning, e.g., use of remote sensing and GIS for flood planning discussed in Chap. 26 contributes to efficient environmental management.

1.5 Objectives and Aims of the Book

This book is intended to be of use to two main groups of readers; those who deal with basic geoinformatics related theory, and those who apply it for environmental related tasks. This is informed by the fact that most environmental problems are inherently geographical (see, e.g., Dasgupta et al. 2005). It is aimed at realizing two main objectives:

- (1) To the geoinformation specialist, who deals with diverse mapping technologies like GNSS, remote sensing and GIS, the book aims at presenting examples of the possible applications of these technologies to environmental monitoring and management. Whereas GNSS is widely used as a tool for spatial data collection for position determination, unlike remote sensing, its role in environmental monitoring is now beginning to be appreciated, see e.g., Awange (2012). Examples are presented of possible applications of these technologies to support monitoring of tsunamis, earthquakes, e.g., Seidel and Randel (2006), rising sea level, flash floods, global warming, conservation measures of endangered species, and many other environmental phenomena that can be monitored with the help of the same. It is hoped that these examples will stimulate further research in the relevant areas in an attempt to meet the needs and challenges of environmental monitoring and management.
- (2) To those in environmental monitoring and management related fields, the book aims at presenting the Geoinformatic concepts of GNSS, remote sensing and GIS in a simplified format. For example, it deliberately moves away from the complex mathematical formulations found in many GNSS books, which often intimidate those whose aim is to simply understand the basics. Where only absolutely necessary are the mathematical details presented with such usage limited to the understanding of particular topics. The book highlights the need for integrating GNSS-based location data with other spatial data derived from, for example remote sensing of the environment and socio-economic data for

the further enhancement of environmental monitoring and management through GIS.

Pursuant to the above aims, in the remaining chapter of Part I we introduce the concepts of geodata and fundamentals of geoinformatics. In Part II we present the basic concepts of environmental geodesy—hopefully in a manner that would be easily understood by environmentalists. This part elucidates the fundamentals of surveying and geodesy, along with modernization of GNSS and characteristics of GPS, before wrapping up with considerations for environmental surveying and surveillance. In Part III we describe the concepts of remote sensing, with optical and microwave remote sensing distinguished. Essentials of photogrammetry and basic concepts in digital photogrammetry are also articulated in Part III. Part IV deals with the basics of GIS including data models and structure, data capture, GIS database, spatial analysis and web GIS. Finally, in Part V of the book we present diverse applications of geoinformatics in monitoring and management of the environment.

References

- Artiola J, Pepper IL, Brusseau ML (eds) (2004) *Environmental monitoring and characterization*. Elsevier Academic Press, San Diego
- Awange JL (2012) *Environmental monitoring using GNSS, global navigation satellite system*. Springer, Berlin
- Awange JL, Sharifi M, Ogonda G, Wickert J, Grafarend EW, Omulo M (2007) The falling Lake Victoria water level: GRACE, TRIMM and CHAMP satellite analysis. *Water Resour Manag*. doi:[10.1007/s11269-007-9191-y](https://doi.org/10.1007/s11269-007-9191-y)
- Barbari M, Conti L, Koostra BK, Masi G, Workman SR (2006) The use of global positioning and geographical information systems in the management of extensive cattle grazing. *Biosyst Eng* 95(2):271–280. doi:[10.1016/j.biosystemseng.2006.06.012](https://doi.org/10.1016/j.biosystemseng.2006.06.012)
- Bonner MR, Han D, Nie J, Rogerson P, Vena JE, Freudenheim Jo L (2003) Positional accuracy of geocoded addresses in epidemiologic research. *Epidemiology* 14:408–412. doi:[10.1097/01.EDE.0000073121.63254.c5](https://doi.org/10.1097/01.EDE.0000073121.63254.c5)
- Burden FR, McKelvie I, Förstner U, Guenther A (2002) *Environmental monitoring handbook*. McGraw-Hill, New York
- Conacher AJ (1978) Resource and environmental management. Some fundamental concepts and definitions. In: Thakur B (ed) *Perspective in resource management in developing countries*. Resource management: theory and techniques, vol 1. Concept Publishing, New Delhi, pp 49–60
- Dasgupta S, Deichmann U, Meisner C, Wheeler D (2005) Where is Poverty-Environment Nexus? Evidence from Cambodia, Lao PDR, and Vietnam. *World Development* 33(4):617–638, doi:[10.1016/j.worlddev.2004.10.003](https://doi.org/10.1016/j.worlddev.2004.10.003)
- Downes BJ, Barnuta LA, Fairweather PG, Faith DP, Keough MJ, Lake PS, Mapstone BD, Quinn GP (2002) *Monitoring ecological impacts: concepts and practise in flowing waters*. Cambridge University Press, Cambridge
- Durner GM et al (2009) Predicting 21st-century polar bear habitat distribution from global climate models. *Ecol Monogr* 79:25–58. doi:[10.1890/07-2089.1](https://doi.org/10.1890/07-2089.1)
- Dymond J, Begue A, Loseen D (2001) Monitoring land at regional and national scales and the role of remote sensing. *JAG* 3:162–175

- Finlayson CM (1996) Framework for designing a monitoring program. In: Tomas Vives P (ed) *Monitoring mediterranean wetlands: a methodological guide*. MedWet Publication, Wetlands International, Slimbridge, UK and ICN, Lisbon
- Fischbach FF (1965) A satellite method for pressure and temperature below 24 km. *Bull Am Meteorol* 46:528–532
- Goldsmith FB (ed) (1991) *Monitoring for conservation and ecology*. Chapman and Hall, New York
- Goncalves RM (2010) Short-term trend modeling of the shoreline through geodetic data using linear regression, robust estimation and artificial neural networks. PhD thesis, Geodetic Sciences Post-graduate Program, Federal University of Parana (UFPR), Curitiba, Brazil, 152 pp
- Goncalves RM, Awange JL, Krueger CP, Heck B, Coelho LS (2012) A comparison between three short-term shoreline prediction models. *Ocean Coast Manag* 69:102–110. doi:[10.1016/j.ocecoaman.2012.07.024](https://doi.org/10.1016/j.ocecoaman.2012.07.024)
- Hebblewhite M, Haydon DT (2010) Distinguishing technology from biology: a critical review of the use of GPS telemetry data in ecology. *Philos Trans R Soc B* 365:2303–2312. doi:[10.1098/rstb.2010.0087](https://doi.org/10.1098/rstb.2010.0087)
- Hofman-Wellenhof B, Lichtenegger H, Collins J (2001) *Global positioning system: theory and practice*, 5th edn. Springer, Wien
- Huete AR (2004) Remote sensing for environmental monitoring. In: Artiola J, Pepper IL, Brusseau ML (eds) *Environmental monitoring and characterization*. Elsevier Academic Press, San Diego
- James LF, Young JA, Sanders K (2003) A new approach to monitoring rangelands. *Arid Land Res Manag* 17:319–328. doi:[10.1080/15324980390225467](https://doi.org/10.1080/15324980390225467)
- Janssen V (2012) Indirect tracking of drop bears using GNSS technology. *Australian Geographer* 43(4) 445–452
- Jensen JR (2005) *Introductory digital image processing: a remote sensing perspective*, 3rd edn. Prentice-Hall, Upper Saddle River
- Larson LW (1996) Destructive water: water-caused natural disasters, their abatement and control. In: IAHS conference, Anaheim, CA, pp 24–28
- Leimgruber P, Christen C, Laborderie A (2005) The impacts of landsat satellite monitoring on conservation biology. *Environ Monit Assess* 106:81–101
- Lein JK (2012) *Environmental sensing: analytical techniques for earth observation*. Springer, New York, 334 pp: doi:[10.1007/978-1-4614-0143-8](https://doi.org/10.1007/978-1-4614-0143-8)
- Lillesand TM, Kiefer RW, Chipman JW (2010) *Remote sensing and image interpretation*. Wiley, New York
- Macarthur R (2004) Geographical information systems and their use for environmental monitoring. In: Artiola J, Pepper IL, Brusseau ML (eds) *Environmental monitoring and characterization*. Elsevier Academic Press, San Diego
- Mackenzie FT (2003) *Our changing planet; an introduction to Earth system science and global environmental change*, 3rd edn. Prentice Hall, New York
- Melbourne WG, Davis ES, Duncan CB, Hajj GA, Hardy K, Kursinski R, Mehan TK, Young LE, Yunck TP (1994) The application of spaceborne GPS to atmospheric limb sounding and global change monitoring. JPL Publication 94-18, JPL, Pasadena
- Richards JA (1994) *Remote sensing digital image analysis: an introduction*. Springer, Berlin
- Study of Critical Environmental Problems (1970) *Man's impact on the global environment*. MIT Press, Cambridge
- Seidel DJ, Randel WJ (2006) Variability and trends in the global tropopause estimated from radiosonde data. *J Geophys Res* 111. doi:[10.1029/2006JD007363](https://doi.org/10.1029/2006JD007363)
- Spellerberg IF (2005) *Monitoring ecological change*, 2nd edn. Cambridge University Press, Cambridge
- Spitzer D (1986) On the application of remote sensing for environmental monitoring. *Environ Monit* 7:263–271
- Steede-Terry K (2000) *Integrating GIS and the global positioning system*. ESRI Press, California

- Taylor MAP, Woolley JE, Zito R (2000) Integration of the global positioning system and geographical information systems for traffic congestion studies. *Transp Res Part C* 8(1–6):257–285. doi:[10.1016/S0968-090X\(00\)00015-2](https://doi.org/10.1016/S0968-090X(00)00015-2)
- Thirgood S, Mosser A, Tham S, Hopcraft G, Mwangomo E, Mlengeya T, Kilewo M, Fryxell J, Sinclair ARE, Borner M (2004) Can parks protect migratory ungulates? the case of the serengeti wildebeest. *Anim Conserv* 7:113–120. doi:[10.1017/S1367943004001404](https://doi.org/10.1017/S1367943004001404)
- Urbano F, Cagnacci F, Clement C, Dettki H, Cameron A, Neteler M (2010) Wildlife tracking data management: a new vision. *Philos Trans R Soc B* 365:2177–2185. doi:[10.1098/rstb.2010.0081](https://doi.org/10.1098/rstb.2010.0081)
- Uriel K (1998) Landscape ecology and epidemiology of vector-borne diseases: tools for spatial analysis. *J Med Entomol* 35(4):435–445
- Vaughan H, Brydges T, Fenech A, Lumb A (2001) Monitoring long-term ecological changes through the ecological monitoring and assessment network: science-based and policy relevant. *Environ Monit Assess* 67:3–28
- Wickert J (2002) Das CHAMP-Radiookkultationsexperiment: algorithmen, Prozessierungssystem und erste ergebnisse. Dissertation, Scientific technical report STR02/07, GFZ Potsdam
- Wiersma GB (ed) (2004) Environmental monitoring. CRC Press, Boca Raton

Chapter 2

Geodata and Geoinformatics

“A human being is part of a whole, called by us the universe, a part limited in time and space. He experiences himself, his thoughts and feelings, as something separated from the rest, a kind of optical delusion of his consciousness. This delusion is a kind of prison for us, restricting us to our personal desires and to affection for a few persons nearest us. Our task must be to free ourselves from this prison by widening our circles of compassion to embrace all living creatures and the whole of nature in its beauty.”

Albert Einstein (1879–1955)

2.1 Dimensions of Space, Time and Scale

Understanding the characteristics of and possibilities in using geodata is premised on proper comprehension of the underlying concepts of space, time and scale, contextualized within the Earth’s framework. Although these concepts are used in everyday parlance, often without much afterthought, they are not trivial at all. For instance, looking back throughout the entire history of mankind, the concepts of space and time have been the subject of animated philosophical, religious and scientific debates. In this section, we attempt to present a background of each of these dimensions of geodata, both independently and collectively, as well as highlight their relevance in influencing the character of geodata.

Space is that boundless, three-dimensional extent in which objects and events occur and have relative position and direction (Britannica 2011). In analytical geometry, one examines “spaces” with different dimensionality and underlying structures. Indeed, the concept of space is considered to be of fundamental importance to an understanding of the physical universe although disagreement continues between

philosophers over whether it is itself an entity, a relationship between entities, or part of a conceptual framework (Wikipedia 2011).

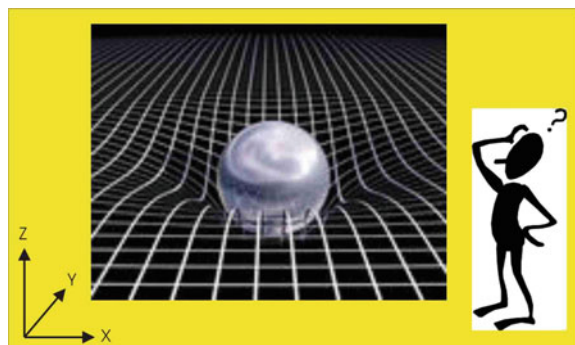
Philosophical debates on the nature, essence and the mode of existence of space date back to antiquity. From treatises like that championed by *Timaeus of Plato* in his reflections on what the Greeks called *khora* (i.e. space), to the physics of *Aristotle* in the definition of *topos* (i.e. place), or to even the geometrical conception of place as “*space qua extension*” by *Alhazen* (El-Bizri 2007).

Many of the classical philosophical assertions were later discussed and reformulated in the seventeenth century, particularly during the early development of classical mechanics. For example, in *Sir Isaac Newton's* view, space was absolute, in the sense that it existed permanently and independent of whether there were any matter in the space (French and Ebison 2007). However, other philosophers like *Gottfried Leibniz* were of the different view that space was a collection of relations between objects, given by their distance and direction from one another (Wikipedia 2011).

Up until around the eighteenth century, and within the framework of *Euclidean geometry*, space was perceived by most mathematicians to be flat. However, between the nineteenth and twentieth centuries mathematicians began to examine *non-Euclidean geometries*, in which space was inferred to be curved, rather than flat. According to *Albert Einstein's* theory of *general relativity*, space around gravitational fields deviates from Euclidean space (Carnap 1995). Furthermore, experimental tests of general relativity have confirmed that non-Euclidean space provides a better model for the shape of space as illustrated in Fig. 2.1.

Turning to the dimension of time, time is considered to be part of the measuring system used to sequence events, to compare the durations of events and the intervals between them, and to quantify rates of change such as the motions of objects (Internet Encyclopedia of Philosophy 2011). The temporal position of events with respect to the transitory present is continually changing. For example, future events become present, then pass further back into the past. In the *Bible*, time is traditionally regarded as a medium for the passage of predestined events. Subsequently, there is an appointed time for everything, see e.g., *Ecclesiastes 3:1–8* (Bible 2011). Evidently, time has been a major subject in religion, philosophy, and science, but defining it in a non-

Fig. 2.1 Concept of non-Euclidean space



controversial manner applicable to all fields of study has consistently eluded the greatest scholars (Wikipedia 2011).

Time is one of the seven fundamental physical quantities defined in the International System of (SI) Units. It is also used to define other quantities, such as velocity. An operational definition of time infers that observing a certain number of repetitions of one or another standard cyclical event (such as the passage of a free-swinging pendulum) constitutes one standard unit such as the second. This view is highly useful in the conduct of both advanced experiments and everyday affairs of life. However, this operational definition ignores the question whether there is something called *time*, apart from the counting activity that transits and can be measured (Wikipedia 2011).

Two contrasting assertions on time divide many prominent philosophers. The first view is that time is part of the fundamental structure of the universe, a dimension in which events occur in sequence. *Sir Isaac Newton* subscribed to this realistic view, and hence it is sometimes referred to as *Newtonian time*, see e.g., Rynasiewicz (1995a, b), Markosian (2002) etc. According to this view, time travel becomes a possibility as other “times” persist like frames of a film strip, spread out across the time line.

The second and opposing view contends that time does not refer to any kind of “container” that events and objects “move through”, nor to any entity that “flows”, but that it is instead part of a fundamental intellectual structure (together with space and number) within which humans sequence and compare events. This assertion, in the tradition of *Gottfried Leibnitz* (Burnham 2006) and *Immanuel Kant* (see e.g., Matthey 1997, McCormick 2006 etc) holds that time is neither an event nor a thing, and thus it is not itself measurable nor can it be traveled.

Temporal measurement has occupied the minds of scientists for a long time and was the prime motivation in the disciplines of navigation and astronomy. Periodic events and periodic motion have long served as standards for units of time. Examples include the apparent motion of the sun across the sky, the phases of the moon, the swing of a pendulum, and the beat of a heart. Currently, the international unit of time, the *second*, is defined in terms of radiation emitted by cesium atoms. Time is also of significant social importance and is often viewed as having economic value as captured by the popular adage *time is money*, as well as personal value, due to an awareness of the limited and finite time in each day and in the human life span (Wikipedia 2011). Consequently, different time scales are employed in different application domains, such as geological time (Harland et al. 1989; Haq 2006; Kulp 1961), biological time (Winfree 2001; Enright 1965; Hochachka and Guppy 1987) etc.

From the above discussion, regardless of the school of thought advanced, it is evident that historically, the dimensions of space and time have been closely related. As a matter of fact, it is virtually impossible to describe either of the two dimensions without inferring the other. Put together, these two dimensions represent the *space-time* concept expressed in Einstein’s special relativity and general relativity theories. According to these theories, the concept of time depends on the spatial reference frame of the observer, and the human perception as well as the measure-

ment by instruments such as clocks are different for observers in relative motion. Subsequently, the past is the set of events that can send light signals to the observer, whilst the future is the set of events to which the observer can send light signals (Wikipedia 2011).

This then brings us to the dimension of scale. The scale of a map is an important metric that defines the level of detail of geoinformation that can be extracted from such a map (see Sect. 19.1). Scale also gives an indication of the resolution in the geodata. In general, a larger scale means that more geodata would be captured, including fuzzy detail that might otherwise be generalized or glossed over at smaller scales. The interpretation of scale is therefore important. For instance, by simply varying the map scale alone, the estimated distance between two points would vary. Many researches have studied the scale dimension and its perception and meaning in different applications, see e.g., Mandelbrot (1967), Fisher et al. (2004), Levin (1992), Tate and Wood (2001) etc. A review of space, time and scale from a geographer's perspective is given in Meentemeyer (1989).

For many years, the dimension of scale was not explicitly integrated into data modeling. Therefore, scale was assumed to be uniform within a spatio-temporal context. This was done ostensibly to keep the whole geo-modeling problem simplified. The fact that classical maps could only be produced at one specific scale probably reiterates this. By convention, national mapping agencies had to designate certain mapping scales for different map coverages. This therefore enabled map users to identify the maps that were suitable for different applications. For example, in typical civil engineering work, whereas a scale of 1:50,000 would be appropriate at the reconnaissance or preliminary planning stage, larger scales of 1:500–1:2,000 would be required at the construction or maintenance phases.

Evidently, the scale dimension has not evoked as much controversy as the twin dimensions of space and time. The issue with the scale dimension has been more to do with the scientific challenge of identifying appropriate data models and structures. Indeed, consideration of scale as an extra dimension of geographic information, fully integrated with the other dimensions, is a fairly recent proposition (Oosterom and Stoter 2010). Whereas 3D space captures the geometrical characteristics of geodata, 4D integrates the temporal representation, with the 5D providing the scale definition. Meentemeyer (1989) avers that most geographic research is now conducted with a relativistic view of space rather than a view of space as a "container". However, spatial scales for relative space are more difficult to define than those for the absolute space of cartography and remote sensing (Meentemeyer 1989).

In concluding this section, it is important to recognize that the five dimensions of space, time and scale are integral to the unambiguous definition of position for they help to fully integrate 5D data modeling. Realizing this would ensure that geodata is used seamlessly with no undesirable overlaps or gaps and assuming consistency across space, time and scale dimensions. In future, probably the existence and relative importance of different classes in diverse applications could also be considered in a more integrated manner as the sixth dimension of geodata—the *semantic* dimension (Oosterom and Stoter 2010).

Table 2.1 Hierarchy of decision making support infrastructure

Level of decision-making support infrastructure	Ease of sharing	Example
Wisdom	Impossible	Policies developed and accepted by stakeholders e.g., ideal use for parcel
↑		
Knowledge	Difficult (especially tacit knowledge)	Personal knowledge about places and issues e.g., adjoining parcel boundaries
↑		
Evidence	Often not easy	Results of spatial analysis of datasets or scenarios e.g., parcel area
↑		
Information	Easy	Contents of a database assembled from raw facts e.g., owner of parcel
↑		
Data	Easy	Raw facts and figures e.g., geographic coordinates

Modified after Longley et al. (2005)

2.2 Geodata

Data is simply defined as any set of raw facts or figures that have been collected, often in a systematic manner, and from which inference(s) may be drawn. Similarly, *information* is defined as any useful data that satisfies some user need(s). This is generally required to support the making of decisions. Apparently, data and information constitute the basic building blocks in the decision-making support infrastructure that also includes *evidence*, *knowledge* and *wisdom* as summarized in Table 2.1.

An *information system* is a combination of technical and human resources, together with a set of organizing procedures that produces information in support of decision-making usually to meet some managerial requirement. Thus an information system should be able to receive, store, process, update, output and distribute data and information. Classical information systems for general management are called *Management Information Systems (MIS)*. They are distinguished from *Geographic Information Systems*, which are information systems that deal with spatially referenced data and are discussed in more detail in Sect. 13.1.

Data is distinguished as *geodata* (or *geospatial* data) if it can be geographically referenced in some consistent manner using for example; latitudes and longitudes, national coordinate grids, postal codes, electoral or administrative areas, watershed basins etc. As mentioned in Sect. 2.1, although geodata is normally defined in 3D in many practical applications, it needs to be redefined in 5D for geodata to be used without any restrictions in space, time or scale. The first three dimensions describe

the geometric characteristics of geodata usually in 3D space. The fourth dimension provides the temporal representation that denotes how geodata has changed over time, while the scale is represented by the fifth dimension. This dimensional view of geodata is important for it ensures that there are no gaps or overlaps in the data. Furthermore, it also maintains the consistency of geodata across space, time and scale dimensions. Section 6.6.1 reviews typical datums used in surveying.

Geodata may be collected by both government organizations as well as private agencies. A key characteristic of this type of data is its potential for diverse and multiple applications. Moreover, geodata can be shared and re-used by different users and applications through the *spatial data infrastructure* (SDI), see e.g., Groot and McLaughlin (2000), Nebert (2004), Maguire and Longley (2005) etc. To infer the correct decision(s), it is imperative that the geodata be *accurate, complete, consistent* and *timely*. Furthermore, it is important that the required geodata be made available and that in addition, it also be allowed to flow unhindered to and between the various users and applications.

2.3 Digital Earth Concept

Digital Earth is the name given to a concept coined by former US vice president Al Gore in 1998, that describes a virtual representation of the Earth that is spatially referenced and interconnected with the world's digital knowledge archives.¹ Furthermore, the greater part of this knowledge store would be free to all via the *Internet*. However, a commercial marketplace of related products and services was envisioned to co-exist, in part in order to support the expensive infrastructure that such a system would require (Wikipedia 2011).

Clearly, many aspects of this vision have been realized, evidenced in part by the popularity of virtual globe geo-browsers such as *Google Earth*² for commercial, social and scientific applications as discussed in Chap. 18. But the Gore speech outlined a truly global, collaborative linking of systems that has yet to be fully realized (Wikipedia 2011). That vision has been continually interpreted and refined by the growing global community of interest. As technological advances have made the unlikely possible, the vision has evolved and become more concrete, and as we better understand the interdependence of the environment and social activities, there is greater recognition of the need for such a system. Digital Earth has come to stand for the large and growing set of web-based geographic computing systems worldwide. These are both useful and promising, but do not yet constitute the envisioned *global commons* (Wikipedia 2011).

¹ In a speech prepared for the California Science Center in Los Angeles on January 31, 1998, Gore described a digital future where school children—indeed all the world's citizens—could interact with a computer-generated three-dimensional spinning virtual globe and access vast amounts of scientific and cultural information to help them understand the Earth and its human activities.

² <http://www.earth.google.com>

The global dimension of the digital Earth concept is perhaps best captured by two excerpts from the Beijing declaration³ on digital Earth, which state as follows (Beijing 2009):

- (a) Digital Earth is an integral part of other advanced technologies including: Earth observation, geo-information systems, global positioning systems, communication networks, sensor webs, electromagnetic identifiers, virtual reality, grid computation, etc. It is seen as a global strategic contributor to scientific and technological developments, and will be a catalyst in finding solutions to international scientific and societal issues;
- (b) Digital Earth should play a strategic and sustainable role in addressing such challenges to human society as natural resource depletion, food and water insecurity, energy shortages, environmental degradation, natural disasters response, population explosion, and, in particular, global climate change.

A consortium of international geographic and environmental scientists from government, industry, and academia brought together by the *Vespucci Initiative for the Advancement of Geographic Information Science, and the Joint Research Center of the European Commission* published a position paper that outlined the eight key next generation digital Earth elements to include the following (Craglia et al. 2008):

- (1) Not one digital Earth, but multiple connected globes/infrastructures addressing the needs of different audiences: citizens, communities, policy-makers, scientists, educationalists;
- (2) Problem oriented: e.g., environment, health, societal benefit areas, and transparent on the impacts of technologies on the environment;
- (3) Allowing search through time and space to find similar/analogous situations with real time data from both sensors and humans (different from what existing GIS can do, and different from adding analytical functions to a virtual globe);
- (4) Asking questions about change, identification of anomalies in space in both human and environmental domains (flag things that are not consistent with their surroundings in real time);
- (5) Enabling access to data, information, services, and models as well as scenarios and forecasts: from simple queries to complex analyses across the environmental and social domains;
- (6) Supporting the visualization of abstract concepts and data types (e.g., low income, poor health, and semantics);
- (7) Based on open access, and participation across multiple technological platforms, and media (e.g., text, voice and multi-media); and
- (8) Engaging, interactive, exploratory, and a laboratory for learning and for multi-disciplinary education and science.

³ Ratified on September 12, 2009 at the 6th international symposium on digital earth in Beijing, Peoples Republic of China.

2.4 Fundamentals of Geoinformatics

Having introduced the 5D datum paradigm that needs to be adequately dealt with to define geodata accurately, consistently, timely and completely so that it can be used without any restrictions in space, time or scale and further, having appreciated the truly global dimension of the digital Earth, to put everything in perspective, it is now appropriate to focus on geoinformatics. Like for all other disciplines elaborated in this book it is only right to begin this discussion with pertinent definitions.

Although geoinformatics is a fairly recent terminology, various definitions of the same have been advanced by different authors. For instance, Raju (2003) describes geoinformatics as “the science and technology dealing with the structure and character of spatial information, its capture, its classification and qualification, its storage, processing, portrayal and dissemination, including the infrastructure necessary to secure optimal use of this information”. Similarly, Ehlers (2003) defines geoinformatics as “the art, science or technology dealing with the acquisition, storage, processing, production, presentation and dissemination of geoinformation”.

The bottom line is that there is no globally accepted definition of geoinformatics. However, as a multidisciplinary field, geoinformatics has at its core different technologies that support the acquisition, analysis and visualization of geodata. The geodata is usually acquired from Earth observation sensors as remotely sensed images, analyzed by geographic information systems (GIS) and visualized on paper or on computer screens. Furthermore, it combines geospatial analysis and modeling, development of geospatial databases, information systems design, human-computer interaction and both wired and wireless networking technologies. Geoinformatics uses geocomputation and geovisualization for analyzing geoinformation. Typical branches of geoinformatics include: *cartography, geodesy, geographic information systems, global navigation satellite systems (GNSS), photogrammetry, remote sensing, and web mapping*. These different disciplines that have been developed over different time epochs form the main subject matter of this book.

By combining the ever-increasing computational power, modern telecommunications technologies, abundant and diverse geodata, and more advanced image analysis algorithms available, and integrating technologies such as remote sensing, GIS and GNSS, many opportunities for application of geoinformatics have been realized. Today, many applications routinely benefit from geoinformatics including; urban planning and land use management, in-car navigation systems, virtual globes, public health, local and national gazetteer management, environmental modeling and analysis, military, transport network planning and management, agriculture, meteorology and climate change, oceanography and coupled ocean and atmosphere modeling, business location planning, architecture and archaeological reconstruction, telecommunications, criminology and crime simulation, aviation and maritime transport etc.

Consequently, geoinformatics has become a very important technology to decision-makers across a wide range of disciplines, industries, commercial sector, environmental agencies, local and national government, research and academia,

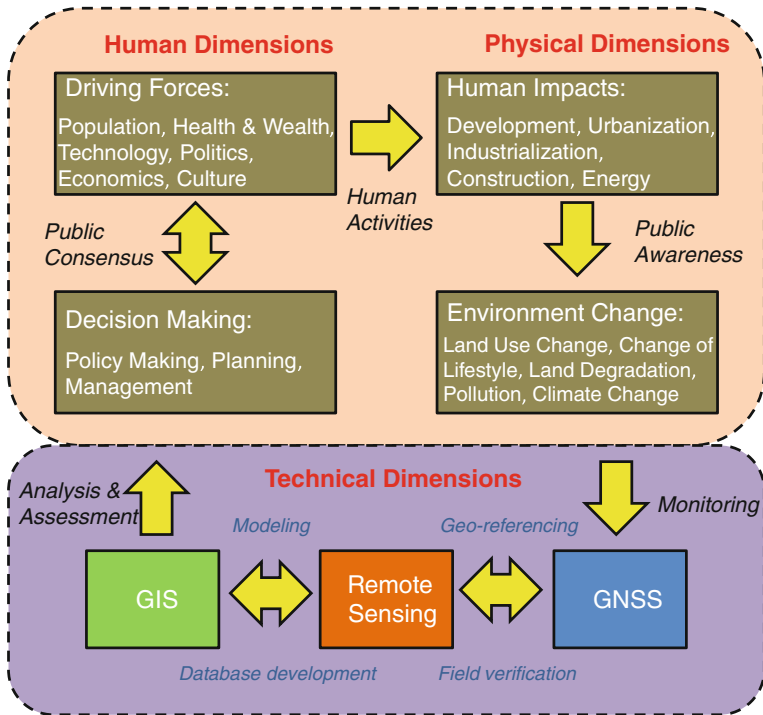


Fig. 2.2 Conceptual framework showing the role of geoinformatics in spatial decision support (Modified after Murai 1999)

national survey and mapping organizations, international organizations, United Nations, emergency services, public health and epidemiology, crime mapping, transportation and infrastructure, information technology industries, GIS consulting firms, environmental management agencies, tourist industry, utility companies, market analysis and e-commerce, mineral exploration etc. Increasingly, many government and non government agencies worldwide are using geodata and geoinformatics for managing their day to day activities. Figure 2.2 shows a conceptual framework that underlines the role of geoinformatics in supporting spatial decision-making.

2.5 Concluding Remarks

Although still unusual in many practical mapping constructs worldwide, a 5D coordinate reference framework is, nonetheless, desirable. This would not only ensure that geodata are defined accurately, consistently, timely and completely, but also guarantee that they are employed without any restrictions whatsoever in terms of space, time and/or scale. There is no doubt that, perhaps more that ever before,

humanity faces a myriad of complex and demanding challenges today. These include natural resource depletion, food and water insecurity, energy shortages, environmental degradation, intermittent natural disasters, population explosion, global climate change etc. To develop pragmatic and sustainable solutions to address these and many other similar challenges requires the use of geodata and the application of geoinformatics.

References

- Beijing (2009) Proceedings of the 6th international symposium on digital earth (ISDE6), Beijing, 9–12 Sept 2009
- Bible (2011) King James version. www.kingjamesbibleonline.org. Accessed 4 May 2011
- Britannica (2011) <http://www.britannica.com/>. Accessed 30 Mar 2011
- Burnham D (2006) Gottfried Wilhelm Leibniz (1646–1716) metaphysics—7. Space, time, and indiscernibles. *The Internet Encyclopedia of Philosophy*
- Carnap R (1995) *An introduction to the philosophy of science*. Courier Dover Publications, New York, 300 pp
- Craglia M, Goodchild MF, Annoni A, Camara G, Gould M, Kuhn W, Mark D, Masser I, Maguire D, Liang S, Parsons E (2008) Next-generation digital earth. *Int J Spat Data Infrastruct Res* 3:146–167
- Ehlers M (2003) Geoinformatics and digital earth initiatives: a German perspective. *Int J Dig Earth* 1(1):17–30
- El-Bizri N (2007) In defence of the sovereignty of philosophy: al-Baghdadi's critique of Ibn al-Haytham's geometrisation of place. *Arab Sci Philos (A historical journal. Cambridge University Press)* 17:57–80
- Enright JT (1965) The search for rhythmicity in biological time-series. *J Theoret Biol* 8(3):426–468
- Fisher P, Wood J, Cheng T (2004) Where is Helvellyn? Fuzziness of multi-scale landscape morphometry. *Trans Inst Br Geogr* 29:106–128
- French AP, Eibson M (2007) *Introduction to classical mechanics*. Chapman and Hall, London, 341 pp
- Groot R, McLaughlin J (eds) (2000) *Geospatial data infrastructure: concepts, cases and good practice*. Oxford University Press, Oxford
- Haq BU (2006) *The geological time table Wallchart*, 6th edn. Elsevier, New York
- Harland WB, Armstrong RL, Craig LE, Smith AG, Smith DG (1989) *A geologic time scale*. Cambridge University Press, Cambridge
- Hochachka PW, Guppy M (1987) *Metabolic arrest and the control of biological time*, ISBN 0-674-56976-8
- Internet Encyclopedia of Philosophy (2011) <http://www.iep.utm.edu/>. Accessed 13 Mar 2011
- Kulp JL (1961) Geologic time scale. *Science* 133(3459):1105–1114. doi:[10.1126/science.133.3459.1105](https://doi.org/10.1126/science.133.3459.1105)
- Levin SA (1992) The problem of pattern and scale in ecology. *Ecology* 73:1943–1967
- Longley PA, Goodchild MF, Maguire DJ, Rhind DW (2005) *Geographic information systems and science*. Wiley, West Sussex
- Maguire DJ, Longley PA (2005) The emergence of geoportals and their role in spatial data infrastructures. *Comput Environ Urban Syst* 29(1):3–14
- Mandelbrot B (1967) How long is the coast of Britain? In: *Statistical self-similarity and fractional dimension*. *Science (New Series)* 156(3775):636–638
- Markosian N (2002) Time. In: Zalta EN (ed) *The Stanford encyclopedia of philosophy*. Oxford University Press, Oxford
- Mattey GJ (1997) Critique of pure reason. In: *Lecture notes: Philosophy 175 UC Davis*

- McCormick M (2006) Immanuel Kant (1724–1804) metaphysics: 4. Kant's transcendental idealism. *The Internet Encyclopedia of Philosophy*
- Meentemeyer V (1989) Geographical perspectives of space, time, and scale. *Landsc Ecol* (Springer) 3(3–4):163–173. doi:[10.1007/BF00131535](https://doi.org/10.1007/BF00131535)
- Murai S (1999) GIS work book: fundamental and technical courses, vols 1–2. National Space Development Agency of Japan (NASDA)/Remote Sensing Technology Center of Japan (RESTEC). Japan Association of Surveyors
- Nebert DD (ed) (2004) Developing spatial data infrastructures: the SDI cookbook. Global spatial data infrastructure (GSDI), Technical Working Group Chair
- Oosterom P, Stoter J et al (2010) 5D data modelling: full integration of 2D/3D space, time and scale dimensions. In: Fabrikant SI (ed) *GIScience 2010, LNCS*, vol 6292. Springer, Berlin, pp 310–324
- Raju PLN (2003) Fundamentals of geographic information systems. In: Sivakumar MVK, Roy PS, Harmsen K, Saha SK (eds) *Workshop: satellite remote sensing and GIS applications in agricultural meteorology, India*
- Rynasiewicz R (1995a) By their properties, causes and effects: Newton's Scholium on time, space, place and motion. Part I: The text. *Stud Hist Philos Sci* 26:133–153
- Rynasiewicz R (1995b) By their properties, causes and effects: Newton's Scholium on time, space, place and motion. Part II: The context. *Stud Hist Philos Sci* 26:295–321
- Tate N, Wood J (2001) Fractals and scale dependencies in topography. In: Tate N, Atkinson P (eds) *Modelling scale in geographical information science*. Wiley, Chichester, pp 35–51
- Wikipedia (2011) <http://en.wikipedia.org/wiki/>. Accessed 28 Aug 2011
- Winfree AT (2001) *The geometry of biological time*. Springer, 777 pp, ISBN 0387989927

Part II
Environmental Geodesy

Chapter 3

Fundamentals of Surveying and Geodesy

“We must admit with humility that, while number is purely a product of our minds, space has a reality outside our minds, so that we cannot completely prescribe its properties a priori.”

Carl Friedrich Gauss (1777–1855)

3.1 Environmental Geodesy

Although the environment has remained at the forefront of scientific interest for well over four decades (e.g., Lein (2012)), it is not until this decade that remote sensing of the environment using geodetic methods started gaining momentum. This has largely been fuelled by the launching and modernization of satellites that enable the environment to be measured, mapped, and modelled. The advent of these satellites have given birth to a new field of “*Environmental Geodesy*”, which can be argued as that branch of geodesy that applies geodetic techniques to monitor the environment and provide information that contribute towards effective management of the environment by supporting appropriate decision making. This is true since geodesy’s primary task is that of measuring the Earth’s surface, a task which could easily find use in environmental applications.

Amongst the geodetic techniques that could be useful to environmental sensing include: Satellite laser ranging (SLR) that are useful in monitoring mass redistribution e.g., postglacial and also in calibrating altimetry satellites; interferometric synthetic aperture radar (InSAR) that are finding use in monitoring vertical deformation and oil leaks; satellite altimetry used in monitoring the melting polar ice and changing sea level; very long baseline interferometry (VLBI) that are useful in plate tectonic studies, etc. Perhaps the most revolutionary techniques that have pushed geodesy to the forefront of sensing the environment are the satellites gravity measurements (e.g., from CHAMP (CHALLENGING Mini-satellite Payload), GRACE (Gravity

Recovery And Climate Experiment) and GOCE (Gravity field and the steady state-of-the ocean circulation explorer, Fig. 20.8). Apart from gravimetric sensing satellites, the GNSS (Global Navigation Satellite System) satellites such as GPS, which are playing an increasingly crucial role in tracking low earth orbiting (LEO) remote sensing satellites at altitudes below 3000 km with accuracies of better than 10 cm, see e.g., Yunck et al. (1990) are increasing in use.

The applications of GNSS to environmental monitoring and management have been documented, e.g., in Awange (2012). In this chapter, basics of surveying and geodesy that underpin environmental geodesy are discussed.

3.2 Definitions: Plane and Geodetic Surveying

Traditionally, surveying is defined as the determination of the location of points on or near the Earth's surface. This is achieved through distances and angular measurements, which are converted into coordinates to indicate the horizontal position, while heights are measured relative to a given reference i.e., the vertical dimension. The advent of computers, however, has necessitated the modernization of the definition of surveying to "the collection, processing and management of spatial information" (Uren and Price 2010).

Surveying plays a pivotal role in determining land ownership, engineering, mapping, marine navigation, and environmental monitoring through height determination of anthropogenic land subsidence (see Sect. 26.10) among other uses. For example, surveying plays a crucial role in monitoring deformation of structures such as dams, bridges, buildings and many others. The main strength of surveying is that it operates locally, at levels by which most development activities take place.

Surveying can take on the form of plane surveying, where a flat horizontal surface is used to define the local surface of the Earth and the vertical is taken to be perpendicular to this surface (Fig. 3.1). Plane surveying, therefore, adopts a horizontal plane as a computational reference and the vertical direction is defined by the local gravity vector, which is considered constant. All measured angles are plane angles, and the method is applicable for areas of limited size. In contrast to plane surveying, *geodetic surveying* uses a curved surface of the Earth as the computational reference, e.g., the ellipsoid of revolution (Fig. 3.2). The ellipsoid of revolution is considered to approximate the figure of the Earth, and forms the surface upon which GNSS positioning is undertaken. Both could be used for environmental monitoring and management at local scale (plane surveying) and global or regional scale (geodetic surveying).

The distinction between plane and geodetic surveying, therefore is that plane surveying assumes a flat horizontal surface of the Earth where the vertical is considered to be perpendicular to this surface. Geodetic surveying on the other hand accounts for the true form of the Earth as illustrated in Fig. 3.2.

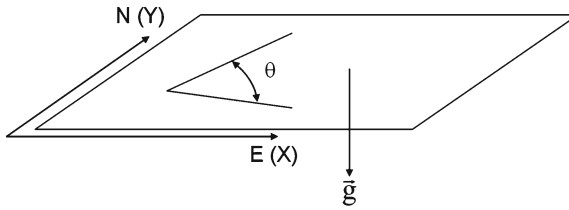


Fig. 3.1 Plane surveying

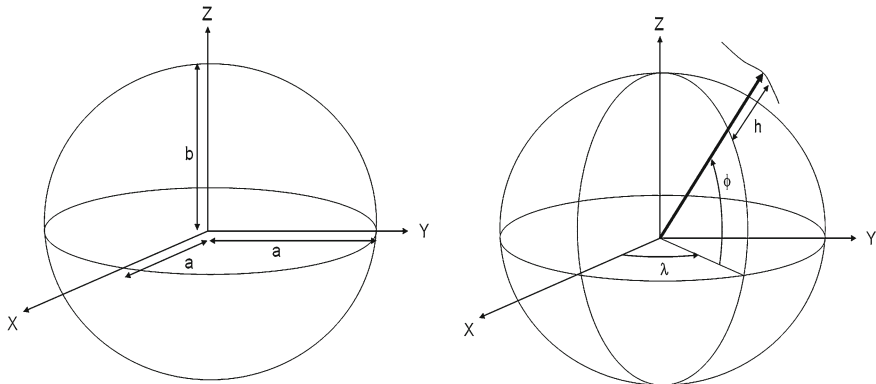


Fig. 3.2 Geodetic surveying based on the ellipsoid of revolution with a and b being the semi-major and semi-minor axes of the ellipsoid respectively. The position of a point on the reference ellipsoid will be defined by the longitude λ , longitude ϕ , and height h

3.3 Types of Measurements

Both plane and geodetic approaches lead to the following types of surveys:

Types of Surveying

Depending on the task at hand, surveying is generally categorized into

- (i) *Cadastral surveying*, which deals with property boundary determination. Whether for property ownership or development of land, knowledge of who owns what property will always be required.
- (ii) *Topographic surveying*, which deals with generation of maps at various scales. These maps support variety of uses, ranging from reconnaissance to assisting flood management in civil engineering, mapping spatially changing features, e.g., changes in wetland perimeter in environmental monitoring, to soil type maps for assisting land management decisions. Chapter 19 explores the role of topographical maps in detail.

- (iii) *Engineering surveying*, which deals mainly with construction, deformation monitoring, industrial and built environment.
- (iv) *Photogrammetric surveying* discussed in Chap. 11, which uses photogrammetric technology for mapping purposes.
- (v) *Control surveying*, which is performed to provide horizontal and vertical controls. These in turn provide a framework upon which subsequent locations are based. This type of survey is more accurately undertaken than the other types of survey and often involve use of more precise equipment.
- (vi) *Mine surveying*, which is undertaken to support mining activities through provision of control points for mining locations. These controls are used for infrastructure construction and also for coordination of points within the mining areas.
- (vii) *Hydrographic surveying* that is undertaken for marine purposes and could also find use in measuring changes in sea level, which is a vital indicator for monitoring the impact of climate change.
- (viii) *Satellite surveying*. Although this can be undertaken locally to support development activities, its functions are globally oriented and will be discussed in detail in the Chap. 5.
- (ix) *Inertial surveying systems*, which consist of three accelerometers that are orthogonally mounted in known directions, relative to inertial space, on a stable platform used to measure changes in the three-dimensional position, as well as, the length and direction of the gravity vector (Cross 1985). An in-depth exposition of this system is presented, e.g., by Cross (1985) who list the advantages of the system as being faster, independent of refraction of the measuring signals, and independent of external organization unlike the global navigation satellite system (GNSS) discussed in Chap. 5 (see Awange (2012)). Like GNSS, the systems are all-weather and all-day but are expensive to purchase, and can only be used in interpolative mode (Cross 1985). Its usage include (Cross 1985): provision of photogrammetric control (see Chap. 11), densification of national control networks, route surveys e.g., for pipelines, powerlines and roads, cadastral surveys, fixing of navigation aids and geophysical surveys. For geophysical surveys, an immediate application that would support environmental monitoring is the measurement of gravity discussed in Chap. 20. In some remote-sensing activities, it can give information about the position and attitude of the sensors and it can be combined with a satellite navigation system to give real-time positions offshore (Cross 1985).

3.3.1 Plane Surveying Measurements and Instruments

Plane surveying measures linear and angular quantities (Fig. 3.3). Linear measurements take the form of horizontal distances, e.g., measured directly by a tape or indirectly using a total station. In measuring horizontal or slope distances with a total station (Fig. 3.4a), use is made of electromagnetic distance measurement (EDM)

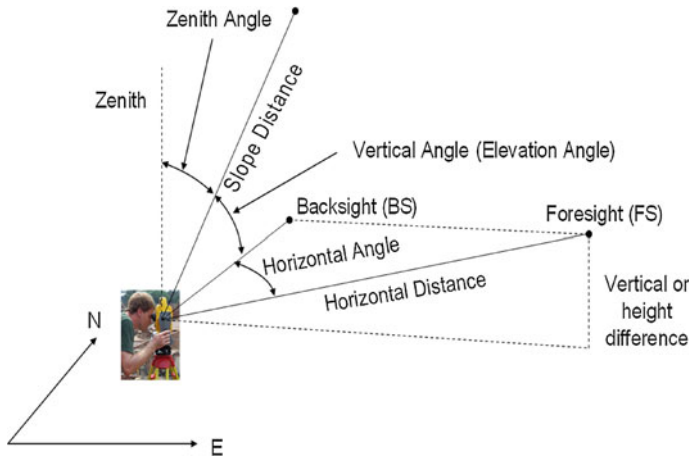


Fig. 3.3 Angular and distance measurements in surveying



Fig. 3.4 (a) Total station (b) Automatic level and staff

(Uren and Price 2010). Indirect measurement of height differences (vertical distance) using a total station makes use of the slope distance and elevation or vertical angle. Height differences are directly measurable using a level (Fig. 3.4b).

Angular measurements are of three types; vertical or elevation angles, zenith angles, and horizontal angles (Fig. 3.3). Vertical or elevation angle to a point is measured with reference to a horizontal plane while the zenith angle is measured with respect to the zenith or vertical direction, where the vertical angle α is given as

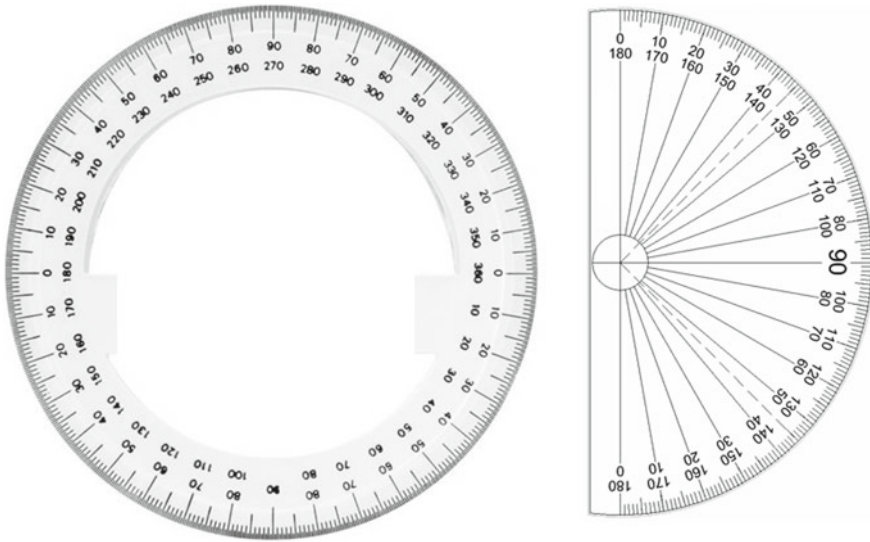


Fig. 3.5 Protractors defining the buildup of a total station. The complete protractor is used for measuring horizontal angles/directions, while the half protractor is used to measure the vertical/zenith angles

$$\alpha = 90^\circ - z$$

where z is the zenith angle. The horizontal angle is obtained in a horizontal plane by taking the difference between two directions. A total station is used to measure the angles discussed above. One can view a total station as made of two protractors. A 360° protractor marked in degrees placed in the horizontal plane and used to measure the horizontal angles, and a half circle protractor in the vertical plane used to measure the vertical/zenith angles (Fig. 3.5).

3.3.2 Geodetic Measuring Techniques

For geodetic surveying, measurement methods that cover wider spatial extent such as continental or the entire globe are essential. Such methods are useful for measuring environmental changes at regional or global scales on the Earth's surface, hydrosphere, cryosphere or the atmosphere. They include but are not limited to global positioning methods, e.g., by Global Navigation Satellite Systems (GNSS) discussed in Chaps. 4 and 5 (see also Awange (2012)), Satellite altimetric methods (Sect. 20.4), Satellite Laser Ranging (SLR) and Lunar Laser Ranging (Sect. 3.4.4), Interferometric Synthetic Aperture Radar (InSAR) discussed in Sect. 9.5, and Very Long Baseline Interferometry (VLBI) discussed in Sect. 3.4.3.

3.3.3 Basic Measuring Principles and Error Management

In surveying as well as geodesy, there are basic measuring principles that must be adhered to in order to achieve the desired outcome that satisfy both the client and the operator (surveyor). These include completing the measuring task within the shortest possible time and at the least possible cost. This may be beneficial to environmental phenomenon that changes within short periods and whose monetary budget for monitoring are limited. Further, the task must be completed according to instruction and using instruments of appropriate precision. The records of the field notes are essential and form part of legal evidence in a court of law in case of disputes. The following should be taken into consideration.

- Field notes are permanent records of work done in the field and must be thorough, neat, accurate and guarded carefully.
- Mistakes in field books are never erased but crossed out with one horizontal line through the middle.
- Specific field note formats exist for different types of surveys. This is particularly important for cadastral surveys, where notes may be used as evidence in court cases.

Finally, for mitigation and management purposes, in order to achieve accurate results, types of errors in surveying measurements and their sources that should be taken care of are:

- Natural
 - Due to the medium in which observations are made.
 - Factors: Wind, temperature, humidity, etc.
- Instrumental
 - Due to imperfections in instrument construction or adjustment.
 - May be reduced or eliminated by calibration and/or observation procedure.
- Personal
 - Limitations in operator ability.
 - Can be improved with practice.
 - Examples: Ability to read vernier scale, ability to accurately point cross-hairs, etc.
- Mistakes, also called gross errors or blunders
 - Usually, but not always, large magnitude.
 - Examples: Reading a tape incorrectly, transposing numbers.
 - Example: A distance of 15.369 m is read and 15.396 is recorded in the field book.

- Systematic (deterministic) errors
 - Errors that follow some physical or geometric law.
 - Their effects can be mathematically modeled and, thus, corrected.
 - Examples: Refraction of the line of sight, thermal expansion of a steel band.
- Random errors (what is left over)
 - Errors that can't be modeled and corrected: random variations.
 - Governed by probabilistic or stochastic models.

3.4 Measuring Techniques

3.4.1 Linear Measurements

Linear measurements deals with distances (slope, horizontal or vertical), which are normally required for plotting the positions of details when mapping and also for scales of the maps (see Chap. 19). Horizontal and vertical distances are useful for mapping, provision of controls, and monitoring spatial and vertical changes of features. Slopes and vertical distances are essential for setting out construction sites, where vertical distances are useful in height transfer from floor to floor in multistory building or in mining, i.e., transferring distances from the surface to underground.

Distance measurements can be undertaken using, e.g., tapes (for short distances) or electromagnetic distance measuring (EDM). Errors associated with tape measurements include instrumental errors (e.g., incorrect length where the tape is either too short or too long), natural errors (e.g., the expansion or contraction of the steel tape caused by temperature changes) or personal errors such as wrong reading of the tape or poor alignment while measuring the distances. EDM is nowadays the most common tool used for measuring distances. It can be classified according to either radiation source (optical or microwave), measurement principle (phase or pulse), or whether a reflector is required or not (i.e., reflectorless). The operating principle involves the signal being emitted from the total station to some reflector, which reflects the signals back to the emitter. The distance is then obtained from the basic equation

$$Speed = \frac{Distance}{Time}.$$

Since the speed of light(c) is known, and the time the signal takes to travel from the emitter and back measured, say Δt , the distance measured by the EDM instrument then becomes

$$d = \frac{c\Delta t}{2}.$$

The division by 2 is due to the fact that the signal travels twice the distance (i.e., from the emitter to the reflector and back). The phase method, where the signal travels

in a sinusoidal form is the most common method of distance measurement found in surveying instruments. However, the pulse method using pulsed laser is becoming more common particularly for reflectorless instruments. Errors associated with EDM are elaborately discussed, e.g., in Uren and Price (2010).

3.4.2 Traversing

Traversing is a survey technique used to determine the planar positions (Easting and Northing: E_B and N_B , Fig. 3.6) of control points or setting out points using measured angle θ and distance d_{AB} (Fig. 3.6). The position of point B obtained relative to that of A is given as

$$E_B = E_A + \Delta E_{AB} = E_A + d_{AB} \sin \theta$$

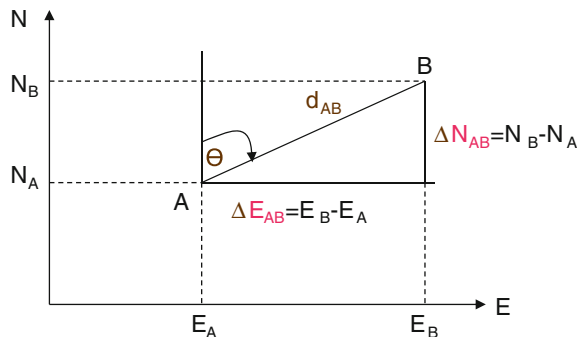
$$N_B = N_A + \Delta N_{AB} = N_A + d_{AB} \cos \theta$$

where E_A , N_A is the known planar position of point A.

Applications of traversing include the establishing of control points useful for construction purposes or for delineating feature boundaries, horizontal control for generation of topographic maps (see e.g., Chap. 19) and also for detail maps for engineering work, establishment of planar positions of points during construction (set-out), for area and volume computations, and ground control needed for photogrammetric mapping discussed in Chaps. 11 and 12.

A traverse can take the form of either open or closed. A closed route can start from a known point and end at another known point (e.g., from A to B in Fig. 3.7a). This type of traverse is also known as link traverse. If the traverse starts from a known point and closes at the same point, then it is known as a loop traverse. An open traverse starts from a known point but does not end at a known point (Fig. 3.7b).

Fig. 3.6 Traversing. d_{AB} is the distance between points A and B while θ is the angle measured from the true North at point A to point B



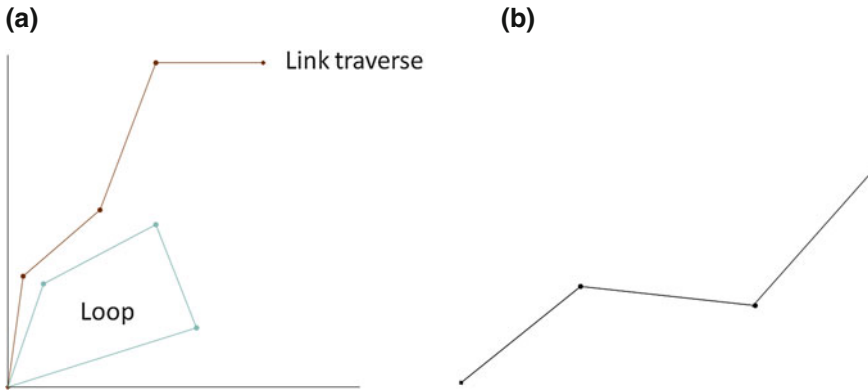


Fig. 3.7 Closed and open traverses. Closed traverse starts from a known point and ends at another known station. Open traverse may start from unknown point and end at another unknown point **a** Closed Traverse **b** Open Traverse

3.4.3 Very Long Baseline Interferometry (VLBI)

Very long baseline interferometry (VLBI) is a geodetic space technique that is used solely, or in combination with other satellite techniques to measure geodetic, astronomical and geodynamic parameters. It was developed in radioastronomy with the objective of studying detail structures of compact radio sources with a higher angular resolution (see e.g., Seeber (2003, p. 485)).

The system was developed in late 1960s and early 1970s and contains at least two antennas fixed at thousands of distance apart (the interferometric base) and the processing unit. The radio telescopes simultaneously receive signals from extragalactic radio sources known as the quasars (Fig. 3.8). These signals are recorded on a magnetic tape for later processing and analysis at a central station.

The time delay between the signals received from the stations are measured using precise atomic clocks and used to determine the baseline vectors (Δx , Δy , Δz) between the stations. Observations to more than 12 radio sources over a period of 24 h is needed to determine the baseline vector (Fig. 3.9).

Modern operations involve eVLBI (Fig. 3.10), where high speed network are used to connect radio telescopes separated by large distances (100–1000s of km) instead of traditional method of recording the received signals on magnetic tapes and shipping the recorded data to a central processor. International collaboration on VLBI service (IVS) exists and brings together those groups working on VLBI.

With an accuracy of less than 30 mm on baseline lengths of 10,000 km, VLBI is one of the most accurate space-based measuring technique and find use in establishing and maintaining Global Reference Frames (e.g., International Celestial Reference Frame (ICRF) and International Terrestrial Reference Frame (ITRF)). It also provides fiducial points for controlling GPS satellites (see Sect. 5.41). Other uses include monitoring plate motions, which may be useful in Earthquake studies, monitoring

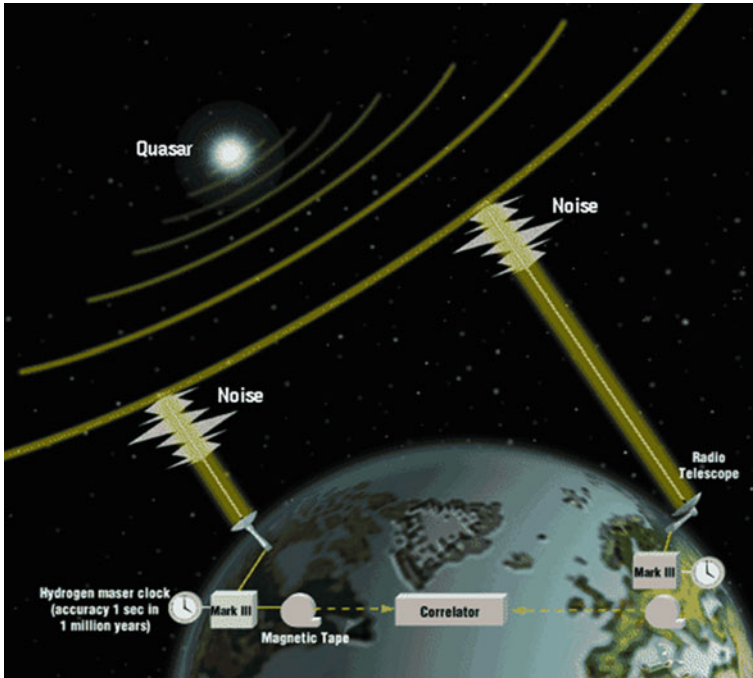


Fig. 3.8 Very Long Baseline Interferometry (VLBI). *Source* <http://lupus.gsfc.nasa.gov/brochure/bintro.html>

the orientation of the Earth, positioning, and supporting international collaboration. It also finds use in establishment of CORS stations discussed in Sect. 6.5. Its advantages include not suffering from satellite orbital errors, being weather independent, being independent of the Earth's gravity field, and not being influenced by the variation of geocenter.

Its shortcoming includes being slow, expensive, and requiring intensive data processing. Its instrumental errors are difficult to handle and the results are not available in real-time. VLBI does not provide absolute coordinates but relative coordinates with respect to some arbitrary selected origin unlike GNSS techniques presented in Chaps. 4 and 5.

3.4.4 Laser Ranging Techniques

Laser ranging techniques include satellite laser ranging (SLR) and lunar laser ranging (LLR). Satellite laser ranging measures precise distances from network of stations to lower altitude satellites such as Laser Geodynamics Satellites (LAGEOS) with an altitude of 5838 km. These lower altitude satellites are fitted with retro-reflectors, i.e., reflectors that reflect the incoming signals in the same direction from which they came. Laser pulses are generated and transmitted to the satellite via an optical

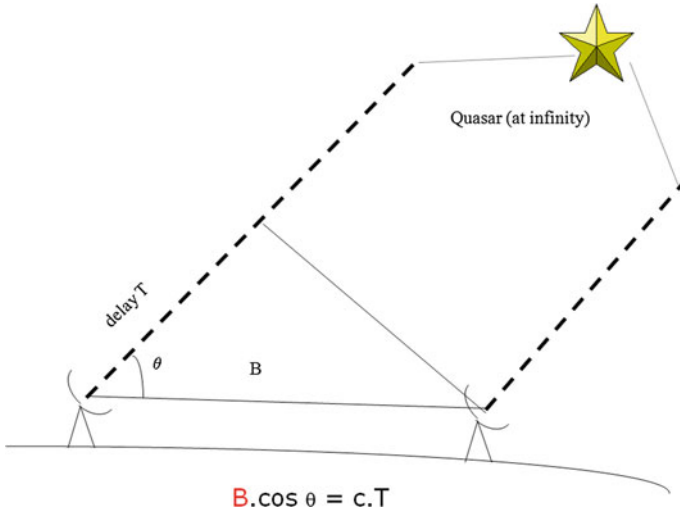


Fig. 3.9 VLBI computations



Fig. 3.10 VLBI antenna. Source <http://lupus.gsfc.nasa.gov/>

system (see Fig. 3.11). The signals are detected by the reflectors on the satellite and send back where they are received by the receiver telescope, analyzed, and the travel time t measured. From this two-way travel time, the distance between the telescopes, receiver, and the satellite d is computed by

$$d = (T/2)c,$$

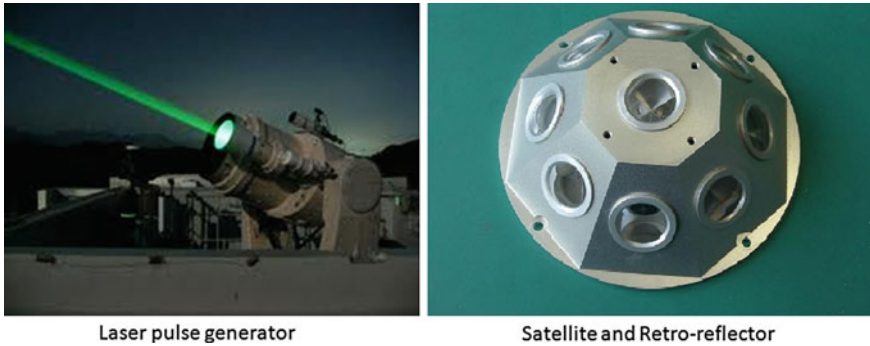


Fig. 3.11 Laser ranging (SLR). *Source* http://www1.kaiho.mlit.go.jp/KOHO/simosato/Photos/laser_thumb.jpg and <http://center.shao.ac.cn/laser3.JPG>

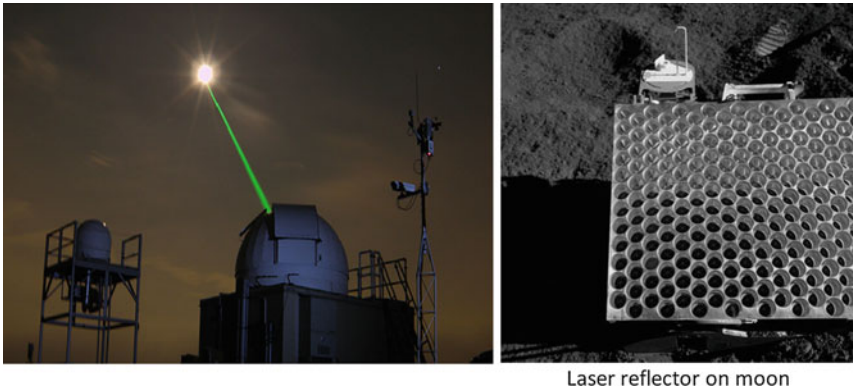
where c is the velocity of propagation (speed of light) and T is the measured travel time of the signal. The accuracy of the system requires accurate orbit of the satellites to which signals are sent and also accurately known SLR stations.

The main components of SLR consist of ground and space equipment. Ground equipment are made up of a generator and transmitter of the laser pulse, including the optical system that sends the pulse. Also in the ground equipment component are a detector and analyser of the returned pulse, including the receiving telescope, and a time-of-flight measuring unit. The space equipment consist of the satellite and retro-reflector (see Fig. 3.11).

SLR can achieve an accuracy of about 1 cm over a baseline of 1000 km. It requires many observations during a single satellite pass and highest accuracy can be obtained through combining multi-days observations. The errors are similar to those of GNSS (Chap. 5), i.e., due to clock and atmospheric. High precision satellite orbits are computed from well known permanent stations such as GPS. The system's advantages include (see e.g., Seeber (2003, p. 485)): high accuracy, long-term series of observations and derived parameters (e.g., absolute heights), independent control of other geodetic techniques, and back-up of active orbit determination systems such as GPS (see, e.g., Sect. 5.41). SLR are also applicable in establishing the CORS stations discussed in Sect. 6.5. The disadvantages are its strong dependence of the suitability of the weather, high cost in building and maintaining ground segments, inhomogeneous data distribution compared to GNSS and VLBI, and no or limited mobility of ground segment that limits operational capability.

Its applications include; positioning used to realize the global reference frames and measure plate tectonics (Sect. 26.7), determination of changes in Earth's gravity field (Sect. 20.3), measuring Earth's orientation parameters, measuring Ocean and Earth body tides, the determination of precise orbits of certain satellites, e.g., altimeter satellites in Fig. 20.10, and the determination of mass redistribution (Sect. 20.3.1).

Lunar laser ranging (LLR) (Fig. 3.12) has the moon acting as the satellite with the three reflectors that were left on the moon following the Apollo missions of July



Laser reflector on moon

Fig. 3.12 Laser Ranging—LLR Source http://www.nasa.gov/images/content/444021main_apollo15_LRRRpart_HI.jpg

1969 (Apollo II), February 1971 (Apollo 14), and July 1971 (Apollo 15) reflecting the received signals. These reflectors form a triangle with sides 950, 1100 and 1250 km well distributed in latitude and longitude. Two reflectors L17 and L21 were deployed by the French, with L21 included in LLR. Compared to SLR, high energy laser are required to “shoot” to the moon which makes the system costly. Only few observatories have LLR capabilities. LLR can achieve about 3 cm root-mean-square and find use in studying mutation and rotation of the Earth, lunar rotation, plate motions (e.g., Sect. 26.7), defining reference frames, and locating GNSS ground control stations as discussed in Sect. 6.5.

3.5 Concluding Remarks

This chapter has presented in a nutshell the basics of surveying and geodesy that underpin the emerging field of *Environmental Geodesy*. Surveying and geodesy form part of the geoinformatic discipline that are useful for sensing the environment at a local as well as global level. Chapters 4–6 extensively cover the global navigation satellite systems (GNSS), particularly the global positioning system (GPS). The GNSS will be shown in part V as the main tools from surveying and geodesy discipline contributing heavily towards environmental monitoring. This does not mean, however, that the other methods treated in this chapter are less important. Indeed, as we shall see, most of these methods are inter-linked. For instance, the establishment of GNSS’ CORS stations require the use of VLBI and SLR (e.g., Sect. 5.4.1). The applications of VLBI, SLR and other methods discussed in this chapter to environmental monitoring will be discussed in the appropriate places of part V. Several books exist that cover surveying and geodesy in extensive detail, see e.g., Grafarend and Awange (2012, and the references therein).

References

- Awange JL (2012) Environmental monitoring using GNSS, global navigation satellite system. Springer, Berlin
- Cross PA (1985) Inertial surveying: principles, methods and accuracy. *Int J Remote Sens* 6(10):1585–1598
- Grafarend EW, Awange JL (2012) Applications of linear and nonlinear models. Springer, Berlin
- Lein JK (2012) Environmental sensing: analytical techniques for earth observation, 334 pp. Springer, Berlin. doi:[10.1007/978-1-4614-0143-8](https://doi.org/10.1007/978-1-4614-0143-8)
- Seeber G (2003) Satellite geodesy. Walter de Gruyter, Berlin
- Uren J, Price WF (2010) Surveying for engineers. Palgrave Macmillan Ltd., New York, pp 816
- Yunck TP, Wu SC, Wu JT, Thornton CL (1990) Precise tracking of remote sensing satellites with the global positioning system. *IEEE Trans Geosci Remote Sens* 28:108–116

Chapter 4

Modernization of GNSS

“By the end of the next decade, there maybe as many as 12 systems in orbit.”

Donald G. DeGryse, Inside GNSS Nov/Dec 2009

4.1 Introductory Remarks

Throughout history, position (location) determination has been one of the fundamental tasks undertaken by humans on a daily basis. Each day, one deals with positioning, be it going to work, the market, sport, church, mosque, temple, school or college, one has to start from a known location and move towards another known destination. Often the start and end locations are known since the surrounding physical features form a reference upon which we navigate ourselves. In the absence of these reference features, for instance in the desert or sea, one then requires some tool that can provide knowledge of position.

To mountaineers, pilots, sailors, etc., the knowledge of position is of great importance. The traditional way of locating one's position has been the use of maps or compasses to determine directions. In modern times, however, the entry into the game by Global Navigation Satellite Systems (GNSS) comprising the US's Global Positioning System (GPS), Russia's Global Navigation Satellite System (GLONASS), the European's Galileo, and the Chinese's Compass have revolutionized the art of positioning, see, e.g., Hofman-Wellenhof et al. (2008). The use of GNSS satellites can be best illustrated by a case where someone is lost in the middle of the desert or ocean and is seeking to know his or her exact location (see, e.g., Fig. 4.1).

In such a case, one requires a GNSS receiver to be able to locate one's own position. Assuming one has access to a hand-held GNSS receiver (e.g., Fig.4.1), a mobile phone or a watch fitted with a GPS receiver, one needs only to press a button and the position will be displayed in terms of geographical longitude and latitude

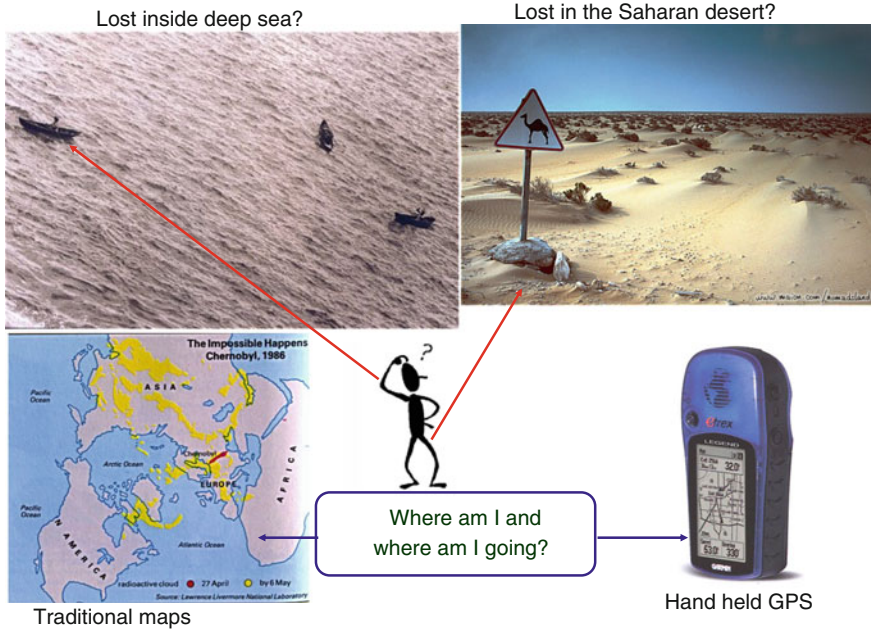


Fig. 4.1 Use of GNSS to position oneself

(ϕ , λ). One then needs to locate these values on a given map or press a button to send his/her position as a short message service (sms) on a mobile phone as is the case in search and rescue missions. Other areas where GNSS find use are geodetic surveying (discussed in Sect. 3.3.2) where accuracies are required to mm level, GIS (Geographic Information System) data capture (e.g., part IV), car, ship and aircraft navigation, geophysical surveying and recreational uses.

The increase in civilian use has led to the desire of autonomy by different nations who have in turn embarked on designing and developing their own systems. In this regard, the European nations are developing the Galileo system, the Russians are modernizing their GLONASS system while the Chinese are launching a new Compass system. All of these systems form GNSS with desirable positional capability suitable for environmental monitoring and management. GNSS are:

1. Global: This enables the monitoring of global environmental phenomena e.g., global warming, changes in sea level, etc.
2. All weather: This feature makes GNSS useful during cloudy and rainy periods, which are still stumbling blocks to radar systems and low Earth orbiting satellites discussed in part II.
3. Able to provide 24h coverage: This enables both day and night observation and can thus enable the monitoring of diurnal environmental phenomena such as the spread of oil from a maritime disaster.

4. Cheaper: As compared to other terrestrial observation techniques such as photogrammetry (Chaps. 11 and 12) or Very Long Baseline Interferometry (VLBI) (Takahashi et al., 2000), GNSS are economical due to the fact that only a few operators are needed to operate the receivers and process data. Less time is therefore required to undertake a GNSS survey to obtain a solution.
5. Able to use a global common reference frame (e.g., WGS 84 Coordinate System discussed in Sect. 6.6.2).

4.2 The GNSS Family

Besides the US owned GPS and the European’s Galileo under development, GNSS family is comprised also of the Russian owned GLONASS and the People’s Republic of China’s Compass. Other than GPS that has been in operation for a long period of time, GLONASS that was first launched in 1982 has also been in operation after attaining full operational capability in 1995. Full constellation should consist of 21 satellites in 3 orbits plus 3 spares orbiting at 25,000 km above the Earth surface. By 2005, only 14 satellites were in orbit. Russia is however planning a new generation of satellites as discussed in Sect. 4.3. A complete constellation of 24 satellites was achieved last December, but Russia intends to keep pushing ahead with its GNSS to attain 30 satellites, complete augmentation system and improved OCX by 2020.¹ Table 4.1 provides a comparison between the GLONASS and GPS systems.

Other systems include augmentation such as the European Geostationary Navigation Overlay Service (EGNOS), Indian Regional Navigation Satellite System (IRNSS) consisting of seven satellites, with the first satellite of IRNSS constellation planned to be launched in 2013 and the full constellation expected

Table 4.1 Comparison between GPS and GLONASS as of March 2011

	GPS	GLONASS
Number of satellites	31	22
Number of orbital planes	6	3
Orbital radius	26,000 km	25,000 km
Orbital period	11h 58m	11h 15m
Geodetic datum	WGS84	SGS84
Time reference	UTC(USNO)	UTC(SU)
Selective availability	Yes	no
Antispoofing	Yes	Possible
Carrier	L1:1575.42 MHz L2:1227.60 MHz	1602.56-1615.5 MHz 246.43-1256.5 MHz
C/A code (L1)	1.023 MHz	0.511 MHz
P-code (L1,L2)	10.23 MHz	5.11 MHz

¹ <http://www.insidegnss.com/node/3010>

in 2014.² The Japanese's Quasi-Zenith Satellite System (QZSS) is a proposed three-satellite regional time transfer system and Satellite Based Augmentation System (see Sect. 6.4.4.2) for the GPS that would be receivable within Japan and cover most of Australia. The first QZSS satellite was launched on 11 September 2010 and a full operational capability is expected by 2013.³ EGNOS is a stand alone system that seeks to augment the existing GPS and GLONASS systems to improve satellite positioning accuracy within Europe. It has its own ground, space, and user segments with support facilities. The Indian based GAGAN (GPS Aided GEO Augmented Navigation) is a regional SBAS system designed to support the functions of the Airports Authority of India for Civil Aviation requirements through an improved accuracy of better than 7 m. The first GAGAN satellite was launched on 21st May 2011 and the second on 29th September 2012.⁴

EGNOs' ground segment is made up of GNSS (GPS, GLONASS, Geostationary Earth Orbiting satellites-GEO), Ranging and Integrity Monitoring Stations (called RIMS) connected to a set of redundant control and processing facilities called Mission Control Center (MCC) that determine the *integrity, pseudorange differential corrections* for each monitored satellite, *ionospheric delays* and generates GEO satellite ephemeris (European Commission and European Space Agency 2002). This information is up-linked to the GEO satellites from the Navigation Land Earth Station (NLES). The GEO satellites then send the correction information to individual users (user segment) who use them to correct their positions. For discussions on more GNSS systems, such as DORIS, PRARE, etc., we refer the reader to Awange (2012); Hofman-Wellenhof et al. (2008); Prasad and Ruggieri (2005).

4.3 Future Missions

GLONASS was designed to have a constellation of 24 satellites, but funding limitations led to its near demise with fewer than originally planned operating (i.e., 22 satellites operating as of March 2011). The Russian government has, however, embarked on a modernization program which will see the deployment of new generation GLONASS-K, GLONASS-M and GLONASS-KM (scheduled for launch in 2015) satellites that will have improved features, e.g., reduced weight, more stable clocks, longer lifespan and improved navigation message.⁵ On 25th of September 2008, the Space Forces successfully launched three GLONASS-M satellites into orbit from the Baykonur launch site bringing the number of GLONASS-M satellites to about 18. The launch of the GLONASS-K satellites with three civilian frequencies, which are supposed to have a longer lifetime than the GLONASS-M satellites (i.e.,

² <http://www.isro.org/scripts/futureprogramme.aspx#Forth>

³ http://www.jaxa.jp/projects/sat/qzss/index_e.html

⁴ <http://www.isro.org/scripts/futureprogramme.aspx#Satellite>

⁵ The System: GLONASS Forecast Bright and Plentiful. <http://www.gpsworld.com/the-system-ilonass-forecast-bright-and-plentiful/>

10 years), and with added integrity components took place on 26th of February 2011, having been delayed from its planned date in December 2010 following the crash of the three GLONASS-M type satellites into the Pacific ocean. GLONASS, like GPS, reserves high accuracy signals for military use while providing free standard accurate signals for civilian use.

Not to be left behind, the Peoples Republic of China launched the first Compass satellite in 2007 and the second one in 2009. By October 2012, the number of Compass satellites in space were 16, with a complete global coverage expected by 2020.⁶ Compass constellation is expected to comprise more than 30 satellites orbiting at an altitude of about 21,150 km (see e.g., Hofman-Wellenhof et al. (2008, p. 402), for details).

4.4 Environmental Benefits of the Expanded GNSS Family

With the receivers undergoing significant improvement to enhance their reliability and the quality of signals tracked, the world will soon be proliferated with various kinds of receivers that will be able to track several or all GNSS satellites. The monitoring and management of environmental aspects could benefit enormously from these enhanced and improved GNSS satellites. First, the possibilities of combining some of the main GNSS satellite systems could impact positively on environmental monitoring by meeting demands of various users.

For example, a receiver capable of tracking both GLONASS and GPS satellites such as Sokkia's GSR2700-ISX receiver has the possibility of receiving signals from a total constellation of more than 40 satellites. When GLONASS attains full operational capability (FOC), with 28 satellites, this will lead to an integrated GPS/GLONASS of more than 50 satellites. Similarly, the design of Galileo is being tailored towards an interoperability with other systems, thereby necessitating compatibility with GPS and GLONASS and potentially leading to a constellation of nearly 80 satellites.

The combination of GPS and Galileo and other GNSS systems will further provide more visible satellites. Consider the proposed Australian CORS stations shown in Fig. 6.15, which will be useful for monitoring the future expected changes in sea level, submergence of land due to groundwater abstraction and other environmental phenomenon [see e.g., Awange (2012)]. As an example, Fig. 4.2 presents GPS satellites that were visible on 15th of March 2007 compared to the situation in Fig. 4.3 to what would have been observed were Galileo satellites also fully operational on that day. As can be seen from Fig. 4.2, the lowest number of satellites visible at any station on that day was 6. When Galileo satellites are included, the minimum number of visible satellites doubles to 12. Thus overall, anywhere on the Australian continent at the aforementioned "snapshot" of time, there would have been enough visible satellites for the proposed CORS network and that the addition of GALILEO

⁶ <http://www.insidegnss.com/node/3246>

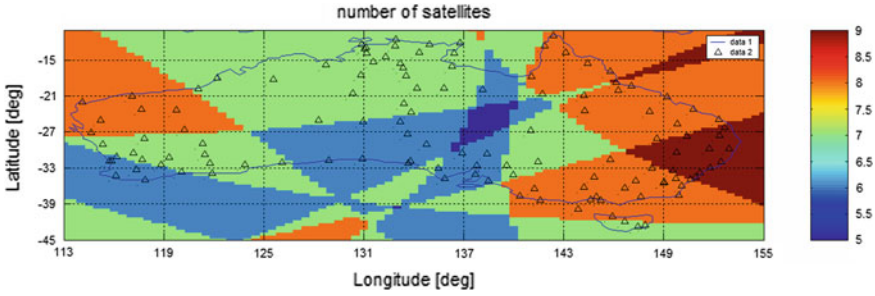


Fig. 4.2 Number of visible GPS satellites over Australia on 15.03.2007. Source Wallace (2007)

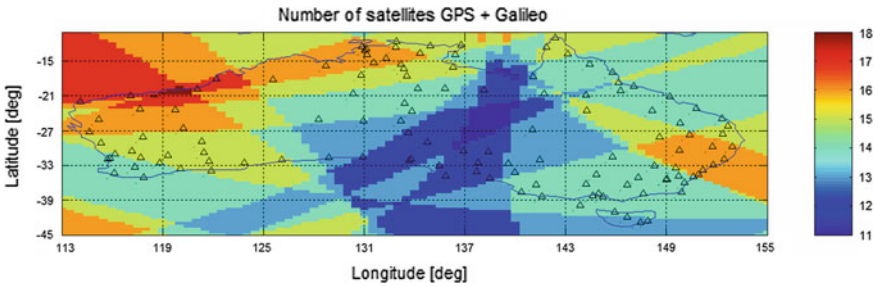


Fig. 4.3 Number of visible GPS+Galileo satellites over Australia on 15.03.2007. Source Wallace (2007)

will greatly improve satellite visibility. Table 4.2 presents the total number of visible Galileo and GPS satellites as reported by the definition phase of Galileo, see e.g., European Commission and European Space Agency (2002). This increase in the number of visible satellites will ensure a better geometry and improved resolution of unknown ambiguity, thereby increasing the positioning accuracies as discussed in Sect. 6.3.

The advantages of combining GNSS systems listed by the EU and EC-ESA (European Commission and European Space Agency, 2002) include:

- Availability: For example, a combination of Galileo, GLONASS and GPS will result in about 60 operational satellites, resulting in the increased availability for

Table 4.2 Maximum number of visible satellites for various masking angles

Receiver elevation masking angle (°)	Number of visible Galileo satellites	Number of visible GPS satellites	Total
5	13	12	25
10	11	10	21
15	9	8	17

Source European Commission and European Space Agency (2002)

the required minimum 4 satellites from 40 % to more than 90 % in normal urban environments worldwide.

- Position accuracy: Allied to an increased availability in restricted environments (urban) is a better geometry of spacecraft and enhanced positioning performance.
- Integrity: In addition to generating ranging signals, augmentation of GNSS with SBAS discussed in (Awange 2012) will enhance the provision of integrity information.
- Redundancy: The combination of services from separate and fully independent systems will lead to redundant observations.

Increased satellite availability from 40 % to more than 90 % in urban environments would benefit satellite environmental monitoring measurements undertaken in urban areas where the effect of multipath and signal reflection from buildings and features are rampant. Redundant observations will be beneficial to environmental monitoring projects that may need continuous measurements (i.e., full system backup).

GNSS systems can be combined with non-GNSS systems such as conventional surveying, Long Range Aid to Navigation (LORAN-C) and Inertial Navigation Systems (INS) to assist where GNSS systems fail, such as inside forests and tunnels. Other benefits that would be accrued through the combination of GNSS system with conventional methods have been listed, e.g., by EU and EC-ESA (European Commission and European Space Agency, 2002) as offering improved signal strength, which provides better indoor penetration and resistance to jamming; offering a limited communication capability; offering a complementary positioning capability to users in satellite critical environments through mobile communication networks; and provision of a means for transferring additional GNSS data through communication systems to enable enhanced positioning performances (e.g., accuracy) as well as better communication capabilities (e.g., higher data rates, bi-directional data links).

4.5 Concluding Remarks

With the anticipated GNSS systems that will comprise various Global Positioning Satellites, environmental monitoring and management tasks requiring use of satellites will benefit from increased number of satellites. Increased number of satellites will have additional advantages compared to GPS system currently in use. Some of the advantages include additional frequencies, which will enable modeling of ionospheric and atmospheric errors to better resolutions; additional signals that will benefit wider range of environmental monitoring and management tasks; and a wider range of satellites from which the users will be able to choose from. GNSS will offer much improved accuracy, integrity and efficiency performances for all kinds of user communities over the world. In the next Chap. 5 is presented more details on GPS. Detailed use of GNSS to environmental monitoring and management is presented in Awange (2012).

References

- Awange JL (2012) Environmental monitoring using GNSS, global navigation satellite system. Springer, Berlin
- European Commission and European Space Agency (2002) Galileo mission high level definition, 3rd issue. http://ec.europa.eu/dgs/energy_transport/Galileo/doc/Galileo_hld_v3_23_09_02.pdf. Accessed 11 Nov 2008
- Hofman-Wellenhof B, Lichtenegger H, Wasle E (2008) GNSS global navigation satellite system: GPS GLONASS; galileo and more. Springer, Wien
- Prasad R, Ruggieri M (2005) Applied satellite navigation using GPS GALILEO and augmentation systems. Artech House, Boston
- Takahashi F, Kondo T, Takahashi Y, Koyama Y (2000) Very long baseline interferometer. IOS press, Amsterdam
- Wallace N (2007) CORS simulation for Australia. Curtin University of Technology. Final year project (unpublished)

Chapter 5

The Global Positioning System

“The number of GPS units and sensors is growing fast, and if geo-referencing was a specialist’s work a few years ago, it is a mainstream “one click matter” today. Software in smart-phones and alike makes it incredibly easy to create geo-referenced data. Location-based services are a fast growing business accordingly and all kinds of geo-related social networking “here I am” applications invade our daily life.”

Erik Kjems

5.1 Introductory Remarks

The Global Positioning System or GPS is the oldest and most widely used GNSS system, and as such will be extensively discussed in this and the next chapter. The development of GPS satellites dates from the 1960s (Hofman-Wellenhof et al. 2001; Leick 2004). By 1973, the US military had embarked on a program that would culminate into the NAVigation System with Timing And Ranging (NAVSTAR) GPS, which became fully operational in 1995. The overall aim was to develop a tool that could be used to locate points on the Earth without using terrestrial targets, some of which could have been based in domains hostile to the US. GPS satellites were therefore primarily designed for the use of the US military operating anywhere in the world, with the aim of providing passive real-time 3D positioning, navigation and velocity data. The civilian applications and time transfer though the predominant use of GPS is, in fact, a secondary role.

The World of Geographically Referenced Information is Facing a Paradigm Shift. Source <http://www.vectorlmedia.com/>.

5.2 GPS Design and Operation

In general, GPS is comprised of *space*, *control* and *user segments*, which are described in the following subsections.

5.2.1 Space Segment

This segment is designed to be made up of 24 satellites plus 4 spares orbiting in a near circular orbit at a height of about 20,200 km above the Earth's surface. As of December 2012, there were 31 operational GPS satellites in space.¹ Each satellite takes about 11 h 58 min to orbit around the Earth [i.e., orbits the Earth twice a day (Agnew and Larson 2007)]. The constellation consists of 6 orbital planes inclined at 55° from the equator, each orbit containing 4 satellites (Fig. 5.1). With this setup, and an elevation of above 15°, about 4 to 8 satellites can be observed anywhere on the Earth at anytime (Hofman-Wellenhof et al. 2001; Leick 2004). This is important to obtain 3D positioning in real-time. The satellites themselves are made up of solar panels, internal components (atomic clock and radio transmitters) and external components such as antenna. The orientation of the satellite in space is such that the solar panels face the sun so as to receive energy to power the satellite while the antennas face the Earth to transmit and receive radio signals.

The launch of GPS satellites has undergone several stages since inception. First launched were Block I prototype satellites, from 1978 to 1985. Powered by solar panels, they weighed 845 kg and were designed with a lifespan of 4.5 years. They, however, exceeded this time span with some operating for more than 10 years. These satellites are now not operational, having been replaced by Block II satellites launched in 1989 and weighing 1,500 kg. They operated until 1996, by which time 27 satellites of Blocks II and IIA ("A" stands for Advanced) had been launched. The last of the Block IIA satellites was launched in 2001. Their life span was designed to be 7.5 years, but some were still operational even after 10 years. By April 1995, GPS had been declared fully operational with the third generation satellites, Block IIR ("R" stands for Replacement), designed to replace the early Block II satellites, being deployed in July 1997.

On 26th September 2005, the first satellite of Block IIR-M ("R" standing for replacement and "M" modernized) was successfully launched. The last of the Block IIR-M satellites was launched on 17/08/2009. The first of the Block IIF ("F" standing for Follow-on) series was launched on 27th May 2010 from Cape Canaveral, Florida, USA. Finally, the launch of Block III satellites scheduled for 2014 is expected to improve the capability of the GPS community and is expected to operate up to 2030 and beyond (Hofman-Wellenhof et al. 2008, p. 324). This would provide a wider window of opportunity for important applications such as *environmental monitoring*

¹ <http://adn.agi.com/SatelliteOutageCalendar/SOFCalendar.aspx>

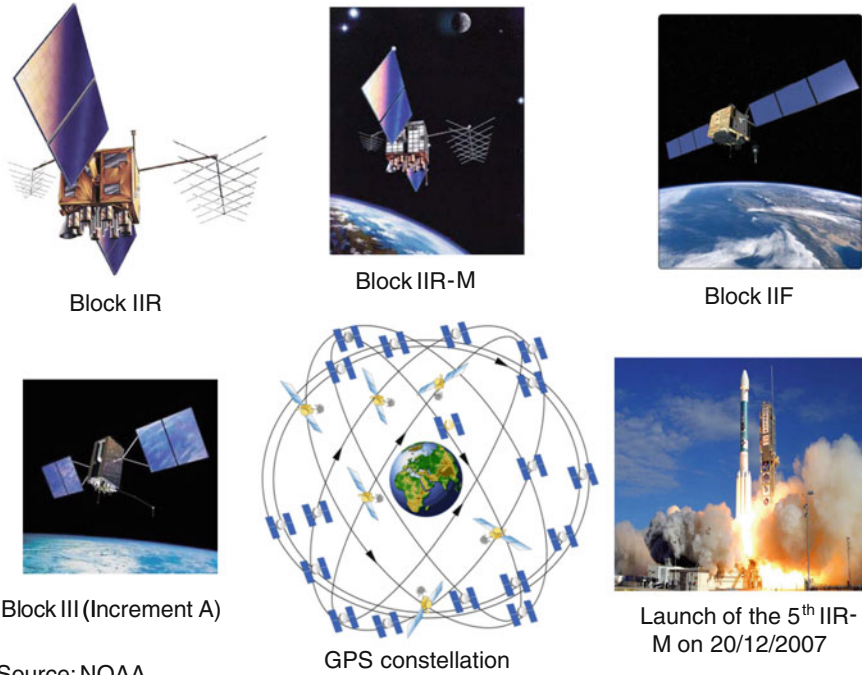


Fig. 5.1 A schematic showing the configuration of the GPS satellites in orbit and the various GPS-blocks

and *management*. Figure 5.1 shows some of these GPS Blocks and the pattern they take in their constellation.

5.2.2 Control Segment

The GPS control segment consists of *master, monitor* and *ground* stations. The master control station is located at Colorado Springs (Schriever Air Force Base, Colorado) with a backup station at Gaithersburg, Maryland. The monitor stations are made up of five stations located at *Colorado Springs, Ascension Island* in the Atlantic Ocean, *Hawaii, Diego Garcia* in the Indian Ocean, and *Kwajalein Island* in the Pacific Ocean. In September 2005, six more monitoring stations of the NGA (National Geospatial-Intelligence Agency) were added to the network, enabling every satellite to be seen by at least two monitoring stations and thus improve the accuracy of the computed satellite orbital parameters (known as *ephemeris*) (see Fig. 5.2).²

² copyright http://www.kowoma.de/en/gps/control_segment.htm



Fig. 5.2 GPS monitoring stations. Source http://www.kowoma.de/en/gps/control_segment.htm

These stations monitor the orbital parameters and send the information to the master control station at Colorado Springs. The information obtained from these monitoring stations tracking the satellites are in-turn used to control the satellites and predict their orbits. This is done through the processing and analysis of the information by the master station, which computes the satellite ephemeris and clock parameters and transmits them to the satellites via the monitoring stations. The satellite ephemeris consists of satellite positions and velocities predicted at given times.

There are several ground stations distributed across the world that augment the control system by monitoring and tracking the satellites in space and transmitting correction information to individual satellites through ground antennas. These stations form the International GNSS Service (IGS) network. The ground control network is therefore responsible for tracking and maintaining the satellite constellation by monitoring satellite health and signal integrity and maintaining the satellite orbital configuration.

5.2.3 User Segment

The user segment consists of receivers (most of which consist of 12 channels), which are either hand-held (also available in wrist watches, mobile phones, etc) or mountable receivers, e.g., in vehicles, or permanently positioned. The availability of 12 channels enables receivers to track and process data from 12 satellites in parallel, thus improving on positioning accuracy (see accuracies for various applications in Chap. 6). These receivers are employed by a wide range of users to meet their daily needs. So wide and varied are the uses of GPS that Awange and Grafarend (2005)

termed it the Global Positioning System (GPS). For military purposes, it is useful in guiding fighter planes, bombers and missiles, as well as naval and ground units.

Civilian use covers a wide range of applications, such as mining, where it is used to guide heavy machinery, or locating positions to agriculture in what has become known as “*precision farming*”. Using GPS and GIS, farmers can integrate location, amount of fertilizer and yield expected and analyze the three for optimum output. Awange and Ong’ang’a (2006) have elaborated the possible use of GPS in lake studies. Modern car tracking companies use GPS to locate stolen vehicles or trucks that have veered away from predestined routes, while in the aviation sector, GPS can be used in both aircrafts and airports to guide landings and take offs. GPS is also widely used in sports such as mountaineering. The list of uses is therefore only limited to our imaginations.

For *environment monitoring*, GPS as one of the GNSS plays a key role as discussed in detail in Awange (2012). For example, GPS plays a vital role in earthquake monitoring and as such is useful for environmental disaster mitigation. It can also map post disaster areas and monitor events such as forest fires and oil spills, and how fast they are spreading. Its application to environmental phenomena such as El Niño, tsunami warning, water vapour monitoring and global warming in what is known as GPS-meteorology promises more benefits to humanity. In recent studies, GPS has contributed to the monitoring of variations in fresh water resources and has together with other satellites established the cause of the 2006 rapid fall in Lake Victoria, see e.g., Awange et al. (2008).

5.3 GPS Observation Principles

In this section, the basic principles upon which GPS operates are presented. More detailed expositions of the operational principles can be obtained in more advanced text books such as Hofman-Wellenhof et al. (2001), Leick (2004) and US Army Corps of Engineers (2007). We begin the section by looking at the structure of the GPS signals.

5.3.1 GPS Signals

Earlier GPS satellites (Blocks II, IIA, and IIR) sent microwave radio signals to receivers that are comprised of

- L1 and L2 carrier frequencies,
- *Coarse Acquisition C/A* and *Precise Acquisition P*-binary codes, and
- the navigation messages.

The precise atomic clocks on-board the GPS satellites generate a fundamental clock rate or frequency f_0 of 10.23 MHz, which is used to generate the two L-band

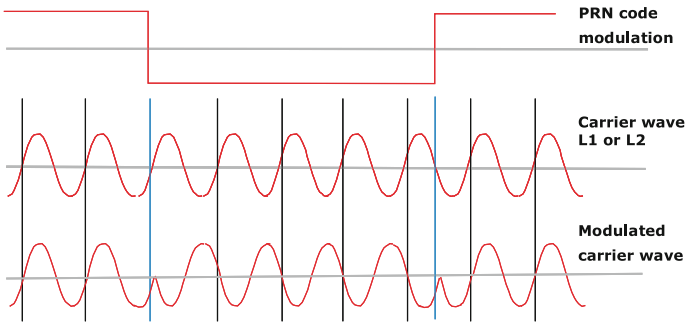


Fig. 5.3 Code modulation in the GPS carrier frequencies

carrier frequencies L1 and L2 through integer multiplication (i.e., $L1 = 154f_0$ and $L2 = 120f_0$). This leads to the frequency of L1 to be 1575.42 MHz with a wavelength of 19 cm and that of L2 as 1227.60 MHz with a wavelength of 24.4 cm. The ranging binary codes C/A-code and P-code are then modulated onto the carrier frequencies (see Fig. 5.3). Each of these ranging codes consists of a stream of binary digits, zeros and ones, known as bits or chips (El-Rabbany 2006, p. 14). Due to the noisy nature of these codes, they are known as Pseudo Random Noise (PRN) but are normally generated using a mathematical algorithm, see e.g., Hofman-Wellenhof et al. (2001).

The L1 frequency carries both the C/A-code and P-code, while the L2 frequency carries only the P-code. The C/A-code modulates at 1 MHz and repeats every 1023 bits while the P-code modulates at 10 MHz and repeats every 7 days, however the P-code is not accessible to civilian users.

Each satellite has a specific C/A-code, which enables the GPS receiver to identify which satellite is transmitting a particular code. For example, a GPS satellite with an ID of PRN 20 refers to a GPS satellite that is assigned to the twentieth week segment of the PRN P-code (El-Rabbany 2006, p. 14). C/A-code is less precise compared to P-code and is reserved for civilian use.

The P-code, with a frequency of 10.23 MHz, is more precise and is reserved for the use of the US military and its allies. P-code repeats itself every week having a wavelength of 29.3 m. The reservation of this code for military use is realized through the addition of an unknown W-code to the P-code to generate a P(Y)-code. This process is called antispoofing (AS).

Besides the ranging C/A-code and P-codes, a GPS satellite will also broadcast navigation messages to its users. The navigation message contains information on the health of the satellite, orbital parameters (satellites broadcast their ephemeris as a function of time), generic ionospheric corrections, satellite clock correction parameters, satellite almanac (essential for mission planning, see Chap. 6), and some information on other satellites. Each message has a 50 Hz frequency and consists of 25 pages (also known as frames) and 5 subframes of data.

Subframe 1 contains GPS week number, satellite accuracy and health, and satellite clock correction terms. Subframes 2 and 3 carry the satellite ephemeris, while

subframe 4 contains ionospheric corrections, satellite health and almanac data for satellites 25 to 32, special messages, satellite configuration flags, ionospheric and UTC data. Subframe 5 contains the satellite health and almanac data for satellites 1–24, almanac reference time and week number. Each subframe is made up of 10 words, and each word is made up of 30 bits. The total message length is therefore 1500 bits.

The advantage of using dual frequencies (L1 and L2) is the ability to mitigate ionospheric errors. The setback with the traditional GPS signal structure is that the civilian user has only access to the L1 carrier frequency. Positioning with L1 alone has the limitation of not being able to use the differencing techniques that combine both L1 and L2 frequencies to minimize *ionospheric errors*. To circumvent this problem, most geodetic high precision GPS receivers adopt techniques such as cross-correlation that do not require the *Y-code* to recover the L2 signal (El-Rabbany 2006, p. 20). These techniques, however, recover L2 signals which are noisier than the original signals. For long baselines, i.e., distances of 100s of km between receivers, use of such L2 signals provides some relief against the effect of the ionosphere. For very short baselines, e.g., <5 km, the ionospheric effects cancel out between the receivers as the atmospheric conditions are almost identical between these receivers. Use of L2 signals could thus be omitted without significant effects.

Modernized GPS satellites (Block IIR-M and Block IIF) are attempting to address this problem through the introduction of the second civilian *ranging code L2C* that will be modulated on the L2 carrier frequency. The L2C signal is already being transmitted by Block IIR-M satellites currently in orbit. This will provide civilians with the capability of combining the two frequencies L1 and L2 to mitigate ionospheric errors. In addition to this civilian frequency, Block IIR-M will also have a new military signal with a new code (M-code on L1M and L2M). Although this is expected to improve autonomous positioning (stand-alone GPS), the additional of the second civil code is found to be insufficient for use in civil safety of life applications, mainly due to the potential interference of ground radars that operate near the GPS L2 band (El-Rabbany 2006, p. 17).

Therefore, in order to meet the needs of safety-of-life in aviation, a third civil code L5 is planned to be incorporated in future block IIF and GPS III satellites in addition to the L2C and the new robust and higher power military M-codes. They will be modulated into the L1 and L2 carrier frequencies. These additional civilian signals are expected to improve positioning accuracy (see, e.g., Fig. 6.7 in p. 83).

5.3.2 Measuring Principle

The starting point is the basic principle of physics that relates the travel time t , distance travelled d , and speed of light c , namely:

$$Distance(d) = Speed(c) \times Time(t). \quad (5.1)$$

If time t can be accurately measured in (5.1), and the speed c is known, then it is possible to obtain the distance d . This basic expression forms the foundation of GPS satellite positioning. GPS receivers situated on the ground or in space accurately measure the time t taken by a signal to travel from the satellites to the receivers. Knowing the speed of light (i.e., $c = 3 \times 10^8 \text{ ms}^{-1}$), the distance from the satellites to the receivers, known as “*pseudoranges*” can be measured. Since the GPS satellites orbit at about 20,200 km above the Earth, it takes around 0.07 s for the signal to travel from the satellites to the receivers.

The satellites generate binary codes that are sent to the receiver, which generates an identical binary code. The receiver generated codes are then compared to those received from the satellites, which lag behind those generated by the receivers. By comparing the two signals (from satellite and receiver), the receivers are able to compute the travel time of the signal. A binary code generated by the satellite takes the form of $+1/-1$ (see Fig. 5.3).

In order to measure the time traveled by the signal accurately, the receiver and satellite clocks must be synchronized and be error free. The clocks, however, normally have errors that are propagated to the measured ranges. Furthermore, clock errors are not the only ones that degrade the measured ranges. The atmosphere, orbital errors, multipath, and other types of errors discussed in Sect. 5.4 also contribute to the degradation of the measured ranges, hence the term *pseudoranges*.

Because the receiver position is given by the three Cartesian coordinates X, Y, Z , one solution of Eq. (5.1) would not suffice, with three such equations being required. This would essentially mean simultaneously observing three satellites in space to obtain position for one epoch. Due to clock errors, however, there is an additional *receiver clock* unknown bias Δt which takes the number of unknowns to four, i.e., $X, Y, Z, \Delta t$. Hence a fourth satellite is needed to determine the receiver clock error Δt , while the satellite clock errors are modeled.

There are two ways by which the distances from the receivers to the satellites are measured. These are:

- (i) Code ranging
- (ii) Carrier phase measurements.

Code pseudorange involves measuring the time lag between the satellite and receiver generated signals using either *C/A-code* or *P-code* (Fig. 5.4). The receiver locks onto the signal and synchronizes a matching code, thereby measuring the delay of the signal, as illustrated in Fig. 5.4. The measured time delay, Δt , is then multiplied by the speed of light c in Eq. 5.1 to generate the pseudorange p . Code pseudoranges can achieve an accuracy of about 5–15 m for *C/A-code* and therefore may suffice for those environmental applications that do not require higher accuracies such as locating a waste dumping site.

For accuracies at cm and mm levels, i.e., those required for monitoring environmental phenomenon such as rising sea level or the movement of tectonic plates, one has to use the carrier-phase measurements (Fig. 5.5).

For *Carrier-phase pseudorange*, *phase lag* instead of time lag is measured. The measuring principle is similar to that used in an EDM (electronic distance

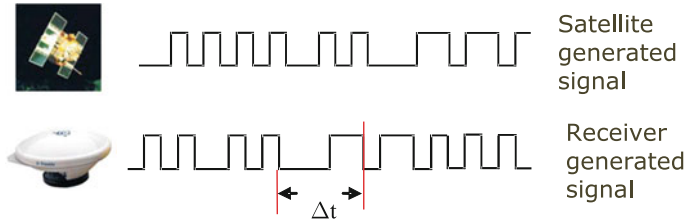


Fig. 5.4 The time difference between the receiver and GPS code signals

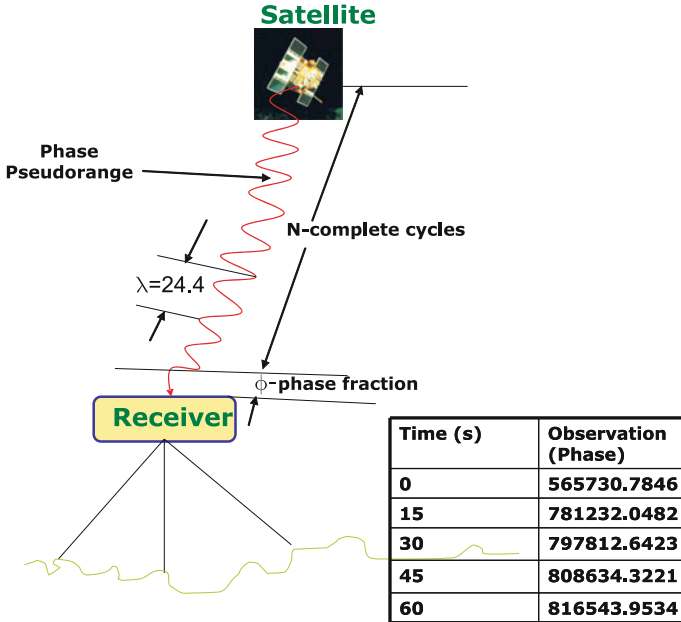


Fig. 5.5 Carrier-phase pseudorange measurement

measurement), see e.g., Irvine and Maclennan (2006). By measuring carrier phase, more precise positioning is possible.

As seen in Fig. 5.5, the complete number of cycles plus the fractional portion (phase) are used in the case of GPS carrier phase pseudorange measurements from the satellites to the receiver. The only difference is that unlike EDM discussed in Sect. 3.4, which is a two way transmission (i.e., the signal is reflected), GPS offers a one way transmission with no reflection of the signals. Since the initial complete number of cycles are not normally known at the time the receiver is switched on, there exists an unknown *integer ambiguity*. The accurate determination of this integer ambiguity underpins the accuracy of the final position derived from the carrier phase measurements. For GPS phase measurements, the one way distance equation becomes

$$pseudorange(p_p) = n\lambda + \phi \quad (5.2)$$

Example 5.1 (Carrier phase measurements) As an illustration, let us consider carrier phase measurements made from the satellite to the receiver for a duration of 1 min (Fig. 5.5). At the time the receiver is switched on (i.e., $t = 0$ s), it generates a random integer number such as (565730) since it does not know the complete number of cycles of the signal from the satellite. As the measurement progresses, the number of cycles increases and the complete number of cycles are accurately counted (if no cycle slips occur, i.e., loss of lock of satellites). After $t = 60$ s, the total number of cycles counted is recorded as 816543.9534. The complete number of cycles measured in 1 min is thus $816543 - 565730 = 250813$ together with the fractional portion of the cycle 0.9534. If 1 cycle of the L2 signal has a wavelength of $\lambda = 0.244$ m, the measured pseudorange P_p will be given by

$$\left. \begin{aligned} P_p &= 250813\lambda + 0.9534\lambda + N\lambda \\ P_p &= 61198.60463 + N\lambda \end{aligned} \right\}, \quad (5.3)$$

where N is the unknown integer ambiguity. If its value is known, then the phase pseudorange could be determined. Since this value is often unknown, it is determined independently or together with the unknown coordinates X , Y , Z and clock parameters as discussed e.g., in Awange (2012).

End of example

In Awange (2012), it is shown how the pseudoranges discussed above are used in the observation equations for generating positions. Detailed discussion of the signal structure and how they are processed can be found, e.g., in Leick (2004), Hofman-Wellenhof et al. (2001, pp. 71–85).

5.4 Errors in GPS Measurements

Just like any other measurement, the accuracy derived from GPS measurements are subject to errors that degrade the quality of the derived parameters, including those of environmental interest. This section considers some of the most significant errors that undermine GPS observations and discusses the means by which these errors could be minimized and/or avoided. As already pointed out in Sect. 5.3.2, these errors lead to pseudorange rather than an accurate range between the satellite and the receiver. Modeling techniques by which these errors are eliminated or minimized are presented, e.g., in Awange (2012).

5.4.1 Ephemeris Errors

As the satellites move along their orbits, they are influenced by external forces such as solar and lunar (moon) gravitational attraction, as well as periodic solar flares (Irvine and MacLennan 2006, p. 180).

For shorter baselines (i.e., distances less than 30 km between two receivers on Earth), orbital errors tend to cancel through differencing techniques (see Awange 2012). Over long baselines however, e.g., over 1,000 km, orbital errors no longer cancel owing to different receivers sensing different components of the error due to significant changes in the vector directions.

As pointed out in Sect. 5.2.2, ground monitoring stations are used to continuously measure the positions of the satellites. Techniques such as satellite laser ranging (SLR), lunar laser ranging (LLR) and Very Long Baseline Interferometry (VLBI) discussed in Sect. 3.4 are used to locate these ground control stations to a very high accuracy. Using the data from the monitoring stations, the master control station predicts satellite positions (broadcast ephemeris), which are transmitted to the user as part of the navigation message together with the data signals during positioning as discussed in Sect. 5.3. The accuracy of the broadcast ephemeris has improved tremendously, i.e., from 20–80 m in 1987 to 2 m currently, see e.g., El-Rabbany (2006, p. 16).

El-Rabbany (2006, p. 16) attributes this improvement to superior operational software and improved orbital modeling. *Broadcast ephemeris* are useful for real-time positioning (i.e., if the GPS receiver is expected to deliver results while collecting measurements in the field). *Precise ephemeris* on the other hand are useful for post processing tasks which are required at a later date. In such cases, the post-processed positions of the satellites by other global tracking stations are available 17 h to 2 weeks later with accuracies of 0.02–0.2 m.

5.4.2 Clock Errors

Satellite clocks are precise atomic clocks (i.e., rubidium and cesium time standards). In contrast, the receivers cannot include atomic clocks since the cost would be too high for users to afford and for safety concerns. Clocks within the receivers are thus less precise and as such subject to errors. This is not to say that the satellite clocks are error free, but that the magnitude of the receiver errors are much higher.

The satellite and receiver clocks also have to be synchronized in order to measure the time taken by the signal to travel from the satellites to the receiver. Since the synchronization is normally not perfect, errors are likely to occur. This error is also known as time offset, i.e., the difference between the time as recorded by the satellite and that recorded by the receiver (see, e.g., US Army Corps of Engineers 2007). The measured range error is then given by

$$R_e = c\delta t, \quad (5.4)$$

where c is the speed of light and δt is the time offset. From (5.4), considering that $c = 3 \times 10^5$ km/s, a clock error of 0.000001 s, for instance, would cause the measured range to be erroneous by 300 m, while an error of 0.001 s would result in a range error of 300 km.

Satellite clock errors are small in magnitude and easily corrected due to the fact that the ground control stations closely monitor the time drift and are able to determine second order polynomials which accurately model the time drift (US Army Corps of Engineers 2007). These second order polynomials are included in the broadcast message. The receiver clock error is determined as a nuisance unknown along with the required coordinate parameters in the observation equation and this explains the need of the fourth satellite as discussed in Sect. 5.3.2.

5.4.3 Atmospheric Errors

The atmosphere is the medium above the Earth by which the GPS signal passes before it reaches the receiver. *Charged particles* in the ionosphere (50–1000 km) and *water vapour* in the troposphere (1–8 km) affect the speed of the GPS signals, leading to an optical path length between the satellite and the receiver and a delay in the corresponding time the GPS signal takes to reach the receiver, see e.g., Belvis et al. (1992). One of the key tasks of geodetic GNSS processing software therefore is to “correct” the ranges between the satellite and the receiver so as to remove the effects of the Earth’s atmosphere, thereby reducing all optical path lengths to straight-line path lengths (Belvis et al. 1992).

The *ionosphere* is made of *negatively charged electrons*, *positively charged atoms* and *molecules* called *ions*. The charged particles are a result of free electrons that occur high in the atmosphere and are caused by solar activity and geomagnetic storms. The number of free electrons in the column of a unit area along which the signal travels between the sending satellite and the receiver make up what is known in GPS literatures as the Total Electron Content (TEC). Free electrons in the ionosphere delay the GPS code measurements, thus making them too long on the one-hand while advancing the GPS phase measurements, making them too short on the other hand, thus resulting in incorrect ranges (i.e., error in the measured ranges) (Hofman-Wellenhof et al. 2001, pp. 99–108; Leick 2004, p. 191).

The size of the delay or advance (which can amount to tens of meters) depends on the TEC and carrier frequency, i.e., the ionosphere is a dispersive medium (Leick 2004, p. 191). The error effect of the ionospheric refraction on the GPS range value depend on sunspot activity, time of the day, satellite geometry, geographical location and the season. Ionospheric delay can vary from 40–60 m during the day to 6–12 m at night (US Army Corps of Engineers 2007). GPS operations conducted during periods of high sunspot activity or with satellites near the horizon produce range results with the highest errors, whereas GPS observations conducted during low

sunspot activity, during the night, or with satellites near the zenith produce range results with the smallest ionospheric errors. Ionospheric effects are prominent over longer baselines (>30–50 km) although high ionospheric activity can affect shorter distances. Ionospheric errors can be significantly reduced through:

1. *Use of dual frequency.* Since signal speed through the ionosphere is dependent on frequency (dispersive medium), ionospheric effects which cause a delay of about 2–80 m can be modeled using frequency combination. They are removed mostly by comparing the signal delays of the $L1$ and $L2$ frequencies and exploiting the known dispersion relations for the atmosphere (Brunner and Gu 1991; Spilker 1980), i.e.,

$$\rho_{IF} = \frac{f_{L1}^2}{(f_{L1}^2 - f_{L2}^2)} \rho_{L1} - \frac{f_{L2}^2}{(f_{L1}^2 - f_{L2}^2)} \rho_{L2} \quad (5.5)$$

and

$$\Phi_{IF} = \frac{f_{L1}^2}{(f_{L1}^2 - f_{L2}^2)} \Phi_{L1} - \frac{f_{L2}^2}{(f_{L1}^2 - f_{L2}^2)} \Phi_{L2}, \quad (5.6)$$

where ρ_{IF} and Φ_{IF} are the *ionosphere-free* pseudorange and phase measurements, respectively. ρ_{L1} and ρ_{L2} are measured pseudoranges while Φ_{L1} and Φ_{L2} are phase measurements at $L1$ and $L2$ carrier frequencies. The resulting observations in (5.5) and (5.6) are known as ionospheric-free observable and hence explain the main reason why GPS uses two frequencies. The disadvantage with using dual frequencies as illustrated above is the increased noise and as such, this approach is useful mainly for longer baselines. For very short baseline (<5 km), where the atmosphere is assumed uniform, the ionosphere error is minimized once differencing techniques are used.

2. *Modeling.* GPS navigation messages contain ionospheric correction parameters that are used in correction models during data processing. Several ionospheric correction models, such as the Klobuchar model, are available in commercial software and can be used to reduce ionospheric error. However, this only gives an approximate value that usually does not remove more than 50% of the error. Moreover, modeling is generally inefficient in handling short-term variations in the ionospheric error.

The second medium, the *troposphere*, also known as the neutral atmosphere, consists of 75% of the total molecular mass of the atmosphere, as well as all of the water vapour and aerosols. The troposphere is a non-dispersive medium, i.e., the refraction is independent of the frequency of the signal passing through it. Tropospheric errors vary significantly with *latitude* and *height* and are dependent on *climatic zone*. The neutral atmosphere is therefore a mixture of *dry gases* and *water vapour*. Water vapour is unique in this mixture because it is the only constituent that possesses a dipole moment contribution to its refractivity, thus leading to separate treatment between the dipole and non-dipole contribution to refractivity by the water vapour and other constituents in the atmosphere (Belvis et al. 1992).

The tropospheric errors thus comprise two parts (see Fig. 20.1, p. 275): the “*hydrostatic part*”, commonly referred to in various GPS text as “dry part”, and the dipole component known as the “*wet part*”. Belvis et al. (1992), while citing Saastamoinen (1972) and Davis et al. (1985), state that the *hydrostatic delay* is generally erroneously referred to as “*dry delay*” in the literature, meaning that they are due to the contribution of dry air. In actual fact, according to Belvis et al. (1992), the dry air contributes mostly to the hydrostatic delay, but there is also the contribution of the non-dipole component of water vapour. They propose the use of the term hydrostatic delay instead of dry delay. In this book, the term hydrostatic delay therefore is adopted.

According to Belvis et al. (1992), both hydrostatic and wet delays are smallest for paths oriented along the zenith direction and increase approximately inversely with the sine of the elevation angle, i.e., either delay will tend to increase by about a factor of 4 from zenith to an elevation of about 15°. Consequently, Belvis et al. (1992) point out that most expressions for the delay along a path of arbitrary elevation consist of the zenith delay multiplied by a mapping function. This mapping function has been shown, e.g., by Davis et al. (1985) to describe the dependence of the delay on elevation angle.

The *hydrostatic part* contributes 90% of the tropospheric error. It is easily modeled out to few millimeter or better given surface pressure. The remaining 10% occurs from the wet part, resulting from the *water vapour*, which depends on the refractivity of the air through which the signal is traveling. The refractivity of air depends on (1) the *density of air molecules* (dry component) and (2) the *density of the water vapour* (wet component). Above 50 km altitude, the density of molecules is very low and hence its effect is small. Although the wet delay is always much smaller than the hydrostatic delay, it is usually far more variable and more difficult to remove (Belvis et al. 1992).

The tropospheric delay therefore depends on *temperature, pressure* and *humidity* and affects signals from satellites at lower elevations more than those at higher elevation. For example, El-Rabbany (2006, p. 55) and Belvis et al. (1992) indicates that tropospheric delay results in pseudorange errors of about 2.3 m for satellites at the zenith (i.e., satellites directly overhead), 9.3 m at 15° elevation and 20–28 m for 5° elevation. Therefore, the lower the elevation angle of the incoming GPS signal, the greater the tropospheric effect because the signal travels a longer path through the troposphere.

Tropospheric delay can be problematic, especially when stations are widely distributed at different altitudes. For example, cold (dense) air can accumulate in mountain basins on clear calm nights whilst mountain tops may be considerably warmer. Tropospheric delay can also exhibit short-term variations, e.g., due to the passing of *weather fronts*. The *hydrostatic part* can be modeled by employing surface meteorological data or by acquiring them from external sources such as the European Center for Medium Weather Forecast (ECMWF) and the National Center for Environmental Prediction (NCEP).

Whereas the hydrostatic delay can be modelled from the surface meteorological data, the wet component cannot be accurately determined in the same manner, but is

instead measured from water vapour radiometers (WVR) (Elgered et al. 1991; Resch 1984; Ware et al. 1986) or by directly estimating the time varying *zenith wet delay* (ZWD) as unknowns from the GPS observations (Herring 1990; Tralli et al. 1988). These estimation techniques usually assume azimuthal symmetry of the atmosphere, and they exploit the form of the elevation dependence of the delay (i.e., the mapping function) and the fact that the delay changes little over short periods of time (Belvis et al. 1992). These analyzes typically constrain the variations in the *zenith wet delay* to between 1 and 20 mm per hour, depending on location and time of year, leading to the recovery of ZWD from GPS data with an accuracy between 5 and 20 mm (Belvis et al. 1992).

In most processing software, ZWD is estimated using Integrated Precipitate Water Vapour (IPWV) models. Many models, e.g., Saastamoinen, Hopfield, and Magnet, have been proposed to model tropospheric errors, see e.g., Hofman-Wellenhof et al. (2001). Some of these models depend on real meteorological data input. However, the best observational principle is to keep the baselines as short as possible.

The discussions in this section have focused on eliminating the effects of atmospheric delay in order to improve the accuracy of positioning. In Chap. 21, we will see that such noise, as geodesists are keen on positioning, are actually valuable environmental monitoring parameters. In essence, *one person's poison is another person's meat!*

5.4.4 Multipath

Consider now a satellite signal that is meant to travel straight to the receiver being reflected by a surface, as shown in Fig. 5.6. The measured pseudorange reaching the receiver ends up being longer than the actual pseudorange had the signal travelled directly. In urban areas, the presence of buildings contribute greatly to the multipath effect. Multipath errors can be avoided by placing the receiver in a place without reflective or refractive surfaces. The best practice is to place the receiver at least 3m from reflecting walls and in addition use GPS antennas with ground panels,

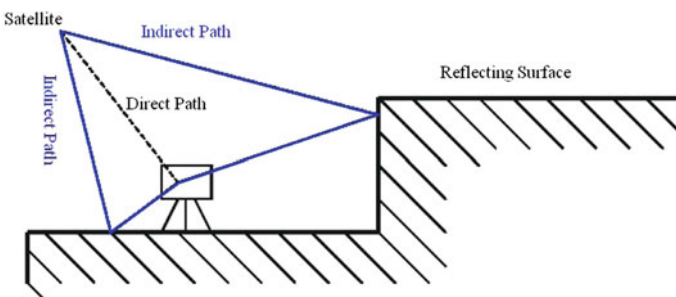


Fig. 5.6 Multipath effect

which discard indirect reflected signals (which are of a lower power). A choke ring antenna also provides a means of reducing multipath while other receivers have in-built filtering mechanisms. Good mission planning (See Sect. 6.3) also helps to reduce the effect of multipath.

5.4.5 Satellite Constellation “Geometry”

Dilution of precision (DOP) depends on the distribution of the satellites in space (see Fig. 6.1 on p. 76). With clear visibility and a large number of satellites, the value of DOP is low, indicating a good geometry. With obstructions and fewer satellites, however, the DOP values becomes high, indicating poor geometry, which may negatively affect positioning accuracy.

Also used to measure the geometric strength is the Position Dilution of Precision (PDOP) which can be used essentially as an expression of the quality of the satellites geometry, which is essential for ambiguity resolution. Usually, a PDOP value of less than 6 but greater than 1 is desirable. For a detailed discussion of this topic, we refer the reader to Sect. 6.3.

5.4.6 Other Sources of Errors

Other sources of errors which may degrade accuracy include hardware errors due to variations in the antenna phase centers with satellite altitude. This error is greater at elevations below 15° but less between 15° and 60°. In addition, there is receiver noise (e.g., signal processing, clock synchronization, receiver resolution, signal noise, etc.) and cycle slips which results when the receivers lose lock on a satellite due to, for example, signal blockage by buildings. Radio interference, severe ionospheric disturbance, and high receiver dynamics can also cause signal loss (El-Rabbany 2006, p. 25).

5.5 Concluding Remarks

In summary, this chapter has presented the basics of GPS satellites by looking at the satellites, signal structure and measurement principle used to obtain position. Position is calculated by accurately measuring the distance of a receiver from the satellite by determining the delay in the radio signal transmitted by the satellite. This delay is measured by matching and comparing the received signals by an equivalent receiver generated signal. More precise measurements use phase instead of timing measurements. The signals, however, are subject to various sources of errors, which have been discussed in this chapter.

In general, the measuring principle and the errors discussed in this chapter are also valid for all the other GNSS systems (GLONASS, Galileo and Compass). They only differ in design, signal structure and coordinate systems (see Sect. 6.6).

References

- Agnew DC, Larson KM (2007) Finding the repeat times of the GPS constellation. *GPS Solutions* 11:71–76
- Awange JL (2012) *Environmental monitoring using GNSS, global navigation satellite system*. Springer, Berlin
- Awange JL, Grafarend EW (2005) *Solving algebraic computational problems in geodesy and geoinformatics*. Springer, Berlin
- Awange JL, Ong’ang’a O (2006) *Lake Victoria-ecology, resource of the Lake Basin and environment*. Springer, Berlin
- Awange J, Sharifi M, Ogonda G, Wickert J, Grafarend E, Omulo M (2008) The falling Lake Victoria water level: GRACE, TRIMM and CHAMP satellite analysis of the lake basin. *Water Resource Management*, 22, 775–796. doi:10.1007/s11269-007-9191-y
- Belvis M, Businger S, Herring TA, Rocken C, Anthes RA, Ware RH (1992) GPS meteorology: remote sensing of water vapour using global positioning system. *J Geophys Res* 97:15787–15801
- Brunner FK, Gu M (1991) An improved model for the dual frequency ionospheric correction of GPS observations. *Manusc Geod* 16:205–214
- Davis JL, Herring TA, Shapiro II, Rogers AE, Elgered G (1985) Geodesy by radio interferometry: Effects of atmospheric modeling errors on estimates of baseline length. *Radio Sci* 20:1593–1607
- Elgered G, Davis JL, Herring TA, Shapiro II (1991) Geodesy by radio interferometry: water vapour radiometry for estimation of the wet delay. *J Geophys Res* 96:6541–6555
- El-Rabbany A (2006) *Introduction to GPS—global positioning system*, 2nd edn. Artech House, Norwood
- Herring T, Davis JL, Shapiro II (1990) Geodesy by radio interferometry: the application of Kalman filtering to the analysis of very long baseline interferometry data. *J Geophys Res* 95(12):561–581
- Hofman-Wellenhof B, Lichtenegger H, Collins J (2001) *Global positioning system: theory and practice*, 5th edn. Springer, Wien
- Hofman-Wellenhof B, Lichtenegger H, Wasle E (2008) *GNSS—Global Navigation Satellite System: GPS, GLONASS, Galileo and more*. Springer, Wien
- Irvine W, Maclellan F (2006) *Surveying for construction*, 5th edn. McGraw-Hill, New York
- Leick A (2004) *GPS satellite surveying*, 3rd edn. Wiley, New York
- Resch GM (1984) Water vapour radiometry in geodetic applications. In: Brunner FK (ed) *Geodetic refraction*. Springer, New York, pp 53–84
- Saastamoinen J (1972) Atmospheric correction for the troposphere and stratosphere in radio ranging of satellites. In: Henriksen SW et al (eds) *The use of artificial satellites for geodesy, geophys*. Monogr. Ser., vol 15. AGU, Washington, DC, pp. 247–251
- Spilker JJ (1980) GPS signal structure and performance characteristics. In: *Global positioning system*, vol 1. The Institute of Navigation, Washington, DC
- Tralli DM, Dixon TH, Stephens SA (1988) Effect of wet tropospheric path delays on estimation of geodetic baselines in the Gulf of California using the global positioning system. *J Geophys Res* 93:6545–6557
- US Army Corps of Engineers (2007) *NAVSTAR global positioning system surveying*. Engineering and Design Manual, EM 1110-1-1003
- Ware R, Rocken C, Hurst KJ (1986) A GPS baseline determination including bias fixing and water vapour radiometer corrections. *J Geophys Res* 91:9183–9192

Chapter 6

Environmental Surveying and Surveillance

“Any measurement must take into account the position of the observer. There is no such thing as measurement absolute, there is only measurement relative”. Jeanette Winterson. In that case, “Measure what is measurable, and make measurable what is not so”.

Galileo Galilei (1564–1642)

6.1 Environmental Monitoring Parameters

In this section, we discuss the *quantitative* and *qualitative data* that could be collected using GNSS satellites, and in so doing, attempt to answer the question “what can GNSS satellites deliver that is of use to environmental monitoring?” The observed parameters necessary for environmental monitoring vary, depending upon the indicators being assessed. Some are *physical variables* such as changes in soil patterns, vegetation, rainfall, water levels, temperature, deforestation, solar and UV radiation. Others are *chemical variables*, e.g., pH, salinity, nutrients, metals, pesticides, while others are *biological variables*, e.g., species types, ecosystem health, and indicator species.

GNSS satellites are useful in measuring physical variables such as atmospheric temperature, pressure, and tropopause heights needed for weather and climate change monitoring, as we will see in Chap. 21. For chemical and biological variables, the main environmental monitoring parameter provided by these satellites is the *position* of the respective variable. Positions are useful not only in providing physical locations, but also in measuring spatial variation in the variables being monitored.

For example, monitoring coastal erosion can be undertaken by the constant monitoring of shoreline positions using GNSS satellites as shown by Goncalves (2010), Goncalves et al. (2012). In other environmental monitoring examples, satellite derived positions could complement other systems to enhance monitoring. For

example, GNSS satellites complement low-flying satellites such as the Gravity Recovery And Climate Experiment (GRACE) to allow more detailed and accurate monitoring of mass redistribution on the Earth's surface. Such mass distribution include, e.g., variations in surface and groundwater at local, regional and global scales, as will be discussed in Chap. 20. For dynamic environmental phenomena, such as variations in deforestation, GNSS satellites could provide efficient tools for measuring such changes by providing time series of their variation in position.

6.2 Design of GNSS Monitoring Survey

In order to achieve maximum benefit from the use of GNSS satellites for environmental monitoring, it is essential that proper measurement procedures be undertaken with clear aims, and objectives. As in all measurements, the quality of the observations will be determined by the purpose and objectives and, to a greater extent, the client's requirements. These objectives and needs will dictate the methods chosen for *data collection*, the *frequency of data collection*, and *temporal* and *spatial* extent. The monitoring design should therefore specify the monitoring variables desired from GNSS satellites, where, when and by whom the data shall be collected. Like other environmental monitoring techniques, GNSS satellite monitoring also requires some *baseline survey* or information upon which any change in the environment could be referred to. In the case of positions, permanent reference stations whose locations are accurately known normally provide such references. Any spatial change (i.e., change in the environmental variable being monitored with regards to position) will then be referred to these points. Measurements can be repeatedly taken at given time intervals (temporal resolution) depending on the monitoring budget and the desired accuracy.

The final accuracy of the collected data will depend on how the errors are handled. For GNSS satellite monitoring, these errors (see Sect. 5.4) could be external (i.e., outside the user's control) or internal (i.e., during the actual measurements). In this Chapter, GNSS measurement procedures that may help minimize errors and achieve meaningful results relevant for environmental monitoring are presented.

GNSS surveys can be divided into three components:

- *Planning and reconnaissance*: This is an essential part of any monitoring campaign. For a GNSS survey, it is essential to plan the measuring campaign in such a manner that the errors discussed in Sect. 5.4 are minimized. For example, it is important that the sky visibility and satellite paths are plotted in a skyplot for the survey area and the desired survey period. The advantage of having sky plots is that the number of satellite visible during the planned observation period and features blocking the satellite are determined in advance. The main objective is to ensure unobstructed view of at least four satellites with a good geometric distribution in the sky. As already indicated in Sect. 5.4.5 (p. 70), satellite geometry is indicated by the dilution of precision (DOP) factor. Reconnaissance provides the opportunity of visiting the survey site prior to the actual GNSS survey and assessing the

availability of existing reference stations (geodetic control) and accessibility to these stations, while at the same time looking out for potential sources of errors such as buildings and trees that can cause multipath errors. The advantage of undertaking reconnaissance and planning prior to a satellite survey is that it can significantly reduce some logistical problems such as setting up a receiver in an area where the signals would be blocked.

- *Undertaking the monitoring survey*: Once the aims and objectives of the environmental monitoring project have been identified and the reconnaissance done, the survey task can be executed through proper *choice of GNSS positioning method*, *undertaking care in the actual survey procedures*, and *avoiding or minimizing errors where possible* (e.g., setting the receiver in an open space that is not very close to buildings to reduce the likelihood of multipath errors).
- *Processing of the data*: In order to obtain the monitoring parameters or baseline information from the GNSS observation, data can be processed in real-time or during post-processing.

6.3 Mission Planning and Reconnaissance

In Sect. (5.3.1), satellite signals were introduced as the measurable quantities that are needed to generate monitoring information. GNSS signals are microwaves that penetrate cloud cover and travel under all weather conditions, but unfortunately cannot penetrate dense *vegetation* canopies or buildings. Because of this, and in order to reduce the detrimental effects of atmospheric refraction and multipath signals, it is desirable that the antenna has as clear view of the sky as possible. An elevation angle of above 15° is often considered suitable to enable a clear sky view, although this could at times be as low as 10° . Some antennas are equipped with a ground plane that blocks unwanted multipath signals from reaching the antenna. Nearby metallic objects, such as fences and power lines, should be avoided where possible in order to prevent imaging, i.e., when metallic objects act as secondary antennas, thereby distorting the positions derived from GNSS satellites. It is therefore recommended that the GNSS observation sites be selected in open areas away from potential sources of multipath and imaging where possible.

As already pointed out in Sect. (5.4.5), the geometrical strength of the satellite constellations will contribute to the quality (accuracy) of the positions obtained. A weaker geometry from satellites close together in the sky as illustrated in Fig. 6.1 (right) will contribute to geometrically weaker solutions while solutions computed by observing satellites evenly distributed in the sky (e.g., Fig. 6.1, left) will lead to geometrically stronger solutions. Both geometric dilution of precision (GDOP) and position dilution of precision (PDOP) are useful in measuring the geometrical strength of a satellite constellation, but PDOP is the most commonly used. PDOP is computed from the positions of the satellites in relation to the receiver and takes a single value, see e.g., Hofman-Wellenhof et al. (2008, pp. 262–266). It is a measure based solely on the geometry of the satellites and therefore can be computed prior

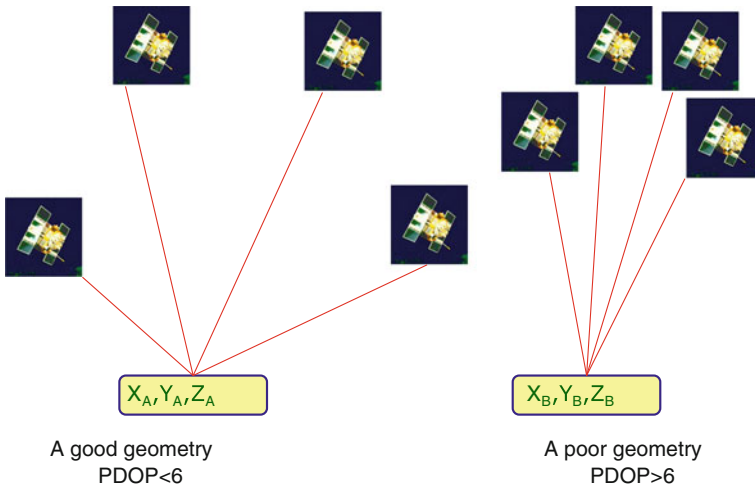


Fig. 6.1 Satellite geometry: *Left* (good geometry); *Right* (poor geometry)

to any observation being taken. A higher PDOP value (i.e., >6) indicates a poor satellite geometry for computing a position. In mission planning therefore, PDOP values are computed and used to indicate the observation window where the satellite constellation is adequate.

Satellite geometry becomes more crucial when one is observing over short occupation times, as is often the case in real-time kinematic (RTK) surveys discussed in Sect. 6.4.6. Whereas satellite geometry can be improved by longer observation period, poor sky visibility combined with a low number of satellites above the horizon can severely compromise static solutions. This essentially means that before a successful GNSS environmental monitoring campaign is undertaken, it is essential to know when bad situations are likely to occur so that they can either be avoided or the survey team prepare itself for a significantly longer period of observation. This knowledge can only be made possible through careful reconnaissance and well executed *mission planning*. Mission planning is thus a very vital component of any GNSS environmental monitoring campaign.

If the only possible observation window gives a PDOP between 6 and 10, it is recommended that the observation time frame be between 30–45 min. For PDOPs greater than 10, it might be necessary to postpone the observations. If, for whatever reason, postponing is not feasible, then the observation period should be made as long as possible, assuming of course that the effects of other errors such as multipath are minimal. If this is not possible, then it may not be possible to achieve as accurate position for this point using satellite positioning as one may wish, regardless of the length of the observation time.

Finally, a word of caution is necessary. PDOP values only indicate when satellites are likely to produce good or bad results and should therefore not be considered as a measure of the actual quality of the positions. Awange (2012) discusses the quality estimation during the post-processing of the satellite data.

The basic stages for planning a GNSS survey are generally as follows:

1. Locate unknown control points and update reference marks information if necessary.
2. Assess the suitability of unknown control points for GNSS positioning and check for multipath sources in the vicinity.
3. If necessary, construct a visibility diagram using a compass and a clinometer (see, e.g., Fig. 6.2). The compass will provide an approximate position from the true North, while the clinometer will give the elevation of features such as buildings and vegetation. This will indicate the satellites likely to be blocked by tall buildings and trees. Such a diagram should also contain information on potential multipath sources.
4. Locate local reference stations. This will provide baseline positioning information.
5. Assess the suitability of these reference stations for satellite surveying and check for multipath sources in the vicinity.

Example 6.1 (Mission planning) In order to decide on the appropriate time to carry out GNSS observations, any mission planning software such as those of Sokkia or Trimble could be used. Most receivers will come with software

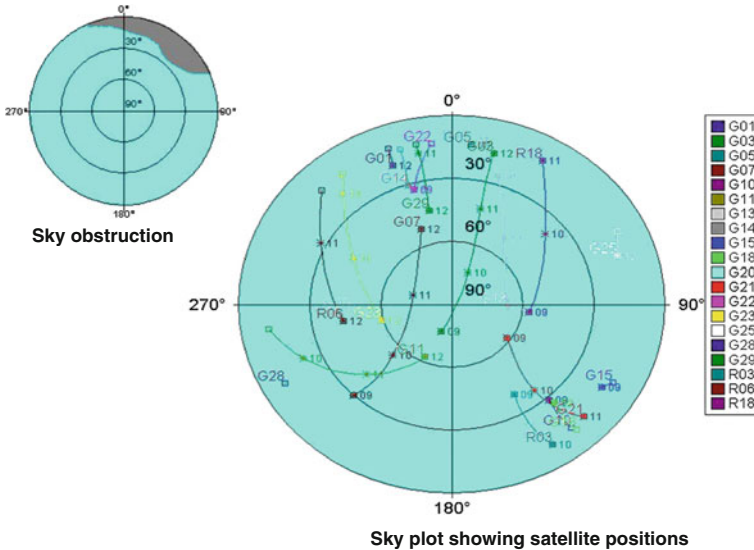


Fig. 6.2 Satellite visibility diagram of Astro deck 8 located at one of the buildings of the Curtin University (Australia) campus on the 16th of May 2008. *Left* Obstructed sky is noted at elevation 28° and azimuth between 0° and 60°. *Right* Satellite travel paths. The colors indicate the individual satellites

which are capable of conducting mission planning that can be used to indicate the position of the satellites during the desired observation time. The software provides DOPs which are useful in indicating the geometrical strength of the satellite constellation as already discussed. The following example illustrates how mission planning can be undertaken using any available commercial software. In general, the operational steps of most mission planning software are similar and will tend to give similar results. Using any planning software, one would generally proceed as follows:

- *Step 1 (Running the software)*: Within the appropriate user window of the software, start by inserting the *dates* over which you wish to undertake the GNSS survey and the *approximate coordinates* of the point for which the receiver will be stationed during the selected day. Approximate coordinates of this station can be entered in terms of latitude and longitude since the satellite constellation varies slowly with distance. You may enter the latitudes and longitudes of your local area for example by selecting your city from an option list which is often provided.
- *Step 2 (Setting the time zone)*: It is convenient when planning the survey to work in local standard time, thus, ensure the time zone is correct.
- *Step 3 (Loading the almanac)*: The almanac contains information about the satellite positions in their orbits and are normally sent as part of the navigation message. GPS receivers collect broadcast ephemerides which are satellite positions broadcast to the receiver by the satellites themselves. For precise positioning, broadcast ephemeris are valid for a maximum of 4 h but are repeated every hour. However, mission planning can use these ephemerides to predict satellite orbits over a period of about a month. Note that the more recent the ephemeris, the more precise are the planning mission results. Most GNSS receivers automatically acquire almanac data during regular operations. One way of accessing the current almanac data is to carry out quick observations (e.g., about 15 min) without necessarily setting up the antenna to survey specifications. The almanac can also be obtained from the Internet.¹
- *Step 4 (Planning graphs)*: Within the mission planning software, graphs giving various types of information for the day specified can be viewed. These graphs will indicate *satellite elevations plotted against time*, *satellite azimuths plotted against time*, *number of available satellites plotted against time*, representation of the *visibility time spans* of individual satellites, separate displays plotting the respective types of *dilution of precision (DOP) against time*, and *satellite tracks* through the time interval being plotted, showing elevations and azimuths in polar coordinates. Figure 6.3 presents an example of visibility time spans of individual satellites for station Astro deck 8 at Curtin University, Australia. A plot of the number of visible satellites and the related DOP is given in Fig. 6.4. Together with the skyplot

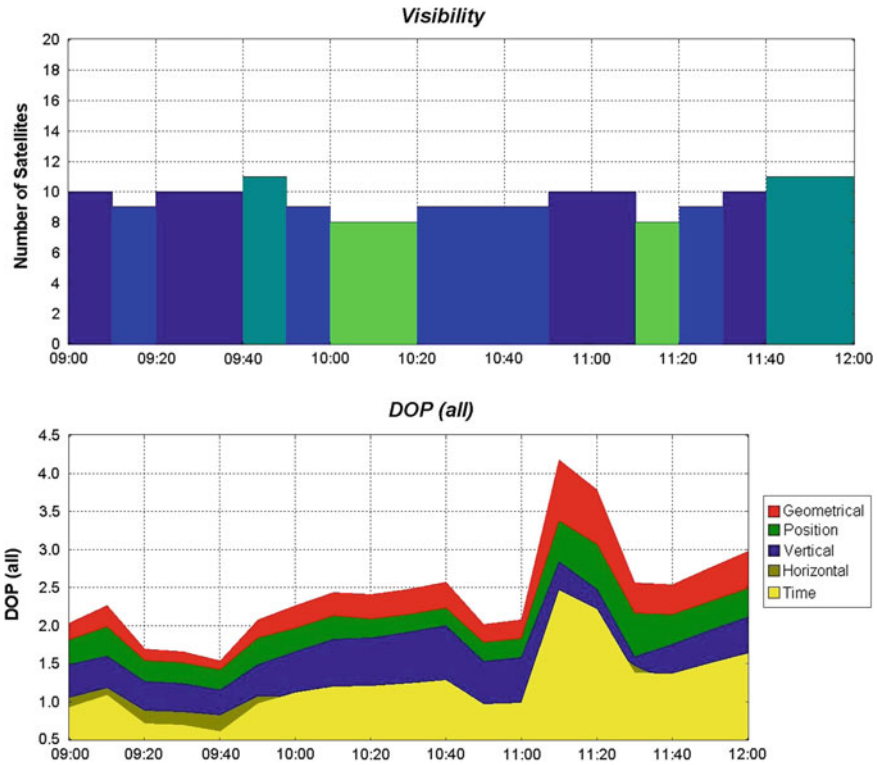


Fig. 6.4 Number of visible satellites (top) and the related DOP (bottom)

6.4 GNSS Field Procedures

Having done the planning, the next step involves the actual procedure for the field measurements. The objective of a given monitoring environmental task will dictate the types of equipment required. If the objectives call for more precise and accurate work, e.g., monitoring rise in sea level (Sect. 26.8), then the correct receivers and field procedure must be adopted. One of the tasks undertaken during a GNSS survey is the setting up of the antenna over some mark. These marks consist of pillars upon which the GNSS receiver is set (e.g., Fig. 6.5) or some marks on the ground, in which case a tripod has to be used (e.g., Fig. 6.6). In older GNSS equipment, the receivers and antennas were separate components but modern equipment such as Sokkia and Trimble incorporate both receivers and antennas in one unit.

Setting up the antenna over a mark should be done as accurately as possible in order to reduce centering errors. The receiver must be *leveled, aligned over each point,* and the *height of its geometrical center above the point recorded.* Antenna heights are normally measured to the phase center. Sometimes, this phase center does not coincide with the geometrical center of the antenna leading to antenna phase center variation (see Sect. 5.4.6). In high precision satellite measurements, this phase center



Fig. 6.5 Reference station, pillar 18 at Curtin University, Australia

variation can lead to errors in the range of millimeters to a centimeter. Most precise (geodetic) receivers possess antenna phase center models which can reduce this effect during the post-processing of the measurements. In relative positioning (Sect. 6.4.2), the error due to phase center variation can be eliminated through the matching of the antennas by aligning both to North.

The most common source of error during the setting up of the antenna is the incorrect measurement of the antenna height. Since GNSS provides three-dimensional positions (recall Sect. 5.3), any error in height determination will propagate to contaminate the lateral position, and vice versa. As a standard practice, comprehensive field notes should be kept, which should include the *station and surveyor's name, start and end times of the survey, type of receivers and antennae used, data file names, satellites used, details of reference marks, potential sources of errors and obstructions and most importantly, the antenna height.*

6.4.1 Single Point Positioning

Depending on the environmental monitoring task at hand, the single point positioning operation can take the form of *absolute point positioning*, also called autonomous positioning in some books, *relative positioning* or *differential positioning*. For absolute point positioning, pseudoranges have to be measured to the satellites whose positions must be known. The accuracy of the positioned point will therefore rely on how well these ranges are measured and how good the satellite positions are



Fig. 6.6 Setting up an antenna and measuring its height at Station John Walker (JW) at Curtin University, Australia

known. It should be pointed out that repeated measurements leading to redundant observations will generally improve range accuracy (US Army 2007).

If the task just requires a simple location of a station, e.g., the location of a *soil analysis pit*, with an accuracy of several meters, then a low-cost, hand-held GNSS receiver will suffice. These kinds of receivers (see, e.g., Fig. 4.1) use *code pseudoranges* and are the ones commonly used for personal navigation in cars, boats, low-accuracy GIS data capture, etc. Hand-held receivers provide absolute positioning to a horizontal accuracy of about 5–15 m (95 % of the time). Decimeter accuracy can be achieved by stationing a receiver over a station of interest and taking observations for 30–45 min. Future modernized GNSS satellites are expected to improve the positioning accuracy by an order of magnitude (see Fig. 6.7). This improvement will come as a result of improved satellite orbit determination, improved receiver technology, additional user signal L2C, which would assist in modelling ionospheric errors, and additional ground monitoring stations.

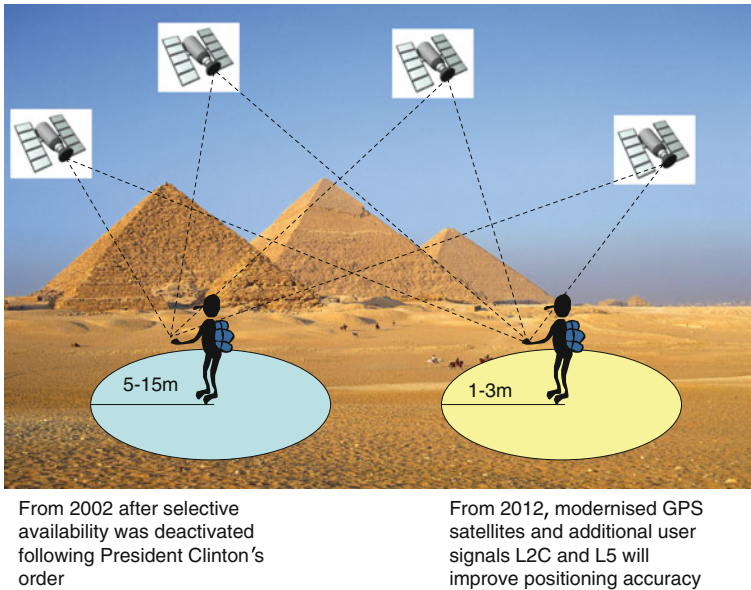


Fig. 6.7 Improved point positioning accuracy following modernization of GNSS satellites and receiver technology

6.4.2 Static Relative Positioning

Where a reference station (i.e., of known position) exists (e.g., Fig. 6.5), the static *relative positioning* method is recommended for higher positioning accuracy. In this mode of operation, *two GNSS receivers* or more are required in order to observe the same satellites simultaneously. Although additional cost is incurred in providing more equipment, the advantage over absolute point positioning is the capability of eliminating or minimizing errors associated with the atmosphere and satellite orbits (see Sect. 5.4) through differencing techniques (see e.g., Awange (2012)).

The method is more effective over short baselines of less than 20 km where the atmospheric errors are assumed to be the same. Using this method, one receiver will be set at a reference (control) station (Fig. 6.5) while the other receiver will be set at an unknown station (e.g., Fig. 6.6). Tracking of satellites must then be simultaneous and synchronized. The observation time would normally take 20 min to 1 h with data being sampled at intervals of 10–15 s. Longer durations of observation benefit from improved satellite geometry leading to better solution of the unknown integer ambiguities $\{N\}$. When the settings are properly done, and errors minimized through proper prior planning, the method is capable of giving coordinate differences (ΔX , ΔY , ΔZ) to a centimeter to millimeter level accuracy. The method is useful in the establishment of higher precision control networks (baseline reference networks) useful for environmental monitoring.

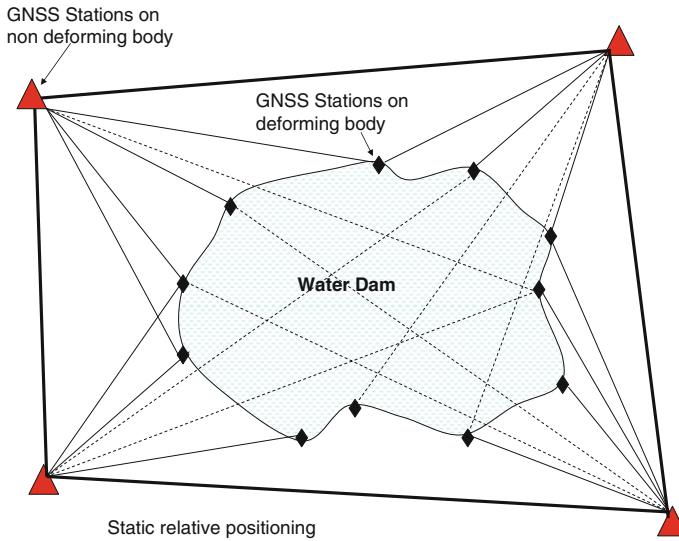


Fig. 6.8 Monitoring of deformation of a dam using static relative positioning. The *triangles* indicate control stations on the non-deforming surface. The *diamonds* indicate GNSS stations around the dam, which are being monitored for horizontal and vertical motion (shift)

The static relative positioning approach is potentially extremely useful for monitoring *environmental spatial variations*, e.g., deformation or land subsidence (e.g., Fig. 6.8). In this case, the control (reference) stations are set on a permanent non-deforming surface far from the deforming site being monitored, while the stations to be monitored are set on the deforming area. Relative positioning using *carrier phase* provides more accurate results to a few cm, depending on the accuracy of the control stations and on how the other errors are managed.

If the observations are undertaken for a longer period of say 1 h, depending on baseline lengths, the improved satellite geometry will enable the calculation of integer ambiguity and also reduce satellite geometry errors leading to more accurate results. Post-processing can also permit the use of *precise ephemeris* obtained within one to two weeks after the actual survey to give very accurate results. For example, the temporal monitoring (i.e., surveillance) of the position of a dam's wall will indicate any spatial changes such as horizontal or vertical shift which can be analyzed to see whether the dam is deforming and posing a potential danger. The static relative positioning method is further useful for densification of existing control networks, monitoring earthquakes through measuring plate movements in crustal dynamics (see Sect. 26.7) and oil rig monitoring (Schofield and Breach 2007, p. 339).

6.4.3 Real-Time GNSS (RTGNSS)

In Sect. 6.4.1, a decimeter accuracy for a stand alone receiver was said to be achievable by taking observations for 30–45 min using code observations. It was also pointed out that future modernized GNSS satellites are expected to improve positioning accuracy as a results of improved satellite orbit determination, receiver technology, additional user signal L2C which would assist in modelling ionospheric errors, and additional ground monitoring stations. Although higher accuracies can be realized through post-processing of data, i.e., as done for precise point positioning (e.g., El-Rabbany (2006, p. 68)), more and more users require these higher accuracies to be achieved in real-time. With such demands, receiver manufacturers are responding by coming up with receivers capable of delivering cm-level accuracy in real-time. More recently, position solution accuracy and speed have advanced to the point where centimeter-precision coordinates are available within seconds, and millimeter precision is available for daily solutions (Hammond et al. 2011).

An example is the NASA Global Differential GPS (GDGPS) System, which is fully operational since 2000. It is a complete, highly accurate, and extremely robust real-time GPS monitoring and augmentation system that uses a large ground network of real-time reference receivers, innovative network architecture, and award-winning real-time data processing software to give decimeter-level (10 cm) positioning accuracy and sub-nanosecond time transfer accuracy anywhere in the world, on the ground, in the air, and in space, independent of local infrastructure.² Another example is the hand-held Mobile Mapper 100 from Ashtech that combines internal high-grade antenna and processing capability to achieve cm-level accuracy.³ This hand-held receiver is suitable for monitoring changes in perimeters and areas of environmental features with spatial variability.

Besides the requirement of real-time GNSS data, other environmental applications such as earthquake monitoring would prefer that such data be delivered at a higher sampling rate (e.g., 1 Hz or higher), and at a low-latency (e.g., an order of seconds or less (e.g., Hammond et al. 2010)). Real-time data allow for real-time science and have a place in an increasingly real-time society. For example, today, it is possible for anyone to receive notification of hypocentral and moment tensor information for earthquakes, placed into geographic and tectonic context, within minutes of their occurrence (Hammond et al. 2010). Hammond et al. (2010) provide an illustration of the benefit of low-latency information as exemplified by people who live in the path of natural hazards and require information about catastrophic events to be delivered as quickly as possible. The ability to detect and characterize events rapidly can make all the difference in the critical minutes to hours that follow an event, as was the case in the catastrophic 2004 Sumatra and 11 March 2011 Tohoku-oki earthquakes and tsunamis where many lives were lost (Hammond et al. 2010, 2011).

² <http://www.gdgps.net/>

³ Mobile Mapper 100. White paper: A break through in hand-held accuracy.

6.4.4 Differential and Augmented GNSS

6.4.4.1 Differential GNSS (DGPS)

In this approach, the procedure is theoretically identical to post-processed static relative positioning using *code pseudoranges*, except that everything happens in real-time. The solutions using differential corrections (DGPS) and post-processed relative positioning using code data both give identical results. Due to the fact that the user obtains realtime results, in addition to the two receivers, a *real-time data link*, e.g., *radio or mobile* is required. The purpose of the data link is to transmit the “*range corrections*” from the reference station to the roving receiver for it to correct its own measured pseudoranges.

In general, a DGPS system will comprise of the *reference sites* whose coordinates are already well known to a higher accuracy, having been already surveyed using GPS carrier phase; a receiver measuring code or carrier phase pseudo-ranges, computing and transmitting the corrections; and a data link for transmitting the differential corrections using different radio frequencies. The reference station also monitors the integrity of the system and is often a permanent site with continuous power supply and automated equipment. There can be several reference sites whose coordinates are known in a DGPS system, of which there are two types:

1. The user’s own independent reference station, which essentially means the user has to purchase an additional receiver, thereby incurring additional costs;
2. Commercially owned reference stations, which charges users to access transmitted signals, e.g., Fugro in Australia.

Users of commercially owned DGPS only require one receiver, a data link and the cost of accessing the data. Japan’s GEONET (GPS Earth Observation Network System) is comprised of more than 1500 receivers dedicated to GNSS-meteorology. In Australia, the National Collaborative Research Infrastructure Strategy (NCRIS) is currently establishing a nation-wide geodetic continuous operating reference stations (CORS) network consisting of 126 stations. These commercially owned systems are discussed in detail in Sect. 6.5.

The *user’s station* is comprised of the receiver, with data link software to apply corrections to its uncorrected pseudoranges. Fax, telephones or mobile phones are also applicable in addition to radio as data links are range dependent, while other systems are line of sight dependent. Data link frequency bands vary depending on the baseline range while the data is transmitted from the reference to a roving station using a standard format called Radio Technical Commission for Maritime Services Special Committee 104 (RTCM SC-104 Format). With DGPS, the achievable accuracy using code pseudorange from a single frequency (L1) is in the range 3–5 m (US Army 2007).

This accuracy, however, is dependent on the closeness between the user’s (rover) and the reference stations. The separation distance should ideally be below 50 km in order to assume that the satellite signals at both the rover and the reference stations are affected by the same errors. Users also have to be aware of data latency (time-delay in the reception of the corrections by the rover, i.e., 0.25–2 s). When

carrier phases are used instead of code measurements, a real-time carrier phase differential GPS is achieved that provides positioning to a few centimeters accuracy (see Sect. 6.4.6).

6.4.4.2 Augmented GNSS

For applications that are more than 1000km from a reference station, the DGPS approach discussed above is limited, thus paving way to *Wide Area Differential GPS (WADGPS)*. WADGPS has a global or regional coverage of reference stations required to model *atmospheric* and *orbital errors* that suffices for long baselines, and are classified into *Ground Based Augmented Systems (GBAS)* and *Satellite Based Augmented Systems (SBAS)*. GBAS, which uses ground-based stations, are useful for real-time applications. For multiple reference stations, RTCM SC-104 pseudorange corrections are received onboard the roving receiver from n reference stations (up to approximately 400km). The pseudorange observations at the roving receiver are combined with each set of corrections to provide n independent solutions that are then combined in a conventional 3D adjustment to provide an additional estimate of the roving receiver's position. The accuracy of the roving receiver, similar to the DGPS case, will depend on its distance from the reference stations. For Government provided GBAS, the services are free to the users while subscription is required for privately delivered GBAS. Examples of GBAS are the Australian Maritime Safety Authority (AMSA) that has been operational since 2002 and offers maritime services to users, and the Nationwide Differential GPS (NDGPS) that is being expanded to cover all surface areas of the United States to meet the requirement of surface users.

SBAS send DGPS corrections to remote areas (e.g., areas out of reach of ordinary DGPS or GBAS such as oceans). Unlike a DGPS system where the data is transmitted via radio links, SBAS transmits data via geostationary communication satellites. These corrections are transmitted on a similar frequency to GPS satellites, thereby alleviating the need for additional software from the users. In Europe, the EGNOS geostationary satellites augment the GPS and GLONASS systems to provide wide area differential corrections. In US, the Federal Aviation Authority (FAA) developed the Wide Area Augmentation System (WAAS) to improve the accuracy, integrity and availability of GPS so that it can be a primary means of navigation for aircraft enroute and for non-precision approaches, thereby improving the real time civil accuracy of GPS to 7 m (Schofield and Breach 2007, p. 362). WAAS is also used in many other civil applications.

Examples of DGPS/WADGPS Companies include Fugro, who operates the Omnistar and Starfix systems, Racal who operates Landstar and Skyfix, and Western Geophysical who operate SARGAS. Other WADGPS systems are as discussed in Sect. 4.2.

6.4.5 Rapid Positioning Methods

Rapid GNSS positioning using carrier phase pseudorange includes techniques such as *rapid static or fast static surveys*, *stop-and-go surveys*, and *kinematic surveys*. Rapid or fast static survey are usually post-processed while stop-and-go and kinematic survey can be used in post-processing or in real-time modes of operation. Whereas for static surveying (see Sect. 6.4.2), ambiguity is resolved through long term averaging and a simple geometric calibration principal resulting in the solution of the linear equation that produces a resultant position, a variety of physical and mathematical techniques have been developed for rapid methods (US Army 2007). The physical methods include:

- Static occupation of a known point (e.g., previously positioned points, i.e., known baselines) for over 30 s.
- Static measurement at another known point on the baseline.
- Static occupation of an unknown baseline (e.g., fast-static occupation time).
- Static occupation of an unknown baseline and swapping of reference-rover receivers for 2–4 min (i.e., between known and unknown points).

A mathematical approach adopted by most GPS systems used today is the ambiguity resolution *on-the-fly* (while moving). This technique is common for most real time kinematic (RTK) applications. *Rapid-static* or *fast-static surveys* are essentially the same as static surveys but make use of shorter station occupation times. In this approach, one or more roving GPS receivers occupies all *unknown stations* while at least one receiver (reference station) is stationary at a known control station all the time (Fig. 6.9). The rapid nature of this type of survey compared to static surveys is due to the rapid solution of the integer ambiguities, making use of *all observable satellites*, *single or both dual-frequency L1/L2*, and *carrier phase data*. Although fast-static relative positioning is accurate and economical where there are many points to be surveyed and offers more efficient positioning than conventional static relative positioning, the accuracy is usually slightly lower at the centimeter level. It is, however, suitable for short baselines where systematic errors such as atmospheric and orbital factors are considered identical and can be differenced.

Due to the special processing algorithm used for solving the integer ambiguities, at least four satellites need to be tracked continuously. The technique is only effective over short (<10–20 km) baselines and the observation occupation time depends on the number and geometry of the satellites visible. Station occupation time vary between 2 and 10 min with a data sampling rate every 5 s, depending on the distance to the base as well as the satellite geometry, see e.g., El-Rabbany (2006, p. 74) and US Army (2007). Redundant observations to more than four satellites with good geometry help improve the solution of the ambiguities and reduce the time required to achieve a sufficiently accurate position. While moving from one station to another, the receiver can also be switched off to conserve power. For static and fast-static satellite surveying, the effect of high PDOPs because of poor geometry is less significant since the observation time is normally longer (2–60 min), thereby guaranteeing a better or improved satellite geometry.

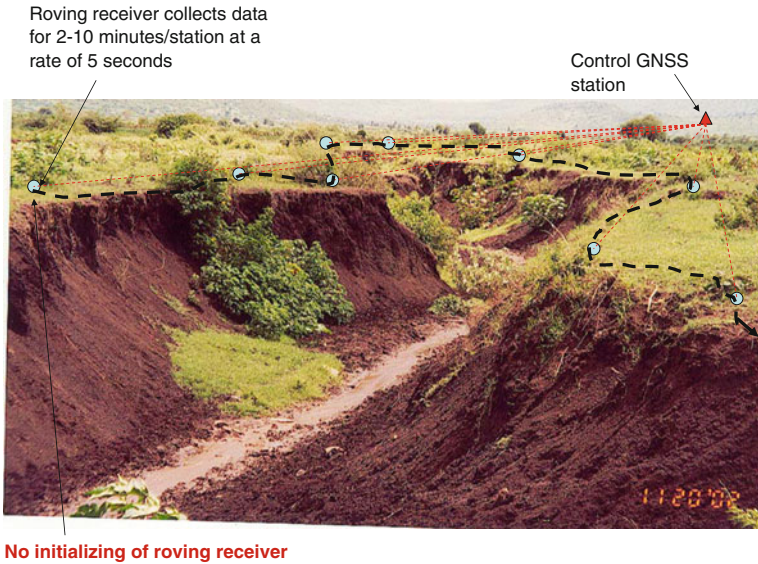


Fig. 6.9 Monitoring of the extent of erosion using fast static positioning. The *triangle* indicate the control station while the *circles* indicate the positions occupied by the roving receiver

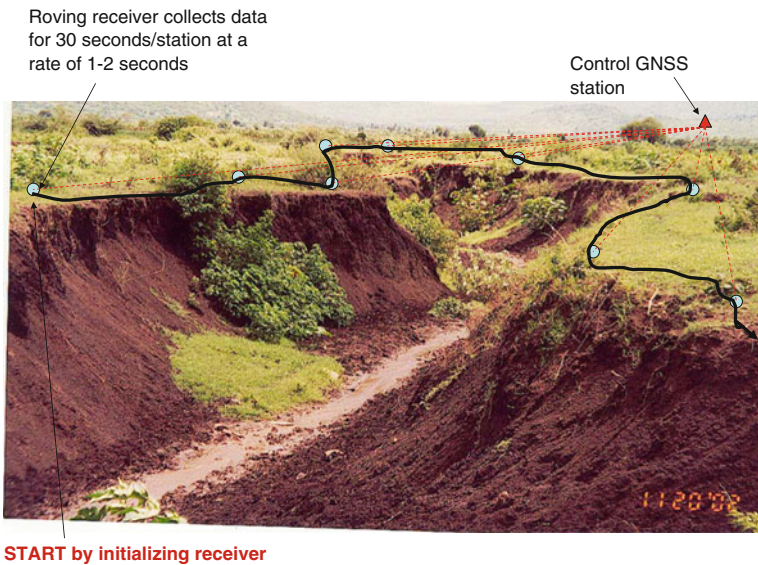


Fig. 6.10 Monitoring of the extent of erosion using the stop-and-go positioning method. The *triangle* indicate the control station while the *circles* indicate the positions occupied by the roving receiver. Initialization has to be done at the first station and a lock on four or more common satellites maintained

The *stop-and-go* method is a mixture of pure kinematic and static positioning. A series of points are positioned with respect to the reference receiver by moving the roving receiver sequentially to the points (see Fig. 6.10). To initialize the survey, the rover receiver has to remain static (e.g., at the first station to be positioned) for a certain time to allow for a solution of the integer ambiguities. The slightly longer period required for the initialization is to enable the satellite geometry to improve. Essentially, the initial static time is the same as that required for a fast-static survey. However, the initialization time can be greatly reduced by the occupation of a known station.

After initialization, the roving receiver is moved to the next station while continuously tracking the common (same) satellite signals. Initialization can also be achieved through reference-rover antenna swapping, by observing static data at another known point on the network, or by observing on a known baseline. At a given station, an observation time of only one or a few epochs (period of observations) is necessary to obtain a precise position as the integer ambiguities are already solved during the initialization phase. The rover typically collects data for a period of 30 s at a sampling rate of 1–2 s before moving to the next station (El-Rabbany 2006, p. 75). In this way, by moving the roving receiver, a series of stations can be coordinated sequentially. Similar to the fast-static survey, the stop-and-go survey technique requires at least four satellites to be continuously tracked. If lock to one of the minimum four satellites is lost, the roving antenna must be re-initialized by *returning the roving receiver to a previously surveyed point, or preferably to a known station.*

With the availability of fast ambiguity resolution techniques, the stop-and-go survey technique is best suited to coordinate a large number of stations (e.g., survey grid or precise mapping). However, there must be open sky in order to avoid frequent loss-of-lock of the satellite signal. It is essential for this technique that the satellites' signals can be continuously tracked throughout the survey. This method has an advantage over static positioning since it reduces observation time and is ideal for topographic surveys, such as the mapping of habitats, since it offers an accuracy of 2–3 cm for a baseline of 10–15 km (real-time or post-processed). The disadvantage of the method is the reliance on locked satellites (i.e., the satellites detected by the receiver) and having to re-initialize once loss of lock occurs.

Kinematic surveying operates with the same principle as the stop-and-go method, only that in this case, there is no stopping but the roving receiver is in continuous motion. Unlike fast static approach, the receiver is not switched off while in motion. In Fig. 6.11 the use of kinematic survey, particularly when a linear feature is being mapped is shown. The accuracy of kinematic surveys is, however, lower than that of stop-and-go, since some of the common errors encountered cancel with improved satellite geometry in stop-and-go.

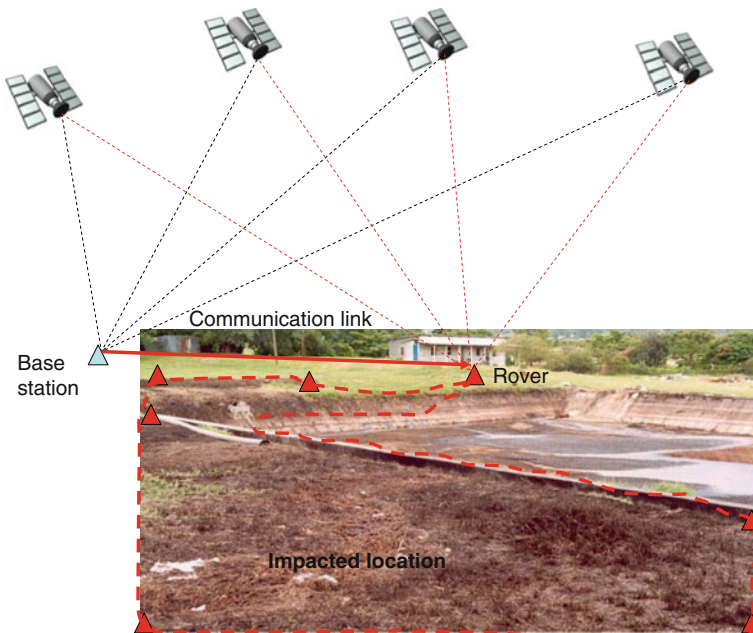


Fig. 6.11 RTK mapping of the boundary of an impacted location to monitor its spatial extent. The base receiver remains stationary and transmits raw data together with its position via the communication link to the roving receiver

6.4.6 Real-Time Kinematic (RTK)

As the name suggests, RTK is capable of delivering real-time positions in the field. Similar to the other rapid positioning techniques discussed above, RTK also requires more than two receivers, with one being placed at a known station (also called base station). Unlike the fast static and stop-and-go, it uses the DGPS principle discussed in Sect. 6.4.4. The base receiver remains stationary and has a transmitting radio link while the roving receiver is in motion and has a receiving radio link (see Fig. 6.11). The base receiver samples data every second and transmits these raw data together with its position via the communications link (e.g., satellites, mobiles or radio) to the roving receiver. Using its radio receiver, the rover receives the transmitted data from the base receiver and uses in-built software to combine and process the GNSS measurements obtained at both the base and roving receivers to obtain its position (El-Rabbany 2006, p. 78).

Some GPS manufacturers provide a hand-held controller that the surveyor can use to operate both the roving and the base receivers. Normally, the surveyor carries the roving receiver attached to the radio link in a back pack. The method requires the fixing of the integer ambiguities at the start of the survey (initialization) before undertaking the survey. Ambiguities can be initialized through the methods discussed

in Sect. 6.4.5. Once the initial ambiguity has been fixed, the roving receiver can be moved. Any loss-of-lock due to obstructions makes a re-initialization necessary.

Most kinematic survey algorithms use the ambiguity resolution on-the-fly as it allows integer resolution while the antenna is moving. With this approach, no initial *static initialization* is required. Once the integer ambiguities have been fixed, all previous measurements can be calculated back to obtain precise coordinates for all positions. This surveying technique, which requires dual frequency observations (L1/L2), makes it possible to perform certain precise environmental monitoring tasks in a kinematic mode, e.g., monitoring a proposed construction of linear features such as roads for the purpose of assisting environmental impact assessment. The integer ambiguity is fixed and preserved for at least four (preferably five) satellites during the motion of the roving receiver. The accuracy of this method is about 2–5 cm with a possibility of improvement if a longer period of station observation (i.e., 30 s) is adopted (El-Rabbany 2006, p. 78). Compared to the kinematic survey which allows post-processing (i.e., post processed kinematic, PPK), the accuracy of RTK is a bit lower. This is due to the time lag in the transmitted data reaching the rover, whereas post-processing enables the matching of data, correcting it for some errors and use of precise ephemeris.

In order not to confuse real-time DGPS and RTK, it should be remembered that DGPS uses code pseudorange corrections, improving the positioning accuracy from 15 to 5 m,⁴ while RTK uses raw carrier phases and codes. RTK facilitates the efficient establishment of a series of points in open areas, and even in areas of some overhead obstructions due to the advent of fast ambiguity resolution techniques. Unlike DGPS, the fundamental principle of RTK is that the carrier phase and code data from the reference station are transmitted to the roving receiver, which then uses the data from both the roving and reference receivers to form double difference observations and compute the position of the rover. Telemetry links form a critical component of RTK systems, over which the data from the reference receiver are transmitted to the rover. High baud rates and high radio frequencies are required, which limit the extent of the surveys. Reference (control) stations can normally be obtained from local surveying offices or the appropriate government agencies. The accuracies of the control points will contribute to the accuracies of the user's derived position, particularly when using relative, DGPS or RTK methods.

Network RTK: Since most RTK systems require the roving receiver to be within 10 km of the base station (assuming similar atmospheric conditions), use of multiple base stations, i.e., network RTK, provides an alternative for baselines more than 10 km long. Ambiguities must still be resolvable within seconds or instantaneously, up to baselines of 50–100 km in length, which requires the consideration of the orbital and atmospheric (tropospheric and ionospheric) errors. An approach currently receiving wide attention around the world uses the virtual reference station. In this approach, the roving receiver is located within the bounds of three or more reference stations and the observation errors modelled according to the approximate position of the

⁴ Some providers, such as FUGRO in Australia, have started using carrier phase pseudorange corrections to deliver sub-centimeter accuracy.

rover. Rizos (2001) identified some advantages of network RTK over single-baseline RTK as:

1. Rapid static and kinematic GPS techniques that could be used over baselines many tens of kilometers in length.
2. Instantaneous (i.e., single-epoch) on-the-fly ambiguity resolution algorithms could be used for GPS positioning, at the same time ensuring high accuracy, availability and reliability for critical applications.
3. Rapid static positioning is possible using lower-cost, single-frequency GPS receivers, even over baselines tens of kilometers in length.

6.5 Environmental Surveillance: CORS Monitoring

In Sect. 1.1, *surveillance* was introduced as the systematic observation of variables and processes with the aim of producing *time series*. Indeed, most environmental events require *continuous monitoring* in order to analyze time series maps. Such environmental processes are those that result in changes with time, such as *plate tectonic motions, land submergence* or *changes in sea levels*. As an example, let us consider a locality like Perth (Australia), which uses ground water for its domestic and industrial activities. In order to monitor the environmental impacts of groundwater extraction, i.e., whether there is some land submergence due to water extraction, continuous observation of locations of known heights can provide time series maps, which can be analyzed to assess any sinking of land.

Currently, GPS stations provide such capability in what is known as a Continuous Operating Reference Station (CORS). CORS data support high-accuracy three-dimensional positioning activities useful in environmental monitoring of spatial motions in time. Its data are also used by geophysicists, meteorologists, atmospheric and ionospheric scientists and others, in support of a wide variety of applications (Snay and Soler 2008). For example, Maryam et al. (2009), Motagh et al. (2007), Anderssohn et al. (2008) undertook surveillance monitoring of land subsidence in northeast Iran using both GPS and InSAR⁵ (discussed in Sect. 9.5) and obtained a 19 cm/year subsidence using both methods (see Sect. 26.10 for more details).

A CORS station is a stationary GNSS receiver, which is continually collecting data from visible GNSS satellites on a 24 h basis in order to produce its three-dimensional coordinates (e.g., Fig. 6.12). CORS networks vary in size ranging from regional, national to global scales (e.g., the International Global Navigation Satellite System Service (IGS)). Each individual CORS station is positioned to a very high degree of accuracy using precise GNSS, satellite laser ranging (SLR), and very long baseline interferometry (VLBI) discussed in Sect. 3.4, thereby enabling them to be used as reference stations to position other points, besides continuously providing their own positions. Individual users can also benefit from CORS networks by acquiring data from the CORS stations within their vicinity to achieve more accurate results (see

⁵ interferometric synthetic aperture radar.



Fig. 6.12 A GEONET GNSS-based CORS station in Japan. *Source* Geospatial Information Authority of Japan

Sect. 6.4.4). Perhaps of importance to environmentalists is the question posed by Rizos (2001):

What if, instead of broadcasting RTK corrections and placing the onus of obtaining a final solution on users and their equipment, users' coordinates are determined by a service provider?

This is the client-server approach envisaged by Rizos (2001) who then states:

Final (position) solutions for all real-time (logged) users could be simply computed as a by-product of the continuous network processes, all the time satisfying the quality and integrity criteria implemented at the network administrator level. Note that improved accuracy and reliability of the user coordinates can be expected if GPS data is processed in the network mode, rather than as individual baselines as is the case for standard RTK-type techniques. In addition, precise ultra-rapid IGS ephemerides can be used in the network computations instead of the broadcast ephemeris.

The feasibility of Rizo's proposed model would enormously benefit environmentalists who would then have to only send their data to a central processing unit and receive their final products in the form of their receiver positions. Such a mode

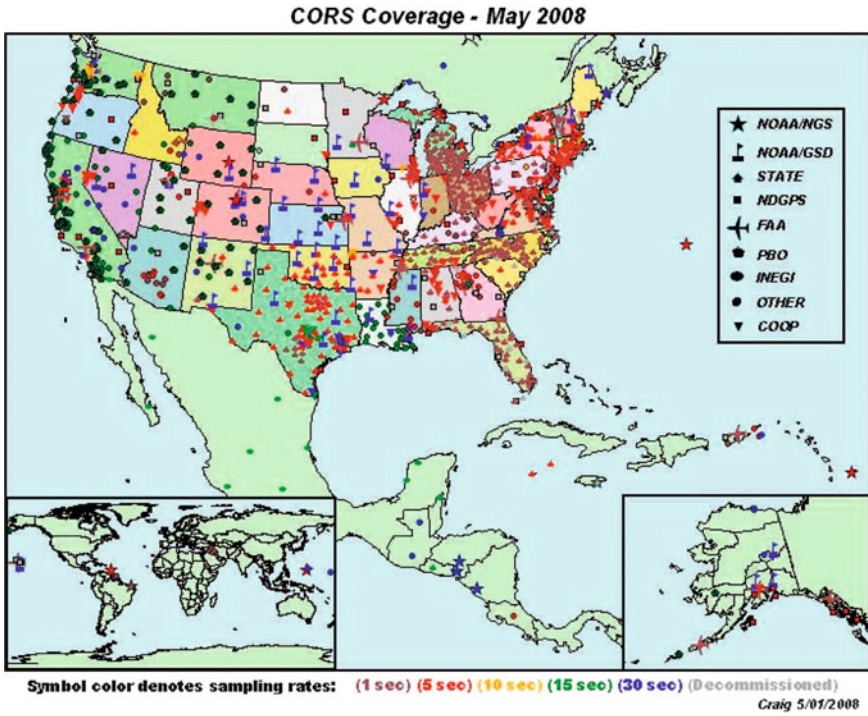


Fig. 6.13 NSRS CORS stations in May 2008. *Source* Snay and Soler (2008)

of GNSS operations already exist. In Australia for example, AUSPOS (Australian online GPS processing service) enables users to send their data to a central processing unit at Geoscience Australia via the Internet (AUSPOS 2006). The processing software thereafter, chooses three CORS stations that are near the user’s observing station and employs them to process the user’s position (Fig. 6.13). The results are then send back to the user via email. In the US, the OPUS (Online Positioning User Service) has performed similar functions as AUSPOS since March 2001 (National Geodetic 2006).

Other examples of CORS-type networks include the Japanese GEONET (e.g., Fig. 6.14), Germany’s Satellite Positioning Service (SAPOS), and the US’s National Spatial Reference System (NSRS, Fig. 6.13), which comprised a network of over 1,350 sites in 2008 and is growing at a rate of about 15 sites per month (Snay and Soler 2008). Snay and Soler (2008) summarize the history, applications, and future prospects of the NSRS CORS network by describing the more important contributions of the CORS system to the scientific community. Some of the uses of CORS documented e.g., by Snay and Soler (2008), which may be of benefit to environmental monitoring tasks include;

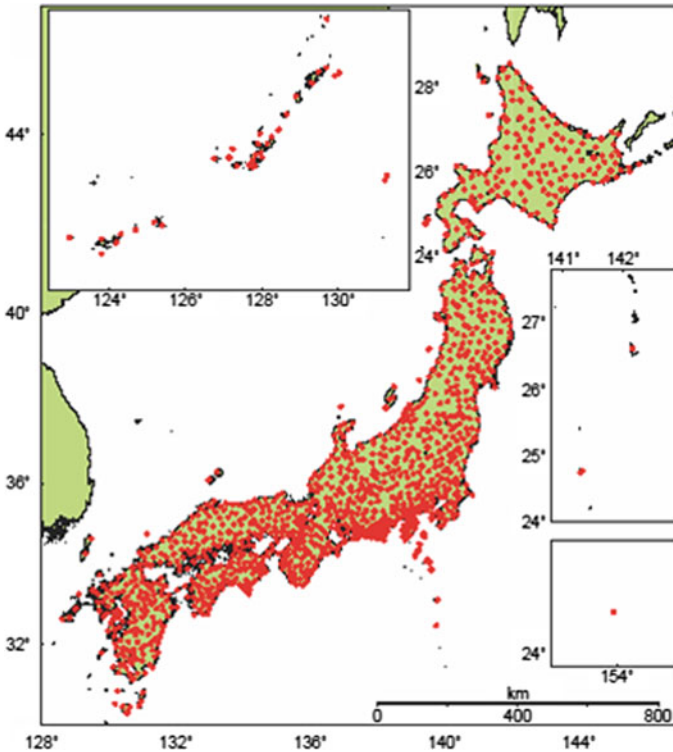


Fig. 6.14 GEONET CORS stations. GEONET data are used in various disaster related meetings and geophysical model estimation of crustal activities and thus are reflected in the decision making process to cope with the disaster as well as the scientific researches. *Source* Matsuzaka (2006)

- Upgrading national geodetic reference systems (e.g., Sect. 6.6). Snay and Soler (2008) report on the upgrading of the US based national geodetic system with the help of CORS coordinates that were held fixed in the adjustment process.
- Assessing GNSS observational accuracies. With a well-established network of CORS stations, it is possible to design experiments that are aimed at improving GNSS positioning methodologies within a relative positioning framework, e.g., Snay and Soler (2008).
- Multipath studies. In this regard, the CORS network could be used for instance to investigate further possibilities of minimizing positioning errors resulting from multipath (discussed in Sect. 5.4.4). Snay and Soler (2008) report on how CORS stations were used to evaluate the amount of multipath occurring at each of the more than 390 sites, where the most and least affected sites were identified in the network, different receiver/antenna combinations compared, and those sites that appeared to be severely affected by multipath more closely investigated.
- Crustal motion monitoring. This could be the most visible environmental monitoring application of CORS stations where the horizontal and vertical motion of the

Earth's surface is monitored to mitigate, e.g., the impacts of earthquakes, tsunamis and other disasters resulting from plate motions, as we will see in Chap. 26. For this, many CORS stations provide velocities that are useful in indicating plate motions and time information.

- Sea level change monitoring. The variations of vertical crustal velocities at CORS sites near tide gauge stations may be used to determine the “absolute” sea level change with respect to the International Terrestrial Reference Frame (ITRF). This type of analysis was impossible to conduct before the proliferation of CORS in coastal areas (Snay and Soler 2008). This application is discussed further in Sect. 26.8.3.
- Atmospheric monitoring. CORS are currently contributing to the new field of GNSS-meteorology (see Sect. 20.2.1). Besides their application to GNSS-meteorology, CORS station could be useful in ionospheric studies as discussed by Snay and Soler (2008).
- Support of remote sensing applications. CORS stations have been used to support remote sensing applications such as the accurate positioning of aircraft employed in aerial mapping in order to improve the reliability of photogrammetric restitution, especially for large-scale aerial surveys over remote or inaccessible terrain. It may then be implemented for geolocating landmarks from the air with digital cameras, as well as being applied to a broad range of mapping technologies, such as scanning radar, light detection and ranging (LiDAR), inertial systems, interferometric synthetic aperture radar, and/or sonar (Snay and Soler 2008). These remote sensing techniques are discussed in detail in part III of this book.

To date, Japan's distribution of CORS stations is the most numerous and densest in the world. This network, known as *GEONET* (Fig. 6.14), is used mainly for geodynamic/geophysical monitoring around Japan where four tectonic plates are interacting with each other, i.e., the monitoring of earthquakes and volcanic hazards (Matsuzaka 2006).

Matsuzaka (2006) points to the fact that 1200 GEONET CORS stations with an average spacing of 20–30 km between stations are operational in order to realize the system's desired use. This network has been operational since 1994 under the control of the Geospatial Information Authority of Japan (GSI), providing precise daily coordinates of all stations, with which displacement and strain rates are calculated nationwide, thereby revealing the various characteristics of tectonic deformation in the Japanese islands (Sagiya 2005). Japan has also undertaken several measures to improve the quality of data collected, including creating a double cylindrical structure of observation pillar to reduce thermal effects, unification of antenna types to reduce multipath and a better analysis strategy to obtain more reliable and accurate solutions (Matsuzaka 2006). A typical GEONET station consists of a 5 m pillar, chokering antenna, 24 h observations, 1 Hz sampling rate and real-time data transfer (see, e.g., Fig. 6.12). These attributes enable Japan to measure *tectonic plate movements* and “slips” occurring along fault lines to a high degree of accuracy (post-processed ± 2 mm) (Matsuzaka 2006).

SAPOS comprises a network of more than 250 CORS stations⁶ run by the German State Survey for the purpose of supporting cadastral surveying, engineering surveying, private industry sector applications (e.g., transport fleet management), emergency guidance systems (e.g., police, fire and radio) and deformation measurements (SAPOS 2009). The average spacing between the stations is 50 km. Various quality control measures carried out allow a precision of the order of 1 cm–5 m in real-time positioning, see e.g., Wolfgang (2005).

The US presents two scenarios of CORS made up of 1450 stations (as of May 2010): the National CORS system made up of over 988 stations and run by the National Geodetic Survey (NGS), and a collaborative network comprising more than 200 organizations.⁷ CORS GPS observational data are freely provided to the user community via the Internet and are capable of supporting high-accuracy positioning requirements. In addition to enhancing geospatial positioning, applications using CORS data include the following (Stone 2006);

- a critical role in defining the nation’s geodetic reference system,
- *the ability to characterize the free electron content of the ionosphere*, and
- *an important source of precipitable water vapour input to meteorological forecasts.*

The last two are environmental monitoring related tasks.

CORS Networks in Australia are at the development stage. Australia-wide, there are several CORS networks in place. The Australian Fiducial Network (AFN) consists of 8 CORS stations, which together with a further 8 CORS stations, both on the Australian continent and offshore, form the Australian Regional GPS Network (ARGN) (Geoscience Australia 2009). The network has reached a global accuracy of a few centimeters, which is sufficient for the designed purpose. Besides this, several Australian states and cities have begun installing their own CORS networks, e.g., Victoria’s VICPOS. Some of the CORS stations in VICPOS are also incorporated in MELBPOS, a CORS network specifically for Melbourne. Sydney also has a specific CORS network named SYDNET.

Densification of the Australian CORS network is currently ongoing, as indicated in Fig. 6.15 that shows the proposed Australian CORS network, which is designed to cater for the needs of most of the populated areas of the country. This network would allow a maximum baseline length of 200 km spatial coverage. To be able to position with the online based AUSPOS, the number of stations that a user can access within the proposed baseline length of 200 km are illustrated in Fig. 6.16.

6.6 Coordinate Reference System

The preceding sections have dwelt with the measurement techniques and variables used with GNSS. What has not been discussed at length is that these measurements have to refer to some coordinate system. From a social perspective, human beings

⁶ http://www.sapos.de/pdf/Flyer/2004Flyer_e.pdf

⁷ <http://www.ngs.noaa.gov/CORS/>

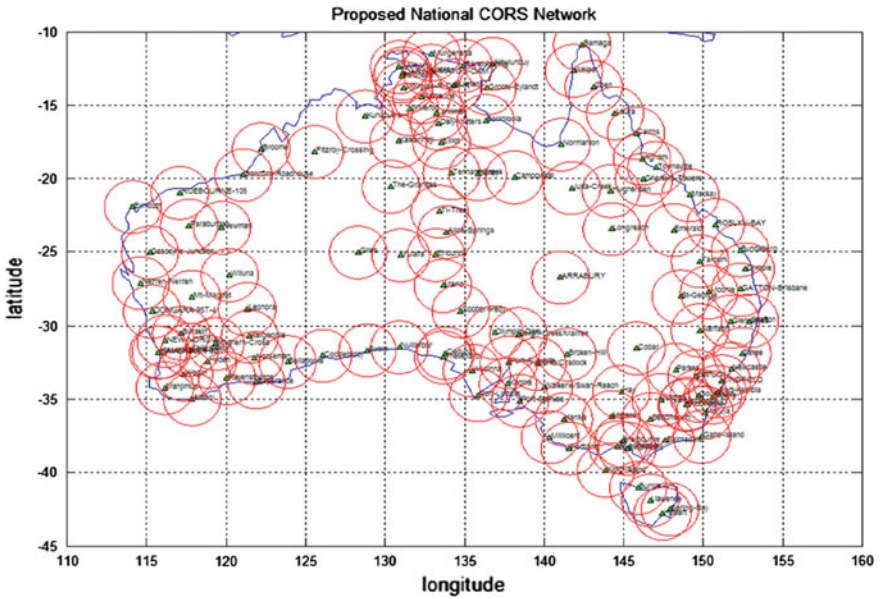


Fig. 6.15 Coverage by the proposed Australian national CORS network (baseline length 200 km). Source Wallace (2007)

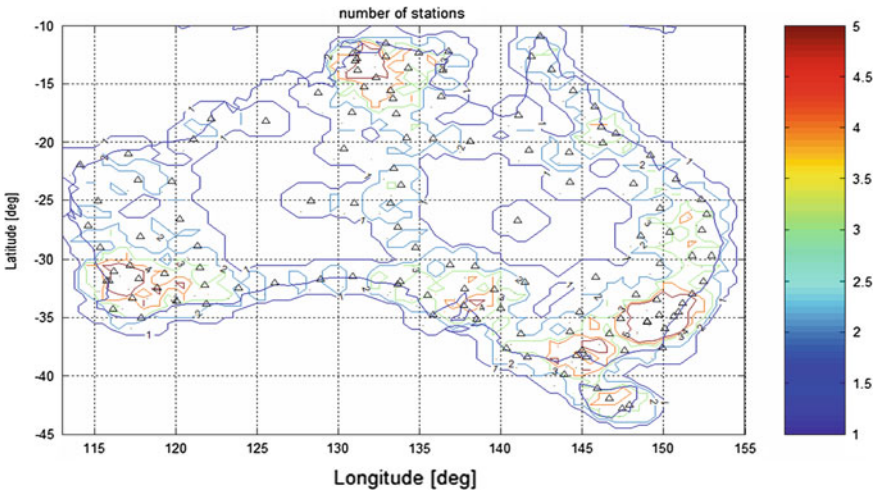
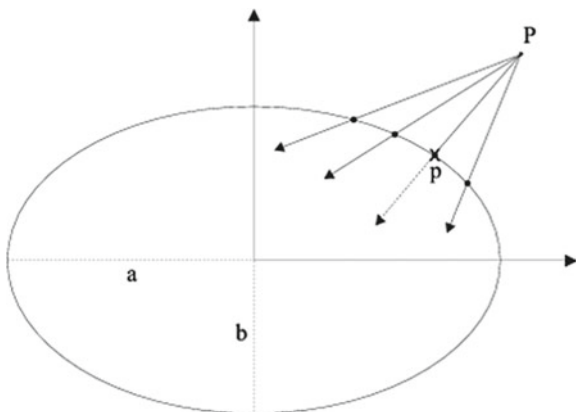


Fig. 6.16 Station overlap for 200km baseline. Source Wallace (2007)

have names that identify them, as do places and biological species. When we talk of GNSS providing locations, how therefore do we refer to them? The answer lies in the concept of a Coordinate Reference System, which is comprised of a *datum*, *coordinate system* and *map projection*.

Fig. 6.17 Reference ellipsoid: Point P on the Earth's topographic surface and its corresponding point p on the *Reference ellipsoid of revolution* with semi-major axis a and semi-minor axis b



6.6.1 Datum

A datum, a *mathematical figure* (ellipsoid) that enables measurements and computations to be undertaken on the surface of the Earth, is defined by its size, shape, location and orientation, and its relation to the geoid by means of geoid undulation and deflection of the vertical (Leick 2004, p. 29). This is necessitated by the fact that the topographical surface of the Earth is irregular and unfit to be used for computations. For simple tasks, a sphere is normally used to approximate the Earth. In more precise work, such as GNSS measurements and computations, an *ellipsoid of revolutions* (e.g., Fig. 6.17) is normally used. An ellipsoid of revolution is simply a bi-axial ellipsoid defined by the axes $\{a, b\}$ rotated around the minor axes $\{b\}$. Besides these axes, the ellipsoid has to have an origin.

For the case where this origin coincides with the center of mass of the Earth, it is called a geocentric ellipsoid. The ellipsoid thus becomes a reference surface for horizontal positioning. A well-positioned reference ellipsoid has two axes defining the dimensions of the ellipsoid, three parameters defining its origin, and three parameters defining the orientation in space. All together, these form a *geodetic datum* (El-Rabbany 2006, p. 48) or simply a *reference ellipsoid*. A geodetic datum as defined above will therefore give the horizontal position (two-dimensional) of any location on Earth.

Some environmental monitoring tasks, such as land subsidence, changes in sea level, or the amount of siltation in a lake, require information on heights with respect to some reference. This reference is often known as the *vertical datum*. Its definition uses the sea level. If sea level in a coastal area is measured by tide gauges and averaged over a period of time (i.e., years), a *mean sea level* MSL is obtained. Now, let us project this MSL through the Earth such that it passes through the continents (e.g., Fig. 6.18), as if there were canals all the way through the continents. The obtained surface is called a *geoid*, and is defined as an equipotential surface approximating mean sea level, and is the *vertical datum*. Height measurements in local systems

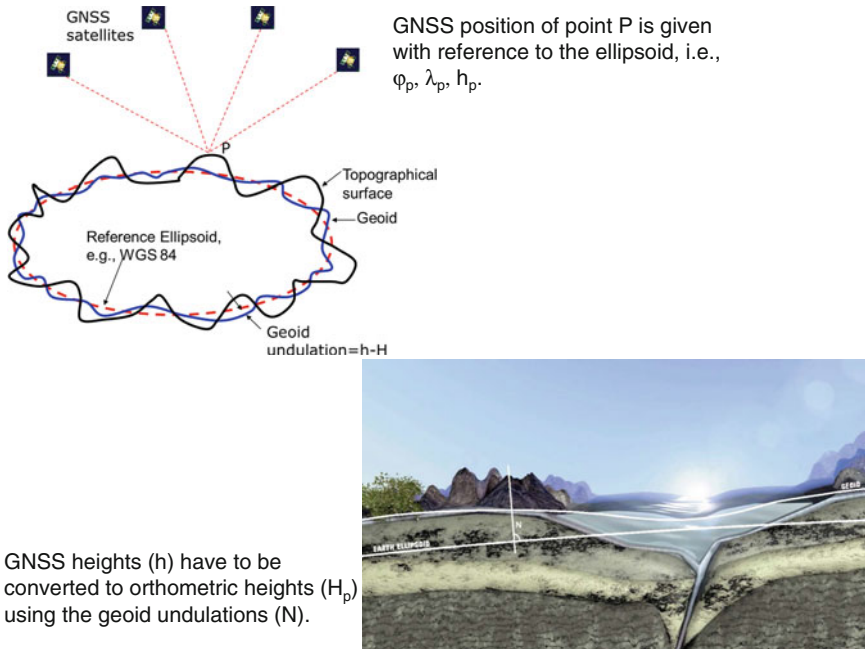


Fig. 6.18 Vertical datum—the geoid

are normally measured with respect to this datum or simply the MSL, hence it is common to give readings above MSL.

Unlike the traditionally used heights (orthometric heights), which are normally referred to MSL as a reference, GNSS heights are normally measured with respect to the reference ellipsoid. The shape of the geoid is complex, determined by the Earth’s gravity field. Therefore, when using GNSS for vertical positioning, knowledge of the geoid-ellipsoid separation (i.e., (N) in Fig. 6.18), is highly desirable, if not essential. For surveys over small areas (e.g., up to 10km), it is often acceptable to use an approximation to the geoid. This method makes use of the fact that the geoid height does not vary that much over these distances.

In traditional surveying methods, the horizontal positions and vertical positions are determined separately. With GNSS positioning, however, both the vertical and horizontal positions are obtained from the same set of measurements. For instance, the position of point P in Fig. 6.18 would be given by GNSS as $\{\phi, \lambda, h\}$. The height h is, however, measured with respect to the reference ellipsoid. Of interest is the height with respect to the geoid, i.e., H . In this case, we have to subtract the geoid undulation N from the measured ellipsoidal GNSS height h to obtain the physical height H above the MSL (geoid).

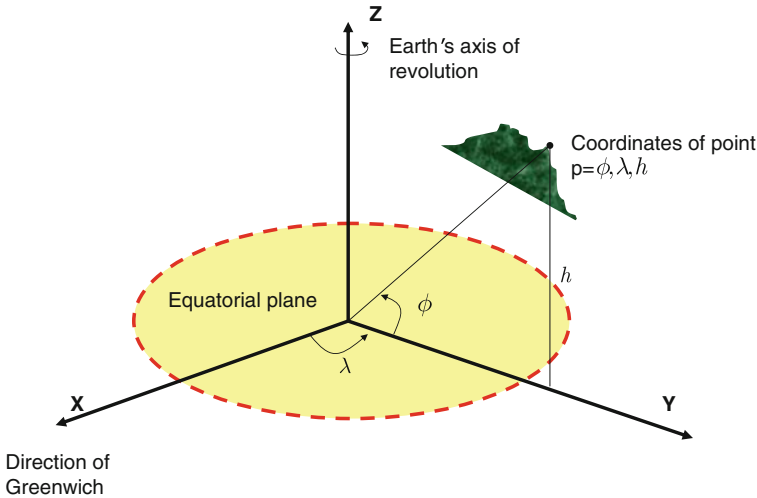


Fig. 6.19 A coordinate system

6.6.2 Coordinate Systems and Transformations

A *coordinate system* is a set of rules that state the correspondence between coordinates and points; a *coordinate* is one of the set of the N numbers individuating the location of a point in an N -dimensional space. A coordinate system is defined once a point of known *origin*, a set of N lines, known as *axes*, all passing through the origin and having a well-known relationship to each other, and a *unit length* are established (Prasad and Ruggieri 2005, p. 17). A coordinate system is thus a set of rules that specify the locations (also called the coordinates of points), see e.g., Fig. 6.19 (El-Rabbany 2006, p. 49). Coordinate systems are normally:

- One-dimension (e.g., the 1D heights or sea level tide gauge readings); two-dimensions (e.g., the 2D position of points in Easting and Northing); or three-dimensions (e.g., the 3D position of points in latitude ϕ , longitude λ , and height h). GNSS positioning will always give 3D coordinates of points either in geographical form (ϕ, λ, h) or Cartesian form (X, Y, Z) . Transformation between geographical and Cartesian are documented, e.g., in Awange and Grafarend (2005), Awange et al. (2010).
- Refer to reference surfaces. Many countries have their own local reference surfaces (i.e., their own origins and axes parameters). For GNSS positioning, the reference surface is always an ellipsoid of revolution (see, definition of datum in Sect. 6.6.1).

A *reference system* is the conceptual idea of a particular coordinate system, whereas a *reference frame* is the practical realization of a reference system through observations and measurements (affected by errors), which means that a reference frame is a list of coordinates and velocities of stations (related to tectonic plate motion) placed in the area of interest, together with the estimated level of errors in

those values (Prasad and Ruggieri 2005, p.18). An example of a 3D geocentric coordinate system is the *Conventional Terrestrial Reference System (CTRS)* whose origin coincides with the center of the Earth. The z -axis points towards the conventional terrestrial reference pole (i.e., mean of the pole during the period 1900–1905), the x -axis points in the direction of the Greenwich meridian and the y -axis is perpendicular to the $x - z$ -plane, thus completing a right-handed system (Fig. 6.19). To be of use, the CTRS must be positioned with respect to the Earth, a task often undertaken by assigning coordinates to selected points (stations) on the Earth’s surface. The assignment of coordinates, i.e., realization, is often achieved using accurate geodetic techniques such as GNSS, VLBI and SLR (e.g., Sect. 3.4).

The *International Terrestrial Reference System (ITRF)* is one of the CTRS commonly used and is realized through GPS and other geodetic measurements of globally distributed stations. It is maintained by the IERS (International Earth Rotation Service) under the auspices of the IAG (International Association of Geodesy) and is updated every 1–3 years to achieve the highest level of accuracy and, often refers to the particular time of updating, e.g., ITRF2005 as per 2005. This therefore means that ITRFs are dynamic in nature with the coordinates changing due to plate tectonic motions. They are only valid for a specific period (epoch) and incorporate velocity information to update other epochs.

The *World Geodetic System (WGS-84)* established in 1984 is a 3D system that is used in GPS positioning in an Earth-Centered Earth-fixed (ECEF) reference frame. It is defined as (Prasad and Ruggieri 2005, p. 22):

- Its origin is at the center of mass, the Z axis points towards the direction of the International Earth Rotation Service (IERS) reference pole (IRP), which corresponds to the direction of the BIH (Bureau International de l’Heure) Conventional Terrestrial Pole (CTP) at the epoch 1984.0 with uncertainty of 0.005.
- The X axis is defined by the intersection of the IERS reference meridian and the plane passing through the origin and normal to the Z axis.
- The Y axis completes a right-handed, ECEF orthogonal coordinate system.

The satellite positions sent via the navigation message discussed in Subsect. 5.3.1, i.e., the broadcast ephemeris, are with respect to the WGS-84 system. Any user whose position values used broadcast ephemeris will thus obtain the receiver’s position in the WGS-84 system (El-Rabbany 2006, p. 52). The WGS-84 system was originally established using a number of Doppler stations and has since been updated to bring it to ITRF as close as possible (El-Rabbany 2006, p. 49). This has since seen the WGS-84 system evolve to being dynamic. If users work with the precise ephemeris obtained from the IGS (International GNSS Service), see e.g., IGS (2009), then their coordinates will be in the ITRF reference system.

Datum transformations are the conversion of coordinates from one form to another, i.e., WGS-84 to local systems. This is necessitated by the fact that old maps in most countries were done in local systems (e.g., separate horizontal and vertical datums). Normally, there exists transformation parameters that are used for these transformations, see e.g., Awange and Grafarend (2005). Most GNSS processing software have in-built transformation algorithms that undertakes this task.

Coordinate transformation is commonly used in photogrammetry, remote sensing and GIS and is adequately addressed in many textbooks, see e.g., Murai (1999), Moffit and Mikhail (1980), Wolf (1980), Luhmann et al. (2011), Schenk (2005) etc. Different types of coordinate transformations can be discriminated. For example, this may entail transformation from one two-dimensional coordinate system (x, y) to another two-dimensional coordinate system (u, v). It may also involve transformation from a two-dimensional coordinate system (x, y) to a three-dimensional coordinate system (X, Y, Z), or even transformation from one three-dimensional coordinate system (X, Y, Z) to another three-dimensional coordinate system (X', Y', Z'). Generally speaking, coordinate transformations are required to among other things:

- (a) Transform different map projections (see Sect. 6.6.3) employed in diverse GIS data sources to a unified map projection in a GIS database;
- (b) Correct and adjust for various systematic errors which occur during map digitization as a result of shrinkage or distortion of the map measured (see Sect. 10.3.1);
- (c) Transform generated stereomodels from an arbitrary coordinate system to an integrated photogrammetric coordinate system during aerial triangulation (see Sect. 11.3.3); and
- (d) Produce geo-coded image through geometric correction of remote sensing imagery (see Sect. 10.3.1).

Basically, coordinate transformation is accomplished through the selection and use of an appropriate transformation model (or mathematical equation), with a set of reference or control points. The control points are selected as *tic marks*, *reséau* or *ground control points*. Furthermore, the number and spatial distribution of the control points is important and is determined by the type of coordinate transformation being undertaken and the desired level of accuracy.

6.6.3 Map Projection

Finally, once the datum (ellipsoid of revolution) and the coordinate system for referencing the locations have been chosen, an appropriate mathematical method of transferring locations from the idealized Earth model to the chosen planar coordinate system must be chosen, a procedure known as *map projection*. Map projections are thus the representation of objects and information on a curved surface in a plane using mathematical and geometric relations (see Fig. 6.20).

6.7 Concluding Remarks

This chapter has presented some of the GNSS field techniques that are essential for measuring key indicators in environmental monitoring. Essentially, kinematic GNSS surveying refers to taking measurements while the receivers are ‘on the move’ and

- Post-processing in PPK enables the use of precise ephemeris from the IGS and the possibility of removing cycle slip errors, thereby giving more accurate results compared to RTK, which uses broadcast ephemeris.
- Advantages of real-time GNSS for environmental monitoring include rapid and efficient data collection that provide results in real-time.

In summary, real-time satellite positioning can be achieved at three levels of accuracy for navigation.

1. Low-accuracy, real-time positions are given by any stand-alone receiver.
2. DGPS uses telemetry of C/A-code pseudorange corrections to give improved $\sim 2\text{--}5$ m positioning and ~ 0.1 m/s velocity accuracies of the roving receiver. This is of use in applications such as airborne magnetic surveying or remote sensing. Real-time DGPS is robust due to its use of the unambiguous codes, which are not as susceptible to loss of satellite lock as the carrier phases.
3. The highest accuracy real-time requirements, ~ 10 cm positioning and ~ 0.01 m/s velocity are offered by real-time pure kinematic relative GPS. Its applications include accurate marine and airborne navigation and precise hydrographic surveying. On land, detailed survey grids can be established in the field to better than 5 cm. This is an example of RTK, where the real-time capability requires only one visit to the field.
4. Kinematic surveys (Sect. 6.4.6) using carrier phases can position the roving receiver with respect to the stationary reference receiver to better than 10 cm.
5. GPS positioning accuracy depending on position mode and measurement types used are listed below:
 - Kinematic point positioning (code) $\sim 15\text{--}20$ m.
 - Static (autonomous) point positioning (code) 5–15 m. Expected to be 3–5 m with current modernization.
 - Kinematic relative positioning (DGPS) 3–5 m.
 - Kinematic relative positioning (carrier phase) < 10 cm.
 - Static relative positioning (code) 0.5–1 m.
 - Static relative positioning (carrier phase) mm-cm level.
 - RTK surveying < 10 cm.

References

- Anderssohn J, Wetzel H, Walter TR, Motagh M, Djamour Y, Kaufmann H (2008) Land subsidence pattern controlled by old alpine basement faults in the Kashmar Valley, northeast Iran: results from InSAR and levelling. *Geophys J Int* 174:287–294. doi:10.1111/j.1365-246X.2008.03805.x
- AUSPOS (2006) Australian online GPS processing service. <http://www.ga.gov.au/bin/gps.pl>. Accessed 14 May 2009
- Awange JL (2012) Environmental monitoring using GNSS, global navigation satellite system. Springer, Berlin
- Awange JL, Grafarend EW (2005) Solving algebraic computational problems in geodesy and geoinformatics. Springer, Berlin

- Awange JL, Grafarend EW, Paláncz B, Zaletnyik P (2010) Algebraic geodesy and geoinformatics, 2nd edn. Springer, Berlin
- El-Rabbany A (2006) Introduction to GPS global positioning system, 2nd edn. Artech House, New York
- Geoscience Australia (2009) Australian Regional GPS Network. <http://www.ga.gov.au/geodesy/argn/>. Accessed 16 May 2009
- Goncalves RM (2010) Short-term trend modeling of the shoreline through geodetic data using linear regression, robust estimation and artificial neural networks. Ph.D. Thesis, Geodetic Sciences Post-graduate Program, Federal University of Parana (UFPR), Curitiba, Brazil, 152 pp
- Goncalves RM, Awange JL, Krueger CP, Heck B, Coelho LS (2012) A comparison between three short-term shoreline prediction models. *Ocean Coast Manag* 69:102–110. doi:[org/10.1016/j.ocecoaman.2012.07.024](https://doi.org/10.1016/j.ocecoaman.2012.07.024)
- Hammond WC, Brooks BA, Bürgmann R, Heaton T, Jackson M, Lowry AR, Anandakrishnan S (2011) Scientific value of real-time global positioning system data. *Eos* 92(15):125–126. doi:[10.1029/2011EO150001](https://doi.org/10.1029/2011EO150001)
- Hammond WC, Brooks BA, Bürgmann R, Heaton T, Jackson M, Lowry AR, Anandakrishnan S (2010) The scientific value of high-rate, low-latency GPS data, a white paper
- Hofman-Wellenhof B, Lichtenegger H, Wasle E (2008) GNSS global navigation satellite system: GPS, GLONASS; Galileo and more. Springer, Wien
- IGS (2009) International GNSS service. <http://igsceb.jpl.nasa.gov/>. Accessed 16 May 2009
- Leick A (2004) GPS satellite surveying, 3rd edn. Wiley, New York
- Luhmann T, Robson S, Kyle S, Harley I (2011) Close range photogrammetry: principles, techniques and applications. Whittles Publishing, Scotland
- Maryam D, Zoj V, Javad M, Iman E, Ali M, Sassan S (2009) InSAR monitoring of progressive land subsidence in Neyshabour, northeast Iran. *Geophys J Int* 178:47–56. doi:[10.1111/j.1365-246X.2009.04135.x](https://doi.org/10.1111/j.1365-246X.2009.04135.x)
- Matsuzaka S (2006) GPS network experience in Japan and its usefulness. Seventeenth United Nations regional cartographic conference, Geographical Survey Institute, Bangkok
- Moffitt FH, Mikhail E (1980) Photogrammetry, 3rd edn. Harper and Row Publishers, New York
- Motagh M, Djamour Y, Walter TR, Wetze H, Zschau J, Arabi S (2007) Land subsidence in Mashhad Valley, northeast Iran: results from InSAR, levelling and GPS. *Geophys J Int* 168:518–526. doi:[10.1111/j.1365-246X.2006.03246.x](https://doi.org/10.1111/j.1365-246X.2006.03246.x)
- Murai S (1999) GIS work book: fundamental and technical courses, volumes 1 and 2, National Space Development Agency of Japan (NASDA)/Remote Sensing Technology Center of Japan (RESTEC), Japan Association of surveyors
- National Geodetic Survey (2006) Guidelines for new and existing continuously operating reference stations (CORS). NOAA, Silver Spring
- Prasad R, Ruggieri M (2005) Applied satellite navigation using GPS, Galileo and augmentation systems. Artech House, Boston
- Rizos C (2001) Alternatives to current GPS-RTK services and some implications for CORS infrastructure and operations. *GPS Solutions* 11(3):151–158
- Sagiya T (2005) A decade of GEONET: 1994–2003 The continuous GPS observation in Japan and its impact on earthquake studies. *Earth Planets Space* 56:xxix-xli
- SAPOS (2009) Satellitenpositionierungsdienst der deutschen Landesvermessung. <http://www.sapos.de/>. Accessed 16 May 2009
- Schenk T (2005) Introduction to photogrammetry. The Ohio State University, Columbus
- Schofield W, Breach M (2007) Engineering surveying, 6th edn. Elsevier, Amsterdam
- Snay R, Soler T (2008) Continuously operating reference station (CORS): history, applications, and future enhancements. *J Surv Eng* 134(4):95–104. doi:[10.1061/\(ASCE\)0733-9453\(2008\)134:4\(95\)](https://doi.org/10.1061/(ASCE)0733-9453(2008)134:4(95))
- Stone W (2006) The evolution of the national geodetic survey's continuously operating reference station network and online positioning user service. http://www.ngs.noaa.gov/PUBS_LIB/Evolution_of_CORS_and_OPUS.pdf. Accessed 16 May 2009

- US Army Corps of Engineers (2007) NAVSTAR global positioning system surveying, engineering and design manual, EM 1110-1-1003, Washington
- Wallace N (2007) CORS simulation for Australia. Curtin University of Technology, Final year project (unpublished)
- Wolf P (1980) Elements of photogrammetry. McGraw Hill Book Co., New York
- Wolfgang D (2005) Funktion und Nutzung des SAPOS-Deutschland-Netzes, Flächenmanagement und Bodenordnung (FuB). http://www.sapos.de/pdf/SAPOS_Deutschland_Netz_klein.pdf. Accessed 16 May 2009

Part III
Remote Sensing and Photogrammetry

Chapter 7

Fundamentals of Remote Sensing

“Know the weather, know the terrain, and your victory will be complete”

Sun Tzu (≈500 BC)

7.1 Basic Concept

Remote sensing is defined as the art, science and technology through which the characteristics of object features/targets either on, above or even below the earth’s surface are identified, measured and analyzed without direct contact existing between the sensors and the targets or events being observed, see e.g., (Jensen 2009; Lillesand et al. 2010; Richards 1994; Murai 1999) etc. This allows for *information* about such object features to be obtained by sensing and recording reflected or emitted energy and processing, analyzing, and applying that information.

Electromagnetic radiation is normally used as the *information carrier* in remote sensing. Such electromagnetic radiation that is either reflected or emitted from targets normally constitutes remote sensing data. This can be detected by a sensor usually on-board airborne (e.g., aircraft or balloon) or space-borne (e.g., satellites and space shuttles) platforms. A comprehensive survey of airborne and space-borne missions and sensors for observing the earth is given in Kramer (2002). As an analogy, of the five basic human senses, three of them namely; sight, hearing and smell may be considered forms of “remote sensing”, where the source of information is at some distance away from the sensors, in this case the eyes, ears and nose respectively. In contrast, however, the other two human senses (i.e., taste and touch) rely on direct physical contact with the source of information.

As shown in Fig. 7.1, the process of remote sensing is characterized by various stages and interactions summarized as follows: (a) an energy source or illumination is used to provide electromagnetic energy to the target of interest, (b) interactions

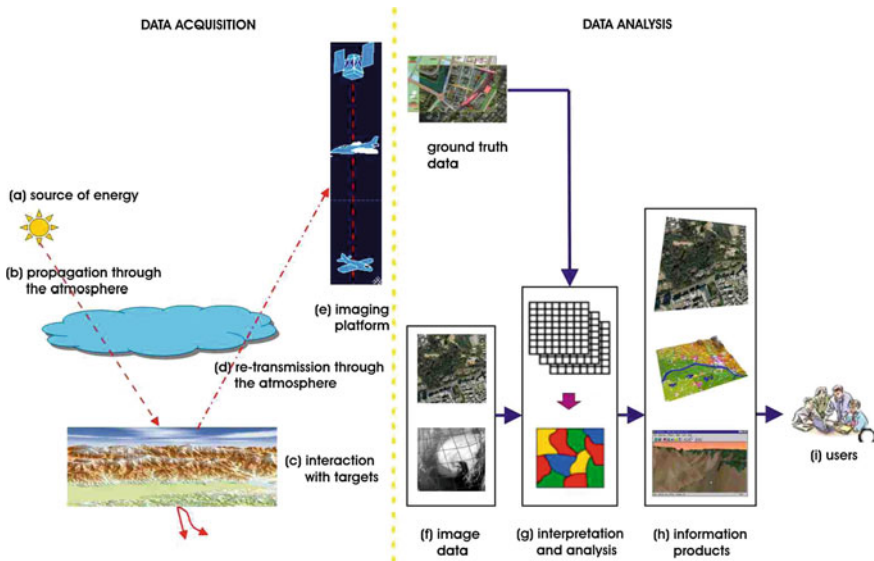


Fig. 7.1 Remote sensing process

between the electromagnetic radiation and the atmosphere, (c) interaction between the target and the electromagnetic radiation, (d) recording of reflected and emitted energy from the target by the sensor, (e) transmission, reception and processing of recorded energy into an image, (f) interpretation and analysis of image to extract desired information and (g) application of the information about the object or target in order to better understand it, reveal some new information, or assist in solving a particular problem.

Although it is now possible to expand the object feature base in image interpretation beyond the traditional spectral domain to include spatial and other dimensions, the practice of remote sensing still relies heavily on the spectral characteristics of objects. Accordingly, each object has a unique spectral signature of reflection or emission dependent on the sun, climate, atmosphere, ground condition, sensor among other factors. This allows the discrimination of the object *type*, *class*, *rank* or *density* to be made through image processing and analysis as illustrated in Fig. 7.2.

Even though the invention of classical photography can be traced way back to around 1860 and balloon photography was pioneered in 1900, strictly speaking, the technology of remote sensing evolved gradually into a scientific discipline only after World War II. Like most other mapping technologies, the early developments in remote sensing were mainly driven by military use, with civilian applications emerging much later. Today, the range of remote sensing applications varies from archeology, agriculture, cartography, civil engineering, meteorology and climatology, coastal studies, emergency response, forestry, geology, geographic information systems, hazards, land use and land cover, natural disasters, oceanography, water resources etc. Furthermore, the introduction of high spatial resolution sensors and the

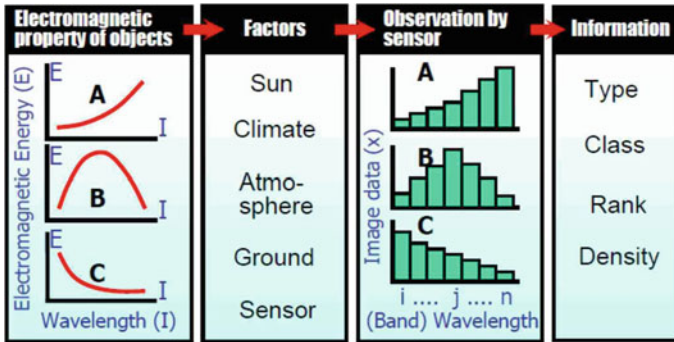


Fig. 7.2 Flow of remote sensing. Source Murai (2004)

development of new image analysis algorithms, has given an impetus to new applications in non-conventional areas like urban mapping, disaster management, location-based services, car and pedestrian navigation etc.

7.2 Principles of Electromagnetic Radiation

7.2.1 Electromagnetic Spectrum

Electromagnetic radiation, whose major source is the Sun, is fundamentally a carrier of electromagnetic energy. The electromagnetic radiation which travels in the form of waves at the speed of light (denoted as c and equals to $3 \times 10^8 \text{ ms}^{-1}$) is known as the electromagnetic spectrum. The waves propagate through time and space oscillating in all directions perpendicular to their direction of travel. According to the quantum wave theory, electromagnetic radiation propagates as a transverse wave comprising of both an electric field (E) and a magnetic field (H). These two fields are located at right angles to each other and travel at the speed of light.

Electromagnetic radiation is defined by four basic elements namely; *frequency* or *wavelength*, *transmission direction*, *amplitude* and *plane of polarization*. It is these four elements which influence the kind of information that can be extracted from electromagnetic radiation. They also effectively determine the characteristics of remote sensing data or images cues such as colors, tones or geometric shape of objects. The wavelength (λ) is defined as the distance between successive crests of the waves. The frequency (μ) is the number of oscillations completed per second. On the other hand, the amplitude defines the maximum positive displacement from the undisturbed position of the medium to the top of a crest. The plane of polarization represents the plane of the electric field and is important in microwave remote sensing (described in Chap. 9).

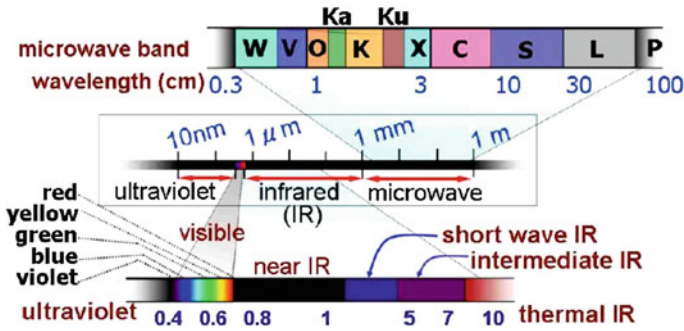


Fig. 7.3 Bands used in remote sensing. Source Murai (2004)

By scientific convention, the *electromagnetic spectrum* is divided into different portions. The major divisions of the electromagnetic spectrum ranging from short-wavelength, high-frequency waves to long-wavelength, low-frequency waves, include gamma rays, X-rays, ultraviolet (UV) radiation, visible light, infrared (IR) radiation, microwave radiation, and radio waves. Because of the spectral absorption characteristic of atmospheric molecules in certain regions of the atmosphere, otherwise referred to as the *blocking effect*, only certain parts of the electromagnetic spectrum are useful in remote sensing. These regions represent the *principal atmospheric windows* and define the bands employed in remote sensing as shown in Fig. 7.3.

The *ultraviolet* or UV portion of the spectrum has the shortest wavelengths which are practical for remote sensing. This radiation is just beyond the violet portion of the visible wavelengths, hence its name. Some rocks and minerals fluoresce or emit visible light when illuminated by UV radiation. The visible spectrum is a very narrow band whose wavelength ranges from between 0.3 and 0.7 μm . However, it is a very important part of the electromagnetic spectrum that is particularly critical in photogrammetry and satellite remote sensing. In addition, the light which our eyes—“ur remote sensors”—can detect is part of the visible spectrum.

The *infrared* (IR) region can be divided into two categories based on their radiation properties—the *reflected IR* and the *emitted or thermal IR*. Radiation in the reflected IR region is used for remote sensing purposes in ways very similar to radiation in the visible portion as shown in Fig. 7.4a. The reflected IR covers wavelengths from approximately 0.7 and 3.0 μm . The thermal IR region is quite different than the visible and reflected IR portions, as this energy is essentially the radiation that is emitted from the earth’s surface in the form of heat (see Fig. 7.4b).

The thermal IR covers wavelengths from approximately 3.0 and 100 μm . The principle of black body radiation is relevant in understanding the operation of thermal remote sensing and is articulated in most classical remote sensing literature, see e.g., Lillesand et al. (2010), Richards (1994) etc. While reflected IR images can yield important information on the health status of crops and vegetation, thermal IR sensors have been employed to support rescue operations in disaster events like earthquakes, fires etc.

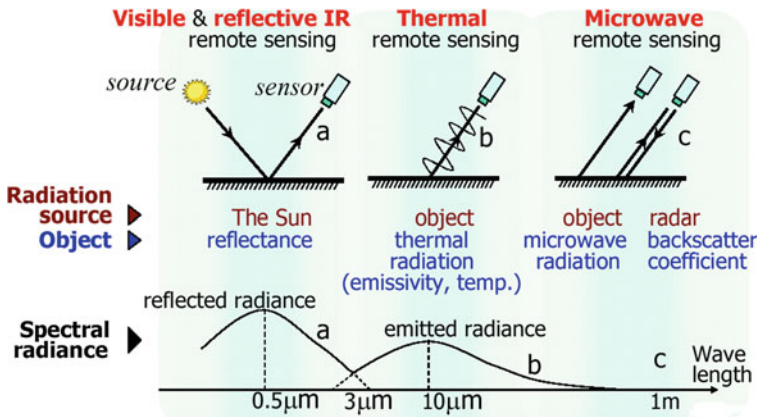


Fig. 7.4 Types of remote sensing. Source Murai (2004)

The *microwave regions* represent the portion of the electromagnetic spectrum that has raised most interest to remote sensing in recent times. It covers a vast wavelength region that extends in wavelength from about 1 mm to 1 m (see Fig. 7.4c). The microwave region is further subdivided into several other bands like P, L, C, X and K bands. Microwave remote sensing uses microwave in both passive and active modes. Microwaves can be emitted from the earth, from objects such as cars and planes, as well as from the atmosphere.

These microwaves can be detected to provide information, such as the temperature of the target that emitted the microwave. Most passive microwave sensors are characterized by low spatial resolution. Active microwave sensing systems such as RADAR provide their own source of microwave radiation that is fired in the form of a radar pulse towards the targets. They are then able to detect and record the energy that is backscattered from the targets as shown in (Fig. 7.4c). More detailed discussion on microwave remote sensing is presented in Chap. 9.

7.2.2 Interaction with the Atmosphere and Targets

As the electromagnetic energy travels through the atmosphere from either the energy source or the target, some *absorption and/or scattering* will inevitably take place. Ozone, carbon dioxide, and water vapour are the three main atmospheric constituents which absorb electromagnetic radiation. As mentioned above, it is only in those regions of the electromagnetic spectrum where no or slight absorption occurs, otherwise referred to as the *principal atmospheric windows*, where meaningful remote sensing can be practiced.

Scattering occurs when particles or large gas molecules present in the atmosphere interact with and cause the electromagnetic radiation to be redirected from its original path resulting in attenuation of the electromagnetic radiation. Scattering is mainly

caused by nitrogen (N_2) and oxygen (O_2) molecules, aerosols, fog particles, cloud droplets, and raindrops. The type of scattering that results is influenced by the relative size of the atmospheric molecules and particles *vis á vis* the wavelength of the incident energy and will thus vary from one atmospheric region to the other. Three different types of scattering can be distinguished: *Rayleigh scattering*, *Mie scattering* and *Non-selective scattering* in the upper, mid and lower atmospheric regions respectively. Whereas Rayleigh scattering is the reason why the sky appears blue, non-selective scattering is the reason for fog and clouds appearing white.

Different types of interactions will occur when the incident electromagnetic radiation finally hits or connects with the targets. The specific type of interaction will depend on the properties of both the target and the wavelength of the incident electromagnetic radiation. *Reflection* occurs when radiation bounces off the target and is then redirected. When the target surface is smooth, *specular reflection* results, where all (or almost all) of the energy is directed away from the surface in a single direction. When the target surface is rough, the energy is reflected almost uniformly in all directions, in which case *diffuse reflection* occurs. Most earth surface features lie somewhere between perfectly specular or perfectly diffuse reflectors.

Absorption occurs when electromagnetic radiation is absorbed by the target. *Transmission* occurs when electromagnetic radiation passes through a target. For any given material, the amount of solar radiation that reflects, absorbs, or transmits varies with wavelength. As discussed in Sect. 7.1, it is this important characteristic of matter that makes it possible to identify different substances or features and distinguish between them on the basis of their *spectral signatures* (spectral curves) in remote sensing.

For demonstration purposes, Fig. 7.5 shows the *spectral reflectance curves* for vegetation, water and dry and wet soils. While vegetation has a unique pattern, the spectral reflectance for soil varies depending on the moisture content with dry soil

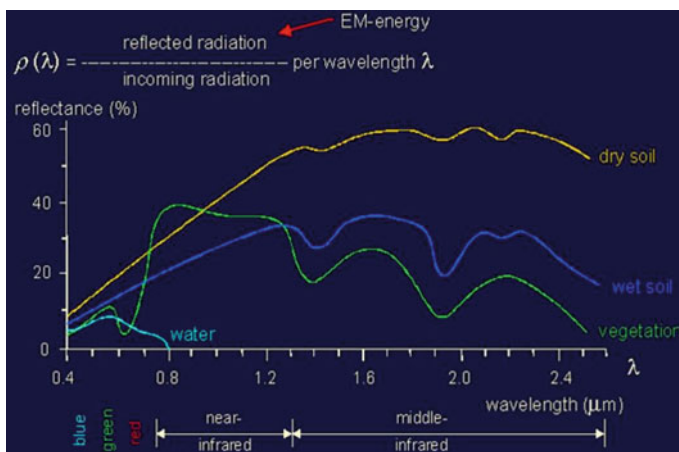


Fig. 7.5 Spectral curves for some features. Source CCRS (2012)

exhibiting higher reflectance than wet soil. The main part of water, except for shorter wavelength is absorbed with less reflection. Furthermore, Fig. 7.5 also shows that the near infra-red band represents the best region within which to distinguish between vegetation and most other object features like water.

7.3 Passive Versus Active Remote Sensing

On the basis of the scope of application and type of electromagnetic radiation employed, remote sensing may be divided into Weng (2010): (a) *satellite remote sensing* (when satellite platforms are employed), (b) *photogrammetry* (when photographic images are used to record reflected visible energy as discussed in Chap. 11), (c) *thermal remote sensing* (when the thermal infrared portion of the electromagnetic spectrum is used), (d) *microwave remote sensing* (when microwave wavelengths are employed as described in Chap. 9). and (e) *LiDAR or laser scanner remote sensing* (when laser pulses are directed toward the target and the distance between the sensor and the target is estimated premised on either the return time for pulse ranging or the phase difference for side tone (continuous wave) ranging as described in Sect. 8.4.

Based on how energy is used and detected, one can distinguish between two different forms of remote sensing (i) passive-and (ii) active remote sensing. Passive remote sensing systems record the reflected energy of electromagnetic radiation or the emitted energy from the Earth, such as cameras and thermal infrared detectors. On the other hand, active remote sensing systems send out their own energy and record the scattered energy received upon interaction with the Earth's surface, such as radar imaging systems and LiDAR.

One of the advantages of active sensors over their passive counterparts is that they can be used during both day and night or in most weather conditions. In addition, active remote sensors are also able to penetrate through cloud cover. This is unlike passive remote sensors for which sunlight is critical to their successful operation and cloud cover is an impedance and is thus undesirable. It is also possible to generate different imagery with different information content for the active remote sensors like radar imagery by simply altering the wavelength (or frequency) and the polarization of the transmitted and received signals.

7.4 Concluding Remarks

From its humble beginning, remote sensing has grown in stature over the past half century or so to influence virtually all aspects of human endeavor and the environment. Coupled with the availability of historical remote sensing (time-series) data, the reduction in data cost and increased spatial resolution, remote sensing technology appears poised to make an even greater impact on many socio-economic and political endeavors of mankind. Notably, the number of remote sensing applications is very impressive today, with many new applications emerging even in non-traditional

areas like urban mapping, disaster management, location-based services, car and pedestrian navigation etc.

To realize the full potential of this mapping technology, however, it is imperative to integrate remote sensing with other related technologies that provide and deliver geospatial data and information such as *Global Navigation Satellite Systems* (GNSS), *inertial mapping units* (IMU) or other *rotation sensors*, *Geographic Information Systems* (GIS), *wireless sensor networks*, *Global System for Mobile Communication* (GSM), and the *Internet*.

In view of the multi-faceted and increasingly complex nature of most problems confronting humanity today, it is critical that the integration of the above technologies be implemented within the framework of a *decision support system* (DSS) elucidated in Sprague (1980), Bhatt and Zavery (2002), Shim et al. (2002), Power (2004) etc. Using disaster as a typical example, whereas mapping technologies like remote sensing, GNSS and GIS would provide the basic support in pre-event preparedness, response and monitoring, and post-reconstruction in disaster management, communication satellites and the Internet would help in disaster warning, relief mobilization and telemedicinal support Jayaraman et al. (1997). To leverage from these diverse technologies and to effectively respond to disasters in a coordinated, efficient and timely manner would call for building of the necessary DSS capability within a GIS platform.

References

- Bhatt GD, Zavery J (2002) The enabling role of decision support systems in organizational learning. *Decision Support Syst* 32:297–309
- CCRS (2012) Canada centre for remote sensing remote sensing tutorial. <http://www.nrcan.gc.ca/earth-sciences/geography-boundary/remote-sensing/fundamentals/>. Accessed 24 July 2012
- Jayaraman V, Chandrasekhar MG, Rao UR (1997) *Managing the natural disasters from space technology inputs*. Elsevier Science Ltd, Great Britain
- Jensen, JR (2009) *Remote sensing of the environment: an earth resource perspective*. Prentice Hall, Saddle River
- Kramer HJ (2002) *Observation of the earth and its environment: survey of missions and sensors*. Springer, Berlin
- Lillesand TM, Kiefer RW, Chipman JW (2010) *Remote sensing and image interpretation*. John, Hoboken
- Murai S (1999) *GIS work book: fundamental and technical courses*. vols 1 & 2. National Space Development Agency, New York
- Murai S (2004) *Remote sensing and GIS courses—distance education*. Japan International Cooperation Agency (JICA)-Net
- Power DJ (2004) Specifying an expanded framework for classifying and describing decision support systems. *Commun Assoc Inf Syst* 13:158–166
- Richards JA (1994) *Remote sensing digital image analysis: an introduction*. Springer, Berlin
- Shim JP, Warkentin M, Courtney JF, Power DJ, Sharda R, Carlsson C (2002) Past, present and future of decision support technology. *Decision Support Syst* 33:111–126
- Sprague RH (1980) A framework for the development of decision support systems. *MIS Q* 4:1–26
- Weng Q (2010) *Remote sensing and GIS integration: theories, methods, and applications*. McGraw-Hill, Boston, p 416

Chapter 8

Optical Remote Sensing

“It is not knowledge, but the act of learning, not possession but the act of getting there, which grants the greatest enjoyment.”

Carl Friedrich Gauss (1777–1855)

8.1 Data Acquisition—Sensors and Systems

There are a large variety of systems for collecting remotely sensed data in operation today. Ramapriyan (2002) asserts these can be categorized in several ways according to the:

- type of instrument (imager, sounder, altimeter, radiometer, spectrometer, etc.);
- mechanics of the instrument (push broom, whisk broom, serial cross-track, parallel cross-track, conical scan, step-staring, etc.);
- sensing mechanism (passive or active);
- viewing characteristics (point-able or fixed, nadir- or off-nadir-looking, single- or multi angle (mono or stereo));
- spectral characteristics measured (panchromatic, multi-spectral, hyper-spectral);
- spatial resolution (high, moderate, low);
- observed wavelength range (UV, visible, near infrared, thermal, microwave, etc.);
- platform (aircraft, spacecraft); and
- altitude (in case of airborne sensors) or orbits (in the case of space-borne sensors (e.g., sun-synchronous, geosynchronous, geostationary, low inclination etc.)).

Against the above background, the design of remote sensing systems principally revolves around the identification of the most appropriate *sensor-platform* combination. As a matter of fact, this arrangement represents a basic and common denominator in virtually all remote sensing systems. Following a user needs assessment the most pragmatic sensor-platform combination is identified in order to deliver the

desired remote sensing data solution to suit specific or generic application(s). In view of the often huge financial and human resources required, as well as the diversity and scope of applications, the design of remote sensing systems is definitely not a trivial exercise.

As discussed in Sect. 7.2, and with regard to the type of sensing mechanism applied, mapping sensors may be classified as either passive or active. Furthermore, they may vary in design from classical frame-based to digital aerial cameras employing either frame or line scanning techniques, and from opto-mechanical to push-broom scanners with stereo and even triplet imaging capability. In defining the most appropriate orbit for a sensor, as mentioned above, several attendant factors need to be considered such as altitude, attitude, orbit or flight course, payload etc. By using Kepler's laws of planetary motion, the characteristics of satellite orbits are defined through several parameters including orbit figure (circular, ellipsoidal etc.), inclination (oblique, polar etc.), period (geosynchronous or sun synchronous), recurrence (recurrent or semi-recurrent) etc.

In retrospect, various factors have continued to drive and impact on the development of remote sensing and GIS in general as illustrated in Fig. 2.2. For instance, developments in space technology have strongly influenced the design of mapping sensors. Furthermore, increased size of charged-couple devices (CCD) sensors and high data transmission rates have all given an impetus to this. The increase in the application of space-derived data into new and often diverse fields has also significantly contributed to the development of mapping sensors.

Usually, most of these new applications have brought with them new demands and challenges. Attempts to address these new use requirements have contributed significantly to the development of remote sensing imaging systems as articulated in Kiema (2001). From a purely political perspective, the easing of prior military restrictions on the availability and use of high spatial resolution imagery (HSRI) to civilians has opened up new business opportunities in mapping.

The vehicle or carrier on which remote sensors are borne is called the *platform*. Pigeons were some of the earlier remote sensing platforms employed in remote sensing. Basically, platforms used in remote sensing may be classified as space-borne, airborne or ground-based. Satellites constitute the principal space-borne platforms employed today. Aircrafts are the most common type of airborne platform used in remote sensing, although helicopters, radio controlled planes and balloons are also employed, especially at lower orbits of up to about 500 m.

Ground-based platforms are used in terrestrial and close range imaging applications. Space-borne platforms are predominant at higher altitude orbits stretching from between 240 and 350 km for space shuttle, to between 500 and 1,000 km for Low Earth Orbiting Satellites (LEOS) usually with sun synchronous orbit and 36,000 km for Geostationary Earth Orbiting Satellites (GEOS). On the other hand, airborne sensors are usually employed at lower altitudes from 10 to 12 km. One can compare remote sensing satellites with the Global Navigation Satellite Systems (GNSS) like the Global Positioning Satellite (GPS), which are essentially Medium Earth Orbiting Satellites (MEOS) and orbit at an altitude of about 20,200 km.

The key factor in the selection of a platform is the altitude which determines the ground resolution if the instantaneous field of view (IFOV) of the sensor is constant. The selection of the appropriate platform also depends on the purpose—which is sometime requested for *a priori*. For example, a constant altitude is required for aerial surveys, while various altitudes are needed to survey vertical atmospheric distribution. Moreover, for aerial photogrammetry, the flight path is strictly controlled to meet the requirement of geometric accuracy. However, helicopter or radio controlled planes are used for a free path approach, for example in disaster monitoring.

There are probably several hundreds of *space utility vehicles* (SUVs) employing different sensor-platform arrangements in operation today. Undoubtedly, the number of such systems is bound to continue growing even further. This prediction is true, especially as more enterprise or domain specific sensors continue to be launched into orbit and as many more countries, including even those in the developing world, begin to recognize the strategic importance and value of investing in space technology.

8.2 Characteristics of Optical Remote Sensing Data

As highlighted in Sect. 7.1, electromagnetic radiation which is either reflected or emitted from objects is what is referred to as remote sensing data. This data can be in either analogue format (e.g., hard-copy aerial photography or video data) or digital format (e.g., a matrix of brightness values corresponding to the average radiance measured within an image pixel). The success of data collection from remotely sensed imagery requires an understanding of four basic image resolution characteristics, namely; spatial, spectral, radiometric, and temporal resolution (Jensen 2005). From the very outset, however, it is important to acknowledge the fact that the interpretation of different sensor performance characteristics is anything but trivia (Joseph 2000).

Spatial resolution is a measurement of the minimum distance between two objects that will allow them to be differentiated from one another in an image and is a function of sensor altitude, detector size, focal size, and system configuration (Jensen 2005). As much as the spatial resolution determines the smallest object that can be perceived in an image, the contrast of an object with respect to the surrounding object also influences its interpretation. The impact of spatial resolution on the pointing accuracy and overall interpretation has been investigated in several works (e.g., Forshaw et al. (1983), Bähr and Vögtle (1998)).

These studies have demonstrated the importance of specifying the *Modulation Transfer Function* (MTF) of an imaging system in order to adequately describe its geometric capability. For aerial photography, spatial resolution is measured in resolvable line pairs per millimeter, whereas for other sensors, it refers to the dimensions (in meters) of the ground area that falls within the instantaneous field of view (IFOV) of a single detector within an array or pixel size (Jensen 2005). Spatial resolution, which defines a sensor's footprint on the ground, determines the level of spatial details that can be observed on the earth's surface from a particular sensor.

Table 8.1 Typical costs of different types of remote sensing imagery. *Source* Kumi-Boateng (2012)

Sensor category	Sensor type	Spatial resolution (m)	Scene coverage (Km ²)	Estimated acquisition cost per Km ² (US\$)	Estimated pre-processing cost per Km ² (US\$)
Coarse resolution (>250m)	NOAA AVHRR	1090	5,760,000	0.00015	0.00008
	Terra MODIS	250	5,428,900	0.00000	0.00005
	Orbview-1	1000	3,750,000	0.00013	0.00006
Medium resolution (10–250)	Landsat MSS	80	34,000	0.00880	0.00440
	Landsat TM 4-5	30	34,000	0.01620	0.00810
	Landsat ETM 7	30	34,000	0.02130	0.01065
	IRS (XS)	23	21,900	0.11400	0.02800
	SPOT 1-3	10	3,600	0.41600	0.15000
	ASTER	15	3,600	0.01520	0.00760
High resolution (<10m)	RADARSAT	10–100	1,000	2.53000	1.20000
	IKONOS	1 (Pan)	121	29.00000	14.50000
	SPOT 5	2.5	3,600	0.73000	0.27000
	IRS	6 (Pan)	4,900	0.33000	0.08000
	Quickbird	0.6 (Pan)	400–1,600	39.00000	19.50000
	Color-IR Photography	10	83	5.50000	2.75000
	Aircraft digital imagery	1	variable	50.00000	25.00000
	AVIRIS	20	99	5.00000	2.50000
LiDAR	0.1	variable	74.00000	37.00000	

Generally speaking, the finer the spatial resolution, the higher the level of detail it records and certainly the more expensive the satellite imagery as shown in Table 8.1.¹ From a practical standpoint, cost is often the most important factor in a remote sensing application as reiterated by Phinn (1998). Coarse spatial resolution data may include a large number of mixed pixels, where more than one land-cover type can be found within a pixel. Whereas fine spatial resolution data considerably reduce the mixed-pixel problem, they may increase internal variation within the land-cover types. Higher spatial resolution also implies need for greater data storage and higher cost and may even introduce difficulties in image processing for a large study area as pointed out by Weng (2010).

The relationship between geographic scale and spatial resolution has been investigated in Quattrochi and Goodchild (1997). From such studies and experience gained over the years, it has been confirmed that high spatial-resolution imagery, such as that employing IKONOS and QuickBird data, is more effective on the local scale. On the regional scale, medium-spatial-resolution imagery, such as that employing Landsat Thematic Mapper/Enhanced Thematic Mapping Plus (TM/ETM+) and Terra Advanced Space-borne Thermal Emission and Reflection Radiometer (ASTER) data, is more common. At the continental or global scale, coarse-spatial-resolution

¹ All the tabulated sensors are passive, except RADARSAT and LiDAR that are active sensors.

imagery, such as that employing Advanced Very High Resolution Radiometer (AHVRR) and Moderate Resolution Imaging Spectrometer (MODIS) data is mundane as shown in Table 8.1.

Each remote sensor is unique with regard to what portion(s) of the electromagnetic spectrum's energy it is able to detect. Different remote sensing instruments record different segments, or bands, of the electromagnetic spectrum. *Spectral resolution* of a sensor refers to the number and size of the bands it is able to record (Jensen 2005). In general, the finer the spectral resolution, the narrower the wavelength range for a particular band. To describe the spectral resolution more precisely, however, it is necessary to define a number of related parameters including the central wavelength, bandwidth size, jointly with the percentage of out-of-band response as noted by Joseph (2000).

The spectral resolution may vary from panchromatic to multi-spectral and even hyper-spectral sensors. Panchromatic sensors record images in either black or white, while multi-spectral sensors detect images in a few bands e.g., visible and reflected infrared. For most high spatial resolution sensors the panchromatic (Pan) and multi-spectral (MSS) channels are usually separated, with the panchromatic channel often having a finer spatial resolution than the multi-spectral channels. Hyper-spectral sensors (imaging spectrometers) are instruments that acquire images in many very narrow contiguous spectral bands. An example of a hyperspectral sensor is MODIS on-board National Aeronautics and Space Administration (NASA)'s Terra and Aqua missions that has a spectral resolution in 36 spectral bands designed to capture data about land, ocean, and atmospheric processes simultaneously.

Radiometric resolution refers to the sensitivity of a sensor to incoming radiance, that is, how much change in radiance there must be on the sensor before a change in recorded brightness value takes place Jensen (2005). Coarse radiometric resolution would record a scene using only a few brightness levels, that is, at very high contrast, whereas fine radiometric resolution would record the same scene using many brightness levels. For example, remote sensors with a radiometric resolution of 8 bits can record data in 256 brightness or gray levels ranging from 0 to 255. The finer the radiometric resolution of a sensor, the more sensitive it is in detecting small differences in reflected or emitted energy.

Temporal resolution defines the duration it takes a sensor to return to a previously imaged location. It is important to note that because of some degree of overlap in the imaging swath of adjacent orbits for most remote sensing satellites, coupled with the increase of this overlap with increasing latitude, some parts of the earth tend to be re-imaged more frequently than others. This is besides the fact that some satellite systems are also able to "point their sensors".

Temporal resolution has an important and critical implication in change detection and environmental monitoring. For instance, many environmental phenomena such as vegetation, weather, forest fires, volcanoes etc. periodically change over time. To monitor the development of crops and vegetation, temporal resolution is an important consideration to be able to detect and explain changes and anomalies. In view of the often sporadic changes in weather patterns worldwide, most weather sensors have a high temporal resolution such as, Geostationary Operational Environmental Satellite

(GOES), 0.5/h; NOAA-9 AVHRR local-area coverage, 14.5/day; and METEOSAT first generation, every 30 min (Weng 2010).

Fine spatial resolution remote sensing image data can be very expensive, with the cost often spiraling to several hundred dollars per square kilometer (see Table 8.1) depending on the type of sensor and the timeliness of the desired data. Given the availability of a wide array of different types of remote sensing data with different characteristics, the selection of the most appropriate data for a particular exercise is not trivial at all. This is further compounded by the fact that in many remote sensors, clear trade-offs exist between different forms of resolution as described in Campbell (2007). In the final analysis, therefore, the selection of the most appropriate remote sensing data in a particular application will be influenced by several factors including: the nature of the specific application, the information or classes of interest that need to be extracted, the sensor characteristics assessed and the available budget.

8.3 High Spatial Resolution Imagery

8.3.1 Development and Characteristics of HSRI

With the onset of space-based mapping, which was incidentally triggered off way back in 1972 with the launch of *Landsat-1*, most of the space-borne sensors that were employed belonged to national mapping and other federal agencies. Despite the fact that mapping applications involving the use of satellite imagery have continued to grow impressively since then, these have, nevertheless, been rather constrained and have never realized the full potential of satellite remote sensing *per se*. This is basically due to the relatively low spatial resolution of most of the earlier satellite imagery. Consequently, photogrammetry (discussed in Chap. 11) continued to be used in applications, like in medium to large scale topographic mapping, where the accuracy offered by satellite imagery was deemed to be inadequate.

The inauguration of high spatial resolution mapping sensors, which was pioneered in 1999 with the successful launch of *IKONOS*, has significantly changed the above scenario (see Table 8.1). The introduction of high spatial resolution imagery (HSRI) addressed the inherent weakness of the earlier generation of satellite imagery and ideally marked the beginning of a new era in space imaging for earth observation as articulated in Fritz (1996), Aplin et al. (1997) etc. With the use of sensors characterized by high geometric fidelity, HSRI have demonstrated remarkable mapping capability as explained in Sect. 8.3.2.

In addition, high spatial resolution mapping sensors have exhibited very rapid cycle of image collection that is flexible enough to satisfy varied customer delivery needs. A distinctive feature of most high spatial resolution commercially-based earth observation satellites is that, unlike the earlier mapping sensors, they are largely owned by different private consortia, often with an international dimension. Fig. 8.1 highlights examples of some typical HSRI.

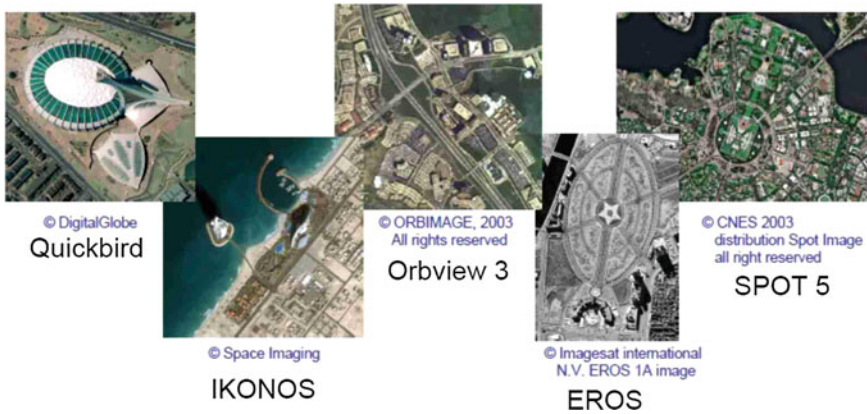


Fig. 8.1 Examples of HSRI. *Source* Murai (2004)

Some of the typical products associated with HSRI include: (i) Geo-coded image: Panchromatic (Pan), Multi-spectral (MS), Pan sharpened etc; (ii) Orthoimage corrected for topography; (iii) Digital Surface Models (DSMs)/Digital Elevation Models (DEMs) from stereo imagery; (iv) Contour line map generated from DEM; (v) Land cover map: auto/semi-automatically produced; (vi) Overlay on GIS; and (vii) 3D landscape animations.

8.3.2 Potential of HSRI

HSRI contain rich spatial information, providing a greater potential to extract much more detailed thematic information (e.g., land use and land cover, impervious surface, and vegetation), cartographic features (e.g., buildings and roads), and metric information with stereoisimages (e.g., height and area) that are ready to be used in GIS (Weng 2010). Murai (2004) deduces the potential of HSRI from the typical products provided to include the following:

- (1) Mapping capability: A ground resolution of 1 m coupled with a pointing accuracy of 0.3 pixel will provide 1:10,000 line drawing map with contour interval of between 2.5 and 5 m. Background image map will also be possible at the scale of 1:5,000 including orthoimage.
- (2) GIS: HSRI can be overlaid as background image on GIS vector data.
- (3) Provision of DEM from stereo imagery.
- (4) Automated feature extraction.
- (5) Fused data products.
- (6) 3D Modeling: This requires stereo imagery to succeed. Moreover, the central perspective projection (see Sect. 11.2), upon which the basic photogrammetric theory is anchored, is not applicable here due to the very narrow field of

view (less than 2°). Instead, *generic* or *replacement* sensor models described in Sect. 12.2 are used. Specifically, two methods have been developed for 3D modeling namely; (a) affine transformation with 6 parameters as shown in Eq. 8.1

$$\begin{aligned}x &= a_1 + a_2X + a_3Y \\y &= b_1 + b_2X + b_3Y\end{aligned}\quad (8.1)$$

where; x, y are the image coordinates; X, Y are the object point coordinates; a_1, a_2, a_3, \dots etc. are the transformation coefficients.

(b) rational function with up to 80 parameters that are provided by the HSRI distributor as exemplified in Eq. 8.2.

$$\begin{aligned}x_{ij} &= \frac{P_{i1}(X, Y, Z)_j}{P_{i2}(X, Y, Z)_j} \\y_{ij} &= \frac{P_{i3}(X, Y, Z)_j}{P_{i4}(X, Y, Z)_j}\end{aligned}\quad (8.2)$$

where; x_{ij}, y_{ij} are normalized image coordinates; X, Y, Z are the object point coordinates (normalized latitude, longitude & height); and $P_{i1}(X, Y, Z)_j = a_1 + a_2Y + a_3X + a_4Z + \dots + a_{19}X^2Z + a_{20}Z^3$

$$P_{i2}(X, Y, Z)_j = b_1 + b_2Y + b_3X + b_4Z + \dots + b_{19}X^2Z + b_{20}Z^3$$

$$P_{i3}(X, Y, Z)_j = c_1 + c_2Y + c_3X + c_4Z + \dots + c_{19}X^2Z + c_{20}Z^3$$

$$P_{i4}(X, Y, Z)_j = d_1 + d_2Y + d_3X + d_4Z + \dots + d_{19}X^2Z + d_{20}Z^3 \text{ and } a_1, a_2, a_3, \dots \text{ etc. are the polynomial coefficients.}$$

(7) Visualization and 3D fly throughs.

Subsequently, the advantages of HSRI include:

- (a) Frequent data acquisition from high temporal resolution;
- (b) Good image quality;
- (c) Simple 3D modeling;
- (d) Access possibility (high mountain, boundary etc.);
- (e) Less number of ground control points (GCPs) are required; and
- (f) No special skill is required.

On the contrary, the disadvantages of HSRI include:

- (a) High cost;
- (b) Cloud coverage;
- (c) Shadows caused by topography, tall buildings, or trees;
- (d) High spectral variation within the same land-cover class, especially in complex landscape, e.g., urban areas;
- (e) Fixed frequency and acquisition time;
- (f) Huge amount of data storage and computer display, which can adversely affect image processing; and
- (g) Less development history.

8.4 Light Detection and Ranging

Although growing in popularity only in recent years, Light Detection And Ranging (LiDAR), otherwise referred to as laser scanning technology, has been in use from around 1972 when the *Airborne Profile Recorder* (APR) was first employed and effectively combined in photogrammetric block adjustment Ackermann (1999). Throughout the 1980s different feasibility studies were conducted with the viability of LiDAR only confirmed following the steady growth of Global Positioning System (GPS) and development of rotational sensors. This then saw the first laser profiling research conducted at the University of Stuttgart, Federal Republic of Germany between 1989–1990 under the direction of Prof. Ackermann in the special research project titled “High Precision Navigation”. Commercial applications of LiDAR commenced later in the early 1990s spearheaded by firms like TopScan,² Toposys³ etc.

As mentioned in Sect. 7.3, LiDAR is essentially an active remote sensing technology that employs Light Amplification by Stimulated Emission of Radiation (LASER). In principle, it operates by firing laser pulses towards the object/target and measuring the range between the sensor and the object based on either the return time for pulse ranging systems or the phase difference for side tone (continuous wave) ranging systems. From a knowledge of the instantaneous position and attitude of the LiDAR sensor, derived from real-time kinematic (RTK) GPS positioning (discussed in Sect. 6.11) and inertial measuring units (IMU) respectively, through simple polar determination, it is possible to compute the three-dimensional coordinates of the object/target. These initial estimates, however, still need to be filtered to correct for noise after which LiDAR data in the form of discrete x, y, and z coordinates are generated and transformed into the desired local coordinate system. Intensity data (images) may also be delivered together with other elevation derived surfaces such as digital elevation model (DEM), digital surface model (DSM) etc. LiDAR data provide fairly good vertical and horizontal resolutions with accuracies of ± 0.3 m reported (Webster et al. 2004).

Unlike other remotely sensed data, LiDAR data focus solely on geometry rather than radiometry (Weng 2010). With the ability to detect and record more than one return for each height point measured (Alharthy and Bethel 2002), LiDAR possesses distinct advantages over most other remote sensing systems. Specifically, most LiDAR allow the recording of the first- and last-pulse returns as shown in Fig. 8.2. The first-pulse returns are registered by surfaces of all ground objects, including both solid and transparent objects, and is extremely useful for detecting penetrable objects such as trees. Starting from individual tree analysis, forest volume and biomass can be estimated subsequently, see e.g., Renslow (2000), Popescue et al. (1998), Secord and Zakhor (2007), Voss and Sugumaran (2008) etc. In contrast, the last-pulse returns are recorded by laser that penetrates through and is finally reflected from non-penetrable objects such as the ground and buildings. While the first pulse LiDAR data is useful for generation of DSMs, the last pulse data is important for producing

² <http://www.toposcan.de>

³ <http://www.toposys.de>

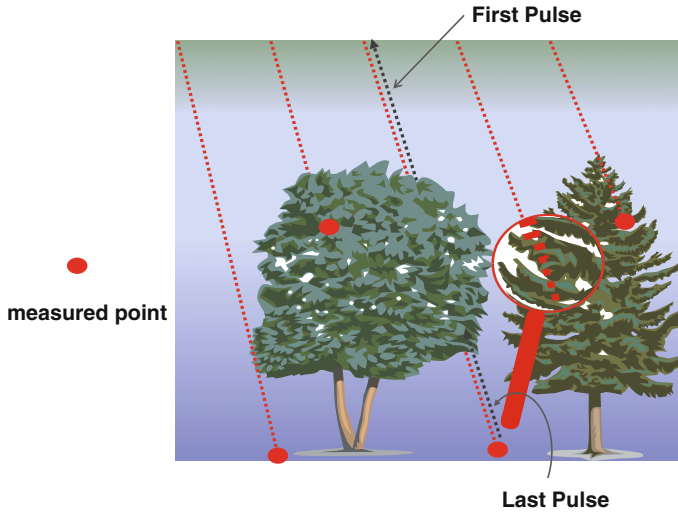


Fig. 8.2 First- and last-pulse measurements

DEMs. The normalized DSM (nDSM), otherwise known as the *normalized height model*, derived from Eq. 8.3, is important in the extraction of urban objects such as buildings and trees.

$$\text{nDSM} = \text{DSM} - \text{DEM} \quad (8.3)$$

Over the years, LiDAR technology has distinguished itself in many applications largely due to its ability to deliver high resolution data, within a short acquisition time and at a lower cost compared with classical methods like photogrammetry, irrespective of weather conditions. LiDAR is today a critical data source in urban studies, especially for extraction of buildings and trees, see e.g., Haala and Brenner (1999), Brunn and Weidner (1997), Clode et al. (2007), Forlani et al. (2006), Miliaris and Kokkas (2007) etc. LiDAR data have also been used in urban planning, telecommunications network planning, and vehicle navigation (Kokkas 2005). To demonstrate its versatility, many urban studies have also examined the extraction of urban objects by fusing LiDAR with high spatial resolution imagery (HSRI), see e.g., Lee et al. (2008), Secord and Zakhor (2007), Voss and Sugumaran (2008), Sohn and Dowman (2005) etc.

Given the diversity and quality of products offered by LiDAR technology, there has been discussion in the literature whether this technology is in competition with or complimentary to older technologies, such as photogrammetry, that leverage on similar outputs, see e.g., Baltsavias (1999), Liu (2008), Schenk and Csatho (2002), Ma (2005) etc. Some of the advantages that LiDAR possesses over photogrammetry include the fact that; (i) it is virtually independent from environmental conditions; (ii) it can operate both during day or night; (iii) it does not need control points and signals; (iv) it does not need expensive mapping equipment; (v) it has a high point density

(1–5 m); and (vi) although it has a higher cost per square kilometer (see Table 8.1), it is still more competitive in terms of both cost and time by between 25–50 % Konecny (2003). Evidently, LiDAR together with HSRI (discussed in Sect. 8.3) provide high impact data sets that will continue to influence many future developments in remote sensing.

8.5 Concluding Remarks

That space technology is expensive business is a matter of fact. This partly explains why for slightly over half a century since their introduction, the earlier generation of earth observation satellites remained the preserve of only a handful of national mapping and federal agencies. However, the ever growing business opportunities present in the space industry seem to have changed this situation in recent times, with several private consortia and companies already fully engaged in the provision of high-end remote sensing imaging data and associated value-added products. This paradigm shift seems to be emerging even as many first world countries continue to cut down on their budgets for space technology, owing largely to the recurrent global financial crisis.

Conversely, we are increasingly witnessing the deployment of many miniature earth observation satellites, particularly in the emerging economies in Asia like China, Korea, Malaysia etc., thanks to innovation and development in nano technology. Murai (2004) contends that these small satellites cover up to about 95 % of the basic functions of large satellites at only about 5 % of the total cost of the same. Furthermore, they also have a relatively short development time and reasonable reliability, besides requiring smaller and cheaper launch vehicles, see e.g., Xue et al. (2008), Kramer and Cracknell (2008), Guelman and Ortenberg (2009) etc.

These attractive propositions will certainly result in many more developing countries leaping into the league of select nations that own earth observation satellites to support assorted human, environmental and other strategic interests and applications. However, like the proverbial two sides of a coin, these new developments will most likely introduce new technical, institutional and legal challenges, such as the need for better measures and procedures to deal with debris mitigation, frequency allocation and satellite registration, among other contemporary space issues.

With the benefit of hindsight, one can postulate that it is unlikely that any one single sensor-platform combination will provide all the data required in remote sensing. What is required today is the development of appropriate sensor networks and webs. Such technologies that are currently being deployed in environmental monitoring, present new opportunities for gathering land surface information that allow the integration of field data collection in remote sensing McCoy (2005), thus amplifying the utility of remotely sensed data (Ho et al. 2005; Porter et al. 2005; Kussul et al. 2009) etc. Additionally, the emergence of a more spatially literate society will no doubt continue to demand for high quality remote sensing data to suit their diverse applications. The quality of the wide array of remote sensing data on offer

will be evaluated on the basis of several factors such as *lineage*, *consistency*, *completeness*, *positional accuracy*, *semantic accuracy*, *temporal accuracy* and *attribute accuracy*, see e.g., Groot and McLaughlin (2000), Devillers and Jeansoulin (2006), Congalton and Green (2009) etc.

Furthermore, the future use of earth sensor data, and through this, the future development of mapping sensors will continue to be influenced by algorithmic advances in various fields including automatic image understanding, data fusion, and data compression (Schiewe 1998). Ultimately, however, the final selection of the most suitable remote sensing data in an application will be made based on several factors including; the specific type of the application, the information or classes to be extracted, the sensor characteristics assessed, and perhaps even more importantly, the available budget (Kiema 2001).

References

- Ackermann F (1999) Airborne laser scanning—present status and future expectations. *ISPRS J Photogramm Remote Sens* 54:64–67
- Alharthy A, Bethel J (2002) Heuristic filtering and 3D feature extraction from LIDAR data. In: *International Archives of Photogrammetry and Remote Sensing (IAPRS)*, Graz, Austria, vol XXXIV, Part 3A:29–34
- Aplin P, Atkinson PM, Curran PJ (1997) Fine Spatial resolution satellite sensors for the next decade. *Int J Remote Sens* 18:3873–3881
- Bähr H-P, Vögtle T (eds) (1998) *Erderkundungssatelliten und ihre Produkte*. Digitale Bildverarbeitung, vol 3. Wichmann Verlag, Heidelberg, pp 29–43
- Baltsavias E (1999) A comparison between photogrammetry and laser scanning. *ISPRS J Photogramm Remote Sens* 54:83–94
- Brunn A, Weidner U (1997) Extracting buildings from digital surface models. *Int Arch Photogramm Remote Sens* 32:27–34
- Campbell JB (2007) *Introduction to remote sensing*, 4th edn. Guilford Press, New York
- Clode S, Rottensteiner F, Kootsookosc P, Zelniker E (2007) Detection and vectorization of roads from LiDAR data. *Photogramm Eng Remote Sens* 73:517–535
- Congalton R, Green K (2009) *Assessing the accuracy of remotely sensed data: principles and practices*. Taylor & Francis Group, Boca Raton
- Devillers R, Jeansoulin R (eds) (2006) *Fundamentals of spatial data quality*. ISTE, London
- Forlani G, Nardinocchi C, Scaioni M, Zingaretti P (2006) Complete classification of raw LiDAR data and 3D reconstruction of buildings. *Pattern Anal Appl* 8:357–374
- Forshaw MRB, Haskell A, Miller PF, Stanley DJ, Townshend JRG (1983) Spatial resolution of remotely sensed imagery: a review paper. *Int J Remote Sens* 4(3):497–520
- Fritz LW (1996) The Era of commercial earth observation satellites. *Photogramm Eng Remote Sens* 1:39–45
- Groot R, McLaughlin J (eds) (2000) *Geospatial data infrastructure: concepts, cases and good practice*. Oxford University Press, New York
- Guelman M, Ortenberg F (2009) Small satellite's role in future hyperspectral earth observation missions. *Acta Astronaut* 64:1252–1263
- Haala N, Brenner C (1999) Extraction of buildings and trees in urban environments. *ISPRS J Photogramm Remote Sens* 54:130–137
- Ho C, Robinson A, Millerm D, Davis M (2005) Overview of sensors and needs for environmental monitoring. *Sensors* 5:4–37

- Jensen JR (2005) *Introductory digital image processing: a remote sensing perspective*, 3rd edn. Prentice-Hall, Upper Saddle River
- Joseph G (2000) How well do we understand earth observation electro-optical sensor parameters? *ISPRS J Photogramm Remote Sens* 55:9–12
- Kiema JBK (2001) *Multi-source data fusion and image compression in urban remote sensing*. Doctor of engineering. Dissertation, University of Karlsruhe. ISBN3-8265-9312-X. Shaker Verlag, pp 130
- Kokkas N (2005) *City modeling and building reconstruction with Socet Set v.5.2* BAE Systems. Customer presentation at the 2005 GXP regional user conference. Cambridge, England, pp 19–21
- Konecny G (2003) *Geoinformation: Remote sensing, photogrammetry*, Geographic Information Systems. Taylor and Francis, London
- Kramer HJ, Cracknell A (2008) An overview of small satellites. *Int J Remote Sens* 29:4285–4337
- Kumi-Boateng B (2012) *A spatio-temporal based estimation of vegetation changes in the Tarkwa mining area of Ghana*. Doctor of philosophy. Dissertation, University of Mines and Technology, Ghana, pp 165
- Kussul N, Shelestov A, Skakun S (2009) Grid and sensor web technologies for environmental monitoring. *Earth Sci Inform* 2(1–2):37–51
- Lee DH, Lee KM, Lee SU (2008) Fusion of LiDAR and imagery for reliable building extraction. *Photogramm Eng Remote Sens* 74:215–225
- Liu X (2008) Airborne LiDAR for DEM generation: some critical issues. *Prog Phys Geogr* 32(1):31–49. doi:[10.1177/0309133308089496](https://doi.org/10.1177/0309133308089496)
- Ma R (2005) DEM generation and building detection from lidar data. *Photogramm Eng Remote Sens* 71(7):847–854
- McCoy R (2005) *Field methods in remote sensing*. The Guilford Press, New York 158p
- Miliareisis G, Kokkas N (2007) Segmentation and object-based classification for the extraction of the building class from LiDAR DEMs. *Comput Geosci* 33:1076–1087
- Murai S (2004) *Remote sensing and GIS courses—distance education*, Japan International Cooperation Agency (JICA)-Net
- Phinn SR (1998) A framework for selecting appropriate remote sensed data dimensions for environmental monitoring and management. *Int J Remote Sens* 19:3457–3463
- Popescue SC, Wynne RH, Nelson RF (2003) Measuring individual tree crown diameter with LiDAR and assessing its influence on estimating forest volume and biomass. *Can J Remote Sens* 29:564–577
- Porter J, Arzberger P, Braun H, Brynat P, Gage S, Hansen T, Lin C, Lin F, Kratz T, Michener W, Shapiro S, Williams T (2005) *Wireless sensor networks for ecology*. *BioScience* 55:561–572
- Quattrochi DA, Goodchild MF (1997) *Scale in remote sensing and GIS*. Lewis Publishers, New York
- Ramapriyan HK (2002) *Satellite imagery in earth science applications*. In: Castelli V, Bergman LD (eds) *Image databases search and retrieval of digital imagery*. Wiley, Chichester
- Renslow M, Greenfield P, Guay T (2000) *Evaluation of multi-return LiDAR for forestry applications*. Project report for the inventory and monitoring steering committee, RSAC-2060/4810-LSP-0001-RPT1
- Schenk T, Csatho B (2002) Fusion of lidar data and aerial imagery for a more complete surface description. *Archives of photogrammetry*
- Schiewe J (1998) Experiences from the MOMS-02-Project for future developments. *Intl Arch Photogramm Remote Sens* 32:533–539
- Secord J, Zakhor A (2007) Tree detection in urban regions using aerial lidar and image data. *IEEE Geosci Remote Sens Lett* 4:196–200
- Sohn G, Dowman I (2005) Data fusion of high-resolution satellite imagery and LiDAR data for automatic building extraction. *ISPRS J Photogramm Remote Sens* 62(1):43–63
- Voss M, Sugumaran R (2008) Seasonal effect on tree species classification in an urban environment using hyperspectral data, LiDAR, and an object-oriented approach. *Sensors* 8:3020–3036

- Webster TL, Forbes DL, Dickie S, Shreenan R (2004) Using topographic LiDAR to map flood risk from storm-surge events for Charlottetown, Prince Edward Island, Canada. *Can J Remote Sens* 30:64–76
- Weng Q (2010) *Remote sensing and GIS integration: theories, methods, and applications*. McGraw-Hill, New York, p 416
- Xue Y, Li Y, Guang J, Zhang X, Guo J (2008) Small satellite remote sensing applications—history, current and future. *Int J Remote Sens* 29:4339–4372

Chapter 9

Microwave Remote Sensing

*“The most beautiful thing we can experience is the mysterious.
It is the source of all true art and all science.”*

Albert Einstein (1879–1955)

9.1 Principles of Microwave Remote Sensing

9.1.1 Basic Concept

Persistent cloud cover, especially within the tropics, offers limited clear views of the Earth’s surface from space. This presents a major impediment to the application of optical remote sensing discussed in Chap. 8 in providing global remote sensing coverage. Moreover, other than thermal sensors, most other optical imaging technologies best operate during day time when there is sufficient sunlight. The microwave region of the EM spectrum represents a principal atmospheric window that can be employed to overcome the above limitations in optical remote sensing. For instance, in view of their much longer wavelengths and contrary to optical sensors, microwaves can easily penetrate through vegetation canopies and even dry soils. In addition, microwave systems offer the user more choice and control over the properties of the incident microwave energy to be applied. Furthermore, they can be operated round the clock even under rainy or poor visibility conditions.

Additionally, whereas optical sensors image only the surface elements of the landscape, microwave image contains volumetric and sub-surface information as well. It is also possible to generate different microwave images with different information content from the same basic dataset by simply altering the wavelength (or frequency) and the polarization of the transmitted and received microwave signals. Thus there is more imaging variety with microwave remote sensing than with optical remote sensing. Against the above background, microwave remote sensors have continued to

be deployed for topographic mapping, landscape change detection and 3D modeling in many parts of the world, especially those regions that cannot be periodically and effectively mapped using optical imaging technologies.

However, Richards (2009) reckons that understanding microwave remote sensing is more difficult than optical remote sensing. This is largely because the technology itself is more complicated and the image data recorded more varied. Consequently, the level of mathematics involved can be fairly complex. With a wide disparity in wavelength between microwave and optical radiation, imaged targets appear different over these two EM bands. In many practical situations, however, microwave image data has been used to complement optical image data, with many operational remote sensing solutions leveraging from the synergy of both systems.

This chapter is intended to give the reader a fairly basic understanding of imaging radar technology. More comprehensive treatment of microwave remote sensing is available in the literature. For example, the three volumes by Ulaby et al. (1981a, b, 1986) provide a comprehensive treatment of the theory of microwave sensing. Besides detailing theoretical concepts, most later works on the subject also focused on applications, see e.g., Henderson and Lewis (1998), Richards (2009). Woodhouse (2006) considers both passive and radar remote sensing, while Wang (2008) adopts a signal processing approach in discussing the theory of microwave remote sensing. There are also many references that focus on specific advancements in microwave technology such as radar interferometry, see e.g., Hanssen (2001), Ferretti et al. (2007) and radar polarimetry, see e.g., Ulaby and Elachi (1990), Massonnet and Souyris (2008), Mott (2007).

As described in Sect. 7.2, microwave is defined as electromagnetic radiation with wavelength ranging from 1 mm to 1 m or frequency ranging from 0.3 GHz (corresponding to 1 m wavelength) to 300 GHz (corresponding to 1 mm wavelength). There are two basic types of microwave remote sensing namely; passive and active microwave remote sensing. Passive microwave remote sensors detect and record microwave radiation emitted from targets. To enable them accomplish this, they usually incorporate a microwave radiometer. On the other hand, active microwave remote sensors detect and record backscattering reflected from transmitted microwave radiation incident upon targets on the ground. To measure this active microwave remote sensors integrate several equipments including microwave radar, microwave scatterometer and microwave altimeter. Passive microwave remote sensing employs a wider range of microwave radiation than active microwave remote sensing. Active microwave remote sensors operate between the microwave band width popularly referred to as the K, X, C, L and P bands as shown in Fig. 9.1. For example, the GNSS techniques discussed in Chaps. 4–6 employ the L-band microwave range, while the gravimetric GRACE sensing satellite discussed in Sect. 20.3.3 uses the K-band microwave.

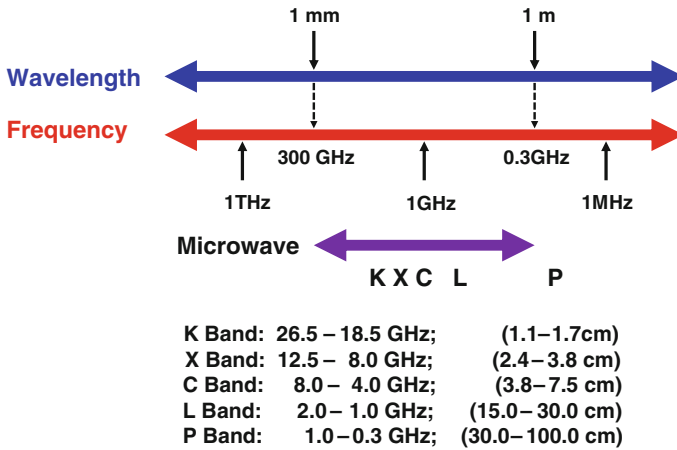


Fig. 9.1 Microwave bands

9.1.2 Radar Backscattering

As shown in Fig. 9.2, different types of radar backscattering or radar return can be distinguished. A detailed discussion of these is given in Richards (2009). The total amount of radar return will depend on both instrumental parameters, such as wavelength, polarization and incidence/look angle, as well as target parameters, such as dielectric constant, surface roughness, moisture content and local incidence angle. *Surface scattering* is usually diffuse scattering that occurs on the surface of a target. Closely allied to this is *sub-surface scattering* that is from reflection near the subsurface due to the penetration ability of microwaves. Of the various factors that influence surface scattering, roughness of a target is the most important one.

Hard targets that include metallic targets like cars, ships, railway tracks, power lines, bridges, industrial plants, corrugated iron sheet roofs etc., exhibit very strong radar return due to their high dielectric constant in the microwave frequency range. Similarly, because of double specular reflection on vertical targets, *corner reflectors*, such as tall buildings, walls etc., result in high radar return when facing towards the sensor. However, they backscatter very low return when facing away from the sensor as they are in radar shadow (see Sect. 9.3). On the other hand, *specular surfaces*, which comprise targets like still water bodies, roads, highways, pavements etc., reflect virtually all incident microwave radiation resulting in very low radar return.

Volume scattering is scattering that occurs within the target itself, and usually consists of multiple bounces and reflections from different components within the target. This happens when microwave radiation passes through relatively soft media such as cloud, rain drops, trees, forests etc. The result is either random, directional or uneven scattering as shown in Fig. 9.2. Classical volume scattering occurs when microwave radiation passes through rain drops in the atmosphere. In this case, the

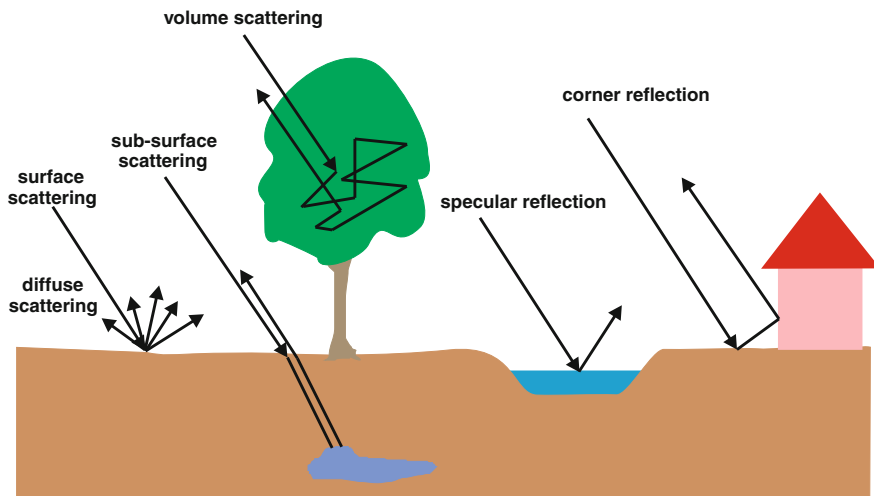


Fig. 9.2 Typical scattering mechanisms

amount of volume scattering recorded will depend on the size of the rain droplets and the intensity of the rainfall itself.

9.1.3 Attenuation of Microwave Signals

As described in Sect. 7.2, the blocking effect or attenuation of incident electromagnetic energy is manifested through the absorption characteristics of the atmosphere. Whereas this is generally considered to be a major impediment in remote sensing, since it delimits the range of principal atmospheric windows, attenuation of microwave is, however, an important factor in the study of atmospheric gases like water vapour, oxygen, ozone etc. (see Sect. 20.2). The amount of attenuation recorded varies depending on the frequency (wavelength) of the microwave as shown in Fig. 9.3a. In general, the higher the intensity of the rainfall the higher the attenuation as shown in Fig. 9.3b. It is based on this understanding and taking cognizance of volume scattering of rain drops that precipitation radars, like that found in the Tropical Rainfall Measuring Mission¹ (TRMM) are designed.

¹ TRMM orbits at an altitude of ≈ 403 km with an inclination of 50° completing 16 revolutions every day. It is designed to monitor and study tropical rainfall in the latitude range $\pm 50^\circ$ over inaccessible areas such as the oceans and un-sampled terrains. The primary instruments contained in TRMM include the microwave imager (TMI), the precipitation radar (PR) and the visible and infrared radiometer System (VIRS) (Kummerow et al. 1998).

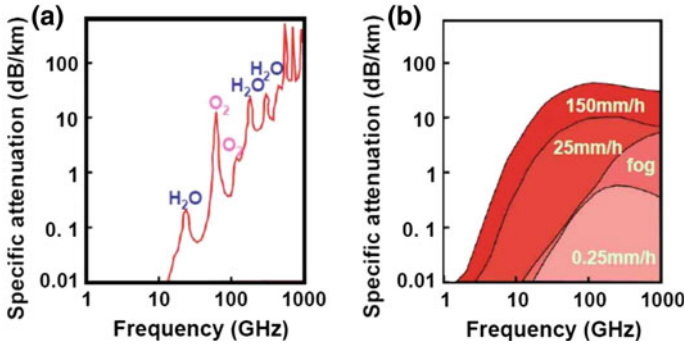


Fig. 9.3 Microwave absorption in the atmosphere. Source Murai (2004)

9.2 Structure of Microwave Systems

9.2.1 Microwave Antenna

Antennae are basic instruments in the structure of any microwave system. In general, the design of antenna for active microwave sensors is different from that for passive microwave sensors. Figure 9.4 shows the radiation pattern of an antenna with respect to the incident angle. It comprises of a main lobe in the central region which represents the main gain for the antenna. However, there are always side lobes on either lateral direction, which produce some sort of noise. The beam width is specified as a range of the main lobe with less than 3 dB in radiation power.

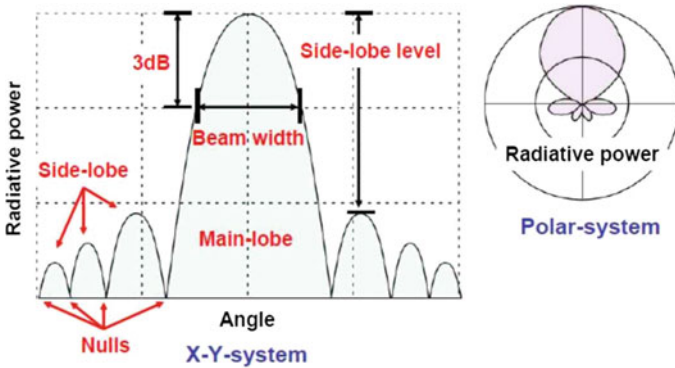


Fig. 9.4 Radiation pattern of an antenna. Source Murai (2004)

Table 9.1 Types of microwave sensors and their application

Sensor	Instrument	Target
Passive sensor	Microwave radiometer	Sea surface temperature, ozone, aerosol, NO _x
Active sensor	Microwave scatterometer	Soil moisture, surface roughness, biomass
	Microwave altimeter	Sea surface topography, geoid, ocean wave height, wind velocity
	Imaging radar	Image of surface, topography and geology

Source Murai (2004)

9.2.2 Microwave Sensors

Table 9.1 presents a summary of the major types of microwave sensors and some of their typical applications. Passive microwave sensors employ microwave radiometers and measure sea surface temperature, ozone, aerosol, NO_x etc. Most active microwave sensors use a combination of instruments comprising of scatterometers, altimeters and imaging radars. Microwave scatterometers are employed to measure soil moisture, surface roughness, biomass etc. Micrometer altimeters are used to measure sea surface topography, geoid, ocean wave height, wind velocity etc., while imaging radars are employed in imaging surface topography, geology etc. The remainder of this chapter focuses on imaging radars. Some examples of microwave sensors on-board satellites is shown in Table 9.2.

Table 9.2 Examples of some microwave sensors

Satellite	Sponsor	Sensor	Year launched
SEASAT-1	USA	SMMR, ALT, SAR	1978
ERS-1	ESA	AMI, RA	1991
ERS-2		ATSR/M	1995
JERS-1	Japan	SAR	1992
RADARSAT-1	Canada	SAR	1995
RADARSAT-2			2007
TRMM	Japan/USA	TMI, PR	1997
ALMAZ-1B	Russia	SAR-10 SAR-70	1998
Aqua	Japan/USA	AMSR-E, AMSU	1999/2000/2002/2006
SRTM	USA	SIR-C/X-SAR	2000
ENVISAT-1	ESA	ASAR, MWR, RA-2	2002
ALOS	Japan	PALSAR	2006
TerraSAR-X	Germany	X-SAR	2007
TanDEM-X			2010

Modified after Murai (2004)

9.3 Radar Imaging and Geometry of SAR

Two distinct types of radar imaging can be distinguished, namely; *Side Looking Aperture Radar (SLAR)* and *Synthetic Aperture Radar (SAR)*. Side Looking Aperture Radar, popularly referred to as *Real Aperture Radar*, is the classical radar with real aperture antenna. As discussed in Sect. 9.2.1, the footprint or resolution of radar imagery depends primarily on the size of the antenna. The larger the antenna is, the higher the resolution and vice-versa. Figure 9.5a is a schematic illustration of the operation of a SLAR. The resolution of the radar image is defined by the pulse length in the range direction, which is orthogonal to the flight direction, and the beam width in the azimuth direction, that is parallel to the flight direction as shown in the figure.

On the other hand, SAR was developed to mimic a desirable long antennae. This is in view of the practical limitation of expanding the size of the real aperture antennae beyond a certain threshold. Basically, SAR operates by simulating a long antennae as illustrated in Fig. 9.5b. This virtual effect is realized through the *Doppler effect* and allows the small antennae with a real and finite beam width (D) to transmit microwave beams in different travel times along the beam width. The result is the creation of a radar image with higher resolution as though a large real aperture antennae was employed. This is shown as the synthetic aperture (L_s) in Fig. 9.5b. Because of this capability, SAR is the more common imaging technology applied in most practical radar applications today.

SAR imaging is achieved through scanning performed by the antennae in a direction orthogonal to the flight/azimuth direction. The scanning width depends on the magnitude of the off-nadir angle. Slant-range distortion occurs since the radar is measuring the distance to features in slant-range rather than the true horizontal distance along the ground (Wolff 2012). This results in image scale difference that varies from near to far range. Three distinct distortion types can be distinguished, namely; *foreshortening*, *layover* and *shadow*. Foreshortening arises when the radar beam reaches the base of a tall feature tilted towards the radar (e.g., a mountain) before it reaches the top as shown in Fig. 9.6a. Consequently, the slope (from point a to point b) will appear compressed and the length of the slope will be represented incorrectly (a' to b') at the image plane.

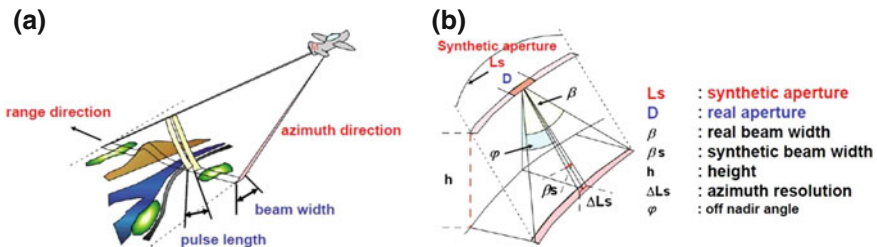


Fig. 9.5 Principle of radar imaging. a Side looking aperture radar (SLAR). b Synthetic aperture radar (SAR) (Source Murai 2004)

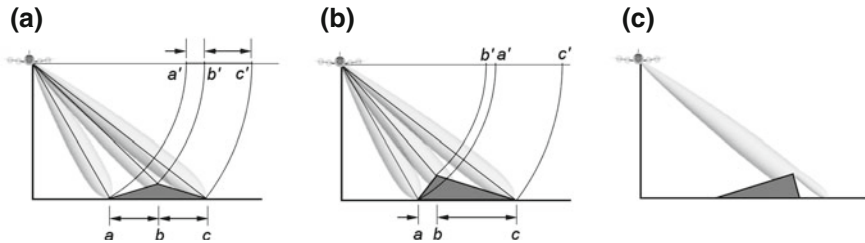


Fig. 9.6 Geometric distortions on radar imagery: **a** foreshortening, **b** layover, **c** shadowing. *Source* Wolff (2012)

Layover occurs when the radar beam reaches the top of a tall feature (b) before it reaches the base (a). The return signal from the top of the feature will be received before the signal from the bottom. As a result, the top of the feature is displaced towards the radar from its true position on the ground, and “lays over” the base of the feature (b' to a') (Wolff 2012). This effect is illustrated in Fig. 9.6b. Radar shadowing occurs when the microwave signals are obscured by terrain topography from hitting the target as shown in Fig. 9.6c. In general, areas with layover and foreshortening have strong radar returns, with no radar return recorded in regions covered by radar shadows.

9.4 Image Reconstruction of SAR Data

The acquisition and processing of SAR data represents not only a fairly complex process, but one that also usually requires considerable time to complete successfully. Indeed, this presents one of the challenges of radar imaging. Similar to the output from all other coherent imaging systems, radar imagery is characterized by noise in the form of *speckle* or “*salt and pepper*” texture. This granular noise is caused by random constructive and destructive interference generated from multiple scattering return that occurs within each SAR resolution cell. Speckle is a direct consequence of the superimposition of the signals re-irradiated by many small elementary scatterers within the resolution cell (Ferretti et al. 2007). Speckle in SAR images complicates the image interpretation problem by reducing the effectiveness of image segmentation and classification. To alleviate deleterious effects of speckle, various ways have been devised to suppress it including use of spatial filtering algorithms (see e.g., Lee et al. 1994; Mueller and Hoffer 1989; Rio 2000), or multi-look processing (see e.g., Lee et al. 1994, 1999; Shi and Fung 1994).

Once the speckle effect has been dealt with, the SAR image can then be reconstructed. This is realized through two basic steps. Firstly, geocoding of the SAR data is performed. This refers to the migration of radar return from an azimuth-range coordinate system, in which it was acquired, into a conventional geo-referenced coordinate system. Secondly, SAR reconstruction also includes the equalization of topographic imaging effects of layover, foreshortening and radar shadow. This is synonymous

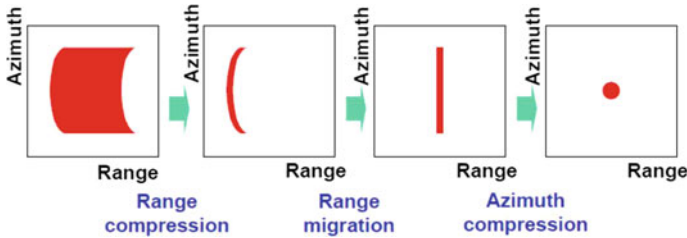


Fig. 9.7 Geocoding of SAR data. Source Murai (2004)

to the correction of various geometric distortions inherent in the radar imagery (see Fig. 9.6, p. 140). Back to SAR geocoding, this is accomplished through various stages as shown in Fig. 9.7. Firstly, *range compression* is performed to obtain compressed SAR data in the range direction. This is followed by rearrangement of the compressed data in the range direction through a process called *range migration*. Finally, *azimuth compression* is carried out which results in the final geocoded SAR data.

9.5 Interferometric SAR

Interferometry is a method of estimating terrain heights using radar that essentially relies on the ability to measure the phase difference of microwaves. In principle, interferometric systems employ two antennas, separated in the range dimension by a small distance, both recording the returns from each resolution cell (CCRS 2012). The two antennas can either be on-board the same platform, as is the scenario with some airborne SARs. Alternatively, interferometric SAR (InSAR) can be acquired from two different passes made with the same sensor, or even from different sensors, as is the case with either airborne or satellite radars. As an example of single-pass interferometry, SRTM² from the USA was outfitted with two radar antennas, one located in the Shuttle’s payload bay and the other at the end of a 60 m mast. Similarly, as an example of two-pass interferometry realized from two distinct radar sensors, TanDEM-X³ from Germany operates together with its sister satellite TerraSAR-X in a cross-track orbit configuration that is closely controlled to allow the two satellites to record data synchronously.

From measurement of the exact phase difference between the two returns, the difference in the path length can be estimated to within an accuracy of the order of the wavelength (i.e., centimeters). Knowing the position of the antennas with respect to the Earth’s surface from Global Navigation Satellite Systems (GNSS), the position of the resolution cell, including its elevation, can be determined (CCRS 2012). Using the phase difference between adjacent resolution cells, different colors

² shuttle radar topographic mission (<http://www2.jpl.nasa.gov/srtm/>).

³ <http://www.dlr.de/eo/en/desktopdefault.aspx/>

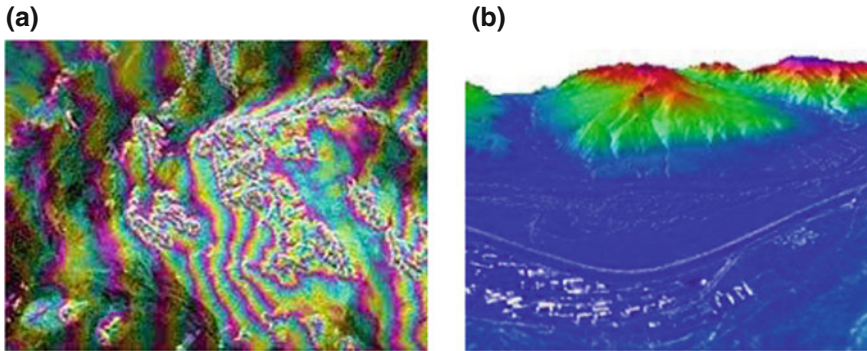


Fig. 9.8 Example of InSAR. **a** The phase difference between adjacent resolution cells is illustrated in this interferogram, with different colors representing variations in height. **b** The information contained in an interferogram can be used to derive topographic information and produce 3D imagery of terrain height. *Source* CCRS (2012)

can be employed to represent variations in height as exemplified in Fig 9.8a. This can then be interpolated to generate a Digital Elevation Model (DEM), otherwise referred to as an *interferogram* or InSAR DEM as shown in Fig. 9.8b. Differential SAR interferometry (DInSAR) can be generated from either interferograms obtained with differential temporal gaps or from coherent topographic interferograms (Mora et al. 2006; Ferretti et al. 2007). DEMs derived from InSAR and DInSAR are very popular sources for height information as evidenced by the numerous applications outlined in Part V of this book.

9.6 SAR Polarimetry

As discussed in Sect. 9.1.1, compared to optical sensors, microwave sensors definitely offer more variety. Radar polarimetry is a typical example of the diversity that is possible with microwave sensors. Essentially, this involves discriminating between the polarizations that a radar system is able to transmit and receive. Most conventional radars transmit microwave radiation in either horizontal (H) or vertical (V) polarization, and similarly receive the backscattered signal at only one of these polarizations. However, multi-polarization radars are able to transmit either H or V polarization and receive both the like- and cross-polarized returns (e.g., HH and HV or VV and VH, where the first letter stands for the polarization transmitted and the second letter the polarization received).

On the other hand, polarimetric radars are able to transmit and receive both horizontal and vertical polarizations. Thus, they are able to receive and process all four combinations of these polarizations: HH, HV, VH, and VV. Each of these “polarization channels” have varying sensitivities to different surface characteristics and properties (CCRS 2012). Hence, resulting imagery will contain different information

content. Consequently, availability of SAR polarimetric data helps to improve the identification of, and the discrimination between features. In addition to recording the magnitude (i.e., the strength) of the returned signal for each polarization, most polarimetric radars are also able to record the phase information of the returned signals. This can be used to further characterize the “polarization signature” or “polarization response plots” thus providing a convenient way of distinguishing and visualizing a target’s scattering properties (CCRS 2012).

Polarimetric SAR has proved useful in several applications including (CCRS 2012): agriculture (for crop type identification, crop condition monitoring, soil moisture measurement, and soil tillage and crop residue identification); forestry (for clear-cuts and linear features mapping, biomass estimation, species identification and fire scar mapping); geology (for geological mapping); hydrology (for monitoring wetlands and snow cover); oceanography (for sea ice identification, coastal wind-field measurement, and wave slope measurement); shipping (for ship detection and classification); coastal zone (for shoreline detection, substrate mapping, slick detection and general vegetation mapping) etc.

9.7 Concluding Remarks

Compared to optical sensors, radar exhibit much longer wavelengths. Hence, unlike optical sensors, microwaves can easily penetrate through targets such as vegetation canopies and even dry soils. In addition, microwaves operate within a much broader EM spectrum that extends between 1 mm and 1 m compared to optical sensors, which function within a very narrow wavelength band of between 0.4 μm to 1 mm. Moreover, whereas optical sensors detect and record only the surface elements of the landscape, radar imagery captures volumetric and sub-surface information as well.

In a nutshell, microwave sensors offer more imaging possibilities and variety than their optical counterparts. However, microwave remote sensing remains more difficult to understand than optical remote sensing. This is basically due to the fact that the technology itself is more complicated and the image data recorded more varied. Against this backdrop, there is need to draw synergy by integrating both microwave and optical remote sensing technologies. This would create a comprehensive imaging tool that is not only versatile, but flexible enough to handle varying user needs in different remote sensing applications.

References

- CCRS (2012) Canada Centre for Remote Sensing tutorial. <http://www.nrcan.gc.ca/earth-sciences/geography-boundary/remote-sensing/fundamentals/>. Accessed 24 July 2012
- Ferretti A, Monti-Guarnieri A, Prati C, Rocca F, Massonnet D (2007) InSAR principles: guidelines for SAR interferometry processing and interpretation. ESA Publications, Ithaca

- Hanssen RF (2001) Radar interferometry: data interpretation and error analysis. Remote sensing and digital image processing book series, vol 2. Kluwer Academic, Dordrecht
- Henderson FM, Lewis AJ (eds) (1998) Principles and applications of imaging radar. Manual of remote sensing, vol 2, 3rd edn. Wiley, New York
- Kummerow C, Barnes W, Kozu T, Shiue J, Simpson J (1998) The tropical rainfall measuring mission (TRMM) sensor package. *J Atmos Oceanic Technol* 15(3):809–817
- Lee J-S, Jurkevich L, Dewaele P, Wambacqb P, Oosterlinck A (1994) Speckle filtering of synthetic aperture radar images: a review. *Remote Sens Rev* 8(4):313–340. doi:[10.1080/02757259409532206](https://doi.org/10.1080/02757259409532206)
- Lee J-S, Grunes MR, de Grandi G (1999) Polarimetric SAR speckle filtering and its implication for classification. *IEEE Trans Geosci Remote Sens* 37(5):2363–2373
- Lee J-S, Miller AR, Hoppel KW (1994) Statistics of phase difference and product magnitude of multi-look processed Gaussian signals. *Waves in random media*, pp 307–319. doi:[10.1088/0959-7174/4/3/006](https://doi.org/10.1088/0959-7174/4/3/006)
- Massonnet D, Souyris J-C (2008) Imaging with synthetic aperture radar, EPFL. Taylor and Francis, Boca Raton
- Mora O, Arbiol R, Pala V, Adell A, Torre M (2006) Generation of accurate DEMs using DInSAR methodology (TopoDInSAR). *IEEE Geosci Remote Sens Lett*. doi:[10.1109/LGRS.2006.879563](https://doi.org/10.1109/LGRS.2006.879563)
- Mott H (2007) Remote sensing with polarimetric radar. IEEE Press Wiley, Hoboken
- Mueller PW, Hoffer RN (1989) Low-pass spatial filtering of satellite radar data. *Photogram Eng Remote Sens* (ISSN 0099-1112) 55:887–895
- Murai S (2004) Remote sensing and GIS courses —distance education. Japan International Cooperation Agency (JICA)-Net
- Richards JA (2009) Remote sensing with imaging radar. Springer, Berlin
- Rio JNR (2000) Spatial filtering of radar data (RADARSAT) for wetlands (brackish marshes) classification. *Remote Sens Environ* 73(2):143–151
- Shi Z, Fung KB (1994) A comparison of digital speckle filters, Geoscience and remote sensing symposium, 1994. IGARSS '94. *Surf Atmos Remote Sens: Technol Data Anal Interpret* 4:2129–2133
- Ulaby FT, Elachi C (eds) (1990) Radar polarimetry for geoscience applications. Artech House, Norwood
- Ulaby FT, Moore RK, Fung AK (1981a) Microwave remote sensing: active and passive. radar remote sensing and surface scattering and emission theory, vol 2. Addison-Wesley, Reading
- Ulaby FT, Moore RK, Fung AK (1981b) Microwave remote sensing: active and passive. Microwave remote sensing and fundamentals. Vol 1, Addison-Wesley, Reading
- Ulaby FT, Moore RK, Fung AK (1986) Microwave remote sensing: active and passive, Volume scattering and emission theory, advanced systems and applications, vol 3. Addison-Wesley, Reading
- Wang BC (2008) Digital signal processing techniques and applications in radar image processing. Wiley, Hoboken
- Wolff C (2012) Radar tutorial. <http://www.radartutorial.eu/20.airborne/ab07.en.html>. Accessed 26 Oct 2012
- Woodhouse IH (2006) Introduction to microwave remote sensing. Taylor and Francis, Boca Raton

Chapter 10

Image Interpretation and Analysis

“A decision is as good as the information that goes into it.”

John F. Bookout, Jr.

10.1 Introductory Remarks

The *interpretation and analysis* of remote sensing imagery involves the identification and/or measurement of various targets or objects in an image in order to extract useful information about them. More specifically, this seeks to extract qualitative (thematic) and quantitative (metric) information from remote sensing data. Qualitative information provides descriptive data about earth surface features like structure, characteristics, quality, condition, relationship of and between objects.

Themes can be as diversified as areas of interest, such as soil, vegetation, and land cover. This may be obtained through either visual image interpretation or computer-based digital image processing. On the other hand, metric information includes location, height, and their derivatives such as area, volume, shape, slope angle etc. Metric information is usually extracted through photogrammetry as discussed in Sect. 11.33 and GNSS discussed in Chaps. 4–6. Many textbooks have tackled the subject of pattern recognition and image analysis sufficiently well, see e.g., Jensen (2005), Richards (1994), Schowengerdt (2007) etc.

As shown in Table 10.1, some of the merits of *visual image interpretation* include the fact that the interpreter’s knowledge is available and understanding of complex images is significantly easier and better. The demerits of visual interpretation include the fact that it can be quite time consuming and human knowledge is not easy to apply. In addition, the results of visual interpretation may also vary with different interpreters as this is a relatively subjective process.

On the other hand, the merits of *digital image analysis* include the relative short processing time required, ability for standardized processing and the fact

Table 10.1 Human interpretation versus digital image processing

Method	Merits	Demerits
Human image interpretation	<ul style="list-style-type: none"> ● Interpreter's knowledge available ● Understanding of complex images is better 	<ul style="list-style-type: none"> ● Time consuming ● Human knowledge is not easy to apply
Digital image processing	<ul style="list-style-type: none"> ● Short processing time ● Standardized processing ● Extraction of physical quantities is possible 	<ul style="list-style-type: none"> ● Human knowledge is difficult to apply ● Contextual information is poor

that extraction of physical quantities like temperature and elevation is possible. The demerits of computer-based image processing includes the fact that human knowledge is hard to apply, while contextual information extraction is poor.

10.2 Visual Image Interpretation

Colwell (1997) defines *photographic interpretation* as the act of examining aerial photographs/images for the purpose of identifying objects and judging their significance. When interpreting or analyzing an image through visual methods two scenarios may arise: (i) direct and spontaneous recognition or (ii) logical inference. Direct and spontaneous recognition refers to the ability of an interpreter to identify objects or phenomena at a first glance. In logical inference, several cues are used in a reasoning process to draw conclusions. The degree of success in the inference depends on the interpreter's professional knowledge and experience as well as the quality of the photographic imagery.

Several basic elements, commonly referred to as interpretation elements or cues, are used in photographic/image interpretation: (1) tone/color, (2) size, (3) shape, (4) texture, (5) pattern, (6) shadow, and (7) association. *Tone* refers to the relative brightness or color of objects in an image. Tone/color is the most important element in photographic/image interpretation. The more light received, the lighter is the image on the photograph. Thus, water, which absorbs nearly all incident light, appears black, whereas a concrete highway which reflects a high percentage of light produces very light tones. Variations in tone also allows the elements of shape, texture, and pattern of objects to be distinguished.

Size provides another important clue in discrimination of objects and features. The size of objects in an image is a function of scale. It is important to assess the size of a target relative to other objects in a scene, as well as the absolute size, to aid in the interpretation of that target. A quick approximation of target size can lead to direct interpretation of an appropriate result more quickly. For example, if an interpreter had to distinguish zones of land use, and had identified an area with

a number of buildings in it, large buildings such as factories or warehouses would suggest industrial use, whereas small buildings would indicate residential use.

Shape refers to the general form, structure, or outline of individual objects. Shape can be a very distinctive clue for interpretation. Generally speaking, whereas human-made features often exhibit straight edges, natural features tend to be more crispy. Straight edge shapes typically represent urban or agricultural (field) targets, while natural features, such as forest edges, are generally more irregular in shape, except where man has created a road or clear cuts. Moreover, a railway may be distinguished from a highway because its shape consists of long straight tangents and gentle curves as opposed to the curvy shape of a highway.

Texture describes the arrangement and frequency of tonal variation in particular areas of an image. Rough textures would consist of a mottled tone where the gray levels change abruptly in a small area, whereas smooth textures would have very little tonal variation. Smooth textures are most often the result of uniform, even surfaces, such as fields, asphalt, or grasslands. *Pattern* refers to the spatial arrangement of visibly discernible objects. Typically an orderly repetition of similar tones and textures will produce a distinctive and ultimately recognizable pattern.

Shadow is also helpful in interpretation as it may provide an idea of the profile and relative height of a target or targets which may make identification easier. However, shadows can also be an impedance to interpretation. For instance, targets that are obscured by shadows are much less (or not at all) discernible from their surroundings. *Association* is a contextual element that takes into account the relationship between other recognizable objects or features in proximity to the target of interest. The identification of features that one would expect to associate with other features may provide information to facilitate identification. Some features are always associated with one another. Indeed, association is one of the most helpful clues in identifying human-made installations.

Besides the above elements, *stereoscopic information* is also critical for successful visual image interpretation, as it allows the perception of depth or relative variation in object heights to be appreciated in a better and more vivid manner. *Stereoscopic vision* is realized when overlapping photographs are oriented to simulate the same basic geometry or orientation that they exhibited during their acquisition (see Sect. 11.3.2). Once this is accomplished by eliminating any existing parallax a *stereo-model* is generated. *Stereoscopes* can then be employed to view the photographs stereoscopically, with the left eye viewing the left image, while the right eye views the right image.

Tone, color and stereoscopic information are referred to as primary interpretation elements. Size, shape, texture, pattern represent the spatial arrangement of tone and color. Height and shape are based on analysis of the primary elements, while association essentially defines contextual relationships between object features.

On the basis of the various interpretation elements, appropriate *interpretation keys* need to be developed. This is necessary in order to reduce the degree of subjectivity in the interpretation. The interpretation keys need to be developed *a priori*, if these do not already exist, before the commencement of the interpretation exercise. They will usually vary from one application domain to the other. In terms of the interpretation procedure itself, it is imperative to make use of existing base maps

to orient the acquired images accordingly. Use is then made of the interpretation keys to identify what the various imaged features represent or even mean semantically. The final interpretation results are then displayed on thematic maps for graphic output.

10.3 Digital Image Processing

As pointed out in Sect. 10.1, digital image analysis has certain distinct advantages over visual image interpretation. For instance, in comparison with visual interpretation, digital image processing requires a relatively short processing time, besides substantially reducing the subjectivity in the interpretation. As a matter of fact, digital image analysis is the only viable interpretation method that can be adopted in the case of *multi-sensor*, *multi-temporal* or *multi-spectral* remotely sensed image data. Given the fact that this type of remotely sensed image data has become the norm rather than the exception, it is unsurprising that digital image processing is increasing becoming the *defacto* image interpretation and analysis technique. Although developed initially based on aerial photographs, the basic elements of image interpretation are nonetheless, also applicable to digital images.

Figure 10.1 gives an overview of digital image processing. This shows that digital image processing can be grouped into: image correction (image pre-processing), image conversion (image conversion/transformation) and image classification procedures. Most classical digital image analysis methods are based on the spectral

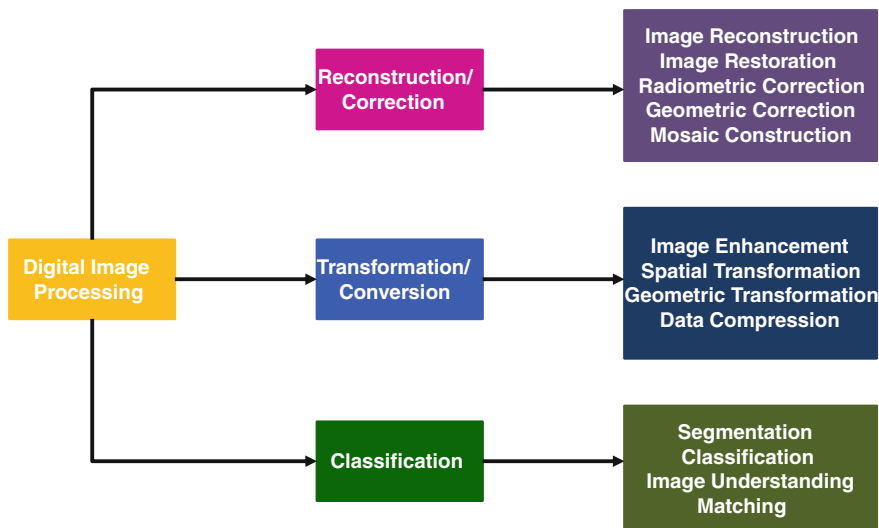


Fig. 10.1 Flow of digital image processing. Source Murai (2004)

characteristics of object features, or put differently, on the tone or color, which is represented as a digital number (i.e., brightness value) in each pixel of the digital image. However, the introduction of multi-sensor and high spatial resolution remote sensing data (see Sect. 8.3) has resulted in an expanded object feature base, beyond the classical spectral feature base, being adopted in digital image analysis. This has seen more interpretation elements like texture, size, shape and even association or contextual relationships being employed in digital image classification.

Digital image processing systems employ several hardware component revolving around either personal computer or networked configurations with several input/output peripherals being shared. This requires appropriate image input devices, image display systems, image processing software, image output systems and storage devices for image data. The image input devices will vary in operation, resolution and accuracy from mechanical, electronic, electronic/mechanical to optical scanning devices. Similarly, image display systems will also vary from the employed projection system to applied stereo viewing concept.

Image processing software varies from proprietary to public domain and open source software. Most of these software will exhibit certain basic functionality such as: file utilities (input and output of various image and vector format), image display (zooming, RGB, image enhancement), overlaying of various data, cursor locator, classification, transformation (geocoding, map projection), DEM generation, atmospheric correction, radar data processing etc. Image output devices will also vary from silver-chloride photography, electro photography, electrostatic recording, thermal transcription, ink jet, laser color plotter etc.

10.3.1 Image Reconstruction/Correction

The preliminary task in digital image processing is to ensure that the image is in digital form. This is necessary when analogue sensors are employed to acquire the image. In such cases, analogue/digital (A/D) conversion is required to convert the analogue data to equivalent digital data using appropriate equipment like a film scanner. Before the image can be transformed or converted and later classified in readiness for mapping, *image pre-processing* is required.

In principle, image pre-processing aims to correct for different types of errors, both systematic and accidental, that may have arisen out of the employment of the sensor-platform combination (imaging system), absorption and scattering characteristics of the atmosphere and due to the earth's curvature and rotation and nature of topography. Image pre-processing, which constitutes a major phase of data processing in remote sensing, includes procedures for image reconstruction, image restoration, radiometric correction, geometric correction and mosaic construction.

Radiometric distortions will arise due to variations in scene illumination and viewing geometry, atmospheric conditions, and sensor noise and response and will vary depending on the specific sensor and platform used to acquire the data and the conditions present during data acquisition. It may also be desirable to convert

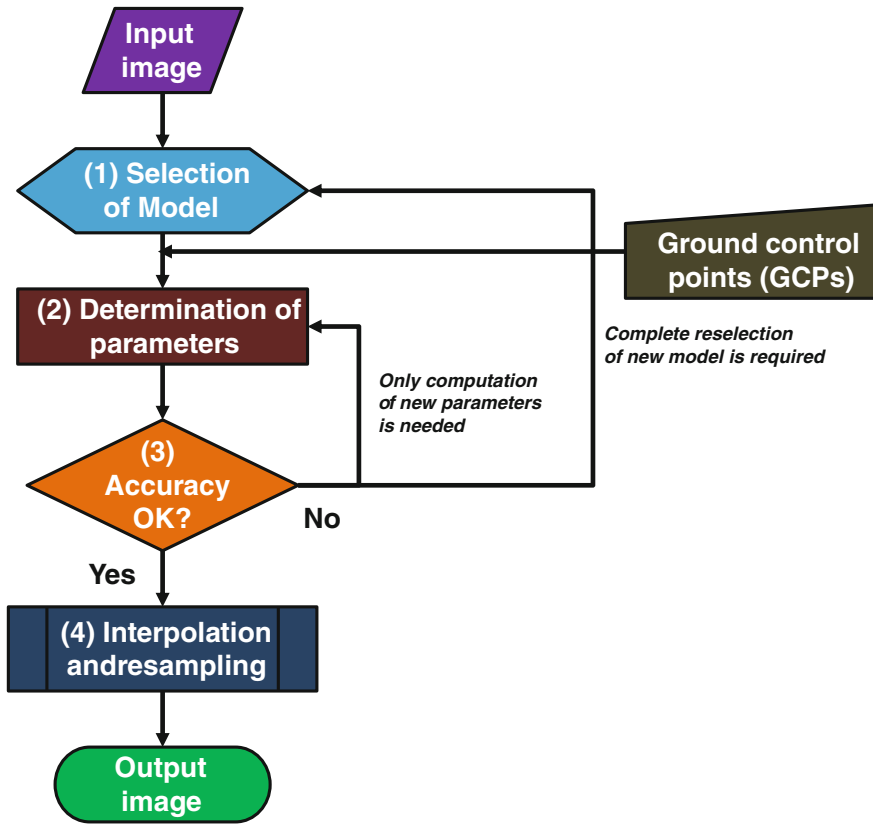


Fig. 10.2 Flowchart of geometric correction

and/or calibrate the data to known (absolute) radiation or reflectance units to facilitate comparison between different data sets. Geometric correction and atmospheric calibration represent the most important steps in image pre-processing.

Geometric distortions may result due to several factors, including: the perspective of the sensor optics; the motion of the scanning system; the motion of the platform; the platform altitude, attitude, and velocity; the terrain relief; and, the curvature and rotation of the earth. One can distinguish between two types of geometric distortions: (i) internal distortions which are geometric errors that result from the sensor's geometry and (ii) external distortions that are geometric errors emanating from platform and ground targets.

To correct for the geometric errors, registration of the imagery to a known ground coordinate system must be performed through a process referred to as *geo-referencing* as shown in Fig. 10.2. Accurate geometric rectification or image registration of remotely sensed data is a prerequisite as explained in Jensen (2005). The first step

in geometric correction requires the selection of an appropriate model like the affine transformation. Sufficient number of well identified, accurate and well distributed *ground control points* (GCPs) obtained e.g., using GNSS are then used to determine the transformation parameters through the process of *digital rectification*.

An accuracy check is then performed to assess whether the resulting errors are within prescribed tolerance levels. Interpolation and re-sampling of the input image using algorithms such as *nearest neighbor*, *bilinear*, and *cubic convolution* is then carried out resulting in the final corrected image. On the other hand, atmospheric calibration is mandatory when spatio-temporal or multi-sensor data are used (Weng 2010). Similarly, the shade effect, predominant especially in rugged or mountainous regions, through which vegetation reflectance is affected by shades caused by topography and canopy, needs to be reduced (Weng 2010).

10.3.2 Image Transformation/Conversion

10.3.2.1 Image Enhancement

The visual interpretability of the corrected or reconstructed image needs to be further enhanced through image conversion or transformation. This is usually an intermediate step after image pre-processing and before image classification and is important to facilitate thematic information extraction. Image conversion or transformation includes procedures for image enhancement, spatial transformation, geometric transformation and data compression. Image enhancement methods can be broadly grouped into three categories: (a) contrast enhancement, (b) spatial enhancement, and (c) spectral transformation.

Contrast enhancement involves changing the original values so that more of the available range of digital values is used, and the contrast between targets and their backgrounds is increased (Jensen 2005). *Histogram equalization* is a typical contrast enhancement method. Spatial enhancement applies various algorithms, such as spatial filtering, edge enhancement, and Fourier analysis, to enhance low- or high-frequency components, edges, and textures.

Major spatial filters with their effects in brackets include the following; sobel (gradient—finite differences), laplacian (differential), median (smoothing), high-pass (edge-enhancement), sharpening (clearer image) etc. Spectral transformation refers to the manipulation of multiple bands of data to generate more useful information and involves such methods as band ratioing and differencing, Principal Components Analysis (PCA), vegetation indices such as the Normalized Difference Vegetation Index (NDVI) and its associated derivatives¹ (see e.g., Omute et al. (2012)).

¹ Vegetation Condition Index (VCI), Standardized Vegetation Index (SVI), Annually Integrated NDVI (AINDVI), NDVI anomaly (NDVIA) etc.

10.3.2.2 Feature Extraction

Feature extraction is an essential first step towards subsequent thematic information extraction (Weng 2010). Many potential variables can be used in image classification. These include variables like spectral signatures, vegetation indices, transformed images, textural or contextual information, spatio-temporal images, multi-sensor images, and ancillary data (Weng 2010). Because of different capabilities in class separability, use of too many variables in a classification procedure may decrease classification accuracy (Price et al. 2002). It is therefore important to select only the critical variables that are most effective for separating thematic classes (Weng 2010).

Selection of a suitable feature extraction approach is especially necessary when hyper-spectral data are used. This is so because of the huge amount of data and the high correlations that exist among the bands of hyper-spectral imagery (Weng 2010). Moreover, a large number of training samples is required in image classification. Many feature extraction approaches have been developed such as *principal components analysis*, *minimum-noise fraction transform*, *discriminant analysis*, *decision-boundary feature extraction*, *non-parametric weighted-feature extraction*, *wavelet transform*, and *spectral mixture analysis*, see e.g., Asner and Heidebrecht (2002), Landgrebe (2003), Lobell et al. (2002), Myint (2001), Neville et al. (2003), Okin et al. (2001), Rashed et al. (2001), Platt and Goetz (2004) etc.

10.3.3 Image Classification

The objective of *image classification* is to match the *spectral classes* in the data to the respective *information classes* of interest. In this regard, information classes are defined as those categories of interest that the image analyst is actually trying to identify in the imagery, such as different kinds of crops, forest types or tree species, geologic units or rock types etc. On the other hand, spectral classes represent groups of pixels that are uniform (or near-similar) with respect to their brightness values in the different spectral channels of the data. Hence, image classification involves assigning all pixels in the image to particular information classes.

Through image classification each pixel or image area is assigned to a corresponding information class with homogeneous characteristics as shown in Fig. 10.3. The resulting classified image is comprised of a mosaic of pixels, each of which belong to a particular theme, and is essentially a *thematic map* of the original image. In practice, however, rarely does a simple one-to-one match between the information and spectral classes exist. Different classifiers employ different rationale like statistical inference to deal with uncertainty in the matching. Conceptually speaking, and from a broad perspective, image classification includes all those procedures for segmentation, classification, image understanding and matching.

Two basic types of image classifications can be distinguished namely: *supervised* and *unsupervised classifications*. In supervised classification the operator defines the clusters during the training process using data obtained from *ground truth*. Clean and

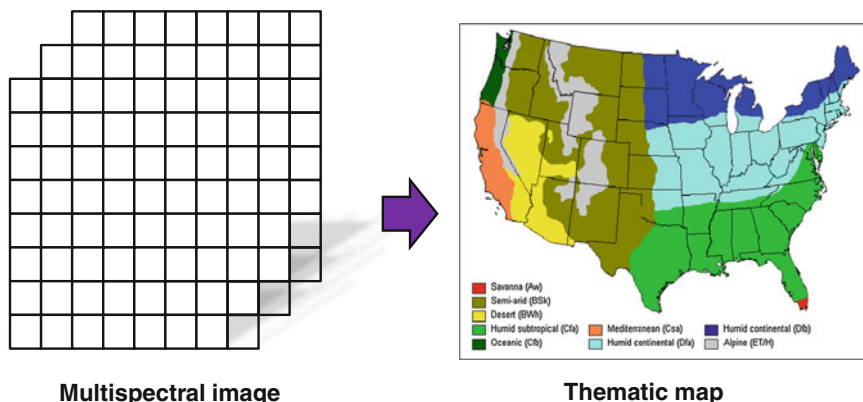


Fig. 10.3 Concept of image classification

homogeneous areas need to be identified for the training data. Unsupervised classification involves a clustering algorithm automatically determining and defining the number of clusters in the feature space using only image characteristics or features. This is often a processor intensive operation. To optimize on available computing resources, most clustering algorithms provide facility for defining the desired number of clusters *a priori*.

As mentioned before, classical image classification involves the application of only the spectral feature base in the classification, in which case only the spectral characteristics of the data is considered. Some of the popular traditional image classifiers employed in remote sensing include: *maximum likelihood*, *minimum distance*, *parallel piped*, *clustering* etc.

Increasingly, and in recent times, however, many image classifiers have tended to employ an expanded feature base that includes diverse features like multi-spectral features, multi-temporal features, texture, height information (e.g., DTM, DSM), indices (e.g., NDVI, turbidity) etc. Similarly, many advanced classification approaches from other application domains, such as *artificial neural network*, *fuzzy-set*, *knowledge-based* or *expert systems*, *contextual classifications* etc., have become widely applied for image classification. A summary of major advanced classification approaches is outlined in Weng (2010) who distinguishes different classification algorithms into: per-pixel algorithms, sub-pixel algorithms, per-field algorithms, contextual-based approaches, knowledge-based algorithms and combination approaches of multiple classifiers.

The recognition of *man-made objects* like buildings and roads from HSRI and LiDAR data offers certain challenges in digital image analysis and is worth specific mention here. For instance, these new data sources require processing functionality that is not currently standard on many systems (Poulter 1995). In general, recognition procedures for man-made objects comprise of several generic procedures including segmentation of potential candidates, reconstruction of geometric description and

attribution of description elements. Cues that are used to recognize such objects include shape description including height information, spectral signature, GIS data etc.

When combined with HSRI and/or LiDAR data, an object oriented analysis shows great potential for extracting the earth surface features, including both thematic and metric information (Weng 2010). Wilkinson (1996) asserts that in order to use this type of data, which is characterized by very high dimensionality, in combination with pre-existing GIS datasets, techniques such as virtual reality for visualization and projection pursuit for data reduction are needed. Moreover, techniques for information/pattern extraction from such remote sensing and GIS datasets and data analysis need much development, for example, self-organizing neural networks, integrated spatial and temporal representation and analysis, and data mining (Wilkinson 1996).

10.4 Concluding Remarks

Image data constitutes the basic raw material that is employed in remote sensing. This needs to be interpreted in order for useful information about the imaged targets or objects to be extracted. Such information can then be used to support the process of planning and decision making in diverse remote sensing applications. Both thematic and metric information can be extracted from remote sensing data through either visual image interpretation or digital image analysis techniques. Each of these methods has its own strengths as well as weaknesses.

However, digital image analysis is the only viable image interpretation method that can be applied in the case of multi-sensor, multi-temporal or multi-spectral image data. Given that this type of data has become the most predominant type of earth observation image data in recent times, especially in most environmental monitoring and management applications, and with the widespread penetration and advancement of observational, information, computing and communication technologies, digital image processing is poised to continue being the *defacto* image interpretation technique employed.

References

- Asner GP, Heidebrecht KB (2002) Spectral unmixing of vegetation, soil and dry carbon cover in arid regions: comparing multispectral and hyperspectral observations. *Int J Remote Sens* 23:3939-3958
- Colwell RN (1997) History and place of photographic interpretation. In: Philipson WR (ed) *Manual of photographic interpretation*. American Association of Photogrammetry and Remote Sensing, Bethesda
- Jensen JR (2005) *Introductory digital image processing: a remote sensing perspective*, 3rd edn. Prentice-Hall, Upper Saddle River
- Landgrebe DA (2003) *Signal theory methods in multispectral remote sensing*. Wiley, Hoboken

- Lobell DB, Asner GP, Law BE, Treuhaft RN (2002) View angle effects on canopy reflectance and spectral mixture analysis of coniferous forests using AVIRIS. *Int J Remote Sens* 23:2247–2262
- Murai S (2004) remote sensing and GIS courses—distance education, Japan International Cooperation Agency (JICA)-Net
- Myint SW (2001) A robust texture analysis and classification approach for urban landuse and land-cover feature discrimination. *Geocarto Int* 16:27–38
- Neville RA, Levesque J, Staene K et al (2003) Spectral unmixing of hyperspectral imagery for mineral exploration: comparison of results from SFSI and AVIRIS. *Can J Remote Sens* 29:99–110
- Okin GS, Roberts DA, Murray B, Okin WJ (2001) Practical limits on hyperspectral vegetation discrimination in arid and semiarid environments. *Remote Sens Environ* 77:212–225
- Omute P, Corner R, Awange JL (2012) The use of NDVI and its derivatives for monitoring lake victorias water level and drought conditions. *Water Resour Manag* 26: 1591–1613. doi:[10.1007/s11269-011-9974-z](https://doi.org/10.1007/s11269-011-9974-z)
- Platt RV, Goetz AFH (2004) A comparison of AVIRIS and Landsat for land use classification at the urban fringe. *Photogramm Eng Remote Sens* 70:813–819
- Poulter M (1995) Integrating remote sensing and GIS: Designs for an operational future. In: Palmer M (ed) Proceedings of a seminar on integrated GIS and high resolution satellite data. Defense Research Agency [DRA/ CIS/(CSC2)/5/26/8/1/PRO/1], Farnborough.
- Price KP, Guo X, Stiles JM (2002) Optimal Landsat TM band combinations and vegetation indices for discrimination of six grassland types in eastern Kansas. *Int Remote Sens* 23:5031–5042
- Rashed T, Weeks JR, Gadalla MS, Hill AG (2001) Revealing the anatomy of cities through spectral mixture analysis of multispectral satellite imagery: a case study of the greater Cairo region. *Egypt. Geocarto Int* 16:5–15
- Richards JA (1994) Remote sensing digital image analysis: an introduction. Springer, Berlin
- Schowengerdt RA (2007) Remote sensing: models and methods for image processing. Elsevier Inc., Amsterdam
- Weng Q (2010) Remote sensing and GIS integration: theories, methods, and applications. McGraw-Hill, New York 416 pp
- Wilkinson GG (1996) A review of current issues in the integration of GIS and remote sensing data. *Int J Geogr Inf Syst* 10:85–101

Chapter 11

Fundamentals of Photogrammetry

“A map is the greatest of all epic poems. Its lines and colors show the realization of great dreams”

Gilbert H. Grosvenor, Editor, National Geographic (1903–1954)

11.1 Definition and Scope

Like in many other disciplines, there is no universally accepted definition of the term *photogrammetry*. The Manual of Photogrammetry (2003) defines photogrammetry as the art, science, and technology of obtaining reliable information about physical objects and the environment through processes of recording, measuring, and interpreting photographic images and patterns of electromagnetic (EM) radiant energy and other phenomena. Notably, the extracted information could be of a geometric, physical, semantic or even temporal nature, although in many photogrammetric applications the geometric information is more relevant. Other popular definitions of this non-contact discipline are given e.g., in Moffit and Mikhail (1980), Wolf (1980), Kraus (1994), Schenk (2005) etc. In a very broad sense, and from a network design point of view, (Fraser 2000) reckons that a photogrammetric system is one that meets the following basic requirements:

- Capability for self diagnosis (quality control);
- Potential for high precision and reliability (redundant sensor data); and
- Task flexibility with respect to 3D object reconstruction functions.

The term *photogrammetry* is developed from the Greek words *phos* or *phot*, which refers to *light*, *gramma*, which means *letter* or something *drawn*, and *metrein*, the noun of *measure*. Strictly speaking, photogrammetry may be considered to be a subset of remote sensing with photogrammetry zeroing in only on the visible part of the EM spectrum, while remote sensing focuses on the entire EM spectrum

(see Sect. 7.1). In practice, however, photogrammetry has often been treated and viewed as a distinct and separate discipline away from remote sensing. The main reason for this perception is ostensibly because photogrammetry developed much earlier than remote sensing. In general, both photogrammetry and remote sensing provide Geographic Information Systems (GIS) with essential geospatial data and information. As a matter of fact, the core topographic information in most GIS databases and Spatial Data Infrastructures (SDIs) today is still essentially produced through photogrammetric procedures.

Depending largely on the type of application, as well as, to some extent, on variables such as the platform and/or sensor types employed, different types of photogrammetry can be distinguished including; aerial photogrammetry, terrestrial and close-range photogrammetry, biostereometrics, industrial photogrammetry, architectural photogrammetry etc. Terrestrial and close-range photogrammetry was the first type of photogrammetry practiced, and even though it has in recent years re-emerged in prominence, in common parlance the term photogrammetry often refers to aerial photogrammetry.

Historically, photogrammetry is a fairly old discipline with the term “photogrammetry” first coined by *Meydenbauer* in 1893. During the early phase of its development, photogrammetry was limited in applications, focusing largely on terrestrial surveys of inaccessible objects like mountains, expeditions, glaciers, buildings etc. Over the years, however, a paradigm shift has occurred in photogrammetry resulting from developments in computing and imaging technologies. This has fundamentally changed the way photogrammetric procedures are implemented from the traditional *plane table photogrammetry* into *analogue photogrammetry*, through *analytical photogrammetry*, and more recently, into *digital (softcopy) photogrammetry* as illustrated in Fig. 11.1. The net effect of this paradigm shift has been improved accuracy and reliability in map restitution. In Table 11.4 (p. 169) is presented a summary of the basic differences between each of these different phases of photogrammetry.

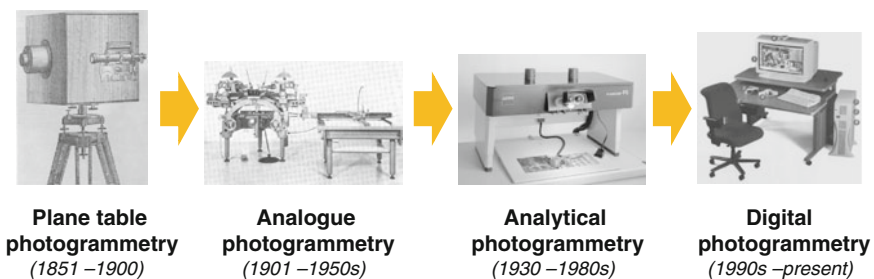
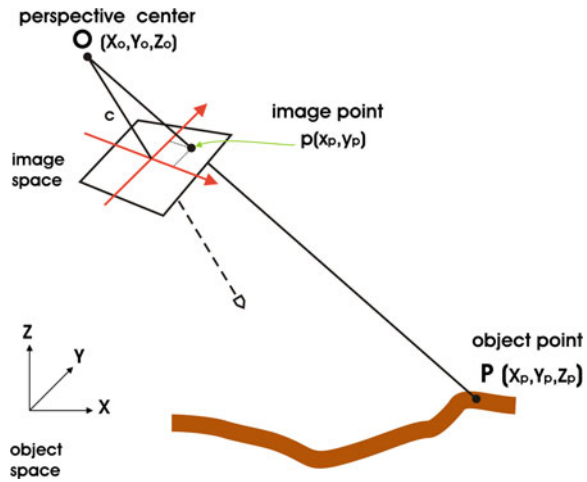


Fig. 11.1 Paradigm shift in photogrammetry

Fig. 11.2 Principle of central perspective projection



11.2 Geometry of Aerial Photography

11.2.1 Central Perspective Projection

In principle, an aerial photograph is imaged on the basis of the *central perspective projection* as shown in Fig. 11.2. This also helps to define the spatial relationship between the image and object spaces. According to the central perspective projection, the object point, perspective center and corresponding image point all lie on a straight line.

The central perspective projection is defined mathematically through the *collinearity condition equations* described through Eqs. 11.1 and 11.2. These are apparently the most important equations in photogrammetry.

$$x_p = -c \frac{r_{11}(X_p - X_o) + r_{12}(Y_p - Y_o) + r_{13}(Z_p - Z_o)}{r_{31}(X_p - X_o) + r_{32}(Y_p - Y_o) + r_{33}(Z_p - Z_o)} \quad (11.1)$$

$$y_p = -c \frac{r_{21}(X_p - X_o) + r_{22}(Y_p - Y_o) + r_{23}(Z_p - Z_o)}{r_{31}(X_p - X_o) + r_{32}(Y_p - Y_o) + r_{33}(Z_p - Z_o)} \quad (11.2)$$

where (x_p, y_p) represent the coordinates of the image point (p) (usually corrected for systematic errors); c is the calibrated focal length; r_{ij} for $i, j = 1, 2, 3$ are the elements of the orthogonal rotation matrix comprising the three angles (ω, ϕ, κ) ; (X_o, Y_o, Z_o) are the coordinates of the perspective center and (X_p, Y_p, Z_p) the coordinates of the object point (P).

The six parameters $(\omega, \phi, \kappa, X_o, Y_o, Z_o)$ constitute the elements of *exterior orientation*, which define the position and attitude of the camera in space. For a single

camera, they are conventionally estimated through the process of *space resection* provided that sufficient control points are available. Once the elements of exterior orientation are determined, every measured image point contributes two collinearity equations while adding three unknown parameters, namely the coordinates of the object point (X_p, Y_p, Z_p) .

Solving for the coordinates of the object point requires that for the same image point, two conjugate points are imaged on corresponding overlapping aerial photographs, otherwise known as *stereopairs*. Therefore, a minimum of a stereopair is required for successful *intersection* of an object point. This provides for stereoscopy in photogrammetry and is particularly critical in the perception of depth and estimation of heights by measuring *stereoscopic parallax* (see Sect. 10.2). Since the collinearity equations are nonlinear, solving for all the above parameters requires that these equations be first linearized using Taylor's series. Procedures for solving these equations without linearization are presented, e.g., in Awange and Grafarend (2005), Awange et al. (2010).

11.2.2 Photographic Scale

The level of information detail that can be extracted from an aerial photograph depends largely on the photographic scale. The photographic scale also has a direct influence on the final map scale and hence the application to which aerial photographs (or even maps) can be put to. For a particular aerial camera, the photographic scale varies depending on the flying height as well as the degree of relief variation. Thus, more hilly terrain will exhibit higher photographic scale variation than fairly level ground. Tilt displacement can also influence scale variation, especially if the amount of tilt is significant.

As shown in Fig. 11.3 the scale of a near vertical photograph can be approximated using Eq. 11.3.

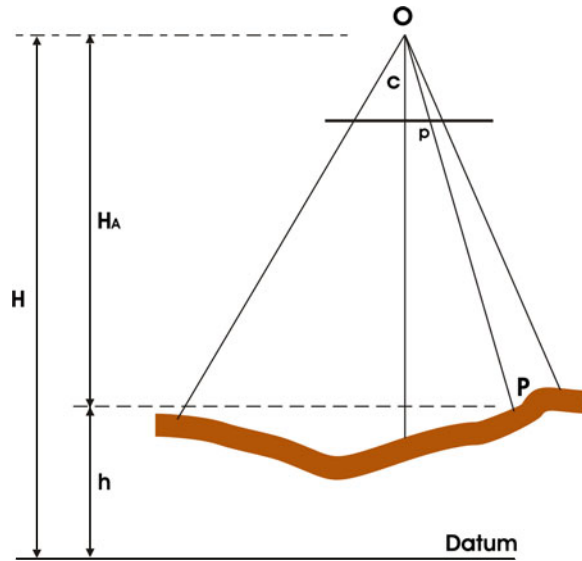
$$s = \frac{c}{H_A} = \frac{c}{H - h} \quad (11.3)$$

where s is the photographic scale, c is the calibrated focal length, H is the flying height above datum, h is the average terrain elevation and H_A is the flying height above average terrain.

11.2.3 Classification of Aerial Photographs

As mentioned in Sect. 11.2.2, on the basis of photographic scale alone, different types of aerial photographs can be distinguished as being better suited for different types of applications than others. In general, therefore, it is important to classify aerial photographs accordingly. By convention, these are classified on the basis of several

Fig. 11.3 Photographic scale



factors including; the orientation of the camera axis, the focal length of the camera, and the type of the emulsion. Using orientation one can differentiate between:

- (1) True vertical photograph: This is a photograph taken with the camera axis perfectly vertical. Such photographs hardly exist in reality.
- (2) Near vertical photograph: A photograph acquired with the camera axis nearly vertical. The deviation from the vertical is called *tilt*. For a near vertical photograph the amount of tilt should not exceed 3° .
- (3) Oblique photograph: A photograph taken with the camera axis intentionally tilted between the vertical and horizontal. A high oblique photograph is tilted so much that the horizon is imaged on the photograph, while a low oblique photograph does not include the horizon.

Whereas vertical photographs are employed in diverse photogrammetric applications, their oblique equivalents are used largely for interpretation work and to deliver *bird's eye views*. The angular coverage is a function of focal length and format size. Standard focal lengths and associated angular coverages are summarized in Table 11.1. While wide angle cameras are the most popular in most photogrammetric mapping applications, super wide angle cameras are used in flat regions. On the other extreme end, narrow angle cameras are used in reconnaissance and intelligence work.

The sensitivity range of emulsion can be used to classify photography into:

- (a) Panchromatic black and white: This is the most widely used type of emulsion for photogrammetric mapping.
- (b) Color: This is mainly used for interpretation purposes. However, color is increasingly being used for mapping applications.

Table 11.1 Classification of aerial photographs based on angular coverage. *Source* Schenk (2005)

	Super wide angle	Wide angle	Intermediate angle	Normal angle	Narrow angle
Focal length (mm)	88	153	210	305	610
Instantaneous field of view (IFOV)	119	82	64	46	24
Photographic scale	7.2	4.0	2.9	2.0	1.0
Ground coverage	50.4	15.5	8.3	3.9	1.0

- (c) Infrared black and white: Since infrared is less affected by haze it is used in applications where weather conditions may not be as favorable for mapping missions (e.g., intelligence).
- (d) False color: This is particularly useful for interpretation, mainly for studying vegetation (e.g., crop disease) and water pollution.

11.3 Photogrammetric Procedures

There are different ways of trying to understand the basic photogrammetric procedure. From a system's perspective, one can look at this as comprising of the three interrelated phases of data acquisition, photogrammetric restitution and photogrammetric output as illustrated in Fig. 11.4. Further discussions in this chapter will be made on the basis of this distinction.

11.3.1 Data Acquisition

11.3.1.1 General Remarks

Although there are different types of cameras designed specifically for use with ground-based and space-based platforms, the discussion hereafter only focuses on airborne-based sensors. The aerial camera is the principle data acquisition tool (sensor) in photogrammetry. It is focused at infinity so that objects on the ground beneath are imaged at a distance equal to the focal length of the taking camera. Today, both analogue frame cameras using film based imaging systems and digital aerial cameras employing charged-couple devices (CCD) are used in photogrammetric data acquisition. As shown in Fig. 11.4, although imagery acquired from analogue cameras need to be first scanned to get these into digital format, digital sensors allow imagery to be directly obtained in digital format ready for processing within a digital environment.

In general, the lens employed in aerial cameras has exceptionally high geometric fidelity. However, it is still imperfect and fails to perfectly replicate the central

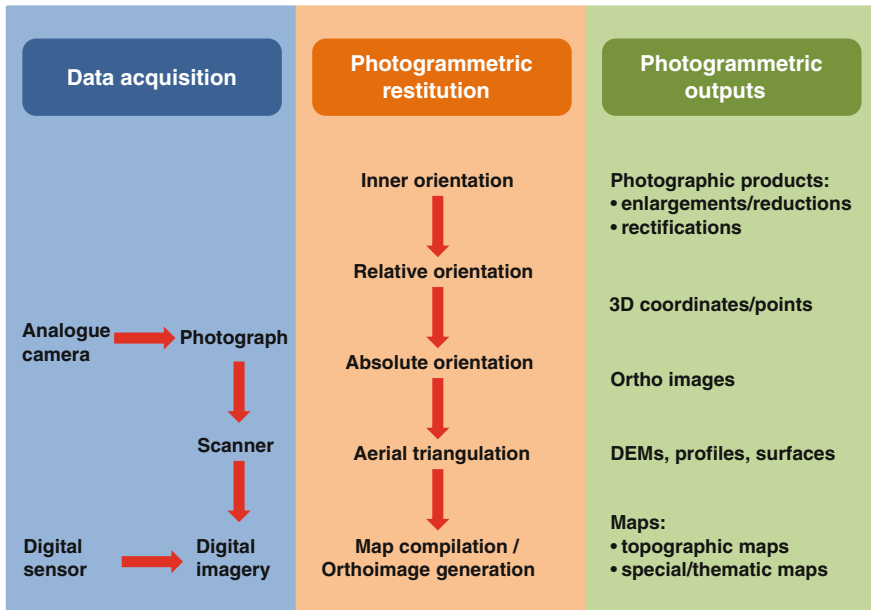


Fig. 11.4 Basic photogrammetric procedure. Modified after (Schenk, 2005)

perspective projection, realizing in practice only an approximation of the same. Hence, there is need to correct resulting aerial imagery for systematic errors incurred during the process of data acquisition, such as tilt and relief displacements, scale variation and film distortion for analogue cameras. In order to procure photography that meets the expected mapping specifications, there is need to carry out a priori photogrammetric project planning as discussed in Sect. 11.3.1.4.

11.3.1.2 Analogue Frame Camera

The most popular type of analogue camera employed in aerial photogrammetry is the frame camera. This is basically a metric sensor that operates by freezing/capturing a square area on the ground in one instance of time when an exposure is made. It normally uses a standard format size of 23 cm × 23 cm. Analogue frame cameras employ film-based systems, which means that the exposed film needs to be processed to develop the photographs once the images are acquired.

The high imaging accuracy of analogue frame cameras is realized through the use of a lens of high geometric fidelity with minimum lens distortion, and the employment of a film flattening device to ensure that the film is held flat against the camera focal plane at the instance of exposure. Camera accessories are also incorporated to ensure proper functioning of the entire analogue sensor. Details of the components of frame analogue cameras are given in Manual of Photogrammetry (2003), Moffit and Mikhail (1980).

11.3.1.3 Digital Aerial Cameras

Compared to the long distinguished history of successful mapping applications using analogue frame cameras dating back from around the 1920s, digital aerial cameras have been in operation for a much shorter period of time from just around the year 2000. The basic difference between these two types of sensors is that digital cameras employ CCDs and no film. In principle, the CCD works by converting photons which fall onto the sensor surface into electrons. These are accumulated in capacitors and converted into digital form for output. Details of this operation are given in most reference books on digital photogrammetry (see e.g., Mikhail et al. 2001; Lindner 2003 etc.).

From a geometric point of view, digital sensors exhibit larger lens distortions and medium accuracy compared to their analogue counterparts and are only stable after warming up. They are of medium resolution compared to silver emulsions employed in analogue cameras. One can distinguish between linear arrays used primarily for satellite or airborne sensors and 2D arrays employed in close range photogrammetric work. Ultimately, the two most important characteristics for digital sensors applicable in photogrammetry are the size of the array and the pixel size. Other important features include the dynamic range, the geometric characteristics (particularly the lens distortion), the transfer of data from the sensor to storage and the time taken to record an image.

During the last decade, competition has been witnessed in the development of digital aerial cameras with single and multiple frame sensors, as well as three-line scanners (TLS) and multiple line scanners. Table 11.2 gives the characteristics of several digital aerial frame cameras including the DMC,¹ UltraCam,² DSS³ and DIMAC⁴ sensors, which are further illustrated in Fig. 11.5. Similarly, examples of digital line scanners comprising the Leica ADS40,⁵ Startlabo StarImager⁶ and JAS 150⁷ are given in Table 11.3, with Fig. 11.6 showing the operating principle of the Leica ADS40 camera.

11.3.1.4 Photogrammetric Project Planning

Planning for a photogrammetric project is the first critical and essential step to consider before execution of aerial photography. Given the area that needs to be mapped, and following a user needs assessment, the photogrammetrist, in consultation with the client, must define the various project parameters, such as overlap and sidelap

¹ <http://www.intergraph.com>

² <http://www.microsoft.com/ultracam>

³ <http://www.applanix.com>

⁴ <http://www.dimacsystems.com>

⁵ <http://www.leica-geosystems.com>

⁶ <http://www.starlabo.co.jp>

⁷ <http://www.jenoptik.com>

Table 11.2 Digital aerial frame cameras

Digital aerial frame camera type	Pixels	Pixel size (μm)	Focal length (mm)
Intergraph DMC	8,000 \times 14,000 pan	12	120
Excel UltraCam _D	7,500 \times 11,500 pan	9	100
Applanix DSS	4,092 \times 4,077	9	55 or 35
DIMAC	up to 4 times 8,984 \times 6,732	9	47–210



Fig. 11.5 Digital aerial frame cameras

Table 11.3 Digital aerial line scan cameras

Digital aerial line scan camera type	Pixels	Pixel size (μm)	View direction in flight direction	Field of view across
Leica ADS40	2 \times 12,000 staggered	6.5	-16°, nadir, 26°	62°
Starlabo StarImager	14,400	5	-23°, nadir, 17°	62°
JAS 150	12,000	6.5	Nadir, $\pm 12^\circ$, $\pm 20.5^\circ$	29°

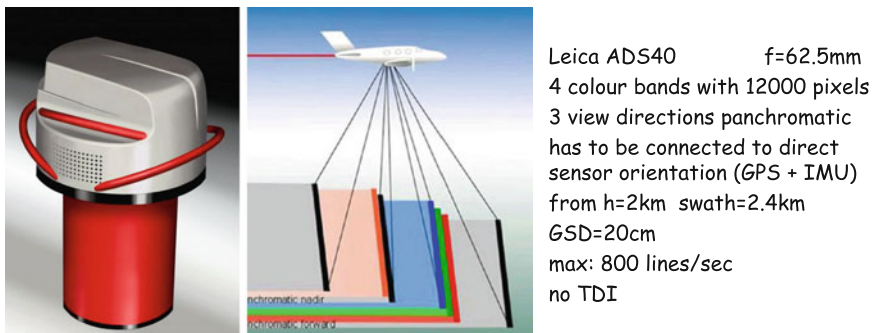


Fig. 11.6 Operating principle of Leica ADS40. Source <http://www.leica-geosystems.com>

requirements, photographic scale, final map scale, instruments to be used etc. These parameters inform the data acquisition, photogrammetric restitution and map compilation procedures that need to be employed.

Basically, photogrammetric project planning consists of three interrelated phases, namely;

- (a) Development of a *flight plan* which must be followed when taking the aerial photographs to be used in the project. The flight lines to be used during the photography are first drawn on a topographic map. This is done with the objective of avoiding gaps in the resultant photography, and taking into account factors like the overlap and sidelap requirements, general orientation of the area to be mapped etc.
- (b) Planning the *ground control* and executing the necessary field surveys to satisfy the accuracy requirements of the project. Photo control is required in photogrammetric restitution. Suitable, sufficient and adequately distributed ground control points whose images clearly appear on the resultant photographs need to be pre-marked or postmarked and coordinated appropriately using e.g., GNSS discussed in Chaps. 4–6.
- (c) Estimating the *costs* involved in the project. Aerial photogrammetry can be fairly expensive and an appropriate budget needs to be provided for the exercise to be successful.

Details of typical computations in photogrammetric project planning are discussed e.g., in Manual of Photogrammetry (2003), Moffit and Mikhail (1980), Wolf (1980) etc. Example 11.1 demonstrates a typical example of photogrammetric project planning.

Example 11.1 (Photogrammetric project planning. (Source: Konecny 2003))

The following is an example on how to quickly estimate the number of photographs required to cover an area to be mapped through photogrammetry. Figure 11.7 shows a typical photogrammetric data acquisition schema. The ground distance between the two exposure centers designated as b is given by:

$$b = a \left(1 - \frac{o}{100} \right) \quad (11.4)$$

where o is the overlap and a is the ground format coverage for an image. For a typical overlap of 60 % the ground distance b is given by:

$$b = a(0.4) \quad (11.5)$$

If the sidelap between the strips p is 30 %, then the ground distance between any two adjacent strips, q , becomes:

$$q = a \left(1 - \frac{p}{100} \right) = a(0.7) \quad (11.6)$$

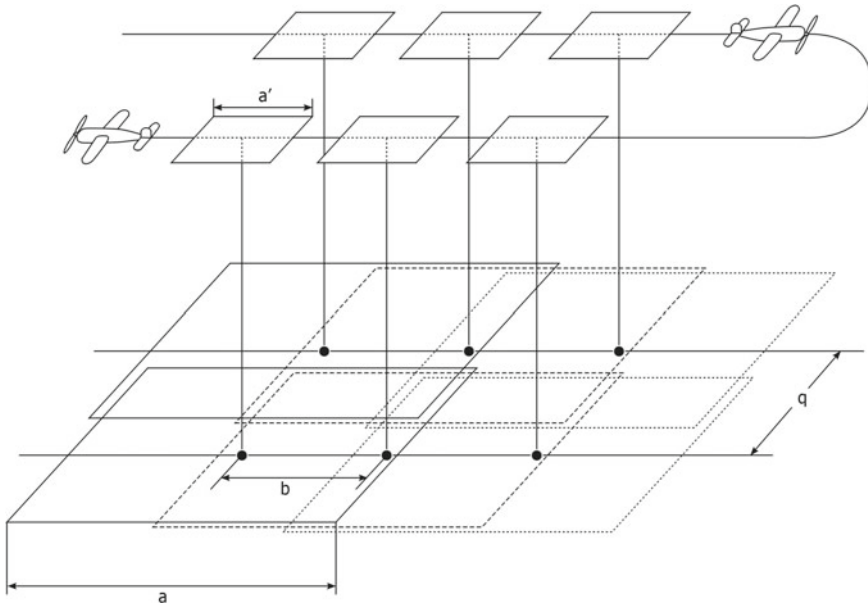


Fig. 11.7 Photogrammetric data acquisition configuration

To calculate the number of photographs required for the entire area it is important to first consider a single model comprising of two overlapping photographs. The net (overlap) area, N , has the dimensions $N = b \cdot q$. Thus, the number of photographs, n , required to cover a total area, B , can be estimated from:

$$n = \frac{B}{N} \tag{11.7}$$

End of Example 11.1

11.3.2 Photogrammetric Restitution

As described in Sect. 11.1, the basic objective of photogrammetry is to extract useful geometric and other information types by analyzing and interpreting photographic imagery. It therefore follows that once the aerial photographs have been acquired they need to be further analyzed and interpreted to extract 3D geoinformation from the iconic 2D imagery. Traditionally, this has been achieved through the process of *photogrammetric restitution* as illustrated in Fig. 11.8. Conceptually, this involves simulation and inversion of the basic photographic process and can be implemented using

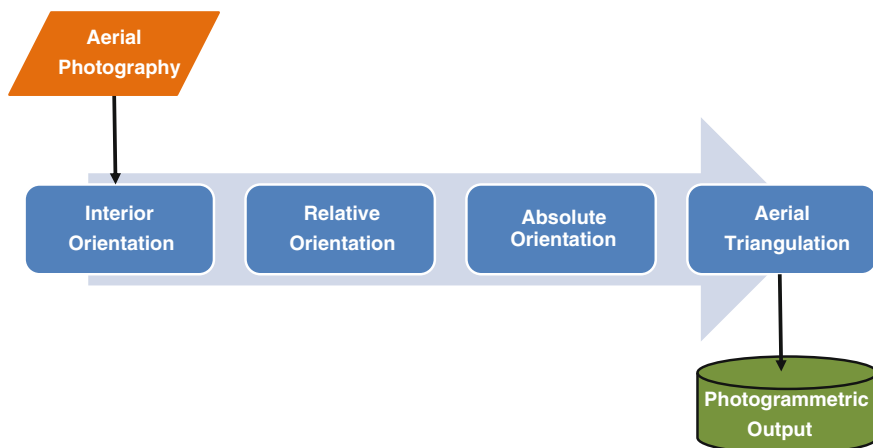


Fig. 11.8 Classical photogrammetric workflow

either plane table-, analogue-, analytical- or digital photogrammetric techniques. Table 11.4 compares the characteristics of these different approaches towards photogrammetric restitution.

The following subsections discuss the different stages in photogrammetric restitution that define the basic photogrammetric workflow. The focus here is only on conceptual ideas and not on implementation issues.

11.3.2.1 Interior Orientation

The main objective of *interior orientation* is to reconstruct the same geometry (or bundle of rays) that existed during image acquisition. In principle, therefore, this endeavors to simulate the photographic process. The elements of interior orientation are conventionally estimated through *camera calibration*. The magnitude and sense of these parameters give an indication by how much the geometry of image formation in the employed camera deviates from a perfect central perspective projection (described in Sect. 11.2.1). The main cause for this deviation is the various systematic errors that are likely to have occurred during image acquisition, including tilt and relief displacements, along with scale variations, film distortions etc. This calls for appropriate mathematical models to be adopted to correct for these error sources.

The interior orientation parameters estimated through camera calibration include: coordinates of the principal point (x_o, y_o), the calibrated focal length (c), radial lens and tangential lens distortion elements, film deformation, atmospheric refraction and earth curvature. The purpose of correcting the image rays for these errors is to ensure that the line from the object space passing through the perspective center to the image space is a straight line, thus fulfilling one of the basic assumption of collinearity condition given in Eqs. 11.1 and 11.2 (p. 159). In addition, it is also

Table 11.4 Comparison of various photogrammetric restitution methods

Characteristic	Description
<i>Plane Table Photogrammetry</i>	
Methodology	Derivation of angles from image points
Users	Surveyors
Auxiliary disciplines	Photography; descriptive geometry; projective geometry; perspective geometry
Origins	da Vinci—basic geometry (c. 1480); Desargues—projective geometry (c. 1625); Lambert—perspective geometry (1759); Daguerre—silver emulsions and photographic exposure (1839); Meydenbauer—photogrammetry terminology coined (1893)
Practical uses	Sebastian Finsterwalder mapping Vernagt Glacier (1888); Lavssedat mapping Paris from rooftops (1851)
Application	Limited to terrestrial surveys of inaccessible objects (e.g., mountains, expeditions, glaciers, buildings)
<i>Analogue Photogrammetry</i>	
Methodology	Reconstruction of stereo-models by optical or mechanical instruments
Users	Photogrammetrists
Auxiliary disciplines	Optics, mechanical tooling, stereoscopy
Origins	Pulfrich—stereocomparator (1901); von Orel—autograph (1907); Gasser plotter—Multiplex (1915)
Practical uses	Stereoplotters by Leica (Wild), Zeiss etc. (1926)
Application	Topographic Mapping (1939-1945); accelerated mapping programs in the 1950s
<i>Analytical Photogrammetry</i>	
Methodology	Integration of computers in stereo restitution
Users	Photogrammetrists
Auxiliary disciplines	Analytical geometry, matrix algebra, least squares adjustment
Origins	Collinearity equations (Gast, 1930); bundle block adjustment (H. Schmid, 1953); analytical plotter (U. Helava, 1957); orthocomp by Zeiss (1980)
Practical uses	Semiautomatic orientation; DEM; analytical aerial triangulation; vector plotting
Application	Improved accuracy and reliability in map restitution
<i>Digital Photogrammetry</i>	
Methodology	Use of scanned analogue images or digital images in pixel format
Users	Geoinformatics specialists
Auxiliary disciplines	Computer science, digital image processing
Origins	Optronics—1970; stereo workstation—1988; digital image matching (Sharp—1965)
Practical uses	Digital orthophotos, space imagery restitution
Application	Integration into GIS

Modified after Konecny (2003)

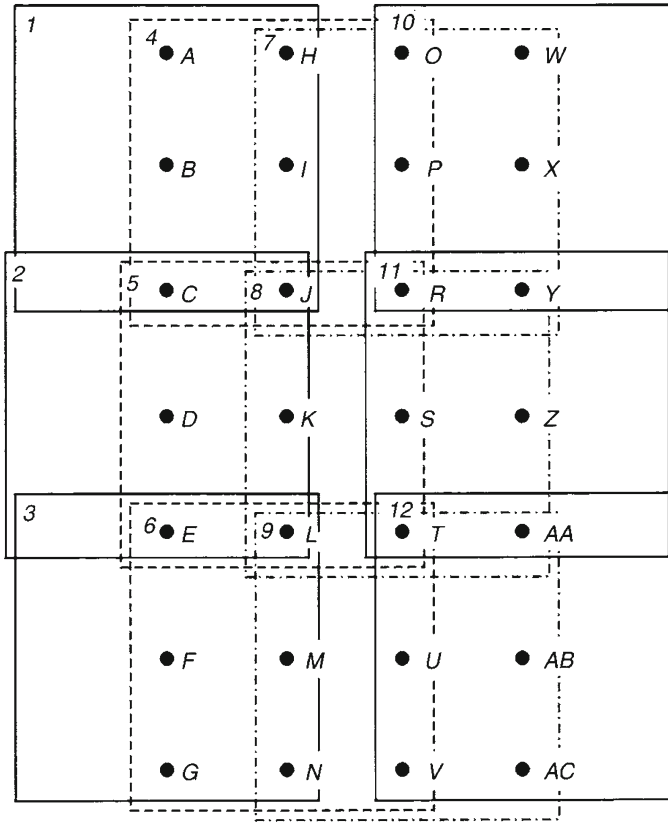


Fig. 11.9 A schematic of a block of aerial photography showing the *von Gruber* location of various control points. These points can be coordinated using GNSS techniques to allow for aerial triangulation

usually important to evaluate the resolution of the entire imaging system through an assessment of the *modulation transfer function* (MTF).

11.3.2.2 Relative Orientation

Relative orientation is the process that follows after inner orientation. The basic objective of relative orientation is to constrain corresponding conjugate rays to ensure that they intersect uniquely in space in order to form a stereomodel. In essence, this attempts to reverse the photographic process by ensuring that the same relative position that the two overlapping images exhibited during image acquisition is maintained. This is realized in practice by removing parallax around six standard locations, otherwise referred to as the *von Gruber* locations, defined within the overlap area (Fig. 11.9). The procedure adopted in the removal of parallax will vary depending on the photogrammetric restitution method applied.

Table 11.5 Stereoscopic viewing methods. *Source* Schenk (2005)

Dimension	Stereoscopic implementation
Spatial	2 monitors + stereoscope
	1 monitor + stereoscope (split screen)
	2 monitors + polarization
Spectral	Anaglyphic
	Polarization
Temporal	Stereo alternate synchronization by polarization

Once parallax has been successfully removed a 3D *stereomodel* that is a scaled replica of the imaged ground underneath is generated. This stereomodel can be viewed *stereoscopically* and even measured. To successfully view the stereomodel, an appropriate viewing (ocular) system that delimits the left eye to view only the left stereopair, and the right eye to view only the right stereopair needs to be in place. Reversing the viewing system results in a *pseudoscopic* view, in which case hills appear as valleys and vice-versa. In principle, stereoscopic viewing can be implemented in different ways as summarized in Table 11.5.

11.3.2.3 Absolute Orientation

The created stereomodel has an arbitrary scale and is not anchored on any existing datum. To overcome both the scale and height datum defects requires that the stereomodel be appropriately scaled and leveled. This is achieved through the use of existing ground controls measured using GNSS during the process of *absolute orientation*. The scaled and leveled stereomodel can then be used in the compilation of maps and production of orthoimages.

11.3.2.4 Aerial Triangulation

After successful relative orientation a stereomodel will be produced from a minimum of every stereopair employed. For a photogrammetric block comprising of several stereopairs, it is necessary to relate multiple stereo images to each other so as to link and connect them up. This is achieved by employing the collinearity model described in Sect. 11.2.1, and using sufficient tie, pass and control points, as shown in Fig. 11.9, in a process referred to as *aerial triangulation* or *aerotriangulation* that seeks to:

- (1) determine the complete exterior orientation parameters of each image in the photogrammetric block that includes the (X_o, Y_o, Z_o) coordinates of the position of the camera in space, as well as the camera attitude (defined through the rotations ω, ϕ, κ); and
- (2) estimate ground coordinates (X, Y, Z) of measured conjugate image points.

The collinearity model can be expanded further to incorporate additional parameters, especially those required to model various systematic error sources, such as

radial and tangential lens distortions. In view of the numerous image points that need to be processed and the substantial number of unknown parameters that need to be estimated, to enhance the reliability of the estimation process, a *bundle adjustment* approach is usually adopted in most practical photogrammetric triangulation. This allows for the simultaneous estimation of all unknown object space coordinates, together with the elements of interior and exterior orientation from the measured image coordinates and provided photogrammetric control within one common bundle adjustment solution. The least squares bundle adjustment solution is particularly attractive because it significantly improves the reliability of the estimation given the high degree of freedom encompassed.

11.3.3 Photogrammetric Output

Photogrammetric products fall generally into three categories, namely; photographic products, computational results and maps. Photographic products are essentially derivatives of single photographs or composites obtained from stereopairs. Supposing that an analogue camera is used, during the exposure of the film a latent image is formed which can be developed into a *negative*. Similarly, *diapositives* and *paper prints* can also be produced (see Fig. 11.10). In addition, *enlargements* may also be obtained to support preliminary design or planning studies.

All the above products are derived from unrectified photographs. Better approximations to a map are *rectifications* that are aerial photographs corrected for tilt displacement. The rectified photographs can be further processed to correct for relief displacement through the process of *differential rectification*. This results in an *orthoimage* that is geometrically identical to a map. Composites are frequently used as a first base for general planning studies. *Photomosaics* are probably the most common composites, but composites derived from orthophotos, called *orthophoto maps* are increasingly being applied. Such photogrammetric products find use, e.g., in soil landscape mapping discussed in Sect. 23.3.1 in p. 383.

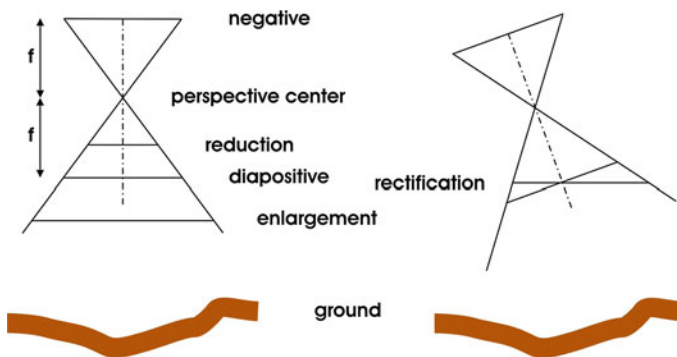


Fig. 11.10 Typical photographic products. Source Schenk (2005)

For computational results, *aerial triangulation* represents a very successful application of photogrammetry that delivers 3D positions of points measured on photographs in a ground coordinate system. *Profiles* and *cross-sections* are typical products in the design of highways from which earthwork quantities are computed. The most popular form for representing height variations of the earth's surface is the *DEM/DTM* (Digital Elevation Model/Digital Terrain Model), e.g., Fig. 19.3 on p. 262.

Ultimately, however, *maps* remain the most prominent product of photogrammetry. They can be produced at various scales and degrees of accuracies depending on the desired mapping application. Unlike aerial photographs that exhibit a central perspective projection, maps are generally produced using an orthographic projection. Planimetric maps contain only the horizontal position of ground features, while topographic maps include elevation data, usually in the form of contour lines and spot elevations. On the other hand, thematic maps emphasize one particular theme e.g., transportation network, geology etc. Details of different types of maps are discussed in Sect. 9.2.

11.4 Concluding Remarks

It is indisputable that photogrammetry has come a long way indeed. In terms of data acquisition, it has transited from the early days, when pigeons were used as platforms for cameras, to the modern era, where digital sensors are employed to acquire image data directly in digital format. With regard to image restitution, photogrammetry has gone through a complete paradigm shift. From the era of plane table photogrammetry, when terrestrial and close range mapping systems were employed to map inaccessible features, to the present time, when digital (softcopy) photogrammetry has come of age. In terms of output, photogrammetry has moved from the era of traditional topographic maps, that were difficult and expensive to revise, to the modern era, where orthophotos can be economically applied to update GIS and CAD data. The next chapter provides insight on how this can be achieved.

Against the above background, it seems reasonable to pose the question; what does the future portend for photogrammetry? This is a very difficult question to answer, even for an optimist. The truth is that photogrammetry today faces, perhaps, its most serious challenge ever as a mapping tool. For instance, compared to LiDAR, photogrammetry is disadvantaged in several ways, especially in terms of flexibility, cost and delivery times as discussed in Sect. 8.4. Nonetheless, as of now, photogrammetry still remains fairly competitive, particularly with regard to accuracy and reliability. However, to effectively compete with other non-contact mapping technologies, photogrammetry will need to be more competitive, specifically in terms of cost and delivery times.

References

- Awange JL, Grafarend EW, Palancz B, Zaletnyik P (2010) Algebraic geodesy and geoinformatics. Springer, Berlin
- Awange JL, Grafarend EW (2005) Solving algebraic computational problems in geodesy and geoinformatics. Springer, Berlin
- Fraser CS (2000) Network design. In: Atkinson KB (ed) close range photogrammetry and machine vision. Whittles Publishing, Caithness
- Konecny G (2003) Geoinformation: remote sensing, photogrammetry, geographic information systems. Taylor and Francis, London
- Kraus K (1994) Photogrammetry, Verd. Duemmler, Bonn
- Lindner W (2003) Digital photogrammetry: theory and applications. Springer, Berlin
- Manual of Photogrammetry (2003) In: McGlone C, Mikhail E, Bethel J (eds) American society of photogrammetry and remote sensing, 5th edn. Bethesda
- Mikhail EM, Bethel JS, McGlone JS (2001) Introduction to modern photogrammetry. Wiley, New York
- Moffit FH, Mikhail E (1980) Photogrammetry, 3rd edn. Harper and Row Publishers, New York
- Murai S (2004) Remote Sensing and GIS Courses—distance education, Japan International Cooperation Agency (JICA)-Net
- Schenk T (2005) Introduction to photogrammetry. The Ohio State University, Columbus
- Wolf P (1980) Elements of photogrammetry. McGraw Hill Book Co., New York

Chapter 12

Digital Photogrammetry

“Imagination is more important than knowledge.”
Albert Einstein (1879–1955)

12.1 Introduction

One of the most fundamental developments in the history of photogrammetry has been the transition from analytical to digital photogrammetry. This was realized in the early 1990s through softcopy-based systems or Digital Photogrammetric Workstations (DPWs). Today, on the one hand, initial applications of digital photogrammetry in performing routine and operational procedures, such as aerial triangulation and map revision, as well as in generating geospatial datasets, including digital elevation models (DEMs) and digital orthophotos, have been essentially standardized. On the other hand, system development in automated feature extraction for diverse geospatial features have been continually improved and refined.

The need for ensuring up-to-date map coverage was, and still remains, a critical issue in many mapping applications worldwide. In the past, map revision posed a basic mapping challenge. The immediate problem was how best to maintain the base map with limited resources and, at the same time, be able to provide an up-to-date map to users. There was also growing need for national base map coverage at larger scales. Historically, traditional techniques could not meet the user demands for timeliness and accuracy. The orthophoto and stereo feature extraction have proved to be viable solutions to the map revision problem, besides fulfilling the need for larger scale base maps.

Digital techniques have become widely available over the last two decades or so. As shown in Fig. 12.1 (p. 177), either scanned analogue images, converted into digital image data with high resolution, or digital images, acquired directly in digital format, constitute the basic input datasets in digital photogrammetry. Each picture element

(pixel) has its known position and measured intensity value, with only one value for black/white imagery, while several such values represent color or multi-spectral imagery.

Evidently, and as discussed in Sect. 11.3.2, most of the photogrammetric restitution procedures, such as relative orientation, are fairly repetitive. In a production environment, such repetitive and often laborious procedures qualify as suitable candidates for automation. One of the attractive reasons for using digital photogrammetry is the ability to apply automation. *Image matching* or *image correlation* (discussed in Sect. 12.4) presents the basic process for automatically determining corresponding conjugate image points on stereopairs and is key to automation in digital photogrammetry.

12.2 Sensor Models

Unlike in both analogue and analytical photogrammetry, where basically only one functional relationship between the image and object space is identified, in digital photogrammetry two sensor models can be distinguished. On the one hand, there is the *physical* or *rigorous sensor model* that is anchored on the basic collinearity condition. This is the classical functional model that is employed in traditional photogrammetry, and is particularly critical for the successful implementation of aerial triangulation. On the other hand, there is also the *generalized* or *replacement sensor model* that can be applied in digital photogrammetry. This later type of model deviates from the physical equivalent in that it does not incorporate information about the sensor position and orientation. Most modern DPWs have the capability of implementing either of the two sensor models.

Majority of the generalized sensor models employ geometries, such as projective geometry, that are different from the central perspective geometry (see Sect. 11.2.1) used in classical photogrammetry. Furthermore, they make use of general polynomials like rational functions (see e.g., Eq. 8.2, p. 126), plus algebraic strategies that are computationally faster to execute than the traditional rigorous sensor model. They are thus appropriate for real-time implementation of subsequent digital photogrammetric outputs and applications, such as DEM generation, orthoimage generation and feature extraction (Agouris et al. 2001). Generalized sensor models are also increasingly attractive in view of the growing number of imaging sensors that are not necessarily designed based on the central perspective projection. This includes remote sensing systems such as high spatial resolution satellite imaging sensors (see Sect. 8.3), LiDAR (see Sect. 8.4) etc.

12.3 Digital Photogrammetric Workstations

The basic requirements of a system for processing digital imagery photogrammetrically will vary depending on the type of application. For example, requirements for topographic mapping are informed largely by the need for recording continuous features, and for being able to view the complete stereo coverage. On the other hand, for close range photogrammetric work, point measurement on smaller images is more critical. Based on the requirements of softcopy map production, the defining characteristics of a DPW include Agouris et al. (2001):

- the ability to store, manage, and manipulate very large image files;
- the ability to perform computationally demanding image processing tasks;
- providing smooth roaming across entire image files, and supporting zooming at various resolutions;
- supporting large monitor and stereoscopic display;
- supporting stereo vector superimposition; and
- supporting three dimensional data capture and edit.

12.3.1 Basic Hardware Requirements

Figure 12.1 shows a schematic of a DPW. According to Schenk (2005), the basic hardware components of a DPW will include the following:

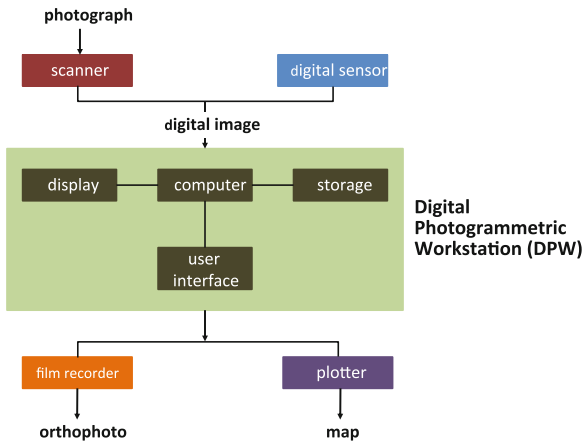


Fig. 12.1 Schematic diagram of digital photogrammetry environment with the DPW as the major component. Modified after Schenk (2005)

- (a) Central processing unit (CPU): This should be reasonably fast considering the amount of computations that need to be performed. Moreover, many processes are best computed within a parallel processing architecture.
- (b) Operating system (OS): Although earlier DPWs ran almost exclusively on Unix or VAX platforms, migration to more economical, modular, scalable, and open hardware architectures provided by PC/Windows-based platforms has been witnessed Agouris et al. (2001). OS with minimum configuration of 64-bit and suitable for real-time processing is required.
- (c) Main memory: Due to the large amount of data that needs to be processed, sufficient memory should be made available e.g., minimum RAM of 6 GB.
- (d) Storage system: This must accommodate the efficient storage of several images and should consist of both fast access storage devices and mass storage media.
- (e) Graphic system: The purpose of the display processor is to fetch data, such as raster (images) or vector data (GIS), process and store it in the display memory and update the monitor. The display system also handles the mouse input and the cursor. At least one or more high end graphic cards should be considered.
- (f) 3D viewing system: This allows the viewing of the photogrammetric model to be done comfortably and possibly in color. For a human operator to view stereoscopically, the left eye must be constrained to view the left image, while the right eye views the right image. Different electro-stereoscopic display and viewing techniques are employed in different DPWs (see Table 11.5, p. 171).
- (g) 3D measuring device: This is used for stereo measurements by the operator. The solution may range from a combination of a 2D mouse and trackball to specialized 3D mouse designs with several programmable function buttons.
- (h) Network: A modern DPW hardly works in isolation. It is usually connected to the scanning system and/or other workstations e.g., GIS. The client/server architecture provides an adequate configuration which allows multiple workstations to share peripherals and other resources (e.g., printers, plotters).
- (i) User interface: This may consist of hardware components such as keyboard, mouse, and auxiliary devices like hand-wheels (to emulate an analytical plotter environment). A crucial component is the Graphical User Interface (GUI).

Additionally, special hardware components may be built into DPWs to deal with special tasks. For instance, near real time operations will require that a special processor dedicated only to such tasks be provided. This would then deal with such characteristics as input from more than one sensor and modeling the behavior of the features in images, as is typical in many robotics and machine vision applications.

12.3.2 Basic Software Requirements

The software in a DPW must cover the normal photogrammetric requirements of orientation and coordinate determination, plus the special requirements of the system application. The standard software requirements include:

- (a) Handling image display: This will encompass display of the whole or part of the image, image manipulation using contrast stretching, density slicing, and movement of cursor/image.
- (b) Measurement to record pixel coordinates.
- (c) Determination of orientation: This will cover inner orientation, application of calibration parameters; relative and absolute orientation and bundle adjustment.
- (d) Transformation: This will include transformation of pixel coordinates to three dimensional model coordinates and model coordinates to other ground coordinate systems.
- (e) Image matching: This is required to cover image matching for automated measurement of fiducial marks; conjugate point determination for relative orientation and other applications; and feature extraction (see Sect. 12.4).
- (f) Digital rectification: This is required for generation of orthoimages.
- (g) Visualization.

In addition, for close range photogrammetric applications some additional functions are necessary (Atkinson 2000):

- (h) Target tracking in image sequences.
- (i) Radiometric and geometric image analysis and MTF determination.

12.4 Image Matching

One of the attractive propositions for using digital photogrammetry is the ability to apply automation. Through automation many routine photogrammetric mapping procedures can be done much faster and with higher precision. Indeed, the biggest gain of digital photogrammetry lies in the potential to automate photogrammetric procedures, outputs and applications, such as aerial triangulation, DEM generation, orthophoto generation etc. The basic process around which automation revolves in digital photogrammetry is *image matching*, sometimes referred to as *image correlation*. Principally, this is the process of automatically identifying corresponding conjugate image points on two or more stereo images.

Two basic image matching methods can be distinguished, namely;

- (1) *Area-based matching*. This is the most popular image matching technique and is particularly suited for images with fairly continuous features. In this method, a search pattern is determined for the feature to be matched. This is then passed over a search window in the conjugate image, with the aim of identifying pixels with similar digital composition as the search pattern as shown in Fig. 12.2. More specifically, the cross correlation between the search pattern and the iterative search windows is compared. A match is deemed to have been realized when the maximum cross correlation coefficient approximating a value of 1 is achieved as described hereunder.

For the pattern matrix, the standard error in gray level variation is given by

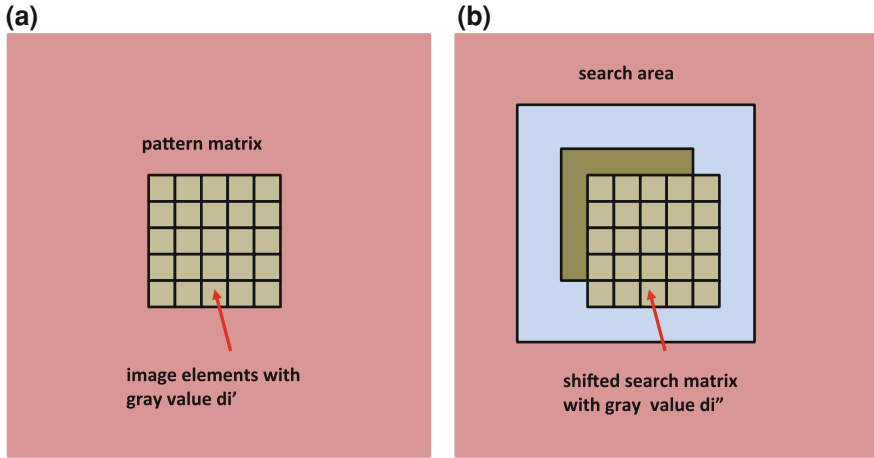


Fig. 12.2 Area-based image matching. **a** Image pattern. **b** Search window

$$\sigma' = \sqrt{\left(\frac{1}{n-1}\right) \sum (d'_{ij} - d')^2} \quad (12.1)$$

where the mean of the gray value differences $d' = \frac{1}{n} \sum_1^n d'_{ij}$.

Similarly, for the search window the standard error in gray level disparity is given by

$$\sigma'' = \sqrt{\left(\frac{1}{n-1}\right) \sum (d''_{ij} - d'')^2} \quad (12.2)$$

with the mean gray level variation $d'' = \frac{1}{n} \sum_1^n d''_{ij}$.

From Eqs. 12.1 and 12.2 the correlation coefficient is given by

$$Covr_{ij} = \frac{1}{n} \sum d'_{ij} \cdot d''_{ij} \quad (12.3)$$

The cross correlation coefficient, r_{ij} then becomes

$$r_{ij} = \frac{Covr_{ij}}{\sigma' \cdot \sigma''} \quad (12.4)$$

- (2) *Feature-based matching*. This is suitable for imagery with many discontinuous features like rivers, roads etc. As the name suggests, feature-based matching is premised on the detection and identification of image features which possess distinct gray value characteristics, either individually or collectively. These may

include features comprising of noticeable primitives, such as points, line segments etc and/or interest points of high gray value variance, such as bright spots, sharp corners etc. Different operators e.g., *Sobel*, *Moravec*, *Förstner* etc may be employed to support feature-based matching.

In terms of implementation, image correlation can be accomplished either on the basis of image-to-image or template-to-image matching. Furthermore, it is possible to combine both area- and feature-based matching techniques to improve on the precision of image correlation. In addition, it is also possible to apply least squares matching algorithms that seek to reduce the minimum sum of squared gray value differences in order to improve the quality of area-based image matching.

12.5 Automated Photogrammetric Mapping

In the following subsections, we present a synopsis of the major procedures, outputs and applications that rely heavily on automation in digital photogrammetry. Since most of these systems still require some measure of human intervention, the terminology “*automated*” is often used to describe their implementation in practice. To produce required geospatial information, digital imagery needs to be oriented and analyzed accordingly. As illustrated in Fig. 11.8 (p. 168) and discussed in Sect. 11.3.2 various different orientations and transformations are required in photogrammetric mapping.

12.5.1 Interior Orientation

Considering that aerial photographs are normally captured in analogue form and subsequently scanned to produce the digital imagery, interior orientation allows for the transformation of pixel coordinates to equivalent photo coordinates and, using camera calibration data, to reconstruct, if necessary, the geometry of the bundle that generated a single image Agouris et al. (2001). Consequently, interior orientation in a DPW comprises of two fundamental transformations:

- (1) Transformation from the digital image pixel coordinate system to the photo coordinate system defined by the fiducial marks, and
- (2) Estimation of the interior orientation parameters through camera calibration.

It is in the first transformation that the automation enabled in digital photogrammetry through DPWs is exploited. To implement this, search windows are first identified from selected image patches in the area surrounding the fiducial marks. This is done either manually, with a human operator pointing using the cursor, or automatically, by means of hierarchical approaches as described in Schickler and Poth (1996). As illustrated in Fig. 12.3a, the refinement of the location or the precise measurement of

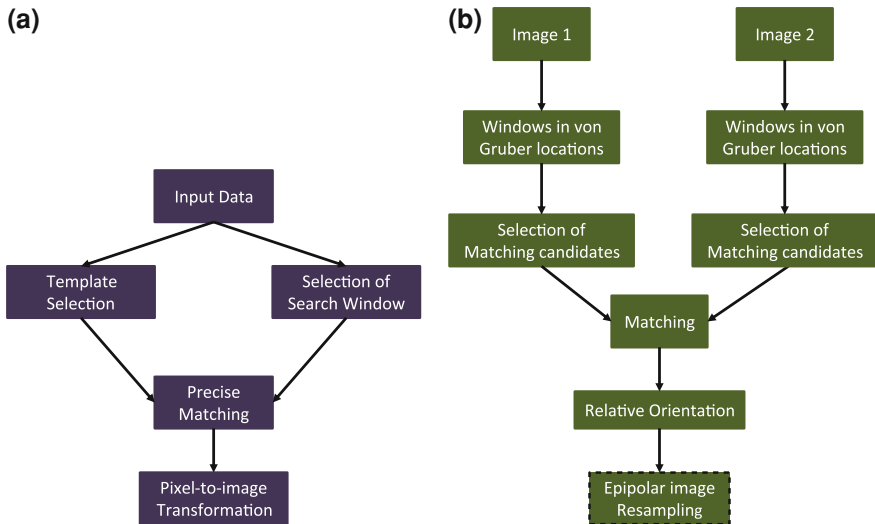


Fig. 12.3 Automated photogrammetric orientation. (Source Agouris et al. 2001) **a** Typical workflow of an automated interior orientation module. **b** Automated conjugate point measurement in a stereopair

the fiducial marks is essentially a matching task that seeks to compare templates of fiducial marks to these search windows Lue (1995). In order to facilitate the performance of automated interior orientation, most DPWs have a database with templates of commonly encountered fiducial marks Agouris et al. (2001).

12.5.2 Relative Orientation

As pointed out in Sect. 11.3.2.2, the basic objective in relative orientation is to make certain that corresponding conjugate rays intersect uniquely in space to form a stereomodel. From a statistical perspective, this requires measurement of a minimum of five (5) conjugate image points at the von Gruber locations (see Fig. 11.9, p. 170). The measurement of conjugate image points in a stereopair is an automated procedure in digital photogrammetric applications (see Fig. 12.3b). Moreover, to increase the redundancy as well as the quality of the relative orientation solution, hundreds of conjugate image points are typically measured in most practical relative orientation procedures employing DPWs.

Consequently, relative orientation is implemented in DPWs through automated *conjugate point measurement*. To begin with, windows in the neighborhood of the von Gruber locations are first selected using approximate information on image overlap. Matching candidates that are suitable for subsequent matching within the selected windows are then identified. These may include features such as distinct primitives (e.g., points, line segments etc.) and/or interest points of high gray value

variance (e.g., bright spots, sharp corners etc.). Appropriate matching techniques, such as area-based matching, can thereafter be applied to establish correspondences, with windows centered on each matching candidate compared to identify conjugate points as those that display the highest correlation values (see Sect. 12.4).

Furthermore, various conditions can be imposed to minimize gross errors or curtail weak matches, thereby improving the overall performance of the matching. These include routines such as setting a minimum threshold on acceptable correlation limits or defining constraints on acceptable parallax ranges Agouris et al. (2001). Once matching of conjugate image points has been accomplished, in order to revert to epipolar geometry and produce *epipolar stereopairs*, y-parallax needs to be removed (as underscored in Sect. 11.3.2.2) through epipolar image resampling. This is illustrated in the final step in Fig. 12.3b and leaves behind only x-parallax, which is interpreted as height difference between image points.

12.5.3 Aerial Triangulation

Relative orientation provides the framework for automated point measurement. As a procedure, it is therefore closely intertwined with aerial triangulation and is implemented in most DPWs, not as a separate module, but as part of a broader point measurement and triangulation module Agouris et al. (2001). Nonetheless, the main objective of aerial triangulation (see Sect. 11.3.2.4) is to relate multiple stereo images within the photogrammetric block to each other. This is achieved by measuring conjugate image points within the stereo coverage in the block, otherwise referred to as tie and pass points, as well as the depicted control points.

Modern DPWs implement aerial triangulation using least squares bundle adjustment algorithms, along with integrating robust estimation techniques. This allows for a rigorous and high quality triangulated solution to be obtained, in addition to the automatic detection of blunders in the measurements. Two different types of measurements can be distinguished using DPWs, namely;

- (1) *Automatic point measurements* that automatically produces numerous measurements of conjugate image points. In order to handle aerial triangulation computational needs, matching tools have been extended from stereo- to multi-stage application Agouris et al. (2001). Furthermore, it is possible to match features automatically to better than ± 0.1 pixel (Atkinson 2000).
- (2) *Interactive point measurements* which allow for user-controlled measurements for the identification and measurement of specific points of interest e.g., ground control points in a semi-automatic manner.

12.6 Generating DEMs and Orthoimages

12.6.1 Automated Generation of DEMs

Once aerial triangulation has been successfully completed within a digital photogrammetric environment, it is possible, thereafter, to extract precise 3D geospatial data and information. Different geospatial products and analyses capabilities can be derived from DPWs to support many diverse applications and different user communities. Besides the classical photogrammetric outputs (see Sect. 11.3.3), foremost among the products derived from digital photogrammetry include Digital Elevation Models (DEMs, see e.g., Fig. 19.3 on p. 262) and orthoimagery.

In general, DEMs are generated in DPWs using *automated terrain extraction* (ATE) procedures. Analogous to conjugate image point measurement employed in relative orientation (see Sect. 12.5.2), ATE uses height matching procedures to generate uniformly spaced grid height (z-) values. Different DPWs employ different heighting correlation strategies defined by diverse key parameters including; terrain relief, cultural content, image quality, shadowing, and desired speed of operation Agouris et al. (2001). It is imperative, however, that after completion of automated DEM generation, the results are reviewed and edited using appropriate post-processing tools. This is necessary in order to detect and remove potential mistakes that may result from poor matching.

12.6.2 Automated Orthoimage Generation

As pointed out in Sect. 11.3.3, orthoimage generation is, in principle, achieved through differential rectification. This essentially involves a special case of image resampling through which the effects of image perspective and relief displacement are removed from the source image. The net result of this is conversion of the image projection from perspective to orthographic, thus allowing the resulting orthoimage uniformly scaled pixels. This makes an orthoimage to be geometrically similar to a planimetric map.

Unlike in analogue and analytical photogrammetry, where orthoimage generation is a time consuming and challenging exercise that normally requires use of dedicated hardware, in digital photogrammetry orthoimage generation is a much simpler automated process. Every DPW software module for orthoimage generation requires as fundamental input, aerial triangulation results and a DEM. Two basic approaches to orthoimage generation include forward and backward projection (Novak 1992). In forward projection, pixels from the source image are projected onto the DEM to confirm their object space coordinates, which are subsequently projected into the orthoimage. In the backward projection, the object space coordinates are projected into the source image to derive the radiometric information for the correspond-

ing orthoimage pixel Agouris et al. (2001). Both these projections require image resampling.

Various factors affect and influence the accuracy of the resulting orthoimage including; the spatial resolution of the source image, the accuracy of aerial triangulation, along with the accuracy and resolution of the DEM (Agouris et al. 2001). For urban scenes, a typical problem with automated orthoimage generation remains the effect of building displacement. This is occasioned by building shadows and results in buildings appearing as if they were “leaning”. Such undesirable effects can be corrected using supplementary stereo images that reveal areas obscured in building shadows in the source image.

12.7 Automated Feature Extraction

By supporting 3D data capture and editing, feature extraction provides the link between photogrammetry and Geographic Information Systems (GIS). Generally speaking, this defines a fairly complicated procedure to automate, with modern DPWs providing for the creation of 3D feature topology from standard vector primitives (described in Chap. 14), object-relational database (explained in Chap. 16) for feature geometry and attributes.

As a basic minimum, feature extraction requires triangulated imagery. The generated DEM can also be used to bolster the feature extraction process, which can be done either in monoscopic (2D) or stereoscopic (3D) mode. Modern DPWs support *automated feature extraction* (AFE) using diverse approaches and algorithms. In the past, most research on AFE algorithms focused on the extraction of man-made features in general, and on buildings (see e.g., Weidner and Förstner 1995; Gulch et al. 1999; Irvin and McKeown 1989; Shufelt 1999; Gruen et al. 1997; Rottensteiner 2001 etc.) and roads (see e.g., Baumgartner et al. 1999; McKeown and Denlinger 1988; Agouris et al. 2002; Mena 2003; Trinder and Wang 1998; Gruen et al. 1997; Harvey et al. 1999 etc.) in particular. The problem of AFE has greatly extended the scope of photogrammetry into the domain of computer vision and artificial intelligence with techniques transcending many disciplines, such as digital image processing, pattern recognition, knowledge-based methods, artificial neural networks, fuzzy logic, etc., having been investigated (see Sect. 10.3.2.2).

12.8 Concluding Remarks

Although it was not the intention, perhaps Sect. 11.4 conjectured a somewhat gloomy picture about the future prospects of photogrammetry. That notwithstanding, however, if we are going to see a renaissance of photogrammetry, it will surely come through digital photogrammetry. By providing an all-inclusive digital environment within which photogrammetric mapping is performed, digital photogrammetry

presents photogrammetry with the chance, yet again, to be competitive as a mapping technology. This is especially in terms of the areas, such as cost and timeliness, in which photogrammetry has increasingly been perceived to be less competitive compared to other mapping technologies like LiDAR.

For instance, by applying image matching, the turn around time incurred in many digital photogrammetric procedures is cut down drastically. Moreover, as conventional products generated through digital photogrammetry, orthoimages and DEMs have already distinguished themselves, not only as attractive and viable map revision inputs, but also valuable basic framework data in spatial data infrastructure (SDI). Similarly, by leveraging on its direct integration with GIS, digital photogrammetry is set to continue offering serious challenge to other competing non-contact mapping technologies, now and into the foreseeable future.

References

- Agouris P, Doucette P, Stefanidis A (2001) Automation and digital photogrammetric workstations. In: McGlone C, Mikhail E, Bethel J (eds) *Manual of photogrammetry*. Am Soc Photogramm Remote Sens 5:949–981
- Agouris P, Doucette P, Stefanidis A (2002) Automated road extraction from high resolution multi-spectral imagery technical report. Digital image processing and analysis laboratory, Department of Spatial Information Science and Engineering. University of Maine, Orono, Maine
- Atkinson KB (ed) (2000) *Close range photogrammetry and machine vision*. Whittles Publishing, Caithness
- Baumgartner A, Steger C, Mayer H, Eckstein W, Ebner H (1999) Automatic road extraction based on multi-stage, grouping and context. *Photogramm Eng Remote Sens* 65(7):777–785
- Gruen A, Baltsavias EP, Henricsson O (eds) (1997) *Automatic extraction of man-made objects from aerial and space images (II)*. Birkhäuser Basel, Basel
- Gulch E, Muller H, Labe T (1999) Integration of automatic processes into semi-automatic building extraction. *Int Arch Photogramm Remote Sens* 32(3):177–186
- Harvey W (1999) Performance evaluation for road extraction. *Bulletin de la Société Française de Photogrammetrie et Télédétection* 153(1999–1):79–87
- Irvin R, McKeown D (1989) Methods for exploiting the relationship between buildings and their shadows in aerial imagery. *IEEE Trans Syst Man Cybern* 19(6):1564–1575
- Lue Y (1995) Fully operational automatic interior orientation. In: *Proceedings of Geoinformatics 1995*, pp 26–35
- McKeown D, Denlinger J (1988) Cooperative methods for road tracking in aerial imagery. In: *IEEE Proceedings of the computer vision and pattern recognition*, Ann Arbor, MI
- Mena JB (2003) State of the art on automatic road extraction for GIS update: a novel classification. *Pattern Recognit Lett* 24(16):30373058
- Novak K (1992) Rectification of digital imagery. *Photogramm Eng Remote Sens* 58(3):339–344
- Rottensteiner F (2001) Semi-automatic extraction of buildings based on hybrid adjustment using surface models and management of building data in a TIS. Ph.D. Dissertation, Vienna University of Technology
- Schenk T (2005) *Introduction to photogrammetry*. The Ohio State University, Columbus
- Schickler W, Poth Z (1996) Automatic interior orientation and its daily use. *Int Arch Photogramm Remote Sens XXXI(B3):746–751*
- Shufelt J (1999) Performance evaluation and analysis of monocular building extraction from aerial imagery. *IEEE Trans Pattern Anal Mach Intell* 21(4):311–326

- Trinder JC, Wang Y (1998) Automatic road extraction from aerial images. *Digit Signal Process* 8(4):215–224
- Weidner U, Förstner W (1995) Towards automatic building extraction from high-resolution digital elevation models. *ISPRS J Photogramm Remote Sens* 50(4):38–49

Part IV
Geographic Information Systems

Chapter 13

Fundamentals of GIS

“Knowing where things are, and why, is essential to rational decision making”

Jack Dangermond, Founder ESRI

13.1 Basic Concept

Geographic Information System (GIS) is defined as a special type of information system that is used to input, store, retrieve, process, analyze and visualize geospatial data and information in order to support decision making, see e.g., Aronoff (1989), Tomlinson (2007), Longley et al. (2005), Konecny (2003), Burrough (1986), Murai (1999) etc. Hence, a GIS is basically a computer-based information system for handling spatially referenced data and information. In the early years after its emergence in the mid 1960s, GIS was viewed essentially as a mere tool—a spatial decision support tool. However, over the years GIS has evolved dramatically from being a simple tool of automated mapping and data management into a sophisticated spatial data-handling and analysis technology and, more recently, into *geographic information science and technology (GIS&T)*.

Weng (2010) articulates that GIS today is far broader and harder to define with many people preferring to define its domain as GIS&T. Moreover, it has become embedded in many academic and practical fields with the net result that the GIS&T field today is largely a loose coalescence of groups of users, managers, academics, and professionals all working with geospatial information. Furthermore, each group has a distinct educational and cultural background and identifies itself with particular ways of approaching particular sets of problems (Weng 2010).

In principle, GIS handles geographic data, which include both spatial and attribute data that describe geographic features. Whereas spatial data describe the location and shape of geographic features and their spatial relationships, attribute data describe

the characteristics of spatial data. Traditional information systems for decision support, like the classical management information systems, were originally designed to handle only non-spatial data such as salary and personnel data, stock inventories, bank account management data etc. On the other hand, geographic location captured through the use of geospatial data is the cornerstone of GIS. In the past, one could without ambiguity distinguish between the characteristics of spatial and non-spatial information systems. Today, however, it is now widely recognized that even traditional information systems could have better utility if the spatial dimension of the data they handle could be extracted and included in the analysis. This has resulted in a narrowing of the divide between spatial and non-spatial information systems, thereby creating many new applications in GIS.

There are several reasons and situations that would occasion the need for a GIS. According to Konecny (2003), these include among others the fact that:

- geospatial data are poorly maintained (especially in many developing countries);
- maps are out of date;
- data and information are inaccurate;
- geospatial data are inconsistent;
- there is no standard;
- there is no data sharing;
- there is no data retrieval service; and
- there is no scientific decision making etc.

Once a GIS is fully implemented, numerous benefits accrue including (Konecny 2003):

- geospatial data are better maintained in a standard format;
- revision and updating are easier;
- geospatial data and information are easier to search, analyze and represent;
- more value added products are output;
- geospatial data can be shared and exchanged;
- overall productivity is improved;
- time and cost are saved; and
- better and informed decisions are made etc.

Some of the generic questions that any serious GIS is expected to answer include:

- (1) Where is it? (*Location question*; identifies the geographic location(s) that satisfy certain conditions)
- (2) What is there.....? (*Basic inventory question*; examines what exists at a particular location)
- (3) What spatial patterns exist? (*Relation question*; analyzes the spatial relationship between objects of geographic features)
- (4) Why there? (*Cause and effect question*; explores various driving factors and consequence(s) thereof)
- (5) What has changed since? (*Trend question*; identifies geographic occurrence or trends that have changed or are in the process of changing)

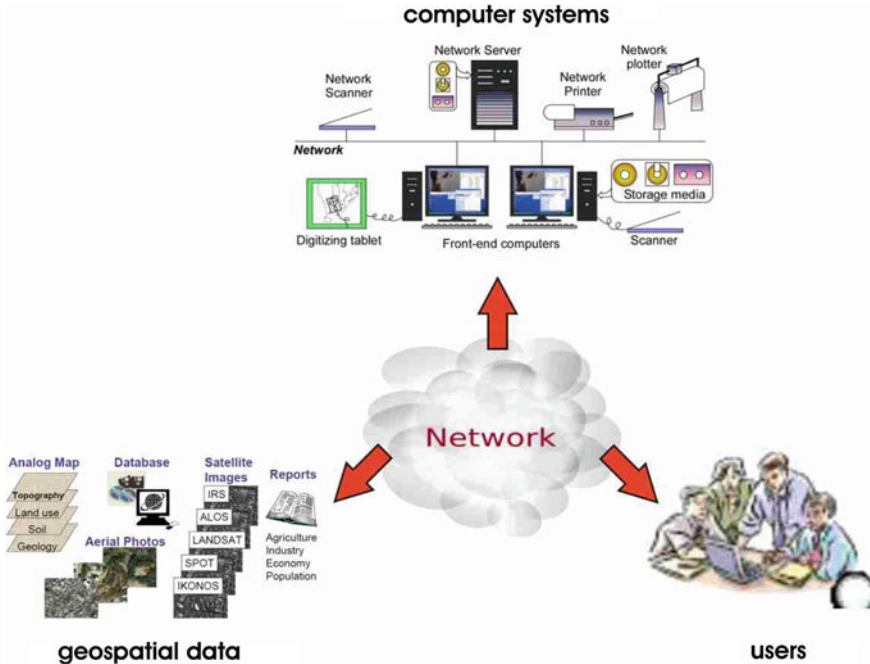


Fig. 13.1 Key components of a GIS

(6) What if? (*Modeling question*; analyzes various scenarios based on model and given conditions e.g., optimum path, a suitable land, risky area against disasters etc.)

13.2 Key Components

The key components of GIS are a computer system, geospatial data and users as shown in Fig. 13.1. A computer system for GIS consists of hardware, software, network and procedures designed to support the data capture, processing, analysis, modeling and visualization of geospatial data. The basic hardware items for GIS includes the host computer, a digitizer, printer, plotter, monitor, keyboard, mouse, plus the associated cabling and external storage media usually in a networked environment.

Besides standard software for mundane tasks like operating system, programming, graphics, networking etc., GIS software will also be required. This falls in the category of application software. There are various types of GIS software available in the market and by extension different GIS systems e.g., Desktop GIS (normal software), Server GIS (expensive software allowing sharing with many users), Web GIS (software using web browser described in Chap. 18), Mobile GIS (working with

Personal Digital Assistant (PDA)) etc. It is important to understand the required computer systems in GIS and identify the required GIS hardware and software characteristics.

A GIS with the best hardware and software combination will still fail if there is inadequate or inappropriate input data. This is true since data is the raw material from which information is processed. Data in a GIS consists of both spatial and attribute data. The data is kept in a database and is managed by a database management system (DBMS). In addition, an appropriate organizational environment is essential for proper functioning of GIS hardware and software. Specifically, organizational procedures must be put in place in order to create awareness about the GIS and fit it appropriately in the overall operations of the concerned organization. Some important issues involved in setting up GIS include the development of standards, access protocols, database administration, quality assurance and system security.

Within the knowledge economy and in many businesses, staff are usually seen as the prime business asset and the factor that differentiates one organization from another. Longley et al. (2005) reiterates that the supply of GIS experts and GIS-literate people is a critical factor in determining the rapidity of up-take of the existing facilities and their successful use. People in GIS consist of staff that operate the system, the users of the system and external consultants that may be called from time to time to advise on different strategic, technical and project issues. For a medium to large GIS establishment, the core GIS team will usually comprise of the following personnel: GIS manager, database administrator, system manager, GIS analyst, GIS programmers, data entry clerks etc. In a fairly small GIS set up, only the GIS analyst, programmer and data entry clerk may be necessary with the GIS analyst doubling as the GIS manager.

At a practical level and in order to function properly the various GIS components need to be synchronized to match the system requirements and desired applications. For instance, the purchase of hardware must be matched with that of software. Similarly, the right human resources must be put in place to transform the geospatial data into information and knowledge for decision support. Resources must also be availed to capture the required geospatial data, which incidentally constitutes the most expensive GIS component as shown in Fig. 13.2a. Installing a GIS can be a fairly expensive

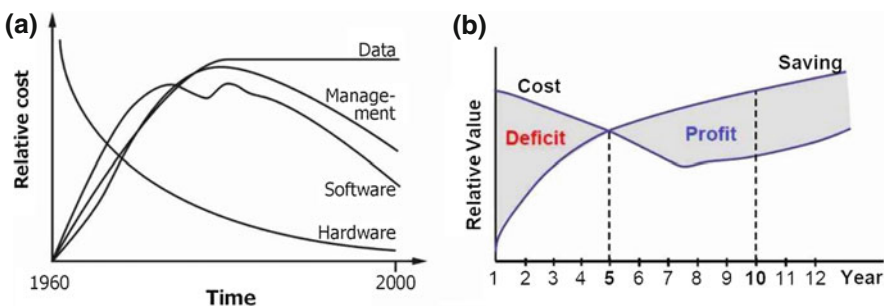


Fig. 13.2 GIS cost aspects. Sources **a** Konecny (2003) and **b** Murai (2004)

exercise requiring significant capital investment for a minimum period of between 5 and 7 years before any profits can be realized as shown in Fig. 13.2b.

13.3 Basic Functions and Applications

There are many software available in the GIS market today. Although the most renowned of these are proprietary in nature, increasingly many open source GIS software are being produced. As a matter of fact, open source GIS is a rich and rapidly expanding field of endeavor as confirmed by Sherman (2008), who carried out a comprehensive survey of open source resources for GIS users, and the impressive list of 356 software and 25 geodatasets available at the freeGIS project website.¹ Despite the fact that different GIS software have different design and architecture, there are certain basic functions that will be characteristic of any serious GIS software as presented in Table 13.1.

Examples of major GIS software with their respective costs are outlined in Table 13.2. One can easily distinguish between open source and freeware GIS software and commercial and proprietary GIS software. For commercial and proprietary GIS software it is important to note that on average an upgrade costs anything between 1/3 and 1/2 of the basic software price. Moreover, each extension module is an added cost and for some GIS software houses it may cost several times more than the basic software. In practice, academic and multiple-user licenses are also available for commercial and proprietary GIS software. As mentioned in Sect. 13.2, to achieve optimal usage, GIS software needs to be matched against the appropriate hardware following an assessment of the user requirements. Ultimately, however, in selecting an appropriate GIS software the total cost of ownership, including the acquisition, maintenance and manpower costs needs to be evaluated.

GIS has evolved today into an integrated multidisciplinary science with many disciplines having contributed to its development in different ways and to varying degrees. Disciplines that traditionally have researched geographic information technologies include cartography, remote sensing, geodesy, surveying, photogrammetry, etc. Additionally, disciplines that traditionally have researched digital technology and

Table 13.1 Basic GIS functions

Basic function	Description
Data input and preprocessing	Map digitizing, map/photo scanning, editing, topology building, format conversion etc
Database management	Data archiving, data retrieval, data updating etc
Spatial analysis	Query, measurements, reclassification, coverage rebuilding, overlay operations, connectivity analysis etc
Graphic output and visualization	Map projection, graphic representation, map production, DEM generation, bird's eye views etc

¹ <http://www.freegis.org>

Table 13.2 Examples of major GIS software in the market (2012)

GIS software	Software house	Single desktop user license cost (US\$)
ArcGIS	ESRI	1,500
Geomedia	Intergraph	1,500
MapInfo	Mapinfo	1,295
ILWIS	ITC (Faculty of Geo-Information Science and Earth Observation, University of Twente)	Free
IDRISI	Clark University	1,250
GRASS	GRASS Information Center	Free
SIS	Cadcorp	–
ER Mapper	ER Mapper	–

information include computer science in general and databases, computational geometry, image processing, pattern recognition, and information science in particular (Weng 2010). Disciplines that traditionally have studied the nature of human understanding and its interactions with machines include particularly cognitive psychology, environmental psychology, cognitive science, and artificial intelligence (Weng 2010).

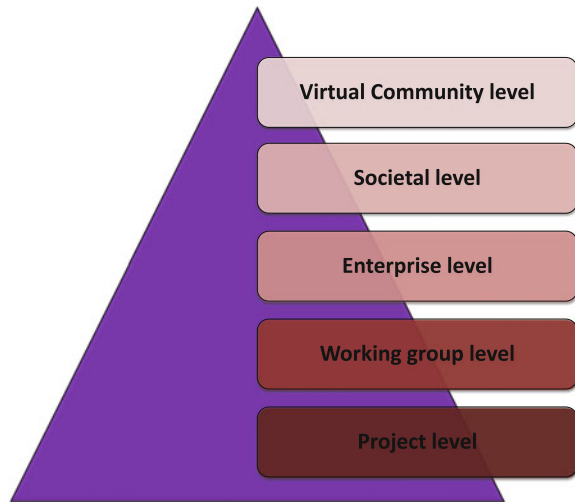
The incredible potential of GIS is perhaps best exemplified by the fact that at least 80% of public and private decision-making is based on some spatial or geographic aspect (Fédération Internationale des Géomètres 2001). As an *enabling technology*, GIS has diverse and almost unlimited potential for applications, ranging from simple to complex, local to global, rural to urban etc. Although GIS was first applied to environmental and natural resource management, it has found application in many classical fields that study physical or human aspects of the earth including geography, global science, sociology, political science, epidemiology, anthropology, demography etc. GIS has also found numerous applications in the area of management and decision making, such as in resource inventory and management, urban planning, land information systems, facilities management, marketing and retail planning, vehicle routing and scheduling etc.

In line with the basic objective of this book, GIS can be used to support environmental monitoring and management in a number of ways, namely;

- (a) Collecting and managing baseline data. Most environmental monitoring activities require that baseline data be collected *a priori* to serve as reference in subsequent monitoring activities (see e.g., Sect. 21.4 for REDD² project baseline mapping).
- (b) Tool for designing and managing monitoring programs. Given the diverse data sets employed in environmental monitoring from different sources e.g., remote sensing, GNSS, desk reports etc., GIS provides a framework for integrating and managing all these different data. Monitoring programs can then be designed and managed using the developed GIS database.

² Reductions in Emissions from Deforestation in Developing countries.

Fig. 13.3 GIS implementation levels



- (c) Managing data requests for multiple users. Environmental monitoring is a multi-disciplinary activity with inputs and requests from different players including the local community. GIS provides a suitable platform for sharing data both horizontally and vertically, especially when integrated within a *spatial data infrastructure* (SDI) framework.
- (d) Analysis and modeling of management and development scenarios. As discussed in Chap. 17, the main strength of GIS lies in spatial analysis. Among other spatial analyses possible, GIS allows the modeling of various “what if” scenarios that enables appreciation of the likely consequences of different developments, without necessarily having to experience them in practice. For example, it is possible to get a graphic visualization of the possible effects of unmitigated forest destruction.

Finally, each application area of GIS requires a special treatment and must examine data sources, data models, analytical methods, problem-solving approaches, and planning and management issues (Weng 2010). Furthermore, depending on the scope of application, GIS can be implemented at different levels ranging from a single project to virtual community level, where for instance cloud GIS solutions are employed, through working group-, enterprise- and societal levels as highlighted in Fig. 13.3.

13.4 Reasons for Success or Failure

The implementation of GIS will either be a success or failure depending on several factors. Tomlinson (2007) summarizes the following six elements as representing the most important factors for implementing a successful GIS:

- (1) *Data input* comprises anything between 70 and 80% of the total cost in GIS. This explains why serious attention should be accorded to the selection and classification of required geospatial data for GIS projects, while taking into consideration the digitizing method to be employed.
- (2) *Maintenance of database* is critical since the quality of decisions made from a GIS depends largely on the quality of the GIS database. It is evident that the maintenance of database is a key issue upon which the success of GIS is centered. In particular, maintaining data quality and routinely updating the system is imperative.
- (3) *Consensus of supporters* is important to the success of GIS projects. Indeed, the supply of GIS experts and GIS-literate people is a critical factor in determining the rapidity of up-take of the existing GIS facilities and their successful use. To achieve success, not only top managers but also other administrative staffs and engineers should support the GIS project. Ideally, GIS should be mainstreamed into the various activities within the organization itself.
- (4) *Customizing software* transforms generic software to customer/application-friendly software. There are various reasons for customizing GIS software including to: add new functionality to applications; embed GIS functions in applications and create specific purpose applications. The tools required for customization of GIS software include availability of an appropriate programming language such as *Visual Basic* or *Java* and an *Integrated development environment* (IDE).
- (5) *Data sharing* is increasingly being appreciated worldwide as an important factor in the economic and effective use of geospatial data in general. This represents one of the important factors that can be relied upon to minimize the total cost of data input and also to maximize the use of the database. Political and administrative problems should be solved to promote the data sharing for a successful GIS. The optimal sharing and standardization of GIS data is best realized once a *spatial data infrastructure* (SDI) has been put in place.
- (6) *Education and training* is very important to understand GIS concept, goals and techniques. They should be organized into three levels for makers, professionals and technologists. However, there is need to modify GIS education and learning to take cognizant of the fact that GIS is now a much broader discipline than simply a collection of tools and techniques. Hence, drawing from the paradigm of geographic information science and technology (GIS&T), more emphasis should be placed upon concepts and methods for geographic problem solving in a computational environment (UCGIS 2003).

Conversely, several reasons have been identified as being responsible for the failure of many GIS projects including (Tomlinson 2007):

- (1) *Lack of vision* and more specifically, the absence of *specific, measurable, achievable, realistic* and *timely* (SMART) objectives will in the long run lead to failure in the implementation of GIS. Precise and specific targets and goals need to be drawn to mitigate against failure.

- (2) *Lack of long term plan* may also contribute towards failure in GIS. Cost-benefit analyses have demonstrated that the full benefits of GIS are only realized after about 5 to 7 years (see Fig. 13.2b, p. 194). This means that the initial phase of implementing GIS is essentially one of capital investment, with the costs incurred far outweighing any possible benefits. However, inability to demonstrate benefits in the interim period may actually lead to unsuccessful GIS. Similarly, poor planning or lack of a long term plan will result in unsuccessful GIS. There is also need to periodically update GIS data and upgrade GIS hardware and software accordingly to match user and system requirements.
- (3) *Lack of system analysis* is likely to precipitate failure in GIS. There is need to adopt a system approach and integrate appropriate restructuring to avoid failure in the implementation of GIS projects. Similarly, un-supportive organizational structure will lead to unsuccessful GIS.
- (4) *Lack of user's access* will in the long run lead to failure. Besides data, users constitute an integral component in GIS (see Sect. 13.2). There is need to equip the different cadres of GIS users with appropriate knowledge, skills and experience through customized training and full user participation. To avoid failure it is also important to provide documentation for all requisite procedures.
- (5) *Lack of support by decision makers* and particularly, lack of executive-level commitment and support, due to one reason or the other, will lead to failure in GIS. Similarly, lack of core funding, or undesirable political pressure, especially where these change rapidly will only lead to unsuccessful GIS.
- (6) *Lack of expertise* is a sure way to failure as GIS is a fairly technical discipline. Inadequate oversight of key participants, inexperienced managers or absence of consultation will no doubt lead to failure in GIS.

13.5 Concluding Remarks

As a special type of information system which basically deals with geospatial data, GIS has proved to be quite a versatile *science and technology* that offers remarkable spatial decision support capability. It is particularly well suited for use in fairly complex practical applications, like those prevalent in environmental monitoring and management, in which several different and sometimes competing factors often characterized by complex relationships, need to be considered in decision making. GIS allows the stochasticity of the different pertinent variables to be brought together within a common framework to make better and informed decisions. Moreover, appropriate models can be integrated to customize and tailor GIS software in order to address and suit specific applications.

Perhaps, one of the foremost advantages of GIS is the ability to investigate worst case scenarios and appreciate the underlying factors in a better and more meaningful way, without having to wait to experience these first in practice. For example, using GIS it is possible to model and examine the possible impact of an oil spill to an ecosystem *a priori*. This would allow for appropriate mitigation measures to be put

in place well in advance to prevent the occurrence of such an environmental disaster, or to deal with the possible consequences by fine tuning response and recovery strategies, if such a disaster was to occur in future.

By and large, the quality of the decisions made from a GIS is influenced largely by the quality of the geospatial data in the GIS database. This data needs to be accurate, complete, consistent and up-to-date. As articulated in this chapter, alongside this basic and critical requirement, various other factors also need to be in place to ensure that GIS succeeds in contributing positively to influencing the way that better, timely and informed decisions are made.

References

- Aronoff S (1989) Geographic information systems: a management perspective. WDL Publications, Ottawa
- Burrough PA (1986) Principles of geographical information systems for land resources assessment. Oxford University Press, New York, 50 pp
- Fédération Internationale des Géomètres (2001) <http://www.fig.net>. Accessed 11 June 2010
- Konecny G (2003) Geoinformation: remote sensing, photogrammetry, geographic information systems. Taylor and Francis, New York
- Longley PA, Goodchild MF, Maguire DJ, Rhind DW (2005) Geographic information systems and science. Wiley, West Sussex
- Murai S (1999) GIS work book: fundamental and technical courses, vols 1–2. National Space Development Agency
- Murai S (2004) Remote sensing and GIS courses—distance education. Japan International Cooperation Agency (JICA)-Net
- Sherman GE (2008) Desktop GIS: mapping the planet with open source tools. The Pragmatic Bookshelf, Raleigh
- Tomlinson RF (2007) Thinking about GIS: geographic information system planning for managers. ESRI Press, New York
- UCGIS (University Consortium for Geographic Information Science) (2003) The Strawman report: development of model undergraduate curricula for geographic information science & technology. Task Force on the Development of Model Undergraduate Curricula, University Consortium for Geographic Information Science
- Weng Q (2010) Remote sensing and GIS integration: theories, methods, and applications. McGraw-Hill, New York 416 pp

Chapter 14

Data Models and Structure

“The sciences do not try to explain, they hardly even try to interpret, they mainly make models. By a model is meant a mathematical construct which, with the addition of certain verbal interpretations, describes observed phenomena. The justification of such a mathematical construct is solely and precisely that it is expected to work—that is, correctly to describe phenomena from a reasonably wide area.”

John von Neumann (1903–1956)

14.1 Introductory Remarks

By convention, data in the real world is deemed to exist in a continuous or analogue form usually in three dimensional space as discussed in Sect. 2.1 Such data needs to be digitized or made discrete before it can be input and processed by a digital computer. A GIS database can be viewed as an abstraction of reality. To convert object features observed or measured in the real world into the digital realm in a GIS database it is necessary to structure the data appropriately. Four (4) different generic types of primitive object features can be distinguished, namely: point features (0-D), line features (1-D), area features/polygons (2-D), and surface features (3-D). Incidentally, when surface features are captured in a discrete or non-continuous manner, this is then referred to as 2.5D. In general, an object feature is defined by three (3) properties in GIS, namely: position, attributes and relationship with other features referred to as *topology*.

The object feature position consists of location data that defines the object’s spatial extent. Feature attributes are data that describe and specify the characteristics of a feature, whereas the object feature relationship describe its neighborhood properties. There are two major types of geometric data models employed in GIS: *vector* and *raster models* (see Fig. 14.1).

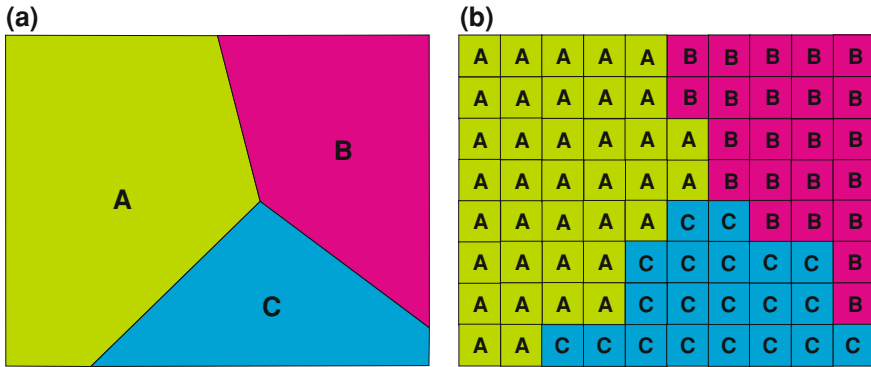


Fig. 14.1 Vector and raster models. **a** Vector model. **b** Raster model

Table 14.1 Comparison between vector and raster models

Model type	Advantages	Disadvantages
Vector	Precise expression Less data volume Full topology Fast retrieval Fast conversion	Complicated structure Difficulty in overlay Difficulty in updating Expensive data capture
Raster	Simple data structure Easy for overlay and modeling Suitable for 3D display Integration of image data Automated data capture	Large data volume Difficulty in network analysis Slow conversion

Source Murai (1999)

- (1) *Vector model* that uses discrete points, lines and/or areas corresponding to discrete objects with name or code number of attributes.
- (2) *Raster model* which employs regularly spaced grid cells set out in a specific sequence.

14.2 Vector and Raster Models

Most of the earlier GIS software ran on either vector or raster platforms and thus supported either one of these two data models. This meant that from the word go, one had to decide *a priori* which one of these two data models one’s GIS would support. Whichever choice one made was informed largely by the the type of analysis that one wanted to perform as each of these formats had its own advantages and disadvantages. Today this limitation is no longer critical in most commercial GIS software. It is thus

possible to convert from vector to raster data format and vice-versa, even though with certain data loss. Nonetheless, it is important to appreciate the strengths and weaknesses of these two data formats as this would inform the environment in which one would perform a particular GIS operation. Table 14.1 compares the advantages and disadvantages of vector and raster data models.

14.3 GIS Topology

A GIS topology is essentially a set of rules and behaviors that model how objects share geometry. Topology is employed for a number of reasons including to ESRI (2005):

- (1) Manage shared geometry (i.e., constrain how features share geometry). For example, adjacent polygons, such as parcels, share edges; street centerlines and the boundaries of census blocks share geometry; adjacent soil polygons share edges etc.
- (2) Define and enforce data integrity rules (e.g., no gaps should exist between parcel features, parcels should not overlap, road centerlines should connect at the endpoints etc.)
- (3) Support topological relationship queries and navigation (e.g., have the ability to identify adjacent and connected features, find the shared edges, and navigate along a series of connected edges).
- (4) Support sophisticated editing tools that enforce the topological constraints of the data model (e.g., ability to edit a shared edge and update all the features that share the common edge).
- (5) Construct features from unstructured geometry (e.g., the ability to construct polygons from lines sometimes referred to as “spaghetti”).

Conventionally, spatial objects in vector data format are geometrically represented by the data primitives: point, line, polygon and surface. For most spatial analysis in GIS, use of only the object geometry, which is defined through the object’s position, shape and size in a specified coordinate system, is not sufficient. Usually, the spatial relationship or connectivity between the various spatial objects defined by the topology is also required. Specifically, vector data structure requires that in addition to the geometry the topology be explicitly encoded. Furthermore, when two GIS layers are overlaid, there is need to update the topology for the new combined map. This is not the case with raster data structure, since the pixel coordinates in both horizontal and vertical dimensions help to uniquely define both the geometry and topology. Hence, unlike the case with the vector data, it is not necessary to explicitly encode the topology in raster data structure.

Various topological relations can be discriminated such as connectivity, adjacency, inclusion etc. Different topological data structures can be distinguished for the basic data primitives of point, line and area. As illustrated in Fig. 14.2 one can make a distinction of point to point relations (is within, nearest to); point to line relations (on

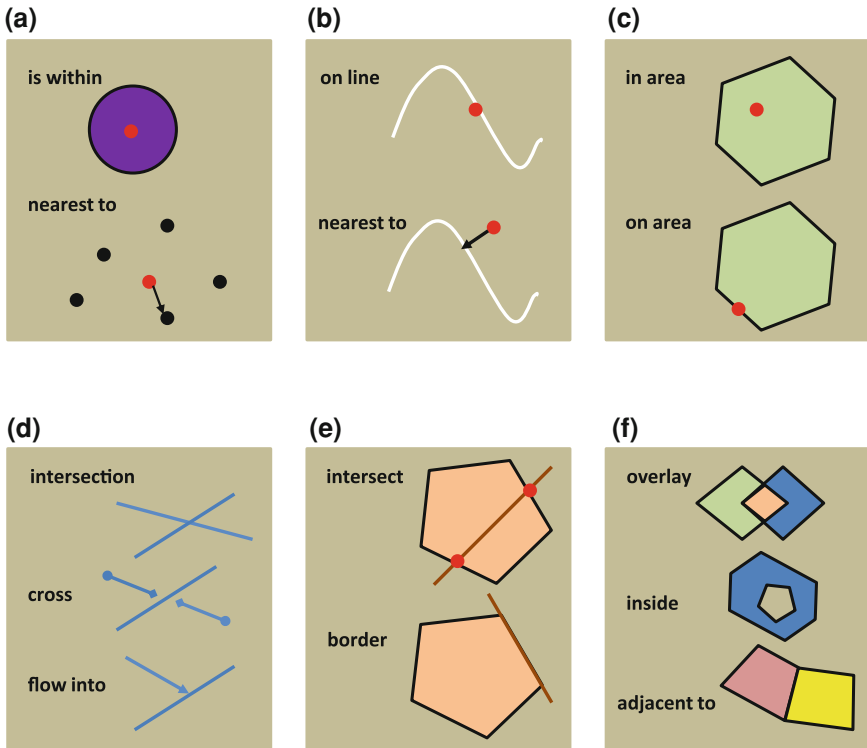


Fig. 14.2 Spatial topological relationships. **a** Point to point relations. **b** Point to line relations. **c** Point to polygon relations. **d** Line to line relations. **e** Line to polygon relations. **f** Polygon to Polygon relations

line, nearest to); point to polygon relations (in area, on area); line to line relations (intersection, cross, flow into); line to polygon relations (intersect, border); and polygon to polygon relations (overlap, inside, adjacent to). Geometric and topological modeling can be built using semantic networks as exemplified in Stilla (1997), Bishr (1998), Mena (2003) etc.

14.4 Concluding Remarks

Geospatial data needs to be appropriately structured before it can be input into a GIS database. One can distinguish between vector and raster data structures. Each of these data structure has its own strengths and weaknesses. Moreover, it is also true that certain GIS analyses are best performed using one data model or the other. For instance, whereas overlays are best handled in raster environment, network analysis is best performed in vector format. In a particular GIS application, therefore, it is

important to identify the best data structure that needs to be employed *a priori*, and thereafter format or restructure the data accordingly. Besides the geometry, topological relationships also need to be encoded, either explicitly or implicitly for vector and raster data respectively.

References

- Bishr Y (1998) Overcoming the semantic and other barriers to GIS interoperability. *Int J Geogr Inf Sci* 12(4):299–314. doi:[10.1080/136588198241806](https://doi.org/10.1080/136588198241806)
- ESRI (2005) GIS topology: an ESRI white paper. p 14
- Mena JB (2003) State of the art on automatic road extraction for GIS update: a novel classification. *Pattern Recogn Lett* 24(16):30373058
- Murai S (1999) GIS work book: fundamental and technical courses. vols 1 & 2. National Space Development Agency, New York
- Stilla U, Michaelsen E (1997) Semantic modelling of man-made objects by production nets. In: Automatic extraction of man-made objects from aerial and space images (II). Monte Verita, Birkhäuser Verlag Basel, pp 43–65

Chapter 15

Input of GIS Data

“Effective GIS applications have little to do with data and everything to do with understanding, creativity and perspective.”
(GeoWorld, Aug. 1996)

15.1 Data Sources for GIS

Precisely because of the expensive cost of GIS data capture and the fact that the procedures involved in this are also fairly time consuming, the sources for GIS data should always be carefully analyzed before selection in order to suit specific GIS application(s). There are many possible sources for GIS data available today. The criteria for assessing the most appropriate sources for GIS data include firstly, collecting only the necessary data and secondly, for cost effectiveness, accepting the minimum data quality that will get the specific GIS job to be successfully accomplished. Moreover, where geospatial data needs to be integrated, it is important that the various sources be critically examined for compatibility. The following data sources are widely used for input of GIS data:

- (1) *Analogue maps and plans* and specifically, both topographic and thematic maps represent some of the basic sources for GIS data. These need to be digitized either manually by digitizers or automatically by scanners. However, analogue maps exhibit many problems such as lack of availability, out of date, inconsistency in map production time, inaccuracy etc.
- (2) *Aerial photographs* represent one of the best sources for updating GIS data. Both quantitative (metric) and qualitative (thematic) GIS data can be extracted through visual image interpretation and photogrammetric restitution techniques described in Sects. 10.2 and 11.3.2 respectively.
- (3) *Satellite imagery* given that they are usually acquired in digital form, can be input directly into a GIS database. They are available for land use classification,

Table 15.1 GIS data sources

Data sources	Method	Equipments	Accuracy	Cost
Analogue map	Manual digitizing	Digitizer	±0.1 mm (on a map)	Low
	Semi-automatic scanning	Scanner	±0.1 mm (on a map)	High
Aerial photos	Analytical photogrammetry	Analogue stereo plotter	±10 cm	High
	Digital photogrammetry	Digital photogrammetric workstation	±10 cm	Very high
Satellite images	Visual interpretation	Image viewer	±1–50 m	Low
	Digital image processing	Image processing system	±1–30 m	High
Ground survey Reports	Field measurement	Total station, GPS	±1 cm	Very high
	Keyboard entry	Keyboard, PC		Low

(Source Murai 1999)

environmental monitoring, digital elevation model (DEM) etc. Most medium and coarse resolution satellite imagery result in maps of scales between 1:50,000 to 1:100,000. On the other hand, HSRI with ground resolution of about 0.6–2 m can be used to produce maps at scales of between 1:5,000 and 1:10,000 and 3D landscape animations (see Sect. 8.3).

- (4) *Ground survey* methods such as traversing and triangulation are usually very accurate, but too expensive to cover expansive areas. Total station together with GNSS have modernized ground surveys (see Chaps. 4–6).
- (5) *Reports and publications* documenting social economic data usually listed in the form of statistics and census with respect to administration units are useful sources of GIS attribute data.

Table 15.1 shows methods, equipments, accuracy and cost for different data sources.

15.2 Data Capture and Editing

On average, *data capture* contributes up to about 80% of the total costs of a typical GIS project. Figure 15.1 shows the general approach adopted in capturing and editing data ready for input into a GIS database as follows:

- (1) *Data identification* is the first step in the capture of GIS data. A user needs assessment is carried out in order to identify the user information needs. This also helps identify the data required for their applications. Subsequently, the appropriate data sources and their location are determined.

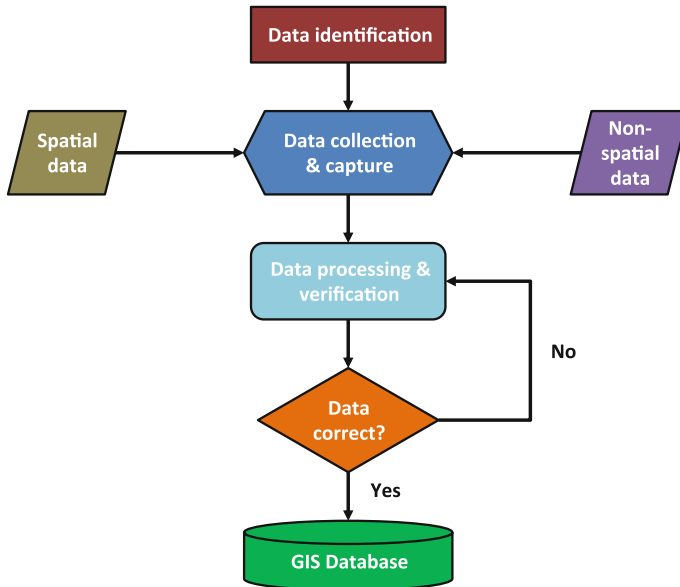


Fig. 15.1 GIS data capture and editing

- (2) *Analogue data collection* is then undertaken since in many cases a lot of the available spatial data is in the form of analogue maps. The identified maps are collected and evaluated on the basis of their quality, complexity and compatibility. Within the framework of *spatial data infrastructure* data quality is defined by factors such as *lineage*, *consistency*, *completeness*, *semantic accuracy*, *temporal accuracy*, *positional accuracy* and *attribute accuracy* (see e.g., Congalton (2009), Groot and McLaughlin (2000) etc). If acceptable the maps may then be prepared for digitization. In projects where digitization will be delayed or extended over a finite period of time, the maps must be stored in optimal temperature and humidity conditions while awaiting digitization. Attribute or non-spatial data often in socio-economic reports or census data also needs to be collected.
- (3) *Analogue data preparation* needs to be then performed. At this stage the object features to be digitized are chosen and feature codes assigned to them. If necessary, they are highlighted for easy recognition. It may also be necessary to reformat the manuscript to conform to the digitization method to be used. Cleaning is needed so as to remove the possibility of noise in the data. For extended digitizing, it may also be prudent to *contact print* the manuscript on more stable material.
- (4) *Digitization* involves the actual conversion of analogue data to digital form according to some chosen data model and structure and then passing onto a digital storage device. One can distinguish between vector and raster methods of digitization as described in the next two subsections. The choice of digitization

method made depends on among others: available instruments, the kind of input data, available finance etc. If no attribute data were entered during digitization, for example in scanning, they are entered at this stage.

- (5) *Editing* is required to remove all the errors incurred during data capture. The digitized data need to be displayed, checked and corrected for any errors or inconsistencies. The process of detecting and correcting errors made at various stages of data capture is known as error editing. This should enable either addition, deletion or change of positional and attribute data. Error editing may be performed in three (3) modes: *batch*, *interactive* or *semi-automatic editing*. Since each of these modes has its own advantages and disadvantages it is important to identify which types of errors are best handled by which editing mode before adopting a particular editing mode. On the other hand, cartographic/cosmetic editing is the cartographic manipulation of the data in order to give the final graphic the expected cartographic appearance e.g., most buildings are expected to have 90° corners.

15.2.1 Vector Data Input

Manual digitizing is the most popular method for vector data input. Some of the advantages of manual digitizing include:

- Relatively cheap hardware and software is required.
- Only viable method when documents must be continuously interpreted as digitizing proceeds.
- Well documented history of success.
- Easy to train operators.

Some of the disadvantages of manual digitization include:

- Operator fatigue and stress mainly due to frequent shifting from one operation to another, which deteriorates the quality of output. Several measures have been attempted to ameliorate this problem with varying success. This includes use of aided tack cursor, voice entry for attributes, introduction of shift working etc.
- Slow progress especially with dense data e.g., contours.

Tablet digitizers with a free cursor connected with a personal computer are the most common device for digitizing spatial features with the planimetric coordinates from analog maps. The analogue map is placed on the surface of the digitizing tablet. The size of digitizer usually ranges from A3 to A0 size.

The basic digitizing operation proceeds as follows:

- (1) The map is affixed onto a digitizing table.
- (2) Control points or tics at four corners of the map sheet should be digitized by the digitizer and input to PC together with the map coordinates of the four corners. Affine parameters and their standard errors are computed and checked against

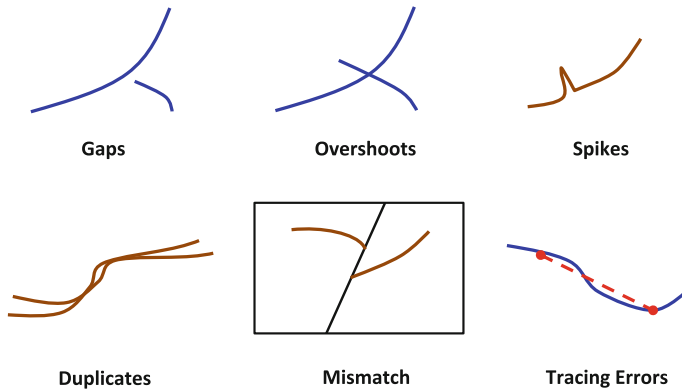


Fig. 15.2 Some typical errors of manual digitizing

acceptable tolerances to confirm whether or not map mounting has been done successfully. If not acceptable, the choice of the tics needs to be varied and the procedure repeated.

- (3) Map features are digitized according to the feature layers and feature code system in either point mode or stream mode either using pre-defined time or distance intervals.
- (4) Editing errors such as small gaps at line junctions, overshoots, duplicates etc., should be made to realize a clean data set without errors.
- (5) Conversion from digitizer coordinates to map coordinates to store in a spatial database.

Major problems of map digitization include the following:

- (a) the map will stretch or shrink day by day which makes the newly digitized points slightly off from the previous points;
- (b) the map itself has errors; and
- (c) discrepancies across neighboring map sheets will produce dis-connectivity.

Inexperienced operators will make a lot of errors and mistakes while digitizing. Some typical errors of manual digitizing are shown in Fig. 15.2.

15.2.2 Raster Data Input

Automatic scanning is the most common method for raster data input. Scanners are used to convert from analog maps or photographs to digital image data in raster format. They sense the gray tone or color values of documents and outputs values in a series of pixels. Digital image data are usually integer-based with one byte gray scale (256 gray tones from 0 to 255) for black and white image and a set of three

gray scales of Red (R), Green (G) and Blue (B) for color image. The following four types of scanners are commonly used in GIS and remote sensing (Murai 1999):

- (1) Mechanical scanner: It is called drum scanner since a map or an image placed on a drum is digitized mechanically with rotation of the drum and shift of the sensor. It is accurate but slow.
- (2) Video camera: Video camera with CRT (cathode ray tube) is often used to digitize a small part of map. This is not very accurate but cheap.
- (3) CCD camera: Area CCD camera (called digital still camera) instead of video camera will be also convenient to acquire digital image data. It is more stable and accurate than video camera.
- (4) CCD scanner: Flat bed type or roll feed/drum type scanner with linear CCD (charge coupled device) is now commonly used to digitize analog maps in raster format, either in mono-tone or color mode. It is accurate but expensive.

Some of the advantages of scanning include:

- It is a fairly fast means of digitizing especially large and dense data sets.
- Minimum strain on operator as the process is largely automatic.
- Resulting data can be readily integrated with remotely sensed image data.

On the other hand, some of the disadvantages of scanning include:

- Relative high cost of hardware and software (although these are continually coming down).
- Very intensive manuscript preparation is required.
- Selective digitizing is not possible.

15.3 Rasterization and Vectorization

As discussed in Sect. 14.2, there are certain GIS analysis that are best performed in either vector or raster environments. However, the data may have been captured in one format or the other. This therefore calls for conversion from vector to raster data format and vice-versa. Numerous algorithms have been developed to enable these conversions that are very useful in practical applications of GIS.

Rasterization refers to conversion from vector to raster data. It is also useful in integrating GIS with remote sensing data. On the other hand, *vectorization* refers to conversion from raster to vector data. It is more complicated and more expensive than rasterization. A typical vectorization algorithm comprises of the following basic steps as shown in Fig. 15.3:

- (a) *Skeletonization* which is the extraction of lines one pixel wide though thinning and is the first step in vectorization.
- (b) *Coordination* through which the pixels defining the vector line are coordinated and the coordinates weeded out for optimum volume.

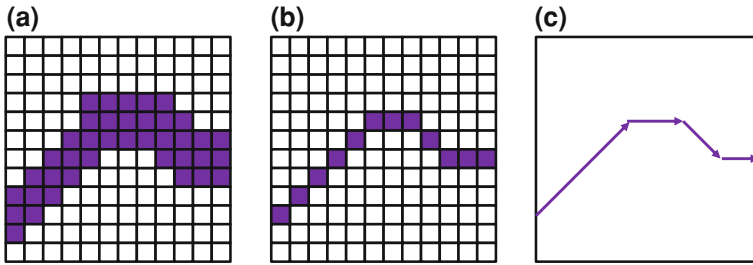


Fig. 15.3 Example of vectorization algorithm: **a** original image: **b** skeletonization: **c** coordination and topology reconstruction

(c) *Topology reconstruction* that allows contextual relationships like adjacency and connectivity to be determined and built in.

15.4 Concluding Remarks

Various possible sources of data for input into a GIS database exist. It is important that the best available combination of data sources be selected to fit a particular application by judiciously examining the quality, completeness, and compatibility of available data among other considerations. The fact that the GIS data capture phase accounts for up to about four-fifths of the entire GIS budget implores the need for prudent investment in data at this critical stage in the construction of a GIS. Data can be captured using either vector or raster based methods, with the most popular techniques being manual digitizing and automatic scanning respectively.

It is also important at this juncture to recognize the growing importance in data sharing, which is incidentally today recognized as one of the keys for a successful GIS (see Sect. 13.4). Within the framework of spatial data infrastructure (SDI), the possibility of using already existing data, provided that it meets the quality expectations of the particular GIS project, should be strongly considered. This calls for the setting up of viable and feasible SDIs at national, regional and global scales.

References

- Congalton R, Green K (2009) Assessing the accuracy of remotely sensed data: principles and practices. Taylor & Francis Group, Boca Raton
- Groot R, McLaughlin J (eds) (2000) Geospatial data infrastructure: concepts, cases and good practice. Oxford University Press, Oxford
- Murai S (1999) GIS work book: fundamental and technical courses vols 1–2. National Space Development Agency, New York.

Chapter 16

GIS Database

“Good design is clear thinking made visible.”

Edward Tufte

16.1 Basic Concept

Once digitized and edited GIS data are stored in a *spatial database*. Evidently, the quality of the decisions made from a GIS will depend on the quality of the data contained in the database. A spatial database is defined as a pool of integrated and structured geospatial data, which is a model of reality, and from which data may be retrieved to provide useful information to users. Hence, a spatial database is comprised of inter-related geospatial data that is maintained efficiently and which is shareable between different GIS applications.

Data management are all the procedures involved in data storage, retrieval, updating, back-up, exchange and archiving. This is needed because of the fact that data processing and use is not instantaneous. Furthermore, data needs to be accessed easily and repeatedly by different users for diverse applications. There are two (2) basic approaches to database management namely; file processing and use of a Database Management System (DBMS). The use of a DBMS is the most popular method. The functions expected of a spatial database include:

1. Consistency with little or no redundancy;
2. Maintenance of data quality including updating;
3. Self descriptive with metadata;
4. High performance by database management system with database language; and
5. Security including access control.

In general, the benefits of employing databases include: little or few redundancy, data security, data sharing, high accessibility, standardization, data contraction, and

access management. In the 1980s, GIS databases were centralized with a *centralized databases*. However, from the 1990s, the network concept arose. This latter conception is more convenient in as far as meeting user needs is concerned with *distributed databases* being employed. Such distributed databases in a network structure present the following benefits:

- (a) Better data storage and updating;
- (b) More efficient retrieval; and
- (c) More efficient output.

16.2 Design Considerations

The design of spatial database will be made by the database manager who is responsible for the following issues:

- Definition of database contents;
- Selection of database structure;
- Data distribution to users;
- Maintenance and updating control; and
- Day-to-day operation.

The following parameters should be considered in designing the spatial database:

1. *Storage media* type should be considered in view of different types of storage media available, the volume, access speed and on-line service.
2. *Partition of data* using an appropriate format should be made in view of the envisaged GIS application. The spatial data may be partitioned on the basis of the administrative boundaries, map sheets, watersheds etc.
3. *Standards* are critical as the format, accuracy and quality should all be standardized. It is also important to address metadata issues.
4. *Change and updating* captured through various commands including “add”, “delete”, “edit” and “update” should be well controlled by the database manager.
5. *Scheduling* of data availability, priorities, data acquisition etc., are all important issues that need to be evaluated and appropriately scheduled.
6. *Security* issues including copyright, back up system and responsibilities should be well managed.

16.3 Database Management System

Date (1983) asserts that a *database management system*(DBMS) represents a set of computer programs that govern access to a database. It provides a number of functions to create, edit, manipulate and analyze spatial and non-spatial data in the

applications of a GIS. Dale and McLaughlin (1989) summarize the objectives of DBMS to include the following:

- Storing of data in formats that are independent of the current or potential application programs;
- Structuring of data so that it can be accessed in a manner independent of its physical structure;
- Controlling access and updating of data to ensure privacy and integrity; and
- Minimizing redundancy in the stored data, thereby reducing storage requirements and increasing consistency of use.

Pursuant to the above objects, the main functions of a database include Murai (2004):

1. *Creating* records of various data types such as integer, real, character, data, image etc.
2. *Operations* including sort, delete, edit, select etc.
3. *Manipulation* like input, analysis, output, reformatting etc.
4. *Query* which is made using a standardized language such as Standard Query Language (SQL).
5. *Programming* which is useful for application programs and includes languages such as Java, C, etc.
6. *Documentation* through which metadata or description of the contents of the database is compiled using languages such as XML.

Behind any DBMS is a logical database model that seeks to capture the often complex spatial relationships between objects. There are five (5) basic types of database models: *hierarchical model*; *network model*; *relational model*; *object-oriented model* and *object-relational model*. Figure.16.1 illustrates the basic differences between the above database models, while Table 16.4 (p. 220) highlights the advantages and disadvantages of different database models.

The hierarchical model is essentially a *top-down* structure where there is a clear “parent-child” relationship between certain data. For example, an administrative database might have data organized by country, province, county and constituency. This organization provides rapid accessing of information within individual branches, but slow comparison of information from separate branches (Dale and McLaughlin, 1989). On the other hand, data is associated by user-defined links in the network model. Such models are desirable when purely hierarchical relations do not fulfill organizational requirements. Compared to hierarchical models, network models allow for the flexible structuring of information to satisfy specific user demands. However, as the number of links increases, the structure becomes very cumbersome to handle in a DBMS as noted by Dale and McLaughlin (1989).

The relational model has been most successful in GIS. It makes use of relational tables to model and link the spatial relationships between objects. Here, data is placed in a table or *relation* which indicates a match between two or more entities. Hence, a database employing the relational model can be thought of as a set of tables, with each table representing specific types of relations. In the conceptualization of

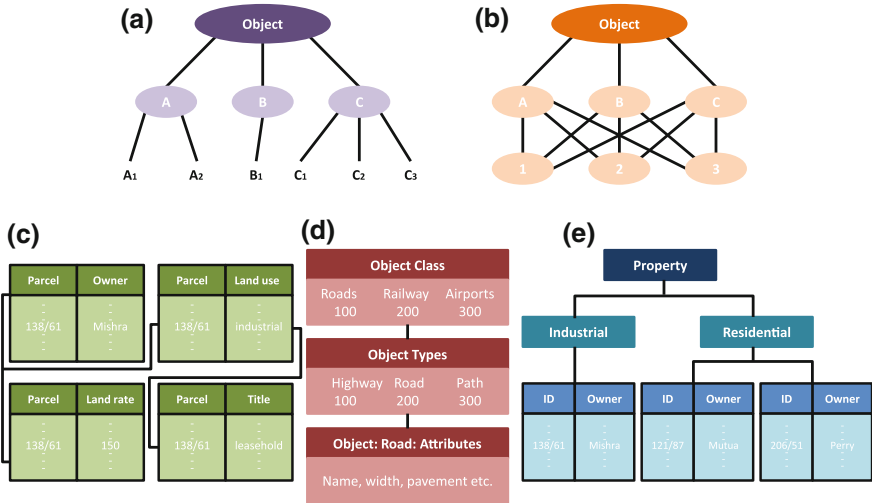


Fig. 16.1 Database management system models. **a** Hierarchical model. **b** Network model. **c** Relational model. **d** Object-oriented model. **e** Object-relational model

Table 16.1 Example of un-normalized tables

Parcel no.	Owner of parcel	Land use type	Annual land rates (US\$)
121/87	Mutua	Residential	50
209/98	Oketch	Commercial	100
127/99	Simiyu	Residential	50
145/79	Tonui	Industrial	150
138/61	Mishra	Industrial	150
207/72	Kimani	Commercial	100
206/51	Perry	Residential	50
152/93	Ali	Commercial	100

relational models, the key(s) of the relation and the prime attribute(s) are important considerations. Once the relations have been captured using appropriate tables there is need to further normalize these in order to reduce data redundancy. This is exemplified through Tables 16.1, 16.2 and 16.3, with the keys comprising “parcel no.” (primary) and “land rates” (secondary) and the attributes including “owner of parcel”, “land use type” and “annual land rate”. Some well known relational DBMSs include *dBase*, *Oracle*, *Informix*, *Sybase*, *PostgreSQL* etc.

The concept of object orientation embraces four components: (i) object-oriented user interface (e.g., icons, dialog boxes, glyphs, etc.), (ii) object-oriented programming languages (e.g., Visual Basic, Visual C etc.), (iii) object-oriented analysis, and (iv) object-oriented database management Lo and Yeung (2002). The object-oriented database model is a logical database model concept characterized by the *inheritance*

Table 16.2 Example of normalized Table 16.1

Parcel no.	Owner of parcel	Land use type
121/87	Mutua	Residential
209/98	Oketch	Commercial
127/99	Simiyu	Residential
145/79	Tonui	Industrial
138/61	Mishra	Industrial
207/72	Kimani	Commercial
206/51	Perry	Residential
152/93	Ali	Commercial

Table 16.3 Example of normalized Table 16.2

Land rates	Land use type	Annual land rates (US\$)
	Residential	50
	Commercial	100
	Industrial	150

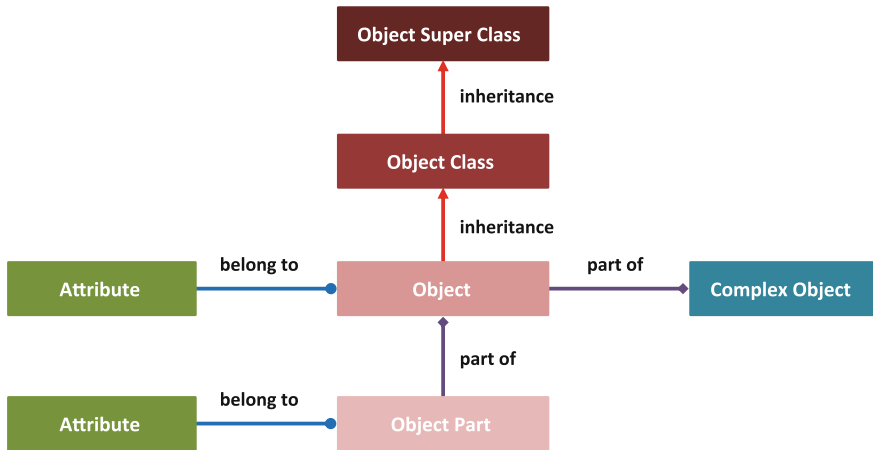


Fig. 16.2 Structure of object-oriented database. *Modified after Murai (2004)*

and *relationship* of data objects. Pursuant to the *General Feature Model* (GFM), spatial information is divided into objects. Furthermore, the database is built by combining these objects. Objects are defined with regard to type, characteristics etc. in the real world. Hence the *class* captures the design of objects. Moreover, objects have functions. Objects and functions are unified through the process of *encapsulation*. Figure. 16.2 highlights the typical object-oriented database structure. Examples of

Table 16.4 Advantages and disadvantages of major DBMS models

DBMS model	Advantages	Disadvantages
Relational database	Simple table structure and user interface, many end-user tools available, easy modification, easy to use table, easy table linkage, fast direct data access, data independence from application, optimized for GIS query and analysis, available large amounts of GIS data, large pool of experienced developers, developer tools, textbooks and consultants	Limited real world representation, limited flexibility of queries and data management, slow sequential access, sometimes difficult to model, complex relationships must be expressed as procedures in every program that accesses the database, performance penalty due to the need to reassemble data structures every time the data is accessed
Object-oriented database	Not necessary to know the inner workings of an object, to allow complex representations of the real world, to support generalization, aggregation, and association, to maintain history in the database, to integrate with simulation modeling techniques, multiple simultaneous updating	Complex models are more difficult to design, import and exchange with other types is difficult, some applications may not be accessible to an object oriented model, slow to execute, difficult description for the natural world, special languages are required for object-oriented database
Object-relational database	Fast execution, uniform repository of geographic data, more accurate data entry and editing, high data integrity, enable to work with more intuitive data objects, simultaneous data editing	Compromise between object-oriented and relational database models, no data encapsulation, limited support for object relationships, difficult to model complex relationships

Source Tomlinson (2007)

commercial object-oriented DBMS include: *ObjectStore*, *Cache*, *Objectivity/DB*, *Smallworld* etc.

The object-relational database model draws from the strengths of both the relational and object-oriented database models. Specifically, the object-relational database is extended by software that incorporates object-oriented behavior, but data are not encapsulated. Database information is still in the form of tables, but some of the attribute columns can include a richer data structure—called an *abstract data type*. Commercial software employing object-relational database model include: *ArcGIS*, *PostGIS* etc.

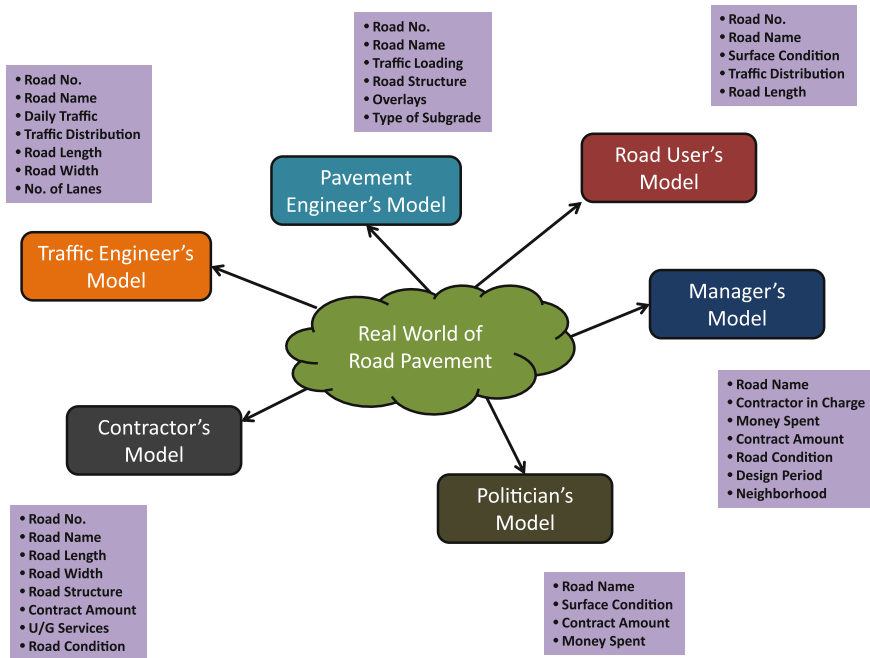


Fig. 16.3 Example of an external model. Source Kiema and Mwangi (2009)

16.4 Design Procedure

Once the spatial database design parameters have been evaluated and the appropriate database model adopted, the *spatial database design process* follows. Conceptually, this is comprised of the following four steps:

1. *External modeling* is the determination of a finite set of potential users of the database, their information needs and data required to satisfy those needs. This comprises the views of the database as seen by the users and focuses mainly on the actual information provided by the database. Figure. 16.3 shows a typical external model designed in the development of a GIS-based Road Pavement Information and Management System.
2. *Conceptual modeling* involves the abstraction of the external model into an Entity-Relation diagram showing all the entities (objects of interest) involved, their attributes (set of properties) and relationships. According to Dale and McLaughlin (1989), the conceptual level can be thought of as the application programmer's view, the data administrator's view or the sum of all the user's views. Figure. 16.4 shows the conceptual model developed from Fig. 16.3.
3. *Logical modeling* revolves around mapping the conceptual model into logical model data management system. For a relational database model, the logical

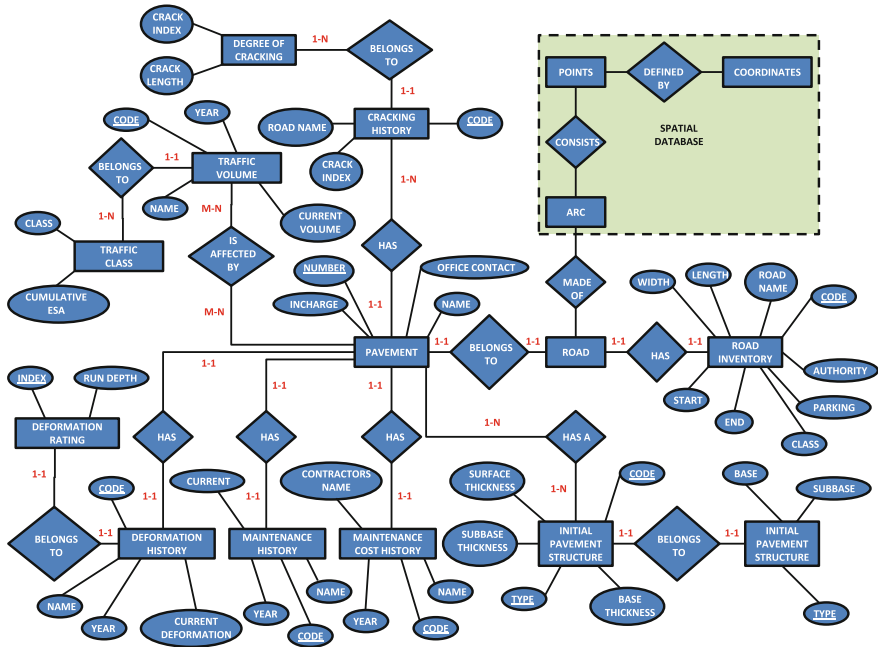


Fig. 16.4 Example of a conceptual model. Source Kiema and Mwangi (2009)

model is in form of tables or relations which must be normalized before application.

4. *Physical modeling* is the actual population of the spatial database. This is hardware and software dependent.

16.5 Concluding Remarks

The GIS database is an abstraction of reality. Ultimately, the quality of the decisions made from a GIS will depend on the quality of the database. This Chapter has attempted in a simple way to define the concept of a spatial database as well as highlight parameters that need to be considered in designing a spatial database. From a functional point of view, the hallmark of a database management system is also outlined. The common five (5) types of database models include: hierarchical, network, relational, object-oriented and object-relational models. Although the relational model is still the most popular DBMS model employed in structuring GIS databases today, it is likely that in future the object-relational model, which leverages on the advantages of both relational and object-oriented databases, will become the most popular GIS database model.

As described in Sect. 2.2, to achieve its full potential, geodata needs to be shared and re-used by different users and applications. This is best done within a framework referred to as *spatial data infrastructure* (SDI), see e.g., Groot and McLaughlin (2000), SDI Cookbook (2004), Maguire and Longley (2005) etc that allows different GIS databases scattered across different geographic locations to be linked and connected. Hence, SDI is all about organizing spatial data and information in an intelligent manner in order to make it useful for gaining knowledge. It is an important construction that is imperative to realizing the full business value of spatial data and information.

References

- Dale P, McLaughlin J (1989) Land information management. Clarendon Press, Oxford
- Date CJ (1983) An introduction to database systems, 3rd edn. Addison Wesley, Munich
- Groot R, McLaughlin J (eds) (2000) Geospatial data infrastructure: concepts cases and good practice. Oxford University Press, New York
- Kiema JBK, Mwangi JM (2009) A prototype GIS-based road pavement information and management system. J Civil Eng Res Pract 6(1). <http://ajol.info/index.php/jcerp/article/view/45192>
- Lo CP, Yeung AKW (2002) Concepts and techniques of geographic information systems. Prentice-Hall, Upper Saddle River
- Maguire DJ, Longley PA (2005) The emergence of geoportals and their role in spatial data infrastructures. Comput Environ Urban Syst 29(1):3–14
- Murai S (2004) Remote sensing and GIS courses—distance education. Japan International Cooperation Agency (JICA)-Net, Shinjuku
- SDI Cookbook (2004) Developing spatial data infrastructures: the SDI cookbook. Global spatial data infrastructure. Nebert, DD (ed). Technical working group chair, GSDI
- Tomlinson RF (2007) Thinking about GIS: geographic information system planning for managers. ESRI Press, New York

Chapter 17

Spatial Analysis

“Everything is related to everything else, but near things are more related than distant things.”

First law of geography—Waldo Tobler

17.1 Introductory Remarks

The most important function of GIS is the analysis of spatial data and their attributes for purposes of decision support. Indeed, *spatial analysis* is the very crux of GIS. It is the means of adding value to geographic data that allows the conversion of data into useful information and knowledge. As a *data mining* procedure, spatial analysis helps the GIS user to reveal inherent anomalies, patterns and relationships in GIS data sets that might not be otherwise apparent. This gives more insight into a place and helps in focusing and prioritizing actions or decisions. Strictly speaking, and at a higher level, one may distinguish between analysis and modeling as shown in Table 17.1. However, for purposes of the discussion here-under, the generic terminology analysis is used.

At a practical level, spatial analysis can be applied to answer questions about the present situation of specific areas and features, which locations satisfy certain conditions or requirements, the change in situation, the trends, the relationship between different spatial variables, the evaluation of various what-if modeling and prediction scenarios. Depending on the type of information sought and the data employed, there are different types of spatial analysis and measurement methods that can be applied. These range from simple queries using arithmetic and logical operations to fairly complicated modeling procedures. Most serious GIS textbooks give some discussion on the important topic of spatial analysis, see e.g., Aronoff (1989), Tomlinson (2007), Longley et al. (2005), Konecny (2003), Burrough (1986), Murai (1999) etc. This chapter attempts to only give an overview of spatial analysis with the reader directed to some of the above references for more detailed presentation.

Table 17.1 Difference between analysis and modeling

Analysis	Modeling
A static approach at one point in time	Multiple stages, perhaps representing different points in time
The search for patterns or anomalies, leading to new ideas	Implementing ideas and hypotheses
Manipulation of data to reveal what would otherwise be invisible	Experimenting with policy options and scenarios

Source Longley et al. (2005)

17.2 Methods and Techniques

17.2.1 Spatial Exploration

Spatial query, also referred to in some literature as *spatial exploration*, is the process of retrieving attribute data without altering the existing data. This is done in accordance with specifications outlined *a priori* by the operator. Normally the specifications are given using *Standard Query Language* (SQL) as follows:

SELECT : attribute name(s)

FROM : table

WHERE : condition statement

The conditional statement is represented by the following three possible types of operators:

- (a) Relational operators e.g., $>$, $<$, $=$;
- (b) Arithmetic operators e.g., $+$, $-$, \times and
- (c) Boolean (logical) operators e.g., *AND*, *OR*, *NOT*, *XOR*.

As a result of a SQL query neither changes occur in the database, nor is any new data produced. Users query a GIS database by interacting with different views of the same data.

17.2.2 Measurements

Measurements are simple numerical values that help to describe geometric aspects of geospatial data. These include algorithms for estimating simple object properties like area, perimeter, centroid, shape, and relational properties like distance or direction. The following parameters can be computed from vector data: area, perimeter, centroid (center of gravity). Equations 17.1–17.3 outline the formula for computing area, perimeter and center of gravity of polygons respectively. Similarly, the shape of

an object can be measured and various shape characteristics computed including roundness, unevenness and flatness factors.

$$Area = \frac{1}{2} \sum_{i=1}^n (x_{i+1} - x_i)(y_{i+1} - y_i), \quad (17.1)$$

where $x_{n+1} = x_1$, $y_{n+1} = y_1$

$$Perimeter = \sum_{i=1}^n \sqrt{(x_{i+1} - x_i)^2 + (y_{i+1} - y_i)^2} \quad (17.2)$$

$$Centroid(X_L) = \frac{1}{6A} \sum_{i=1}^n (y_i - y_{i+1})(x_i^2 + x_i x_{i+1} + x_{i+1}^2)$$

$$Centroid(Y_L) = \frac{1}{6A} \sum_{i=1}^n (x_i - x_{i+1})(y_i^2 + y_i y_{i+1} + y_{i+1}^2) \quad (17.3)$$

17.2.3 Reclassification

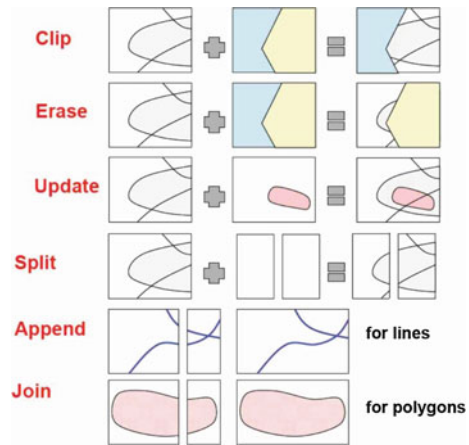
As a more generic term, *transformations* are simple methods of spatial analysis that change data sets, combining them or comparing them to obtain new data sets and new insights. They use simple geometric, arithmetic or logical rules and include operations that convert raster data into vector data and/or vice-versa. More specifically, *reclassification* is the process of reassigning new thematic values or feature codes to units of spatial features. This results in merging existing polygons into new reclassified polygons. A set of “reclassify attributes”, “dissolve the boundaries” and “merge the polygons” are used frequently in aggregating area or polygon objects Murai (1999). Reclassification is executed through the following procedures:

- (a) *Generalization* is reassignment of existing data into smaller number of classes. This will result in a reduction of the level of detail;
- (b) *Ranking* involves valuation of attributes based on an evaluation model or table specified;
- (c) *Re-selection* is selection of features to be kept and removal of unselected features.

17.2.4 Coverage Rebuilding

Coverage rebuilding is a boundary operation to create new coverage and topology that are identified and selected by users. Boundary operations include the following six commands: *clip*, *erase*, *update*, *split*, *append* and *join*. Examples of these commands are illustrated in Fig. 17.1.

Fig. 17.1 Examples of coverage rebuilding commands.
 Source Murai (2004)



17.2.5 Overlay

Rarely will only one factor or one layer be sufficient in ordinary spatial analysis involving typical GIS analysis such as suitability analysis, risk management, potential evaluation, etc. Usually, more than two layers will need to be overlaid together as several factors will need to be considered for a solution. One can distinguish between overlay of raster and vector data. Overlay of raster data is easier than that for vector data.

17.2.5.1 Overlay of Raster Data

Overlay of raster data with more than two feature/map layers is easier compared with overlay of vector data, since it does not include any topological rebuilding but involves only pixel-by-pixel operations. In general, two different methods for raster-based overlay can be distinguished, namely:

- (1) *Weighting point method* in which basically two layers with the values of P_1 and P_2 respectively are overlaid with the weight of w_1 and w_2 respectively as shown in Eq. 17.4:

$$P = w_1 P_1 + w_2 P_2, \quad (17.4)$$

where $w_1 + w_2 = 1.0$

The weighting point method is only available when the attributes have numerical values which can be operated arithmetically.

- (2) *Ranking method* through which at first the attributes of the two layers are categorized into several classes like five ranks as excellent (5), better (4), good (3), poor (2), and bad (1) before a specific purpose of overlay. Then the two different

layers of A and B are overlaid by following one of the three ranking tables, namely:

- (a) *Minimum ranking* where a lower rank is taken as the new rank of the overlaid pixel as the safety rule;
- (b) *Multiplication ranking* in which the two ranks are multiplied because of more influential effect rather than additional effect; and
- (c) *Selective ranking* through which experts can set up combined ranks depending on professional experience.

17.2.5.2 Overlay of Vector Data

Overlay of vector data is more complicated because it must update the topological tables of spatial relationships between points, lines and polygons. Overlay of vector data results in the creation of new line and area objects with additional intersections or nodes that need topological overlay. Three basic types of vector overlay can be distinguished:

- (1) *Point in polygon overlay* in which points are overlaid on polygon map as shown in Fig. 17.2a. Topology of point in polygon is captured through “is contained in” relationship. Point topology is a new attribute of polygon for each point.
- (2) *Line on polygon overlay* through which lines are overlaid on polygon map with broken line objects as shown in Fig. 17.2b. Topology of line on polygon is realized by “is contained in” relationship. Line topology is the attribute of old line ID and containing area ID.
- (3) *Polygon on polygon overlay*, which allows two layers of area objectives to be overlaid resulting in new polygons and intersections as shown in Fig. 17.2c. The number of new polygons are usually larger than that of the original polygons. Polygon topology is a list of original polygon IDs.

17.2.6 Connectivity Analysis

Connectivity analysis defines the methods used to analyze the connectivity between points, lines or polygon in terms of distance, area, travel time, optimum paths etc. Connectivity analysis consists of the following analyses:

- (1) *Proximity analysis* that involves measurement of distances from points, lines or boundaries of polygons. One of the most popular proximity analysis is based on “buffering”, by which a buffer can be generated around a point, line or area with a given distance. Generally, buffering is easier to generate for raster data than for vector data. Proximity analysis is not always based on distance, but can also be undertaken based on variables such as time or traffic volume. As an example, from the framework of school mapping, see e.g., Ministry of Education (2011),

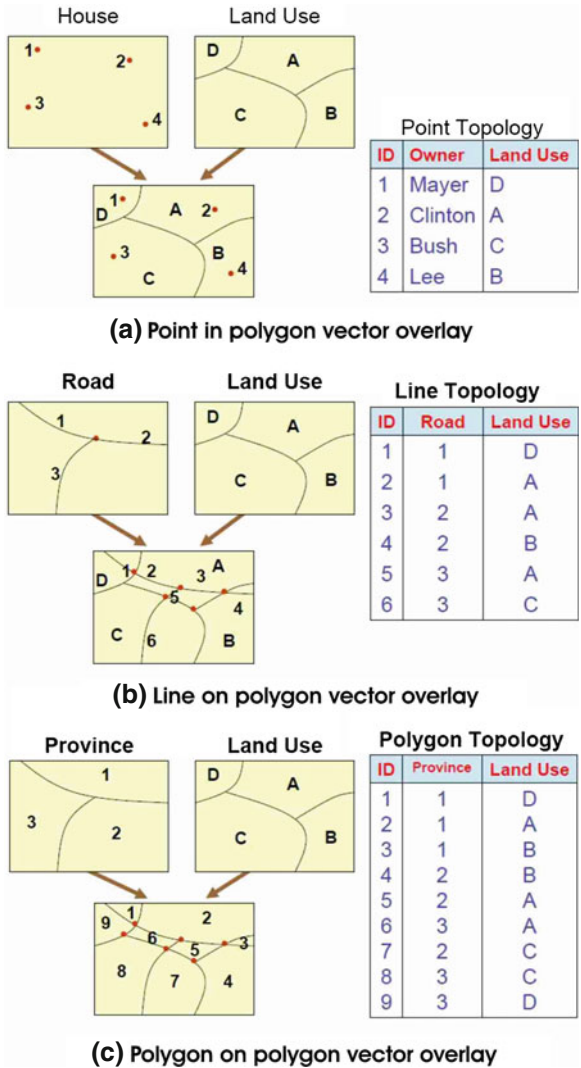


Fig. 17.2 Overlay of vector data. Source Murai (2004)

Mulaku and Nyadimo (2011), Galabawa et al. (2002), Fig. 17.3 shows proximity analysis performed based on distance to analyze the optimality in the location of a district education office.

In more sophisticated proximity analysis, it is possible to convert input points to an output feature class of *Thiessen or Voronoi polygons*. These polygons have the unique property that each polygon contains only one input feature point, and furthermore, any location within a specific polygon is closer to its associated

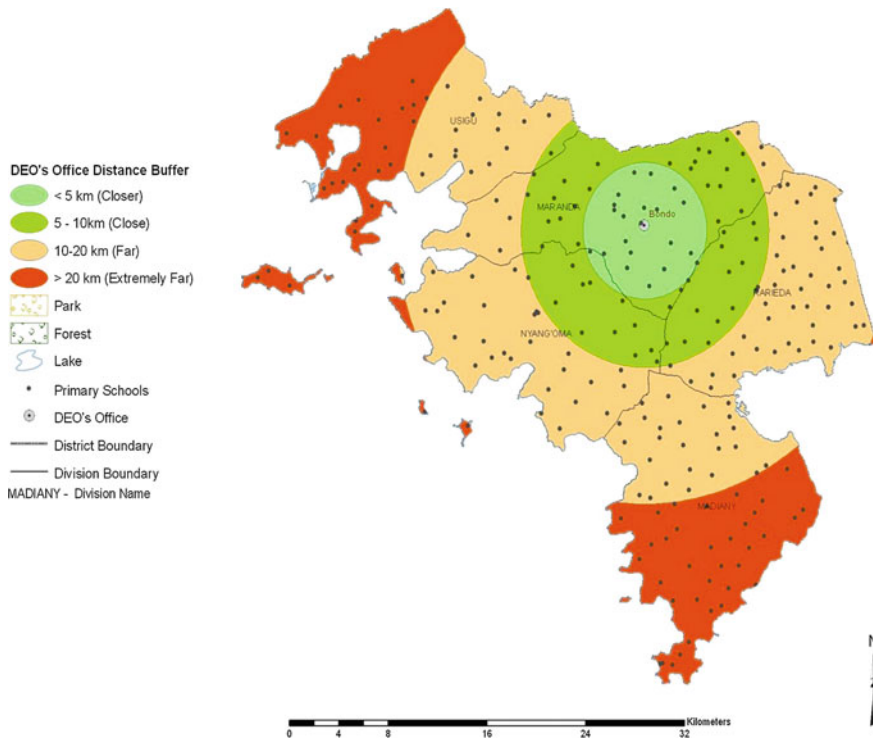


Fig. 17.3 School buffer map. Point buffering is done at 5 km intervals to illustrate the relative location of various primary schools from the District Education Officer's (DEO's) office in Bondo, Kenya. By integrating the location data and performance statistics over the years it is possible to evaluate whether correlation exists between school performance and the distance from DEO's office. This can help to establish, for instance, whether schools located more than 20 km away are performing equally well like those located less than 5 km away from the DEO's office or if they are disadvantaged. Such information can be used as the basis of informing decision about subdivision of the area under the DEO's jurisdiction to enhance performance in line with the basic objectives in the provision of education services. *Source* Ministry of Education (2011)

polygon's point than to the point of any other polygon. Thiessen polygons are constructed from *delaunay triangulation* discussed in Chew (1989), Liu (2008), Fortune (1992), Hjelle and Daehlen (2006). These polygons allow the spatial delineation of points that exhibit similar proximal characteristics as exemplified in the ArcGIS¹ snapshot shown in Fig. 17.4.

- (2) *Network analysis* which includes determination of optimum paths using specified decision rules. The decision rules may be based on variables like minimum time or distance, maximum correlation occurrence or capacity etc. Practical GIS solutions to this problem are normally solved in a raster environment using a *multi-criteria analysis* (MCA) approach, sometimes referred to as *multi-criteria*

¹ <http://www.esri.com/software/arcgis>

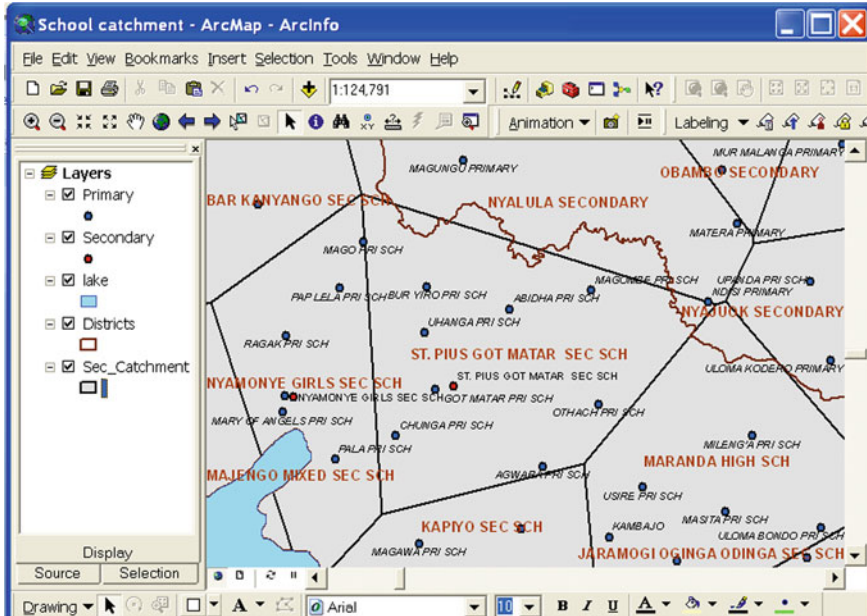


Fig. 17.4 School catchment map. From delaunay triangulation and using Thiessen or Voronoi polygons it is possible to identify and delineate regions with primary schools that constitute the basic catchment for secondary schools as this example of part of Siaya County, Kenya shows. This school mapping information can then be used in micro-planning to ensure equity in the provision of education services and efficiency in the utilization of educational facilities. *Source* Ministry of Education (2011)

decision making. There are several MCA techniques in operation in various countries, see e.g., Lahdelma (2000), Munier (2004). Examples of these techniques include *Analytical Hierarchy Process (AHP)*, *Mathematical Programming (MP)*, *Additive Weighting* and *Concordance Analysis* presented in Annandale and Lantzke (2000), Munier (2004), Ministry of Environment and Energy (1990) etc. Malczewski (2006) conducts a survey of GIS-based multi-criteria decision analysis. More details of MCA are given in Subject. 28.3.2.

In general, MCA methods allow estimation of the overall cost based on several pertinent factors and taking into account their respective individual and combinational weights. Conceptually, each cell is assigned a *friction value* equal to the cost or time associated with moving across the cell in the horizontal or vertical directions. Friction values can be obtained from a number of sources. For instance, land-use and land-cover data might be used to differentiate between forest and open space. Hence, a power line might be given a higher cost in forest because of the environmental impact (felling of trees), while its cost in open space might be allocated based on visual impact. Example 17.1 demonstrates the application of the AHP approach in MCA.

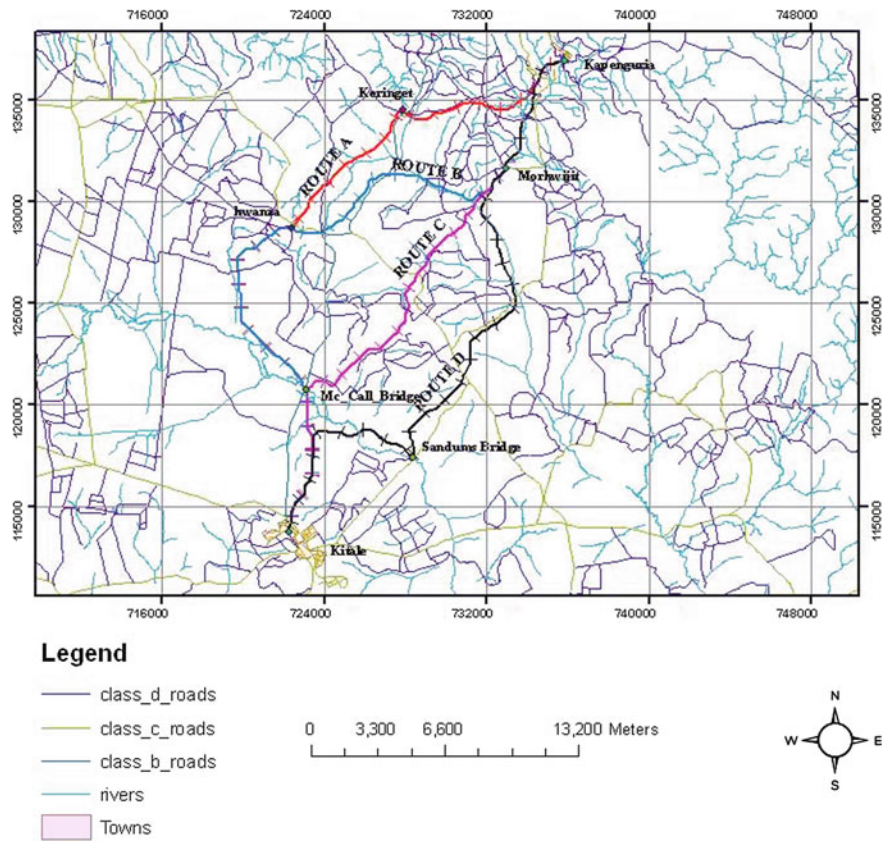


Fig. 17.5 Feasible routes. Source Kiema et al. (2007)

Example 17.1 (Railway route feasibility analysis. Source: Kiema et al. (2007)) The following is an example of a typical multi-criteria GIS-based railway route feasibility analysis between two towns in Kenya. These two towns lie on the proposed railway link between Kenya and South Sudan namely, Kitale (origin) and Kapenguria (destination). According to Saxena and Arora (1981), an ideal railway route should fulfill the following basic requirements:

- (1) *Safety* is a critical issue and the track should be aligned so as to ensure that goods and passengers are transported with minimal chances of accidents and derailment.
- (2) *Aesthetics* although not an overriding factor, is nonetheless, still important. The railway line should be constructed to provide a memorable and pleasant railway journey to train passengers by keeping the track within beautiful natural surroundings.

- (3) *Economy* is central as from an engineering perspective, the track should be as short and direct as possible with minimal construction, maintenance and operating costs.
- (4) *Linking of centers* is critical as a new railway line should connect and inter link important towns and cities so as to provide the necessary transportation services.

In view of the above alignment requirements, minimal evaluation factors and constraints were identified as follows:

- (a) *Slope* of terrain is considered very critical in railway routing as it directly influences the construction and operating costs. The higher the slope, the higher the costs and vice-versa.
- (b) *Soil* that are susceptible to erosion and unconsolidated materials cost more to construct a railway line on. Poorly drained soils are also undesirable for railway line construction. It is therefore comparatively cheaper to construct a railway on ground with soil that is unconsolidated and well drained. Rocky grounds should be avoided as they increase construction costs due to heavy excavation that would be required.
- (c) *Proximity to rivers* is an important consideration since railways should be constructed as far away from rivers as possible for several reasons including: to avoid constructing many bridges that may arise because of the meandering of the rivers; rivers have the propensity to flood and this could cause damage to the railway line; and rivers often change their course and this could cause re-routing of the railway.
- (d) *Land use/land cover* that are varied in category respond differently in terms of their suitability to passing a railway line through them with regard to construction and operation costs.
- (e) *Important towns and cities* is an important factor as town centers form important obligatory nodes and the track should pass through important town centers for economic, social and political reasons. Quarries and human habitats are found in the neighborhood of town centers and therefore construction materials and labor are easily available. Even though a town center may neither be economically nor industrially active, socio-political considerations may still constrain the construction of a railway line through it.
- (f) *Areas the route must not pass through* include those areas in which the railway track must be completely avoided since they would result in very high construction and operation costs. They would also most likely pose a danger to the safety in operations of the rail vehicles. Such undesirable areas include: areas with ground slopes greater than 4.5%; areas within 100m of the centerlines of rivers; flood plains or swampy grounds; and areas within 50m of the centers of existing roads (to minimize accidents).

Table 17.2 Route performance against various evaluation factors

Factor	Route A	Route B	Route C	Route D
Cut and fill volume (m ³)	2,032,524.8	568,068.8	649,984.3	589,148.2
Distance (km)	36.7	38.7	30.4	35.0
Rivers crossed	10	13	10	9
Road intersections	2	14	10	8
Environmental factors	0.095	0.160	0.278	0.467
Overall score	0.116	0.234	0.253	0.397
Rank	4	3	2	1

Source Kiema et al. (2007)

Figure 17.5 shows the alternative routes based on the above multiple criteria superimposed on the cost layer. After comparison of the various options the optimal route is determined as summarized in Table 17.2.

End of Example 17.1

17.3 Concluding Remarks

Spatial analysis constitutes the most important function that is at the very heart of any GIS. This is actually the process that allows GIS data to be transformed into useful information and knowledge upon which decisions can be made. There are different spatial analyses methods and techniques that can be performed ranging from simple queries to complex modeling. At a higher level of discernment, one may even distinguish between analysis and modeling. Nonetheless, it is important to note that certain spatial analysis are best performed using either vector or raster data models.

References

- Annandale D, Lantzke R (2000) Making good decisions: a guide to using decision-aiding techniques in waste facility siting. Institute for Environmental Science, Murdoch University, Perth
- Aronoff S (1989) Geographic information systems: a management perspective. WDL Publications, Ottawa
- Burrough PA (1986) Principles of geographical information systems for land resources assessment. Oxford University Press, New York 50p
- Chew LP (1989) Constrained delaunay triangulations. *Algorithmica* 4(1–4):97–108. doi:[10.1007/BF01553881](https://doi.org/10.1007/BF01553881)

- Fortune S (1992) Voronoi diagrams and delaunay triangulations. Computing in Euclidean geometry. World scientific publishing co, Singapore
- Galabawa JCJ, Agu AO, Miyazawa I (2002) The impact of school mapping in the development of education in Tanzania: an assessment of the experiences of six districts. *Eval Prog Plann* 25(1):23–33
- Hjelle O, Daehlen M (2006) *Triangulations and applications*. Springer-Verlag, New York, p 234, ISBN: 978-3-540-33260-2
- Kiema JBK, Dangana MA, Karanja FN (2007) GIS-based railway route selection for the proposed Kenya-Sudan railway: case study of Kitale-Kapenguria section. *J Civil Eng Res Prac* 4(1):79–90
- Konecny G (2003) *Geoinformation: remote sensing, photogrammetry*. Geographic information systems. Taylor and Francis, London
- Lahdelma R, Salminen P, Hokkanen J (2000) Using multicriteria methods in environmental planning and management. *Environ Manag* 26:595–605
- Liu Y (2008) *Computations of delaunay and higher order triangulations, with applications to splines*. PhD Dissertation, University of North Carolina, Chappel Hill
- Longley PA, Goodchild MF, Maguire DJ, Rhind DW (2005) *Geographic information systems and science*. John Wiley, West Sussex
- Malczewski J (2006) GIS-based multicriteria decision analysis: a survey of the literature. *Int J Geogr Inf Sci* 20(7):249–268
- Ministry of Education, Republic of Kenya (2011) *Spatial analysis of school mapping data*. Basic and analytical reports, Oakar services ltd
- Ministry of Environment and Energy, Government of Ontarion (1990) *Evaluation methods in environmental, assessment*, pp. 3–12, 33–51, 112–137
- Mulaku GC, Nyadimo E (2011) GIS in education planning: the Kenyan school mapping project. *Surv Rev* 43(323):567–578
- Munier N (2004) *Multicriteria environmental assessment. A practical guide*. Kluwer Academic Publishers, Dordrecht
- Murai S (1999) *GIS work book: fundamental and technical courses, vol 1 & 2*. National Space Development Agency, Japan
- Murai S (2004) *Remote sensing and GIS courses—distance education*. Japan International Cooperation Agency (JICA)-Net, Japan
- Saxena SC, Arora S (1981) *A text book of railway engineering*. Dhanpat Rai and Sons, Delhi
- Tomlinson RF (2007) *Thinking about GIS: geographic information system planning for managers*. ESRI Press, New York

Chapter 18

Web GIS and Mapping

“Thanks to ... a range of Web-based services, the average citizen is able to be a consumer and a producer (aprosumer) of geographic information.”

Michael Goodchild et al. (2012)

18.1 The Web and its Influence

The Internet and web-based technology has dramatically influenced the access to and dissemination of information among communities, locally and globally. This is no less true in the domain of geographic information systems (GIS) which have traditionally been constrained in terms of information access and the communities that use them. Geospatial data has traditionally been captured and managed within individual and separate organizational databases with access by a limited number of expert users. Now, with the integrated use of the web, not just geospatial data, but also the functionality of GIS can be accessed globally by citizens and non-experts.

The web brings together different users with the ability for geospatial data to be retrieved from separate databases, accessed by multiple applications such as GIS, digital earth viewers and map servers, and integrated with the location of mobile devices that also can directly access the web (see Fig. 18.1). This combination is very rich and powerful in that users all over the world, connected to any fixed or mobile device on the web, can access multiple applications and associated data from anywhere and anytime.

Invited Chapter

by

Prof. Bert Veenendaal of the Department of Spatial Sciences, Curtin University (Australia).

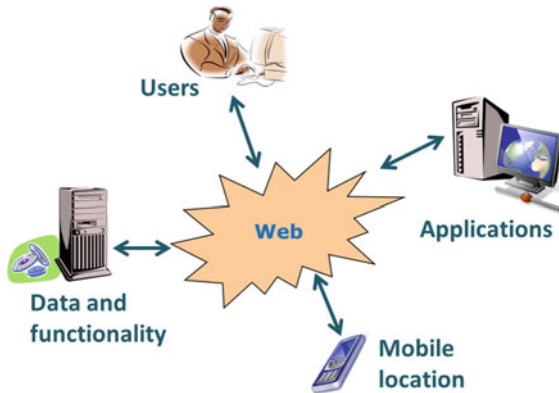


Fig. 18.1 Use of the web for convergence of users, applications, data, functionality and location

The advent of digital earth technologies, such as Google Earth, Microsoft Virtual Earth, ESRI ArcGIS Explorer and NASA World Wind, have opened up geospatial imagery and other data to the average citizen who can, not only access this information via the web, but also be able to contribute and add information of their own. The range of information being integrated in such an environment, as well as the functionality permitted on this information continues to expand so that much of what an expert user can access in a GIS is now able to be interacted with by non-expert users using a virtual globe browser online (Goodchild et al. 2012; Craglia et al. 2012; Li et al. 2011).

18.2 Concept and Applications of Web GIS

Web GIS can be defined simply as a GIS that uses web technologies (Fu and Sun 2011). This can practically be realized in a number of ways. Firstly, GIS software systems are increasingly being extended to incorporate access to the web including the ability to retrieve geospatial data in real-time from other web-based databases and services, and provide web-based interfaces from which the GIS can be driven. Secondly, web GIS applications are being established apart from desktop proprietary systems and incorporate much of the functionality and data that would normally be expected in a GIS. These online GISs range from interactive maps with some limited interaction for manipulating the view, to more sophisticated systems that provide a greater range of GIS functionality.

As an example, Fig. 18.2 illustrates an interactive web mapping interface showing imagery of a region near Brisbane in Queensland, Australia, before and after the January 2011 flood disaster. The user can manipulate the vertical black slider bar to the left and right over the image to reveal and compare the two images covering the same region. Although simple in concept, the interface is very effective in showing the extent of inundation and of the damage that occurred through the disaster event.



Fig. 18.2 Example of an interactive web map showing before/after imagery in the flood disaster for an area near Brisbane, Australia in January 2011 (Source ABC News (2011))

Interestingly, this interactive map was used by ABC News in Australia on their web site (ABC News 2011).

In the more recent January 2013 flood in Queensland, Australia, ABC News again used an interactive map (ABC 2013). However, this time it had the look and feel of the digital earth interfaces with the map view being driven through mouse controls and having some map control buttons superimposed on the image map (see Fig. 18.3).

Web mapping and web GIS are being used for an increasingly diverse range of purposes and applications. The purposes range from access to data, dissemination of data, browsing of geographic regions and datasets, access to information in proximity to a user, comparing change at a geographic location over time, to even accessing real-time information such as live traffic feeds, real-time temperature and rainfall, and current petrol or gas prices. Applications of web GIS and mapping include disaster recovery and management, travel planning and navigation, regional and national interactive atlases, resource information repository, community health information and customized mapping interfaces catering for selected interest groups or projects.

For example, Geoscience Australia's MapConnect online provides users with access to Australian topographic and resources data Geoscience Australia (Geoscience Australia 2012). Users can utilize the online mapping interface to browse the data, view it online and download it using the interactive map selection process (see Fig. 18.4). Users can manipulate the map view by panning, zooming, selecting themes such as 250K topographic maps, global map, geology and geomorphology, and groundwater, as well as selecting geospatial layers such as land cover, land use, vegetation and elevation. They can perform some basic functions such as measuring and drawing, searching and also download or order digital data and maps.

Brisbane overview

Double-click to zoom | Drag to pan | Hover for controls

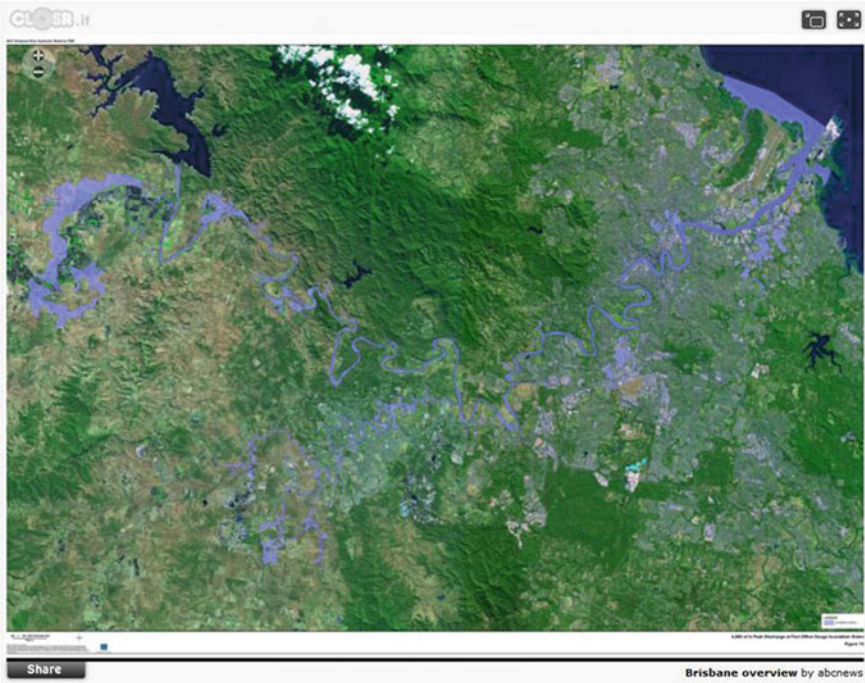


Fig. 18.3 Example of an interactive web map for the January 2013 floods in the region of Brisbane, Australia (Source ABC (2013))

18.3 The Development of Web Mapping

The provision of maps on the web has undergone a number of developments over the past several decades. What started as the provision of images of maps embedded in HTML web pages accessed via an Internet browser are now highly interactive web maps that have the look and feel of a GIS map window and retrieve imagery and GIS data automatically in the background or on an as needed basis (Fu and Sun 2011).

A very early web map, called Map Viewer and built by Xerox Parc, used hyperlinks to provide the user with options of predefined viewing scales, layers, zoom levels and coordinate systems in a series of static hyperlinked HTML pages (Putz 1994). In essence, each combination of user option was embedded as an image in a different HTML page. When accessed, it gave the impression of some dynamic response to a user chosen option for map viewing.

With the development of dynamic HTML with client and server side scripting, it became possible to change information within a specific HTML web page dynamically by generating new HTML or images within the same document. The advent of

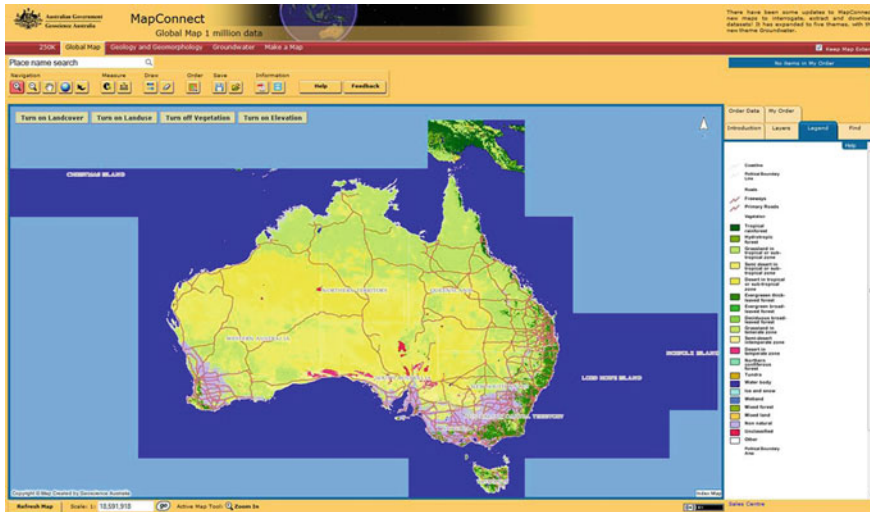


Fig. 18.4 Example of the interactive online map interface of MapConnect (Source Geoscience Australia (2012))

AJAX technology allowed the content of a web page to be loaded dynamically and in the background while the user is able to simultaneously interact with the page. For web mapping, this meant that appropriate image data could be loaded in the background while the user was simultaneously engaging with the interface to toggle on/off map layers, zoom in or out the current geographic view and pan around the map.

A major development in web mapping was realized with the release of Google Earth in 2006.¹ Users could access, not just 2D, but 3D data over the surface of the earth using an interface that was very intuitive and easy to use for the average non-technical user. This development in essence marked the start of an era of access to geospatial data by the global community (Goodchild et al. 2012).

An example of a modern online and interactive web map is The Atlas of Canada (see Fig. 18.5). This web map, considered to be the first online atlas, comprises a legend from which layers can be selected, and provides basic map manipulation tools for panning and zooming, similar to the functionality found within a desktop GIS. Some of the earliest online maps had buttons or sliding bars to facilitate user interaction. However, the user interface has changed to resemble more closely that of a typical desktop GIS with a legend down the side and icons above to manipulate the map view. More recently, the user interface has taken on the look and feel of the digital earth interfaces such as is used in Google Maps and Google Earth, with which many users globally are now familiar. Note that, as shown in Fig. 18.5, the current version of The Atlas of Canada uses the slider bar for zooming and the directional

¹ <http://www.earth.google.com>



Fig. 18.5 Example of a modern web map interface—The Atlas of Canada (Source Government of Canada (2013))

arrows for panning, in addition to the usual functions of the mouse buttons and scroll wheel that enable the same functionality.

18.4 Web Services

Often we think of the web as a set of pages that can be opened up in a browser and provide text and multimedia to read, watch or listen to. However, when presenting maps on the web, there are potentially many diverse sources of data which can be combined in some way to produce the resulting map which can be interacted with and manipulated. In fact, access to both data and functionality can be established through the creation and provision of a web service.

A web service is an interoperable component that provides a defined interface and protocol to deliver a service across the web (Booth et al. 2004). The service is implemented using a client-server model. As illustrated in Fig. 18.6, the server provides

Fig. 18.6 Web services client-server model

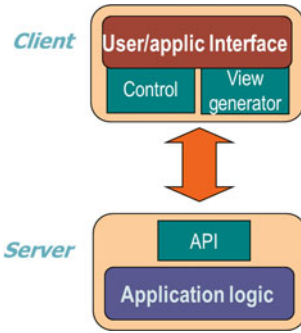
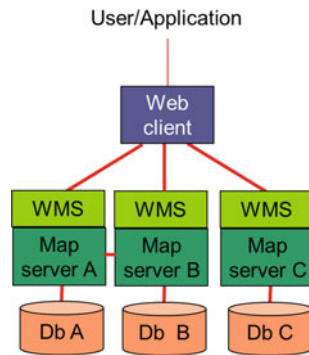


Fig. 18.7 Utilizing the common WMS standard interface to access multiple web mapping services



a service which is performed by the application logic, and defines an application programming interface (API) that describes the requests, parameters and responses that make up the interface (Jones and Purves 2008). The client interacts directly with the user and generates the view that the user sees. Depending on the action that the user initiates, the client puts forward a request to the server, receives the response from the server and then displays it in the browser view to back to the user. For example, if the user requests a map displaying land cover imagery over the central African continent, then the client Internet browser will request that map from a map server. The map server will assemble the map or associated data and return that to the client where it will then be displayed in the map view window within a browser page for the user to visualize.

To facilitate interoperability for geospatial data and functions, the Open Geospatial Consortium (OGC) has developed a number of standard specifications for geospatial web services (OGC 2013). These OGC standards include the Web Map Service (WMS) that provides an assembled map as an image document, Web Feature Service (WFS) that provides geospatial vector-based data using an XML format, Web Coverage Service (WCS) that provides raster-based data, Web Processing Service (WPS) that performs a specified geoprocessing function and responds with the results, and Catalogue Services for the Web (CSW) which provides catalog services for geospatial data on the web. These standards enable users or applications on the client side to



Fig. 18.8 Accessing a WMS geospatial web service from the WA Atlas web map

utilize a common interface when retrieving information from one or multiple servers. Fig. 18.7 illustrates how the WMS standard can be utilized by a client, such as an Internet browser, to retrieve map data from multiple map servers using precisely the same protocol for access.

Geospatial web services can be accessed from within a web page via an Internet browser or from an application program such as a GIS software package, or even from another web service via a web services chain. For example, the WA Atlas (Western Australia) provides an online web map interface with a range of data layers available by default (WA Atlas 2013). However, the user can specify further datasets by linking via a WMS interface; this dynamically accesses data layers from other WMS map servers and presents them within the WA Atlas map window. Fig. 18.8 illustrates how Public Drinking Water Source areas data is dynamically retrieved from a WMS map server and overlaid with other layers (e.g. roads, towns, rivers, etc.) in the map view.

Many web services have APIs that are customized to the types of services provided and go beyond and outside of the existing standards. For instance, most of the virtual globe providers define their own API which provides a means for browsers and applications to directly access these services from within a web page. For example, the Geoscience Australia Earthquake Hazards 2012 online map displays earthquake

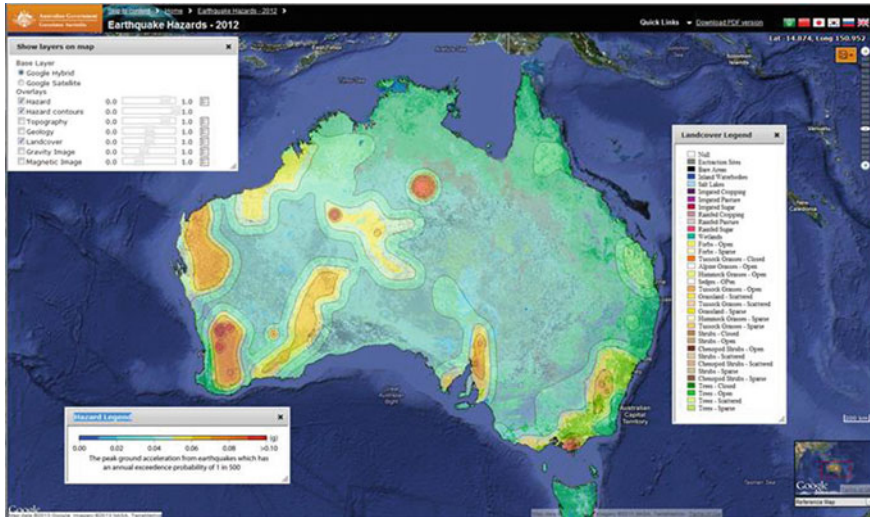


Fig. 18.9 Earthquake hazards 2012 web map utilizing Google Earth imagery in the background (Source Geoscience Australia (2013))

hazard risk on top of additional geospatial layers such as topography, geology, land cover, gravity image or magnetic image (see Fig. 18.9). The background to the map view is imagery from Google using the Google Maps API.² So by linking in to the Google Maps data and functionality (e.g. basic map manipulation tools) using a web service API, a developer is able to extend this with more information, providing the user with options for layer selection, layer viewing opacity, legends, etc.

18.5 Mobile and cloud-based GIS

A fascinating development alongside the web is mobile technology and their use of location. Not only do cell phones and other mobile devices such as laptops, tablet computers and car navigation systems have access to the cellular network and web, but they are also able to access geographic location via a global navigation satellite system (GNSS) such as the United States GPS system (see Chaps. 4 and 5). This allows the current mobile location to be integrated into any web-based or mobile application.

The number and range of applications, particularly on mobile devices, that access the location of the mobile device (user) are increasing rapidly. For example, there are mobile applications that use the current location (and movement in location) to

² <http://developers.google.com>

determine current speed and direction,³ popular nearby restaurants,⁴ position and path of the sun,⁵ mapping tracker and manager of fitness activities,⁶ plane finder using augmented reality to point the mobile phone camera in the direction of an airplane in flight,⁷ tracking the location of mobile devices,⁸ etc. This small sample of mobile applications reflects the diversity of applications and means in which the in-built GPS position is being used in interesting and indeed astounding ways that were not previously imagined.

The location used by an application on a mobile device can be the location of the mobile device, or the location of objects and events. Often, non-geographic information about desired objects or events need to be utilized in order to obtain their location. In the case of a home, the street address can be used to derive a location using a process referred to as *geocoding*. More generally, location can be derived from feature names, GPS positioning (e.g., Chap. 5), IP addresses of devices on the Internet, triangulation of WiFi or cell phone devices based on multiple receiving stations and signal strengths, in a process referred to as *geolocating* (Veenendaal et al. 2011). Once the location of objects or events is known, it can be linked or viewed in relation to other objects or events in proximity. When these features and/or event locations are used in conjunction with the current location of a user (mobile device) that is making a request on their mobile device, the information provided can be very rich in content, instant in real-time, and relatively simple to obtain.

Figure 18.10 illustrates how the process works. Users may put forward a request or run an application via their mobile device or some other device on the Internet. The request may be relative to the current location of the mobile device (either their own or of that elsewhere geographically located), for example, querying a nearby restaurant or tracking the movement of a vehicle. The mobile device, such as a mobile phone or car navigation system, obtains its current location using GPS and sends this to the application. The application may request the location of other features by geolocating or by retrieval from a database on the web, possibly through another online application used to perform the appropriate geolocating or query function. This information is then analyzed by the application and the result is returned to the user or mapped via the application on the device they are using.

Mobile geospatial applications are also very useful as a platform for crowd-sourcing from mobile users and bringing together information at geographic locations or regions. In such situations as natural disaster events, it is crucial to obtain and map information to assist in disaster response and recovery in a timely and coordinated manner.

³ <https://itunes.apple.com/au/app/speedometer-free-speed-limit/id557871911?mt=8>

⁴ <http://www.urbanspoon.com/mobile-downloads>

⁵ <http://www.sunseeker.com/iappint.php>

⁶ <http://runkeeper.com>

⁷ <http://my.pinkfroot.com/page/plane-finder-ar-track-live>

⁸ <https://itunes.apple.com/au/app/find-my-iphone/id376101648?mt=8>

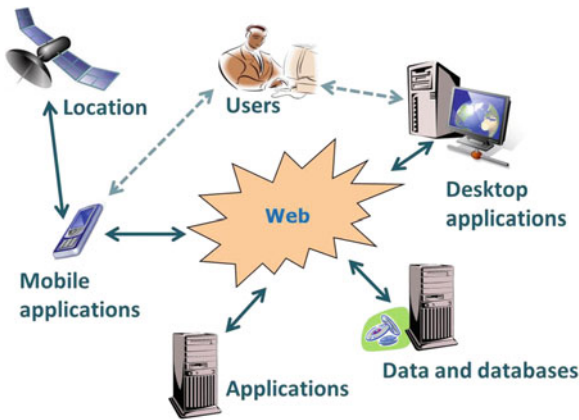


Fig. 18.10 Integrating mobile location into applications in a web environment

The Australia Broadcasting Company experimented with crowd sourcing using the Ushahidi open source platform⁹ for the floods crisis events in Queensland, Australia (ABC 2013). Information such as messages and photos are sourced from people on the ground using Twitter, SMS, email and the web, and are mapped and viewed via an online interactive map. Figure 18.11 illustrates a crowd sourced map of a region near Brisbane, Queensland showing messages plotted as points. The message selected is a call by the Brisbane City Council for volunteers to assist in the response effort during the December 2010–January 2011 flood disaster. This same platform integrating social networking data, location and online mapping, has been used in numerous disaster situations including the Christchurch, New Zealand earthquake and Japan tsunami and earthquake events of 2011.¹⁰

As the amount and demand for geospatial information and functionality continues to rise by an increasingly more diverse and geographically dispersed audience, it is not difficult to understand that an increasing amount of data storage and processing infrastructure is required to facilitate this. A solution that is becoming more utilized is a cloud server that maintains and manages the data and functionality services somewhere out there on the Internet, in the cloud (Li et al. 2011). This is an attractive solution in that the hardware infrastructure is outsourced and the software and data infrastructure can be accessed from anywhere on the web.

As an example, the City of Banff in Canada launched an online web mapping site¹¹ that is hosted on ESRI's ArcGIS Online¹² cloud-based GIS. Although it is not directly visible to the user, the map resides on a cloud server using a web GIS

⁹ <http://www.ushahidi.com>

¹⁰ <http://blog.ushahidi.com/2011/03/16/crisis-mapping-japans-earthquake-and-how-you-can-help>

¹¹ <http://www.banffmaps.ca>

¹² <http://www.arcgis.com/home>

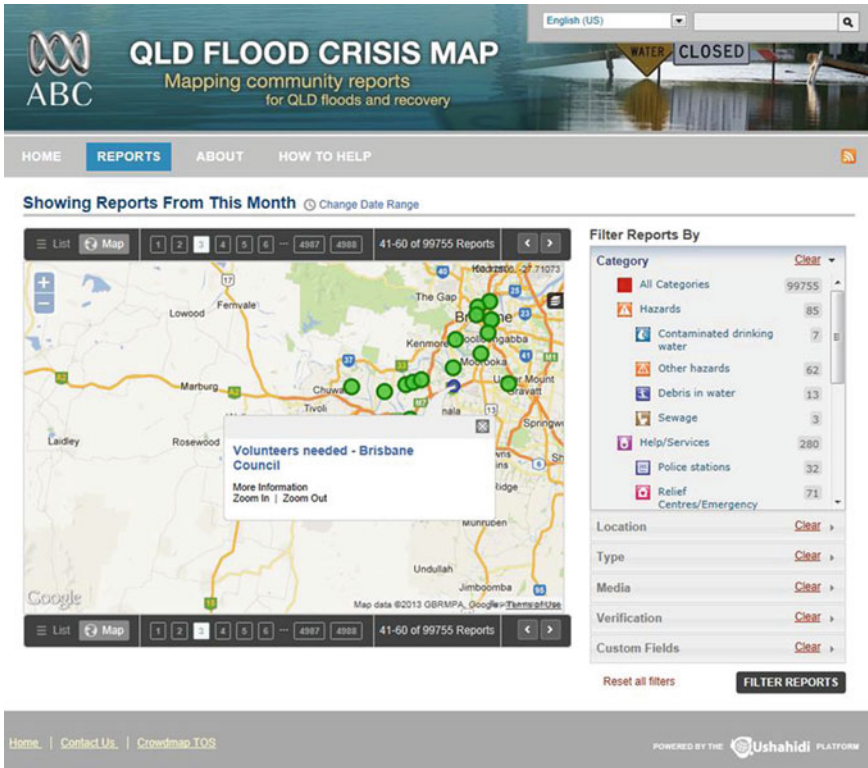


Fig. 18.11 Using crowd-sourced data to compile an online web map as the Queensland flood disaster of 2010/11 unfolded (Source ABC (2013))

platform that makes it easy to implement and able to be accessed from a range of fixed and mobile devices on the web. The map can be shared with only specified users or groups, or more broadly with the general public. All the basic map manipulation and data layer tools are available together with a choice of base maps delivered from another server in the cloud. Cloud-based infrastructures, services and solutions will continue to develop to meet the ever-increasing demands on access to web-based geospatial and GIS information and services (Craglia et al. 2012).

18.6 Concluding Remarks

Web based GIS and mapping technologies are rapidly developing to meet the increasing demands of users and the global community linked via the web. This is an exciting development that is facilitating the use of geospatial information into many and diverse applications. Whereas GIS has traditionally been confined to specialist systems manipulated by specialist professionals, the web has projected GIS into a

global environment and transforming it to meet the needs of the global community and public.

Through the social networked and instant access to information age in which we live, geospatial applications will continue to evolve and be integrated into many applications and work flows across existing and new communities and disciplines. Whether users realize it or not, whether it is explicit or not, web and cloud-based geospatial information and GIS will remain a fundamental and integral part of what we do, when and, importantly, where.

References

- ABC News (2011) Brisbane floods: before and after. Australian Broadcasting Corporation. <http://www.abc.net.au/news/specials/qld-floods>. Accessed 31 Jan 2013
- ABC News (2013) Interactive: Brisbane flood maps. Australian Broadcasting Corporation. <http://www.abc.net.au/news/2013-01-28/interactive-brisbane-flood-maps-released-2013/4487438#overview>. Accessed 31 Jan 2013
- ABC (Australian Broadcasting Corporation) (2013) Qld flood crisis map: mapping community reports for QLD floods and recovery. Australia Broadcasting Corporation. <https://queenslandfloods.crowdmap.com/reports>. Accessed on 31 Jan 2013
- Booth D, Haas H, McCabe F, Newcomer E, Ferris C, Orchard D (2004) Web services architecture. World Wide Web Consortium (W3C) Working Group
- Craglia M, de Bie K, Jackson D, Pesaresi M, Remetej-Flpp G, Wang C, Annoni A, Bian L, Campbell F, Ehlers M, van Genderen J, Goodchild M, Guo H, Lewis A, Simpson R, Skidmore A, Woodgate P (2012) Digital earth 2020: towards the vision for the next decade. *Int J Digit Earth* 5(1):4–21
- Fu P, Sun J (2011) Web GIS: principles and applications. ESRI Press, Redlands
- Geoscience Australia (2012) Topographic mapping: MapConnect. Geoscience Australia, Commonwealth of Australia. <http://www.ga.gov.au/topographic-mapping/mapconnect.html>. Accessed 29 Jan 2013
- Geoscience Australia (2013) Earthquake hazards 2012. <http://www.ga.gov.au/darwin-view/hazards.xhtml>. Accessed 29 Jan 2013
- Goodchild MF, Guo H, Annoni A, Bian L, de Bie K, Campbell F, Craglia M, Ehlers M, van Genderen J, Jackson D, Lewis AJ, Pesaresi M, Remetej-Flppj G, Simpson R, Skidmore A, Wang C, Woodgate P (2012) Next-generation digital earth. *Proc Nat Acad Sci U.S.A* 109(28):11088–11094
- Government of Canada (2013) The atlas of Canada. Government of Canada. <http://atlas.nrcan.gc.ca/site/english/toporama/index.html>. Accessed 29 Jan 2013
- Jones CB, Purves RS (2008) Web-based geographic information systems. In: Wilson JP, Fotheringham AS (eds) *The handbook of geographic information science*. Blackwell, London
- Li S, Veenendaal B, Dragievi S (2011) Advances, challenges and future directions in web-based GIS mapping services. In: Li S, Dragievi S, Veenendaal B (eds) *Advances in web-based GIS, mapping services and applications*. Taylor & Francis Group, London. ISBN 978-0-415-80483-7
- OGC (2013) Open geospatial consortium. <http://www.opengeospatial.org>. Accessed 29 Jan 2013
- Putz S (1994) Interactive information services using world-wide web hypertext. First international conference on the world-wide web, 25–27 May, Geneva Switzerland, published in computer networks and ISDN systems vol 27:2, p 273–280, Elsevier Science BV
- Veenendaal B, Delfos J, Tan T (2011) Geolocating for web-based geospatial applications. In: Li S, Dragicevic S, Veenendaal B (eds) *Advances in web-based GIS, mapping services and applications*. CRC Press, Taylor & Francis Group, London. ISBN 978-0-415-80483-7
- WA Atlas (2013) WA Atlas. <https://www2.landgate.wa.gov.au/bmvf/app/waatlas>. Accessed 29 Jan 2013

Part V
Applications to Environmental Monitoring
and Management

Chapter 19

Maps in Environmental Monitoring

“The science of map making, known as cartography, is now intimately related to environmental monitoring because maps are generated from remote sensing, including aerial photography and satellites, as well as from field surveying and observations.”

D. M. Hendricks (2004)

19.1 Introductory Remarks

A map is an abstraction of reality that creates a model of the world or a part thereof, effectively projecting the curved surface of the earth onto a plane surface. Unlike images that model reality at an iconic level of representation, maps accomplish the same at a symbolic level. Maps are important communication, navigation and decision support tools. They also serve as mechanisms for both storage and communication of spatial data and information. In general, maps are required to document and describe resources and the environment. Furthermore, they are an indispensable instrument for planning sustainable development. Hence, they have an important role to play in many economic, environmental and social activities.

Cartography is the art, science and technology of making maps or charts. Traditionally, maps have been produced by plotting features on paper at a given scale, calling upon a variety of cartographic skills. The advent of computers, satellite data, and geographic information systems (GIS), however, has revolutionized the art of map production, with the modern day cartographer required to master computer skills for the purpose of not only the production, but also the management of digital maps within the framework of *digital cartography*. Many studies have been conducted on the visualization of geospatial data using digital cartography, see e.g., Kraak and Ormeling (2003); Konecny (2003); MacEachren and Kraak (1997) etc.

The paradigm shift in cartography has resulted in change in (Kraak and Ormeling 2003): (i) goals of map use, with maps being transformed from mere tools for information retrieval to being applied in the exploration and discovery of information; (ii) target audience where maps are increasing being developed for individual applications unlike in the past where they served the general public and (iii) flexibility of use from inflexible static products to highly manipulable dynamic outputs. On the overall, this has resulted in maps being transformed from static and physical, inflexible documents to dynamic and interactive spatial information tools.

The transition in map production into the digital era has in turn had a significant impact on environmental monitoring in that maps that took years to be updated can now be updated within minutes, hence permitting the monitoring of activities or phenomena that are changing at a higher temporal rate, e.g., the BP oil spillage in the Gulf of Mexico in 2010. So profound are the changes such that cartography is now intimately related to environmental monitoring due to the fact that maps can now be generated from remote sensing data (i.e., aerial photographs and satellites), in addition to field observation techniques such as surveying and GNSS (Hendricks 2004).

Applications of maps often dictate the scales at which they are produced. Scale is related to space and temporal dimensions as discussed in Sect. 2.1, and its perception and meaning in different applications has been extensively studied, see e.g., Mandelbrot (1967); Fisher et al. (2004); Levin (1992); Tate and Wood (2001) etc. A scale is a relationship between the distance on a map and the equivalent distance on the ground and is often expressed as a ratio $1:x$ or fraction $1/x$ or using graphical representation, where x is a numerical value. The smaller the value of x , the larger the value of the fraction $1/x$, leading to a large scale map that, while covering a smaller area contains a great deal of detail. In contrast, the larger the value of x , the smaller the fraction $1/x$, leading to a small scale map that often covers large areas, but with lesser detail since many features become glossed together.

The appropriate map scale will depend on the level of detail that needs to be extracted from the map, which is a function of the type of application and size of the area that needs to be mapped. In general, a map at a scale $1/1,000$ (1:1000) would be a large scale map, typical of most engineering related maps (also called plans) that depict features such as dams, buildings, pipelines, etc. Small scale maps would typically be at ratio of 1:50,000 and are normally topographic maps covering almost a whole country or sections thereof. Environmental monitoring applications would typically take on both large and small scale maps, depending on the application at hand, as will be discussed in various sections of the book.

19.2 Types of Maps

Maps can exist either in digital format on interactive display devices, or in hard-copy form on paper and other allied media. One can distinguish between formal maps created according to well-established cartographic conventions e.g., topographic or

thematic maps, on the one hand, or transitory maps and map like visualizations e.g., Digital Elevation Models (DEMs), flythroughs etc. on the other hand. In the following sections only the formal type of maps are discussed further.

19.2.1 Thematic Maps

A category of maps that finds use in environmental monitoring are *special purpose maps*, also known as *thematic maps*, which are theme specific, e.g., vegetation maps that show the distribution of plant communities, flood control maps that are used to depict areas prone to floods, soil maps that show the soil types and locations, and climate maps that show the climatic indicators of temperature and precipitation.

19.2.2 Topographic Maps

Topographic maps are *general purpose maps* that are created according to well established cartographic conventions and standards. They have long been used in some form or another to define the cultural and natural features of a landscape. Production of topographic maps requires the execution of topographic surveys, whose purpose is to gather data about the natural and man-made features of an area of interest, in particular the spatial distribution of elevation, to give a three-dimensional representation of the area. Topographic maps are used for a wide range of applications, including cadastre, e.g., Jacobs (2005), engineering, e.g., US Army Corps of Engineers (2007), earthworks, e.g., Garget (2005), archaeology, e.g., Kvamme et al. (2006), land-deformation monitoring, e.g., Gili et al. (2000), basic landscape and geological mapping, e.g., Reynolds et al. (2005); Lavine et al. (2003), while topographic information in a digital database serves as a fundamental layer for GIS, e.g., Braun et al. (2001).

19.3 Maps and their Environmental Applications

There are various types of maps, ranging from engineering plans, which could be useful in environmental monitoring tasks, e.g., in dam monitoring to avoid environmental disasters such as that which was witnessed in 2010 in Hungary, where there was a dam burst and sludge outflow with severe environmental consequences, to topographic maps that show the form and elevation of terrain at various scales. Land provides the base upon which *social, cultural* and *economic* activities are undertaken.

In environmental monitoring, environmental impact assessments (EIA) and audits (EA), topographic maps play an essential role in providing a means by which the locations of sampling sites may be selected, in assisting with the interpretation of

physical features, and in indicating the impact or potential impact on an area due to changes in the system being monitored (e.g., spatially changing features such as wetlands).

The role of topographic maps in supporting environmental monitoring has been highlighted, e.g., by Hendricks (2004), who identifies the use of topographic maps as the provision of a means for determining the nature of landforms, hydrology and, in some cases, the vegetation of an area. Topographic maps also find use in environmental monitoring that support EIA or EA legislations. Most of the environmental monitoring of spatially changing features such as small water bodies required in support of EIA and EA may not require very high accuracies and as such, topographic maps with horizontal accuracies of up to 3 m could suffice, see, e.g., US Army Corps of Engineers (2007, Table 4.3b) .

In Germany, for example, deep hard-coal mining activities by the company “Deutsche SteinkohleAG” (DSK) resulted in subsidence movements, thereby necessitating high demands on planning and monitoring since such effects entailed lasting changes and influences on the environment (Fischer and Spreckels 1999). To minimize possible effects, extensive environmental compatibility studies were performed and detailed prognosis carried out to satisfy EIA legal requirements. In these studies, topographic maps were used to make a prognosis and to forecast the effect of mining excavations (Fischer and Spreckels 1999).

Fischer and Sreckels (1999) report on the limitations of the photogrammetric measurements and high-resolution digital terrain models (DTMs) that described the topographic situation, information on biotopes and the actual land-cover, and propose a multi-temporal satellite data set. They suggest that for environmental changes occurring over wider spatial areas (e.g., 1,500 km²), topographic maps generated from such multi-temporal remote sensing methods are advantageous compared to those from photogrammetric methods. In another example, Ji et al. (2001) show how thematic maps generated using remote sensing were useful in monitoring urban expansion, which contributes to the loss of productive farmlands in China. Similarly, Shalaby and Tateishi (2007) applied remote sensing and GIS generated maps to monitor land-cover and land-use changes in the north-western coastal zone of Egypt. Their results indicated that a very pronounced land cover change took place as a result of tourism and development projects during the study period.

For monitoring environmental changes occurring over smaller areas (e.g., Jack Finney Lake discussed in Sect. 19.3.1.2), the use of remote sensing and photogrammetry techniques to generate topographical maps is quite expensive and as such, the use of conventional methods such as total station or GNSS-generated topographical maps may be a more feasible approach. This is demonstrated, e.g., in the work of Fischer and Spreckels (1999) who show how a GNSS system provided results whose accuracy in height was nearly identical and within the precision of remote sensing methods, and thus could be useful in detecting mining-induced subsidence, enabling the updating of monitoring data at regular intervals.

Another example is presented, e.g., in Gili et al. (2000) where GNSS-generated topographic maps are shown to have the capability to support environmental monitoring of the Vallcebre landslide in the Eastern Pyrenees (Spain), which had been

periodically monitored using terrestrial photogrammetry and total station methods since 1987. Gili et al. (2000) found that the GNSS generated topographic maps allowed greater coverage and productivity with similar accuracies (i.e., 12–16 mm in the horizontal, and 18–24 mm in elevation) as obtained by classical surveying methods.

The examples given above illustrate the major influence on topographic surveys that has resulted from the development of GNSS systems. The possibility of incorporating all the information that may be made available from such an increase in satellite coverage has the potential to deliver much greater accuracies (e.g., below 1–3 m autonomous positioning level accuracy or up to mm level accuracies for relative positioning approaches), and increased reliability and availability to the spatial information industry. This could in turn support environmental monitoring tasks, most of which require accuracies no greater than the cm-level. In the next section, the applicability of RTK presented in Sect. 6.4.6 to small-scale topographic surveys that may be necessary for supporting environmental monitoring will be discussed.

Compared to conventional methods for generating topographic maps, GNSS has the advantage of being less expensive in terms of time and labor and can provide adequate accuracies for most types of topographical surveys. These advantages are only evident, however, as long as the user has the skill and knowledge to use the system, and satellite visibility is adequate. In particular, knowledge of possible error sources is important in successfully applying GNSS.

19.3.1 GNSS-Derived Topographic Maps

In the past, conventional photogrammetry (see Chap. 11) was employed in the production of topographic maps. Today, the development of digital photogrammetry (discussed in Chap. 12) has enabled the automatic generation of orthoimages and production of associated orthoimage maps to be mainstreamed. Besides containing all the spatial features documented in a standard topographic map, an orthoimage map additionally captures vital textural information. Moreover, as pointed out in Sect. 12.1, orthoimage and stereo feature extraction, which are now standard automated procedures in digital photogrammetry, have provided a viable solution to the revision of basic topographic maps, in addition to fulfilling the need for larger scale base maps.

Although topographic maps have many vital uses as discussed in Sect. 19.3, new areas of application requiring the rapid continuous generation of topographic maps continue to emerge, thanks to the use of GNSS in the production of such maps. One of these areas includes land management (e.g., *precision farming*, and *soil erosion modeling and assessment*), where, for example Bakhsh et al. (2000) use soil attribute and topographic maps to establish field yield variability. These applications require substantial and accurate topographic data in order to deliver meaningful results that will inform decision makers on *soil* and *water conservation* practices. To be able to monitor yield variation with respect to topographical features, traditional surveying methods for generating topographic maps, such as the use of total stations instruments

are not sufficient to rapidly generate the substantial amounts of data (horizontal position and elevation) required hence the attraction of GNSS.

Surveys using DGPS and RTK modes of GNSS to map *topographic attributes* of two fields in Northeast Kansas were performed by Schmidt et al. (2003) to compare the two systems. The two fields selected for the study were 24 ha in area and 31 ha with a relief of 19–23 m respectively. Elevation data was obtained using RTK with 3–50 m intervals with the relatively uniform areas having greater intervals. Elevation was also obtained using DGPS at 4–14 m intervals. The elevation data was then interpolated to a 5 m grid. A Trimble MS750 receiver that was used for the RTK survey had a typical vertical accuracy of 1–2 cm. A reference station was established in each field prior to logging elevation data using an AgGPS 170 Field Computer. Digital elevation models (DEMs) were then created from the RTK and DGPS data using the Spatial Analyst Extension in ArcView GIS 3.2. Topographic maps with 10-m cells developed with the DGPS elevation were nearly identical to those developed from the RTK, except for depicting small topographic features such as terraces. Therefore, the RTK system was found to be suitable for producing *topographic maps* of the fields as the depiction of smaller topographic features was not necessary.

As well as the use of topographic maps to provide tagging of site-specific information to a unique location (x, y) in *precision farming*, the elevation data (z) derived from these topographic maps has the potential to be used for topographic analysis such as the delineation of *flow paths*, *channels*, and *watershed boundaries* (Renschler et al. 2002). For instance, Fraisse et al. (2001) applied topographic maps to delineate subfield management zones using the statistical method of Principal Component Analysis (PCA) (see Sect. 10.3.3). Renschler et al. (2002) provide an analysis of the impact of the accuracy of six alternative topographic data sources on watershed topography and delineation in comparison to GNSS measurements using a survey-grade cm-accuracy.

Tokmakidis et al. (2003) produced a GNSS-topographic map and digital terrain model (DTM) for Kilkis, Northern Greece, for land management purposes using RTK techniques. The produced topographic maps and DTM were compared with existing topographic maps that were obtained from conventional photogrammetric techniques, with differences of a few centimeters up to a meter being noted. They also compared heights of contour lines crossed by the GNSS measuring lines where differences of 0.6 m were observed. They concluded that the magnitude of the differences could be considered to be realistic, keeping in mind that changes in the landscape over a period of 25 years could be greater than the difference in the values they obtained, due to farming activities, constructions, etc. The DTM generated from photogrammetry showed sufficient reliability for accuracies of the order of one meter, while the GNSS technique proved to be a very efficient method of capturing data with an accuracy of a few centimeters in order to produce a reliable DTM.

Topographic maps generated by rapid GNSS methods such as stop-and-go and RTK (see Sect. 6.4.5) could also be used for monitoring environmental changes resulting from the implementation of projects following EIA approvals. Resource conservation and disaster management are other possible areas of the application of GNSS to land management (Monico 2004). These applications require topographic

maps that can rapidly be generated, see e.g., Clark and Lee (1998). It is apparent from the examples mentioned above that GNSS can be used for a variety of topographic surveys sufficient for environmental monitoring.

Since topographic maps provide different information and accuracies depending on the specific client or end-user, their generation will vary in *size* and *scale*. Typically, these maps are characterized by a quantitative representation of *relief*, usually using contour lines. The accuracy required for survey data is such that there be no plotable error. The *rule of thumb* in cartography, reiterated by Hall (1994), states that a hand drawn line on a sheet of paper should be within ± 0.25 mm. Consequently, if a survey is to be undertaken at a scale of 1:1,000, all measurements must be sufficiently accurate to ensure that the relative positions of any point with respect to any other point in the survey can be plotted to a planimetric accuracy within ± 0.25 mm at survey scale, which for a 1: 1,000 map scale would represent ± 25 cm.

GNSS-generated topographic maps with such accuracies could be rapidly produced using the RTK approach discussed in Sect. 6.4.6. El Mowafy (2000) noted that the horizontal positions using the RTK method can be achieved to the cm-level of accuracy. The determination of the heights compared to the horizontal measurements, however, is inherently less precise and less accurate. Moreover, GNSS derived ellipsoidal heights must be transformed into a local vertical datum (e.g., the Australian Height Datum (AHD) for Australia, see e.g., Featherstone and Stewart (2001)).

19.3.1.1 Case Study of Edinburgh Oval, Curtin University

GNSS has been presented, e.g., by Schloderer et al. (2010) as a rapid method for monitoring spatial changes to support environmental monitoring decisions and policies. In what follows, a brief discussion of their work is presented to highlight the capabilities of GNSS to generate topographic maps. In their work, Schloderer et al. (2010) set the *base receiver* on a pillar (see Fig. 6.5, p. 81) due to its central location within the survey site (Fig. 19.1) and open unobstructed sky view.

To validate the GNSS-based method, a comparison was made of results from a small-scale topographic survey using RTK and total station survey methods at Jack Finney Lake, Perth, Australia. The accuracies achieved by the total station in their study were 2 cm horizontally and 6 cm vertically, while RTK also achieved an accuracy of 2 cm horizontally, but only 28 cm vertically. While the RTK measurements were less accurate in the height component compared to those from the total station method, they were still capable of achieving accuracies sufficient for a topographic map at a scale of 1:1,750 (Fig. 19.2) that could support environmental monitoring tasks such as identifying spatial changes in small water bodies or wetlands. The time taken to perform the GNSS survey, however, was much shorter compared to the total station method, thereby making it quite suitable for monitoring spatial changes within an environmental context, e.g., dynamic mining activities that require rapid surveys and the updating of the monitored data at regular intervals.

The resulting 3D DTM are presented in Fig. 19.3. Such DTM find use in flood forecasting as discussed in Sect. 26.4.4. Some discrepancies between the contour



Fig. 19.1 Edinburgh Oval, Curtin University's study area with control peg network. *Source* <http://maps.google.com/maps>

maps can be noticed for areas covered with trees (Fig. 19.2). This is due to the inability of the GNSS system to take observations under dense tree cover. The contours displayed on the total station map would therefore be more reliable in these areas.

Lengths of some chosen features were measured on the maps in Fig. 19.2 and compared to the actual ground measurements. The deviations from the actual distances are plotted in Fig. 19.4. The results highlight the fact that GNSS can be used to achieve accuracies suitable for a topographic map at a scale of 1:1,750. For example, a difference in the length measured between the two techniques of the sports pavilion wall of 1.61 m measured on the ground corresponds to a 1 mm difference on the topographic maps. The largest differences were found when measuring the faces of buildings due to the fact that the GNSS receiver cannot be directly positioned on the building corner due to multipath errors. GNSS observations could only be taken some distance away from the building at a point with adequate satellite visibility. However, the building was still positioned on the 1:1,750 topographic map with sufficient accuracy.

Figure 19.4a indicates that both the GNSS and total station techniques have similar accuracies in the horizontal dimension. However, the largest variabilities in the RTK measured distances (Fig. 19.4b) occurred where observations were taken in the proximity of areas of dense tree cover, which would have reduced satellite visibility and introduced multipath errors (see Sect. 5.4.4, p. 69). The results of Fig. 19.4c show the expected outcome of lower accuracies and precisions of the GNSS elevations compared to those of the total station. Multipath could have been one of the

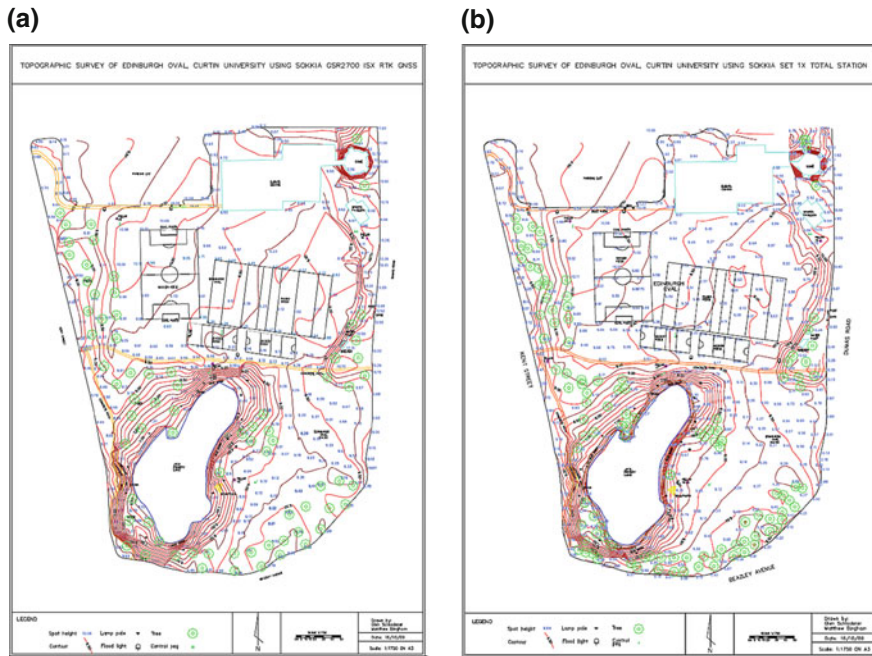


Fig. 19.2 Topographic maps of Edinburgh Oval, Curtin University, Perth, Australia produced from GNSS and total station topographical surveys. **a** GNSS topographical map. **b** Total station topographical map

more significant sources of errors due to the presence of large obstructions within the survey area. For example, control point 5 was located near tall pine trees to the west and point 6 was located near a building to the north. Figure 19.4d shows that the distances measured from each of the topographic maps are strongly correlated with $r^2 = 1$, where r is the fraction of the variance in the total station or RTK measurements that is accounted for by a linear fit of the total station to RTK measurements. More than 99% of the variability in RTK was accounted for by the total station horizontal distances with the coefficient of determinant r^2 value equal to 1.

19.3.1.2 Application to the Monitoring of Lake Jack Finney

The area of the Lake Jack Finney was determined from the RTK survey and compared with areas determined from Google Earth Pro imagery for the years 2000, 2005, and 2009 (Fig. 19.5; Schloderer et al. 2010). The trend shown by the Google images suggests that the lake is gradually shrinking over time, as indicated by the decreasing lake areas from 2000 to 2008 (Fig. 19.6). The data obtained from the RTK survey in 2009 follows this trend with a smaller area compared with 2008.

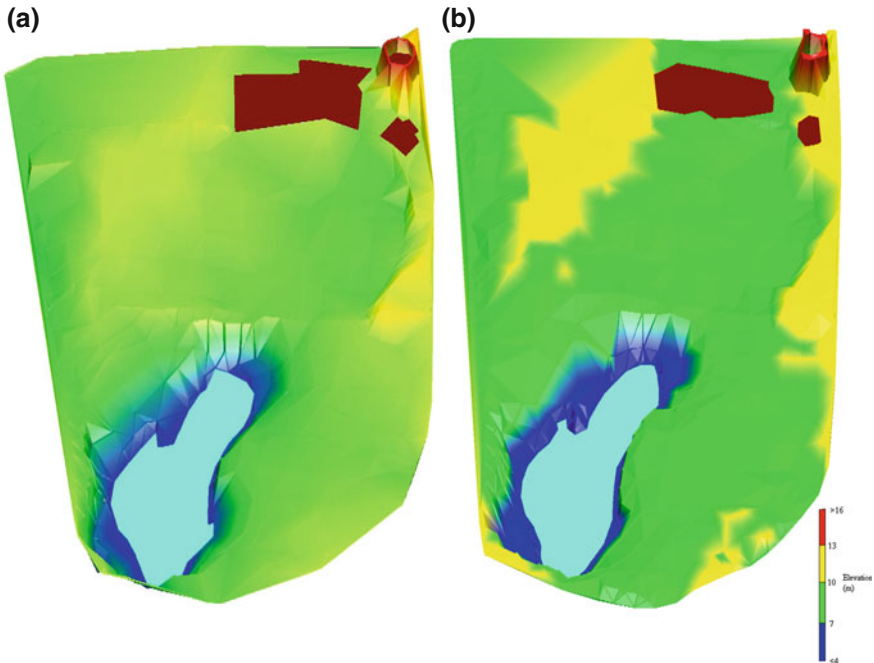


Fig. 19.3 Digital Terrain Models (DTM) of Edinburgh Oval, Curtin University, Perth, Australia produced from GNSS and total station topographical surveys. **a** GNSS's DTM. **b** Total station's DTM

Figure 19.6 describes the decrease in the surface area of the lake found from the GNSS measurements at a rate of 194 m^2 a year, with a correlation of 0.9. Although ideally more data would have been accessible, making for a more accurate and meaningful model to quantify the shrinking size of the lake, the usefulness of the GNSS method is apparent. Since Google Maps are normally not updated frequently enough to be suitable for such monitoring tasks, this again emphasizes the need for rapid and reliable GNSS methods.

As a check on the area obtained from GNSS measurements, Fig. 19.7 compares the GNSS generated surface area to that measured by the total station, with the GNSS-derived area being 148 m^2 greater. This difference comes from the GNSS recording of fewer points around the lake due to the heavy tree cover, while the total station recorded all necessary points to accurately define the edge of the lake. A further comparison of the lake area found by GNSS (Fig. 19.7, left) with that from the total station (Fig. 19.7, right) shows additional differences. Points A, B, C and D are shown on Fig. (19.7, left) as specific points of difference. Point A represents a spot where the GNSS could not measure the necessary point due to dense tree coverage to complete the curve of the lake, hence the lake appears to dip back whereas the total station (on the right) located the required point and completed the curve. Point B is perhaps the most significant point where the image derived from GNSS demonstrates

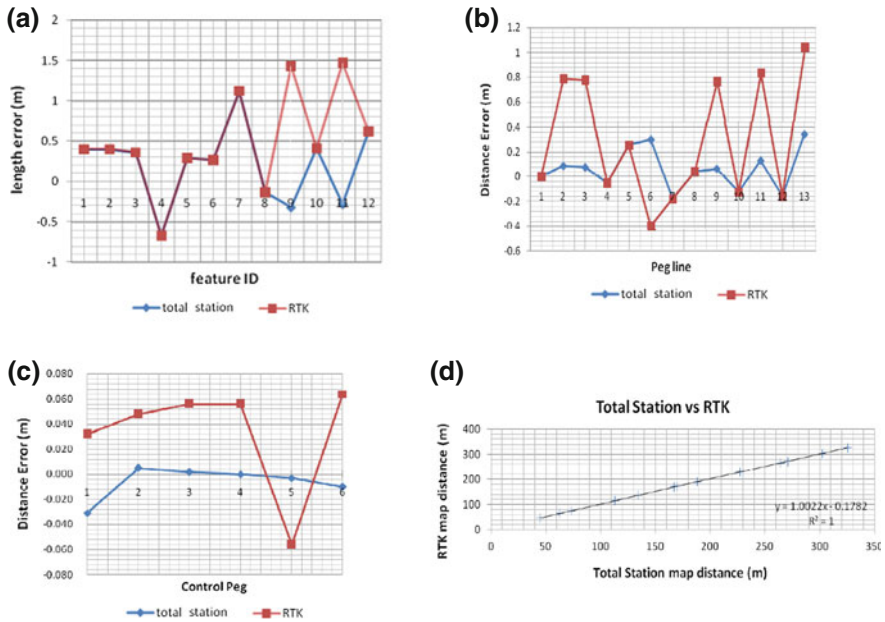


Fig. 19.4 **a** Error distribution for lengths of features measured on the total station and RTK topographic maps. **b** Error distribution for distances between control pegs interpreted from total station and RTK topographic maps compared with ground control distances. **c** Comparison of vertical heights. **d** Regression analysis of distances interpreted from 1:1,750 topographic maps produced from the total station and RTK surveys

a poor definition of the edge of the lake. As before, this was due to large trees blocking the satellite signal. Comparing the image generated from GNSS to the one derived from total station, it is clear that the total station performed a much better job of mapping the area than the GNSS. The same situation applies to point C with large trees blocking the satellite signals, again leading to a poor definition of the edge of the lake. Point D is an area where the converse of above happens. There were tall reeds that prevented the line of sight to the prism even when set at the maximum pole height of 2.1 m. However, with the RTK system, an observation was possible.

With the changing surface area of the lake over time and the effectiveness of each method to define these changes, this is just one area of application that is possible for GNSS.

This example shows that GNSS can be used for the surveys needed for environmental applications such as wetland management, especially where small to moderate spatial coverages are envisaged. In such applications, instead of using expensive satellite imagery, GNSS can be used to map waterlines quickly and accurately to monitor the growth or recession of water bodies over time.

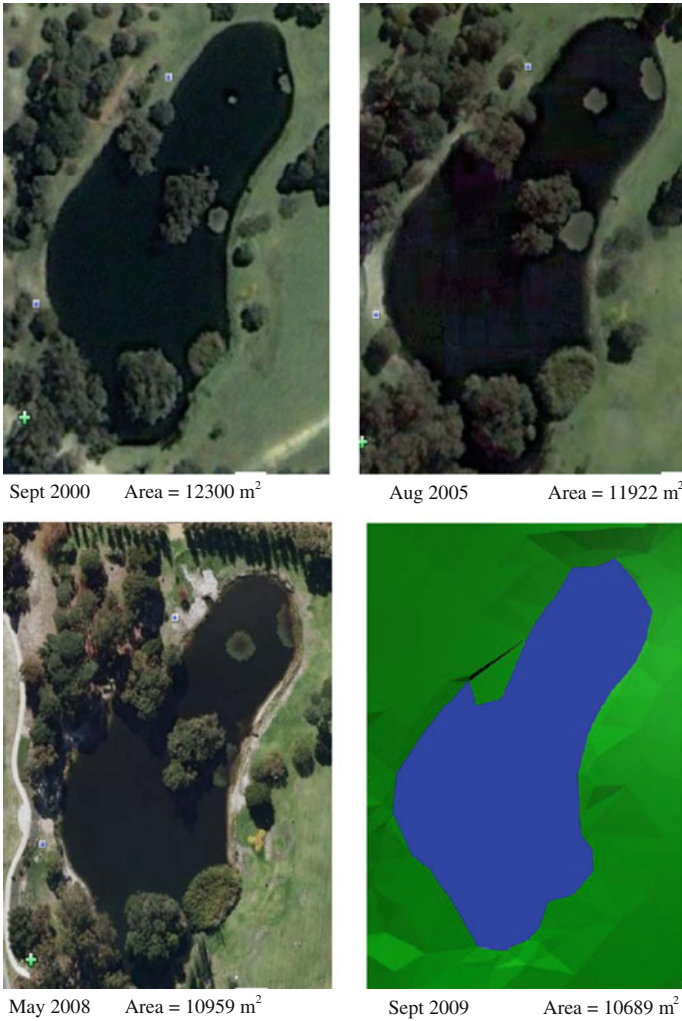


Fig. 19.5 Comparison of the area of Jack Finney Lake during the years 2000, 2005, and 2008 as measured from Google Earth satellite imagery, and from the RTK generated model. *Source* Google Earth Pro

19.4 Concluding Remarks

Topographic maps are conventionally produced using photogrammetric techniques, which are fairly competitive from both an accuracy and cost point of view, especially when large areas need to be mapped and digital photogrammetric techniques discussed in Chap. 12 are applied. In applications requiring higher accuracy, high resolution satellite imagery can be applied. The example of Schloderer et al. (2010)

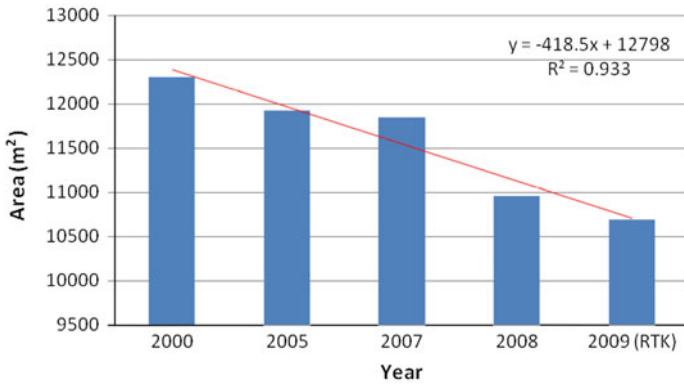


Fig. 19.6 Spatial variation of Jack Finney Lake over time. By March 2011, the lake had dried up

demonstrates that GNSS is also capable of achieving a level of accuracy sufficient to develop a reliable topographic map at a scale of 1:1,750, which suffices for most environmental monitoring purposes. At this scale, given that the GNSS-generated topographic map achieved a planimetric accuracy of 2 cm and a vertical accuracy of 28 cm, it would be useful for most types of environmental monitoring, except where heights need to be more accurate than 28 cm, such as land subsidence monitoring (see Sect. 26.10).

It should be pointed out, however, that this accuracy is not the absolute achievable value, since GNSS accuracy depends on many factors, which include satellite avail-



Fig. 19.7 Lake Jack Finney (September 2009). *Left* GNSS. *Right* Total station. The points marked on the left-hand figure are discussed in the text

ability and visibility, signal blockage from trees and buildings, the effects of multipath errors, and the experience of the observers, to name just a few. These error sources could have contributed to the relatively low accuracy achieved. The results, however, still indicate the potential of GNSS to generate topographic maps capable of supporting the environmental applications listed in Schloderer et al. (2010, Table 3), although we must point out that this is not conclusive, given the problems of error sources and limited data.

In the examples presented, the time taken to perform the topographical surveys was much shorter using GNSS compared with the total station method, where the need for multiple setups and a traverse to establish control on the multiple stations greatly increased the time taken. The GNSS accuracies achieved, when compared against typical accuracies desired for particular survey tasks were found not to meet the required accuracies for cadastral work, utility surveys, land deformation surveys, or archaeological surveys that require cm to mm-level accuracies, but was sufficient for environmental monitoring tasks that does not require such high accuracies, such as the mapping of spatial changes in small water bodies, e.g., Jack Finney Lake.

Therefore, for environmental monitoring of areas with adequate satellite visibility throughout the survey area, and fewer obstructions introducing multipath errors, in the generation of topographic maps that serve as a preliminary reconnaissance tool for environmental studies, or to quickly examine the changing spatial dimensions of a feature, such as a small water body during an environmental audit, GNSS is recommended. It should be noted, however, that GNSS is capable of providing higher accuracies as discussed in Chap. 6.

References

- Bakhsh A, Jaynes DB, Colvin TS, Kanwar RS (2000) Spatio-temporal analysis of yield variability for a cornsoybean field in Iowa. *Trans ASAE* 43(1):31–38
- Braun M, Simões JC, Vogt S, Bremer UF, Blindow N, Pfender M, Saurer H, Aquino FE, Ferron FA (2001) An improved topographic database for King George Island: compilation, application, and, outlook. *Antarct Sci* 13(1):41–52
- Clark RL, Lee R (1998) Development of topographic maps for precision farming with kinematic GPS. *Trans ASAE* 41(4):909–916
- El-Mowafy A (2000) Performance analysis of the RTK technique in an urban environment. *Aust Surv* 45(1):47–54
- Featherstone WE, Stewart MP (2001) Combined analysis of real time kinematic GPS and its users for height determination. *J Surv Eng* 127(2):31–51
- Fischer C, Spreckels V (1999) Environmental monitoring of coal mining subsidences by airborne high resolution scanner. In: *Proceedings of the IEEE international geoscience and remote sensing symposium 1999 (IGARSS '99)*, pp 897–899. doi:[10.1109/IGARSS.1999.774478](https://doi.org/10.1109/IGARSS.1999.774478)
- Fisher P, Wood J, Cheng (2004) Where is Helvellyn? Fuzziness of multi-scale landscape morphometry. *Trans Inst Br Geogr* 29:106–128
- Fraisse CW, Sudduth KA, Kitchen NR (2001) Delineation of site-specific management zones by use of unsupervised classification of topographic attributes and soil electrical conductivity. *Trans ASAE* 44(1):155–166

- Garget D (2005) Testing of robotic total station for dynamic tracking. University of Southern Queensland. <http://eprints.usq.edu.au/>. Accessed 20 Aug 2009
- Gili JA, Corominas J, Rius J (2000) Using global positioning techniques in landslide monitoring. *Eng Geol* 155(3):167–192
- Hall B (1994) Environmental mapping systems locationally linked databases. Riversinfo. Precision Info. http://www.precisioninfo.com/rivers_org/au/archive/?doc_id=1. Accessed 20 Aug 2009
- Hendricks DM (2004) Maps in environmental monitoring. In: Artiola J, Pepper IL, Brusseau ML (eds) Environmental monitoring and characterization. Elsevier Academic Press, San Diego
- Jacobs PG (2005) Assessing RTK GPS for a suburban survey practice, University of Southern Queensland, Faculty of Engineering and Surveying. <http://eprints.usq.edu.au/546/1/PeterJACOBS-2005.pdf>. Accessed 28 Jan 2010
- Ji CY, Liu Q, Sun D, Wang S, Lin P, Li X (2001) Monitoring urban expansion with remote sensing in China. *Int J Remote Sens* 22(8):1441–1455. doi:10.1080/01431160117207
- Kraak M-J, Ormeling F (2003) Cartography: visualization of geospatial data. Pearson Education, Harlow
- Konecny G (2003) Geoinformation: remote sensing, photogrammetry, geographic information systems. Taylor and Francis, London
- Kvamme K, Ernenwein E, Markussen C (2006) Robotic total station for microtopographic mapping: an example from the Northern Great Plains. *Archaeol Prospect* 13:91–102. Wiley Interscience. <http://www.interscience.wiley.com>. Accessed 13 Aug 2009
- Lavine A, Gardner J, Reneau S (2003) Total station geologic mapping: an innovative approach to analyzing surface-faulting hazards. *Eng Geol* 70:71–91. doi:10.1016/S0013-7952(03)00083-8
- Levin SA (1992) The problem of pattern and scale in ecology. *Ecology* 73:1943–1967
- MacEachren AM, Kraak M-J (1997) Exploratory cartographic visualization: advancing the agenda. Pergamon. *Comput Geosci* 23(4):335–343
- Mandelbrot B (1967) How long is the coast of Britain? In: statistical self-similarity and fractional dimension. *Sci N Ser* 156(3775):636–638
- Monico JFG (2004) United nations office for outer space affairs GNSS web pages. *GPS Solut* 8:112–114
- Renschler CS, Flanagan DC, Engel BA, Kramer LA, Sudduth KA (2002) Site specific decision-making based on rtk GPS survey and six alternative data sources: watershed topography and delineation. *Trans ASAE* 45(6):1883–1895
- Reynolds W, Young F, Gibbings P (2005) A comparison of methods for mapping golf Greens. *Spat Sci Queensland* 2007(4):33–36. ISSN 1032–3848
- Schloderer G, Bingham M, Awange JL, Fleming KM (2010) Application of GNSS-RTK derived topographical maps for rapid environmental monitoring: a case study of Jack Finney Lake (Perth, Australia). *Environ Monit Assess* 180(1–4):147–161. doi:10.1007/s10661-010-1778-8
- Schmidt JP, Taylor RK, Gehl RJ (2003) Developing topographic maps using a sub-meter accuracy global positioning system. *Appl Eng Agric* 19(3):291–300
- Shalaby A, Tateishi R (2007) Remote sensing and GIS for mapping and monitoring land cover and land-use changes in the Northwestern coastal zone of Egypt. *Appl Geogr* 27:28–41. doi:10.1016/j.apgeog.2006.09.004
- Tate N, Wood J (2001) Fractals and scale dependencies in topography. In: Tate N, Atkinson P (eds) Tokmakidis K, Spatalas S, Pikridas C (2003) A comparison of a digital terrain model obtained from GPS and classical data. In: Proceedings of international symposium on modern technologies, education and professional practice in the Globalizing World, November, Sofia, Bulgaria, pp 30–35
- US Army Corps of Engineers (2007) Control and topographic surveying. Engineering and design manual, EM 1110-1-1005

Chapter 20

Satellite Environmental Sensing

“GNSS data provide the opportunity to observe Earth system processes with greater accuracy and detail, as they occur.” W.C. Hammond et al. (2011)

20.1 Introductory Remarks

GNSS satellites such as GPS are playing an increasingly crucial role in tracking low earth orbiting (LEO) remote sensing satellites at altitudes below 3000 km with accuracies of better than 10 cm (Yunck et al. 1990). These remote sensing satellites employ a precise global network of GNSS, GRACE (Gravity Recovery And Climate Experiment) and Altimetry ground receivers operating in concert with receivers onboard the LEO satellites, with all estimating the satellites’ orbits, GPS orbits, and selected ground locations simultaneously (Yunck et al. 1990). In this chapter, we illustrate the role played by GNSS satellites in measuring changes in the Earth’s atmosphere, its gravity field, and surfaces (e.g., ice layer density). These changes are found by measuring *refractivity, inter-satellite distances, and reflected signals* (i.e., multipath), respectively.

The last two decades has seen the emergence of GNSS remote sensing techniques that are capable of monitoring changes in the global tropopause height and in so doing, contribute to monitoring *global warming* as we shall see in Chap. 21. GNSS satellites in conjunction, with LEO, e.g., the GRACE, have been used to derive vertical atmospheric profiles of, e.g., *temperature, height, and pressure*, in what is known as GNSS radio occultation (RO) or GNSS-Meteorology (Wickert 2002). Foelsche et al. (2007) point to its potential to overcome problems associated with traditional data sources (e.g., radiosondes) due to their unique combination of *high accuracy and vertical resolution, long-term stability and all-weather global coverage* that is not feasible with other systems.

Indeed, Schmidt et al. (2005) compared RO data from CHAMP (CHALLENGING Mini-satellite Payload) with radiosonde measurements and found an agreement within less than 0.5 K (i.e., in the measured temperature profiles). In another study of global tropopause height changes over a period of 7 years (2001–2007) using CHAMP and GRACE, Schmidt et al. (2008), found a trend of $+(23 - 44)$ m/decade, which is consistent with the results published by Seidel and Randel (2006) based on radiosonde data. The six operational COSMIC (Constellation Observing System for Meteorology, Ionosphere, and Climate) satellites, launched in 2006, have significantly increased the availability of GNSS meteorology data for climate studies, see e.g., Anthes et al. (2008).

In the next section, a brief look at the basics of GNSS remote sensing of the atmosphere is presented, with the interested reader referred to Wickert (2002), Wickert et al. (2005), and Awange (2012) for more detailed discussions on the application of GNSS to monitoring the environment. In Chap. 21, it will be demonstrated how it could be used to enhance tropopause monitoring and in doing so, contribute towards monitoring climatic change related to global warming. In Sect. 20.2, GNSS remote sensing of the atmosphere for weather forecasting and climatic modeling is presented. Section 20.3 then presents GRACE applications for sensing changes in the gravity field caused by mass changes. These mass changes are caused, e.g., by changes in local, regional or global total water storage, changes in cryosphere, or changes in sea level. Section 20.4 treats the application of altimetry, which makes use of the measurement of the delay time between the signals that reach the LEO satellite receiver directly from the GNSS transmitter and those that are reflected, e.g., by the sea surface. Section 20.5 looks at the possibility of using GNSS reflected signals, also known as multipath (see Sect. 5.4.4), to monitor changes in surfaces before concluding in Sect. 20.6.

20.2 Sensing the Atmosphere Using GNSS

As stated in part II of the book, some GNSS satellites, such as GPS and GLONASS, were primarily designed to be used by the military with the primary objective of obtaining accurate *positions* of points on the Earth from space. In order to obtain these positions, we saw that the signals emitted by GNSS satellites have to traverse the ionosphere and neutral atmosphere to be received by ground-based GNSS receivers. One of the major obstacles to positioning with GNSS discussed in Sect. 5.4.3 was the *signal delay* caused by atmospheric refraction.

As opposed to geodesists whose interest is to estimate *ionospheric* and *tropospheric* delays only to eliminate them, *meteorologists* and *environmentalists* could use these ionospheric and tropospheric delays for *weather forecasting*, *climate studies* (e.g., sea, land, and ice level changes), *hazard predictions* and *early warning systems* (see e.g., Awange 2012). Belvis et al. (1992) presents a win-win situation for professionals in both geodesy and environmental studies; for a geodesist,

accurate knowledge of the atmospheric delay will improve the vertical accuracy, which in turn is of great interest to environmental scientists studying *global climate change*, which may be reflected in changes in the atmospheric delay. Or to put it another way, “one scientist’s noise is another scientist’s signal”.

Currently, the NASA Deep Space Network (DSN) uses near-real-time tropospheric delay estimates based on real-time global differential GNSS (GDGPS discussed in Sect. 6.4.3) to calibrate the radio signals from spacecraft in support of deep space navigation. Real-time global ionospheric total electron content (TEC) maps are derived at JPL and by the Air Force Weather Agency (AFWA) based on GDGPS tracking data.¹ Hammond et al. (2010) point out that GNSS measurements have the potential to contribute to tropospheric weather and climatic modeling, and/or weather forecasting in up to four different ways; (i) integrative measurement of atmospheric water vapour in GPS signal delays, (ii) localized sensing of soil moisture and snow depth from satellite to antenna multipaths, (iii) large-scale sensing of water mass from elastic deformation signals, and (iv) imaging of hydrometeor scattering.

For the ionosphere, where almost all aspects of ionospheric research uses GNSS observations (i.e., the measured *total electronic content* (TEC) from the differential delay of the two L1 and L2 signals), higher sampling rates of real-time GNSS will benefit studies of travelling ionospheric disturbances and other wave phenomena, including disturbances from *earthquakes* and *tsunamis*, while lower latency will aid in the development of operational forecasting for space weather, with significant implications for global communications systems and satellite maintenance (Hammond et al. 2011).

This section examines how GNSS satellites could be used to remote sense various atmospheric parameters as their signals pass through the different portions of the atmosphere. The goal is to show how atmospheric parameters such as the TEC in the ionosphere, tropospheric *temperatures*, *pressures* and *water vapour* could be measured by GNSS satellites, and related to meteorological (weather and climatological) applications, and hence to develop the field of *GNSS-meteorology*. In what follows, we start by presenting the background to GNSS-meteorology before discussing the environmental parameters that could be derived from it. The measuring techniques and the potential applications to environmental monitoring are also discussed.

20.2.1 Background to GNSS Meteorology

Melbourne et al. (1994) suggested that the complicating effect of the atmosphere on GNSS signals could be inverted to remote sense the atmosphere using space-borne techniques. He proposed that LEO satellites be fitted with GNSS receivers and be used to track the signals of rising or setting GNSS satellites (occulting satellites).

¹ <http://www.gdgps.net/applications/index.html>

The proposed technology has the potential to play a major role in complementing existing techniques, e.g., radiosondes. Atmospheric profiles from GNSS remote sensing have been tested in numerical weather prediction (NWP) models and the results were found to be promising (Healey et al. 2003). Indeed, Kuo et al. (2000) demonstrated using GPS/MET (GPS/meteorology space trial mission) data that the accuracy of global and regional analysis of weather prediction could be significantly improved. Also encouraging were the results of Steiner et al. (2001) who showed that highly accurate measurements and fine vertical resolution around the tropopause would be employed to monitor climatic change over the next decades.

Several atmospheric sounding missions have been launched aboard LEO satellites, e.g., CHAMP, which is no longer active, but whose data are available, GRACE, and COSMIC (Anthes et al. 2008). The latest entry is the European owned European organization for the exploitation of METeorological SATellites (EUMETSAT), which is installed with a GNSS occultation receivers GRAS (GNSS Receiver for Atmospheric Sounding). Combined, these missions provide more than 5000 occultation data daily. Future possibilities for atmospheric sounding missions may have satellites the size of a laptop with GNSS receivers the size of a credit card, e.g., Yunck (2003). The planned LEO satellite missions, together with the increasing number of GNSS satellites, promises a bright future for atmospheric studies, which would in turn benefit environmental monitoring. Indeed, such atmospheric sounding missions promise to provide daily global coverage of thousands of remotely sensed data that will be vital for weather, climatic and atmospheric studies.

Space-borne GNSS-meteorology, which we discuss in detail in Sect. 20.2.3.1 is just one part of this new technique. The other component is the ground-based GNSS-meteorology, which will be discussed in Sect. 20.2.3.3. Overviews of this new technique have been presented, for instance, in Anthes (2004), Foelsche et al. (2006). In ground-based GNSS-meteorology, a dense GNSS network (e.g., GEONET, Fig. 6.14 on p. 96) is used to measure precisely GNSS path delays caused by the ionosphere and the neutral troposphere traversed by the GNSS signals. These path delays are then converted into TEC and integrated precipitable water vapour (IPWV) values. Conversion to IPWV requires prior information of surface pressure or estimates along the GNSS ray path. These create a continuous, accurate, all weather, real-time lower and upper atmospheric data set with a variety of opportunities for atmospheric research (Ware et al. 2000a).

Use of the GNSS-derived atmospheric precipitate water vapour (PWV) in real-time weather forecasting has, however, been slow due to the fact that forecasters preferred high-rate and low-latency measurements. However, increased availability of high-rate sampling and low-latency GNSS products, e.g., those discussed in Sect. 6.4.3, together with greater station densities, is posed to change the forecasters' perception and lead towards future GNSS water vapour sensing using high-rate, low-latency data from GNSS receivers (Hammond et al. 2010).

20.2.2 GNSS-Derived Atmospheric Parameters

What exactly are the parameters in the atmosphere measurable by GNSS that are of interest to environmental monitoring?

This section attempts to answer this question by examining the effect of the atmosphere on the GNSS signals as they pass through it from the satellites to the receivers. Understanding these effects would in turn enable us know exactly the parameters that could be remotely sensed by GNSS signals. The key to understanding the atmospheric signals of interest is to look at the GNSS signal delays.

The atmosphere acts as a medium through which the GNSS signals travel from the satellites to the receivers. If the atmosphere was a vacuum, the GNSS signal would travel in a straight line. But since the atmosphere is made up of various layers of different densities, the GNSS signal instead curves before reaching the receiver. Hence, the distance increases and the velocity of the radiowaves decreases, thus delaying the signal. This GNSS signal delay is what is measured, as will be discussed in the next section. Once the delay has been measured, it is converted into the required atmospheric parameters; *refractivity, bending angles, temperatures, pressures, water vapour and geopotential heights*. In measuring these atmospheric signals, GNSS-meteorology has the advantages of;

- (a) being *global*,
- (b) *stable*, owing to the stable GNSS oscillators, and
- (c) use of radio frequencies that can *penetrate* clouds and dust, unlike other remote sensing techniques such as optical-based (Chap. 8) whose signals are blocked by clouds.

Next, the relationship between the GNSS signal and refractivity as it traverses the troposphere from an altitude of 40 km to the antenna is presented. This will enhance our understanding of how GNSS satellites remotely sense these environmental attributes. Belvis et al. (1992) classify the effects of the atmosphere on GNSS signal into two parts:

- *First*, there is a reduction in the speed of propagation of the GNSS signals in a region of finite density compared to that in a vacuum, leading to an increase in the time taken by the signal to reach the receiver. This increase in time can be expressed in terms of *excess path length*, leading to an *optical delay*.
- *Second*, the signals travel in a curved path instead of a straight line due to the refractive effects of the atmosphere's changing density (Snell's laws) (see, Fig. 20.2) leading to a *geometrical delay*.

Both the *optical* and *geometrical delays* are attributed to variations in the *index of refraction n* along the path taken by the signals. The excess path length ΔL is given by (Belvis et al. 1992)

$$\Delta L = \int_L n(s)ds - G, \quad (20.1)$$

where $n(s)$ is the refractive index as a function of position s along the curved path L , and G is the straight-line geometrical path length through the atmosphere (i.e., the path that would be taken by the signal in a vacuum). Equation (20.1) can be expressed as

$$\Delta L = \int_L [n(s) - 1]ds - [S - G], \quad (20.2)$$

where S is the path length along L . In Eq. (20.2), $\int_L [n(s) - 1]ds$ represents the reduction in speed, i.e., optic delay while $[S - G]$ is due to the bending effect, i.e., geometric delay. The bending term $[S - G]$ is smaller, about 1 cm or less, for paths with elevations greater than about 15° (Belvis et al. 1992). In addition, rather than the refractive index in n above, which is numerically close to unity, refractivity, given by

$$N = (n - 1)10^6 \quad (20.3)$$

is usually used, leading to

$$N = 77.6 \frac{P}{T} + \left(3.73 \times 10^5 \frac{P_w}{T^2} \right) - \left(40.3 \times 10^6 \frac{n_e}{f^2} \right) + 1.4w, \quad (20.4)$$

where P denotes the total atmospheric pressure in {mbar}, T is the atmospheric temperature in K, P_w is the partial pressure of water vapour in {mbar}, n_e is the number of electron density per cubic meter {number of electron/ m^3 }, f is the transmitter frequency in Hz, and w is the liquid water content in g/m^3 . The three main contributors to *refractivity*, as was discussed in Sect. 5.4.3, are:

- The *dry neutral atmosphere* (called the hydrostatic component, i.e., the first component on the right-hand-side of Eq. (20.4), dependent mainly on *dry air* and also the *non-dipole component of water vapour*. From this component, GNSS-derived vertical profiles of temperatures and pressures used for global warming monitoring are obtained.
- *Water vapour* (also called the wet or moist component, i.e., the second component on the right-hand-side of Eq. (20.4), dependent on the *dipole component of water vapour*). GNSS are used to measure water vapour through the estimated zenith wet delay (ZWD) as discussed below. The GNSS-derived water vapour are useful both for weather forecasting in numerical weather prediction (NWP) models and also in climate change studies.
- The *free electrons* in the ionosphere (i.e., the third component on the right-hand-side of Eq. (20.4)). GNSS plays a key role in providing slant TEC² derived through the differencing of the L1 and L2 frequency phase delay. GPS estimates of slant TEC are by far the most plentiful observations of ionospheric processes and provide

² Total electronic contents.

the bulk of global spatial sampling, so global models necessarily rely on them heavily (Hammond et al. 2010).

GNSS Measurement of Water Vapour

The first two items of Eq. (20.4) are summarized in Fig. 20.1. The contribution of the *free electrons* leading to refraction effects on the signals in the ionosphere are corrected for using signals at two frequencies for which these effects are substantially different, taking advantage of the dispersive nature of the ionosphere. This leaves the last term of Eq. (20.4), which is normally very small and is often neglected, see e.g., Belvis et al. (1992). The first two terms of Eq. (20.4) are indicated by Resch (1984) to be accurate to about 0.5% under normal atmospheric conditions. Thayer (1974) provided an improved version (Belvis et al. 1992) of Eq. (20.4), expressed as (Leick 2004, p. 301)

$$N = k_1 \frac{P_d}{T} Z_d^{-1} + k_2 \frac{P_{wv}}{T} Z_{wv}^{-1} + k_3 \frac{P_{wv}}{T^2} Z_{wv}^{-1}, \tag{20.5}$$

where

- $k_1 = (77.60) \text{ K mbar}^{-1}$, $k_2 = (69.5) \text{ K mbar}^{-1}$, $k_3 = (370100) \text{ K}^2 \text{ mbar}^{-1}$,
- P_d is the *partial pressure of dry air* (in mbar), with the dry gases of the atmosphere in decreasing percentage of volume being N_2 , O_2 , Ar , CO_2 , Ne , He , Kr , Xe , CH_4 , H_2 , and N_2O , representing 99.96% of the total volume,

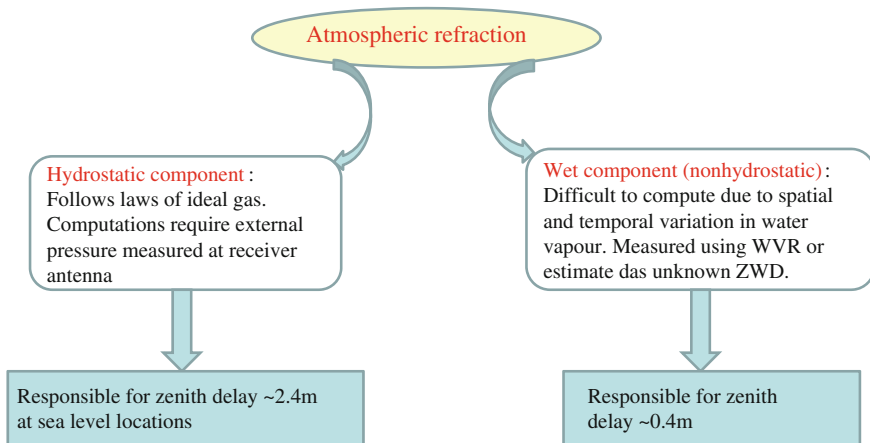


Fig. 20.1 Components of tropospheric refractivity. WVR (water vapour radiometers) and ZWD (zenith wet delay) help in determining the wet component

- P_{wv} is the partial pressure of water vapour (water vapour content is highly variable, but rarely exceeds 1 % of the mass of the atmosphere),
- T is the absolute temperature in degrees Kelvin (K),
- Z_d^{-1} and Z_{wv}^{-1} are the *inverse compressibility factors* for dry air and water vapour, respectively, that account for small departures in the behavior of moist atmosphere from an ideal gas.

Thayer's (1974) modified Eq. (20.5) leads to the retrieval of refraction with an accuracy of about 0.02 % (Davis et al. 1985). Leick (2004, p. 301) provides an explanation of Eq. (20.5) as follows: the first term is the sum of the *distortion* of the electron charges of the dry gas molecules under the influence of a magnetic field, the second term expresses the same effect, but for water vapour, while the third term describes the permanent dipole moment of the water vapour, i.e., it is a direct result of the geometry of water vapour's molecular structure. The *first term* of Eq. (20.5) is then divided into two parts to give (Leick 2004, p. 301):

1. the refractivity of an ideal gas in hydrostatic equilibrium, i.e., *hydrostatic refractivity*, which is the larger component and can be accurately computed if the surface total pressure is available, and
2. a function of *partial water vapour pressure*. This is the smaller component of the two and has to be either measured or estimated (e.g., Fig. 20.1).

The division is achieved using the equation of the state of a gas

$$p_i = Z_i \rho_i R_i T, \text{ for } i = \{d, wv\}, \quad (20.6)$$

with ρ_i being the mass density and R_i the specific gas constant. In Eq. (20.6), the subscripts d , and wv represent dry gas and water vapour, respectively. Using this equation in (20.5), it is immediately noticeable that the term P_d in the first part can be replaced. This introduces the density term ρ_d which can then be replaced by the total density ρ and partial density of water vapour ρ_{wv} . Replacing this partial density of water vapour ρ_{wv} by Eq. (20.6) leads to the division of the first term as (Leick 2004, p. 301)

$$k_1 \frac{P_d}{T} Z_d^{-1} = k_1 R_d \rho - k_1 \frac{R_d}{R_{wv}} \frac{P_{wv}}{T} Z_{wv}^{-1}, \quad (20.7)$$

which clearly indicates that the refractivity of the hydrostatic term is due to both dry gas and partial water vapour, as had been previously stated, e.g., by Belvis et al. (1992). When (20.7) is substituted into Eq. (20.5) and combined with the second term of (20.5), one obtains

$$N = k_1 R_d \rho + k_2' \frac{P_{wv}}{T} Z_{wv}^{-1} + k_3 \frac{P_{wv}}{T^2} Z_{wv}^{-1}, \quad (20.8)$$

and

$$k_2' = k_2 - k_1 \frac{R_d}{R_{wv}} = k_2 - k_1 \frac{M_{wv}}{M_d}, \quad (20.9)$$

with M_i , $i = \{d, wv\}$ being the molar mass. Equation (20.8) essentially provides the hydrostatic (N_d) and wet refractivity (N_{wv}) terms, respectively, as

$$N_d = k_1 \frac{P}{T}, \tag{20.10}$$

and

$$N_{wv} = k_2' \frac{P_{wv}}{T} Z_{wv}^{-1} + k_3 \frac{P_{wv}}{T^2} Z_{wv}^{-1}. \tag{20.11}$$

Integrating (20.5) along the zenith direction using (20.10) and (20.11) gives the zenith hydrostatic delay (ZHD) and the zenith wet delay (ZWD), respectively, as (Leick 2004, p. 301)

$$ZHD = 10^6 \int_{antenna}^{\infty} N_d(h) dh, \tag{20.12}$$

$$\boxed{ZWD = 10^6 \int_{antenna}^{\infty} N_{wv}(h) dh}. \tag{20.13}$$

For satellites that are not vertically overhead, i.e., not in the direction of the zenith, the hydrostatic and wet delays in (20.12) and (20.13) have to be converted into the equivalent slant delays through

$$\begin{aligned} SHD &= ZHD \cdot m_{f_h}(\alpha) \\ SWD &= ZWD \cdot m_{f_{wv}}(\alpha), \end{aligned} \tag{20.14}$$

leading to the slant total delay (STD) expressed as

$$STD = SHD + SWD, \tag{20.15}$$

where m_{f_h} and $m_{f_{wv}}$ are mapping functions and α is the elevation angle. Note that the zenith angle ($90 - \alpha$) could also be used. The simplest relation between the wet delay (SWD) along a line of elevation angle α and the ZWD is given through the simple Pythagorean

$$\boxed{SWD = \frac{ZWD}{\sin(\alpha)}}. \tag{20.16}$$

The most commonly used mapping function is Niell's (1996). Using the zenith angle z , Niell's mapping functions $m_{f_h}(z)$ and $m_{f_{wv}}(z)$ are given by (Niell 1996)

$$m_{f_h} = \frac{1 + f_1}{\cos(z) + f_2} + h \left(\frac{1}{\cos(z)} - \frac{1 + f_3}{\cos(z) + f_4} \right), \tag{20.17}$$

and

$$mf_{wv}(z) = \frac{1 + f_5}{\cos(z) + f_6}, \quad (20.18)$$

where

$$\begin{aligned} f_1 &= \frac{a}{1 + \left(\frac{b}{1+c}\right)} \\ f_2 &= \frac{a}{\cos(z) + \left(\frac{b}{\cos(z)+c}\right)} \\ f_3 &= \frac{a_h}{1 + \left(\frac{b_h}{1+c_h}\right)} \\ f_4 &= \frac{a_h}{\cos(z) + \left(\frac{b_h}{\cos(z)+c_h}\right)} \\ f_5 &= \frac{\tilde{a}}{1 + \left(\frac{\tilde{b}}{1+\tilde{c}}\right)} \\ f_6 &= \frac{\tilde{a}}{\cos(z) + \left(\frac{\tilde{b}}{\cos(z)+\tilde{c}}\right)}, \end{aligned}$$

where a , b , and c are the coefficients of the hydrostatic mapping function given in Niell (1996, Table 3), while \tilde{a} , \tilde{b} , and \tilde{c} are the coefficients of the wet mapping function in Niell (1996, Table 4). Tropospheric delay is thus shortest in the zenith direction where the elevation angle $\alpha = 90^\circ$, but increases as the elevation angle decreases.

From the STD, which can be estimated from GPS observations, the measurable signals of interest to environmental monitoring are the *precipitable water* (PW) and the *integrated water vapour* (IWV). Let us now consider that for each receiver of the continuous operating reference stations (CORS; see Sect. 6.5), for a known station, the range between the satellite and the receiver will be accurately known. If the other errors discussed in Sect. 5.4 are properly modeled, the remaining residual errors of the observations will be due to STD, see e.g., Leick (2004). These STD could then be used to estimate ZWD given a proper mapping function and assuming that the ZHD has been accurately obtained from surface meteorological measurements. The estimation of ZWD from GNSS observation equations can take on the form of (Belvis et al. 1994; Rocken et al. 1993):

- (i) *Least squares solution* (e.g., Awange 2012), where the ZWDs are obtained as unknowns, i.e., the deterministic approach from which one parameter is estimated per station per specified time interval. This approach involves constraining the value of the ZWD and perhaps its rate of change, to keep it within a reasonable set of bounds (Belvis et al. 1994).

- (ii) Estimation as a *stochastic process* using a Kalman filter (Tralli and Lichten 1990), where the temporal variation of ZWD is assumed not to change by a large amount over a short period of time. The stochastic filter estimation of ZWD requires a proper choice of the stochastic process that represents its fluctuation. One common choice is the first-order Gauss-Markov process and the stochastic noise is chosen so as to constrain the variation of the ZWD to between 1 and 20 mm per hour, depending on location and the time of the year (Belvis et al. 1994).

As we shall see in Sect. 21.3.2, NWP models require precipitable water and as such the conversion of the GNSS measured ZWD to precipitable water vapour (PWV) and integrated water vapour (IWV) is necessary. Askne and Nordius (1987) have shown that it is possible to relate IWV and the measured ZWD. The relationship is presented by Belvis et al. (1994) as

$$IWV \approx \zeta ZWD \tag{20.19}$$

and

$$PWV = \frac{\zeta ZWD}{\rho}, \tag{20.20}$$

where ρ is the total density. In (20.19) and (20.20), the value of the constant ζ , i.e., the ratio IWV/ZWD, varies between 5.9 and 6.6 and is given by Leick (2004, p. 301) as

$$\frac{1}{\zeta} = 10^{-6} \left(\frac{k_3}{T_m} + k'_2 \right) R_{wv}, \tag{20.21}$$

where T_m is the weighted mean temperature of the atmosphere given by

$$T_m = \frac{\int \frac{P_{wv}}{T} Z_{wv}^{-1} dh}{\int \frac{P_{wv}}{T^2} Z_{wv}^{-1} dh}. \tag{20.22}$$

In estimating PWV from (20.20), the largest source of error is attributed to the mean temperature T_m which varies with *location, height, season, and weather*. Belvis et al. (1994) provided a total error budget of the estimated ZWD of ~ 10 mm random error and ~ 10 mm long-term bias. This was based on the comparison of the results of Very Long Baseline Interferometry (VLBI, e.g., Sect. 3.4), GNSS (Chaps. 4–6), and WVR (water vapour radiometers, e.g., Chap. 8), with the error component divided as follows (Belvis et al. 1994):

- (a) 5 % error due to the inversion from path delay to IWV in non-arid areas.
- (b) Errors of less than 10 mm in path delay arising from carrier-phase measurements and propagated through the Kalman filtering estimation method.
- (c) Errors of the order of 3 mm in ZWD under normal ionospheric conditions arising from the use of dual-frequency signals for range correction (i.e., ionospheric correction).

- (d) Less than 1% (23 mm) errors in hydrostatic delay as a result of atmospheric dynamics. Proper station calibration, however, can potentially reduce this error to less than 1 mm.
- (e) Multipath errors will depend on the type of antenna, elevation angle of the satellites and the environment in which the antenna is located. Belvis et al. (1994) suggest that since this error is normally less than 100 mm for elevation angles of 15° , it is likely to perturb the zenith delay measurement by less than 20 mm.
- (f) The contribution of ionospheric effects on the signal will generally be below the total error budget.

20.2.3 GNSS Remote Sensing Techniques

Over the years, research efforts have been dedicated to modeling atmospheric refraction in order to improve on GNSS positioning accuracy by accounting for the excess path delay in Eq. (20.2). As we discussed in Sect. 5.43, modeling of the propagation delay is done separately for the *ionosphere* and *troposphere*. For the ionosphere, Eqs. (5.5) and (5.6) on p. 67 are applied to eliminate most of the ionospheric delay. For the tropospheric delay on the other hand, we saw that the troposphere is a non-dispersive medium and that its delay could not be eliminated by the linear combination of dual-frequency observations, but must instead be measured or estimated. In the next sections, we present both space and ground based GNSS remote sensing methods and related missions, which are essential in measuring the atmospheric parameters discussed in Sect. 20.2.2.

20.2.3.1 Space-Borne GNSS Remote Sensing

GNSS radio occultation (GNSS-RO) takes place when a transmitting satellite, setting or rising behind the Earth's limb, is viewed by a LEO satellite as illustrated in Fig. 20.2. GNSS satellites send radio signals that pass through successively deeper layer of the Earth's atmosphere and are received by LEO satellites. These signals are bent and retarded, causing a delay in their arrival at the LEO.

Figure 20.2 shows the occultation geometry where the signal transmitted from a GNSS to a LEO satellite passes through dispersive layers of the ionosphere and atmosphere, and in so doing senses them. As the signal is bent, the total bending angle, α , an impact parameter, a , and a tangent radius, r_t , define the ray passing through the atmosphere. The *refraction angle* is accurately measured and related to the atmospheric parameters; temperature, pressure and water vapour via the refractive index in Eq. 20.4. Use is made of radio waves where a GNSS receiver on-board a LEO satellite measures, at the required sampling rate, the dual-band carrier-phases (L1 and L2), the C/A-code and P-code group delay (see Sect. 5.3.1) (Melbourne et al. 1994). The data is then processed to remove errors arising from short-term oscillator

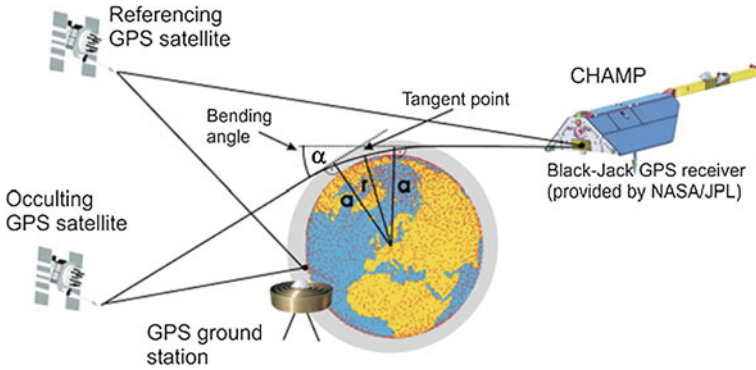


Fig. 20.2 GNSS radio occultation. Use is made of (i) an occulting satellite, (ii) a non-occulted GNSS satellite and (iii) a ground-based GNSS station to determine the bending angle α from which the vertical profiles of temperature and pressure are determined, e.g., from Eq. 20.4 on p. 274. Source Wickert (2002)

and instabilities in the satellites and receivers. This is achieved by using at least one ground station and one satellite that is not being occulted, leading to a Doppler shift (see Fig. 20.2). Once the observations have been corrected for possible sources of errors, the resulting *Doppler shift* is used to determine the refraction angle α .

The variation of α with a during an occultation depends primarily on the vertical profile of the atmospheric refractive index, which is determined globally by *Fermat's principle* of least time and locally by *Snell's law*

$$n \times \sin\phi = \text{constant}, \tag{20.23}$$

where ϕ denotes the angle between the gradient of refraction and the ray path. The Doppler shift is determined by projecting spacecraft velocities onto the ray paths at the transmitter and receiver so that atmospheric bending contributes to its measured value. Data from several GNSS transmitters and post-processing ground stations are used to establish the precise positions and velocities of the GNSS transmitters and LEO satellites. These derived positions and velocities are used to calculate the Doppler shift expected in the absence of atmospheric bending (i.e., were the signal to travel in a straight line). By subtracting the *expected* shift from the measured shift, one obtains the excess Doppler shift. Assuming local symmetry and with Snell's law, the excess Doppler shift, together with satellites' *positions* and *velocities*, are used to compute the values of the bending angles α with respect to the impact parameters a . Once computed, these bending (refraction) angles are related to the refractive index by

$$\alpha(a) = 2a \int_{r=r_0}^{r=\infty} \frac{1}{\sqrt{n^2 r^2 - a^2}} \frac{d \ln(n)}{dr} dr, \tag{20.24}$$

which is then inverted using Abel's transformation to give the desired refractive index

$$n(r_0) = \exp \left[\frac{1}{\pi} \int_{a=a_0}^{a=\infty} \frac{\alpha(a)}{\sqrt{a^2 - a_0^2}} da \right]. \quad (20.25)$$

If the atmospheric temperature T and pressure P are provided from external source, e.g., from models and synoptic meteorological data, then the vertical water vapour density could be recovered from GNSS remote sensing data using Eq. (20.4) (Melbourne et al. 1994).

To demonstrate the capability of the method, the following examples show that the temperature profiles measured by GNSS around the tropopause region (8–17 km) gives accurate results comparable to the traditional radiosonde method.

Example 20.1 (Validating GNSS derived atmospheric parameters (Khandu et al. 2010)) In Fig. 20.3, GNSS-derived temperature profiles from LEO missions (COSMIC, CHAMP and GRACE) are compared with the profiles of the closest radiosondes in Australia. The radiosonde launched from Learmonth Airport (22.24°S, 114.09°E) on 14th June 2005 was within 70 km and 40 min from the CHAMP measurement, whereas the radiosonde launched from Hobart Airport (42.84°S, 147.50°E) on 20th December 2006 was within 12 km and 1.25 h from the COSMIC measurement. The radiosonde from Weipa Aero location and the GRACE RO profile were located within 92 km, with time difference of 1.25 h from each other.

A visual examination of Fig. 20.3 indicates that the COSMIC RO temperature profile agrees very well with its corresponding radiosonde profile with almost no deviation from the radiosonde data. The temperature profiles from the CHAMP satellite have been shown, e.g., by Schmidt et al. (2004) to agree

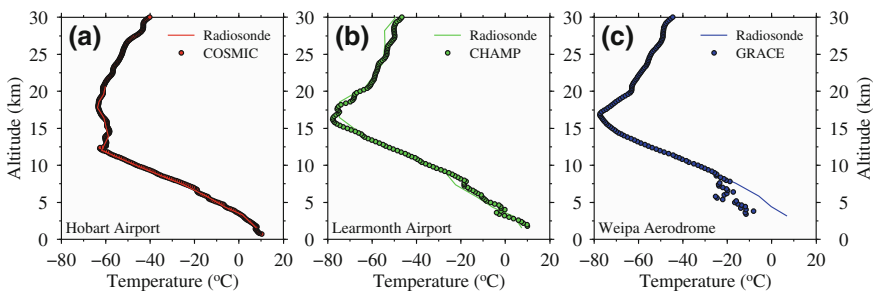


Fig. 20.3 GNSS-RO soundings observed on **a** 20 December 2006 over Hobart Airport [42.84°S, 147.50°E] using COSMIC RO data, **b** 14 June 2005 over Learmonth Airport in Western Australia [22.24°S, 114.09°E] using CHAMP RO data and **c** on 8 September 2006 over Weipa Aero using GRACE data [12.68°S, 141.92°E]. Source Khandu et al. (2010)

well in the upper troposphere and lower stratosphere. However, looking at Fig. 20.3, below 5 km, the CHAMP profiles do not fit the radiosonde data as well as those for the COSMIC profiles due to the effect of water vapour. The GRACE temperature profile agrees well with the corresponding radiosonde measurement above 8 km, while below 8 km it is also affected by water vapour like the CHAMP profiles.

End of Example 20.1

Example 20.2 (Comparison of profiles between 7–30 km height (Khandu et al. 2010)) GNSS-derived temperature profiles between 7–30 km were then compared to those from the radiosonde observations between 2001 and 2006. The comparison method was based on a maximum spatial separation of 100 km and a temporal difference of 3 h between the GNSS-RO measurements and the radiosonde (e.g., Schmidt et al. (2004) use values between 3 h and a distance of 300 km, which they state would mean near constant weather). A distance of 100 km was chosen to account for the spatial drift of the radiosondes, which can reach as far as 200 km from its initial position Ray et al. (2006). Temperatures are compared at 14 standard pressure levels l of the radiosonde data files between 850 and 20 hPa.

The mean temperature deviation at each pressure level $\overline{\Delta T(l)}$ and its standard deviation $\sigma_{\Delta T}(l)$ are calculated according to Eqs. (20.26) and (20.27) (Wickert 2004).

$$\overline{\Delta T(l)} = \frac{\sum_{i=1}^{M(l)} T_{D(LEO)}(i, l) - T_{Radiosonde}(i, l)}{M(l) - 1} \tag{20.26}$$

$$\sigma_{\Delta T}(l) = \sqrt{\frac{1}{M(l) - 1} \sum_{i=1}^{M(l)} (T_{D(LEO)}(i, l) - T_{Radiosonde}(i, l))^2}, \tag{20.27}$$

where $M(l)$ denotes the number of data points at each pressure level. The index i indicates the individual pairs of LEO satellite and radiosonde data, $T_{D(LEO)}$ is the dry temperature derived from the LEO data while $T_{Radiosonde}$ is the temperature given by radiosonde measurements. Temperature deviations exhibiting more than 20 K were ignored to eliminate the influence of outliers.

Figure 20.4 compares the deviation between the radiosonde and CHAMP, GRACE and COSMIC profiles, as well as the number of profiles. 80 CHAMP profiles from September 2001 to December 2006 were found to occur within 100 km and a time delay of less than 3 h of a radiosonde profile. The results of

the comparisons indicate a temperature bias of less than 1 K for the complete height interval between 9 and 26 km, with a standard deviation of less than 2 K. Between 11 and 26 km the bias is less than 0.5 K with a standard deviation of 1–2 K. The bias of the CHAMP temperature in the lower troposphere (altitude < 7.5 km) is largely due to the presence of water vapour, see also Foelsche et al. (2007), Kuo et al. (2005), Wickert (2004). The larger bias between CHAMP and radiosonde data is less than 0.5 K in the upper troposphere and lower stratosphere where there is little or no water vapour. Biases between CHAMP RO data and radiosonde data are all negative for all the altitude levels between 1.5 and 26 km.

Only 18 profiles from GRACE RO data from January 2006 to October 2007 were found within the defined spatial and temporal limits. Nevertheless, the bias is less than 3 K between the altitude range of 9 and 20 km, showing that GRACE RO data agrees well over this range with the radiosonde measurements. Below 9 km, like the CHAMP data, the GRACE temperature profiles are also affected by the presence of water vapour. However, the bias in the GRACE temperatures could be due to the lower number of GRACE profiles meeting the selection criteria.

COSMIC RO data from April 2006 to December 2006 were also used for these comparisons, with 54 COSMIC RO profiles meeting the criteria. From Fig. 20.4, it can be seen that the bias between CHAMP and COSMIC RO data agree well between 10.7 and 25 km, with the difference in the bias over this altitude range being less than 0.5 K. CHAMP RO data displays a lower standard deviation than COSMIC data between 10 and 18 km, with a standard deviation of less than 1.5 K. Below 7.5 km, CHAMP temperatures show a large negative bias whereas the bias from the COSMIC temperature remains constant.

From these three GNSS-RO data sets, the COSMIC temperature data provided a good correlation of data with much smaller standard deviations, with CHAMP and GRACE having higher standard deviations below 10 km. This example highlights the possibility of GNSS satellites being used to remote sense the atmosphere at the heights between 7 and 25 km with accuracies that will suffice for the environmental monitoring of the atmosphere, specifically the tropopause, an issue that will be discussed in detail in the next chapter. Further readings are, e.g., Khandu et al. (2010) and Awange (2012).

End of Example 20.2

Next, we look at the LEO satellite missions that make the GNSS space borne remote sensing possible. Several missions are currently operational, but we will present only the three most commonly discussed.

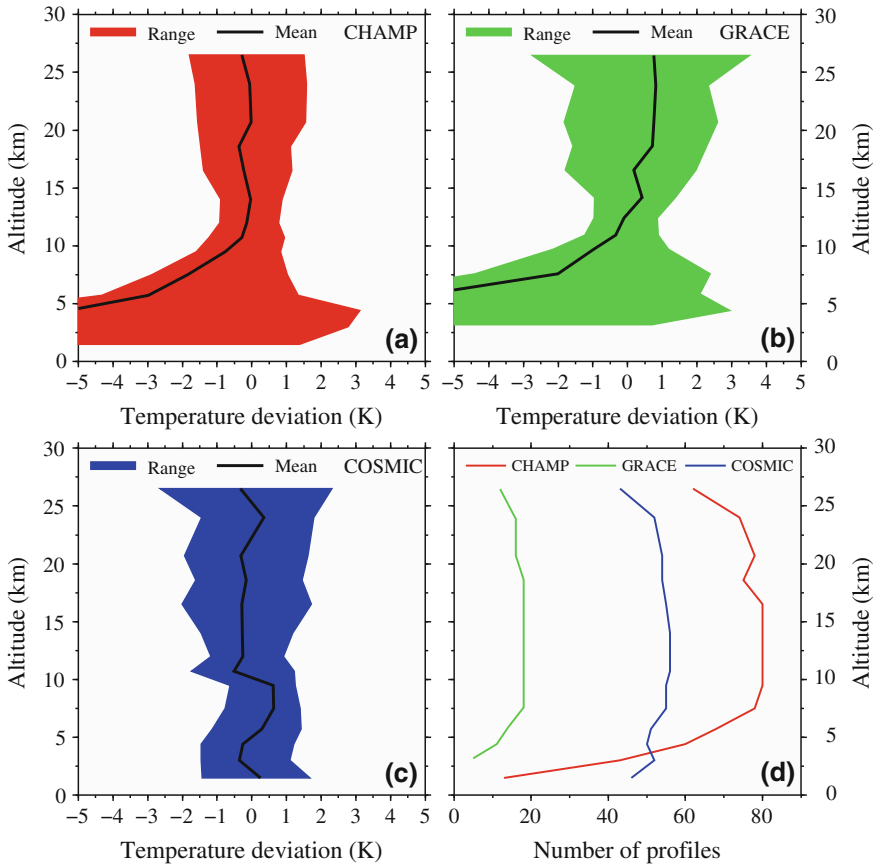


Fig. 20.4 Comparison of the deviations between GNSS-RO profiles **a** CHAMP, **b** GRACE, and **c** COSMIC profiles. **d** Number of profiles from each satellite. *Source* Khandu et al. (2010)

20.2.3.2 GNSS Radio Occultation Missions

The three LEO missions covered in this work; CHAMP, GRACE, and COSMIC, jointly contributed a total of 2,478,829 profiles between 2001 and 2008 that were analyzed (Arras et al. 2010). The German CHAMP (Fig. 20.9, left) satellite was launched on July 15, 2000 into an almost circular and near polar orbit (with an inclination of 87°) at an altitude of about 454 km (Wickert et al. 2002). The GNSS radio occultation on board CHAMP was activated on February 11, 2001, and since then nearly 541,527 occultations were recorded worldwide by 2008 (Arras et al. 2010). Having been in operation for more than a decade, CHAMP ended its mission on 19th of September 2010. CHAMP data can however still be obtained from GFZ

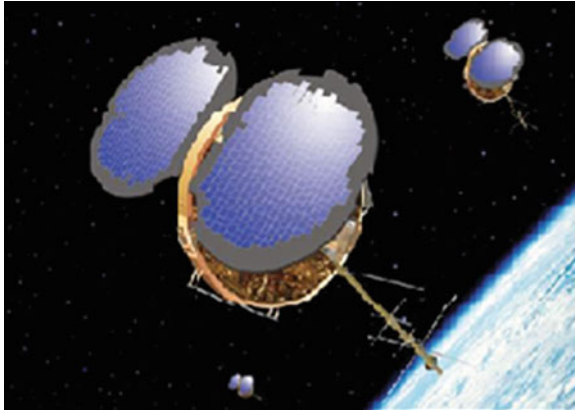


Fig. 20.5 The COSMIC satellites. *Source* <http://www.cosmic.ucar.edu>

(German Research Centre for Geosciences), the Jet Propulsion Laboratory (JPL) or the University Corporation for Atmospheric Research (UCAR).³

CHAMP Level 3 data (version 005) from GFZ data contains Abel inverted profiles of refractivity derived from the vertical profiles of bending angles. They also contain the environmental monitoring indicators of air temperature, air density, air pressure, bending angles, positions (latitudes, longitudes), heights above mean sea level, impact parameters, and signal to noise ratios (SNR) up to 30 km above mean sea level with a vertical resolution of 200 m.

Radio occultation measurements by GRACE satellites (Fig. 20.9, right), discussed in detail in Sect. 20.3.3, were first recorded during a 25 h period on July 28/29, 2004 (Beyerle et al. 2005; Wickert 2004). Atmospheric profiles derived from GRACE show nearly identical characteristics as those from the ECMWF (European Center for Medium-Range Weather Forecasts) (Wickert et al. 2009). The GRACE satellites had recorded over 141,987 occultations worldwide as of 2008 (Arras et al. 2010). The BlackJack GNSS receiver present in the GRACE satellites enables deep atmospheric sounding into the lower troposphere. The GRACE level 2 data, obtainable from GFZ, is equivalent to that from CHAMP, with the same vertical resolution of 200 m.

GNSS limb sounding reached new heights after the launch of the COSMIC mission (see, Fig. 20.5) into a near circular orbit on April 15, 2006, e.g., Anthes et al. (2008), Cheng et al. (2006). COSMIC, a constellation of six identical micro-satellites, is a joint mission between the National Space Organization (NSPO) of Taiwan and UCAR in the United States, with the main goal of obtaining vertical profiles in near-real time of temperature, pressure, and water vapour in the neutral atmosphere and electron density in the ionosphere (Cheng et al. 2006). One major change in the COSMIC data compared to CHAMP and GRACE is the improved data quality, with higher yields in the lower troposphere (below 7 km; cf. Figs. 20.3 and 20.4). This is

³ via <http://www.cosmic.ucar.edu>.

made possible by the use of the OpenLoop (OL) signal tracking technique by the Black Jack GNSS receiver (Wickert et al., 2009). OL signal tracking, which was not available in previous missions, allows for the tracking of rising occultation and deeper penetration into the lower troposphere.

The COSMIC mission provides about 2200 profiles per day on average and by 2008, it had recorded about 1,796,315 (Arras et al. 2010; Wickert et al. 2009). Level 2 COSMIC data can be obtained from both UCAR⁴ and NSPO.⁵ It contains the environmental monitoring indicators of refractivity, air temperature, water vapour, air pressure, height above mean sea level, and the position (latitude and longitude) from mean sea level to 400 km. The tropopause region from COSMIC (like CHAMP Level 3 data) contains temperatures, in which the water vapour is neglected. Level 2 COSMIC atmospheric profiles are provided with a vertical resolution of 100 m. In the following example, the number and distribution of GNSS-RO measured over Australia by 2008 from these missions are presented.

Example 20.3 (Distribution of GNSS-RO over Australia by 2008 Khandu et al. (2010)) The distribution of the GNSS-RO events depends on the geometry of the orbits of the LEO satellites and the transmitting GNSS satellites. CHAMP RO events occurred more commonly in high latitudes, with the exception of the poles, with a relatively low distribution in the equatorial regions, e.g., Foelsche et al. (2007), Tsuda and Hocke (2004). From the start of September 2001 to April 2008 for example, Australia was covered by 8,472 CHAMP RO profiles, averaging about 108 occultations per month, except for July 2006 (Fig. 20.6). Figure 20.6 indicates that the occultations are well distributed over Australia, although with fewer data in the far north, a fact already pointed out by Tsuda and Hocke (2004). It can be seen from Fig. 20.6 that the COSMIC occultations are also well distributed across the region. Like CHAMP RO data, the COSMIC RO profiles are also fewer nearer to the equator (8°S–15°S).

End of Example 20.3

20.2.3.3 Ground-Based GNSS Remote Sensing

Whereas GNSS receivers are onboard LEO satellites (e.g., CHAMP and GRACE) in space-borne GNSS remote sensing, they are fixed to ground stations in the case of ground-based GNSS remote sensing (Fig. 20.7). As we indicated in Sect. 5.4.3, the contribution of the *hydrostatic part*, which can be modeled and eliminated very accurately using surface pressure data or three-dimensional numerical models, is about 90 % of the total delay, while that of the wet delay is highly variable with

⁴ via <http://www.cosmic.ucar.edu>.

⁵ via <http://www.tacc.cwb.gov.tw>.

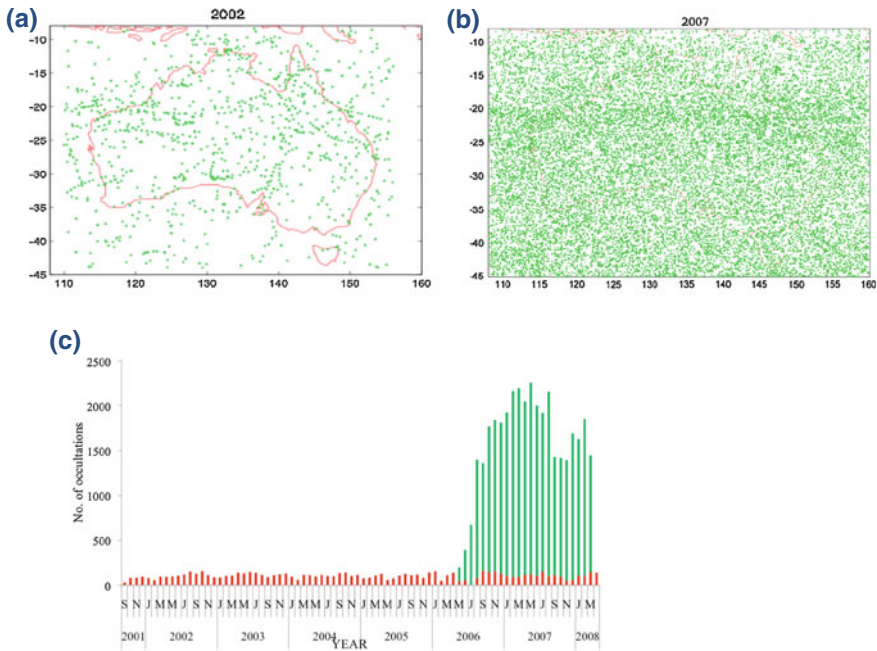


Fig. 20.6 Number of radio occultations over Australia from **a** CHAMP in 2002, **b** COSMIC in 2007, and **c** total number of occultations for CHAMP and COSMIC from 2001 to 2008. It can be seen that COSMIC provided a very dense coverage within its two years of existence. *Source* Khandu et al. (2010)

little correlation to surface meteorological measurements, see also Chen and Herring (1997) and Davis et al. (1985).

Assuming that the *wet delay* can be accurately derived from GNSS data as discussed in Sect. 20.2.2, and that reliable surface temperature data are available, the wet delay can be converted into an estimate of the total atmospheric water vapour P_w present along the GNSS ray path, as suggested by Belvis et al. (1994). This atmospheric water vapour P_w , termed *precipitable water* in GNSS-meteorology, is obtained using Eq. (20.20) on p. 279.

Using several receivers to track several satellites (see Fig. 20.7), a three-dimensional distribution of water vapour and its temporal variation can be quantified. For example, the Japanese GEONET CORS network (Fig. 6.14 on p. 96) is dedicated to ground-based GNSS meteorology, e.g., Anthes (2004) and Tsuda et al. (1998). The dense network of GNSS receivers is capable of delivering information about atmospheric water vapour content, which is useful to meteorological monitoring (e.g., climate studies and weather forecasting discussed in Sect. 21.5). Hansen et al. (1999) point out that maps of the water vapour distribution associated with, for example, a precipitating cloud, a partly precipitating cold front, or horizontal convective rolls, reveal quantitative measurements that are not observable with conventional methods.

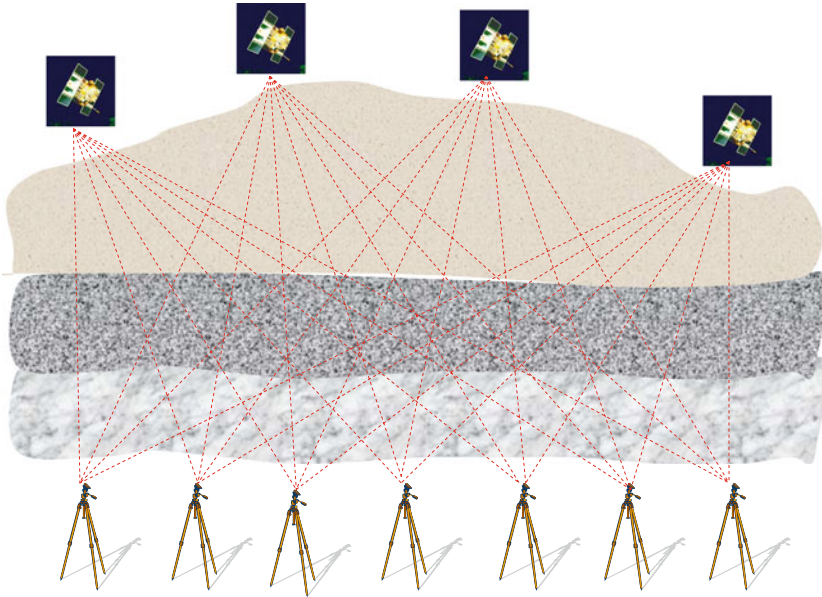


Fig. 20.7 Schematic diagram showing the remote sensing of water vapour via ground-based GNSS receivers. Figure 6.12 on p. 94 presents an example of a GEONET ground-based station. Source Awange (2012)

Example 20.4 (Global validation of GNSS-derived water vapour (Heise et al. 2006)) Heise et al. (2006) provides an overview of the *data processing and retrieval* of vertical refractivity, temperature and water vapour profiles from GNSS radio occultation observations. They also undertook a global validation of CHAMP water vapour profiles with radiosonde data and obtain a bias of about 0.2 g/kg and a standard deviation of less than 1 g/kg specific humidity in the lower troposphere, thus demonstrating the potentials of GNSS-derived CHAMP retrievals for monitoring the mean tropospheric water vapour distribution on a global scale.

End of Example 20.4

20.3 Remote Sensing of Gravity Variations

In the subsections that follow, it is explained how GNSS satellites (particularly GPS) support LEO satellites used to monitor variations in gravity field, which are in turn used to remote sense the changes in stored water at continental scales. The most

significant success of a LEO satellite is evidenced in the GRACE satellites discussed in Sect. 20.3.3. A possible use of GNSS satellites to measure variations in water mass is illustrated by Tregoning et al. (2009) whose predictions derived from GRACE measured fields show a correlation with GNSS measured deformations, suggesting the possible use of such deformations to infer changes in stored water potential on much shorter temporal and spatial scales than GRACE provides (and with low-latency), while averaging over much larger spatial scales than afforded by multipath amplitude measurements (Hammond et al. 2010).

20.3.1 Mass Variation and Gravity

Two types of gravity field variation exists. The *first* is the long-term, also known as mean gravity field, which is due to the static part of the gravity field. The variation is constant over a very long time interval. Its study is useful in understanding the solid structure of the Earth, ocean circulation, and in achieving a universal height measuring system. In this respect, GNSS satellites are used to position LEO satellites such as GOCE (Gravity field and the steady state-of-the-ocean circulation explorer, Fig. 20.8), which maps changes in gravity using state-of-the-art gradiometer with improved accuracy, see e.g., Hirt et al. (2011). GOCE data is expected to benefit other studies such as those concerned with earthquakes, changes in sea level, and volcanoes.⁶

The *second* type of variation of the Earth's gravity field is associated with those processes that occur over shorter time scales, such as atmospheric circulation or the hydrological cycle. This is known as the *time-varying gravity field* and is the component which enables the monitoring of, for example, variations in water resources and the melting of the polar ice.

By removing the effects of the other processes that cause changes in the gravity field, changes in *terrestrial water storage* can thus be inferred from the observed temporal changes in the terrestrial gravity field. By assuming the density of water as 1.00 g/cm^3 , and following the relation of Pool and Eychaner (1995), Ellett et al. (2006) present the relationship between changes in stored water and gravity as

$$\Delta S = 0.419 \Delta g, \quad (20.28)$$

where water storage change ΔS is given in units of cm of water and gravity change Δg is in units of microGal (10^{-6} cm/s^2). From Eq. (20.28), it is seen therefore, that monitoring variations in the gravity field can enable hydrological changes to be monitored.

⁶ See, e.g., http://www.esa.int/esaCP/SEMV3FO4KKF_Germany_0.html.

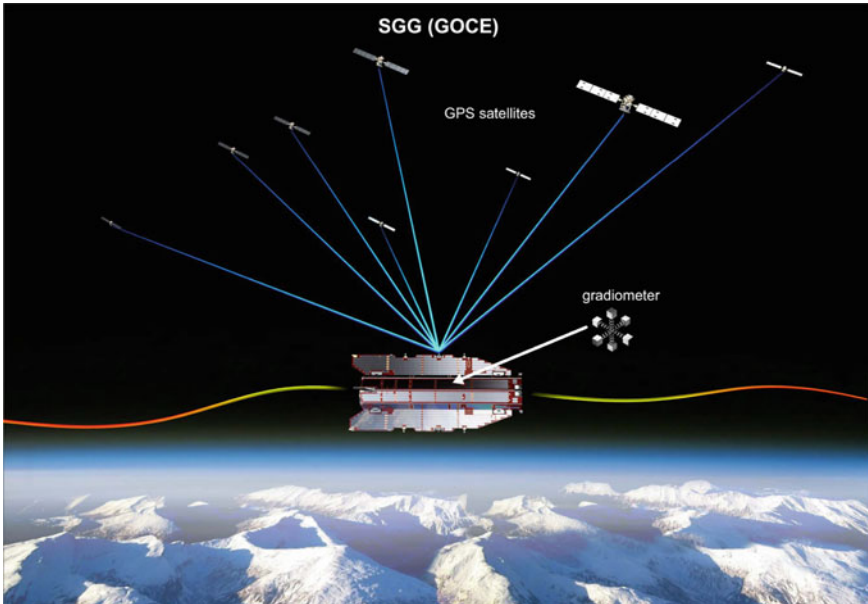


Fig. 20.8 GNSS satellites track the GOCE satellite in space, thus contributing to the determination of its position (© ESA). The GOCE satellite’s accurate determination of the static gravity field is expected to contribute towards studies of changes in sea level, earthquakes, and volcanoes. Figure modified by D. Rieser Rieser (2008)

20.3.2 High and Low Earth Orbiting Satellites

At the broadest conceptual level, LEO satellites’ gravity field missions observe (either directly or indirectly) gradients in the Earth’s external gravitational field. This is essentially done through differential measurements between two or more points, thus largely eliminating spatially correlated errors (cf. differential GPS in Chap. 6). When done from space, two approaches can be used, e.g., Awange et al. (2009), Rummel et al. (2002):

1. Satellite-to-satellite tracking (SST), or
2. A dedicated gravity gradiometer on board a satellite, coupled with SST.

The SST methods can use either low-low inter-satellite tracking (ll-SST, see Fig. 20.9, right), where two LEO satellites track one another and additional observations in terms of high precision ranges and range rates between the two satellites are taken, or high-low inter-satellite tracking (hl-SST, see Fig. 20.9, Left), where high-Earth orbiting satellites (notably GPS) track a LEO satellite. The low-low mode, compared to the high-low mode, has the advantage of signal amplification leading to a higher resolution of the obtained gravity variations, up to the medium wavelength spectrum of a few hundred km in spatial extent (Awange et al. 2009). Taking this further,

a combination of ll-SST and hl-SST is conceptually better still, as is currently demonstrated by the GRACE mission (Fig. 20.9, right) with a baseline length between the two satellites of about 220 km. This is treated in detail in the next section.

In order to detect temporal gravity field variations at smaller spatial scales, the satellite(s) being tracked must be in as-low-as-possible orbits (close to the mass source), with the satellites being as free as possible from the perturbing effects of atmospheric drag (Awange et al. 2009). In addition, so-called de-aliasing models (for correcting short-term—6 h—variations due to atmosphere and ocean mass variations) have to be used to mitigate the propagation of unwanted signals (e.g., leakage from the oceans) into the derived gravity solutions, e.g., Schrama and Visser (2007).

20.3.3 Gravity Recovery and Climate Experiment

The GRACE mission, launched on 17th of March 2002, consists of two near-identical satellites following one another in nearly the same orbital plane (about 400 km altitude) separated by a distance of 220 km; the so-called tandem formation

GNSS tracking a low satellite, e.g., CHAMP.

GNSS tracking 2-low satellites, which are tracking each other, e.g., GRACE.

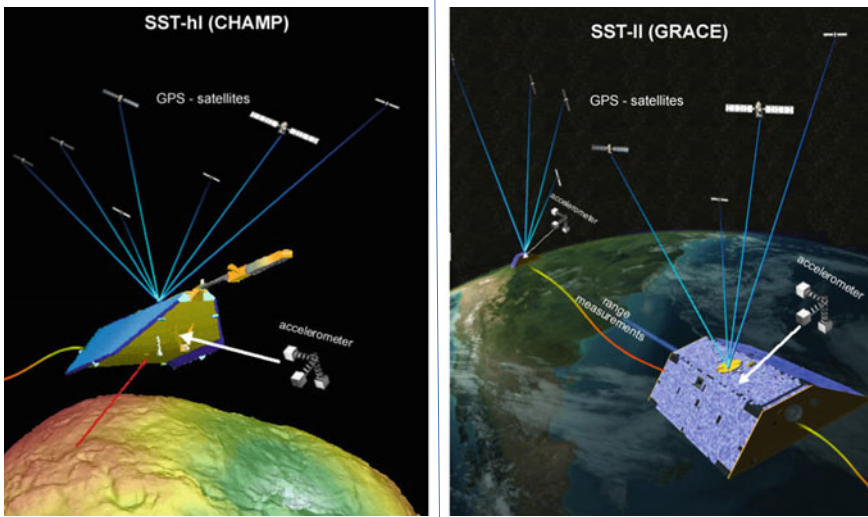


Fig. 20.9 Left SST-hl realized with CHAMP (© GFZ Potsdam ([2.2]). Right A combination of ll-SST and hl-SST realized with GRACE and GNSS satellites (© GRACE—CSR Texas ([2.2]). Figures modified by D. Rieser Rieser (2008)). GNSS satellites are used in determining the positions of these satellites in space. For the GRACE satellites (right) inter-satellite distances can be computed from these positions and compared to the measured K-band distances, thus providing additional independent information

(see Fig. 20.9, right). The ll-SST is measured using K-band ranging, coupled with hl-SST tracking of both satellites by GNSS (GPS; Fig. 20.9, right). GNSS receivers are placed on GRACE satellites to measure occulted signals, and also to determine the orbital parameters of GRACE satellites required in order to determine gravity changes. On-board accelerometers monitor orbital perturbations of non-gravitational origin.

GRACE mission processes GNSS data to contribute to the recovery of long-wavelength gravity field, remove errors due to long-term onboard oscillator drift, and aligns measurements between the two spacecraft (Prasad and Ruggieri 2005, p. 200). The timing function of GNSS for precision orbit determination, in terms of position and velocity as a function of time, enable orbits to be determined within an accuracy better than 2 cm in each coordinate (Prasad and Ruggieri 2005, p. 200). These precise locations of the two satellites in orbit allows for the creation of gravity maps approximately once a month.⁷ These gravity maps, when converted to total water storage maps, are useful for monitoring changes in stored water potential as demonstrated in Chap. 22.

The Earth's gravity field is mapped by making accurate measurements of changes in the distance between the satellites, using GNSS and a microwave ranging system. These changes in the distances between the two satellites occur due to the effect of the gravity (mass concentration) of the Earth. As the lead satellite passes through a region of mass concentration, it is pulled away from the trailing satellite (Fig. 20.9, right). As the trailing satellite passes over the same point, it is pulled towards the lead satellite thus changing the distance between the satellites.

Time-variable gravity field solutions are obtained by the exploitation of GRACE observation data over certain time intervals, i.e., every month Luthcke et al. (2006); Tapley et al. (2004), or less, e.g., Bruinsma et al. (2010) and Lemoine et al. (2007). There are a number of institutions delivering GRACE products, each applying their own processing methodologies and, often, different background models. The mission is currently providing scientists with an efficient and cost-effective way to monitor time-varying component of the gravity field with unprecedented accuracy and in the process yield crucial information about the distribution and flow of mass within the Earth system. The process causing gravity variations that are currently being studied by GRACE include (Ramillien et al. 2004);

- changes due to surface and deep currents in the ocean leading to more information about ocean circulation, e.g., Chambers et al. (2004), Wahr et al. (2002),
- changes in groundwater storage on land masses, relevant to water resource managers, e.g., Ramillien et al. (2004), Rodell and Famiglietti (1999), Tiwari et al. (2009), Werth (2009) and Rodell et al. (2009), see also Chap. 22,
- exchanges between ice sheets or glaciers and the oceans, needed for constraining the mass balance of the global ice regime and sea level change, e.g., Baur et al. (2009), Velicogna (2009), see also Sect. 21.5.4,
- air and water vapour mass change within the atmosphere, vital for atmospheric studies, e.g., Boy and Chao (2005), Swenson and Wahr (2002), and

⁷ <http://www.csr.utexas.edu/grace/publications/brochure/page11.html>

- variations of mass distribution within the Earth arising from, e.g., on-going glacial-isostatic adjustments and earthquakes, e.g., Barletta et al. (2008), Tregoning et al. (2009).

Currently, river basins of the order of $400,000 \text{ km}^2$ in area can be successfully studied using the GRACE products (Swenson et al. 2003). In general, to understand how the GRACE satellites monitor changes in fresh water (all groundwater, soil moisture, snow, ice, and surface waters), first, the larger effect of the mass of the Earth, i.e., the static gravity field discussed in Sect. 20.3.1, which is always a constant G_0 corresponding to nearly 99% of the total field, is computed from a static model [e.g., *GGSM01S* (Tapley et al. 2004)] and removed by subtracting it from the monthly gravity field ($G(t)$) measured by GRACE at a time t (Ramillien et al. 2005), i.e.,

$$\Delta G(t) = G(t) - G_0, \quad (20.29)$$

to give the monthly time-variable gravity field $\Delta G(t)$. Changes mostly related to the atmosphere and ocean, which occur over timescales shorter than one month, are then removed using models, see e.g., Wahr et al. (1998). Remnant atmospheric and oceanographic effects that last for more than one month can be removed using atmospheric and ocean circulation models before water storage change can be analyzed. The resulting difference in Eq. (20.29), which is called the gravity field anomaly is usually due to changes in stored water. If we consider $\overline{\Delta C}_{nm}(t)$ and $\overline{\Delta S}_{nm}(t)$ to be the normalized Stokes coefficients expressed in terms of millimeters of geoid height, with n and m being degree and order respectively, the time-variable geoid in (20.29) is then expanded in-terms of spherical harmonic coefficients (see Heiskanen and Moritz 1967) as

$$\Delta G(t) = \sum_{n=1}^N \sum_{m=0}^n (\overline{\Delta C}_{nm}(t) \cos(m\lambda) + \overline{\Delta S}_{nm}(t) \sin(m\lambda)) \overline{P}_{nm}(\cos(\theta)), \quad (20.30)$$

where N is the maximum degree of expansion, θ is the co-latitude, λ the longitude and \overline{P}_{nm} the fully normalized Legendre polynomial (Heiskanen and Moritz 1967). From the gravitational spherical harmonic coefficients (20.30), the equivalent water thickness is computed using the following steps:

1. The gravitational residual coefficients are converted into the surface density coefficient differences by (Wahr et al. 1998)

$$\begin{pmatrix} \Delta \check{C}_{lm}(M_j) \\ \Delta \check{S}_{lm}(M_j) \end{pmatrix} = \frac{\rho_{\text{avg}}}{3\rho_w} \frac{2l+1}{1+k'_l} \begin{pmatrix} \Delta \overline{C}_{lm}(M_j) \\ \Delta \overline{S}_{lm}(M_j) \end{pmatrix}, \quad (20.31)$$

where k'_l is the load Love number of degree l , $\rho_{\text{avg}} = 5517 \text{ kg/m}^3$ the average density of the Earth, and $\rho_w = 1000 \text{ kg/m}^3$ the density of water.

2. The spatial variation of the surface density is then computed through

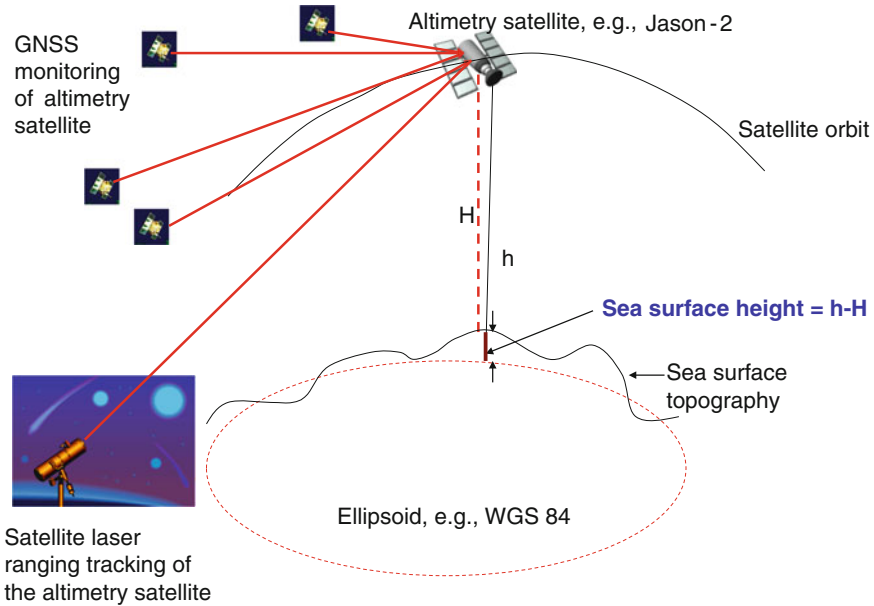


Fig. 20.10 GNSS in support of monitoring changes in sea level through the determination of the altimetry satellites’ precise orbit. From the precise orbital parameters, the height component h is useful in determining changes in sea level through the difference $\{h - H\}$, where H is measured by multiplying the speed of light with the time taken by the signals to travel from and to the satellite divided by 2, since the same distance is covered twice. *Source* Awange (2012)

$$\Delta\sigma(\theta, \lambda, M_j) = R\rho_w \sum_{l=1}^{l_{\max}} \sum_{m=0}^l [\Delta\check{C}_{lm}(M_j) \cos m\lambda + \Delta\check{S}_{lm}(M_j) \sin m\lambda] \bar{P}_{lm}(\cos \theta), \tag{20.32}$$

where $R = 6378137$ m is the radius of the Earth and $\Delta\sigma$ is in kg/m^2 .

3. Finally, the changes in total water storage (TWS) are calculated by

$$\text{TWS}(\phi, \lambda, M_j) = \frac{\Delta\sigma(\theta, \lambda, M_j)}{\rho_w} = \frac{\Delta\sigma(\theta, \lambda, M_j)}{1000} \text{ [meters]}. \tag{20.33}$$

The first steps in the analysis of GRACE data would provide an estimate of the changes in total water storage. In the second step, the changes can then be separated into their various components as discussed, e.g., in Ramillien et al. (2004, 2005) to obtain changes in the respective components (e.g., groundwater, surface water, soil moisture, and ice).

The GRACE satellites have now well exceeded their planned 5 year life-span, however, plans are underway to launch a GRACE follow-on mission around 2015 given the excellent results that have been delivered so far, see e.g., Arras et al. (2010).

The follow up mission may use lasers to measure inter-satellite distances, instead of the traditional microwave, and thus improve the measuring accuracy.

20.4 Satellite Altimetry

20.4.1 Environmental Sensing Using Satellite Altimetry

Satellites altimetry (Fig. 20.10) operates in two steps:

- *First*, the precise orbit of the satellite, i.e., its position, is determined. Through this, its *height* above the Earth is obtained.
- *Second*, range measurements are made by obtaining the time an emitted signal (radar or laser) travels to the Earth's surface and reflected back to the satellite.

GNSS contributes to the *first step* where height is determined. This is achieved through GNSS' receiver onboard the space satellites that enables monitoring of ranges and timing signals from GNSS satellites (see Chaps. 4–6). The observed GNSS ranges provide precise and continuous tracking of the spacecraft, thereby delivering its position $\{\phi, \lambda, h\}$ at any time. The height component h is useful in determining the measured height (see Fig. 20.10). Besides GNSS tracking, other approaches such as satellite laser ranging (SLR; see Sect. 3.4) and DORIS (Doppler Orbitography and Radio positioning Integrated by Satellite) are also used to ensure that precise orbit determination is achieved.

In the *second step*, the Earth's surface heights (e.g., ocean surface, glaciers, and ice sheets) are measured using ranges from the space altimetry satellite to the surface of interest. Radar altimeters send microwave signals to the Earth's surface and measures the time taken by the reflected signals to travel back. Using Eq. (5.1), the distance from the satellite to the Earth's surface is derived. Since the signals pass through the atmosphere from and to the satellites, they are affected by the atmosphere (see Sect. 5.4.3) and as such, atmospheric corrections again have to be made. The sea surface height is then obtained by subtracting the measured ranges in step 2 from the GNSS-derived satellite heights in step 1 (Fig. 20.10).

20.4.2 Satellite Altimetry Missions

The first true satellite altimetry mission was TOPEX/Poseidon, developed by NASA and the Centre National d'Etudes Spatiales (CNES) and launched on 10 August 1992. Its mission ended in 2006 after 13 years of operation, providing 11 years of data. It was followed by Jason-series (Jason-1 was launched on 07/12/2001 and Jason-2 on 20/20/2008). Both TOPEX/Poseidon and Jason-1 were dedicated to measuring global mean sea level from space. TOPEX/Poseidon orbited at 1336 km above the

Earth and covered the global oceans every 10 days, measuring the heights of the ocean surface directly underneath the satellite with an accuracy of 2–4 cm or better when averaging over several measurements (Pugh 2004). Jason-2 is expected to be replaced by Jason-3 (proposed for launch in 2013–2014), and subsequently Jason-CS (Continuity of Service). Combined, all these satellites will provide long-term series of data capable of undertaking *climatological studies* resulting from changes in sea level.

ICESat (launched on January 12, 2003) uses a 1064 nm-laser operating at 40 Hz to make measurements at 172 m intervals over ice, ocean, and land (Abdalati et al. 2010). It combines state-of-the-art laser ranging capabilities with precise orbit and attitude control and knowledge, provides very accurate measurements of ice sheet topography and elevation changes along track. It has the specific objective of measuring changes in polar ice as part of NASA's Earth Observing System.

By observing changes in ice sheet elevation, it is possible to quantify the growth and shrinkage of parts of the ice sheets with great spatial detail, thus enabling an assessment of ice sheet mass balance and contributions to sea level. Moreover, because the mechanisms that control ice sheet mass loss and gain in accumulation, surface ablation, and discharge presumably have distinct topographic expressions, ice sheet elevation changes also provide important insights into the processes causing the observed changes (Abdalati et al. 2010). The ICESat-2 is expected to be a follow-on mission to ICESat (Fig. 20.11) with improved laser capability compared to ICESat and will have the objectives of measuring ice sheet changes, sea ice thickness, and vegetation biomass. Achieving these objectives will contribute to the following (Abdalati et al. 2010):

- Contribute to the development of predictive models that capture both dynamic and surface processes.
- Since the thickness distribution of sea ice controls energy and mass exchanges between the ocean and atmosphere at the surface, and the fresh water fluxes associated with melting ice serve as stabilizing elements in the circulation of the North Atlantic waters, basin-scale fields of ice thickness are therefore essential to improve our estimates of the seasonal and inter-annual variability in regional mass balance, the freshwater budget of the polar oceans, and the representation of these processes in regional and climate models.
- Its capability of producing a vegetation height surface with 3 m accuracy at 1 km spatial resolution, assuming that off-nadir pointing can be used to increase the spatial distribution of observations over terrestrial surfaces. This sampling, combined with a smaller footprint of 50 m or less, would allow characterization of vegetation at a higher spatial resolution than ICESat, and is expected to provide a new set of global ecosystem applications.
- In addition, the atmospheric measurement capability of ICESat-2, even at near-IR wavelengths, will enable global measurements of cloud and aerosol structure to extend the record of these observations beyond those provided by the current lasers onboard ICESat.

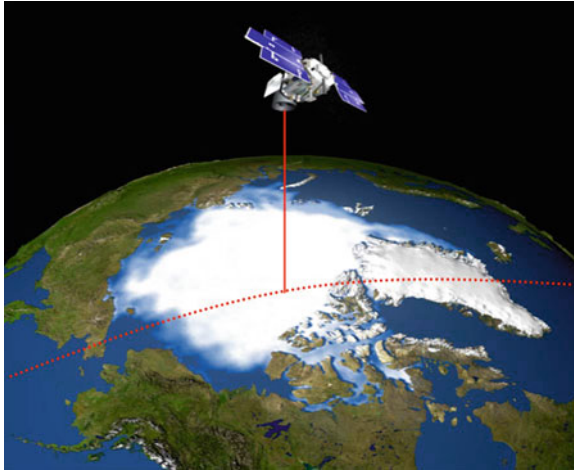


Fig. 20.11 Schematic diagram of ICESat on a transect over the Arctic. ICESat uses a 1064 nm-laser operating at 40 Hz to make measurements at 172 m intervals over ice, oceans, and land. *Source* Abdalati et al. (2010)

As will be discussed further in Sect. 26.5.5, satellite altimetry provide sea surface heights (SSH) that are useful in monitoring climate variability associated to El Niño-Southern Oscillation (ENSO). SSH also find use in providing (i) wave heights that are being used to study tropical cyclones⁸ (ii) ocean heat that feed the tropical cyclone,⁹ and (iii) wind speed that aids in monitoring of hurricane storm surge.¹⁰

20.5 Sensing Using GNSS Reflected Signals

In Sect. 5.4.4, multipath signal was presented as a reflected GNSS signal that is a nuisance when positioning with GNSS and as such needs to be eliminated. Whereas this reflected signal on the one hand is a nuisance for positioning, for environmental monitoring purposes, it could be useful in monitoring sea-wind retrieval, seawater salinity detection, ice-layer density measurements and other remote sensing applications, see, e.g., Yang et al. (2009).

In this approach, also known as the GNSS-reflection (GNSS-R) remote sensing, the microwave signals reflected from various surfaces are received and processed

⁸ See e.g., JPL publications in <http://sealevel.jpl.nasa.gov/newsroom/featurearchive/index.cfm?y=2010>.

⁹ See <http://sealevel.jpl.nasa.gov/newsroom/featurearchive/index.cfm?FuseAction=ShowNews&NewsID=353>.

¹⁰ See e.g., <http://sealevel.jpl.nasa.gov/newsroom/spotlights/index.cfm?FuseAction=ShowNews&NewsID=294>.

to extract useful environmental information about those surfaces. As can be seen in Fig. 5.6 on p. 69, GNSS satellites transmit signals to the receiver, but some signals are reflected by nearby surfaces. These reflected signals are also received by the receivers, either situated on land or placed on LEO satellites such as GRACE, as discussed in Sect. 20.2.3.2. These reflected microwave signals are the ones processed in GNSS-R remote sensing.

The possibility of using GNSS reflected signals for remote sensing sea surface heights was proposed by Martín-Neira (1993), who used fixed-platform experiments to demonstrate that GNSS-reflection altimetry performed to an accuracy of ~ 20 m over the ocean, 450 m above Crater Lake, and 10 m over a pond, see e.g., Lowe et al. (2002b, and the references therein). According to Lowe et al. (2002b), such GNSS altimetry would involve an orbiting receiver that obtains position and timing information from the GNSS constellation as usual, but measures ocean height using the arrival time of GNSS signals reflected from the surface. The advantage over mono-static radar altimeters is that the receiver could produce about 10 simultaneous measurements (~ 20 when Galileo becomes fully operational), distributed over an area thousands of km across-track (Lowe et al. 2002b). Studies of GNSS-reflections from space include, e.g., Lowe et al. (2002a,b).

Such GNSS remote sensing using reflected signals find use, e.g., in monitoring the depths of Antarctica's thick dry snow thus complementing the L-band radiometric observations (Cardellach et al. 2012), and the provision of altimetric precision and spatial resolution necessary to map mesoscale eddies, which has been the most prominent limitation of conventional radar altimeters (Lowe et al. 2002b). Other applications of GNSS-R remote sensing include water reservoir level and ocean monitoring (Egido et al. 2009; Gleason et al. 2005). In addition, over the last few years, there has been increasing interest in this technique for applications such as soil moisture monitoring, where the observations relating to the flux of water to- and from- the land surface can be gleaned from GNSS multipath measurements of, e.g., snow depth and soil moisture (Larson et al. 2009, 2008). These measurements derive changes in the properties of a site's environment from changes in the amplitude and frequency of the multipath interference (relating, respectively, to attenuation properties and position of reflective surfaces) (Hammond et al. 2010). These developments have led to the establishment of new research themes targeting the measurement of land bio-geophysical parameters (Egido et al. 2009).

The advantages of GNSS-R remote sensing over traditional satellite scatterometry and radar altimetry are given, e.g., by Yang et al. (2009) as follows:

- no additional transmitter,
- plenty of signal sources, which in the future will include GPS, Galileo, GLONASS, and Beidou/Compass,
- use of spread-spectrum communication technology to enable the receiver to receive weak signals, and
- wide range of uses for such things as sea-wind retrieval, seawater salinity detection, ice-layer density measurement, humidity measurement of land, and the detection of moving objects.

20.6 Concluding Remarks

GNSS remote sensing and its application to environmental monitoring is a new and active area of research. The data that has been collected so far has provided several environmental (atmospheric) properties that were hitherto difficult to fathom. The new technique clearly promises to contribute significantly to environmental studies. When the life span of the various missions (e.g., GRACE) is reached, thousands of data sets will have been collected that will help to unravel some of the complex nature of atmospheric and environmental phenomena. From the analysis of water vapour trapped in the atmosphere and tropopause temperature, climate change studies will be significantly enhanced. This will be discussed further in Chap. 21.

References

- Abdalati W, Zwally HJ, Bindschadler B, Csatho B, Farrell SL, Fricker HA, Harding D, Kwok R, Lefsky M, Markus T, Marshak A, Neumann T, Palm S, Schutz B, Smith B, Spinhirne J, Webb C (2010) The ICESat-2 laser altimetry mission. *Proc IEEE* 98(5):735–751. doi:[10.1109/JPROC.2009.2034765](https://doi.org/10.1109/JPROC.2009.2034765)
- Anthes RA, Bernhardt PA, Chen Y, Cucurull L, Dymond KF, Ector D, Healy SB, Ho SP, Hunt DC, Kuo YH, Liu H, Manning K, McCormick C, Meehan TK, Randel WJ, Rocken C, Schreiner WS, Sokolovskiy SV, Syndergaard S, Thompson DC, Trenberth KE, Wee TK, Yen NL, Zeng Z (2008) The COSMIC/FORMOSAT-3 mission: early results. *Bull Am Meteorol Soc* 89(3):313–333
- Anthes RA (2004) Application of GPS remote sensing to meteorology and related fields. *J Meteorol Soc Jpn* 82(18):259–596
- Arras C, Jacobi C, Wickert J, Heise S, Schmidt T (2010) Sporadic E signatures revealed from multi-satellite radio occultation measurements. *Adv Radio Sci* 8:225–230. doi:[10.5194/ars-8-225-2010](https://doi.org/10.5194/ars-8-225-2010)
- Askne J, Nordius H (1987) Estimation of tropospheric delay for microwaves from surface weather data. *Radio Sci* 22:379–386
- Awange JL, Sharifi MA, Baur O, Keller W, Featherstone WE, Kuhn M (2009) GRACE hydrological monitoring of Australia. Current limitations and future prospects. *J Spatial Sci* 54(1):23–36. doi:[10.1080/14498596.2009.9635164](https://doi.org/10.1080/14498596.2009.9635164)
- Awange JL (2012) Environmental monitoring using GNSS, global navigation satellite system. Springer, Berlin
- Barletta V, Sabadini R, Bordon A (2008) Isolating the PGR signal in the GRACE data: impact on mass balance estimates in Antarctica and Greenland. *Geophys J Int* 172(1):18–30. doi:[10.1111/j.1365-246X.2007.03630.x](https://doi.org/10.1111/j.1365-246X.2007.03630.x)
- Baur O, Kuhn M, Featherstone W (2009) GRACE-derived ice-mass variations over Greenland by accounting for leakage effects. *J Geophys Res* 114(B06407). doi:[10.1029/2008JB006239](https://doi.org/10.1029/2008JB006239)
- Belvis M, Businger S, Herring TA, Rocken C, Anthes RA, Ware RH (1992) GPS meteorology: remote sensing of water vapour using global positioning system. *J Geophys Res* 97:15787–15801
- Belvis M, Businger S, Chiswell S, Herring TA, Anthes RA, Rocken C, Ware RH (1994) GPS meteorology: mapping zenith wet delays onto precipitable water. *J Appl Meteorol* 33:379–386
- Beyerle G, Schmidt T, Michalak G, Heise S, Wickert J, Reigber C (2005) GPS radio occultation with GRACE: atmospheric profiling utilizing the zero difference technique. *Geophys Res Lett* 32(L13806). doi:[10.1029/2005GL023109](https://doi.org/10.1029/2005GL023109)
- Boy J-P, Chao B (2005) Precise evaluation of atmospheric loading effects on Earth's time-variable gravity field. *J Geophys Res Solid Earth* 110(B8): 4–12. doi:[10.1029/2002JB002333](https://doi.org/10.1029/2002JB002333)

- Bruinsma S, Lemoine J, Biancale R, Valès N (2010) CNES/GRGS 10-day gravity field models (release 2) and their evaluation. *Adv Space Res* 45(4):587–601. doi:[10.1016/j.asr.2009.10.012](https://doi.org/10.1016/j.asr.2009.10.012)
- Cardellach E, Fabra F, Rius A, Pettinato S, D'Addio S (2012) Characterization of dry-snow sub-structure using GNSS reflected signals. *Remote Sens Environ* 124:122–134. doi:[10.1016/j.rse.2012.05.012](https://doi.org/10.1016/j.rse.2012.05.012)
- Chambers D, Wahr J, Nerem R (2004) Preliminary observations of global ocean mass variations with GRACE. *Geophys Res Lett* 31(L13310). doi:[10.1029/2004GL020461](https://doi.org/10.1029/2004GL020461)
- Cheng CZ, Kuo Y-H, Anthes RA, Wu L (2006) Satellite constellation monitors global and space weather. *EOS Trans Am Geophys Union* 87(17):166. doi:[10.1029/2006EO170003](https://doi.org/10.1029/2006EO170003)
- Chen G, Herring TA (1997) Effects of atmospheric azimuthal asymmetry on the analysis of space geodetic data. *J Geophys Res* 102(B9):20489–20502
- Davis JL, Herring TA, Shapiro II, Rogers AE, Elgered G (1985) Geodesy by radio interferometry: effects of atmospheric modeling errors on estimates of baseline length. *Radio Sci* 20:1593–1607
- Egido A, Delas M, Garcia M, Caparrini M (2009) Non-space applications of GNSS-R: from research to operational services. Examples of water and land monitoring systems. In: *IEEE international geoscience and remote sensing symposium IGARSS*, Cape Town, pp 170–173
- Ellett KM, Walker JP, Western AW, Rodell M (2006) A framework for assessing the potential of remote sensed gravity to provide new insight on the hydrology of the Murray-darling basin. *Aus J Water Resour* 10(2):89–101
- Foelsche U, Borsche M, Steiner AK, Gobiet M, Pirscher B, Kirchengast G, Wickert J, Schmidt T (2007) Observing upper troposphere-lower stratosphere climate with radio occultation from the CHAMP satellite. *Clim Dyn* 31:49–65
- Foelsche U, Kirchengast G, Steiner AK (2006) *Atmos climate. Studies by occultation methods*. Springer, Berlin
- Gleason S, Hodgart S, Sun Y, Gommenginger C, Mackin S, Adjrard M, Unwin M (2005) Detection and processing of bistatically reflected GPS signals from low earth orbit for the purpose of ocean remote sensing. *IEEE Trans Geosci Remote Sens* 43(6):1229–1241. doi:[10.1109/TGRS.2005.845643](https://doi.org/10.1109/TGRS.2005.845643)
- Hammond WC, Brooks BA, Bürgmann R, Heaton T, Jackson M, Lowry AR, Anandakrishnan S (2010) The scientific value of high-rate, low-latency GPS data, a white paper
- Hammond WC, Brooks BA, Bürgmann R, Heaton T, Jackson M, Lowry AR, Anandakrishnan S (2011) Scientific value of real-time global positioning system data. *Eos* 92(15):125–126. doi:[10.1029/2011EO150001](https://doi.org/10.1029/2011EO150001)
- Hanssen RF, Weckwerth TM, Zebker HA, Klees R (1999) High-resolution water vapour mapping from interferometric radar measurements. *Science* 283:1297–1299
- Healey S, Jupp A, Offiler D, Eyre J (2003) The assimilation of radio occultation measurements. In: Reigber C, Lühr H, Schwintzer P (eds) *First CHAMP mission results for gravity, magnetic and atmospheric studies*. Springer, Heidelberg
- Heise S, Wickert J, Beyerle G, Schmidt T, Reigber C (2006) Global monitoring of tropospheric water vapour with GPS radio occultation aboard CHAMP. *Adv Space Res* 37(12):2222–2227
- Heiskanen WA, Moritz H (1967) *Physical geodesy*. Freeman and Company, San Francisco
- Hirt C, Gruber T, Featherstone WE (2011) Evaluation of the first GOCE static gravity field models using terrestrial gravity, vertical deflections and EGM2008 quasigeoid heights. *J Geodesy* 85:723–740. doi:[10.1007/s00190-011-0482-y](https://doi.org/10.1007/s00190-011-0482-y)
- Khandu, Awange JL, Wickert J, Schmidt T, Sharifi MA, Heck B, Fleming K (2010) GNSS remote sensing of the Australian tropopause. *Climatic Change* 105(3–4): 597–618, doi:[10.1007/s10584-010-9894-6](https://doi.org/10.1007/s10584-010-9894-6)
- Kuo Y-H, Schreiner WS, Wang J, Rossiter DL, Zhang Y (2005) Comparison of GPS radio occultation soundings with radiosonde. *Geophys Res Lett* 32. doi:[10.1029/2004GL021443](https://doi.org/10.1029/2004GL021443)
- Kuo Y-H, Sokolovski SV, Anthes RA, Vandenberghe F (2000) Assimilation of the GPS radio occultation data for numerical weather prediction. *Terr Atmos Oceanic Sci* 11:157–186
- Larson KM, Gutmann ED, Zavorotny VU, Braun JJ, Williams MW, Nievinski FG (2009) Can we measure snow depth with GPS receivers? *Geophys Res Lett* 36(17). doi:[10.1029/2009GL039430](https://doi.org/10.1029/2009GL039430)

- Larson KM, Small EE, Gutmann ED, Bilich AL, Braun JJ, Zavorotny VU (2008) Use of GPS receivers as a soil moisture network for water cycle studies. *Geophys Res Lett* 35(L24405). doi:[10.1029/2008GL036013](https://doi.org/10.1029/2008GL036013)
- Leick A (2004) *GPS satellite surveying*, 3rd edn. Wiley, New York
- Lemoine F, Luthcke S, Rowlands D, Chinn D, Klosko S, Cox C (2007) The use of mascons to resolve time-variable gravity from GRACE. In: Tregoning P, Rizos C (eds) *Dynamic planet*. Springer, Berlin, pp 231–236
- Lowe ST, LaBrecque JL, Zuffada C, Romans LJ, Young L, Hajj GA (2002) First spaceborne observation of an earth-reflected GPS signal. *Radio Sci* 37(1):1007. doi:[10.1029/2000RS002539](https://doi.org/10.1029/2000RS002539)
- Lowe ST, Zuffada C, Chao Y, Kroger P, Young LE, LaBrecque JL (2002) 5-cm-Precision aircraft ocean altimetry using GPS reflections. *Geophys Res Lett* 29(10):1375. doi:[10.1029/2002GL014759](https://doi.org/10.1029/2002GL014759)
- Luthcke S, Rowlands D, Lemoine F, Klosko S, Chinn D, McCarthy J (2006) Monthly spherical harmonic gravity field solutions determined from GRACE inter-satellite range-rate data alone. *Geophys Res Lett* 33(L02402). doi:[10.1029/2005GL024846](https://doi.org/10.1029/2005GL024846)
- Martin-Neira M (1993) A passive reflectometry and interferometry system (PARIS): application to ocean altimetry. *J ESA* 17(4):331–335
- Melbourne WG, Davis ES, Duncan CB, Hajj GA, Hardy K, Kursinski R, Mehan TK, Young LE, Yunck TP (1994) *The application of spaceborne GPS to atmospheric limb sounding and global change monitoring*. JPL Publication, Pasadena, pp 94–18
- Niell AE (1996) Global mapping functions for the atmosphere delay at radio wavelengths. *J Geophys Res* 101(B2): 3227–3246
- Pool DR, Eychaner JH (1995) Measurements of aquifer-storage change and specific yield using gravity surveys. *Ground Water* 33(3):425–432
- Prasad R, Ruggieri M (2005) *Applied satellite navigation using GPS GALILEO and augmentation systems*. Artech House, Boston
- Pugh D (2004) *Changing sea levels. effect of tides, weather and climate*. Cambridge University Press, New York
- Ramillien G, Cazenave A, Brunau O (2004) Global time variations of hydrological signals from GRACE satellite gravimetry. *Geophys J Int* 158(3):813–826. doi:[10.1111/j.1365-246X.2004.02328.x](https://doi.org/10.1111/j.1365-246X.2004.02328.x)
- Ramillien G, Frappart F, Cazenave A, Gtner A (2005) Time variations of land water storage from an inversion of two years of GRACE geoids [rapid communication]. *Earth Planet Sci Lett* 235(1–2):283–301. doi:[10.1016/j.epsl.2005.04.005](https://doi.org/10.1016/j.epsl.2005.04.005)
- Ray M, Tido S, Conor S, Wang S (2006) Impact of balloon drift errors in radiosonde data on 57 climate statistics. *J Clim* 19(14):3430–3442
- Resch GM (1984) *Water vapour radiometry in geodetic applications in geodetic refraction*. Springer, New York
- Rieser D (2008) *Comparison of GRACE-derived monthly surface mass Variations with rainfall data in Australia*. MSc thesis, Graz University of Technology
- Rocken C, Ware R, Hove TV, Solheim F, Alber C, Johnson J, Belvis M, Businger S (1993) Sensing atmospheric water vapour with the global positioning system. *Geophys Res Lett* 20(23):2631–2634
- Rodell M, Famiglietti JS (1999) Detectability of variations in continental water storage from satellite observations of the time dependent gravity field. *Water Resour Res* 35(9):2705–2724. doi:[10.1029/1999WR900141](https://doi.org/10.1029/1999WR900141)
- Rodell M, Felicogna I, Famiglietti JS, (2009) Satellite-based estimates of groundwater depletion in India. *Nature* 460: 999–1003, doi:[10.1038/nature08238](https://doi.org/10.1038/nature08238)
- Rummel R, Balmino G, Johannessen J, Visser P, Woodworth P (2002) Dedicated gravity field missions—principles and aims. *J Geodyn* 33(1):3–20. doi:[10.1016/S0264-3707\(01\)00050-3](https://doi.org/10.1016/S0264-3707(01)00050-3)
- Schmidt T, Wickert J, Beyerle G, Reigber C (2004) Tropical tropopause parameters derived from GPS radio occultation measurements with CHAMP. *J Geophys Res* 109:D13105. doi:[10.1029/2004JD004566](https://doi.org/10.1029/2004JD004566)

- Schmidt T, Heise S, Wickert J, Beyerle G, Reigber C (2005) GPS radio occultation with CHAMP and SAC-C: global monitoring of thermal tropopause parameters. *Atmos Chem Phys* 5:1473–1488
- Schmidt T, Wickert J, Beyerle G, Heise S (2008) Global tropopause height trends estimated from GPS radio occultation data. *Geophys Res Lett* 35:L11806. doi:[10.1029/2008GL034012](https://doi.org/10.1029/2008GL034012)
- Schrama EJO, Visser P NAM (2007) Accuracy assessment of the monthly GRACE geoids based upon a simulation. *J Geodesy* 81(1):67–80. doi:[10.1007/s00190-006-0085-1](https://doi.org/10.1007/s00190-006-0085-1)
- Seidel DJ, Randel WJ (2006) Variability and trends in the global tropopause estimated from radiosonde data. *J Geophys Res* 111. doi:[10.1029/2006JD007363](https://doi.org/10.1029/2006JD007363)
- Steiner AK, Kirchengast G, Foelsche U, Kornbluh L, Manzini E, Bengtsson L (2001) GNSS occultation sounding for climate monitoring. *Phys Chem Earth* 26:113–124
- Swenson S, Wahr J (2002) Estimated effects of the vertical structure of atmospheric mass on the time-variable geoid. *J Geophys Res* 107(B9):219. doi:[10.1029/2000JB000024](https://doi.org/10.1029/2000JB000024)
- Swenson S, Wahr J, Milly PCD (2003) Estimated accuracies of regional water storage variations inferred from the gravity recovery and climate experiment (GRACE). *Water Resour Res* 39(8):1223. doi:[10.1029/2002WR001736](https://doi.org/10.1029/2002WR001736)
- Tapley BD, Bettadpur S, Ries JC, Thompson PF, Watkins MM (2004) GRACE measurements of mass variability in the earth system. *Science* 305:503–505. doi:[10.1126/science.1099192](https://doi.org/10.1126/science.1099192)
- Thayer D (1974) An improved equation for the radio refractive index of air. *Radio Sci* 9:803–807
- Tiwari V, Wahr J, Swenson S (2009) Dwindling groundwater resources in northern India, from satellite gravity observations. *Geophys Res Lett* 36:L18401. doi:[10.1029/2009GL039401](https://doi.org/10.1029/2009GL039401)
- Tralli DM, Lichten SM (1990) Stochastic estimation of tropospheric path delays in global positioning system geodetic measurements. *Bull Geod* 64:127–159
- Tregoning P, Ramillien G, McQueen H, Zwartz D (2009) Glacial isostatic adjustment and nonstationary signals observed by GRACE. *J Geophys Res* 114:B06406. doi:[10.1029/2008JB006161](https://doi.org/10.1029/2008JB006161)
- Tregoning P, Watson C, Ramillien G, McQueen H, Zhang J (2009) Detecting hydrologic deformation using GRACE and GPS. *Geophys Res Lett* 36(L15401). doi:[10.1029/2009GL038718](https://doi.org/10.1029/2009GL038718)
- Tsuda T, Heki K, Miyazaki S, Aonashi K, Hirahara K, Tobita M, Kimata F, Tabei T, Matsushima T, Kimura F, Satomura M, Kato T, Naito I (1998) GPS meteorology project of Japan-exploring frontiers of geodesy. *Earth Planet Space* 50(10):1–5
- Tsuda T, Hocke K (2004) Application of GPS occultation for studies of atmospheric waves in the middle atmosphere and ionosphere. In: Anthens et al. (eds). *Application of GPS remote sensing to meteorology and related fields*. *J Meteorol Soc Jpn* 82(1B):419–426
- Velicogna I (2009) Increasing rates of ice mass loss from the Greenland and Antarctic ice sheets revealed by GRACE. *Geophys Res Lett* 36(L19503). doi:[10.1029/2009GL040222](https://doi.org/10.1029/2009GL040222)
- Wahr J, Jayne S, Bryan F (2002) A method of inferring changes in deep ocean currents from satellite measurements of time-variable gravity. *J Geophys Res* 107(C12):3218. doi:[10.1029/2002JC001274](https://doi.org/10.1029/2002JC001274)
- Wahr J, Molenaar M, Bryan F (1998) Time variability of the earth's gravity field: hydrological and oceanic effects and their possible detection using GRACE. *J Geophys Res Solid Earth* 103(B12):30205–30230. doi:[10.1029/98JB02844](https://doi.org/10.1029/98JB02844)
- Ware H, Fulker D, Stein S, Anderson D, Avery S, Clerk R, Droegmeier K, Kuettner J, Minster B, Sorooshian S (2000a) SuomiNet: a real time national GPS network for atmospheric research and education. *Bull Am Meteorol Soc* 81:677–694
- Werth S, Güntner A, Petrovic S, Schmidt R (2009) Integration of GRACE mass variations into a global hydrological model. *Earth Planetary Sci Lett* 27(1–2):166–173. doi:[10.1016/j.epsl.2008.10.021](https://doi.org/10.1016/j.epsl.2008.10.021)
- Wickert J (2002) *Das CHAMP-Radiookkultationsexperiment: Algorithmen, Prozessierungssystem und erste Ergebnisse*. Dissertation, Scientific Technical Report STR02/07, GFZ Potsdam
- Wickert J (2004) Comparison of vertical refractivity and temperature profiles from CHAMP with radiosonde measurements. Danish Meteorological Institute, Copenhagen
- Wickert J, Beyerle G, Hajj GA, Schwieger V, Reigber C (2002) GPS radio occultation with CHAMP: atmospheric profiling utilizing the space-based single differencing technique. *Geophys Res Lett* 29(8). doi:[10.1029/2001GL013982](https://doi.org/10.1029/2001GL013982)

- Wickert J, Beyerle G, König K, Heise S, Grunwaldt L, Michalak G, Reigber C, Schmidt T (2005) GPS radio occultation with CHAMP and GRACE: a first look at a new and promising satellite configuration for global atmospheric sounding. *Ann Geophys* 23:653–657
- Wickert J, Michalak G, Schmidt T, Beyerle G, Cheng CZ, Healy SB, Heise S, Huang CY, Jakowski N, Köhler W, Mayer C, Offiler D, Ozawa E, Pavelyev AG, Rothacher M, Tapley B, Arras C (2009) GPS radio occultation: Results from CHAMP, GRACE and FORMOSAT-3/COS MIC. *Terr Atmos Ocean Sci.*, 20:35–50, doi:[10.3319/TAO.2007.12.26.01\(F3C\)](https://doi.org/10.3319/TAO.2007.12.26.01(F3C))
- Yang D, Zhou Y, Wang Y (2009) Remote sensing with reflected signals. GNSS-R data processing software and test analysis. *Inside GNSS*, Sept/Oct, pp 40–45
- Yunck TP (2003): The promise of spaceborne GPS for earth remote sensing. In: International workshop on GPS meteorology, 14–17 January 2003, Tsukuba, Japan
- Yunck TP, Wu SC, Wu JT, Thornton CL (1990) Precise tracking of remote sensing satellites with the global positioning system. *IEEE Trans Geosci Remote Sens* 28:108–116

Chapter 21

Weather, Climate and Global Warming

“All across the world, in every kind of environment and region known to man, increasingly dangerous weather patterns and devastating storms are abruptly putting an end to the long-running debate over whether or not climate change is real. Not only is it real, it’s here, and its effects are giving rise to a frighteningly new global phenomenon: the man-made natural disaster.”

Barrack Obama, April 3, 2006

21.1 Introductory Remarks

In order to fully appreciate the contribution of geoinformatics in monitoring climate change caused by increase in temperature, a distinction between *weather* and *climate*, on one hand, and *climate variability* and *climate change*, on the other hand, is essential. Burroughs (2007) points out that weather is what is happening to the atmosphere at any given time (i.e., what one gets), whereas climate is what would be expected to occur at any given time of the year based on statistics built up over many years (i.e., what one expects).

From these definitions, it follows that *changes in the climate* constitute shifts in meteorological conditions lasting a few years or longer, and may involve a single parameter, e.g., temperature or rainfall, but usually accompany more shift in weather patterns that might result in a shift to, say, colder, wetter, cloudier and windier conditions (Burroughs 2007). If meteorological observations, e.g., of temperature are taken over time, a series of its annual averages could be developed. This series would indicate that over the period of measurements the average value remains effectively constant but fluctuates considerably from observation to observation. This fluctuation about the mean is a measure of *climate variability* (Burroughs 2007). Now, if a linear or cyclic trend is fitted onto the variability, the effect of climate change could be analyzed.

Human activities of all kinds contribute to increased emission of quantities of gases to the atmosphere. Of particular importance is *carbon dioxide* (CO₂), a greenhouse gas that is said to contribute about seven thousand million tones to the carbon already present in the atmosphere (Houghton 2005). Greenhouse gases, such as carbon dioxide and *water vapour*, play a key role in naturally warming the surface of the planet by acting as a blanket that shields the Earth by trapping, in the atmosphere, direct heat radiated by the sun. Whereas this maintains the Earth's temperature balance, the downside is that the energy radiated back into space from the Earth is also trapped by the same greenhouse gases, thereby further warming the Earth. In fact, increase in carbon dioxide contributes to increased temperature, which in turn leads to increased water vapour in the atmosphere thereby providing more blanketing and causing the Earth to be even warmer.

Increase in greenhouse gas concentration in the Earth's atmosphere, particularly carbon dioxide, caused by burning fossil fuels such as oil and coal, and by clearing forests, are believed to be the primary cause of the rise in the Earth's temperature. With rapid industrialization in the world and in the absence of efforts to curb the rise in emission of carbon dioxide, the global average temperature is expected to rise by about 3° in a century (i.e., 0.03° annually) (Houghton 2005). Such a change would potentially lead to the melting of ice masses (IPCC 2007), which may also lead to increased rates of flow in the ice streams (Krabill et al. 2004), dislocation of plants and animals from their habitats, and the spread of diseases such as malaria (Martens et al. 1995; Martens 1998; Uriel 1998). There is therefore a wider agreement that continuous *increases* in greenhouse gas concentrations in the lower atmosphere is well known to intensify the warming effect, which in turn has a serious impact on the *global climate change*.

While there is little doubt that the Earth's surface temperature has risen by 0.74 K over the past century, see e.g., Steffen et al. (2005), our understanding of the upper atmosphere's temperature evolution is still not clear. In an effort to understand the impact of increasing greenhouse gas concentrations in the atmosphere, the tropopause has seen intense monitoring over the last 30 years using weather-balloons (i.e., radiosondes) and re-analyses (e.g., European Center for Medium range Weather Forecasting, ECMWF). For instance Santer et al. (2003, 2004) and Sausen and Santer (2003) have shown that changes in tropopause height is a useful and sensitive indicator of human effects on climate. The heights of the tropopause rise with increased temperature in the troposphere due to global warming (IPCC 2007). Santer et al. (2003) estimated that nearly 80% of the rise in tropopause height between the period 1979 and 1999 is attributed to human-induced greenhouse concentrations in the atmosphere.

The importance of the troposphere and lower stratospheric temperature evolution in understanding the cause of climate change was further highlight in the IPCC's assessment report (IPCC 2007). This chapter examines the contribution of GNSS satellites to monitor the troposphere and in so doing contribute to monitoring of global warming. In Sect. 21.5.4, its contribution to monitoring cryospheric changes resulting from global warming is discussed.

21.2 Impacts of Weather and the Changing Climate

21.2.1 Weather Related Impacts

The unpredictability of weather and its socio-economic dimensions is a major factor in the destruction of properties, which in many cases leads to, or enhances poverty (see, e.g., Agola and Awange 2013). Extreme weather events affects food security in households and as such proper weather forecasts are necessary to ensure food production as it may help to determine what crops to plant in a particular season. However, food production is not the only aspect that suffers from adverse weather. For example, some diseases are weather dependent, see e.g., Nyakwada (2000).

Some of the seasonal variations and extreme weather and climatic anomalies have been associated with the *El Nino Southern Oscillation* (ENSO) phenomenon and the Indian Ocean Dipole (IOD), e.g., Atheru et al. (2000), which lead to anomalous rainfall that results in large losses in the economy. Other weather-related impacts include hailstorm destruction of crops, lightning strikes, thunderstorms, seasonal floods, frost damage, and strong winds. These impacts also often result in the loss of lives and properties, and the mass displacement of people, as witnessed in the floods that ravaged Pakistan and Eastern parts of Australia in 2010–2011. Also common as a result of extreme weather events are erosion, siltation, and increase in water-borne diseases.

To reduce the impacts of these factors, considerable research, awareness, monitoring and finance for the mitigation of weather and climate hazards is needed to implement sustainable climate and weather mitigation initiatives. The simplest and cheapest methods of addressing these problems almost solely takes into account public awareness and information about weather and climate and their roles in life quality. The awareness and information gap is better filled by following the weather *forecasts* issued by meteorological departments and climate-based organizations (Otengi 2000).

Weather and climate forecast information generated by various models has the potential to assist in the fight against poverty by allowing early planning for the mitigation of the adverse effects of droughts and persistent floods (Okoola 2000). The desire to reduce the negative impacts of weather necessitates that forecasters work together with the general population and provide them with timely warnings. In order for the forecasters to provide sufficiently accurate predictions, they would need not only to understand and be familiar with *prediction models*, but also the *long-term* trends in weather and climate. These would in turn lead to forecasting conditions that influence our behaviour and livelihoods. GNSS satellites have started playing a major role in *numerical weather prediction* (NWP) models, as will be discussed in Sect. 21.3.2.

21.2.2 Climate Related Impacts

Though climate change is one of the greatest challenges facing humanity, not all the climate change ends up being adverse. While some parts of the world experience more frequent and more severe droughts, floods, or significant sea level rise, in other places, crop yield may increase due to the fertilization effect of carbon dioxide (Houghton 2005). That said, it is the adverse effects that are of great concern to mankind today. In the last decade alone, we have witnessed the melting of glaciers and polar ice caps (e.g., Sect. 21.5.4), increased numbers of severe storms, hurricanes and typhoons wrecking havoc (Emanuel 2005), and severe wide spread droughts threatening farming and water resources. For example, in its January 2007 monthly statement on the Australian drought, the Bureau of Meteorology (BoM) reported the year 2006 as having been one of the driest on record for most parts of southern Australia. The drought, see e.g., Fig. 21.1, which persisted in many parts of Australia until the time of the writing of this book (2012), has been made worse by increased temperature, e.g., Ummenhofer et al. (2009). Two widely felt consequences of the drought are:

- A drop in farming output, leading to a reduction in the nation’s overall economic growth, and
- a decline in stored fresh water (surface and ground) suitable for human consumption, industrial and mining applications, as seen from media interest. For instance, on the dwindling water resource in Australia, Phillips (2006) wrote: “*With a growing population and a drying climate, Australia—like many rich nations—is running out of water. Solutions are not easy nor cheap ... and may require cities to tap their sewers*”.



Fig. 21.1 Severe drought in Australia (2007): Sheep wondering what to eat! Source [http://en.wikipedia.org/wiki/File:Riverina_Sheep_\(during_drought\).jpg](http://en.wikipedia.org/wiki/File:Riverina_Sheep_(during_drought).jpg)

The Intergovernmental Panel on Climate Change (IPCC 2007) assessment report points to the fact that the rate of global average warming over the past 50 years (i.e., 0.13 ± 0.03 K per decade) was almost double compared to the past 100 years (0.07 ± 0.02 K per decade). These findings further paint a gloomy picture for countries such as Australia where the impact of global warming is already being felt. In fact, in 2005, Steffen et al. (2005) already issued an alert that Australia would be faced with the impact of climate change on its water quantity due to decreased precipitation over parts of the continent. More astonishing for Australia was the IPCC (2007) projection of an increase in drought over the continent and a further decline in fresh water resources over the next two decades.

These impacts of climate change could be monitored through various proxy indicators such as tree rings, ice cores, ocean sediments, pollen records, boreholes, speleothems and corals, see e.g., Burroughs (2007). Global sea level is an indicator of climate change, as it is sensitive to both the *thermal expansion* of the oceans and a reduction in the volume of land-based *ice* (Mitrovica et al. 2009). The influence of climate change on terrestrial water supply has already been noticed, e.g., by Magadza (1996) who analyzed the sensitivity of major African rivers to climate change. Magadza (1996) examined changes in Zimbabwe's main water storage facilities during the 1991–1992 drought cycles, and established that storage had dwindled to less than 10% of its installed capacity. Jallow et al. (1996) and Li et al. (2007) also studied the impact of climate change on water supplies. In their study of the flow of the Gambian river, Jallow et al. (1996) found that the Gambia river flow was very sensitive to climate change. Based on the results of river flow responses and vulnerability analysis, climate variables alone were found to cause a 50% change in runoff in the Gambia river catchments (Jallow et al. 1996). Li et al. (2007) noted that the primary climate indicators of precipitation and temperature influenced the fluctuation of Lake Qinghai water levels.

In general, Manneh (1997) points out that a 1% change in rainfall results in a 3% change in runoff, which in-turn reduces the lake's recharge. Since lake level fluctuations have been shown to track drought episodes, e.g., Beaudoin (2009), Mistry and Conway (2003) investigated the climatological factors responsible for the rise in the lake level, and found that there was a significant correlation between the lake's rainfall series and its levels. They also pointed out that there was a time lag of 1–2 years between rainfall episodes and the water level peaks of the lake. Since the rainfall time series are based on land-based observations, and the lake itself is roughly one quarter of the whole basin, the lake level variability is partially explained by the over-lake rainfall. Awange et al. (2008) investigated whether the fall in Lake Victoria water levels were attributed to climate change. In Chap. 22, the use of GNSS to monitor changes in fresh water levels will be discussed, while Chap. 26 will look at how changing sea levels can be monitored using GNSS to mitigate potential disasters associated with rising sea levels.

21.3 Water Vapour

21.3.1 Significance

Section 5.4.3 discussed the effects of atmospheric delay on the measured GNSS signals, the desire by the geodesist to eliminate it in order to improve their positioning accuracies, and ended by stating that *one person's poison is another person's meat!* In this section and subsequent ones, we demonstrate how this geodesist's *poison* becomes an environmentalist's *meat*. We start by looking at water vapour.

Atmospheric *water vapour* is the gaseous state of water once evaporation takes place and plays a key role in weather forecasting. Its significant role in weather forecasting was pointed out by Belvis et al. (1992) who noted that the limitations in the analysis of water vapour are the major source of error in short-term (0–24 h) forecasts of precipitation. The global composition of water vapour in air is on average roughly equivalent to a layer of liquid water covering the Earth to a thickness of around 25 mm (Brutsaert 2005, p. 23). The thickness of this layer provides the total liquid equivalent of water vapour in an atmospheric column at a given location and is often referred to as *precipitable water* (Brutsaert 2005, p. 23). The spatial distribution of water vapour in the atmosphere varies with latitude as well as vertical elevation. Water vapour concentrations vary until an elevation of 9 km at the poles, and until more than 16 km at the equator, decreasing rapidly with elevation (Tao 2008), with 50% found within the lowest 1–2 km (Brutsaert 2005, p. 23). According to Brutsaert (2005, p. 23), current data indicates that the amount of precipitable water vapour near the poles is less than 5 mm, and close to 50 mm at the equator.

Water vapour plays a key role in environmental phenomena since it provides the means by which *moisture* and *latent heat* are transported. This makes it a key environmental monitoring parameter since knowing its spatial and temporal distribution accurately could significantly enhance weather analysis and forecasting at local, regional and global scales. This could provide early warning systems with adequate information to mitigate the effects of *hurricanes* and *typhoons*. Unfortunately, water vapour fields are inadequately defined, thereby contributing immensely towards hampering the accurate *prediction of weather* and *modeling of climatic change*. Trenberth and Guillemot (1996) attribute this inadequacy to *sparsity of water vapour observations*, combined with the high spatial and temporal variability of water vapour fields.

The critical role played by *water vapour* in the global climate system are listed, e.g., by Brutsaert (2005, p. 23) as *first*, it is a vital component of the hydrological cycle, enabling the movement of evaporated water from the oceans to land where it falls as rain. *Second*, it provides the medium for energy transfer during evaporation (i.e., from Earth to the atmosphere) and during condensation, thus providing the energy required for atmospheric circulation. *Third*, it plays a significant role in controlling the amount and type of cloud cover due to its concentration and spatial distribution. These clouds then play a role in the distribution of solar radiation. *Fourth*, it is a greenhouse gas and contributes to global warming by trapping the radiated energy

from the Earth. Ware et al. (2000, p. 23) adds the role of water vapour in the chemistry of the lower atmosphere to the list, while the vital role of water vapour in atmospheric processes ranging from global climate change to micro-meteorology are pointed out, e.g., by Rocken et al. (1993).

Traditional techniques for monitoring water vapour include *radiosondes*, *surface based humidity sensors*, *surface and satellite based radiometers*, and *research aircraft* (Ware et al. 2000, p. 23). According to Elliot and Gaffen (1991), radiosondes measure temperature and humidity with an accuracy of about 0.2 °C and 3.5%, respectively, and that the performance deteriorates in cold-dry regions. Surface-based radiometers are comprised of upward-looking water vapour radiometers (WVR) that measure the microwave energy emitted by the atmosphere (i.e., microwave radiation produced by water vapour) against the cold background of space and uses it to estimate the zenithal integrated water vapour (IWV) along a given line of sight using retrieval coefficients. These coefficients are derived from the *regression analysis* of *radiosonde data* and are functions of location and climate variations (Belvis et al. 1992; Rocken et al. 1993). Space-based WVR are downward-looking and measure microwave emissions from the atmosphere against the background of the underlying Earth's hot surface. Because of the hot surface, the derived IWV are greatly affected by the large variability in the surface brightness temperature, leading to the method being inefficient for land since the temperatures of the hot background are quite variable and difficult to determine (Belvis et al. 1992).

Belvis et al. (1992) further state that satellite-based WVR are affected by clouds and as such may be more useful over the ocean. In fact, they reckon that both systems complement each other, with the ground-based WVR providing good temporal, but poor spatial coverage while space-based WVR provide good spatial, but poor temporal coverage. Operating both systems could therefore be of significant benefit to environmental monitoring since it could lead to improved short-term weather forecasting (1–12 h) with the benefit of mitigating environmental catastrophes caused by episodic events such as *flash floods*. The shortcomings of the methods, however, are that both are affected by rain, which absorbs and scatters the emitted microwaves. Also, like the radiosonde method, they too are expensive to operate, and are limited in high-latitude areas like the Arctic (Tao 2008). GNSS monitoring of water vapour discussed in Sect. 20.2 promises to provide more data, that hopefully will lead to enhanced monitoring of potential environmental catastrophes as well as the prediction of longer-term climatic change.

21.3.2 Numerical Weather Prediction

In order to understand the role that could be played by GNSS satellites in weather forecasting, it is essential at this point to introduce the concept of mathematically predicting the weather using supercomputers. Prediction of weather, referred to as *numerical weather prediction* (NWP) can be traced back to the work of *Vilhelm Bjerknes* in 1904 (Bjerknes 1904) who proposed the representation of weather as a

problem in mechanics and physics. NWP is an initial/boundary value problem, i.e., the future state of the atmosphere is determinable through model simulations (forecasts) if its present state (*initial conditions*), and appropriate and lateral *boundary conditions* are known (Kalnay 2003, p. 136).

In this approach, Bjerknes (1904) identified a nonlinear system of equations consisting of seven variables as necessary to characterize weather at any given location $\{x, y, z\}$ and time t in the Earth's atmosphere. These nonlinear equations make up *models* that seek to employ the current state of the weather to produce meteorological information for future times at a given *location*. Before the advent of the computers, the solution of this system of equations was extremely difficult, as evident by the works of Charney (1955), Charney et al. (1950), and Richardson (2007). With the increased powers of modern supercomputers, however, the solution of these numerical weather prediction models have become a routine task. Besides improved computing power, other factors that have enhanced NWP include (Kalnay 2003):

- The improved representation of small-scale physical processes within the models. These include clouds, precipitation, turbulent transfer of heat, moisture and radiation.
- The use of more accurate methods of data assimilation, which results in improved initial conditions for the models.
- The increased availability of data, especially satellite and aircraft data, over the oceans and the Southern Hemisphere.

One common characteristic of nonlinear systems of equations is that they can fail to have exact solutions, thereby necessitating alternative solutions, see e.g., Awange and Grafarend (2005) and Awange et al. (2010). For NWP models, these systems of nonlinear equations are solved numerically through *global* or *regional circulation models* (GCMs). Global models are useful in forecasting weather changes for 2 days or more (i.e., *medium range forecasts*). At the National Center for Environmental Protection (NCEP), for example, global models are run through 16 days everyday (Kalnay 2003, p. 11). Due to the fact that global models cover the entire Earth, the resulting solution is generally poor, thus necessitating the use of more focused high resolution regional models for *short-range forecasts* (1–3 days).

Both global and regional circulation models require some *initial tautology values* (present state of the atmosphere) in order to simulate (forecast) the future state of the weather. Methods for determining these initial starting values are presented in details, e.g., in Daley (1991) and Kalnay (2003). Here, a summary of one of these methods, the 3D-Var, is presented. Normally, initial values obtained from ± 3 h *observations* (e.g., radiosonde data, weather satellites, surface weather or radiance, etc.) are normally of few orders, e.g., 10^5 compared to 10^7 for the degree of freedom of the circulation models. Clearly, they are insufficient to initialize the models. This necessitates the use of additional information known as *first guesses* to generate the *initial conditions* for the forecast. According to Bergthorsson and Döös (1955), these first guesses provide the *first estimate* of the state of the atmosphere at all grid points. The initial approach adopted for obtaining the first guesses use *climatology* data which are obtained by averaging observational data ranging over a long period

of time from a variety of observing systems (Bergthorsson and Döös 1955; Poli 2006). These first guesses are later complemented by a short range forecast obtained numerically by running a model from an old set of initial conditions (Bergthorsson and Döös 1955). With improved weather forecasting, the use of short-range weather forecasting as a first guess is universally adopted in operation systems called the *analysis cycle* (Fig. 21.2) (Kalnay 2003, p. 138).

The *observations*, *climatology* and short-range forecasts are then combined through some method of *data assimilation* to produce the ‘*best estimate*’ of the current state of the weather (initial values) called the *analysis*, which are used in the NWP models as illustrated in Fig. 21.2. In atmospheric science, therefore, an analysis is a detailed representation of the state of the atmosphere that is based on observations (Dole et al. 2008). More generally, Dole et al. (2008) state that an analysis may also be performed for other parts of the climate system, such as the oceans or land surface, and is often displayed as a map depicting the values of a single variable, such as air temperature, wind speed, or precipitation, or of multiple variables for a specific time period, level, and region. The daily weather maps that are presented in newspapers, television, and numerous other sources are familiar examples of this form of

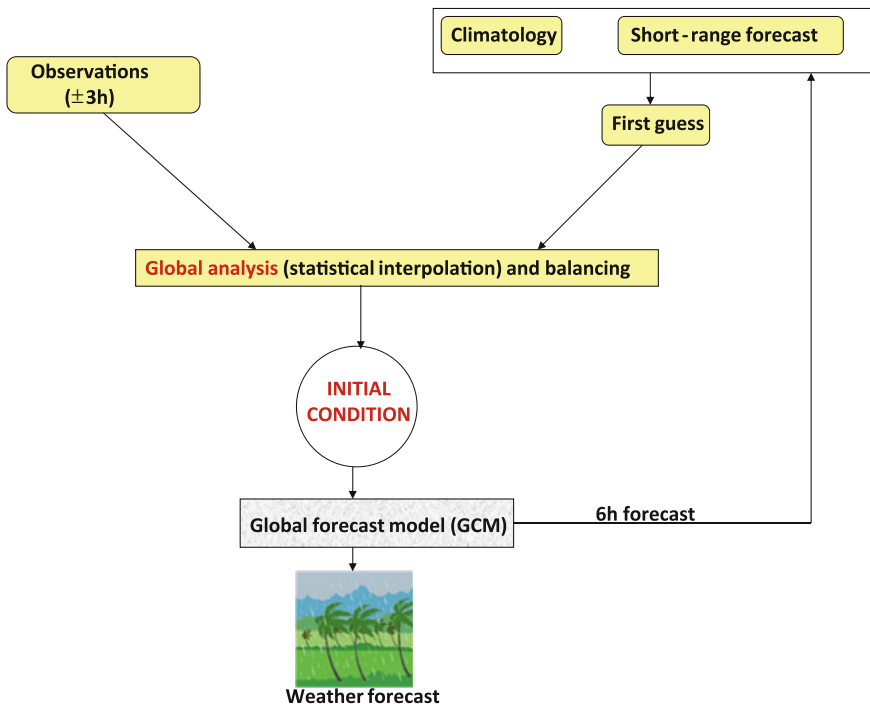


Fig. 21.2 Global data assimilation with 6-h forecast. A global 6-h cycle is performed at 00, 06, 12, and 18 UTC. For regional models, the observation times change from $\pm 3\text{h}$ to $\pm 30\text{min}$, while the forecast data changes from 6 h to 1 h. *Source* Awange (2012)

analysis (Dole et al. 2008). Analyses are also performed at levels above the Earth's surface in order to provide a complete depiction of atmospheric conditions throughout the depth of the atmosphere. This type of analysis enables atmospheric scientists to locate key atmospheric features, such as the jet stream, and plays a crucial role in weather forecasting by providing initial conditions required for models used for weather prediction (Dole et al. 2008). Currently, operational NWP centers produce initial conditions through a statistical combination of observations and short-range forecasts (Kalnay 2003).

Data assimilation, as illustrated by Fig. 21.2, and whose purpose is to use all available information to determine as accurately as possible the state of the atmospheric flow (Talagrand 1997), can be achieved in several ways, see e.g., Kalnay (2003). One approach that operates in a statistical way is the 3D-Var, which minimizes the cost function $J_0[\xi]$ constructed as the sum of (Kalnay 2003, p. 15)

$$J_0[\xi] = \frac{1}{2} \{ (\mathbf{y} - f(\xi))^T \Sigma_y^{-1} (\mathbf{y} - f(\xi)) + (\xi - \tilde{\xi})^T \Sigma_\xi^{-1} (\xi - \tilde{\xi}) \}, \quad (21.1)$$

where the first term of J_0 measures the distance between the newly created initial conditions ξ and the assimilated observations \mathbf{y} (i.e., the first term on the right-hand-side). The second term on the right-hand-side measures the distance between the newly created initial conditions (analysis) and the first guess and is essential for constraining the initial conditions to ensure that they are close to the first guess (Poli 2006). The observation operator f maps the initial conditions ξ through interpolation and transformation into the observation space \mathbf{y} . The variance-covariance matrices Σ_y^{-1} and Σ_ξ^{-1} perform the function of adjusting observational errors and first-guess errors, respectively. Assimilating new data types requires accurate knowledge of the variance-covariance matrices, and an accurate, yet computationally efficient, mapping operator f , whose tangential linear model is also required in order to minimize the total cost function (Poli 2006).

In Eq. (21.1) only two terms have been presented for the cost function J_0 . Other formulations of J_0 may include an optional *third term*, which is added to balance the initial conditions. An extension to the 3D-Var model is the 4D-Var model, which includes within its cost function, the distance to the observation over the time window. For detailed discussions about this model and others, plus a wealth of references on NWP and data assimilation, we refer the reader to Daley (1991) and Kalnay (2003).

21.4 Carbon Sequestration and Estimation of Vegetation Carbon Stocks

It is widely acknowledged that through the process of photosynthesis, vegetation transforms atmospheric carbon dioxide (CO_2) into carbohydrates. The carbohydrates are then stored in various carbon stocks such as plant tissues during growth, some of which may also be transferred to the soil as dead organic matter and as secondary

productivity, see e.g., Jiang et al. (2002), Myneni et al. (2001), Patenaude et al. (2005) etc. The entire process of capturing and up-taking carbon from the atmosphere by vegetation for storage is referred to as *carbon sequestration*. This process contributes towards ensuring global carbon balance.

Vegetation has been identified as having the potential of up-taking (sink) or releasing (source) carbon at any defined time through its pools. Three (3) major types of carbon pools have been associated with vegetation including (see e.g., Houghton 2005; Kumi-Boateng 2012):

- (1) *Above ground biomass*—trees (live or dead);
- (2) *Necromass*—herbaceous plant, litter; and
- (3) *Below ground biomass*—soil and roots.

The importance of carbon sequestration in maintaining global carbon equilibrium cannot be overemphasized. Consequently, land use land cover (LULC) change occasioned mostly through deforestation is considered a significant global concern. This is due to its associated losses of biomass leading to significant decline in net carbon stocks (Bonino 2006). Deforestation does not only transfer carbon stocks directly to the atmosphere by combustion and decomposition, but also destroys the valuable mechanism for controlling atmospheric CO₂ (Tutu 2008).

Forests sequester and store more carbon than any other terrestrial ecosystem and serve as an important *natural brake* on climate change. When forests are cleared or degraded, their stored carbon is released into the atmosphere as CO₂ (Gibbs et al. 2007). Tropical deforestation is estimated to have released between 1 and 2 billion tonnes of carbon per year during the 1990s, accounting for roughly 15–25% of annual global greenhouse gas emissions, see e.g., Fearnside and Laurance (2003), Houghton (2005), Malhi and Grace (2000) etc.

Gibbs et al. (2007) postulate that the inclusion of deforestation projects was initially excluded from the 2008–2012 first commitment period of the Kyoto Protocol because of concerns about diluting the focus then on fossil fuel reductions, sovereignty and challenges in available methods to measure emission reductions. More recently, however, the importance of including emission reductions from tropical deforestation in future climate change policy has grown. Indeed, the United Nations Framework Convention on Climate Change recently agreed to study and consider a new initiative, led by forest-rich developing countries, that calls for economic incentives to help facilitate Reductions in Emissions from Deforestation in Developing countries (REDD) (Kumi-Boateng 2012).

The REDD concept provides financial incentives designed to help developing countries voluntarily reduce national deforestation rates and associated carbon emissions below a baseline (based either on a historical reference case or future projection). Furthermore, countries that demonstrate emission reductions may be able to sell those carbon credits on the international carbon market or elsewhere. These emission reductions could simultaneously combat climate change, conserve biodiversity and protect other ecosystem goods and services (Gibbs et al. 2007).

Baseline mapping, which is essentially a historical mapping analysis coupled with simulation of future carbon scenarios, is fundamental in any REDD project. This is

normally undertaken for an entire country and in practice employs land use land cover (LULC) maps derived from diverse remote sensing systems. From these maps, the historical land cover change of the project area can be assessed and deforestation rates and patterns evaluated. Remote sensing and GIS techniques are usually employed to accomplish this. Determination of the proximate causes and underlying forces of such deforestation is then carried out. This is achieved by interpretation and analysis of the historical trends and locations of deforestation, with a view to identifying and establishing the specific agents, drivers and factors behind the deforestation in a particular case.

It is these agents, drivers, and factors, together with policy guidelines that inform the carbon road-map for a particular country, that are used to model potential future scenarios for conserving carbon. This is done within a GIS environment and software modules have been developed to specifically guide any REDD project. An example is found in IDRISI¹ which includes a complete land analysis toolkit, compatible with international requirements, for mapping historical baselines and modeling future scenarios, as well as a REDD modeling facility to estimate and monitor Green House Gas (GHG) emission reductions due to REDD project implementation.

21.5 Environmental Monitoring Applications

In the next subsections, areas of possible applications of geoinformatics to weather and climate that can contribute to environmental monitoring are presented.

21.5.1 Weather Monitoring Applications

GNSS remote sensing data that are capable of being used for assimilation discussed in Sect. 21.3.2 include; *water vapour, raw amplitude and phase, bending angles, refractivity, temperature and humidity* (Kuo et al. 2000; Poli 2006; Syndergaard et al. 2006). Discussions on the possible assimilation of GNSS data into NWP models are presented, e.g., in Healey and Thépaut (2006), Healey et al. (2005) and Poli (2006). Poli et al. (2008) discuss the effect of GNSS-derived data on NWPs by looking at the influence of European ground-based GNSS-derived zenith total delay (ZTD) data (e.g., summation of Eqs. 20.12 and 20.13 on p. 277) introduced into the Météo-France global forecasting and assimilation system. They report that over three different seasons, the benefits of including such data was most apparent in *improved predictions of temperature and wind*, and especially, in superior quantitative *precipitation forecasts* over France. For space-based GNSS remote sensing (Sect. 20.2.3.1), they report some positive impact on the analysis of the Southern Hemisphere's tropopause. They conclude that these demonstrated benefits has resulted in Météo-France using

¹ <http://www.clarklabs.org/applications/REDD.cfm>

ZTD-derived from European ground-based GNSS networks and GNSS space-based remote sensing data since September 2006 and September 2007, respectively, to update its operational weather prediction analysis.

Furthermore, the success of GNSS data assimilation for stratospheric temperature forecasts and the advantages of GNSS remote sensing data in comparison to other satellite data for assimilation into NWP models are presented by Poli (2006) as:

1. Being all-weather, though the lower 5 km of the atmosphere is generally affected by the presence of water vapour that limits the application of GNSS (see Fig. 20.4 on p. 285),
2. the ability to monitor the Earth from an angle, thus providing higher vertical resolution (less than 1 km). The disadvantage with this, though, is the provision of horizontal resolution elongated in the direction of the ray that makes it difficult to use in models such as ECMWF² and Météo France 4DVAR, which assumes vertically-averaged observations,
3. yielding observations that are independent of surface type, and
4. providing data that relates to altitude as opposed to pressure, as in other techniques.

The potential of water vapour being used for meteorological forecasting have been outlined, e.g., in Baker et al. (2001). For environmental monitoring of weather-related hazards, GNSS remote sensing may potentially play the following roles (Melbourne et al. 1994):

1. *Derive water vapour*: Precise analysis of water vapour content will contribute to the data required by hydrologists to enhance their predictions of local torrential rains that normally cause damage and havoc, see e.g., Awange and Fukuda (2003). Knowledge of water vapour density in the lower troposphere will also be useful for the following:
 - Providing data that could be directly assimilated into meteorological models (NWP) to enhance the predictability and forecasting of weather. The increase in the number of CORS networks (See Sect. 6.5) is already providing the possibility of regional monitoring of IWV. This is achievable by estimating the ZWD in the vicinity of CORS stations and converting them to IWV by means of Eq. (20.19 in p. 279). This unprecedented monitoring of IWV will provide useful data for operational *weather forecasting*, and studies in *atmospheric storm systems*, *atmospheric chemistry* and the *hydrological cycle*.
 - Resolving the distribution of water vapour via tomographic techniques, e.g., Flores et al. (2000).
 - Correcting the wet delay component for both Synthetic Aperture Radar (SAR) and GNSS positioning, thus benefiting applications requiring precise positioning such as crustal deformation monitoring.
 - Monitoring global warming by determining the latent heat suspended in the atmosphere, since water vapour is one of the most important greenhouse gases. Whereas Randall and Tjemkes (1991) indicated that long-term measurements

² European Centre for Medium-Range Weather Forecasts.

of global IWV could provide a source of information for global and regional *climate change studies*, Belvis et al. (1994) pointed to the theorists' belief that global warming will cause changes in the total water vapour content of the atmosphere, a change which would be easily detectable as compared to the associated changes of atmospheric temperatures.

- The radiative forcing due to water vapour and clouds inferred from humidity estimates.
 - Improved inputs for weather forecasting, climate and hydrology. Water vapour is essential for short-term (0–24 h) forecasting of precipitation. Currently, the lack of up-to-date atmospheric water vapour content is the major source of error in short-term weather forecasting (Hanssen et al. 1999).
2. Enhance disaster mitigation measures, in that the provided data will contribute to the much-needed information required to improve the forecasting of catastrophic weather around the world.

21.5.2 Climate Change Monitoring Applications

The provision of *accurate, long-term, and consistent* data to sustain and expand the observational foundation for climate studies is one of the high-priority areas for action to improve the ability to detect, attribute and understand *climate variability and changes* (Foelsche et al. 2006b; IPCC 2001). GNSS remote sensing is fast emerging as a promising climate monitoring tool capable of meeting the requirements above due to the following properties (Stendel 2006):

- *Global coverage of radio occultation (RO) data.* GNSS-RO observations (e.g., Sect. 20.2.3.1; Fig. 20.2 on p. 280–281) have a fairly uniform distribution around the world, both over land and ocean, in contrast to radiosondes and aircraft measurements. This is true for longer averaging periods (as is required for climate monitoring), whereas for shorter, e.g., daily periods, observations tend to cluster due to the sun-synchronous orbits of the LEO satellites.
- *Self-calibrated nature.* GNSS-RO observations are free of instrumental biases since the observations depend on the measurement of time, not of radiation intensities. If double-differencing is applied, the measurements are also essentially self-calibrating. These long-term stability properties imply that it is possible to compare two data sets separated by several years and taken by different sensors, which is not at all straight forward for current microwave sounders.
- *All weather capability.* They can be used in all weather conditions, in particular in cloudy areas, which will not be covered adequately, even by future advanced infrared sounders. Furthermore, the observational quality and sampling characteristics are virtually the same over all geographical regions and at all times.
- They have a relatively high vertical resolution (1 km or better) compared to existing and planned passive infrared and microwave sounders, and thus addressing the

main limitation of these systems. This is true for both temperature and water vapour measurements.

- Quantities that are key observable for climate change, such as near tropopause geopotential heights (Schröder et al. 2003) or refractivity itself can be obtained almost totally independent of conventional measuring systems. Only surface pressure needs to be taken from other sources.
- The unprecedented time stability, accuracy and resolution of GNSS-RO data offers a new possibility to identify spurious trends in radiosonde, Microwave Sounding Units (MSU)/Advanced Microwave Sounding Units (AMSU) and reanalysis data sets discussed in Sect. 21.5.3.1.

The possibilities of using GNSS remote sensing as a tool for monitoring climate change is documented, e.g., in the works of Kursinski et al. (1997), Melbourne et al. (1994) and Yuan et al. (1993). Recognizing the advantages of *global coverage of RO data, self-calibrated nature, high accuracy, and all-weather capability* listed above, recent studies have centered on the possibilities of utilizing it for climate studies, see e.g., Foelsche et al. (2006a,b) and Leroy et al. (2006). For example, the use of refractivity and geopotential heights as global warming parameters have been suggested by Leroy (1997), Schröder et al. (2003) and Stendel (2006). Leroy et al. (2006) states that a good climate monitoring tool must help address the physics of a climate model so as to make it better able to predict future climates, and suggest that GNSS remote sensing be used to provide benchmark for climate models.

Poli et al. (2008), however, caution that though the potential for using GNSS observations for climate studies is significant, detailed sensitivity studies are required in order to evaluate the effects of possible sources of interruption in measurements as well as trends in the stability in the time-series measurements being collected. They reckon that since the atmospheric observations are capable of being used for climate change monitoring, they should be highly accurate and have long-term stability. According to Poli et al. (2008), although the signal delay measured by GNSS offers unmatched meteorological calibration, thanks to the atomic clocks on-board the satellites, the measured GNSS atmospheric delays are not usable directly for climate change monitoring, as they must be converted to other quantities, as was discussed in Sect. 20.2.3.1. Each stage of the conversion could introduce errors that may degrade the atomic calibration aspect.

If successful, however, GNSS remote sensing could benefit climate change monitoring in the following ways (Melbourne et al. 1994):

1. *Precisely derive vertical temperature and pressure profiles*: These will be useful in the following ways:
 - (a) By combining them with other observations of ozone densities and dynamic models, our understanding of the conditions that lead to the formation of polar stratosphere clouds will be improved. It will also help us to be able to understand the chemical reactions that lead to ozone loss.
 - (b) The precisely measured *temperature* will enable the monitoring of *global warming* and the *effect of greenhouse gases*. This is made possible as the

change in surface temperatures caused by an increase in greenhouse gas concentration is generally predicted to be largest and therefore most apparent at high latitudes. Precise temperatures can therefore be used to map the structure of the stratosphere, particularly in the polar regions where temperature is believed to be an important factor in the minimum levels of ozone observed in spring.

- (c) Accurate high-vertical resolution *temperature* reconstructions for the upper troposphere will increase our understanding of the conditions under which cirrus clouds form. Cirrus clouds will generate a positive feedback effect if *global warming* displaces a given cloud layer to a higher and colder region. The colder cloud will then emit less radiation, forcing the troposphere to warm in order to compensate for the decrease.
 - (d) Accurate temperature retrievals from GNSS meteorological measurements combined with high-horizontal resolution temperatures derived from the nadir-viewing microwave radiometers will provide a powerful data set for climate studies of the Earth's lower atmosphere. This can be achieved by using the derived profiles to monitor trends in the upper troposphere and lower stratosphere where the GNSS meteorological technique yields its most accurate results.
 - (e) The measured *pressure* is expected to contribute to the monitoring of *global warming*. This is because pressure versus geometrical height is potentially an interesting diagnostic of the troposphere's climatic change since the height of any pressure surface is a function of the integrated temperature below.
 - (f) The *temperature* in the upper troposphere/tropopause influences the amount of energy radiated out to space. In Sect. 21.5.3, the GNSS monitoring of the tropopause to support the monitoring of climate change will be pursued further.
 - (g) Contribute towards *climatic studies*: By comparing the observed temperatures against the predicted model values, a method for detecting and characterizing stratospheric climatic variations as well as a means for evaluating the performance of model behavior at stratospheric altitudes will be developed and the existing ones tested.
2. Enhance geodynamic studies: The study of the gravitation effects of atmospheric pressure, water vapour and other phenomena will contribute towards the determination of high-resolution local geoids (see Sect. 6.6.1), which are vital for monitoring crustal deformation. The transient drift that occurs over time in the estimation of crustal deformation from GNSS measurement will therefore be corrected for.
 3. With an abundance of GNSS remote sensing data, accuracies better than 1–2 K in temperature given by GNSS meteorological missions (e.g., COSMIC, GRACE, etc.) will be realized.

21.5.3 Monitoring of Global Warming

The layer separating the troposphere and stratosphere is known as the *tropopause*. It is vital to the gaseous exchange between the two layers due to its different characterization with respect to chemical composition and stability. Its height above the Earth's surface normally varies from about 17 km at the equator to about 8 km above the poles, and is influenced by the variation in temperature between the two layers (IPCC 2007; Santer et al. 2003). When the stratosphere warms because of, for example, the absorption of radiation by volcanic aerosols, a lowering of the tropopause height occurs. If the troposphere warms due to, say increases in greenhouse gas concentrations (e.g., carbon dioxide) and stratospheric ozone depletion, the tropopause height increases (IPCC 2007; Sausen and Santer 2003). Indeed, IPCC (2007) noted that most of the observed warming over the last 50 years is likely to have been due to the increase in greenhouse gas concentrations in the lower troposphere.

Evidence of tropospheric warming has been reported, e.g., in Christy et al. (2000, 2003), Mears et al. (2003), and Vinnikov and Grody (2003). For instance, Christy et al. (2003) estimated a global trend of $+0.09$ K/decade from satellite-based Microwave Soundings Unit (MSU) over a 25-year period. Vinnikov and Grody (2003) on the other hand showed a trend of $+0.22 \pm 0.26$ K/decade, which is much higher than the findings of Christy et al. (2003) and Mears et al. (2003), although because of large uncertainty, one cannot definitively say that there is an upward trend.

Santer et al. (2003) identified two different factors that play a key role in the change of tropopause heights, namely *natural forcing* and *anthropogenic forcing*. The anthropogenic forcing include increased greenhouse gas concentration (mainly carbon dioxide), direct scattering of sulphate aerosols, and stratospheric ozone. The natural forcing are the changes in solar irradiance and volcanic aerosols. Santer et al. (2003) estimated that human-induced changes in ozone and greenhouse gases accounted for 80 % of the rise in tropopause height during the period 1979–1999. Radiosonde observations over the past 50 years, e.g., Seidel and Randel (2006), indicate a strong link between climate change and tropopause variability. Global tropopause height indicates an upward trend with decreasing temperature and pressure (Sausen and Santer 2003; Schmidt et al. 2008). During the period 1979–2001, Santer et al. (2004) observed a global increase in tropopause height of 200 m in ECMWF reanalysis, which was mostly caused by tropospheric warming. Similarly, Seidel and Randel (2006) observed a global tropopause trend of 64 ± 21 m/decade using 25 years of radiosonde measurements (1980–2004).

There are many definitions and concepts that are available to identify the tropopause region, e.g., Pan et al. (2004), depending on its latitudinal position and the availability of atmospheric data (such as temperature, pressure, water vapour). Currently, five different definitions are accepted and widely used for identifying the tropopause. These are: *the lapse-rate tropopause* (LRT); *cold point tropopause* (CPT); *the ozone tropopause* (OT); *the isentropic potential vorticity* (IPV) tropopause; and *the 100 hPa pressure level* (PLT). Of these, the LRT has been identified as a key indicator of climate change, see, e.g., Santer et al. (2003).

Previous investigations, e.g., Santer et al. (2003, 2004) and Sausen and Santer (2003), based on LRT height trends, indicate significant increases in the tropopause's height, which is consistent with model prediction used to estimate the impact of increasing greenhouse gases. The definition of the LRT has been outlined by the World Meteorological Organization (WMO 1957) as “the lowest level at which the lapse rate decreases to 2 K/km or less, provided also the average lapse rate between this level and all higher levels within 2 km does not exceed 2 K/km”. This definition has the advantage of being applicable globally and can easily be calculated from the vertical profiles of the atmospheric temperature (Shea et al. 1994).

Whereas surface temperature observations are necessary to monitor daily temperature trends, *monitoring tropopause parameters* (such as temperature and height) is vital for studying changes in the atmosphere as a result of global temperature rise.

21.5.3.1 Traditional Tropopause Monitoring Techniques

Various traditional techniques (e.g., radiosondes, weather analyzes) have been applied by different countries to monitor the tropopause parameters (such as temperatures and heights) over the past 100 years. A brief overview of the existing methods used and their limitations are provided below.

Radiosondes: This is a balloon-borne instrument, also called weather balloon that is traditionally used for collecting weather information along a vertical profile. The Bureau of Meteorology of the United States used radiosondes as early as the 1930s to monitor upper air conditions. A global radiosonde network had been established by 1940s and more than 1000 radiosonde stations had been installed by 1991 by 92 nations (Ware et al. 1996). Radiosonde can be launched in any type of weather, but severe thunderstorms and heavy precipitation can lead to system failures. Under ideal conditions and careful calibration, radiosondes are found to provide temperature observations accurately to about 0.5 K (Shea et al. 1994). Although radiosondes provide soundings with high vertical resolution, global coverage is not feasible with sparse to non-existent data over the oceans and the Southern Hemisphere (Rocken et al. 1997; Schmidt et al. 2008). With fairly low temporal resolution (12-h frequency), the accuracy of the data obtained from this system is affected by instrumental changes, see e.g., Ware et al. (1996).

Although several investigations using radiosonde data sets have been done for a few regions (Anel et al. 2006; Highwood et al. 2000; Nagurny 1998; Randel et al. 2000; Seidel et al. 2001; Varotsos et al. 2004), no studies were performed with regards to global tropopause trends using radiosonde data until 2006. Seidel and Randel (2006) used radiosonde data sets to study global tropopause changes during the period 1980–2004. They divided the globe into seven 29.7° bands to study tropopause trends based on 100 stations around the world. Their findings indicated highly significant tropopause changes during the study period, where the height of the LRT increased by 64 ± 21 m/decade, which is 160 m over 25 years of observations. The increase in tropopause height was associated with a temperature decrease of 0.46 ± 0.09 K/decade and these changes were accompanied by a slight

tropospheric warming ($+0.036 \pm 0.066$ K/decade) and strong stratospheric cooling (-0.77 ± 0.21 K/decade). However, this study was based on a fairly low number of stations which may not provide reliable trends due to instrumental differences across the globe and limited redundancy (IPCC 2007; Ware et al. 1996). Moreover, the stratospheric cooling indicated by Seidel and Randel (2006) appears to contradict the findings of Santer et al. (2004).

The problem with tropopause analysis using radiosondes is that when global estimates based solely on radiosondes are presented, considerable uncertainties exist, see e.g., Agudelo and Curry (2004). Having a denser network of radiosonde stations encompassing even the oceans would be desirable to yield a more reliable global trend, but unfortunately this does not exist nor is it practical.

Satellite-borne Microwave Sounding Units (MSU): These units (e.g., NOAA-N³) have played an important role in providing meteorological information since their first launch in the early 1960s (Ware et al. 1996). The first satellite capable of producing temperature and water vapour soundings was Nimbus III, launched in 1969, followed by NOAA-2 in 1972. Later, these were superseded by Advanced Microwave Sounding Units (AMSU), which began operating in mid 1998 (IPCC 2007). Details of MSU data can be found, e.g., in Christy et al. (1998) and Spencer et al. (1990).

Satellite-borne microwave sounders emit microwaves into the atmosphere, which are then measured and inverted into temperature profiles (and water vapour). These are important sources of data for the lower atmosphere (stratosphere and troposphere) and have been used in several studies of global atmospheric change, see e.g., Christy et al. (2000, 2003), Mears et al. (2003), Parker et al. (1997) and Vinnikov and Grody (2003). The global atmospheric temperature data sets constructed from the satellite MSU measurements of NOAA were used by Christy et al. (2000, 2003) and Mears et al. (2003) to monitor stratosphere-troposphere temperature changes from 1979–1988. A comparison of satellite data with those from radiosondes show reliable trends and have proved to be an important tool for global climate change monitoring. Global time series constructed from MSU records show a global cooling of the stratosphere of -0.32 to -0.47 K per decade and a global warming of the troposphere of 0.04 – 0.20 K per decade for the period 1979–2004 (IPCC 2007).

Satellite-based MSUs and AMSUs are designed to measure short-term temperature changes in the atmosphere and are not suited for the detection of long-term changes since MSU and AMSU data are contaminated by instrumental and orbital drift and coarse vertical resolutions (Anthes et al. 2000). The vertical profiles obtained from the satellite data often *miss* the tropopause region due to insufficient vertical resolution (Ware et al. 1996). Hence, the use of data sets from MSU and AMSU for long-term climate change monitoring has been under considerable scrutiny and debate, see e.g., Christy et al. (2003) and Vinnikov and Grody (2003). Nonetheless, satellite data sets serve as an important data source for weather models and analyzes (e.g., ECMWF).

³ see e.g., http://www.nasa.gov/mission_pages/noaa-n/main/index.html.

Reanalyses: In Sect. 21.3.2, we introduced the concept of analysis and its role in weather prediction and forecasting. Reanalysis, therefore, is an objective, quantitative method for producing a high-quality sequence of analyzes that extends over a sufficiently long-term period to have values for climate research applications, as well as, for other purposes (Dole et al. 2008). An important goal of most reanalysis efforts to date has been to provide an accurate and consistent long-term data record of the global atmosphere (Dole et al. 2008). In certain cases, a reanalysis may be performed for a single variable, such as precipitation or surface temperature, however, in many modern atmospheric re-analyses, the goal is to develop an accurate and physically consistent representation of an extensive set of variables (e.g., wind, temperatures, pressures, etc.) required to provide a comprehensive, detailed depiction of how the atmosphere has evolved over an extended period of time, typically, decades (Dole et al. 2008).

Weather models and re-analyses data are consistently used by researchers to investigate global tropopause changes, e.g., IPCC (2007) and Sausen and Santer (2003). They can also be used to validate data sets from radiosondes and satellites, e.g., Santer et al. (2004) and Schmidt et al. (2005). Global reanalysis such as ERA-40 (ECMWF) provides comprehensive information about climate. The vertical profiles of temperature, pressure, etc. retrieved from the reanalysis models can be used to infer tropopause parameters, as shown in the works of Santer et al. (2003, 2004). Sausen and Santer (2003) and Santer et al. (2003) estimated a tropopause pressure trend of -1.82 hPa/decade for 1979–1997 and -2.16 hPa/decade during the period 1979–2000 in the NCEP/NCAR reanalysis, indicating an increase in the height of the tropopause. Santer et al. (2003) also reported a global mean trend of -1.13 hPa/decade over 1979–1993 in the ECMWF reanalysis. Santer et al. (2004) observed a tropopause height increase of 200 m in the ERA-40 (provided by ECMWF) reanalysis during the observation period 1979–2001.

However, the drawbacks of reanalysis data are that the change in the estimated climate trends may be affected by changes in the observation system over time, and that climate trends proposed by different reanalysis may vary due to differences in the underlying processing techniques.

21.5.3.2 Sensing The Tropopause Using GNSS

The application of GNSS remote sensing to the monitor the tropopause, as presented in Chap. 20, is sure to improve global monitoring of climate change resulting from global warming, especially with more GNSS satellites being planned (see Chap. 4) and with the vertical resolution of the profiles acquired from LEO satellites continuously improving. For example, CHAMP improved its vertical resolution from 200 m to 100 m and its horizontal resolution too (Wickert et al. 2009). Although a long-term study of global tropopause trend using GNSS-RO (e.g., GRACE and COSMIC) data is still not possible due to their short lifespan, Schmidt et al. (2008) estimated a global trend based on the CHAMP satellite's profiles during the period May 2001 to December 2007 (80 months). They obtained a trend of 26–44 m/decade

with trend errors varying between 19 and 21 m, a value which is in good agreement with the radiosonde observations, between 1980 and 2004, both of which indicate a maximum trend around 30°S and between 30°N and 50°N, e.g., Seidel and Randel (2006). However, discrepancies occur in the tropics, which may be associated with the poor RO data distribution (Wickert et al. 2005) and fewer radiosonde stations due to oceanic areas (Free and Seidel 2005).

GNSS tropopause data sources: RO measurements obtained from LEO satellites are processed at various institutions (e.g., GFZ, UCAR) into different products for various uses. Level 3 CHAMP data, Level 2 COSMIC data and GRACE data are essential for tropopause analysis. These data and their sources are discussed in Sect. 20.2.3.2.

Example 21.1 (GNSS monitoring of the Australian tropopause (Khandu et al. 2010)) Australia is a large relatively flat region extending from the tropics to mid-latitudes [8°S–46°S; 108°E–160°E]. The total land area of Australia is 7.7 million square kilometers (Pittcock 2003). Its climate is characterized by varying rainfalls (seasonal, annual and decadal time series) and worsening drought conditions. Australia's climate is strongly influenced by the surrounding oceans, which includes tropical cyclones and monsoon rains in northern Australia, mid-latitude storms in the south causing floods, and prolonged droughts and bushfire outbreaks notably in the mid-latitude zones (Pittcock 2003). The population distribution is fairly uneven with more than 80 % of the settlements being near the coastal areas (Pittcock 2003). The average surface temperature of Australia has warmed by 0.9 K since 1950, with significant regional variations (Bureau of Meteorology 2009). The mean annual temperature anomaly follows an upward trend showing a warming of 1 K over the last 100 years.

In the recent years, Australia, like many other countries in the world, has begun to feel the effects of increasing greenhouse gases leading to regional warming. The rising temperature in Australia thus speeds up the rate of evaporation, enhancing the effect of drought.

Khandu et al. (2010) demonstrated the significance of GNSS remote sensing of the Australian tropopause through their study of changes in the tropopause heights and temperatures (Fig. 21.3). Since the latitude of Australia ranges from 8°S to 46°S, the tropopause height also varies, ranging from around 8 km (mid-latitude) to 17 km (equatorial region) (Wickert et al. 2009). Khandu et al. (2010) applied 80 months (September 2001–April 2008) of CHAMP and 23 months (May 2006–March 2008) of COSMIC satellite RO data to analyze the Australian tropopause structure (height and temperature trends) as shown in Figs. 21.4, 21.5, and 21.6. Their analysis of tropopause height and temperature anomalies indicated a height increase over Australia as a whole of approximately 4.8 ± 1.3 m between September 2001 and April 2008 for CHAMP, with a corresponding temperature decrease of -0.019 ± 0.007 K. They observed a

similar pattern of increasing height/decreasing temperature when determining the spatial distribution of the tropopause height and temperature rate of change over Australia.

Although only a short period of data was considered in Khandu et al. (2010), a function of the operating time of these satellites, their results nonetheless were consistent with those of Schmidt et al. (2008) and Seidel and Randel (2006), and showed an increase in the heights of the tropopause over Australia during that period, and thus may indicate regional warming. Several mechanisms could be responsible for these changes, such as an increase in the concentration of greenhouse gases in the atmosphere, and lower stratospheric cooling due to ozone loss, both of which have been observed during the last decades.

How these rates vary over all of Australia is illustrated in Fig. 21.6 that shows the rate of change of (a) tropopause heights and (b) tropopause temperatures derived from the combined CHAMP and COSMIC data sets between September 2001 and April 2008. There is a general autocorrelation between the two sets of results as one would expect (e.g., increasing height/decreasing temperature). Much of Australia displays trends of 0–0.1 km/year of increasing tropopause height, with a corresponding temperature decrease of 0 to –0.3 K/year. These values are much higher than those presented earlier (see further discussions in Khandu et al. (2010)).

End of Example 21.1

21.5.4 Sensing Cryospheric Changes

The cryosphere, the subsystem of the Earth characterized by the presence of snow, ice, and permafrost, is fundamental to changes occurring in the Earth's environment, e.g., global warming as a result of the melting snow cover, glaciers, and sea ice that produces more warming due to decreased albedo associated with the greater extent and duration of the dark surface (Slaymaker and Kelly 2007). Some of the occurrences in the Earth's polar region (Greenland and Antarctic) could have far reaching consequences on the environment and as such require constant monitoring, which can be achieved through remote sensing using of satellite altimetry such as NASA's ICESat-2 (ice, cloud, and land elevation satellite) proposed for launch in 2015 (see Sect. 20.4.1) and GRACE satellites, e.g., Baur et al. (2009), Velicogna (2009), see also Sect. 20.3.3.

For instance, the Greenland and Antarctic ice sheets are reported to be losing mass at an increasing rate. Fast flowing outlet glaciers and ice streams carrying most of the mass flux from the interiors of the vast Greenland and Antarctic ice sheets toward the ocean have accelerated dramatically, the sea ice that covers the Arctic Ocean has decreased in areal extent far more rapidly than climate models have predicted

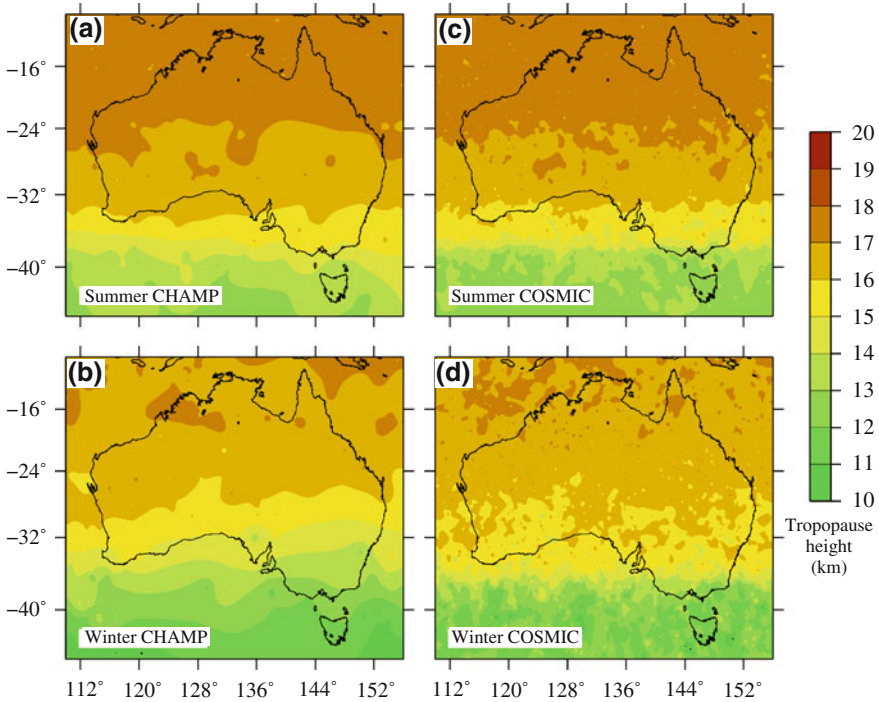


Fig. 21.4 Tropopause heights (in km) derived from CHAMP and COSMIC RO data from between 2006 and 2007. **a** CHAMP results for summer, **b** CHAMP results for winter, **c** COSMIC results for summer, and **d** COSMIC results for winter. *Source* Khandu et al. (2010)

and history in the last few years, leading to improvements in measurements of gross flow velocities, rates of surface snowfall, and isostatic adjustment associated with glacial mass change. In particular, RTGPS (Sect. 6.4.3) can contribute to a better understanding of the dynamics of glaciers by allowing researchers to collect and analyze glacier flow data along with the ocean and atmospheric data (Hammond et al. 2010).

21.5.5 Geoinformatics Support of International Environmental Agreements

21.5.5.1 Background to the Kyoto Protocol

The United Nations Framework Convention on Climate Change (UNFCCC) became operational on 21st March 1994 in response to scientific evidence that the Earth was warming due to increased atmospheric content of CO_2 and other greenhouse gases.

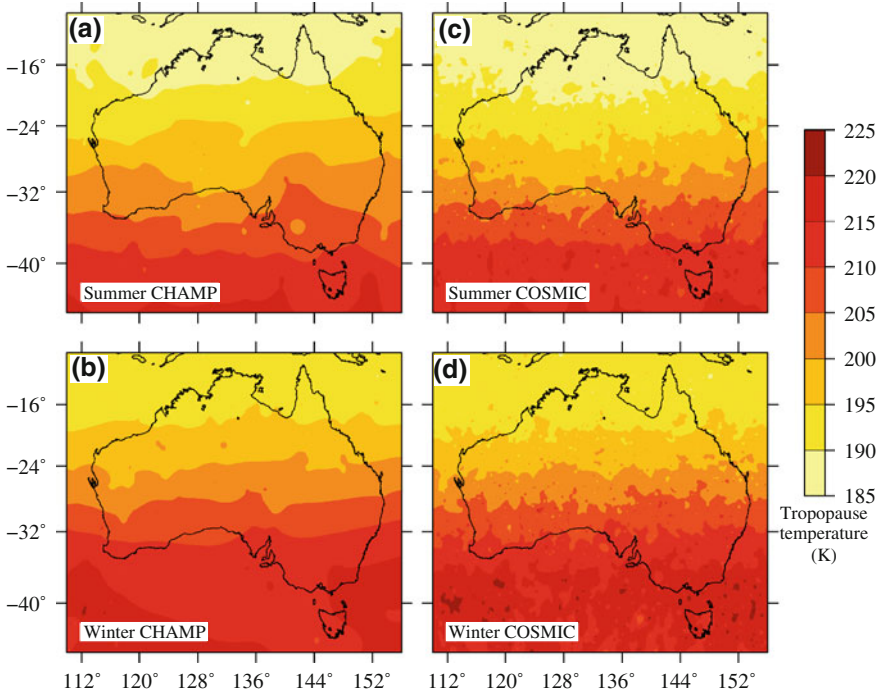


Fig. 21.5 Tropopause temperatures (in K) derived from CHAMP and COSMIC RO data from between 2006 and 2007. **a** CHAMP results for summer, **b** CHAMP results for winter, **c** COSMIC results for summer, and **d** COSMIC results for winter. *Source* Khandu et al. (2010)

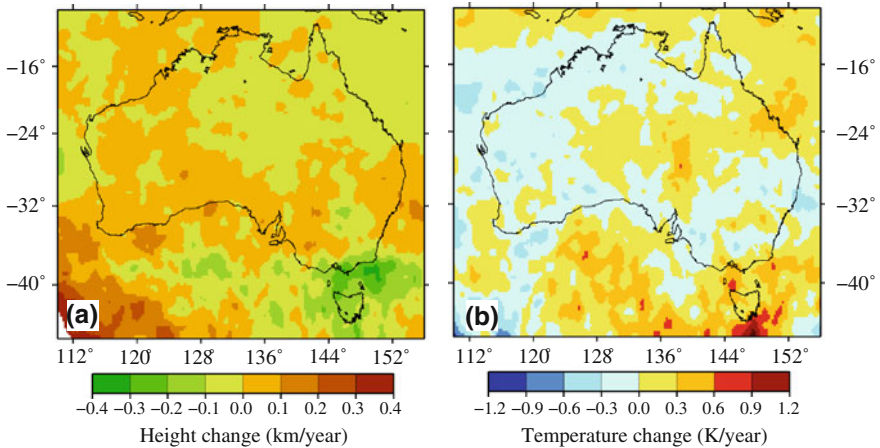


Fig. 21.6 Rate of change in **a** the tropopause heights and **b** tropopause temperatures between September 2001 and April 2008. *Source* Khandu et al. (2010)

In 1997, the *Kyoto Protocol*, an extension of UNFCCC but with more legal binding powers, was passed (UN 1998). At the 2012 Doha climate change talks, Parties to the Kyoto Protocol agreed to extend the Kyoto Protocol to 2020.⁴

In Article 3 of the protocol, quantifiable legal binding commitments are imposed on member countries to the treaty to limit or reduce their greenhouse gas emissions by at least 5% below the 1990 level during the commitment period 2008–2012 (UN 1998; UNFCCC 2007). This means that all member countries are required to periodically carry out and submit an inventory of their respective carbon emissions. Section 3 states that the balance between carbon emission and carbon sinks resulting from direct human-induced, land-use/cover change and forestry activities, limited to afforestation, reforestation and deforestation since 1990, *measured as verifiable changes in carbon stocks in each commitment period*, shall be used to meet the commitments under the Article of each Party included in the protocol.

Furthermore, the greenhouse gas emissions by sources and removal by sinks associated with those activities shall be reported in a transparent and verifiable manner and reviewed in accordance with Articles 7 and 8 (UN 1998). Article 5 states that methods to be used to ensure compliance should be those approved by the *Intergovernmental Panel on Climate Change (IPCC)*. Vegetation is listed in the Article as a measured variable, thereby requiring techniques with the capacity to provide regional as well as global, spatial coverage. Remote sensing, GIS and GNSS satellite methods offer such capabilities.

21.5.5.2 Geoinformatics in Support of Kyoto Protocol

Between 20th and 22nd October 1999 two working groups of the International Society of Photogrammetry and Remote Sensing (ISPRS), together with the University of Michigan, convened to discuss possible areas in which geoinformation could be used to support the Kyoto protocol (Rosenqvist et al. 1999). The groups identified five (5) areas where remote sensing technology could be used. In these areas, GNSS georeferencing would be required to validate the data and support the remote sensing efforts. Remote sensing data has the potential to provide observational and historical data and information about certain features like forests. Such data and information can then be processed and stored in a GIS (see Sect. 1.3) to provide scientific evidence and knowledge, which benefits monitoring compliance with the Articles of the protocol. The 5 identified areas are (Rosenqvist et al. 1999, 2003):

Provision of systematic observation of relevant land cover (Articles 5 and 10): Rosenqvist et al. (1999) observed that multi-spectral systems, in particularly sensors that include mid-infrared bands such as Landsat TM,⁵ ETM+⁶ and SPOT

⁴ <http://www.bbc.co.uk/news/science-environment-20653018>

⁵ Thematic mapper.

⁶ http://landsat.gsfc.nasa.gov/about/L7_td.html

HRVIR,⁷ are suited for the mapping of vegetation. The delineation of fragmented forest lands and smaller patches of forest being used to map vegetation would require high resolution data. To provide mapping of larger spatial coverage (e.g., Australia), higher-resolution data could be complemented by coarse resolution sensors, e.g., NOAA AVHRR⁸ (Richards et al. 2000).

For countries within the tropics, high resolution mapping of vegetation will have to reckon with limitations imposed by cloud cover, smoke and haze. In such situations, coarser resolution sensors with higher temporal repeat cycles or a combination of optical and active microwave data (e.g., Chaps. 8 and 9) could be adopted. Regional and local scales could also benefit from multi-band/polarimetric and interferometric radar systems that have the advantage of being all weather, besides providing data day and night and achieving spatial resolutions of about 50–100 m (Rosenqvist et al. 1999). Radar systems, however, suffer from sensitivity to terrain undulation and hydrological conditions on the ground. Another potential technique for mapping vegetation and its potential to absorb CO₂ is LiDAR⁹ (see Sect. 8.4).

Support to the establishment of the 1990 carbon stock baseline (Article 3): Since 1990 was chosen as a baseline, Landsat TM and SPOT HRV¹⁰ sensors, in operation in 1990, are useful. High resolution data for compiling national coverage maps to support the establishment of the carbon stock baseline is possible, though expensive (Rosenqvist et al. 1999). Rosenqvist et al. (1999) suggests the use of SAR¹¹ data (see Sect. 9.3) for the quantification of component biomass (leaves, branches, stems) of the extensive areas of woodlands that occur throughout parts of Australia, Africa and South America, for which the establishment of a 1990 baseline could be supported.

Detection and spatial quantification of changes in land cover (Articles 3 and 12): Article 3.3 focuses on the detection and spatial quantification of afforestation, reforestation and deforestation during the commitment period of 2008–2012, while Article 3.4 (to be implemented in coming phases) focuses on greenhouse gas balances in agriculture, soils, land-use changes and forestry (UN 1998). Article 12 concerns a clean development mechanism that allows trading in CO₂. To support Article 3.3, repetitive collection of data is required, preferably annually, at specific seasons and at a spatial resolution of the minimum area of interest (Rosenqvist et al. 1999). Panchromatic and multi-spectral remote sensing data can detect and spatially quantify deforestation activities. Partial deforestation resulting from logging will require higher spatial resolution data.

Reforestation (characterizing developmental phase in forests, i.e., from non-forest to forest) and afforestation events (characterized by small patches outside forests) both require high-resolution repetitive multi-spectral measurements. Fire

⁷ High-Resolution Visible and Infrared (imaging instrument). See <http://www.cnes.fr/web/CNES-en/7114-home-cnes.php>.

⁸ Advanced Very High Resolution Radiometer.

⁹ Laser Infrared Detection And Ranging.

¹⁰ High Resolution Visible.

¹¹ Synthetic Aperture Radar.

events could be detected using coarse resolution optical sensors that provide daily coverage. Long-wavelength active microwave systems are also useful since they interact with forests at the branch and trunk level and are essential in separating the contributions from the ground and forests (Rosenqvist et al. 1999). The presence of cloud cover will, however, remain an impediment in some areas. The application of LiDAR to repeatedly characterize structural attributes at specific location could also be valuable, see e.g., Blair et al. (1999).

Trading in CO₂, for instance, could be supported by the use of passive remote sensing. Under such a system, sensors could be placed within the emission source to transmit the collected digital data. The locations of such emission source could be obtained using GNSS, which also helps in mapping forest fires as discussed in Sect. 26.3. As an example, by classifying time series based Landsat and Aster data and applying this in conjunction with ground based inventory data for a mining area in, Tarwa, Ghana, Kumi-Boateng (2012) recorded a total of $1,250.93 \pm 7 \text{ Mg/km}^2$. Furthermore, this study estimated that an average of 961.13 Gg of carbon (equivalent to 45.77 Gg carbon per year) was lost between 1986 and 2007 due to mostly changes in the land-use land cover.

Quantification of above ground vegetation biomass stocks and associated changes therein (Articles 3 and 12): ICESat and its follow on ICESat-2 are expected to contribute in this regard by measuring tree heights (see Sect. 25.3, Fig. 25.8, p. 427–430). Indirect estimation using vegetation indices based on photosynthetically active radiation (PAR) is proposed by Rosenqvist et al. (1999). The use of multispectral sensors to measure PAR for the prediction of net primary production (NPP) presented as units of Carbon is demonstrated, e.g., by Prince and Goward (1995), Kumi-Boateng (2012) etc. The use of active microwave systems and LiDAR to support this Article is still an active area of research. Ranson et al. (1997) demonstrated that radar sensors having full multi-band, polarimetry, and interferometric capabilities are capable of detecting biomass above the ground.

Mapping and monitoring of sources of anthropogenic Methane CH₄ (Articles 3, 5 and 10): Although 6 greenhouse gases are listed in the protocol, see e.g., UN (1998), the more lethal CH₄ was considered by the working groups to be second in importance after CO₂. Sources of CH₄ include irrigated rice paddies, aquaculture and hydroelectric reservoirs. High-resolution optic sensors could be used to detect and spatially quantify open water bodies while repetitive measurements could be employed in the irrigated rice paddies. However, repetitive measurements would most likely be affected by cloud cover, thereby necessitating the use of SAR (Le Toan et al. 1997). The physical locations of these sources, i.e., their boundaries could be mapped using rapid GNSS positioning methods discussed in Chap. 6, Sect. 6.4.5.

21.6 Concluding Remarks

This chapter has highlighted the potential of GNSS measurements to contribute to weather forecasting and climate change monitoring through integrative measurement of atmospheric parameters (temperature, pressure and water vapour) in GPS signal delays as discussed in Chap. 20. The success is largely due to the sensitivity of the microwave frequencies used in GNSS in the presence of water vapour whose estimation along GNSS signal propagation paths is discussed in Sect. 21.3. Because water vapour is key to energy transport and buoyancy, assimilation of water vapour measurements is vital to weather modeling. Operational weather forecasts routinely assimilate observations of relative humidity along with pressure and temperature collected using radiosondes, rocketsondes and surface meteorological sensors. In most continental regions, such measurements sample adequately to prevent significant aliasing of pressure and temperature fields (which co-vary on large spatial and temporal scales) but can under-sample the relatively short temporal and small spatial-scale variability of humidity (Hammond et al. 2010). GNSS-derived water vapour data will thus become more useful for weather and climate applications as RTGPS networks (see Sect. 6.4.3) provide data with low latency and high reliability (Hammond et al. 2011).

The rising troposphere temperature due to global warming increases the height of the tropopause. Therefore, information on tropopause height trend is vital for monitoring global warming. This chapter has explained how GNSS remote sensing of signal delays discussed in Chap. 20 are useful in monitoring global warming. Its atmospheric profiles match those from radiosonde measurements (i.e., temperature accurate to 1 ± 1.5 K in the tropopause region), and are suitable for use in the analysis of the tropopause for the studies of climate change. The tropopause, analyzed in Schmidt et al. (2008), Seidel and Randel (2006) and Khandu et al. (2010), provided examples of the capability of the method.

It is evident from recent climate change conferences (like the one held in Durban in 2011) that parochial political and economic interests have taken center-stage for a few countries—who incidentally are some of the largest polluters. This has made the acceptance of major climate policies and protocols aimed at reducing carbon emissions, especially after the landmark Kyoto protocol, that more difficult to achieve at the global arena. That notwithstanding, however, the worldwide acceptance and implementation of such climate policies and protocols will still require resolution of concomitant scientific challenges. Foremost among these challenges is that of identifying feasible and pragmatic methods for estimating national-level carbon emissions from e.g., deforestation and degradation in especially developing countries. To quantify such emissions, there is need to know the area of cleared forest and the amount of carbon that was originally stored in those forests. When applied in conjunction with ground based data, remote sensing provides a pragmatic tool that can be used in the assessment of carbon stocks in many developing countries.

References

- Abdalati W, Zwally HJ, Bindschadler B, Csatho B, Farrell SL, Fricker HA, Harding D, Kwok R, Lefsky M, Markus T, Marshak A, Neumann T, Palm S, Schutz B, Smith B, Spinhirne J, Webb C (2010) The ICESat-2 laser altimetry mission. *Proc IEEE* 98(5):735–751. doi:[10.1109/JPROC.2009.2034765](https://doi.org/10.1109/JPROC.2009.2034765)
- Agola NO and Awange JL (2013) Globalized poverty and environment.
- Agudelo PA, Curry JA (2004) Analysis of spatial distribution in tropospheric temperature trends. *Geophys Res Lett* 31(L22207): doi:[10.1029/2004GL02818](https://doi.org/10.1029/2004GL02818)
- Anel JA, Gimeno L, Torre LDI, Nieto R (2006) Changes in tropopause. *Naturwissenschaften*. doi:[10.1007/S00114-006-0147-5](https://doi.org/10.1007/S00114-006-0147-5)
- Anthes RA, Rocken C, Kuo YH (2000) Applications of COSMIC to meteorology and climate. *Terr Atmos Ocean Sci* 11:115–156
- Atheru ZKK, Ogallo LA, Ambenje PG (2000) Regional climate forecasts for enhanced food production to alleviate rural poverty around the Lake Victoria region. KMFRI, Nairobi, pp 28–30
- Awange JL, Fukuda Y (2003) On possible use of GPS-LEO satellite for flood forecasting. The international civil engineering conference on sustainable development in the 21st century—“the civil engineer in development”, 12–16 August 2003, Nairobi, Kenya
- Awange JL, Grafarend EW (2005) Solving algebraic computational problems in geodesy and geoinformatics. Springer, Berlin
- Awange JL, Ogallo L, Kwang-Ho B, Were P, Omondi P, Omute P, Omulo M (2008) Falling Lake Victoria water levels: Is climate a contribution factor? *J Clim Change* 89:287–297. doi:[10.1007/s10584-008-9409-x](https://doi.org/10.1007/s10584-008-9409-x)
- Awange JL, Grafarend EW, Paláncz B, Zaletnyik P (2010) Algebraic geodesy and geoinformatics, 2nd edn. Springer, Berlin
- Awange JL (2012) Environmental monitoring using GNSS, Global Navigation Satellite Systems. Springer, Berlin, New York
- Baker HC, Dodson AH, Penna NT, Higgins M, Offiler D (2001) Ground-based GPS water vapour estimation: potential for meteorological forecasting. *J Atmos Solar-Terr Phys* 63(12):1305–1314
- Baur O, Kuhn M, Featherstone W (2009) GRACE-derived ice-mass variations over Greenland by accounting for leakage effects. *J Geophys Res* 114(B06407). doi:[10.1029/2008JB006239](https://doi.org/10.1029/2008JB006239)
- Beaudoin AB (2002) On the identification and characterization of drought and aridity in postglacial paleoenvironmental records from the northern great plains. *Géogr Phys Quat* 56(2–3):229–246. E-SCAPE contribution 3. Note: Volume dated 2002, but published in 2004
- Belvis M, Businger S, Herring TA, Rocken C, Anthes RA, Ware RH (1992) GPS Meteorology: remote sensing of water vapour using global positioning system. *J Geophys Res* 97:15787–15801
- Belvis M, Businger S, Chiswell S, Herring TA, Anthes RA, Rocken C, Ware RH (1994) GPS Meteorology: mapping zenith wet delays onto precipitable water. *J Appl Meteorol* 33:379–386
- Bergthorsson P, Döös B (1955) Numerical weather map analysis. *Tellus* 7:329–340
- Bjerknes V (1904) Das Problem der Wettervorhersage, betrachtet vom Standpunkt der Mechanik und der Physik. *Meteor Zeits* 21:1–7
- Blair JB, Rabine D, Hofton M (1999) The Laser Vegetation Imaging Sensor (LVIS): a medium-altitude, digitization only, airborne laser altimeter for mapping. *ISPRS* 54:115–122
- Bonino EE (2006) Changes in carbon pools associated with a land-use gradient in the Dry Chaco, Argentina. *For Ecol Manag* 223:181–189
- Brutsaert W (2005) Hydrology. An introduction, 4th edn. Cambridge University Press, New York
- Bureau of Meteorology, Australia (2009) Australia’s climate change and variability. http://www.bom.gov.au/silo/products/cli_chg/. Accessed 25 Oct 2009
- Burroughs WJ (2007) Climate change: a multidisciplinary approach, 2nd edn. Cambridge University Press, Cambridge
- Charney JG (1955) The use of primitive equations of motion in numerical prediction. *Tellus* 7:22–26
- Charney JG, Fjørtoft R, von Neuman J (1950) Numerical integration of the barotropic vorticity equation. *Tellus* 2:237–254

- Christy JR, Spencer RW, Lobl ES (1998) Analysis of the merging procedure for the MSU daily temperature series. *J Clim* 11:2016–2041
- Christy JR, Spencer RW, Braswell WD (2000) MSU tropospheric temperatures: dataset construction and radiosonde comparisons. *J Atmos Ocean Technol* 17:1153–1170
- Christy JR, Spencer RW, Norris WB, Braswell WD, Parker DE (2003) Error estimates of version 5.0 of MSU-AMSU bulk atmospheric temperatures. *J Atmos Ocean Technol* 20(5):613–629
- Daley R (1991) *Atmospheric data analysis*. Cambridge University Press, Cambridge
- Dole RM, Hoerling M, Schubert S (eds) (2008) *Reanalysis of historical climate data for key atmospheric features: implications for attribution of causes of observed change*. A report by the U.S. Climate Change Science Program (CCSP) and the Subcommittee on Global Change Research. National Oceanic and Atmospheric Administration, National Climatic Data Center, Asheville, NC, 156 pp
- Elliot WP, Gaffen DJ (1991) On the utility of radiosonde humidity archives for climate studies. *Bull Am Meteorol Soc* 72:1507–1520
- Emanuel K (2005) Increasing destructiveness of tropical cyclones over the past 30 years. *Nature* 436:686–688
- Fearnside PM, Laurance WF (2003) Determination of deforestation rates of the world's humid tropical forests. *Science* 299:10–15
- Flores A, Ruffini G, Rius A (2000) 4D tropospheric tomography using GPS slant wet delay. *Ann Geophys* 18:223–234
- Foelsche U, Kirchengast G, Steiner AK (2006a) *Atmosphere and climate. Studies by occultation methods*. Springer, Berlin
- Foelsche U, Gobiet A, Steiner AK, Borsche M, Wickert J, Schmidt T, Kirchengast G (2006b) Global climatologies based on radio occultation data: the CHAMPCLIM project. In: Foelsche U, Kirchengast G, Steiner A (eds) *Atmosphere and climate studies by occultation methods*. Springer, Berlin, pp 303–314
- Free M, Seidel DJ (2005) Causes of differing temperature trends in radiosonde upper air data sets. *J Geophys Res* 110. doi:[10.1029/2004JD005481](https://doi.org/10.1029/2004JD005481)
- Gibbs HK, Brown S, Niles JO, Foley JA (2007) Monitoring and estimating tropical forest carbon stocks: making REDD a reality. *Environ Res Lett* 2:23–45
- Hammond WC, Brooks BA, Bürgmann R, Heaton T, Jackson M, Lowry AR, and Anandakrishnan S (2010) The scientific value of high-rate, low-latency GPS data. A white paper
- Hammond WC, Brooks BA, Bürgmann R, Heaton T, Jackson M, Lowry AR, Anandakrishnan S (2011) Scientific value of real-time global positioning system data. *Eos* 92(15):125–126. doi:[10.1029/2011EO150001](https://doi.org/10.1029/2011EO150001)
- Hanssen RF, Weckwerth TM, Zebker HA, Klees R (1999) High-resolution water vapour mapping from interferometric radar measurements. *Science* 283:1297–1299
- Healey SB, Thépaut JN (2006) Assimilation experiment with CHAMP GPS radio occultation measurements. *Quart J R Meteorol Soc* 132:605–623. doi:[10.1256/qj.04.182](https://doi.org/10.1256/qj.04.182)
- Healey SB, Jupp AM, Marquardt C (2005) Forecast impact experiment with GPS radio occultation measurements. *Geophys Res Lett* 32: L03804.1–L03804.4
- Highwood EJ, Hoskins BJ, Berrisford P (2000) Properties of the Arctic tropopause. *Meteorol Soc* 126:1515–1532
- Houghton RA (2005) Above ground forest biomass and the global carbon balance. *Global Change Biol* 11:945–958
- IPCC (Intergovernmental Panel on Climate Change) (2001) *Climate change 2001: the scientific basis*. Cambridge University Press, Cambridge, 881 pp
- IPCC (Intergovernmental Panel on Climate Change) (2007) *Contribution of Working Group I to the fourth assessment report*
- Jallow BP, Barrow MKA, Leatherman SP (1996) Vulnerability of the coastal zone of the Gambia to sea level rise and development of response options. *Clim Res* 6:165–177
- Jiang H, Apps MJ, Peng CH, Zhang YL, Liu JX (2002) Modelling the influence of harvesting on Chinese boreal forest carbon dynamics. *For Ecol Manag* 169:65–82

- Kalnay E (2003) Atmospheric modeling, data assimilation and predictability. Cambridge University Press, Cambridge
- Khandu, Awange JL, Wickert J, Schmidt T, Sharifi MA, Heck B, Fleming K (2010) GNSS remote sensing of the Australian tropopause. *Climatic Change* 105(3-4): 597-618, doi:[10.1007/s10584-010-9894-6](https://doi.org/10.1007/s10584-010-9894-6)
- Krabill WE, Hanna P, Huybrechts W, Abdalati J, Cappelen B, Csatho B, Frefick E, Manizade S, Martin C, Sonntag J, Swift R, Thomas R, Yungel J (2004) Greenland ice sheet: increased coastal thinning. *Geophys Res Lett* 31:L24402. doi: [10.1029/2004GL021533](https://doi.org/10.1029/2004GL021533)
- Kumi-Boateng B (2012) A spatio-temporal based estimation of vegetation changes in the Tarkwa mining area of Ghana. Doctor of Philosophy. Dissertation, University of Mines and Technology, Ghana, 165 pp
- Kuo Y-H, Sokolovski SV, Anthens RA, Vandenberghe F (2000) Assimilation of the GPS radio occultation data for numerical weather prediction. *Terr Atmos Ocean Sci* 11:157-186
- Kursinski ER, Hajj GA, Schofield JT, Linfield RP, Hardy KR (1997) Observing Earth's atmosphere with radio occultation measurements using global positioning system. *J Geophys Res* 102(D19): 23429-23465
- Le Toan T, Ribbes F, Floury N, Wang LF, Ding KH, Kong JA, Fujita M, Kurosu T (1997) Rice crop mapping and monitoring using ERS-1 data based on experiment and modeling results. *IEEE Trans Geosci Remote Sens* 35:41-56
- Leroy SS (1997) Measurements of geopotential heights by GPS radio occultation. *J Geophys Res* 102:6971-6986
- Leroy SS, Dykema JA, Anderson JG (2006) Climate benchmarking using GNSS occultation. In: Foelsche U, Kirchengast G, Steiner A (eds) *Atmosphere and climate studies by occultation methods*. Springer, Berlin, pp 287-301
- Li XY, Xu HY, Sun YL, Zhang DS, Yang ZP (2007) Lake-level change and water balance analysis at Lake Qinghai, West China during recent decades. *Water Resour Manag* 21:1505-1516. doi:[10.1007/s11269-006-9096-1](https://doi.org/10.1007/s11269-006-9096-1)
- Magadza CHD (1996) Climate change: some likely multiple impacts in southern Africa. In: Downing TE (ed) *Climate change and world food security*. Springer, Heidelberg, pp 449-483
- Malhi Y, Grace J (2000) Tropical forests and atmospheric carbon dioxide. *Trends Ecol Evol* 15:332-337
- Manneh A (1997) Vulnerability of the water resources sector of The Gambia to climate change. In: Republic of the Gambia: final report of The Gambia/U.S. Country study program project on assessment of the vulnerability of the major economic sectors of the Gambia to the projected climate change. Banjul, The Gambia (unpublished)
- Martens WJM (1998) Health impacts of climate change and ozone depletion: an ecoepidemiologic modeling approach. *Environ Health Perspect* 106:241-251
- Martens WJM, Niessen LW, Rotmans J, Jetten TH, McMichael AJ (1995) Potential impact of global climate change on malaria risk. *Environ Health Perspect* 103:458-464
- Mears C, Schabel M, Wents F (2003) A reanalysis of MSU channel 2 tropospheric temperature trend. *J Clim* 16(22):3560-3664
- Melbourne WG, Davis ES, Duncan CB, Hajj GA, Hardy K, Kursinski R, Mechan TK, Young LE, Yunck TP (1994) The application of spaceborne GPS to atmospheric limb sounding and global change monitoring. JPL Publication, Pasadena, pp 94-18
- Mistry VV, Conway D (2003) Remote forcing of East African rainfall and relationships with fluctuations in levels of Lake Victoria. *Int J Clim* 23:67-89
- Mitrovica JX, Gomez N, Clark PU (2009) The sea-level fingerprint of West Antarctic collapse. *Science* 323(5915):753. doi:[10.1126/science.1166510](https://doi.org/10.1126/science.1166510)
- Myneni RB, Dong JR, Tucker CJ, Kaufmann RK, Kauppi PE, Liski J, Zhou L, Alexeyev V, Huges MK (2001) A large carbon sink in the woody biomass of Northern forest. *Proc Natl Acad Sci* 98:14784-14789
- Nagurny AP (1998) Climatic characteristics of the tropopause over the Arctic Basin. *Ann Geophys* 16:110-115

- Nyakwada W (2000) The use of weather and climate forecasts by rural people to enhance food production. In: Akunda E, Mango C, Oteng'i SBB et al (eds) Sustainable environmental management for poverty alleviation in the Lake Victoria Basin. KMFRI, pp 38–42
- Okoola RE (2000) Climate change as related to food production for the alleviation of rural poverty in the Lake basin region. In: Akunda E, Mango C, Oteng'i SBB et al (eds) Sustainable environmental management for poverty alleviation in the Lake Victoria Basin. KMFRI, pp 43–45
- Otengi SBB (2000) Weather and climate hazards that affect food production in the Lake Victoria Basin. In: Akunda E, Mango C, Oteng'i SBB et al (eds) Sustainable environmental management for poverty alleviation in the Lake Victoria Basin, Kisii, 3–5 Oct 1995. KMFRI, pp 24–27
- Pan LL, Randel WJ, Gary BL, Mahony MJ, Hintsä EJ (2004) Definitions and sharpness of the extratropical tropopause: a trace gas perspective. *J Geophys Res* 109. doi:[10.1029/2004JD004982](https://doi.org/10.1029/2004JD004982)
- Parker DE, Gorden M, Cullum DPN, Sexton DMH, Folland CK, Rayner N (1997) A new global gridded radiosonde temperature database and recent temperature trends. *Geophys Res Lett* 24:1499–1502
- Patenaude G, Milne R, Dawson TP (2005) Synthesis of remote sensing approaches for forest carbon estimation: reporting to the Kyoto Protocol. *Environ Sci Policy* 8(2):161–178
- Phillips S (2006) Water crisis. *COSMOS*, issue 9, June 2006. <http://www.cosmosmagazine.com/issues/2006/9/>
- Pittcock B (2003) Climate change: an Australian guide to the science and potential impacts. Climate change, Australian Greenhouse Office, Canberra
- Poli P (2006) Assimilation of GNSS radio occultation data into numerical weather prediction. In: Foelsche U, Kirchengast G, Steiner A (eds) Atmosphere and climate studies by occultation methods. Springer, Berlin, pp 195–204
- Poli P, Pailleux J, Ducrocq V, Moll P, Rabier F, Mauprivez M, Dufour S, Grondin M, Lechat-Carvalho F, De Latour A, Issler J, Ries L (2008) Weather report. Meteorological applications of GNSS from space and on the ground. *InsideGNSS* 3(8):30–39
- Prince SD, Goward S (1995) Global primary production: a remote sensing approach. *J Biogeogr* 22:815–835
- Randall DA, Tjemkes S (1991) Clouds, the Earth's radiation budget and the hydrological cycle. *Palaeogeogr Palaeoclimatol Palaeoecol* 90:3–9
- Randel WJ, Wu F, Gaffen DJ (2000) Interannual variability of the tropical tropopause derived from radiosonde data and NCEP reanalyses. *J Geophys Res* 105:15509–15524
- Ranson KJ, Sun G, Weishample JF, Knox RG (1997) Forest biomass from combined ecosystem and radar backscatter. *Remote Sens Environ* 59:118–133
- Richards TS, Gallego J, Achard F (2000) Sampling for forest cover change assessment at the pantropical scale. *Int J Remote Sens* 21:1473–1490
- Richardson LF (2007) Weather prediction by numerical process, 2nd edn. Cambridge Mathematical Library (the first edition appeared in 1922), Cambridge
- Rocken C, Ware R, Hove TV, Solheim F, Alber C, Johnson J, Belvis M, Businger S (1993) Sensing atmospheric water vapour with the global positioning system. *Geophys Res Lett* 20(23):2631–2634
- Rocken C, Anthes R, Exner M, Hunt D, Sokolovski S, Ware R, Gorbunov M, Schreiner S, Feng D, Hermann B, Kuo Y-H, Zou X (1997) Analysis and validation of GPS/MET data in the neutral atmosphere. *J Geophys Res* 102:29849–29860
- Rosenqvist Å, Imhoff M, Milne A, Dobson C (eds) (1999) Remote sensing and the Kyoto Protocol: a review of available and future technology for monitoring treaty compliance. Report of a workshop, Ann Arbor, Michigan, USA, 20–22 Oct 1999
- Rosenqvist A, Milne T, Lucas R, Imhoff M, Dobson C (2003) A review of remote sensing technology in support of the Kyoto Protocol. *Environ Sci Policy* 6(5):441–455
- Santer BD, Wehner MF, Wigley TML, Sausen R, Meehl GA, Taylor KE, Ammann C, Arblaster J, Washington WM, Boyle JS, Bruggemann W (2003) Contributions of anthropogenic and natural forcing to recent tropopause height changes. *Science* 301:479–483

- Santer BD, Wigley TML, Simmons AJ, Kallberg PW, Kelly GA, Uppala SM, Ammann C, Boyle JS, Bruggemann W, Doutriaux C, Fiorino M, Mears C, Meehl GA, Sausen R, Taylor KE, Washington WM, Wehner MF, Wentz FJ (2004) Identification of anthropogenic climate change using a second-generation reanalysis. *J Geophys Res* 109. doi:[10.1029/2004JD005075](https://doi.org/10.1029/2004JD005075)
- Sausen R, Santer BD (2003) Use of changes in tropopause height to detect influences on climate. *Meteorol Zeits* 12(3):131–136
- Schmidt T, Heise S, Wickert J, Beyerle G, Reigber C (2005) GPS radio occultation with CHAMP and SAC-C: global monitoring of thermal tropopause parameters. *Atmos Chem Phys* 5:1473–1488
- Schmidt T, Wickert J, Beyerle G, Heise S (2008) Global tropopause height trends estimated from GPS radio occultation data. *Geophys Res Lett* 35:L11806. doi:[10.1029/2008GL034012](https://doi.org/10.1029/2008GL034012)
- Schröder T, Leroy S, Stendel M, Kaas E (2003) Stratospheric temperatures probed by microwave sounding units or by occultation of the global positioning system. *Geophys Res Lett* 30. doi:[10.1029/2003GL017588](https://doi.org/10.1029/2003GL017588)
- Seidel DJ, Randel WJ (2006) Variability and trends in the global tropopause estimated from radiosonde data. *J Geophys Res* 111. doi:[10.1029/2006JD007363](https://doi.org/10.1029/2006JD007363)
- Seidel JD, Ross RJ, Angell JK, Reid GC (2001) Climatological characteristics of the tropical tropopause as revealed by radiosondes. *J Geophys Res* 106:7857–7878
- Shea DJ, Wifley SJ, Stern IR, Hoar TJ (1994) An introduction to atmospheric and oceanographic data. NCAR Tech. Note
- Slaymaker O, Kelly REJ (2007) The cryosphere and global environmental change (Environmental systems and global change series), 1 edn. Wiley-Blackwell, New York
- Spencer RW, Christy JR, Grody NC (1990) Global atmospheric temperature monitoring with satellite microwave measurements: methods and results 1979–84. *J Clim* 3:1111–1128
- Steffen W, Sanderson A, Tyson PD, Jger J, Matson PA, Moore BIII, Oldfield F, Richardson K, Schellnhuber HJ, Turner BLII, Wasson RJ (2005) Global change and the earth system: a planet under pressure. Springer, Berlin
- Stendel M (2006) Monitoring climate variability and change by means of GNSS data. In: Foelsche U, Kirchengast G, Steiner A (eds) *Atmosphere and climate studies by occultation methods*. Springer, Berlin, pp 275–285
- Syndergaard S, Kuo Y-H, Lohmann MS (2006) Observation operators for the assimilation of occultation data into atmospheric models: a review. In: Foelsche U, Kirchengast G, Steiner A (eds) *Atmosphere and climate studies by occultation methods*. Springer, Berlin, pp 205–224
- Talagrand O (1997) Assimilation of observations, an introduction. *J Meteorol Soc Jpn (Spl Issue)* 75(1B):191–209
- Tao W (2008) Near real-time GPS PPP-inferred water vapour system development and evaluation. MSc thesis, UCGE Reports No. 20275. <http://www.geomatics.ucalgary.ca/research/publications>. Accessed 26 Aug 2009
- Trenberth K, Guillemot C (1996) Evaluation of the atmospheric moisture and hydrological cycle in the NCEP Reanalyses. NCAR Technical Note TN-430, Dec 1996
- Tutu BD (2008) Assessing the effects of land-use/cover change on ecosystem services in Ejisu-Juaben District, Ghana. MSc thesis, International Institute for Geo-Information Science and Earth Observation, Enschede, 88 pp
- Ummenhofer C, England M, McIntosh P, Meyers G, Pook M, Risbey J, Gupta A, Taschetto A (2009) What causes southeast Australia's worst droughts? *Geophys Res Lett* 36:L04706. doi:[10.1029/2008GL036801](https://doi.org/10.1029/2008GL036801)
- UN (1998) Kyoto Protocol to the United Nations framework convention on climate change. <http://unfccc.int/resource/docs/convkp/kpeng.pdf>. Accessed 14 July 2010
- UNFCCC (2007) Kyoto Protocol reference manual on accounting of emissions and assigned amounts. Framework convention on climate change. http://unfccc.int/kyoto_protocol/items/2830.php
- Uriel K (1998) Landscape ecology and epidemiology of vector-borne diseases: tools for spatial analysis. *J Med Entomol* 35(4):435–445

- Varotsos C, Cartalis C, Vlamakis A, Tzanis C, Keramitsoglou I (2004) The long-term coupling between column ozone and tropopause properties. *J Clim* 17:3843–3854
- Velicogna I (2009) Increasing rates of ice mass loss from the Greenland and Antarctic ice sheets revealed by GRACE. *Geophys Res Lett* 36:L19503. doi:[10.1029/2009GL040222](https://doi.org/10.1029/2009GL040222)
- Vinnikov KY, Grody NC (2003) Global warming trend of mean tropospheric temperature observed by satellites. *Science* 302:269–272
- Ware H, Fulker D, Stein S, Anderson D, Avery S, Clerk R, Drogemeier K, Kuettner J, Minster B, Sorooshian S (2000) Real-time national GPS networks: opportunities for atmospheric sensing. *Earth Planet Space* 52:901–905
- Ware R, Exner M, Feng D, Gorbunov M, Hardy K, Herman B et al (1996) GPS sounding of atmosphere from low earth orbit: preliminary results. *Bull Am Meteorol Soc* 77:19–40
- Wickert J, Beyerle G, König K, Heise S, Grunwaldt L, Michalak G, Reigber C, Schmidt T (2005) GPS radio occultation with CHAMP and GRACE: a first look at a new and promising satellite configuration for global atmospheric sounding. *Ann Geophys* 23:653–657
- Wickert J, Michalak G, Schmidt T, Beyerle G, Cheng CZ, Healy SB, Heise S, Huang CY, Jakowski N, Köhler W, Mayer C, Offiler D, Ozawa E, Pavelyev AG, Rothacher M, Tapley B, Arras C (2009) GPS radio occultation: Results from CHAMP, GRACE and FORMOSAT-3/COSMIC. *Terr Atmos Ocean Sci.*, 20:35–50, doi:[10.3319/TAO.2007.12.26.01\(F3C\)](https://doi.org/10.3319/TAO.2007.12.26.01(F3C))
- WMO (1957) Definition of tropopause. World Meteorological Organisation, Geneva
- Yuan LL, Anthes RA, Ware RH, Rocken C, Bonner WD, Bevis MG, Businger S (1993) Sensing climate-change using the global positioning system. *J Geophys Res* 98(D8):14925–14937

Chapter 22

Water Resources

“Several authors, politicians, leaders of international organizations and journalists have cautioned the world community that the increasing scarcity of freshwater resources might lead to national and international conflicts. When relating this to climate change forecasts—most of which indicate that climate change will have a significant impact on the availability of freshwater resources, on water quality, and on the demand for water—this is alarming news for humankind as it threatens human security.”

Molen and Hildering (2005)

22.1 Status and Impact of Diminishing Fresh Water Resources

Fresh water is one of the basic necessities without which human beings cannot survive since water is key to the sustainability of all kinds of lifeforms. Water has multiple uses namely; nutritional, domestic, recreational, navigational, waste disposal and ecological as it is a habitat for living and non-living organisms (biodiversity) etc. And, because it is indispensable to different sectors including manufacturing, agriculture, fisheries, wildlife survival, tourism and hydroelectric power generation, it is a vital factor of economic production. For many countries, most freshwater endowments encompass surface waters, groundwater, wetlands and glaciers. Surface water bodies include lakes, rivers, swamps, springs, dams and water pans dispersed within different basins. In general, people living in the vast arid and semi-arid parts of the world rely heavily on groundwater resources. Furthermore, groundwater is also an important supplementary source of water for many urban households in most developing countries.

At a global scale, although much of the Earth is covered by water, most of it is unsuitable for human consumption, since 96% of it is found in the saline oceans.

According to the U.N., only 2.5 % of the roughly 1.4 billion cubic kilometers of water on Earth is freshwater, and approximately 68.9 % of the freshwater is trapped in glacial ice or permanent snow in mountainous regions—the Arctic and Antarctica. Roughly 30.8 % is groundwater, much of which is inaccessible to humans, and the remainder 0.3 % comprise surface waters in lakes and rivers (UNEP 2002). Of these 0.3 % available for human and animal consumption, much is inaccessible due to unreachable underground locations and depths (Hofman 2004).

Although Rijsberman (2006) argues that at a global scale, and from a supply and demand perspective, it is still debatable whether water scarcity is fact or fiction, it is incontestable that fresh water is increasingly becoming a scarce resource and shortages could drive conflict as well as negatively hit food and energy production (Jury and Vaux 2007) (see Fig. 22.1). Moreover, it is estimated that by 2050, about two billion people will be short of water, a potential cause of conflict (IRIN 2006). So vital are water resources that it is difficult to discuss any monitoring of the environment without it. Evidently, the management of water resources conflicts, focusing on negotiation, mediation and decision-making processes, in order to prevent, manage and resolve water conflicts is emerging as a contemporary and topical research issue.

Physical water scarcity is evident in densely populated arid areas in many parts of Central and West Asia, and North Africa with projected availabilities of less than 1000 m³/capita/year (Rijsberman 2006). This has a wide range of negative impacts and ramifications. For instance, it results in higher incidences of waterborne, water-related or sanitation-related diseases such as malaria, diarrhoea and skin infections. In addition, as has been pointed out before, increasing cases of water conflicts, especially between pastoralist and farming communities along lower and upper river basins, as witnessed in water stressed countries like Kenya (Carolina 2002) (with a renewable fresh water per capita endowment estimated at about 548 m³/capita/year (World Bank 2003)), are also likely to heighten food insecurity. On the gender scale, since women are the primary collectors, users and managers of water for domestic use in most developing countries, water scarcity disproportionately affects them because it is they who have to trek long distances, often all day, in search of water. Against

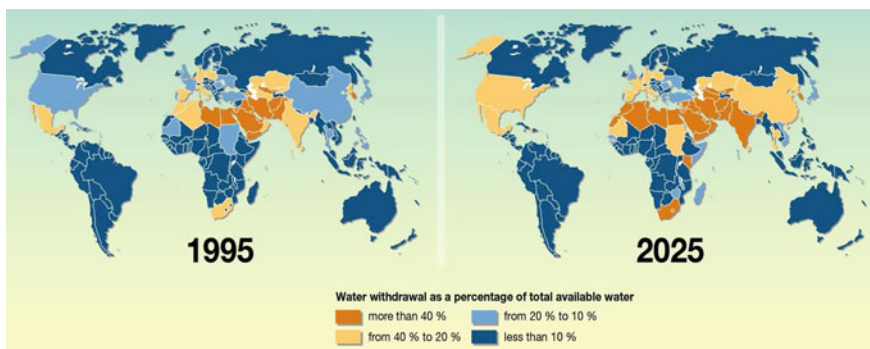


Fig. 22.1 Increased global water stress. *Source* Rekaewicz (2006)

the above background, is the growing realization today that availability of sufficient, accessible and quality potable water is not only a matter of great socio-economic and political importance, but also one of fundamental human rights, see e.g., Birnie and Boyle (1993), Gleick (1999), Zehnder et al. (2003), Schelton (1991) etc.

22.2 Monitoring Variation in Fresh Water Resources

The importance of water as a resource, therefore, calls for sound environmental conservation measures that enhance its protection and management. It is in relation to this that the World Bank, as an emerging priority of its lending framework, decided to broaden the development focus in its 1993 “Water resource management policy paper” to include the *protection* and *management* of water resources in an environmentally sustainable, socially acceptable, and economically efficient manner (World Bank 2003). The protection and management of water resources calls for an elaborate and well established management and monitoring program.

Information about water resources and the environment is inherently geographic. Maps, whether on paper or in digital GIS formats, continue to be the medium for the expression of engineering plans and designs. This is because we are basically concerned about the spatial distribution and character of the land and its waters. Johnson (2009) argues that weather patterns, rainfall and other precipitation, and resultant water runoff are primary driving forces for land development, water supplies, and environmental impacts and pollution. Our water resources systems comprise dams and reservoirs, irrigated lands and canals, water supply collection and distribution systems, sewers and storm water systems, and floodplains. These systems are designed in response to a complex mix of topography and drainage patterns, population and land use, sources of water, and related environmental factors (Johnson 2009).

In general, the planning and engineering design processes used in the development and management of water resources involve different levels of data abstraction. Data are collected and used to characterize the environment at some level of detail, or scale. In seeking to make decisions about plans and designs, data must be collected to describe the resource, and procedures or models must be developed to predict the resultant changes. These data and models help us understand the real world, and this understanding guides our decision making (Johnson 2009).

According to Taylor and Alley (2001), essential components of a water level monitoring program include; *selection of observation wells, determination of the frequency of water level measurements, implementation of quality assurance, and establishment of effective practices for data reporting*. In selecting the observation wells, the authors state that the decisions made about the number and locations of observation wells are crucial to any water-level data collection program (Taylor and Alley 2001). In regard to locations, GNSS satellites could contribute in generating a fast and accurate survey of well location-based data. These data could then be integrated with other information such as water level in a GIS system to enhance the

accessibility of water level data, where the GIS plays the role of depicting the locations of the observed wells relative to pertinent geographic, geologic, or hydrologic features, e.g., Taylor and Alley (2001).

Taylor and Alley (2001) present areas where the monitored ground water levels could be used. Some of these include: determination of the hydraulic properties of aquifers (aquifer tests); mapping of the altitude of the water table or potentiometric surface; monitoring of the changes in groundwater recharge and storage; monitoring of the effects of climatic variability; monitoring of the regional effects of groundwater development; statistical analysis of the water level trends; monitoring of the changes in groundwater flow directions; monitoring of the groundwater and surface water interaction; and numerical (computer) modeling of groundwater flow or contaminant transport.

Information on the spatial and temporal behavior of terrestrial water storage, therefore, is crucial for the management of local, regional and global water resources. This information will (Rieser et al. 2010):

- Enhance sustainable utilization of water resources by, e.g., farmers, urban consumers, miners, etc.
- Guide water resource managers and policy makers in the formulation of policies governing its sustainable use, conservation and management. In particular, state water managers are more informed in regulating the utilization of water, e.g., for industrial and irrigation purposes.
- Benefit local environmental monitoring, management policies and practices that ensures a balance between sustainable utilization and environmental conservation and protection. Changes in water availability impacts upon the environment in several ways, e.g., any significant imbalance in its level affects the ecological system by influencing salinity, land subsidence and the vulnerability of wetlands ecosystem among others.
- Benefit various government agencies at various levels (national, provincial, and local) by providing data that enhances and compliments their work. Such agencies include departments of *water*, *agriculture*, *weather forecasting* and *climate* studies, and so forth.

The conservation and management of water is of paramount importance in areas with arid or semi-arid climates, which include many parts of Australia, especially in times of severe drought, as experienced in Murray Darling Basin (Rieser et al. 2010). In 2006, Australia faced its worst drought in a century as seen from daily reports that were emerging in both the local and international media. A more grim picture of the future of the water situation for Australia was to follow from the IPCC (2007) report, which stated that Australia's water crisis will worsen in the coming years due to drought! There clearly exists an urgent need to have efficient monitoring technique(s). One such technique that monitors changes in stored water, is the use of GRACE satellites (Sect. 20.3.3), which is demonstrated in the examples to follow.

Timely and precise information on the changes in stored water at smaller (localized) scales of economical values, e.g., urban consumption, agriculture, industries,

and mining to within 10–14 days (so far achievable by GRACE satellite) will enhance sustainable conservation and management of this precious *dwindling* resource.

The availability of techniques that delivers information on the changes in stored water at a more local scale, is the first step towards realizing an efficient water society. Water resource managers are able to make decisions based on timely and accurate knowledge; thereby saving considerable resources that are often spent as a penalty of inefficient decisions based on a lack of information. In the south-western wheat belt of Australia, for example, accurate knowledge of changes in stored water will be beneficial to the sustainable utilization of water, while at the same time realizing the economic contribution of wheat farming to the overall Gross Domestic Product (GDP). A blind focus on the GDP's growth without paying attention to the state of salient contributors such as water stored in aquifers is detrimental, since a fall in the amount of the available water in such areas would definitely mean reduced yields.

Since the entire system of stored water is coupled within the hydrological cycle (Fig. 22.2), hydrologists will be in a position to better understand their local hydrological cycle, thanks to information at localized levels. Hydrologists will also be able to use such information to refine and calibrate local-scale models, e.g., rainfall runoff models (Ellett et al. 2005), for further improvement in their hydrological cycles. This will also contribute to our understanding of the impacts of climate change on regional and global hydrological cycles. For the geodetic community, knowledge of the changes in local stored water is vital for assessing the impact of groundwater on the stability of continuously operating GNSS monuments (e.g., Fig. 6.12 on p. 94), which in turn affects the overall accuracy of geodetic networks (see Sect. 6.5).

Environmental studies also have a chance of greatly benefiting from information about changes in stored water. It is widely acknowledged that stored water (surface and groundwater) plays a key role in sustaining natural biodiversity and the functioning of the environment as a whole. Knowledge of the changes in water level is therefore essential for the very survival of the entire ecosystem, which could be adversely affected by extreme change in stored water. In wetlands, for example, some vegetation and ecosystems have been known to respond to water level fluctuations (Casanova 1994).

Accurate monitoring of changes in stored water at smaller wetland scales will thus help in the preservation and conservation of such wetland ecosystems. Changes in water level also brings with it environmental phenomena such as salinity, compacting of aquifers due to the removal of water causing land subsidence, and changes in the properties of the top 5 cm of soil. Information on changes in stored water thus contributes enormously to the environmental conservation and protection. Remote sensing and GIS can be used to monitor the water quality. This is possible by employing multispectral, multitemporal image data and analyzing parameters such as the distribution of suspended sediment, turbidity and chlorophyll. These indicators can be determined through regression analysis.

22.3 Gravity Field and Changes in Stored Water

In Sect. 6.6.1, we introduced the concept of the *geoid* (Fig. 6.18 on p. 101) as a fundamental physical surface to which all observations are referred to if they depend on *gravity*, and whose shape is influenced by inhomogeneous mass distribution within the interior of the Earth (Leick 2004, p. 29). In the discussion that follows, the concept of *gravity field variations* discussed in Sect. 20.3 is related to hydrological processes. Measurements of the time-varying gravity field by LEO satellites, e.g., GRACE discussed in Sect. 20.3.3 are the key to the contribution of space monitoring of changes in water levels at basin scales. Such techniques now enable the monitoring of groundwater recharge, which is the most important element in groundwater resources management and could also be applicable to monitoring salinity management measures at the catchment level (see Sect. 23.4.2). For example, in 2009, GRACE satellites showed that north-west of India's aquifers had fallen at a rate of 0.3048 m yr^{-1} (a loss of about 109 km^3 per year) between 2002 and 2008.¹

22.3.1 Gravity Field Changes and the Hydrological Processes

The hydrological cycle (Fig. 22.2) refers to the pathway of water in nature, as it moves in its different phases through the atmosphere, down over and through land, to the ocean and back to the atmosphere (Brutsaert 2005). The associated variations in gravity field are therefore caused, e.g., by

- the redistribution of water in the oceans, including e.g., El Niño and Southern Oscillation (ENSO) events,
- movement of water vapour and other components in the atmosphere,
- seasonal rainfall; snow and subsequent drying and melting,
- groundwater extraction, or
- drying and filling of lakes, rivers, and reservoirs.

22.3.2 Sensing Changes in Stored Water Using Temporal Gravity Field

The potential of using the relationship between temporal gravity changes and hydrology (Fig. 22.2) was first recognized by Montgomery (1971) who estimated specific yield through a correlation between gravity and water-level changes (Leirião et al. 2009). In 1977, Lambert and Beaumont (1977) used a gravity meter to correlate groundwater fluctuations and temporal changes in the Earth's gravity field. Goodkind (1986) recorded observations from seven super conducting gravimetric stations

¹ The Economist, September 12th 2009, pp. 27–29: Briefing India's water crisis.

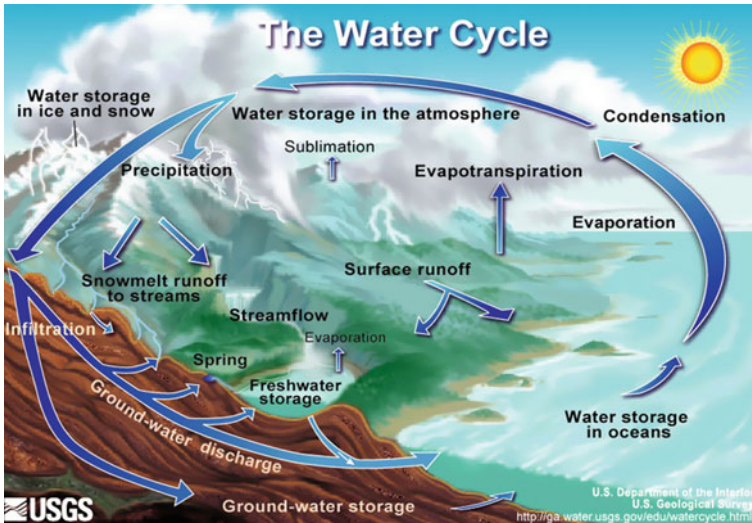


Fig. 22.2 Components of hydrological cycle that lead to temporal variations in the gravity field.
 Source US Geological Survey (USGS)

to examine non-tidal variations in gravity and noted that at one of the stations (Geysers geothermal station), much of the variation could be correlated with rainfall and seismic activity. Such measurements had not been possible before the advent of superconducting gravimeters, thus providing evidence of the existence of temporal variation in gravity.

In 1995, while estimating the atmospheric effects on gravity observations around Kyoto, Mukai et al. (1995) noted that changes in gravity around the station could have been caused by changes in underground water. In the same year, Pool and Eychaner (1995) assessed the utility of temporal gravity-field surveys to directly measure *aquifer-storage* changes and reported gravity changes of around $100\text{--}134\ \mu\text{Gal}$, equivalent to $2.4\text{--}3.2\text{m}$ of water column, considering infinitely extended sheet approximation. Their results from the analysis of changes in stored water in the aquifer indicated an increase in the gravity field of $158 \pm 6\ \mu\text{Gal}$ when the water table rose by about 17.7m , providing further evidence of the possibility of using temporal gravity-field surveys to monitor changes in stored aquifer water. In fact, according to Bower and Courtier (1998) who analyzed the effect of precipitation on gravity and well-levels at a Canadian absolute gravity site, 90% of the gravity variation was found to be due to the effects of precipitation, evapotranspiration and snow-melt.

The last decade has also recorded increased use of temporal gravity field studies in monitoring changes in stored water, see e.g., (Ellett et al. 2006). It saw the beginning of satellite missions dedicated to monitoring temporal variations in the gravity field. Smith et al. (2005) investigated the ability of ground-based gravity meters to monitor changes in soil moisture storage.

Moving from local tests to regional, a different application of gravity surveys was investigated by Damiata and Lee (2002), who simulated the gravitational response to aquifer hydraulic testing. The synthetic system was composed of an unconfined shallow aquifer and the purpose of the investigation was to assess the potential of the gravity measurements for detecting groundwater extraction. Draw-down due to pumping causes a decrease in mass and consequently in gravity measured at the surface. The results showed that the gravitational response to aquifer testing could be used to monitor the spatial development of the draw-down cone. For the configuration considered in the investigation, the signal was of the order of tens of μGals and could be detected up to several hundred meters away from the pumping well.

Water storage changes, such as changes in soil moisture, snow and ice cover, surface and groundwater, including deep aquifers, can be monitored either by in-situ observations or indirectly through changes in gravity (Tapley et al. 2004). While in-situ observations provide valuable localized information, they suffer from limited spatial coverage for regional to continent-wide studies (Rodell et al. 2004). Any change in water storage also manifests itself in a change in the gravity field. This property can be used to infer water-storage changes from time-variable gravity observations as demonstrated by Rodell and Famiglietti (1999) for 20 globally distributed drainage basins of sizes varying from 130,000 to 5,782,000 km^2 to assess the detectability of hydrological signals with respect to temporal and spatial variations. Space-borne techniques can provide time-variable gravity observations on a regional and global scale, thus allowing for large-scale water storage monitoring and the ability to close the 'gaps' between locally limited in-situ observations (Ellett et al. 2005).

Since the launch of the GRACE satellite mission in 2002 (see Sect. 20.3.3), a new powerful tool for studying temporal gravity field changes has become available, and numerous articles assessing the potential of GRACE recovering hydrological signals have been published, see e.g., Awange et al. (2009, and the references therein). Tapley et al. (2004) provided early results of the application of the GRACE products for detecting hydrological signals in the Amazon-Orinoco basin. Following these results, numerous other authors have subsequently applied GRACE to detect hydrological signals in various situations and locations, see references in (Awange et al. 2009).

For instance, Ramillien et al. (2004, 2005) and Andersen et al. (2005) investigated the potential of inferring inter-annual gravity field changes caused by continental water storage changes from GRACE observations between 2002 and 2003, and compared these changes to the output from four global hydrological models. It was possible to correlate large scale hydrological events with the estimated change in the gravity field for certain areas of the world to an accuracy of 0.4 Gal, corresponding to 9 mm of water, see also Andersen et al. (2005), Neumeier et al. (2006) and Yan et al. (2002).

Syed et al. (2008) examined total basin discharge for the Amazon-Orinoco and Mississippi river basins from GRACE, while Rodell et al. (2006) estimated groundwater storage changes in the Mississippi basin. Crowley et al. (2006) estimated hydrological signals in the Congo basin, while Schmidt et al. (2006) and Swenson et al. (2003, 2006) used GRACE to observe changes in continental water storage.

Winsemius et al. (2006) compared hydrological model outputs for the Zambezi River Basin with estimates derived from GRACE. Monthly storage depths produced by the hydrological model displayed larger amplitudes and were partly out of phase compared to the estimates based on GRACE data. Likely reasons included leakage produced by the spatial filtering used in the GRACE data, and the difficulty to identify the time of satellite overpass as opposed to simply averaging over the whole period. Awange et al. (2008) used GRACE to study the fall of Lake Victoria's water level in Africa. This last example will be elaborated upon in more detail in Sect. 22.4.1.2.

As already discussed in Sect. 20.3.3, GRACE satellites detect changes in the Earth's gravity field by measuring changes in the distance between the two satellites at a 0.1 Hz sampling frequency. The variation in the distance between the two twin satellites caused by gravitational variations above, upon, and within the Earth all have an effect on the satellites. This variation in gravity could be due to *rapid* or *slow* changes caused, for example by the redistribution of water in the oceans, the movement of water vapor and other components in the atmosphere, the tidal effect of the Sun and Moon, and the displacement of the material by earthquakes and glacial isostatic adjustment. The data therefore must be processed to isolate these effects so as to retain only those which correspond to the process of interest, in this case, terrestrial water storage changes, see e.g., Bettadpur (2007). Equation (20.33) is used to compute changes in stored water. In the following examples, the applications of GRACE satellites to monitor stored water resources are illustrated. It should be emphasized once more that GNSS do not directly measure changes in water storage but contributes as discussed in Sect. 20.3.3.

22.4 Examples of Geoinformatics-Based Monitoring of Changes in Stored Water

22.4.1 The Nile Basin

The Nile Basin (Fig. 22.3) is one of the Earth's most impressive examples of the influence of topography and climate on the flow conditions of a water system. The Nile has two major tributaries, the White Nile and the Blue Nile, the latter being the source of most of the river's water. The White Nile rises in the Great Lakes region of Eastern Africa, and flows northwards through Uganda and the South Sudan. The Blue Nile starts at Lake Tana in the Ethiopian highlands, flowing into Sudan from the southeast and meets the White Nile at Khartoum in Sudan. From there, the Nile passes through Egypt and ends its journey by flowing into the Mediterranean Sea.

A basin as large as the Nile, which crosses such a wide latitude range (from $\sim 5^\circ\text{S}$ to ca. 31°N) cannot be expected to experience homogeneous climatic and rainfall patterns over its extent. In addition, variations in the geology and soils of the basin strongly influence groundwater availability. Significant rainwater deficits and the variable duration of the rainy seasons over yearly to decadal time scales results in

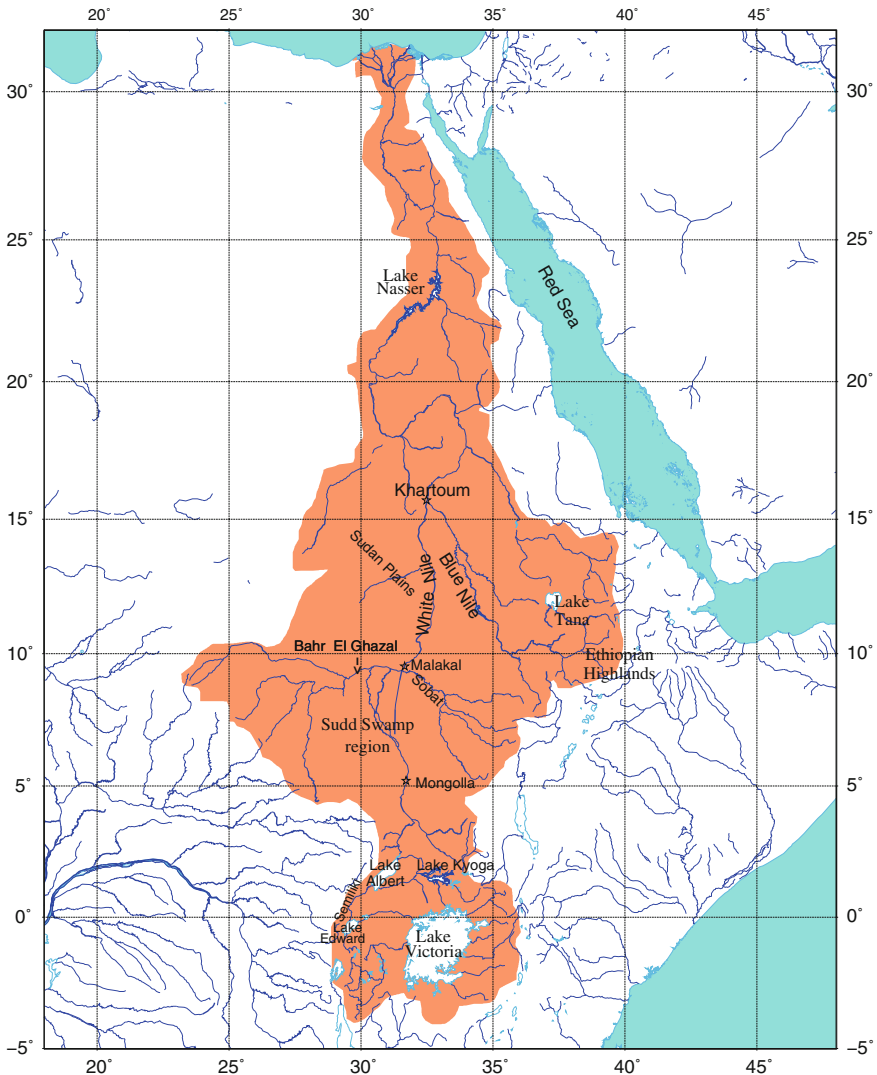


Fig. 22.3 The Nile basin (brown shaded region) with the major features and place names as discussed in the text. *Source* Awange (2012)

hydrological deficits that are not necessarily reflected in a direct response of the base flow, e.g., Owor et al. (2009).

The East African lake region includes the countries of Burundi, Rwanda, Uganda, Kenya and Tanzania, and is the home to Lake Victoria, the world's second largest freshwater lake, and the source of White Nile (Awange JL and Ong'ang'a 2006). From Lake Victoria, the waters are discharged to Lake Kyoga, which also receives water from its surrounding 75,000 km² catchment before flowing on to Lake Albert.

In addition to the waters received from Lake Kyoga, Lake Albert is supplied by its upstream Semiliki basin and the Lake Edward sub-basin (Fig. 22.3). Together, Lakes Edward, Albert, and George form the western edge of the Nile Basin, comprising an area of 48,000 km², of which 7,800 km² is open water (Yates and Strzepek 1998). In the Sudd swamp region, the supply to the Nile benefits from two other basins, the Bahr-El-Ghazal (500,000 km²) to the west and the Sobat (150,000 km²) to the east, before exiting at Malakal.

The Ethiopian highlands are comprised of twelve significant sub-basins aggregated into four primary basins; Lake Tana (200,000 km², the main headwaters of Blue Nile, although it contributes less than 10 % of the total Blue Nile flow), the upper Blue (150,000 km²), the lower Blue (60,000 km²), and the Dinda-Raghad (70,000 km²). All together, they cover almost 480,000 km² and contribute approximately 65 % of the river Nile's total water (Yates and Strzepek 1998).

Lake Nasser region: The Egyptian desert starts from Khartoum, where the Nile flows northward towards Egypt through Lake Nasser (formed by the Aswan dam) and then to the Mediterranean Sea. Yates and Strzepek (1998) reported a net loss of water between the joining of the Atbara river with the Nile north of Khartoum, and Lake Nasser due to evaporation and seepage.

22.4.1.1 Challenges Facing the Basin's Waters

The Nile river basin is one of the largest in the world, with an area of about 3,400,000 km² (almost one-tenth of Africa) and traversing some 6,500 km from south to north as it winds its way across the boundaries of eleven countries: Tanzania, Uganda, Kenya, Rwanda, Burundi, Democratic Republic of Congo (DRC), Eritrea, Ethiopia, Sudan, South Sudan, and Egypt, e.g., Sahin (1985). As it flows through these countries, it supports a livelihoods of over 200 million people.

The Nile's water resources, however, have come under threat from both anthropogenic and natural factors, e.g., Hamouda et al. (2009). Anthropogenic influences have been fueled by the increasing human population that has put pressure on domestic water needs, the supply of hydroelectric power, all coupled with the need to sustain economic growth. However, not only are the demands on water increasing, but the available water supplies appear to be decreasing, with environmental degradation of the upper Blue Nile catchment having increased throughout the 1980s (Whittington and McClelland 1992). Whittington and McClelland (1992) found that about 86 % of the annual Nile river flow into Egypt originates from Ethiopia, and warn of significant implications for Egypt and Sudan should Ethiopia undertake any potential extractions; this issue emphasizes the need for cooperation between the three Blue Nile riparian states.

Natural factors include the changing climate, which has been the subject of numerous studies, e.g., (Yates and Strzepek 1998, and the references therein). Therefore, a combination of human population growth, unsustainable water usage and development, and desertification are just some of the factors that threaten the Nile's ability to supply crucially needed water to the people of the basin.

The present-day state of the stored water variations and their relations to climate variability (e.g., El Niño and Southern Oscillation (ENSO) and the Indian Ocean Dipole (IOD)) in the Nile Basin are, however, also not well understood. Most studies dealing with the Nile Basin to date, however, have dealt mainly with modeling the impacts of climate change (e.g., Beyene et al. (2010), Conway (2005)), with very little being reported on how to monitor the spatial and temporal variations in the stored water (surface, groundwater and soil moisture) of the basin in a holistic manner, and linking them to climate variability. The reason for such few studies, e.g., Bonsor et al. (2010), Senay et al. (2009) has been partly attributed to its large size, as well as the lack of appropriate monitoring techniques that could cover such a vast spatial extent. For instance, the hydrological water balance involves the flow of surface water, the movement of deeper groundwater, and the coupling of the land, ocean and atmosphere through evaporation and precipitation. Monitoring these components requires an accuracy and completeness of geographical data coverage that challenges conventional measurement capabilities.

Using GRACE, GLDAS (Global Land Data Assimilation System),² and TRMM (Tropical Rainfall Measuring Mission)³ data for the period 2002–2011, Independent Component Analysis (ICA) method, e.g., (Forootan and Kusche 2011), is applied in the examples below to localize the Nile Basin's hydrological signals into their respective sources. In Fig. 22.4, it is seen that the dominant signal associated with the Lake Victoria Basin is localized for all the three data set. This clearly shows the contribution of the Lake Victoria basin to the Nile waters. An analysis of the correlation between these signals and climate variability indicate a strong correlation (0.85) between the GRACE's total water storage and ENSO for the period 2006–2011. This confirms the known fact that climate variability, particularly ENSO, influences the changes in stored water of Lake Victoria Basin, and should be taken into consideration in evaluating the basin's hydrology. Section 22.4.1.2 discusses Lake Victoria Basin in more detail.

Figure 22.5 shows the localization of the signals within the Ethiopian highlands, thus indicating the importance of the region to the Nile basin. The Blue Nile receives its waters mainly from the heavy rainfall in the region as seen from the TRMM results (Fig. 22.5; IC5). Any land use patterns that could alter the use of water within the region would be capable of significantly impacting upon the entire Nile Basin. GRACE signals show a correlation of 0.52 with ENSO while GLDAS show 0.44 with ENSO and 0.4 with the Indian Ocean Dipole (IOD) index. Compared to Lake Victoria basin, the correlation to climate variability is not so strong, nonetheless, the fact that the changes in the stored water in the Ethiopian highlands is influenced by climate variability is noticeable. Figure 22.6 shows the localization of the signals within the Bahr-El-Ghazal region, which also contributes water to the River Nile by joining the tributaries from Sobat around Malakal (see Fig. 22.3). Both GRACE and GLDAS signals show a correlation of 0.68 with ENSO respectively, thus indicating that the

² <http://disc.sci.gsfc.nasa.gov/services/grads-gds/gldas>

³ http://trmm.gsfc.nasa.gov/data_dir/data.html

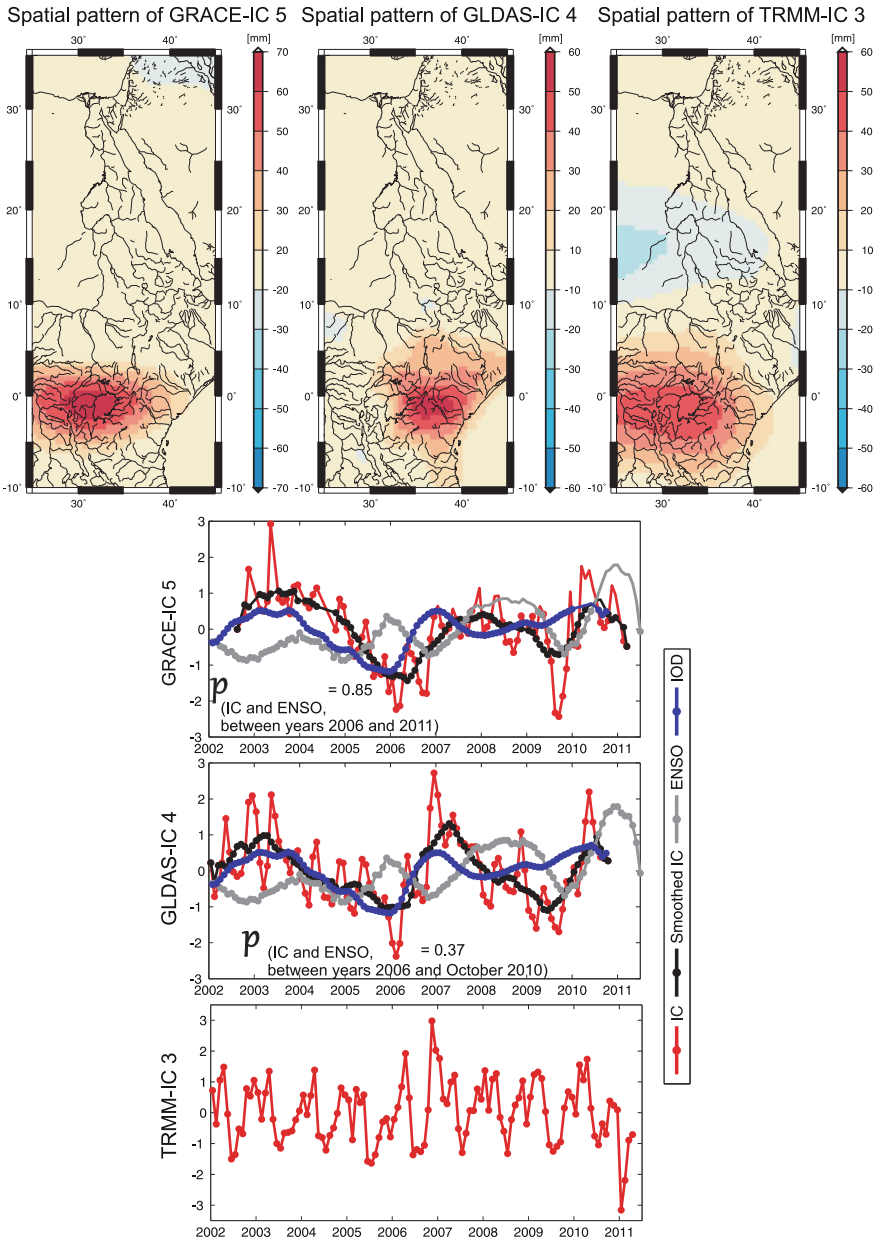


Fig. 22.4 ICA analysis of the GRACE, GLDAS, and TRMM data for the Nile basin. In this figure the signals are localized within Lake Victoria basin in all the data set

Spatial pattern of GRACE-IC 4 Spatial pattern of GLDAS-IC 3 Spatial pattern of TRMM-IC 5

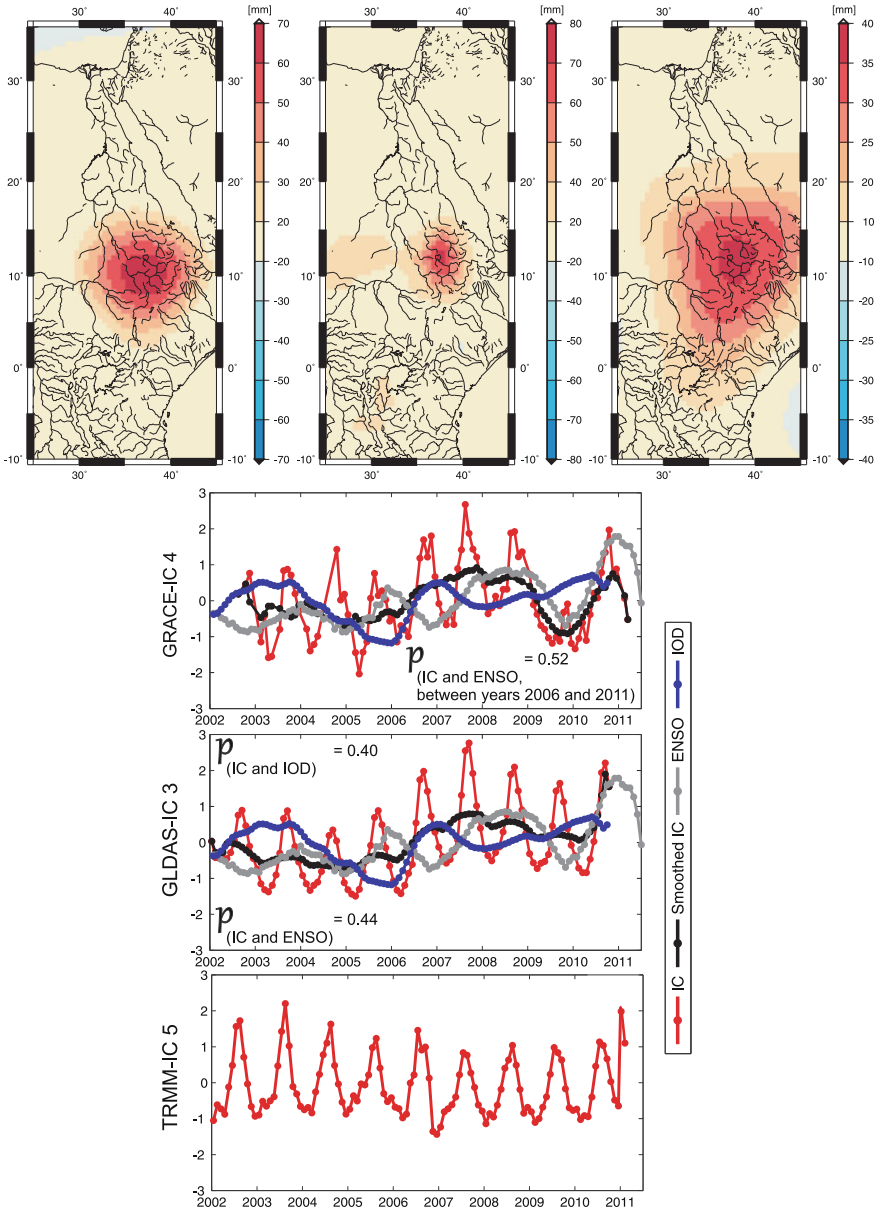


Fig. 22.5 ICA analysis of the GRACE, GLDAS, and TRMM data for the Nile basin. In this figure the signals are localized within the Ethiopian highlands in all the data set

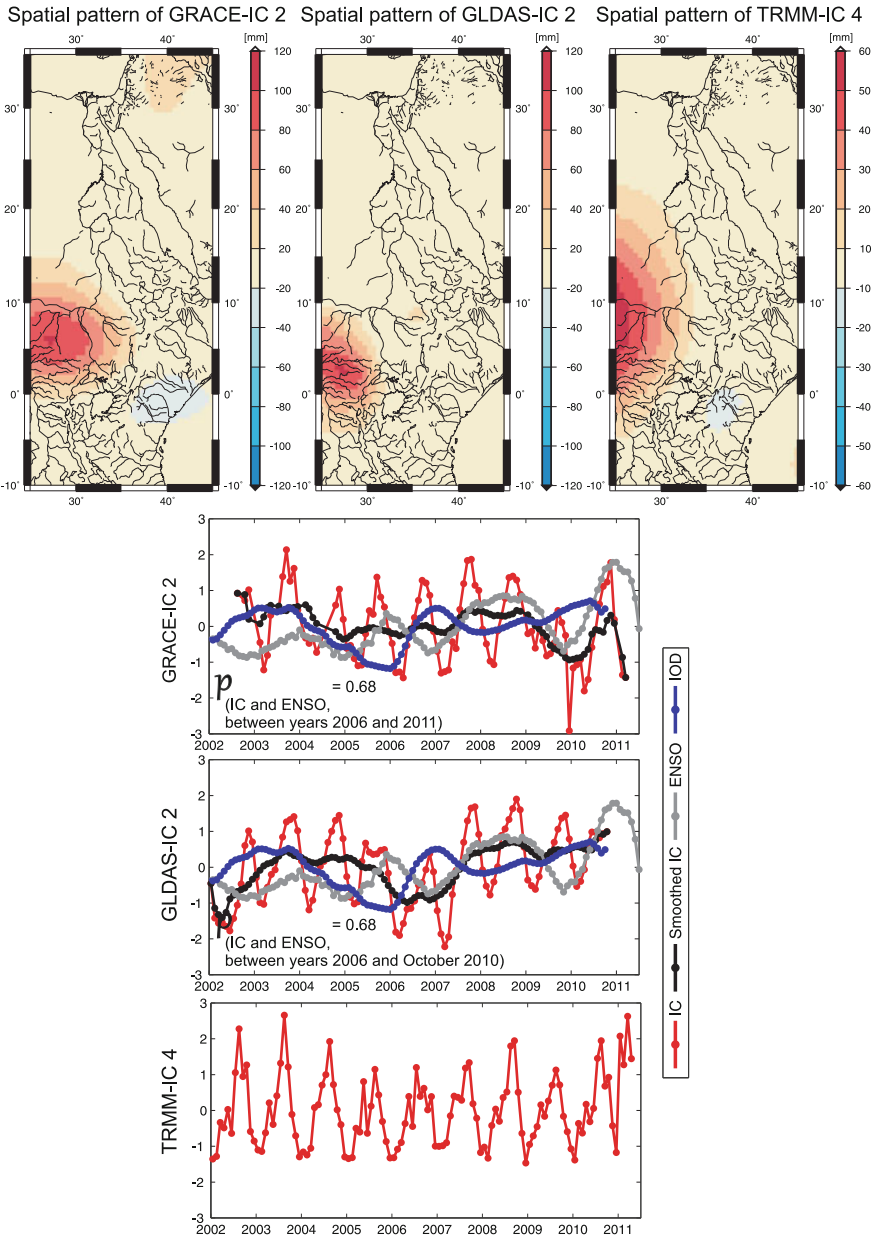


Fig. 22.6 ICA analysis of the GRACE, GLDAS, and TRMM data for the Nile basin. In this figure the signals are localized within the Bahr-el-Ghazal region in all the data set

Spatial pattern of GRACE-IC 6

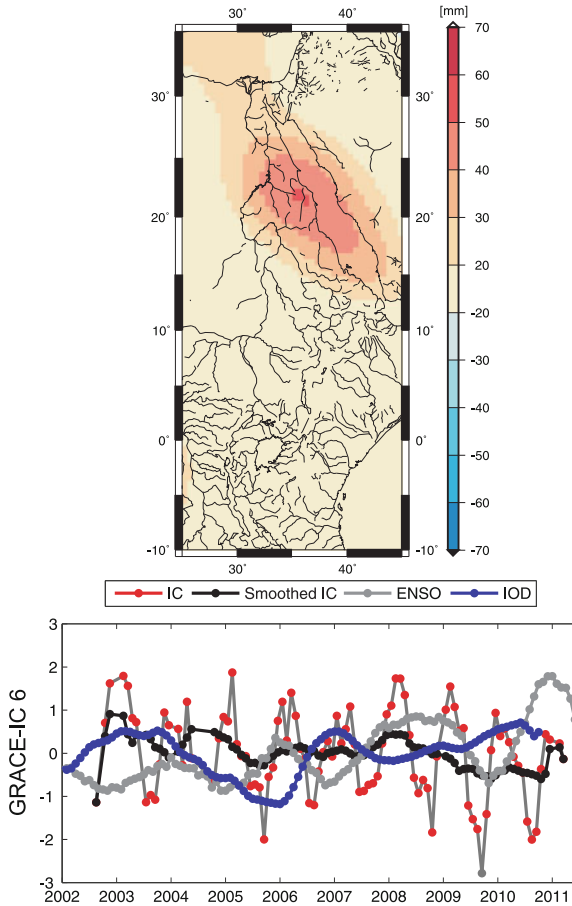


Fig. 22.7 ICA analysis of the GRACE, GLDAS, and TRMM data for the Nile basin. In this figure the signals are localized within the Lake Nasser region in GRACE data set

variability of the stored water is influenced by climate variability. Finally, Fig. 22.7 shows the dynamics around Lake Nasser along the Red Sea. More discussion on this region is presented in Awange et al. (2013).

Positive correlations between the changes in total water storages and IOD corresponding to cool waters in the Indian Ocean associated with large scale circulation changes that leads to above average rainfall in East Africa leading to flooding, while Indonesia and several parts of Australia experience drought have been documented e.g., (Becker et al. 2010; Garcia-Garcia et al. 2011). This is true for the Lake Victoria Basin, the Ethiopian highlands and the Bar-El-Ghazal regions which are also related to ENSO. For the Lake Nasser region, the effect of climate variability is negligible. For the definitions and measured indices of ENSO and IOD, see Sect. 26.4.5.

22.4.1.2 Lake Victoria Basin

Lake Victoria (Fig. 22.8), the world’s third largest lake and the largest in the developing world, is a source of water for irrigation, transport, domestic and livestock uses, and supports the livelihood of more than 30 million people who live around it (Awange JL and Ong’ang’a 2006). Nicholson (1998, 1999) documents its significance as an indicator of environmental and climate change over long-term scales. Since the 1960s, the lake level had experienced significant fluctuation, see e.g., (Nicholson 1998, 1999). From 2001 to 2006, however, Lake Victoria’s water level showed a dramatic fall that alarmed water resource managers as to whether the lake was actually drying up. Kull (2006) reported that the lake’s levels fell by more than 1.1 m below the 10 year average.

With the receding of the lake waters, acres of land that were lost to the floods of the 1960s were fast being reclaimed, creating sources of conflicts between man and wildlife. In some beaches, e.g., Usoma in Kenya, wetlands that were once breeding places for fish were dying up, leaving areas of land as playing fields for children and farmland. Ships were now forced to dock deep inside the lake, while the landing bays needed to be extended. Those who directly depended on the lake waters for domestic use were forced to go deeper into the lake to draw water, thus exposing women and children to water-borne diseases and risks of snakes and crocodiles.



Fig. 22.8 Lake Victoria basin. Source Kayombo and Jorgensen (2006)

Water intakes that supplied major towns and cities had to be extended deeper into the lake, thus causing more financial burden to the municipalities that were already strained financially (Awange et al. 2008).

With 80% of Lake Victoria water coming from direct rainfall, changes in the lake level are directly related to the variation in the water stored in its basin, which contributes around 20% in the form of river discharge. A decrease in stored basin water was therefore suspected to contribute to the drop in the lake level. An analysis of the stored water in the Lake Victoria basin in relation to rainfall and evaporation was therefore necessary as a first diagnosis. This would provide water resource managers and planners with information on the state and changing trend of the stored water within the basin. Such basin scale observations could only be achieved through the use of satellites such as GRACE. Conventional methods for studying variations in stored water such as the Artificial Neural Network, GIS and remote sensing could not diagnose the problem, see e.g., Awange et al. (2008).

Having been motivated by the potential of the GRACE satellites, Awange et al. (2008) undertook a satellite analysis of the entire lake basin in an attempt to establish the cause of the decline in Lake Victoria's water levels. The GRACE and CHAMP satellites (Fig. 20.9 on p. 292) together with data from the TRMM satellite were employed in the analysis. Using 45 months of data spanning a period of 4 years (2002–2006), the GRACE satellite data were used to analyze the gravity field variation caused by changes in the stored waters within the lake basin. Figure 22.9 presents the annual variation of the geoid in the lake's basin during the high rain season months of March, April and May (MAM) for the period 2002–2006. The GRACE

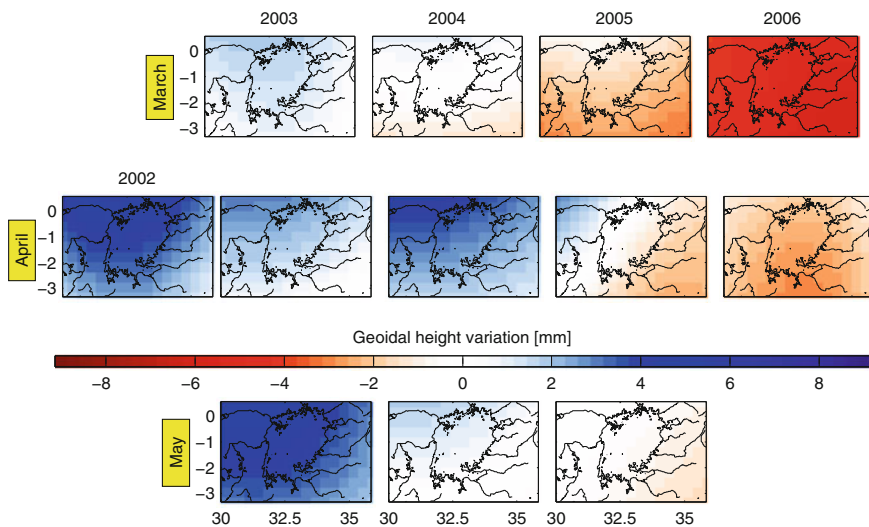


Fig. 22.9 Inter-annual comparison in the geoid during the high rainy season of MAM from 2002–2006. The figure indicates a decline in total water storage in the Lake Victoria basin during this period. *Source* Awange et al. (2008)

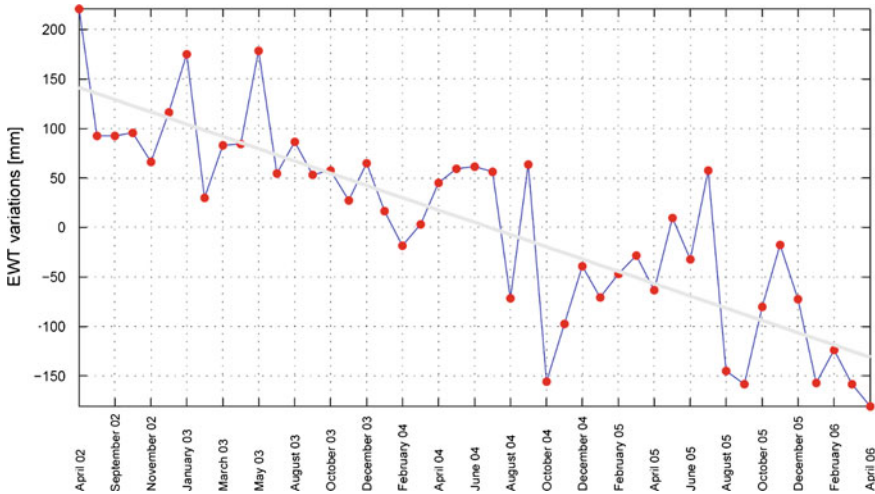


Fig. 22.10 Lake Victoria basin total water storage (equivalent water thickness) changes between 2002–2006, as seen by the GRACE satellite. The figure indicates that the GRACE satellites observed a general decline in the lake’s basin waters over this period (cf. Fig. 26.13 on p. 470 obtained from satellite altimetry). *Source* Awange et al. (2008)

results indicated that the basin’s total water storage dramatically decreased at a rate of 6.20 mm/month. These changes are expressed in equivalent water thickness (also known as total water storage (TWS)) in Fig. 22.10. For the period 2002–2006, the results indicate a general decline in the lake basin’s water level at a rate of 1.83 km³/month (Awange et al. 2008).

To validate the GRACE results, TRMM Level 3 monthly data for the same period of time were used to compute mean rainfall at a spatial resolution of 0.25° × 0.25° (25 × 25 km), as shown in Fig. 22.11, from which the rainfall trends were analyzed (Fig. 22.12). To assess the effect of evaporation, GNSS remote sensing data (59 CHAMP satellite occultations) for the period 2001–2006 were analyzed to define if tropopause warming took place (see the approach in Chap. 20). The results indicated that the tropopause temperature fell in 2002 by about 3.9 K and increased by 2.2 K in 2003 and remained above the 189.5 K value of 2002. The tropopause heights showed a steady increase from a height of 16.72 m in 2001 and remained above that value reaching a maximum of 17.59 km in 2005, an increase in height by 0.87 m. Temperatures did not, therefore, increase drastically to cause massive evaporation. TRMM results indicated the rainfall over the basin (and directly over the lake) to have been stable during this period (see Figs. 22.11 and 22.12). Since rainfall over the period remained stable, and temperatures did not increase drastically to cause increased evaporation, the remaining major contributor during the period 2002–2006 was suspected to be discharge from the expanded Owen Falls dam. Awange et al. (2008) concluded, thanks to the GRACE and GNSS satellites, that the fall in Lake Victoria’s water level between 2001 and 2006, also noted in Sect. 22.4.1, was due to

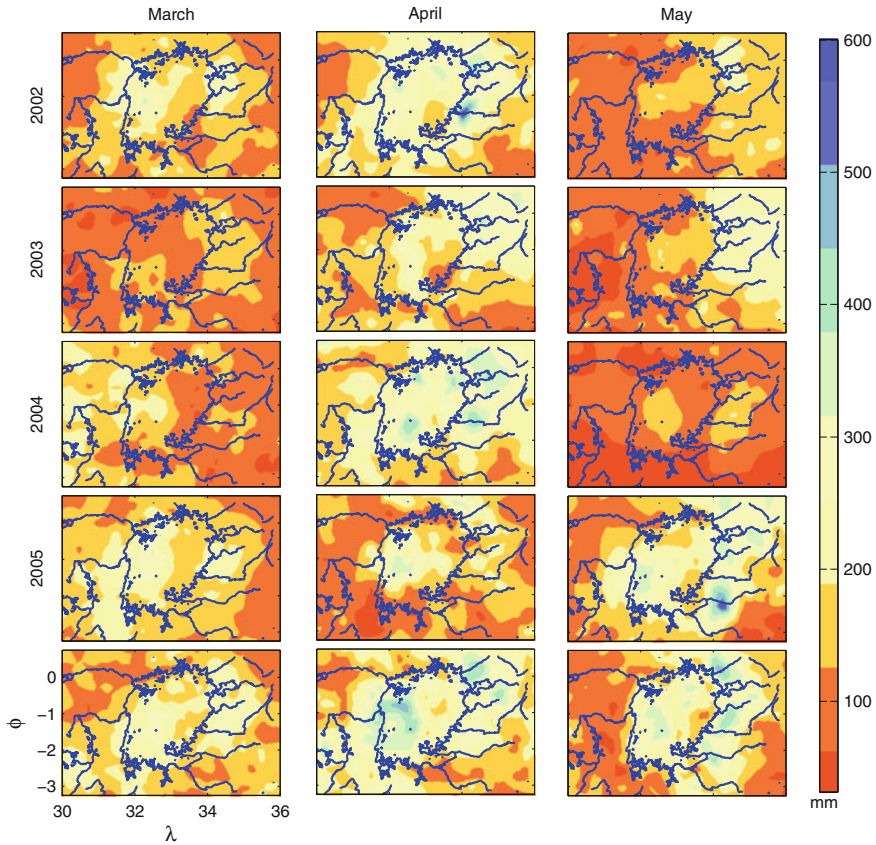


Fig. 22.11 Inter-annual comparison of rainfall over the Lake Victoria basin during the high rainy season of MAM from 2002–2006 using TRMM results. *Source* Awange et al. (2008)

human impact on the basin's environment (i.e., expanded dam) as opposed to natural factors.

In a related work, Swenson and Wahr (2009) used satellite gravimetric and altimetric data to study trends in water storage and lake levels of multiple lakes in the Great Rift Valley region of East Africa for the years 2003–2008. GRACE total water storage estimated by Swenson and Wahr (2009) corroborated the findings of Awange et al. (2008) that the lake's water level had declined by as much as 60 mm/year, while their altimetric data indicated that levels in some large lakes in the East African region dropped by as much as 1–2 m. Swenson and Wahr (2009) concluded that the largest decline occurred in Lake Victoria and, like Awange et al. (2008), attributed this to the role of human activities.

Both the findings of Awange et al. (2008) and Swenson and Wahr (2009) provide evidence that the GRACE satellites (supported by GNSS) could be used to provide independent means of assessing the relative impacts of climate and human activities

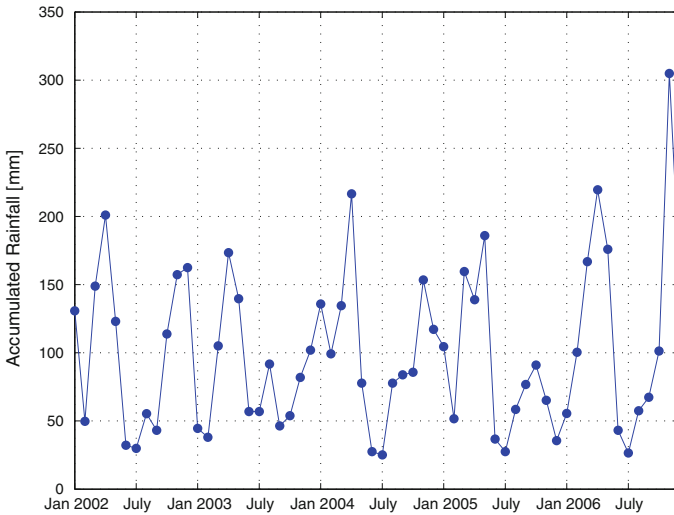


Fig. 22.12 Time series of rainfall 2002–2006 for the lake Victoria basin as observed by the TRMM satellite. *Source* Awange et al. (2008)

on the balance of stored water that does not depend on in-situ observations, such as dam discharge values, which may not be available to the public domain.

22.4.1.3 Application of GNSS to LVB Water Conflict Resolution

Let us revisit Fig. 4.1 on p. 48 where we have three boats with fishermen from each of the three East African countries that border Lake Victoria. If the three boats were in the middle of the Lake, with no visible land mark on the horizon, the fishermen would be at a loss to know which country owns that portion of the lake. In this case, they will not know whether they are in Kenyan, Ugandan or Tanzanian territory. Fishermen have frequently found themselves in this situation and the end result has often been conflict, leading to arrests and the confiscation of boats and fishing equipment. In such cases, hand-held GNSS receivers and a map could easily resolve such a dilemma. A real-case scenario is illustrated by Misingo Island in Fig. 22.13,⁴ which is an island currently disputed between Kenya and Uganda due to it being home to the dwindling Nile Perch (*Lates niloticus*) fish. Owing to uncertainty about the boundary, GNSS receivers were used by a team of surveyors from both countries to mark the boundary and establish that the disputed island belongs to Kenya.

⁴ Source: <http://www.nation.co.ke>.



Fig. 22.13 The disputed Mgingo Island in Lake Victoria (*right*). GNSS was used to establish that the island belongs to Kenya, thus resolving a territorial dispute between Kenya and Uganda. *Source* Daily Nation, Kenya

22.4.2 Understanding the Decline of Lake Naivasha, Kenya

22.4.2.1 The Lake Naivasha Basin

Lake Naivasha ($00^{\circ} 40' S - 00^{\circ} 53' S, 36^{\circ} 15' E - 36^{\circ} 30' E$) is the second largest fresh water lake in Kenya with a maximum depth of 8 m. It is situated in the Central African Rift Valley at an altitude of 1890 m above sea level and is approximately 80 km northwest of the Kenyan capital, Nairobi. Its basin (Fig. 22.14) lies within the semi-arid belt of Kenya with mean annual rainfall varying from about 600 mm at the Naivasha township to some 1,700 mm along the slopes of the Nyandarua mountains, with open water evaporation estimated to be approximately 1,720 mm/year (Becht 2005). Mount Kenya and the Nyandarua Range capture moisture from the monsoon winds, thereby casting a significant rain shadow over the Lake Naivasha basin (Becht 2005). Unlike Lake Victoria, which has its highest rainfall during the March-April-May (MAM) wet season, e.g., Awange et al. (2008), Lake Naivasha basin experiences its highest rainfall period during April-May-June (AMJ). There is also a short rainy season from October to November. The lake's levels therefore follow this seasonal pattern of rainfall cycle, with changes of several meters possible over a few months. Imposed upon this seasonal behaviour are longer-term trends, for example, there has been a change in the lake's water level of 12 m over the past 100 years (Becht 2005).

The lake is fed by three main river systems: the Gilgil, the Malewa and the Karati, the last of which only flows during the wet season (see Fig. 22.15). There is also a groundwater inlet into the lake from the north, and an outlet to the south, which when combined with the river systems and the biochemical and geochemical sedimentation processes that remove ions such as sulphates and carbonates from the water, results in the freshness of the lake (Everard and Harper 2002; Harper et al. 1990). Becht et al. (2005) state that whereas a small portion of the groundwater evaporates and escapes in the form of fumaroles in the geothermal areas, the remaining water flows into Lakes

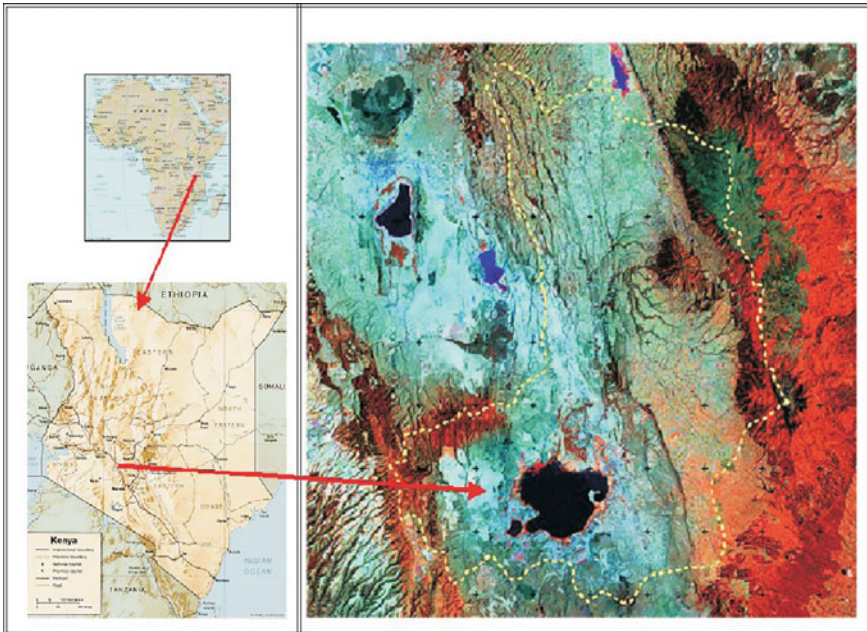


Fig. 22.14 Location map of the Lake Naivasha Basin. *Source* Becht (2005)

Magadi and Elementaita, taking thousands of years to reach them. The basin's water balance has been calculated from a model based upon long-term meteorological observations of rainfall, evaporation and river inflows (Becht 2002). This model reproduced the observed level from 1932 to 1982 with an accuracy of 95% of the observed monthly level, differing by 0.52 m or less (ILEC 2005). This pattern was, however, noticed to deviate after 1982 and by 1997, the difference had reached 3–4 m (Becht 2005). In fact, the onset of this reduced ability to model the lake's level coincided with the increase in horticultural and floricultural activities.

In general, three contemporary global water issues can be identified as occurring in this region, namely *water scarcity/availability*, *water quality*, and *water security*. Several previous works have focused on the problem of water quality and competition for water resources within the area. Water quality studies have endeavored to analyze the physical, chemical and biological characteristics of the water, which represents a measure of the condition of water relative to the requirements of one or more biotic species and/or to any human need or purpose. Most studies have concluded that the main causative factors for the deterioration of the water quality of Lake Naivasha are the large quantities of sediment inflow from the catchments of the Malewa and Gilgil rivers, polluting inflows from Naivasha town and the intensive floriculture enterprises adjacent to the lake, see e.g., Becht (2007). These pollutants include high levels of phosphates, nitrates, pesticide residues and other agro-chemicals.

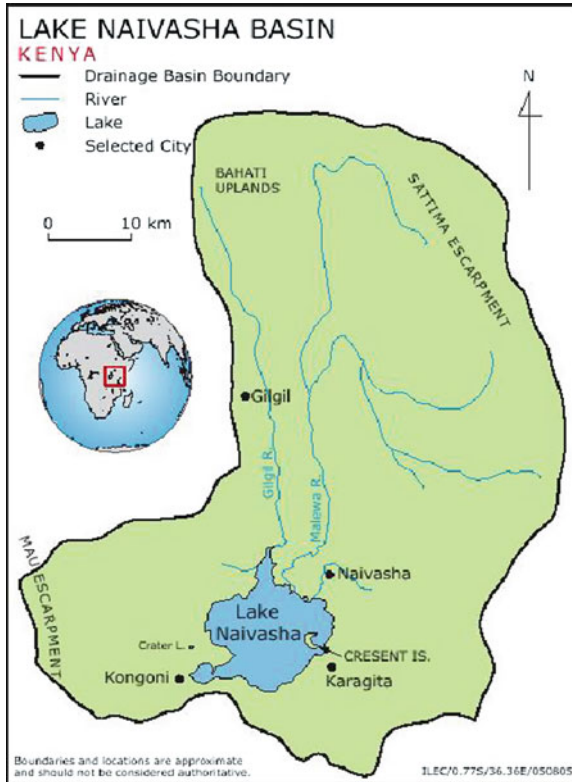


Fig. 22.15 The Lake Naivasha drainage system. Three rivers flow into the Lake; Gilgil, Malewa, and Karati. The Lake's outlet is through an underground system to the south. *Source* Becht (2005)

The use of GNSS in monitoring water pollution discussed in Sect. 27.2 could also be applied to Lake Naivasha to map the sources of point pollutants. Although water security issues are a reality in the Lake Naivasha basin, few studies have been done to better understand the underlying issues. Carolina (2002) asserts that the area of Lake Naivasha basin is of high economic and political importance to Kenya, which presents a wide variety of economic activities around the water resources with many different stakeholders often competing for the water resources.

The flower industry in Kenya has experienced a phenomenal growth, maintaining an average growth rate of 20% per year over the last decade. It is an industry that is the second largest export earner for Kenya, employing between 50,000–60,000 people directly and 500,000 others indirectly through affiliated services (KFC 2011). Although flowers are now grown in many areas with temperate climate and an altitude above 1,500 m in Kenya, the region around Lake Naivasha still remains the nation's main floriculture farming center. The foremost categories of cut flowers exported from Kenya include: roses, carnations, statice, alstromeria, lilies and hypericum. Indeed, Kenya is arguably the largest exporter for flowers in the world, supplying

over 35 % of cut flowers to the world's largest market—the European Union (KFC 2011).

22.4.2.2 Impacts of Flower Farming

Lake Naivasha (Kenya) is the only freshwater lake in the Great Rift Valley of East Africa in an otherwise soda/saline lake series (Everard et al. 2002). In fact, it is the freshness of the water of Lake Naivasha that is the basis for its diverse ecology (Harper et al. 1990). However, recent years have seen a rapid decline in its extent to the point where questions are being raised in the local media as to whether the lake is actually dying.

So unique is Lake Naivasha in the chain of East African Rift Valley lakes that in 1995 it was declared a Ramsar site due to its importance as a wetland. Lake Naivasha and its basin supports a rich ecosystem, with hundreds of bird species, papyrus fringes filled with hippos, riparian grass lands where waterbuck, giraffe, zebra and antelopes graze, dense patches of riparian acacia forest with buffaloes, bushbuck and other species, swampy areas where waterfowl breed and feed and, at the same time, magnificent views of the nearby volcanoes (Becht 2005). The lake also supports local fishery and tourism, and is used for recreation, water sports, subsistence farming and hunting. The surrounding lands are dominated by the cultivation of flowers, vegetables, fruit and cereals, as well as power generation (Becht 2002).

In fact, the *floriculture* industry in this area provides large quantities of flowers that are exported to Europe and other countries of the world. The growth in the flower industry has been favored by the permeable and fertile soils, low rainfall, reliable supply of good quality water, favorable climatic conditions, availability of cheap labor, and easy access to Nairobi airport (Becht 2005). Since much of the water used in the flower farms comes from irrigation, the only source, therefore, is the lake and its basin. The lake and basin also supply drinking water to Nakuru (of which Naivasha is part of, with a population of about 1.6 million as per the 2009 census) located 160 km north west of Nairobi.

The study of fluctuations in Lake Naivasha's water levels has been carried out, e.g., by Nicholson (1998), Richardson and Richardson (1972). Richardson and Richardson (1972), for instance, state that the lake was nearly twice as extensive in the 1920s as it was in 1960–1961. Nicholson (1998) noted trends of lower levels during the first half of the 19th century, very high levels during the last decades of the 19th century, with a rapid decrease occurring during the 20th century. He further points out that the lake returned to a relatively large extent during the 1960s, but this ended in the 1970s, a fact also stated by Richardson and Richardson (1972) who point out that the wetter years beginning in 1961 saw a sharp rise in the levels of Lake Naivasha, as well as of Lakes Elmenteita and Nakuru. The decrease in the lake's water level between 1920s and 1960s is attributed by Richardson and Richardson (1972) to a slight trend of decreasing rainfall during this period, averaging 5 mm/year over the basin, between 1920 and 1949 (see also Sansome (1952)), as well as an increase in human consumption from river influent and boreholes.

In the 1980s, the fall of the lake's level continued, with the local Olkaria geothermal power station and subsurface drainage thought to be the main culprits (Darling et al. 1990). But then, there was little notice taken of the influence of the flower farms, since the first farms had just started in the early 1980s, see e.g., Becht (2005). However, during the 1990s, over 100 km² of land around lake Naivasha was converted to floriculture for the European-cut flower trade, e.g., ILEC (2005). With this growth came an influx of workers leading to a greater extraction of water from the lake, local aquifers, and the inflowing rivers for the agriculture, floriculture and domestic use by the rapidly increasing population (ILEC 2005).

At this point, the impact of such development on the lake's resources begun to be felt, with its size shrinking due to this direct extraction from the lake and also indirectly from closely connected aquifers. In the work of Abiya (1996), the exploitation of the resources of Lake Naivasha is said to pose serious threats to the fragile lake ecosystem and its biodiversity. Abiya (1996) considered the dynamics of the changing lake ecosystem, the imminent threats to this system, and the community-based approach towards the sustainable utilization of the lake. Their study showed that the sustainable use of the lake was not going to be fully realized without a sound management plan, and recommended the enactment of consolidated environmental legislation in Kenya, which will enable the strengthening of environmental conservation and the protection of natural resources (Abiya 1996). This in turn has led to other proposals for the sustainable use of the lake and basin (e.g., Everard and Harper (2002), Harper et al. (1990)).

In the last decade, the lake's level has continued to drop with floriculture being blamed for excessive water extraction from the lake and aquifers, and the small holder farms in the upper catchment being blamed for nutrient loadings, see e.g., ILEC (2005), Mekonnen and Hoekstra (2010), leading to outcry in both the local and international media that this Ramsar site could be dying as a result of the very resource that it supports, see e.g., Mekonnen and Hoekstra (2010). For example, Mekonnen and Hoekstra (2010) observed that the total virtual water exported in relation to the cut flower industry from the Lake Naivasha basin was 16 Mm³/yr during the period 1996–2005. Other factors that have also been proposed as influencing Lake Naivasha's water changes include irregular rainfall patterns (Harper et al. 1990), and trade winds (Vincent et al. 1979). All of these discussions therefore point to the need for the *reliable mapping* of the lake and its basin in order to properly understand the dynamics of this area. This need for accurately monitoring the lake was captured by Becht and Harper (2002), who state that there is an urgent need to accurately measure all abstractions and provide consistent, reliable, hydrological and meteorological data from the catchment, so that a 'safe' yield may be agreed upon by all stakeholders and a sustainable use of the lake waters achieved.

However, lack of reliable basin mapping techniques hampered the proper mapping of changes in the lake basin, while also not allowing accurate predictions of the likely future situation, despite modeling methods being used to calculate its water balance, e.g., Becht (2002). The situation is compounded by the fact that Lake Naivasha has no surface outlet that could assist in hydrological monitoring, and the fact that

changes in its water level occur rapidly, over the order of several meters over just a few months, shifting the shoreline by several meters (Becht 2005).

The emergence of satellite based methods offers the possibility of providing a broader and more integrated analysis of the lake and its basin. Using products from the GRACE gravity mission, changes in the stored water in the region extending from the Lake Naivasha basin to Lake Victoria may be assessed to determine whether the changes are climatic or human induced. Changes in precipitation can be examined by the analysis of products from TRMM, allowing the determination of how much of the fluctuations in Lake Naivasha are related to changes in precipitation behavior.

The fluctuations in the water level of Lake Naivasha can be determined using both ground-based tide gauge observations and satellite altimetry data (TOPEX/Poseidon and Jason-1; see Sect. 20.4). These results may in turn be related to the use of satellite imagery (e.g., Landsat) and change detection techniques to map the shoreline changes of Lake Naivasha, analyzing the trend of changes over the period of interest, and correlating shoreline changes with proposed causes. In general, the combination of different data sets, both space-borne and ground based, provide a valuable contribution to understanding the hydrological behaviour of the East African Great Lakes region, e.g., (Becker et al. 2010).

Example 22.1 (Satellite-based monitoring (Awange et al. 2013)) Several different types of space-borne observations were used in Awange et al. (2013): (1) GRACE gravity-field products (2) precipitation records based on TRMM products (3) satellite remote sensing (Landsat) images (4) satellite altimetry data and (5) flower production data. In addition, data from an in-situ tide-gauge station were used. The results of Awange et al. (2013) confirm that Lake Naivasha has been steadily declining with the situation being exacerbated from around the year 2000, e.g., Fig. 22.18, with water levels declining at a rate of -10.2 cm/yr and a shrinkage in area of -1.04 km²/year (see e.g., Fig. 22.16 where GNSS was used to *geo-reference* the satellite imagery). This rapid decline can be traced largely to anthropogenic activities, a proposal supported by a coefficient of correlation R^2 value of 0.976 between the quantity of flower production and the lake's level for the period 2002–2010 (Figs. 22.17 and 22.18), a period during which such production doubled, see e.g., Fig. 22.19. These results, supported by the use of GNSS show that there is therefore a need for those different communities and interest groups that depend upon Lake Naivasha to better formulate their management plans, a need which can exploit results such as those presented in Awange et al. (2013).

End of Example 22.1

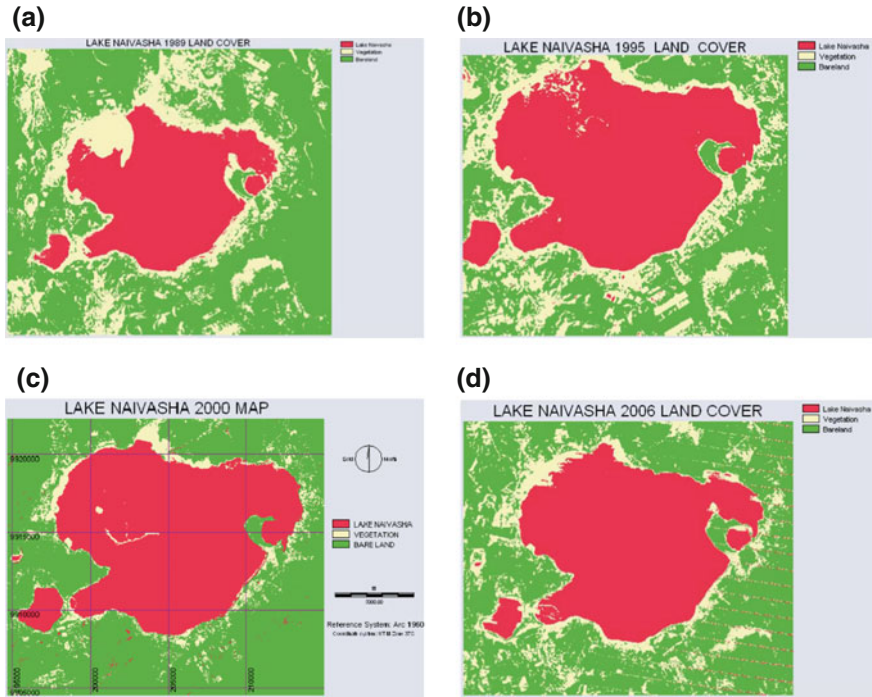


Fig. 22.16 Surface-type classification results for the considered Landsat images. **a** 1989, **b** 1995, **c** 2000 and **d** 2006. GNSS satellites were used to georeference the satellite images. *Source* Awange et al. (2013)

22.4.3 Water, a Critical Dwindling Australian Resource

Warning of Australia's acute water problem (see e.g., Fig. 22.20) had already been sounded by the National Land and Water Resource Audit (NLWRA (2001)), which reported that Australian water resources were scarce and in high demand by agricultural, industrial and urban users. The alarming finding of the report was the fact that 26 % of the river basins and 34 % of the groundwater management units in Australia were approaching or beyond sustainable extraction limits.

The NLWRA highlighted the need for information that could assist in improving water resource management and conservation. Steffen et al. (2005) issued a further alert that Australia would be faced with the impacts of climate change on its water quantity due to decrease in precipitation over parts of Australia.

Even though the need for up-to-date information on stored water resource to support policy formulation and management issues had already been realized, e.g., NLWRA (2001), and specifically with the prevailing drought conditions in Australia, the lack of appropriate techniques that offered high spatial and temporal resolution monitoring of changes in stored water remained a stumbling block (Ellett et al. 2005). The problem was further compounded by the fact that groundwater suitable for human

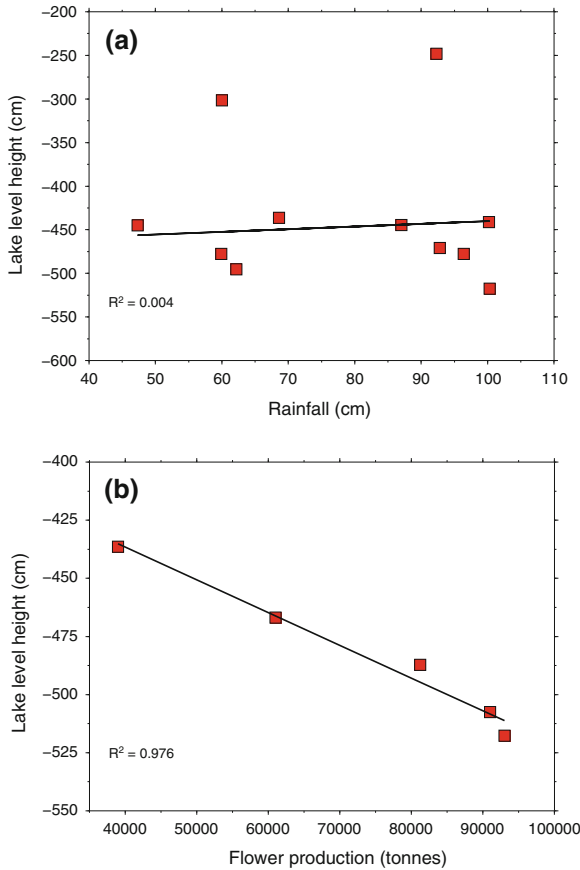


Fig. 22.17 Comparing annual average lake levels with **a** TRMM rainfall and **b** flower exports. The *solid lines* are fitted linear trends, along with their correlation coefficient. A strong correlation coefficient (0.976) is noticed between the Lake’s level and flower export between 2002–2010, the period when the flower export picked (see Fig. 22.19). *Source* Awange et al. (2013)

consumption and utility is normally trapped inside aquifers (see Sect. 22.1) that are beyond reach of modern remote sensing methods. With the introduction of GRACE satellites (Sect. 20.3.3), however, the situation changed.

Example 22.2 (Monitoring changes in Australia’s stored water (Awange et al. 2011)). In order to use the GRACE satellite for monitoring the variation in Australia’s stored water, Awange et al. (2011) investigated the regional $4^\circ \times 4^\circ$ mascon (mass concentration) GRACE solutions provided by GSFC (Goddard Space Flight Center, NASA) for their suitability for monitoring Australian hydrology, with a particular focus on the Murray-Darling Basin (MDB).

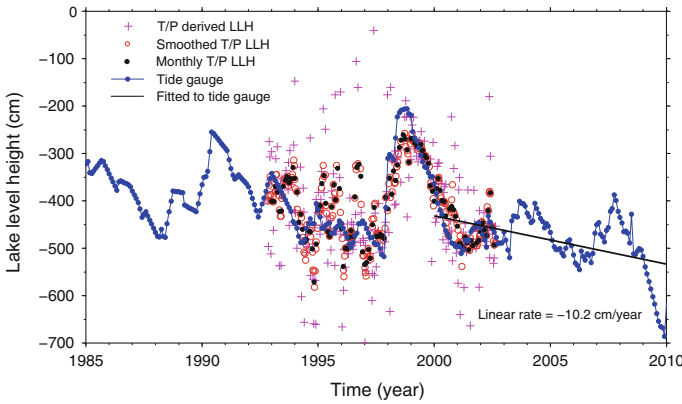


Fig. 22.18 Time Series of lake level height (LLH) changes for Lake Naivasha as provided by satellite altimetry (T/P), and a tide gauge. GNSS satellites support the satellite altimetry as discussed in Sect. 20.4. *Source* Awange et al. (2013)

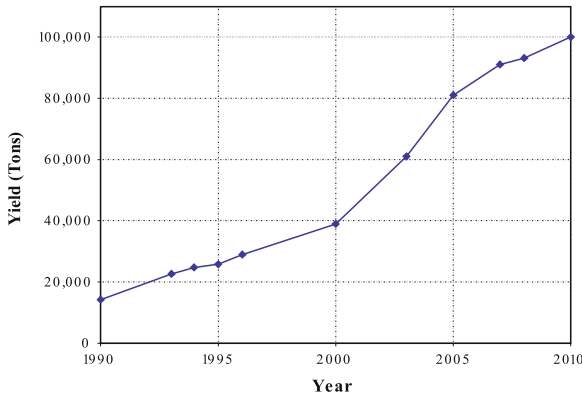


Fig. 22.19 Annual flower exports from Kenya. *Source* Awange et al. (2013)

Using Principal component analysis (PCA) and multi-linear regression analysis (MLRA), the main components of the spatial and temporal variability in the mascon solutions over both the Australian continent as a whole and the MDB in particular were analyzed and the results compared to those from global solutions provided by CSR (the Center for Space Research, University of Texas at Austin) and CNES/GRGS (Centre National d'Études Spatiales/Groupe de Recherche de Geodesie Spatiale, France) and validated using TRMM, water storage changes predicted by the WaterGap Global Hydrological Model (WGHM) and ground-truth (river-gauge) observations. The results of Awange et al. (2011) indicated that for the challenging Australian case with weaker hydrological signals, all the solutions gave similar results.

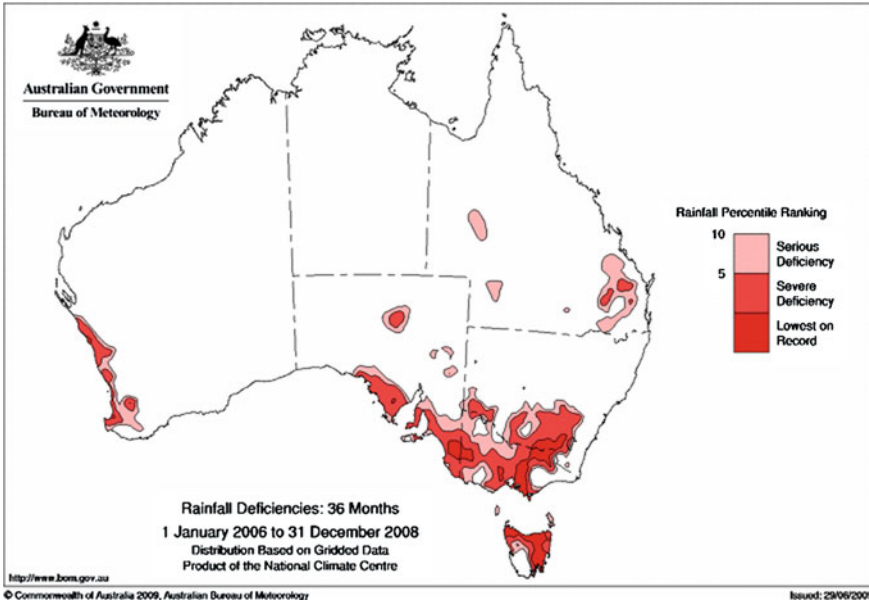


Fig. 22.20 Rainfall deficiencies for the period 1st January 2006 to 31st December 2008 (3 years, Source BOM)

For the PCA results in Fig. 22.21, the Australia-wide case was considered mainly to compare the different GRACE releases among themselves and with TRMM and WGHM time-series. The results of the PCA analysis for the first two modes are shown in Fig. 22.21. It was noticed that most of the variability were contained in the first mode (>50%), while considering the first 2 modes accommodates between 63% (for CNES/GRGS) and 81% (for mascon) of the total variability of each signal. The 1st mode (upper panel, Fig. 22.21) shows similar behavior among all data sets, with all data displaying a general north-south varying empirical orthogonal function (EOF) pattern and strong annual signal in the principle components (PC), indicative of seasonal variations. The annual signal is also apparent in the 2nd PC mode (lower panel, Fig. 22.21), especially for the GRACE time-series, although less so for the filtered TRMM and WGHM results.

The dominant signal in northern Australia is a result of the annual monsoonal rains, and is much stronger than that in the southern part of the continent. Therefore, the 1st mode is dominated by changes in the north, which may lead to smaller hydrological changes in the south being excluded from this mode. The northern signal is very obvious in the 1st mode EOF patterns for all data sets examined, and also in the 2nd mode EOF for the mascon, CNES/GRGS,

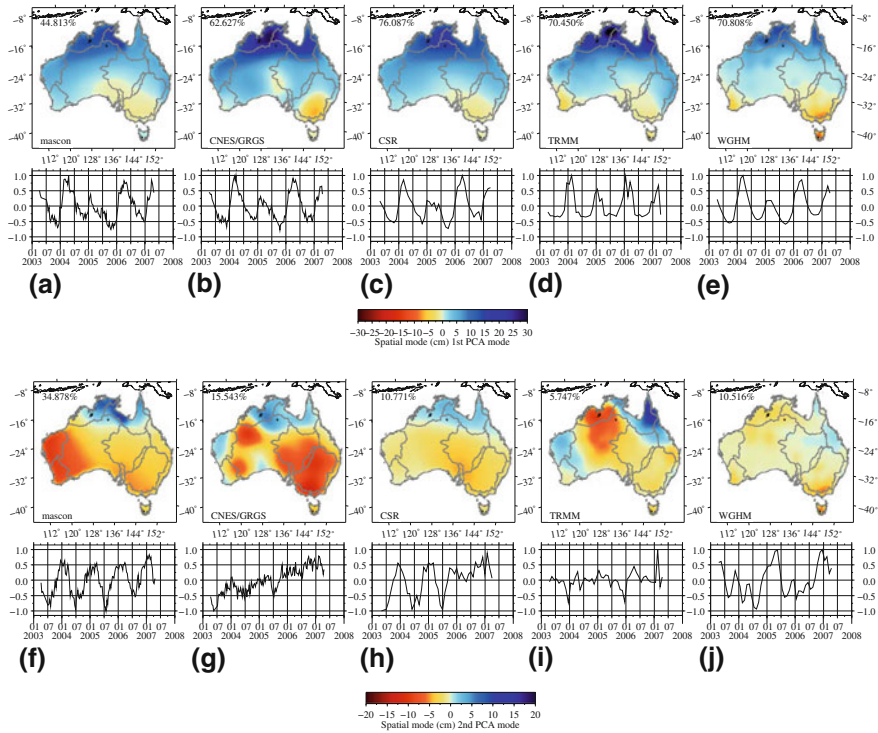


Fig. 22.21 Results of the PCA applied to the whole of Australia for the 1st and 2nd modes. *Top rows (a–e)* the 1st mode results, *bottom rows (f–j)* the 2nd mode results. **a, f** mascon, **b, g** CNES/GRGS, **c, h** CSR, **d, i** TRMM and **e, j** WGHM. Australia’s drainage divisions (from the Australian Bureau of Meteorology, see the Acknowledgments) are marked by the gray boundaries (Lambert conformal conic projection). *Source* Awange et al. (2011)

CSR and TRMM time-series. The PC of the 2nd modes also appears to show strong linear trends in the time-series, especially for the CNES/GRGS and CSR results. For both the 1st and 2nd modes, Central Australia shows a relatively low signal, a consequence of the aridity of this area having small hydrological changes. The shift in the seasons that receive the high rainfall (summer in the north, winter in the south) can be seen by the opposite signs in the signals given by the EOF (time-series in the upper panels, Fig. 22.21).

The Australia-wide results therefore show that all the GRACE solutions provided similar results and were able to identify the major climatological features of Australia, in particular the dominance of the monsoonal rainfall over northern Australia, and the offset (~6 months) between the northern and southern wet seasons, as well as the areas of mass gain (northern Australia) and loss (the MDB in the southeast and southwest Western Australia). In Forootan et

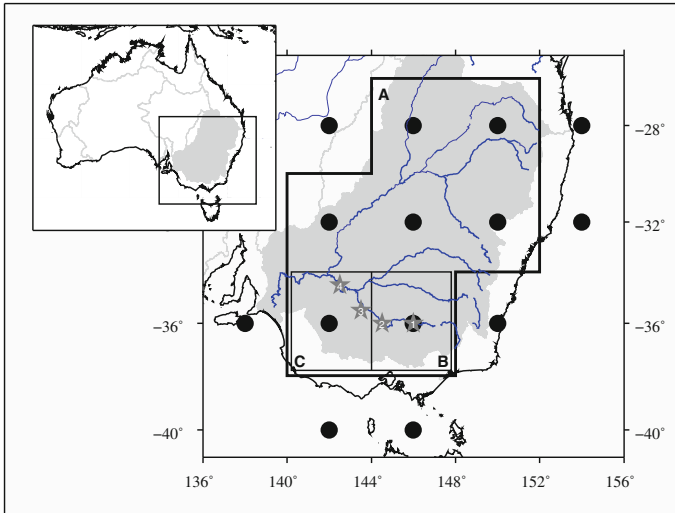


Fig. 22.22 Location map of the Murray-Darling Basin (MDB). The grey shading marks the basin's extent, with Australia's other river basins also outlined in grey. Black filled circles are the centres of the mascon grid cells provided by GSFC ($4^\circ \times 4^\circ$ grid). The thick black-bordered area (a) covers most of the MDB, while the finer black-bordered areas (b and c) are examined with respect to ground-truth data in the form of river-gauge data (numbered stars). The river-gauges are at Yarrowonga (1), Swan Hill (2), Euston (3) and Torrumbarry (4). *Source* Awange et al. (2011)

al. (2012), changes in Australia's stored water in relation to climate variability of ENSO and IOD are treated.

End of Example 22.2

Example 22.3 (Localized Murray-Darling Basin. *Source*: Awange et al. (2011)). Awange et al. (2011) further examined the MDB to determine how the GRACE solutions performed for more localized areas, since the MDB is one of Australia's most important regions for agricultural production and is an area that has been severely affected by the drought conditions (Leblanc et al. 2009; Ummenhofer et al. 2009). First, they examined the area outlined in Fig. 22.22 denoted as A, which is defined by the mascon grid elements that cover much of the MDB. Figure 22.23 compared the inferred stored water variation from each data set.

Examining the three GRACE solutions in Fig. 22.23 over the time period covered by the mascon solutions (grey shaded area), Awange et al. (2011) noted

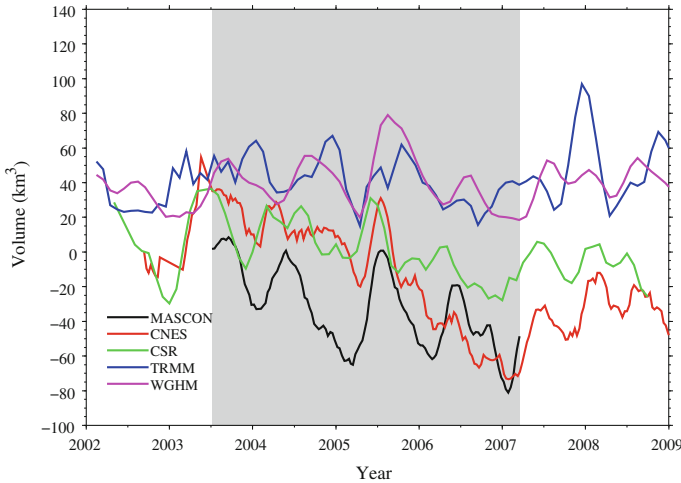


Fig. 22.23 The change in water storage over the MDB, as outlined by sector A in Fig. 22.22 for the data sets used in this work. A three-month moving average has been applied to each time-series. The gray shading marks the time span over which the mascon solutions are available. Cross-correlations between pairs of data sets are listed in Awange et al. (2011)

that the time-series generally follow each other reasonably well, as also shown by the resulting cross correlation values, i.e., CSR and CNE/GRGS, being global solutions, appear to be in closer agreement with each other ($R = 0.83$), than when compared to the mascon (mascon to CNES/GRGS, $R = 0.70$, and mascon to CSR, $R = 0.74$). The correlation between GRACE solutions is relatively high (>0.7), although much poorer when the GRACE solutions are compared to the TRMM and WGHM time-series (<0.5).

End of Example 22.3

22.5 Concluding Remarks

GRACE satellites have been recognized as having the potential to provide the first space-based estimate of changes in terrestrial water storage. Such information will, in essence, assist water managers in conserving and controlling the utilization of dwindling water resources in a sustainable way. Water is arguably one of the most precious resources in the world, therefore, it is logical to try to monitor its distribution as efficiently as possible, and GRACE provides such opportunity. This is because one of the environmentally important signals detected by GRACE is the temporal gravity field variation induced by changes in the distribution of water on and below

the Earth's surface, i.e., hydrology, e.g., Awange et al. (2009). Satellite altimetry provides the possibility of monitoring sea or lake surface heights as was demonstrated for Lake Naivasha. GNSS plays a pivot role in supporting these satellites as discussed in Chap. 20. GNSS also plays a major role in providing location-based information for monitoring groundwater wells, and source of water pollutants as discussed in Chap. 27. Its application in the management of coastal water resources is presented in Chap. 24.

References

- Abiya IO (1996) Towards sustainable utilization of lake Naivasha, Kenya. *Lakes Reserv Res Manag* 2(3–4):231–242. doi:[10.1111/j.1440-1770.1996.tb00067.x](https://doi.org/10.1111/j.1440-1770.1996.tb00067.x)
- Andersen OB, Seneviratne SI, Hinderer J, Viterbo P (2005) GRACE-derived terrestrial water storage depletion associated with the 2003 European heat wave. *Geophys Res Lett* 32(L18405):2–5. doi:[10.1029/2005GL023574](https://doi.org/10.1029/2005GL023574)
- Awange JL (2012) Environmental monitoring using GNSS, global navigation satellite system. Springer, Berlin
- Awange JL, Forootan E, Fleming KM, Kiema JBK, Ohanya S, Heck B (2013) Understanding the decline of Lake Naivasha using satellite-based methods. *Adv Water Res* (in press)
- Awange JL, Fleming KM, Kuhn M, Featherstone WE, Heck B, Anjasmara I (2011) On the suitability of the 4° × 4° GRACE mascon solutions for remote sensing Australian hydrology. *Remote Sens Environ* 115:864–875. doi:[10.1016/j.rse.2010.11.014](https://doi.org/10.1016/j.rse.2010.11.014)
- Awange JL, Sharifi MA, Baur O, Keller W, Featherstone WE, Kuhn M (2009) GRACE hydrological monitoring of Australia. Current limitations and future prospects. *J Spat Sci* 54(1):23–36. doi:[10.1080/14498596.2009.9635164](https://doi.org/10.1080/14498596.2009.9635164)
- Awange JL, Sharifi M, Ogonada G, Wickert J, Grafarend EW, Omulo M (2008) The Falling Lake Victoria Water Level: GRACE, TRIMM and CHAMP Satellite Analysis. *Water Res Manag*. doi:[10.1007/s11269-007-9191-y](https://doi.org/10.1007/s11269-007-9191-y)
- Awange JL, Ong'ang'a O (2006) Lake Victoria-ecology, resource of the Lake Basin and environment. Springer, Berlin
- Becht R (2007) Environmental effects of the floricultural industry on the Lake Naivasha Basin. ITC, Netherlands
- Becht R, Odada EO, Higgins S (2005) Lake Naivasha : experience and lessons learned brief. In: Lake basin management initiative: experience and lessons learned briefs. including the final report: Managing lakes and basins for sustainable use, a report for lake basin managers and stakeholders. Kusatsu : International Lake Environment Committee Foundation (ILEC) 2005:277–298
- Becht R, Haper DM (2002) Towards an understanding of human impact upon the hydrology of Lake Naivasha, Kenya. *Hydrobiologia* 488(1–3):1–11. doi:[10.1023/A:1023318007715](https://doi.org/10.1023/A:1023318007715)
- Becker M, Llowel W, Cazenave A, Güntner A, Crétaux J-F (2010) Recent hydrological behaviour of the East African Great Lakes region inferred from GRACE, satellite altimetry and rainfall observations. *Comptes Rendus Geosci* 342(3):223–233. doi:[10.1016/j.crte.2009.12.010](https://doi.org/10.1016/j.crte.2009.12.010)
- Bettadpur S (2007) UTCSR Level-2 Processing Standards Document for Level-2 Product Release 0004. Gravity Recovery and Climate Experiment (GRACE) Rev 3.1, GRACE 327–742 (CSR-GR-03-03). Center for Space Research, The University of Texas at Austin.
- Beylene T, Lettenmaier DP, Kabat P (2010) Hydrologic impacts of climate change on the Nile River Basin: implications of the 2007 IPCC scenarios. *Clim Change* 100:433–461. doi:[10.1007/s10584-009-9693-0](https://doi.org/10.1007/s10584-009-9693-0)
- Birnie P, Boyle A (1993) International law & the environment. *Camb law J* 52(3):540 (Cambridge university press)

- Bonsor HC, Mansour MM, MacDonald AM, Hughes AG, Hipkin RG, Bedada T (2010) Interpretation of GRACE data of the Nile Basin using a groundwater recharge model. *Hydrol Earth Syst Sci Discuss* 7:4501–4533. doi:[10.5194/hessd-7-4501-2010](https://doi.org/10.5194/hessd-7-4501-2010)
- Bower DR, Courtier N (1998) Precipitation effects on gravity measurements at the Canadian absolute gravity site. *Phys Earth Planet Inter* 106:353–369
- Brutsaert W (2005) *Hydrology. An introduction*, 4th edn. Cambridge University Press, New York
- Carolina BF (2002) Competition over water resources: analysis and mapping of water-related conflicts in the catchment of Lake Naivasha (Kenya). MSc thesis, ITC
- Casanova MT (1994) Vegetative and reproductive responses of charophytes to water-level fluctuations in permanent and temporary wetlands in Australia. *Aust J Mar Freshw Res* 45:1409–1419
- Conway D (2005) From headwater tributaries to international river: observing and adapting to climate variability and change in the Nile Basin. *Global Environ Change* 15:99–114. doi:[10.1016/j.gloenvcha.2005.01.003](https://doi.org/10.1016/j.gloenvcha.2005.01.003)
- Crowley JW, Mitrovica JX, Bailey RC, Tamisiea ME, Davis JL (2006) Land water storage within the Congo Basin inferred from GRACE satellite gravity data. *Geophys Res Lett* 33:L19402. doi:[10.1029/2006GL027070](https://doi.org/10.1029/2006GL027070)
- Damiata BN, Lee TC (2002) Gravitational attraction of solids of revolution—part 1: vertical circular cylinder with radial variation of density. *J Appl Geophys* 50(3):333–349. doi:[10.1016/S0926-9851\(02\)00151-9](https://doi.org/10.1016/S0926-9851(02)00151-9)
- Darling W, Allen D, Armannsson H (1990) Indirect detection of subsurface outflow from a rift valley lake. *J Hydrol* 113(1–4):297–306
- Ellett KM, Walker JP, Western AW, Rodell M (2006) A framework for assessing the potential of remote sensed gravity to provide new insight on the hydrology of the Murray-Darling Basin. *Aust Water Resour* 10(2):89–101
- Ellett KM, Walker JP, Rodell M, Chen JL, Western AW (2005), GRACE gravity fields as a new measure for assessing large-scale hydrological models. In: Zenger A, Argent RM (ed) MODSIM 2005 international congress on modelling and simulation society of Australia and NewZeland, December 2005, pp. 2911–2917. ISBN: 0-9758400-2-9
- Everard M, Harper DM (2002) Towards the sustainability of the Lake Naivasha Ramsar site and its catchment. *Hydrobiologia* 488(1–3):191–203. doi:[10.1023/A:1023390430571](https://doi.org/10.1023/A:1023390430571)
- Everard M, Vale JA, Harper DM, Tarras-Wahlberg H (2002) The physical attributes of the Lake Naivasha catchment rivers. *Hydrobiologia* 488(1–3):13–25. doi:[10.1023/A:1023349724553](https://doi.org/10.1023/A:1023349724553)
- Forootan E, Kusche J (2011) Separation of climate-driven signals in time-variable gravity using independent component analysis (ICA). *J Geodesy* 86:477–497. doi:[10.1007/s00190-011-0532-5](https://doi.org/10.1007/s00190-011-0532-5)
- Forootan E, Awange J, Kusche J, Heck B, Eicker A (2012) Independent patterns of water mass anomalies over Australia from satellite data and models. *Remote Sens Environ* 124:427–443. doi:[10.1016/j.rse.2012.05.023](https://doi.org/10.1016/j.rse.2012.05.023)
- Garcia-Garcia D, Ummenhofer CC, Zlotnicki V (2011) Australian water mass variations from GRACE data linked to Indo-Pacific climate variability. *Remote Sens Environ* 115:2175–2183. doi:[10.1016/j.rse.2011.04.007](https://doi.org/10.1016/j.rse.2011.04.007)
- Gleick PH (1999) The human right to water. *Water Policy* 1:487–503
- Goodkind JM (1986) Continuous measurement of nontidal variations of gravity. *J Geophys Res* 91(B9): 9125–9134
- Hamouda MA, Nour El-Din MN (2009) Vulnerability assessment of water resources systems in the Eastern Nile Basin. *Water Resour Manag* 23:2697–2725. doi:[10.1007/s11269-009-9404-7](https://doi.org/10.1007/s11269-009-9404-7)
- Harper DM, Mavuti KM, Muchiri SM (1990) Ecology and management of Lake Naivasha, Kenya, in relation to climatic change, alien species' introductions, and agricultural development. *Environ Conserv* 17(04):328–336
- Hofman AR (2004) The connection: water and energy security. <http://www.iags.org/n0813043.htm>. Accessed 25 August 2010
- IPCC (Intergovernmental Panel on Climate Change) (2007), Contribution of Working Group I to the Fourth Assessment Report

- ILEC (International Lake Environment Committee) (2005) Managing lakes and their basins for sustainable use. A report for the lake basin managers and stakeholders, International Lakes Environmental Committee Foundation, Kusatsu, Japan
- IRIN humanitarian news and analysis, UN office for coordination of humanitarian affairs (2006). Global: The global water crisis: managing a dwindling resource. <http://www.irinews.org>. Accessed 25 Sept 2011
- Johnson LE (2009) Geographic information systems in water resources engineering. CRC Press Taylor Francis Group, Boca Raton. ISBN 978-1-4200-6913-6
- Jury WA, Vaux HJ Jr (2007). The emerging global water crisis: managing scarcity and conflict between water users. *Advances in agronomy*, Elsevier Inc., vol 95, p 77. doi:10.1016/50065-2113(07)95001-4
- Kayombo S, Jorgensen SE (2006) Lake Victoria: experience and lessons learned brief. International Lake Environment Committee, Lake Basin Management Initiative, Kusatsu, Japan. http://www.ilec.or.jp/eg/lbmi/reports/27_Lake_Victoria_27February2006.pdf. Accessed 25 Sept 2011
- KFC (Kenya Flower Council) (2011) Kenya Flower Council. <http://www.kenyaflowercouncil.org>. Accessed 25 July 2010
- Kull D (2006) Connections between recent water level drops in Lake Victoria, dam operations and drought. <http://www.irm.org/programs/nile/pdf/060208vic.pdf>. Accessed 25 Sept 2011
- Lambert A, Beaumont C (1977) Nano variation in gravity due to seasonal groundwater movements: implications for the gravitational detection of tectonic movements. *J Geophys Res* 82(2): 297–306
- Leblanc M, Tregoning P, Ramillien G, Tweed S, Fakes A (2009) Basin-scale, integrated observations of the early 21st century multiyear drought in southeast Australia. *Water Resour Res* 45:W04408. doi:10.1029/2008WR007333
- Leick A (2004) GPS satellite surveying, 3rd edn. Wiley, New York
- Leirião S, He X, Christiansen L, Andersen OB, Bauer-Gottwein P (2009) Calculation of the temporal gravity variation from spatially variable water storage change in soils and aquifers. *J Hydrol* 365:302–309
- Mekonnen MM, Hoekstra AY (2010) Mitigating the water footprint of export cut flowers from the Lake Naivasha Basin, Kenya. Value of Water Research Report Series No. 45, UNESCO-IHE, Delft, The Netherlands
- Molen I, Hilderling A (2005) Water: cause for conflict or co-operation? *ISYP J Sci World Aff* 1(2):133–143
- Montgomery EL (1971) Determination of coefficient of storage by use of gravity measurements. Ph.D. Thesis, University of Arizona, Tucson
- Mukai A, Higashi T, Takemoto S, Nakagawa I, Naito I (1995) Accurate estimation of atmospheric effects on gravity observations made with a superconducting gravity meter at Kyoto. *Phys Earth Planet Inter* 91(1–3):149–159
- Neumeyer J, Barthelmes F, Dierks O, Flechtner F, Harnisch M, Harnisch G, Hinderer J, Imanishi Y, Kroner C, Meurers B, Petrovic S, Reigber C, Schmidt R, Schwintzer P, Sun HP, Virtanen H (2006) Combination of temporal gravity variations resulting from superconducting gravimeter (SG) recordings, GRACE satellite observations and global hydrology models. *J Geodesy* 79(10–11):573–585. doi:10.1007/s00190-005-0014-8
- Nicholson SE (1998) Historical fluctuations of Lake Victoria and other lakes in the Northern Rift Valley of East Africa. In: Lehman JT (ed) *Environmental change and response in East African lakes*. Kluwer, Dordrecht, pp 7–35
- Nicholson SE (1999) Historical and modern fluctuations of lakes Tanganyika and Rukwa and their relationship to rainfall variability. *Clima Change* 41:53–71. doi:10.1023/A:1005424619718
- NLWRA (National Land and Water Resource Audit) (2001) Water resources in Australia. A summary of the National Land and Water Resource Audit's Australian water resources assessment 2000. Surface water and groundwater—availability and quality
- Owor M, Taylor RG, Tindimugaya C, Mwesigwa D (2009) Rainfall intensity and groundwater recharge: empirical evidence from the Upper Nile Basin. *Environ Res Lett* 4:035009. doi:10.1088/1748-9326/4/3/035009

- Pool DR, Eychaner JH (1995) Measurements of aquifer-storage change and specific yield using gravity surveys. *Ground Water* 33(3):425–432
- Ramillien G, Cazenave A, Brunau O (2004) Global time variations of hydrological signals from GRACE satellite gravimetry. *Geophys J Int* 158(3): 813–826. doi:10.1111/j.1365-246X.2004.02328.x
- Ramillien G, Frappart F, Cazenave A, Gntner A (2005) Time variations of land water storage from an inversion of two years of GRACE geoids [rapid communication]. *Earth Planet Sci Lett* 235(1–2):283–301. doi:10.1016/j.epsl.2005.04.005
- Rekacewicz P (2006) Increased global water stress. *Vital water graphics 2. Le monde diplomatique*. <http://www.grida.no/publications/vg/water2/page/3289.aspx>. Accessed 15 April 2012
- Richardson JL, Richardson AE (1972) History of an African rift lake and its climatic implications. *Ecol Monogr* 42(4):499–534. doi:10.2307/1942169
- Rijsberman FR (2006) Water scarcity: fact or fiction. *Agric Water Manag* 80:522
- Rieser D, Kuhn M (2010) Relation between GRACE-derived surface mass variations and precipitation over Australia. *Aust J Earth Sci* 57(7):887–900. doi:10.1080/08120099.2010.512645
- Rodell M, Chen J, Kato H, Famiglietti JS, Nigro J, Wilson CR (2006) Estimating groundwater storage changes in the Mississippi River basin (USA) using GRACE. *Hydrogeol J* 15(1):159–166. doi:10.1007/s10040-006-0103-7
- Rodell M, Famiglietti JS, Chen J, Seneviratne SI, Viterbo P, Holl S, Wilson CR (2004) Basin scale estimates of evapotranspiration using GRACE and other observations. *Geophys Res Lett* 31:L20504. doi:10.1029/2004GL020873
- Rodell M, Famiglietti JS (1999) Detectability of variations in continental water storage from satellite observations of the time dependent gravity field. *Water Resour Res* 35(9):2705–2724. doi:10.1029/1999WR900141
- Sahin M (1985) *Hydrology of the Nile Basin*. Developments in water science, vol 21. Elsevier, New York, p 575
- Sansome HW (1952) The trend of rainfall in East Africa. *E. Afr. Meteorol. Dep., Tech. Mem.* 1, 14 p
- Schmidt R, Schwintzer P, Flechtner F, Reigber C, Güntner A, Döll P, Ramillien G, Cazenave A, Petrovic S, Jochmann H, Wünsch J (2006b) GRACE observations of changes in continental water storage. *Global and Planet Change* 50(1–2):112–126. doi:10.1016/j.gloplacha.2004.11.018
- Senay GB, Asante K, Artan G (2009) Water balance dynamics in the Nile Basin. *Hydrol Process* 23:3675–3681. doi:10.1002/hyp.7364
- Schelton D (1991) Human rights, environmental rights, and the right to environment, 28 *Stan. Journal of International Law*, Heinonline
- Smith AB, Walker JP, Western AW, Ellett KM (2005) Using ground based measurements to monitor changes in terrestrial water storage. 29th Hydrology and water resources symposium (CD Rom), Institute of Engineers Australia
- Steffen W, Sanderson A, Tyson PD, Jger J, Matson PA, Moore BIII, Oldfield F, Richardson K, Schellnhuber HJ, Turner BLII, Wasson RJ (2005) *Global change and the earth system: a planet under pressure*. Springer, Berlin
- Swenson S, Wahr J (2009) Monitoring the water balance of Lake Victoria, East Africa, from space. *J Hydrol* 370:163–176. doi:10.1016/j.jhydrol.2009.03.008
- Swenson S, Wahr J, Milly PCD (2003) Estimated accuracies of regional water storage variations inferred from the gravity recovery and climate experiment (GRACE). *Water Resour Res* 39(8):1223. doi:10.1029/2002WR001736
- Swenson S, Yeh PJ-F, Wahr J, Famiglietti J (2006) A comparison of terrestrial water storage variations from GRACE with in situ measurements from Illinois. *Geophys Res Lett* 33:L16401. doi:10.1029/2006GL026962
- Syed T, Famiglietti J, Rodell M, Chen J, Wilson C (2008) Total basin discharge for the Amazon and Mississippi River basins from GRACE and a land-atmosphere water balance. *Water Resour Res* 44:W02433. doi:10.1029/2006WR005779

- Tapley BD, Bettadpur S, Ries JC, Thompson PF, Watkins MM (2004) GRACE measurements of mass variability in the Earth system. *Science* 305:503–505. doi:[10.1126/science.1099192](https://doi.org/10.1126/science.1099192)
- Taylor CJ, Alley WM (2001) Ground-water-level monitoring and the importance of long-term water-level data. U.S. Geological Survey Circular 1217, Denver, Colorado
- Ummerhofer C, England M, McIntosh P, Meyers G, Pook M, Risbey J, Gupta A, Taschetto A (2009) What causes southeast Australia's worst droughts? *Geophys Res Lett* 36:L04706. doi:[10.1029/2008GL036801](https://doi.org/10.1029/2008GL036801)
- UNEP (2002) A world of salt: total global saltwater and freshwater Estimates. <http://www.unep.org/dewa/assessments/ecosystems/water/vitalwater/freshwater.htm>. Accessed 25 Aug 2010
- Vincent CE, Davies TD, Beresford UC (1979) Recent changes in the level of Lake Naivasha, Kenya, as an indicator of equatorial westerlies over East Africa. *Clim Change* 2(2):175–189. doi:[10.1007/BF00133223](https://doi.org/10.1007/BF00133223)
- World Bank (2003) Water resource and environment. Davis R, Hirji R (eds). Technical Note G.2, Lake Management
- Whittington D, McClelland E (1992) Opportunities for regional and international cooperation in the Nile Basin. *Water Int* 17(3):144–154. doi:[10.1080/02508069208686134](https://doi.org/10.1080/02508069208686134)
- Winsemius HC, Savenije HHG, van de Giesen NC, van den Hurk B, Zapreeva EA, Klees R (2006) Assessment of gravity recovery and climate experiment (GRACE) temporal signature over the upper Zambezi. *Water Resour Res* 42:W12201. doi:[10.1029/2006WR005192](https://doi.org/10.1029/2006WR005192)
- Yan JP, Hinderer M, Einsele G (2002) Geochemical evolution of closed-basin lakes: general model and application to Lakes Qinghai and Turkana. *Sediment Geol* 148(1–2):105–122. doi:[10.1016/S0037-0738\(01\)00212-3](https://doi.org/10.1016/S0037-0738(01)00212-3)
- Yates DN, Strzepek KM (1998) Modelling the Nile Basin under climate change. *J Hydrol Eng* 3(2):98–108. doi:[10.1061/\(ASCE\)1084-0699\(1998\)3:2\(98\)](https://doi.org/10.1061/(ASCE)1084-0699(1998)3:2(98))
- Zehnder AJB, Yang H, Schertenleib R (2003) Water issues: the need for action at different levels. *Acquatic Sci Res Across Boundaries*. 65(1):1–20. doi:[10.1007/s000270300000](https://doi.org/10.1007/s000270300000)

Chapter 23

Land Management

“The Earth provides enough to satisfy every man’s needs, but not every man’s greed.”

Mahatma Gandhi (1869–1948)

23.1 Introductory Remarks

Land provides the base upon which *social, cultural* and *economic* activities are undertaken and as such is of significant importance in environmental monitoring. Social, cultural and economic activities have to be planned and managed in such a way that the sustainable use of land resources is enhanced. Sustainable land use ensures that economic and socio-cultural activities do not benefit at the expense of the environment (see Sect. 28.5). Monitoring of *changes* in land through indicators could help in policy formulation and management issues for the betterment of the environment. Some of the vital indicators for land management include vegetation, soil quality and health, biosolids and waste disposed on land, land evaluation, land use planning, contaminated land, integrity of the food supply chain, mine closure completion criteria, and catchment management, in particular water balance, salinity, eutrophication, and riparian/wetland vegetation. This Chapter presents the possibility of using geoinformatics to enhance the monitoring of some of these indicators.

23.2 Reconnaissance and Validation

Before any field measuring campaign is undertaken, pre-field preparations are essential. At this initial stage, all available data sets and imagery required for the project need to be acquired and a desk study undertaken in preparation for the

field work. *Topographic maps* (Chap. 19), *aerial photographs* (Chap. 11), *satellite imagery* (Chap. 7) and any *existing reports* normally provide the main sources of information for determining land use capability. Maps, photographs and coarse resolution satellite imagery such as *Landsat* from varying time span can be visually examined and inspected (Chap. 10) to identify any potential land use changes that may have occurred during the time interval under consideration. During the desk study, existing reports need to be examined to extract any relevant information.

Field reconnaissance entails the pre-visitation of a survey area before the actual survey. Hand-held GNSS receivers (see, e.g., Fig. 4.1 on p. 48) are useful for georeferencing as well as in providing navigation services. For example, if the crew members require to visit a specific location, they could easily use the navigation function of a hand-held GNSS receiver to reach the desired location or to identify the derived feature. In addition, *still* or *video images* may be taken to capture important spatial information. It is possible today to employ *digital cameras* that integrate both GNSS and GIS, thus allowing images acquired in the field to not only be directly georeferenced, but also uploaded directly into existing GIS databases. This may even allow elementary GIS spatial analysis (Chap. 17) to be undertaken in *real-time* during the field reconnaissance.

Terrain evaluation to identify *relief changes* within the study area and any landmark features, e.g., remnant vegetation (Fig. 23.1), is important as this may be useful in georeferencing. Hand-held GNSS receivers that position to within 3–15 m are useful for georeferencing tasks. This is because the spatial dimension of most land features under investigation are normally larger than the 15 m accuracy typical for positioning using single frequency hand-held receivers.



Fig. 23.1 Ground-truthing using aerial photos: example of remnant vegetation at Mt. Kokeby, Australia. This could be located using a hand-held GNSS receiver similar to that shown in Fig. 4.1 on p. 48

23.3 Monitoring of Land Conditions

23.3.1 *Soil Landscape Mapping*

Soil maps define mapping units where a particular soil type is believed to be located. On the other hand, *soil landscape mapping* is a survey of land resources, which delineates repeating patterns of landscapes and associated soil types and differs from soil mapping in that the landscape component is an explicit part of the mapping Schoknecht et al. (2004). Uses of land resource data collected during a soil-landscape mapping program include Schoknecht et al. (2004); reducing the risk in decision-making (ensuring that changes in land management are the result of land resource information that reduces the uncertainty about the impact of different strategies), improving our understanding of biophysical processes, designing large-scale land use changes (e.g., targeted re-vegetation to control dry land salinity), environmental regulation and trading systems, mapping and monitoring land conditions to support national policies on natural resource management support of international agreements (e.g., Kyoto Protocol demands for predictions of the distribution and dynamics of soil carbon over a range of scales), and support of environmental management systems. For example, Pieri (1997) used GNSS to collect spatial data needed for planning sustainable land management. Using GNSS information, photographs and photo mosaics, simple information such as field boundaries, farmers' appreciation of soil productivity or constraints (using, e.g., indigenous classification of soils), and land use rights were collected and registered. The report proposed the use of GNSS to spatially reference all physical and social information in land management planning.

Schoknecht et al. (2004) divided the information about the soils and landscapes of Western Australia into point data stored in a soil profile database, which is comprised of site specific information such as soil profile descriptions, the results of laboratory analysis and photographs, map unit polygons stored as digital lines, boundaries drawn around areas containing similar soil and landscape patterns, and a map unit database that contained descriptions of the map unit polygons and related them to broad areas rather than a specific point. In both point and polygon data, GNSS satellites played an important role during the data collection process, with GIS used to provide the spatial database.

23.3.2 *Provision of Point Data*

Field surveys for soil landscape mapping involves occupying selected sites identified during a preliminary survey and reconnaissance. Factors influencing the selection of these sites include ease of access and the changing landscape. Representative soils from these selected sites are examined in soil pits with samples taken for chemical and physical analysis. Besides the examination of the soil, other physical descriptions of the site, such as slope and vegetation, are also recorded.

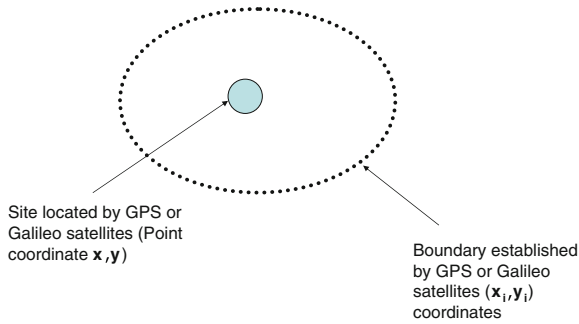


Fig. 23.2 Schematic description of how GNSS can provide site and boundary locations. These values can easily be integrated in a GIS system to enhance analysis

The important contribution of GNSS satellites in this process would be the provision of the site locations, which can be achieved using a hand-held receiver as shown in Fig. 23.2. This allows point data information on which all the landscape information relating to a specific site, such as; site *description*, soil *profile* description, soil *classification*, soil *profile's chemical*, and *physical properties* are related. The site description consists of information such as slopes measured using clinometers, landform patterns and elements of the survey area, the surrounding vegetation (e.g., Fig. 23.1), land surface and use. All these attributes can be input into a GIS database. An example of mapping soil characteristics that significantly affects crop production, e.g., clay content, organic matter content, nutrient content, and plant available water, is illustrated, e.g., in the work of Brubaker et al. (1993).

23.3.3 Provision of Polygon Data

Since the aim is to produce the soil landscape maps, the boundary of the maps are traced on aerial photographs or satellite imagery and then captured digitally using computer-aided mapping systems (e.g., in a GIS). This is done by either scanning the photographs or by keying in directly the two dimensional x, y coordinates. The boundary coordinates $\{x_i, y_i\}$ that form the map unit polygon are provided through satellites or ground surveying methods and are then mapped onto those of adjoining surveys. GNSS satellites provides control and tie points needed to match these boundaries (i.e, orienting the aerial photographs). For example, Fig. 11.9 on p. 170 indicates control points that are selected, marked, and accurately surveyed using GNSS positioning techniques discussed in Sect. 6.4.2. These points are then captured by aerial photographs and the GNSS positions compared with those of the photograph to control the quality of the maps derived from the photographs.

Alternatively, points could be located in older photographs and their positions established using GNSS receivers to control the quality of the digital maps derived

from these photographs. Tie points on the other hand are common points that appear on different overlapping photographs. They too could be located using GNSS satellites, and together with the control points provide the base upon which landscape maps could be prepared. Point data and map unit polygons form map unit databases that relate to the entire landscape. Use of such digital maps include precision farming discussed in Sect. 23.5.1. Details of the actual geoinformatics procedures needed to generate maps are discussed in Chap. 19.

23.4 Monitoring of Land Degradation

Bell (1997) classifies land degradation as both a local and global problem. Locally, the individual land owners are faced with the problem of declining land productivity while globally, the increase in population poses a threat to the fertile land and decreasing resources. The demand for increased food production for feeding the increasing population must increasingly be met from increased production per unit area Bell (1997). Another emerging global challenge is the increasing conversion of productive agricultural land to other usage such as biofuel production leading to reduced food production and increased food prices. For instance, the contribution of biofuel production has been associated, e.g., by Kgathi et al. (2012) to influence increase in food prices. This is due to the fact that food availability is affected if food crops or productive resources such as land, labour, water are diverted from food production to that of biofuel (e.g., Kgathi et al. 2012). Indeed, identifying the serious effects of land degradation on the environment leads to increased efforts in quantifying the problem, developing possible solutions, and engaging with the community to resolve these problems Bell (1997).

Land degradation can be seen through the effect of salinity, water erosion, wind erosion, waterlogging, remnant vegetation decline, sub-soil compaction, soil structure decline, structural decline, fertility decline, eutrophication, acidification and water repellence Lantzké and Fulton (1993). The main cause of these forms of land degradation has been attributed to water, which is often an off-farm impact as a result of water recharge, water discharge, water runoff and flooding, e.g., Bell (1997).

23.4.1 Soil Erosion Monitoring

Soil erosion occurs through the process of detachment, transportation and the deposition of soil. The net effect is the loss of fertile top soil for agriculture, siltation of streams and lakes, eutrophication of surface water bodies, and the loss of aquatic biodiversity Onyando et al. (2005). Mackenzie (2003, p. 393) points out that an estimated 480 billion tons of topsoil have been lost to the world's farmers by erosion in the past few decades. Of this, 18 billion tons are said to be transported by rivers to oceans annually, while the rest moves to other terrestrial ecosystems.

In order to minimize the impact of soil erosion, it is essential that management practices take into consideration the magnitude and *spatial distribution* of soil erosion. Soil erosion models such as the Universal Soil Loss Equation (USLE) Hudson (1985) and its modified version (Revised Universal Soil Loss Equation RUSLE, e.g., Onyando et al. (2005)) have been developed to estimate the rate of soil erosion. Determination of soil erosion, however, poses a challenge due to the contribution of biophysical factors (e.g., soil and climate) and the interactions between them. The limitation of these models is their inability to cope with the large amount of data that describes the heterogeneity of the natural system Pandey et al. (2007). Within the scope of these models, remote sensing finds use in mapping and assessing the landscape attribute that control soil erosion such as land use/land cover, soil type, relief, slope, drainage etc.

Multi-temporal satellite images are useful in studying seasonal land use dynamics that contribute to soil erosion. Satellite imagery also provide information on erosion features such as gullies and vegetation cover, and also contribute in the generation of Digital Elevation Models (DEM), e.g., Fig. 19.3 on p. 262, useful for soil erosion models. This is achieved through the analysis of stereoscopic and microwave (SAR) data. Lufafa et al. (2003) combined aerial photo interpretation and interpretation of Landsat TM images of 1994 to generate land use/land cover maps using the normalized digital vegetation index (NDVI). Parameters of the land use/land cover maps were then inserted in the USLE model to predict the rate of soil erosion.

In Onyando et al. (2005), multi-spectral image processing is used to extract thematic information from Landsat TM (bands 2, 3 and 4) data to generate land cover maps from which parameters for the USLE model are derived. Supervised classification using maximum likelihood is adopted. Other studies that have generated land cover maps useful for soil erosion include Ismail and Ravichandran (2007); Lu et al. (2004); Pandey et al. (2007). In Lu et al. (2004), geometric rectification of the images was achieved using ground reference data collected from topographic maps. As was discussed e.g., in Chap. 19, GNSS-derived topographical maps could be useful. Besides, GNSS could also provide DEM (see e.g., Fig. 19.3), and also in providing location-based data for generating spatial distribution of soil erosion (as shown e.g., in Fig. 6.9 on p. 89).

23.4.2 Salinity Monitoring: The Catchment Approach

Salinity can be classified into primary and secondary salinity. Over millions of years, salt from the ocean has been collected and deposited by wind and rain across landscape, with few rivers returning this salt to the sea. This led to a gradual accumulation of salt, which eventually became part of the natural landscape termed *primary salinity*.¹ *Secondary salinity* of soil, or ‘salinization’, results from rise in water table, which is often caused by changing land use actions such as land clearing or irrigation,

¹ http://www.environment.sa.gov.au/education/pages/modules/land/salinity_02.html

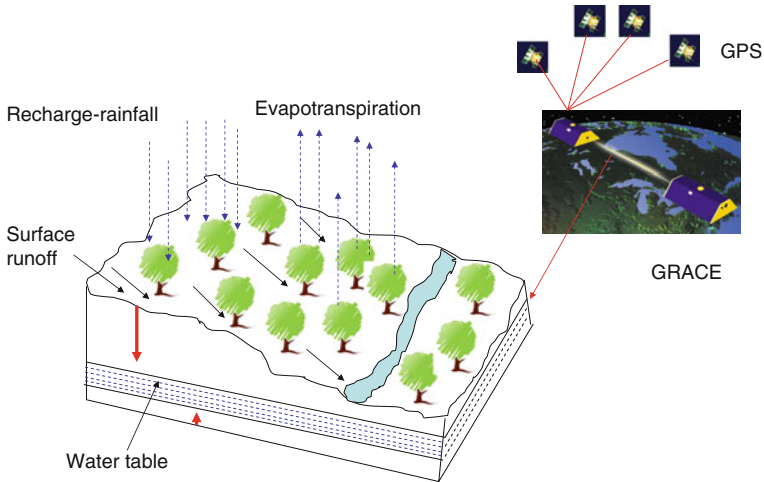


Fig. 23.3 With natural vegetation, the water balance is maintained, groundwater levels are low, less recharge, less runoff and salinity is curbed

where the term ‘water table’ refers to underground water (or groundwater), which may be very deep, but can be quite close to (or at) the surface.

The major origin of salt causing secondary salinity is rainfall which has deposited large amount of salt over ten thousands of years. Other contributors are weathering of minerals in the underlying bedrock and marine sediments. The processes leading to *secondary salinity* are traced to the altered water balance due to the fact that deeply rooted perennial native vegetation, which helped maintain the groundwater balance (e.g., Figs. 23.3 and 23.4) has been replaced by pastures and crops that do not use enough rainfall to lower water tables and significantly reduce salinity.

The clearing of such vegetation has seen increased recharge at a much faster rate than would otherwise occur naturally. The excess water not used by vegetation seeps into the soil, past the root zone, and contributes to increase in stored groundwater. With time, the groundwater water table rises and in the process dissolves the solid salt stored deep in the soil. When the water table reaches within 1–2 m of the soil surface, salt enters the plant root zone and growth is affected. This process is called *dryland salinisation* and has been reported, e.g., in NLWRA (2001) to affect a significant proportion of agricultural soils in south-western Australia.

Apart from the dryland salinity, there is also *irrigation salinity*, which is caused by the recharge of groundwater by excessive irrigation and leakage from irrigation channels. This again causes water tables to rise and in so doing brings salt to the root zones. Besides vegetation clearing and irrigation, the local landscape (i.e., geology and topography) and groundwater aquifer characteristics also play an important role in the susceptibility of land to salinization. In both dryland and irrigation salinity, saline groundwater near the soil surface kills native vegetation and reduces biodiversity, thus threatening the overall health of natural ecosystems (see Fig. 23.5).

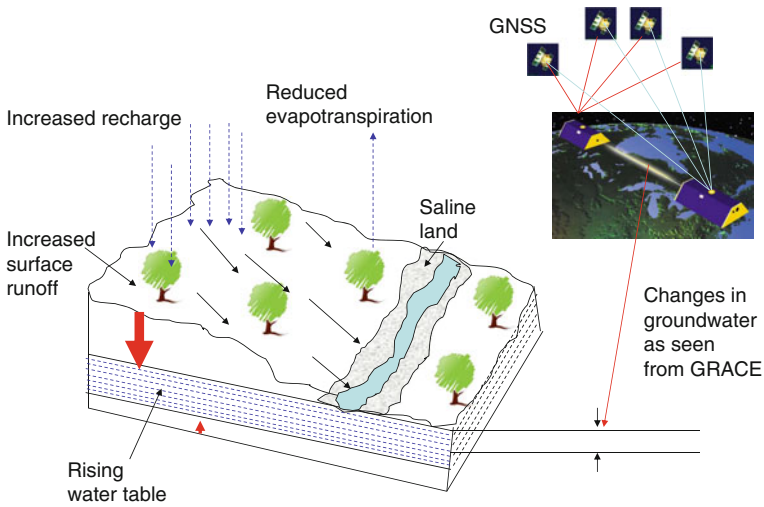


Fig. 23.4 With vegetation cleared, the water balance is disturbed. Groundwater levels rise, recharge increases with increased runoff and salinity increases. GRACE satellites discussed in Sect. 20.3.3 could provide a possible means of measuring changes in water level at catchments having sufficient spatial resolution for its use



Fig. 23.5 Impacts of salinity at Mt. Kokeby, Australia

It also results in the loss of agricultural productivity, deteriorates the quality of drinking water, and damages infrastructure such as roads and buildings.

In the Murray-Darling Basin (MDB) in Australia for example, agricultural production is reported to account for approximately 40 % of the total production in Australia Ellett et al. (2005). This high level of agricultural production comes despite MDB's high aridity and low runoff compared to other major river basins Ellett et al. (2006). This comes at the expense of irrigation, which uses about 75 %

of the total water used in Australia, and extensive clearing of native vegetation for cropping and pastoral land use (Ellett et al., 2005).

As already illustrated in Fig. 23.4, vegetation clearing leads to salinity as does extensive irrigation. Since both irrigation and clearing of the MDB has occurred to sustain agricultural productivity, the landscape and river systems have been dramatically altered leading to several undesirable effects, including increased salinity, diminished biodiversity and ecosystem degradation Ellett et al. (2006). The number of land parcels falling victims to salinity seems to be on the rise, calling for integrated catchment-based remedies. For instance in New South Wales (Australia), over 500,000 hectares of land were estimated to be impacted by salinity in the year 2000, with a projection of 2–4 million hectares by 2050 if changes in land use are not enacted Ellett et al. (2006).

Management Options: Management of salt-affected land (or potentially salt-affected land) must be based at least on a whole catchment approach, e.g., Read (2001). Catchment management involves all those activities related to the *capacity to produce and maintain* runoff and groundwater with desirable quality and quantity characteristics, and by reducing the undesirable consequences of land use on stream behavior Bell (1997). Catchment management should, therefore, be holistic in outlook, i.e., it should involve the consideration of all aspects of the physical and socio-economic environments that impinge on the catchment, its resources, and their use. Management of *discharge* areas will differ from the *recharge* areas. Discharge areas are part of the landscape where groundwater approaches or reaches the soil surface. Recharge areas on the other hand are part of the landscape where water passes below the root zone and adds to the groundwater (see Fig. 23.4).

Management of discharge areas aims at obtaining production (i.e., of salt tolerant shrubs or pasture) from the area, while at the same time reducing the salt-affected land. Actions taken on, or immediately around, discharge areas can take the form of engineering remedies such as digging drains or banks, to biological methods such as planting shrubs, grasses or trees or a combination of both engineering and biological. Management of salt-affected areas to alleviate the problem uses four principles Bell (1997); *increase water use, decrease surface evaporation, decrease water-logging, and increase leaching* of salt.

Management of recharge areas essentially leads to the prevention of salinity with the objective being to reduce recharge water (Fig. 23.4) reaching groundwater. This can be achieved by increasing plant water use and by using engineering means to divert excess water from the saline areas to avert ponding and water-logging. One approach for achieving this is to plant deep rooted plants with the ability to use water throughout the year. This approach has been found to yield fruit in some parts of Western Australia (WA). For instance, Greenwood et al. (1985) found that at North Bannister, the annual evaporation from trees (*Eucalyptus cladocalyx*, *E. globulus* and *E. maculata*) was some seven times the evaporation from grazed pasture Read (2001). Planting trees and shrubs on recharge areas of agricultural catchments is also being advocated by the Department of Agriculture in WA. While it is not economic to indulge in large scale plantings, there are often areas in catchments which can be identified as “specific recharge areas” Nulsen (1984), which are small,

make a major contribution to recharge, and do not produce economic crops or pastures, but can be used for planting trees or shrubs. Encouraging extensive planting, especially in high recharge zones, of deep-rooted perennial plants (trees, shrubs and pastures) is, therefore, one of the clearest mechanism to fight salination.

Plants such as barley and lupins are also known to have high water uptake owing to their deep roots and are encouraged for prevention. The difference in plant water usage is attributed to *rooting depth*, *leaf area index*, and *biomass*. For example, barley, and lupin have root penetration down to 2.5 m. Barley also has been shown to attain the highest leaf area index, followed by lupins, wheat and clover. Lupins have been shown to have higher transpiration rates than wheat and pasture in late winter due to greater biomass. The disadvantage with the plants approach is that they are not annual crops and are unable to utilize water throughout the year, thus rain which fall outside of the growing season still seep into the soil Bell (1997).

Example 23.1 (Geoinformatics support of salinity management) This can possibly be achieved in two basic ways:

1. In the first instance, remote sensing and photogrammetry could be employed to map the spatial extent of affected areas. Given their penetration abilities, microwave remote sensing sensors would be better suited for this. GNSS hand-held receivers could then be used in monitoring salt-tolerant pasture areas through the mapping of the boundary of salt-tolerant pasture species (e.g. barley). The GNSS data could then be input into a GIS database for monitoring purposes.
2. The second approach would be the monitoring of changes in groundwater as illustrated in Fig. 23.4. For large spatial coverage, use of piezometers may not suffice and hence the requirement of space techniques. The monitored variations in groundwater could then be correlated with the re-vegetation measures to assess the impacts of replanting of trees or retained native vegetation to curb salinity. In this particular scenario, GNSS plays the supportive role to GRACE remote sensing satellite (see, e.g., Chap. 20). It should be mentioned, however, that the resolution of the catchment area must be suitable for use of GRACE. Other components of the total water storage such as surface water and soil moisture need to be isolated to leave only the groundwater. Soil moisture could be measured using microwave scatterometers (see Table 9.1 on p. 138). This overall approach of using GRACE satellites, however, remains an ambitious proposal to be tested.

End of Example 23.1

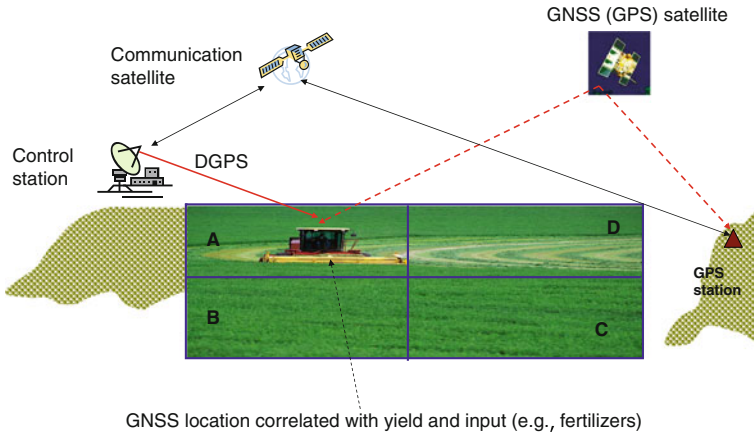


Fig. 23.6 Application of GNSS to precision farming

23.5 Role of Geoinformatics in Precision Farming

23.5.1 Precise Farming

Traditionally, farming normally treats the “*whole field*” as a single (homogeneous) entity upon which decisions (based on field averages) have been made. Inputs (e.g., fertilizers) are then applied uniformly across the field. Modern farming methods (also known as precision farming), however, divide large pieces of land into smaller segments that are managed separately to optimize productivity (see, e.g., Fig. 23.6) through the use of GNSS.

Precision farming is the gathering of information dealing with *spatial* and *temporal variation* within a field with the aim of using the information to manage inputs and practices. This is made possible by linking *computers, mobile sensors, GNSS, GIS* and other devices Grisso et al. (2003). It is a comprehensive approach to farm management and has the following goals and outcomes; *increased profitability and sustainability, improved product quality, effective and efficient pest management, energy, water and soil conservation, surface and groundwater protection, yield rates, pest infestation management, and other factors that affect crop production* Grisso1 et al. (2002). To achieve these outcomes, farm managers base their decisions on the requirements of each zone to control input resources. *GNSS and GIS can be used to control the input of these zones* as discussed, e.g., in Steede-Terry (2000, Chap. 9).

Precision farming allows the management of various zones, with the zone having a higher potential for economic return receiving more inputs, if needed, than less productive zones so as to achieve maximum economic return for each input Grisso1 et al. (2002). Dobermann and White (1999) refer to precision farming as site specific crop management and discuss how GNSS satellites are applicable to nutrient management.

Precise farming attempts to increase food production per unit area and as such, requires proper land utilization and management of the input resources, e.g., *fertilizers* to maximize the yield. When this is done in a manner such that the environment is protected and conserved, and social values also promoted, it can lead to *sustainable agriculture*, whose indicators are *state of resource*, *biophysical* and *economic* trends.

For instance, the application of GNSS to *precision farming* have been shown to include soil sample collection, chemical application controls, and harvest yield monitoring El-Rabbany (2006, p. 142). The applications of GNSS for soil sampling was discussed in Sect. 23.3.1. Spraying of the field from airplanes could be integrated using aerial guidance systems in such a way that the field sprayer is guided using a moving map display. Based on the sprayer's location, the system will apply the chemical at the correct locations, with minimal overlap, and automatically adjust the chemical's use rate, thus increasing the efficiency of chemical and fuel usage El-Rabbany (2006, p. 14). The position of these field spots could be provided by GNSS as discussed in Sect. 23.3.3.

Example 23.2 (Trimble's AgGPS) Trimble (<http://www.trimble.com>) has developed the AgGPS system, which combines in-field guidance using GPS satellite receivers and intelligent farm management. The AgGPS field positioning systems enable field guidance at a higher accuracy, allowing farmers the possibility of collecting information on tillage, cultivation, irrigation, topography and infestations, which can then be mapped and analyzed in a GIS to provide a better understanding of the elements affecting farm operations and management Buick (2006). The system can be tailored for site specific applications such as yield mapping and variable rate management. Buick (2006) lists the primary reasons why many farmers are considering (or reconsidering) numerous site-specific precision agriculture practices as the net gain in sustainable agriculture, i.e., *economic*, *environmental* and *sociological* paybacks from GNSS-guidance and automated steering systems, and the decrease in the cost of GNSS machine control systems. With more GNSS satellites on the way, this cost is expected to be even lower.

End of Example 23.2

23.5.2 Farm Topographic Maps

A farm topographic map is an example of maps (see Sect. 19.3.1) produced using either DGPS or RTK methods of GNSS positioning discussed in Subsects 6.4.4.1 and 6.4.6 respectively. They are useful in depicting topographical features such as elevation, landscape, drainage, soil attributes, slopes etc. Since spatial yield variability is usually related to topographical features, see e.g., Cassel et al. (1996); Jones

et al. (1989); Kravchenko and Bullock (2000); Schmidt et al. (2003); Timlin et al. (1998); Yang et al. (1998) etc., the availability of high accurate GNSS *farm topographic maps* should enhance *operational efficiency* and lead to better, improved *agricultural and environmental management*. For instance, such maps should lead to improved management of agricultural inputs such as fertilizers, and in water deficient countries such as Australia, contribute to better management of surface and groundwater.

Example 23.3 (Controlled Traffic Farming (CTF) Solutions) Controlled Traffic Farming (CTF) Solutions is an Australian-based organization that seeks to provide solutions on focusing on efficient and effective use of *farm resources* to maximize production and minimize *environmental impacts* such as *soil erosion* and *water-logging*. (see <http://www.ctfsolutions.com.au/> [Accessed on 8-09-2009].) CTF Solutions collects topographic data using a 2 cm auto steer operations during the period which the tractor is in the field undertaking farm operation or by using a vehicle with an antenna mounted on it. In order to collect gridded data for the purpose of generating elevations, the vehicle is driven at regular swath intervals (width of 20–40 m) with the GNSS receiver logging data at 5–10 m intervals. Besides these regular grids, data for other features of environmental interest, such as flood runners and erosion washers, are also collected.

Fig. 23.7 GNSS topographical map taken in 2004 by CTF overlaid on a high resolution IKONOS imagery. *Dark red* colours indicate areas of poor drainage affected by water-logging. Source <http://www.ctfsolutions.com.au>

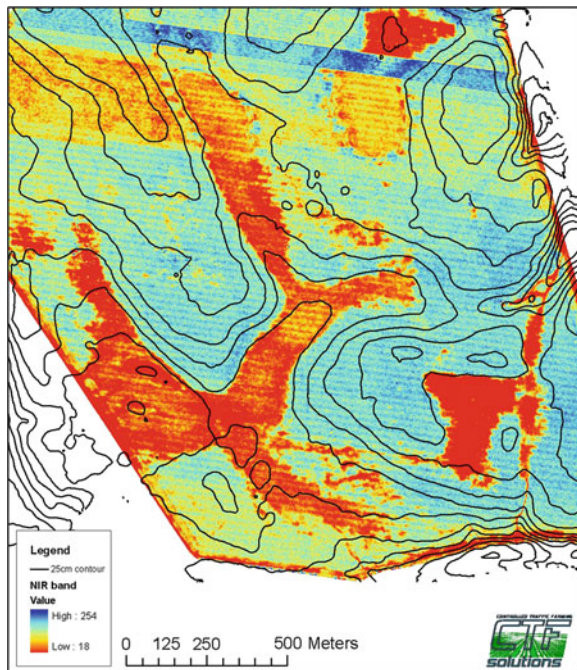




Fig. 23.8 GNSS topographical map taken by CTF overlaid on a high resolution IKONOS imagery. The *left* figure was taken in April 2004 (see Fig. 23.7) above. The *right* figure indicates the same area in August 2006 after drainage was undertaken in 2005. Source <http://www.ctfsolutions.com.au>

The data is then analyzed using a GIS system to generate topographic maps (see, e.g., Fig. 19.2 on p. 261).

An illustration of the CTF Solution's application of GNSS (RTK approach) is presented in Fig. 23.7, where CTF's RTK collected topographical data at 25 cm contour interval are overlaid on a high resolution IKONOS imagery. (© Geoeye 2004 NIR band.) The figure essentially shows that low lying areas of production have suffered significant crop loss due to water-logging (Tim, pers. comm).

Following the results outlined in Fig. 23.7, drainage was undertaken on the paddock in 2005 and GNSS together with high resolution imagery once again applied to monitor the environmental impact of water-logging in 2006 (Fig. 23.8). In 2004, this water-logging cost the farmers in the order of Australian \$50,000 in lost production (Tim, pers. comm). The combination of GNSS and high resolution imagery was the key to the success, otherwise each monitoring method on their own would not have told the whole story (Fig. 23.8). This example, therefore, provides a good illustration of the role played by geoinformatics in monitoring *environmental impacts* on farms.

End of Example 23.3

23.6 Concluding Remarks

This chapter has presented the possibility of using geoinformatics to support land management measures. Discussions have been made on pertinent land management issues including reconnaissance and validation, monitoring of land conditions and land degradation, together with precision farming. It is clear from the discussion that the area of precision farming has received a greater share of GNSS application compared to other areas of land management. In general, however, the uses of GNSS satellites are more vital in areas of land management that requires information on positions and spatial coverage. With more GNSS satellites being launched, they are expected to become more useful to land management, particularly when coupled with GIS and/or remote sensing methods.

References

- Bell RW (1997) Introduction. In: Bell RW (ed) Land management unit reader. Murdoch University, Perth, pp 3–7
- Brubaker SC, Jones AJ, Lewis DT, Frank K (1993) Soil properties associated with landscape position. *Soil Sci Soc Am J* 57(1):235–239
- Buick R (2006) GPS guidance and automated steering renew interest in precision farming techniques. White paper, Westminster
- Cassel DK, Kamprath EJ, Simmons FW (1996) NitrogenSulfur relationships in corn as affected by landscape attributes and tillage. *Soil Sci Soc Am J* 88(2):133–140
- Dobermann A, White PF (1999) Strategies for nutrient management in irrigated and rainfed lowland rice systems. In: Balasubramanian V, Ladha JK, Denning GL (eds) Resource managements in rice Systems: nutrients. Kluwer Academic Publishers, Netherlands
- Greenwood EAN, Klein JL, Beresford JD, Watson GD (1985) Differences in annual evaporation between grazed pasture and Eucalyptus species in plantations on a saline farm catchment. *J Hydrol* 78:261–278
- Grisso RB, Oderwald R, Alley M, Heatwole C (2003) Precision farming tools: global positioning system (GPS). Virginia Cooperative Extension (VCE), publication, Blacksburg, pp 442–503
- Grissol RB, Alley M, McClellan P, Brann D, Donohue S (2002) Precision farming: a comprehensive approach. Virginia Cooperative Extension (VCE) publication, Blacksburg, pp 442–500
- Ellett KM, Walker JP, Rodell M, Chen JL, Western AW (2005) GRACE gravity fields as a new measure for assessing large-scale hydrological models. In: Zenger A, Argent RM (eds) MODSIM 2005 international congress on modelling and simulation, modelling and simulation society of Australia and New Zealand, pp 2911–2917. ISBN: 0-9758400-2-9
- Ellett KM, Walker JP, Western AW, Rodell M (2006) A framework for assessing the potential of remote sensed gravity to provide new insight on the hydrology of the Murray-Darling Basin. *Aust J Water Resour* 10(2):89–101
- Hudson N (1985) Soil Conservation. Batsford Academic and Educational, London
- El-Rabbany A (2006) Introduction to GPS global positioning system, 2nd edn. Artech House, Boston
- Ismail J, Ravichandran S (2007) RUSLE2 model application for soil erosion assessment using remote sensing and GIS. *Water Resour Manag* 15:41–54
- Jones AJ, Mielke LN, Bartles CA, Miller CA (1989) Relationship of landscape position and properties to crop production. *J Soil Water Cons* 44(4):328–332

- Kgathi DL, Mfundisi KB, Mmopelwa G, Mosepele K (2012) Potential impacts of biofuel development on food security in Botswana: A contribution to energy policy. *Energy Policy-Elsevier* 43:70–79
- Kravchenko AN, Bullock DG (2000) Correlation of corn and soybean grain yield with topography and soil properties. *Agron J* 92(1):75–83
- Lantze N, Fulton I (1993) Soils of the northam advisory district. The darling range and West Kokeby Zone. *Agric WA Bull* 3:42–57
- Lu D, Li G, Valladares GS, Batistella M (2004) Mapping soil erosion risk in Rondonia, Brazilian Amazonia: using RUSLE, remote sensing and GIS. *Land Degrad Dev* 15:499–512
- Lufafa A, Tenywa MM, Isabirye M, Majaliwa MJG, Woomer PL (2003) Prediction of soil erosion in a Lake Victoria basin catchment using GIS-based universal soil loss model. *Agric Syst* 76:883–894
- Mackenzie FT (2003) *Our changing planet; an introduction to earth system science and global environmental change*, 3rd edn. Prentice Hall, New Jersey
- Nulsen RA (1984) *Saltland management—the catchment approach*. Western Australia Department of Agriculture. Farmnote 133/84, Australia
- Onyando JO, Kisoyan P, Chemelil MC (2005) Estimating the potential of soil erosion for river Perkerra catchment in Kenya. *Water Resour Manag* 19:133–143
- Pandey A, Chowdary VM, Mal BC (2007) Identification of critical erosion prone areas in the small agricultural watershed using USLE, GIS and remote sensing. *Water Resour Manag* 21:729–746
- Pieri C (1997) Planning a sustainable land management: the hierarchy of user needs. *ITC J* 3(4):223–228
- Read V (2001) *Salinity in Western Australia a situation statement*. Resour Manag Tech Rep No.81 3:223–228. ISSN 0729-3135
- Schmidt JP, Taylor RK, Gehl RJ (2003) Developing topographic maps using a sub-meter accuracy global positioning system. *Appl Eng Agric* 19(3):291–300
- Schoknecht N, Tille P, Purdie B (2004) *Soil landscape mapping in South-Western Australia. Overview of methods and outputs*. Resource management technical report 280, Department of Agriculture, Government of Western Australia
- Steede-Terry K (2000) *Integrating GIS and the global positioning system*. ESRI Press, California
- Timlin DJ, Pachepsky Y, Snyder VA, Bryant RB (1998) Spatial and temporal variability of corn grain yield on a hillslope. *Soil Sci Soc Am J* 62(3):764–773
- Yang C, Peterson CL, Shropshire GJ, Ottawa T (1998) Spatial variability of field topography and wheat yield in the Palouse region of the Pacific Northwest. *Trans ASAE* 41(1):17–27

Chapter 24

Marine and Coastal Resources

Shoreline and beach surveys can today benefit from the state-of-the-art GNSS monitoring techniques, which directly offer both two- and three-dimensional data sets within a short period of time.

Morton et al. (1993)

24.1 Marine Habitat

24.1.1 Background

Marine habitats are comprised of zones termed *coastal terrestrial*, *open water*, and the *ocean bottom* until several meters deep. Besides fish, these habitats are home to diverse flora and fauna, with swathes of sandy beaches and sand dunes spread across the globe critical for the survival of many endangered species e.g., turtles, dugongs, migratory birds etc. Several physical parameters, e.g., temperature, salinity, tides, currents, winds, etc., play a major role in defining the marine habitat. Malthus and Mumby (2007) have listed marine ecosystem to comprise *mangroves*, *seagrasses*, *coral reefs*, *lagoonal microbial mats*, *shoreline features*, *sub-littoral zone benthos* and *overlying water column features*. So delicate are most of these features such that some of them, for example, mangroves could serve as indicators of coastal change (Blasco 1996). The spectral reflectance of these features can be measured using remote sensing to provide synoptic data at various spatio-temporal scales. Such data are essential requirements for marine and coastal managers to be able to address issues facing these diverse and delicate habitats.

In most countries, these environments are either being degraded or not inventoried. This is due partly to their inaccessibility and partly due to their large spatial coverage, leading to high costs when applying conventional methods. Remote sensing and GIS offer possibilities of mapping and inventorying marine habitats, thus enhancing

the understanding of their unique characteristics. Malthus and Mumby (2007) have indicated that remote sensing could be used to reveal how patterns change across a near-continuum of spatio-temporal scales, details of which are useful in identifying the scale at which disturbance such as El Niño-Southern Oscillation (ENSO) causes changes in the marine environment. In what follows, we examine some of the ways in which geoinformatics could be used to support mapping of marine habitats.

24.1.2 Geoinformatics-Based Monitoring of Marine Habitats

The presentation in this section shows the complementary nature of remote sensing, GIS and GNSS methods in supporting monitoring of marine habitats. Remote sensing techniques applicable to monitoring of marine habitats include, e.g., aerial photography, airborne optical sensors, microwave remote sensors (radar systems) e.g., Synthetic Radar Aperture (SAR), and optical satellite-based sensors. Analysis tools include empirical models and multi-spectral classifications. Remote sensing and GIS techniques are useful in discriminating marine habitats as demonstrated, e.g., by Call et al. (2003) who discriminate coral reef habitats. Held et al. (2003) applied hyperspectral and radar techniques to map tropical mangroves. Discrimination of marine habitats requires that the radiative transfer properties of the marine environment be well understood. Effective use of remote sensing to monitor water quality will require an established relationship between water color and constituent bio-optical water quality parameters such as suspended organic matter and dissolved organic matter (Malthus and Mumby 2007). Karpouzli et al. (2003) have highlighted the need to understand the spatial and temporal variations in optical water quality parameters and their influence on inherent and apparent optical properties.

Owing to the high spatial diversity of marine habitats, high spatial and spectral resolution data are required to discriminate between features. Moderate resolution sensors, e.g., Landsat ETM¹ and SPOT are limited by poor spatial and temporal resolution, spectral capabilities, and important signatures falling outside visible bands. Held et al. (2003) and Call et al. (2003) demonstrate that sub-pixel-scale mixing prevent accurate identification of features leading to coarse descriptive levels of mapping. One possible way of improving the performance of moderate resolution sensors would be the combination of optical and microwave sensors as described by Held et al. (2003), who combined these sensors for the case of mapping mangroves. In this case, increased classification accuracies with the use of multi-sensor data was possible.

Due to the optical similarity in the reflectance between the bottom and top marine features, leading to subsequent confusion during classification of remotely sensed data, care must be taken in distinguishing different classes (e.g., vegetation) on the basis of spectral reflectance. To overcome this challenge, higher-spectral resolution imagery is needed to perceive the subtle differences, see, e.g., Call et al. (2003).

¹ http://landsat.gsfc.nasa.gov/about/L7_td.html

Malthus and Mumby (2007) point out that classification based on high-spectral resolution airborne data tends to provide the best results. They advocate the necessity to better understand the depth limits to which useful above surface spectral signatures can be derived, but still allow the discrimination of habitat types, as does the relationship to varying water column optical properties. In this regard, Call et al. (2003) demonstrated that the point at which a spectral signature begins to resemble a water column's optical properties rather than substrate for a coral reef system is 7 m. However, this applies for certain locations only, in others, such as Ningaloo Marine Park in Australia, it is 15 or 20 m.

As already pointed out, one of the major shortcomings of remote sensing technique in mapping marine habitat is the poor spatial resolution of traditional sensors (e.g., 30 m in Landsat). Call et al. (2003) identified a spatial resolution of 4 m as critical for mapping seagrass in their littoral system. Therefore, High-resolution sensors (discussed in Sect. 8.3), like IKONOS and QuickBird, could be of use in such applications. Mumby et al. (1997) evaluated Landsat MSS², Landsat TM³, SPOT XS, CASI (Compact airborne spectrographic imager), SPOT (Pan) and a combination of Landsat TM and SPOT (Pan) to map Caribbean coral reefs. Landsat MSS was the least accurate sensor, while CASI was found to be more accurate than satellites sensors and aerial photographs. They noted that maps with detailed habitat information had a maximum accuracy of 37% when based on satellite imagery, 67% based on aerial photography and 81% based on CASI. In tropical regions, characterized by prolonged cloud cover, low accessibility, high temperature and high humidity, digital airborne colour and infrared photography are useful (Malthus and Mumby 2007).

Besides using optical remote sensing as a stand alone tool, a combination with other methods such as acoustic, SAR and LiDAR⁴ could be useful. Optical, SAR and LiDAR will cover above surface, while acoustic could be used for sub-surface studies. In this combination, LiDAR would offer high data density for bathymetry, optical spectral information with degree of penetration into water column and wide spatial coverage, and SAR the structural components of the habitat (onshore and sub-surface), which are less visible in optical sensors. This could be enhanced by the incorporation of knowledge-based classification algorithms (Sect. 10.3.3) to improve accuracies of classification (Malthus and Mumby 2007).

Ground truthing and georeferencing can be achieved using GNSS, where positions of selected marked features on a remotely sensed image are determined, e.g., using hand-held GNSS receivers. Besides ground truthing, GNSS is also useful in providing orientation for aerial photographs (e.g., Fig. 11.9 on p. 170). Validation of classification results obtained from processing remotely sensed image data is essential. This could be achieved through, e.g., matching signatures to defined biotopes; assessing changes between images; and applying the results in coastal zone management. Moreover, once the remote sensing data has been processed, they provide attributes that together with other data can be used in a GIS system to generate

² Multispectral Scanner.

³ Thematic Mapper.

⁴ Light Detection and Ranging.

a marine habitat georeferenced system. This system can be edited, updated, and queried, which greatly benefits marine habitat management.

Example 24.1 (Application to microbiology monitoring program Schiff and Weisberg (2001) conducted an inventory to assess the number, type, spatial distribution, and costs of microbiological monitoring programs in southern California marine waters from Point Conception to the US/Mexico border. The location of each sampling site was determined using GNSS, while the estimates of geographic coverage were determined using GIS techniques. A list of organizations that conduct microbiological monitoring in marine waters was compiled by contacting all city and county public health agencies and regional water quality control boards in Southern California. Monitoring organizations were then surveyed to ascertain the following information about each sampling site: station name, location (latitude/longitude, general description, water body type), depth of sampling, analytes measured, analytical methods, and sampling frequency by season. Where latitude and longitude data were unavailable, the sites were revisited and the position of the sampling sites found using DGPS (Sect. 6.4.4.1). The relative distribution of sampling effort among habitat types was assessed by differentiating sampling sites into offshore and shoreline strata. Shoreline sites were further differentiated into eight categories: (1) high-use sandy beaches, (2) low-use sandy beaches, (3) high-use rocky shoreline, (4) low-use rocky shoreline, (5) perennial freshwater input areas, (6) ephemeral freshwater input areas, (7) embayment, and (8) restricted access areas.

End of Example 24.1

24.2 Shoreline Monitoring and Prediction

24.2.1 Definition and Scope

A shoreline is defined as the boundary between the continent and the portion adjacent to the sea where there is no effective marine action beyond the maximum reach of the waves, and is identified by cliffs, the boundary between the vegetation and the seashore, by the rocks, or by any other feature that determines the beginning of the continental area (see e.g., Soares et al. (1995) and Suguio (1992)). In Fig. 24.1, four examples of different scenarios that define the position of a shoreline are presented as follows; in (a), the shoreline is the boundary between the vegetation and the seashore while in (b), (c), and (d), the shoreline is the boundary between the continent and the portion adjacent to the sea where there is no effective marine action beyond the maximum reach of the waves, characterized by urban settlement and problems of coastal erosion.



Fig. 24.1 Examples of definition of a shoreline; **a** the shoreline is the boundary between the vegetation and the seashore while in **(b)**, **(c)**, and **(d)**, the shoreline is the boundary between the continent and the portion adjacent to the sea where there is no effective marine action beyond the maximum reach of the waves, characterized by urban settlement and problems of coastal erosion. *Source* Goncalves (2010)

Shorelines are known not to be stable and vary over time causing the effects of *progradation* (i.e., a shoreline moving towards the sea due to deposit) or *retrogradation* (i.e., a shoreline moving towards the land due to wave erosion). *Long-term changes* can be related to changes in sea level, sediment supply, wave energy, and geological controls (contemporary and antecedent), causing movements in the position of a shoreline over a period of centuries and millennia. *Short-term changes*, on the other hand, occur over time scales of 80 years or less and are related to daily, monthly, and seasonal variations in tides, currents, wave climate, episodic events and anthropogenic factors (see, e.g., Demarest and Leatherman (1985), Galgano et al. (1998) and Galgano and Douglas (2000)). Very rapid (episodic) changes in shoreline location can also occur as a result of (tropical) storms and hurricanes and can move a shoreline more than 30m in a day (Gibeaut et al. 2001). Fenster et al. (1993) describe shoreline movement as a complex phenomenon and the difficulties involved in distinguishing long-term shoreline movement (signal) from short-term changes (noise), although for long-term analysis, the effect of storms are not treated as outliers, hence they are considered in the temporal data distribution, e.g., Fenster et al. (2000). The complexity of the definition of a shoreline, mapping, and subsequent utilization are discussed, e.g., in Boak and Turner (2005) and Li et al. (2001). Ma et al. (2003) and Di et al. (2003) employ high resolution satellite imagery to perform 3D shoreline extraction and mapping.



Fig. 24.2 An example of environmental degradation of a coastal area through erosion. *Source* Goncalves (2010)

Monitoring and prediction of shorelines is vital for environmental and resource management. Most coastal areas are known to experience soil erosion (see Fig. 24.2), which in some cases, lead to the disappearance of beaches, destruction of cliffs by gullies, or submersion of parts of the coast. Yet beaches have been known to be a source of revenue for those countries that attract tourism along their coasts. Environmental management is therefore essential in realizing the long term durability of such coastal areas. One way of realizing efficient management of beaches is through constant monitoring of the coastal shorelines. Through continuous monitoring, policy and decision makers are informed of the behavior of forcing and response parameters of shorelines. These forces are, e.g., changes in the forces that move the sand, namely wind, waves, and currents.

Monitoring is therefore essential in improving the database of information on shorelines evolution in an area, thereby indicating the trend in beach loses as demonstrated by Fig. 24.3. Metropolitan Borough of Sefton (2002) have listed the benefits of shoreline evolution information as; *providing input to shoreline review plans, planned maintenance of coastal defenses, achievement of high government level targets, determination of appropriate design criteria for coastal works, biodiversity action plan, implementations of habitats directive, and leisure and amenity management of shoreline areas*. Shoreline information have also been used to support other monitoring studies, e.g., in microbiological monitoring of marine recreational waters, see e.g., Schiff and Weisberg (2001), while accurate interpretation of its movement trends and precisely quantifying the rates of movement are necessary to accurately predict its future positions (Morton et al. 1993).



Fig. 24.3 Impacts of shoreline erosion in Matinhos District in the coast of Paraná State, Brazil in 2007. *Source* Goncalves (2010)

24.2.2 Monitoring

Traditionally, monitoring of shorelines and beach dynamics has been undertaken using surveying techniques such as traversing and levelling (see Sect. 3.4) where shoreline positions are determined in addition to the height information that are linked to a nearby monument. To infer the rate of erosion, these positions and height information are compared to subsequent beach surveys to yield a two-dimensional cross-sectional area, which represents the amount of beach erosion and deposition that occurred between the surveys. A three-dimensional volumetric change in the beach is derived from the profiles by integrating between adjacent cross-sectional areas (Morton et al. 1993). Morton et al. (1993) lists the setbacks of these traditional approach as (i) loss of the reference monument upon which the heights are referenced through, e.g., erosion (ii) errors in the generation of the cross-sections since subsequent surveys may not traverse the same course, (iii) amount of time required to undertake the extensive survey, and (iv) the errors incurred in generating a three-dimensional volumetric data from a two-dimensional cross-sectional data.

To remedy these setbacks, shoreline and beach surveys can today benefit from the state-of-the-art GNSS monitoring techniques, which directly offer both two and three-dimensional data set within a short period of time, see e.g., Morton et al. (1993)

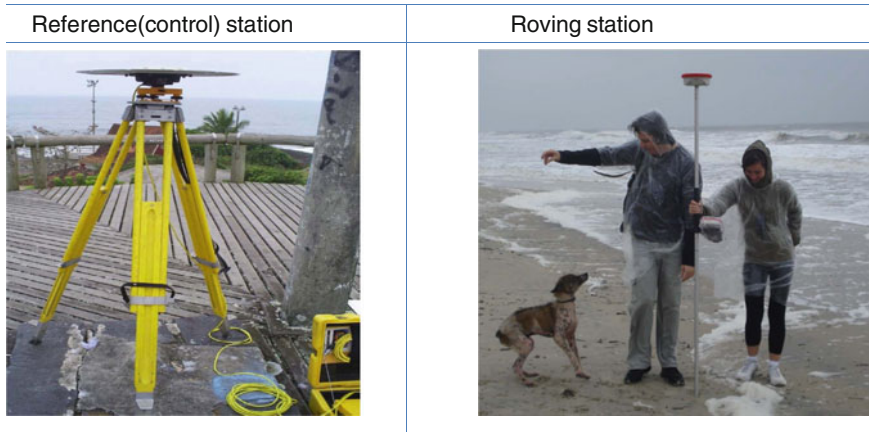


Fig. 24.4 *Left* Base station in Matinhos. Source: Goncalves (2010). *Right* Real-time GNSS shoreline monitoring. A roving GNSS receiver is used to provide shoreline's location-based data relative to the reference station whose position is known using one of the rapid positioning techniques discussed in Sect. 6.4.5. Source Goncalves (2010)

and Goncalves et al. (2012). Other mapping techniques that have benefited shoreline monitoring are photogrammetry, remote sensing, and LiDAR. These methods have been elaborately discussed, e.g., in Gorman et al. (1998). White and Asmar (1999) provide an illustration where the Thematic Mapper (TM) image is used to monitor the changing position of the Nile Delta coastline. To enhance these monitoring mapping tools, GIS techniques are now being used to analyze changes in natural phenomenon according to the evolution in time using spatio-temporal dynamic models in a Coastal Geographic Information System (CGIS). For example, CGIS has been used by Li et al. (2001) to monitor the Malaysian shoreline. With respect to GNSS satellites, the following roles are foreseen:

- (1) Providing orientation to aerial photographs (e.g., Fig. 11.9) and ground truthing data for remote sensing satellites.
- (2) Provision of *real-time* monitoring of positional data of the shoreline that informs the decision making of environmental (coastal) managers (see, e.g., Fig. 24.4, right).
- (3) Provision of *historical data* needed for computing the parameters of the predictive models as discussed in the next section.

Sect. 19.3.1.2 illustrates how GNSS could be applied to monitor shoreline changes.

24.2.3 Prediction

Whereas shoreline monitoring is essential as already discussed, predicting its future position is equally vital to support the *environmental impact assessment* and

management of programs such as predicting increased shoreline erosion (Hecky et al. 1984) and building setbacks to serve as protection for a time comparable to the expected lifetime of new coastal structures, usually 30 or 60 years (Crowell et al. 1997). According to Morton et al. (1993), predicting future rates of coastal erosion and land loss progressed from a purely academic exercise to one of environmental importance since many coastal states and government agencies relied on technical data to determine construction setback lines and insurance hazard zones. This led to the establishment of elaborate networks of closely spaced beach profile monuments that were periodically revisited to assess magnitudes and rates of shoreline movement that were used to establish building zones and to create construction control lines Morton et al. (1993). Going back to Fig. 24.3 for example, if the shorelines had been predicted before the roads were developed, such environmental degradation could have been avoided by constructing the roads further inland.

Crowell et al. (1997) states, however, that determining adequate setbacks requires estimating long-term shoreline changing trends from historical data. Fenster et al. (1993) developed a predictive method that detects short-term changes in the long-term trend and identifies linear or high-order polynomial models that best fit the data according to the minimum description length (MDL) criterion. In this method, only linear models are extrapolated.

Douglas et al. (1998) stressed the need to incorporate long-term erosion trends and historical records of storms, including their impact on shoreline position and beach recovery, in predictive models. Exploiting the relationship between shoreline and sea-level changes (i.e., using series of sparsely sampled sea level values as surrogate data for shoreline changes), they developed an algorithm to evaluate several predictive methods, such as the end-point method, linear regression, and minimum description length criterion. They evaluated several well-known shoreline prediction algorithms and established that linear regression gave superior results. Predictions shaped or influenced by higher-order polynomial schemes can sometimes be superior to those obtained from linear regressions, but they can also be extremely inaccurate (Crowell et al. 1997). Use of modern more accurate surveying measurement techniques such as photogrammetry and GNSS have also been shown to improve the quality of forecasts. Douglas and Crowell (2000) demonstrated that this is achievable even if the inherent variability of shoreline position indicators remains at the level of many meters.

The linear regression models that are usually used to predict shoreline positions work well when the underlying linearity and normal distribution assumptions are fulfilled. In some cases, however, the sources of data, particularly photogrammetric data are of a poor quality. Indeed, this fact is acknowledged, e.g., by Douglas et al. (1998) who point out that some data used in predicting shorelines are at times temporally poorly sampled historical shoreline positions, resulting in the violation of the linear regression assumptions. In others instances, the transformation process used to bring all the data into a common coordinate system (e.g., Sect. 6.6.2) may be poorly done, such that the resulting extracted shoreline positions used for predictive purposes are themselves inaccurate. In such cases, therefore, modern techniques such as GNSS provide *fast, efficient* and *accurate* means for data capture that support shoreline

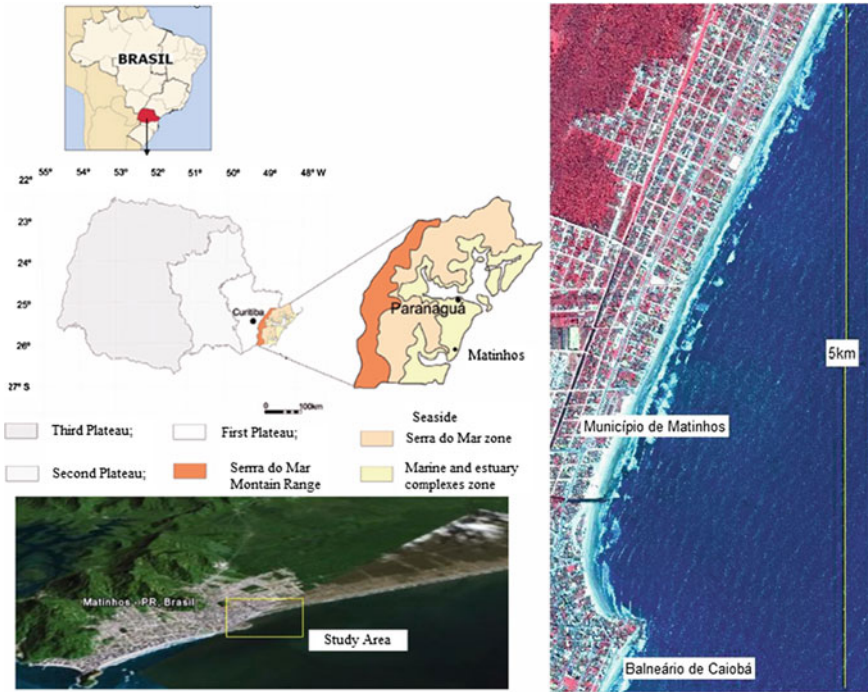


Fig. 24.5 Matinhos District in the coast of Paraná State, Brazil. *Source* Goncalves (2010)

prediction. In the following example, the use of GNSS in supporting predictions of shoreline positions is illustrated.

Example 24.2 (Shoreline prediction of Matinhos Beaches in Paraná, Brazil) Goncalves (2010)

Background of Matinhos: Matinhos District is located along the coast of Paraná State, Brazil (Fig. 24.5). The coastal region of the State of Paraná, located between the 25–26° S and 48–49° W, is formed by the Serra do Mar mountain range, extensive coastal plains, and estuary complexes.

Exploitation of the Matinhos shoreline started as early as 1920, but the first settlement begun in 1948 with a hotel built on the sandy shore. By 1949, a murrum road had been constructed near the shore (see Fig. 24.6). The settlement in Matinhos occurred near the shore, whereby in some oceanic beaches, the settlement was characterized by constructions on the shoreline or over the sand, leading to the destruction of dunes, wetlands, and forcing rivers to change course. This was as a result of unplanned settlement that did not take the morphology and coastal dynamic environment into consideration, see e.g., Pierrri et al. (2006). For instance, Fig. 24.7 indicates that the main road in front of the

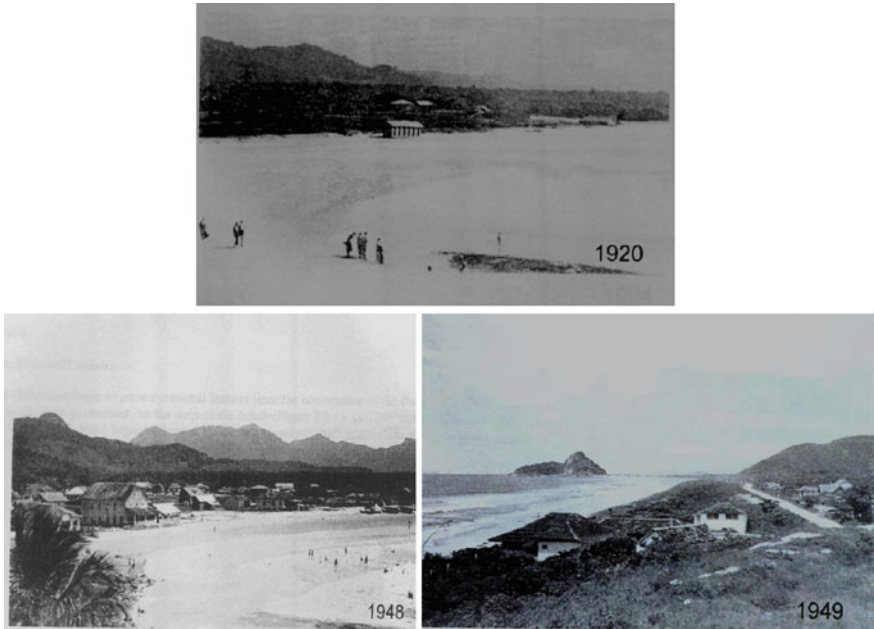


Fig. 24.6 Photos of the Matinhos shore in 1920, 1948, and 1949. *Source* Angulo et al. (2000)



Fig. 24.7 Vertical aerial photo taken in 1953. *Source* Pierri et al. (2006)

beach called Atlantic Avenue in Matinhos was planned to run alongside the shoreline in 1953, but has been faced with soil erosion problems.

Coastal erosion started in the 1970s and to date, this environmental degradation continues to be fueled further by the expanding development as illustrated in Fig. 24.7. Figure 24.8 shows the walls of concrete and rocks being used as protective tools against the encroaching ocean, but every year over the past



Fig. 24.8 Photos of the shore in 1981, 1994, and 1995. Walls of concrete were applied as protective tools against the encroaching ocean. *Source* Angulo et al. (2000)



Fig. 24.9 Houses destroyed by an ocean storm in May 2000, and removal of the houses and dune reconstruction in 2004. *Source* Pierri et al. (2006)

decades, storms have destroyed them, exposing the coastal settlement to erosion. For the past 40 years, this beach has continued to languish under these problems. According to Pierri et al. (2006), the process of coastal erosion once started has the tendency to grow and is often difficult to reverse thereby calling for prevention as the best cure. When the problems start, depending on the



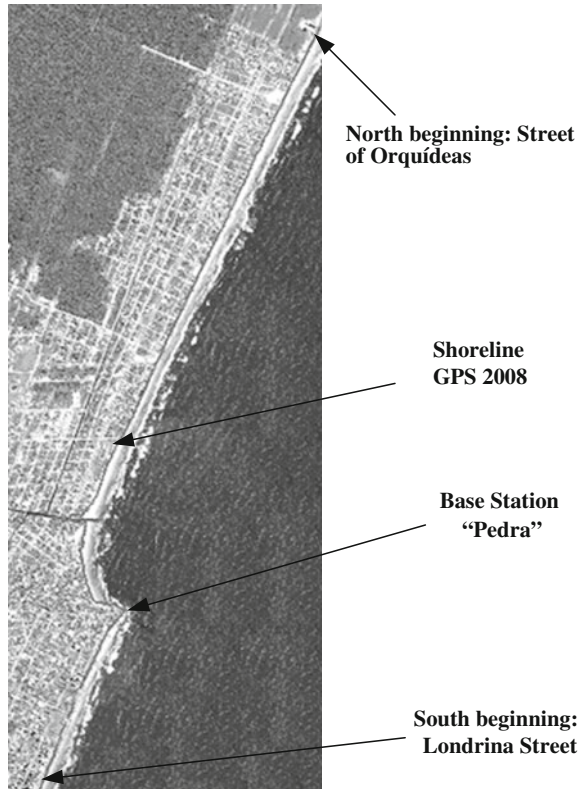
Fig. 24.10 Effects of an episodic event in Matinhos (May, 2001). *Source* Krueger (2002)

settlement of the shore, the best solution can be the removal of any “offside” structures.

In Matinhos, removal of houses was performed on an informal settlement in the central beach after the ocean storm of May 2000, which destroyed several houses. After four years there was a restoration of the beach and dune systems, as can be seen by comparing photographs taken at different times in Fig. 24.9. In May 2001, another storm struck the shore of Matinhos (Fig. 24.10), destroying sidewalks, much of the waterfront promenade, and some fishing families were displaced (Krueger 2002). Figure 24.3 on p. 403 shows the situation at Matinhos in 2007, indicating that the problems of coastal erosion are still present.

Prediction of Matinhos’ shoreline: In order to monitor or predict shoreline position of Matinhos, a combination of various data sources and tools were employed. For example, use was made of aerial photographs and GNSS (GPS) surveys for the years 2001, 2002, 2005 and 2008, to compare short-term prediction models (*robust parameter estimation, neural network and linear regression*). GNSS data from a geodetic survey of the shoreline in Matinhos was collected using the kinematic relative positioning method (see Sect. 6.4.2). The reference (base) receiver was stationed at Pedra ($25^{\circ} 49'05''$ S, $48^{\circ} 31'49''$ W) as shown in Fig. (24.4, left). The southern GNSS survey began near Londrina Street, while the northern survey began near the Street of the Orquideas (see Fig. 24.11). For this survey, dual frequency (L1 and L2) GNSS receivers were employed for the years 2001, 2002, 2005 and 2008 (see Fig. 24.12, right), compared to earlier results obtained through photogrammetric restitution (see Fig. 24.12, left). Figure 24.13 indicate the residual between the predicted shoreline for 2007 compared to the actual shoreline position measured using GNSS.

Fig. 24.11 Location of the base station and the extent of the shoreline mapping.
Source Goncalves (2010)



The result of this comparison showed residuals of less than 8 m between the predicted values for the year 2007 and the measured values using GNSS. The deviation was within the desired accuracy for predictive models of short-term shorelines, thus indicating the capability of GNSS to provide input data for predictive models and also in validating the shoreline prediction models. For more discussion on this example, the reader is referred to Goncalves et al. (2012)

End of Example 24.2

24.3 Concluding Remarks

Marine habitats represent some of the most fragile ecosystems that need to be carefully protected in order to conserve biodiversity. This chapter has demonstrated the potential of geoinformatics in monitoring and managing both marine and coastal

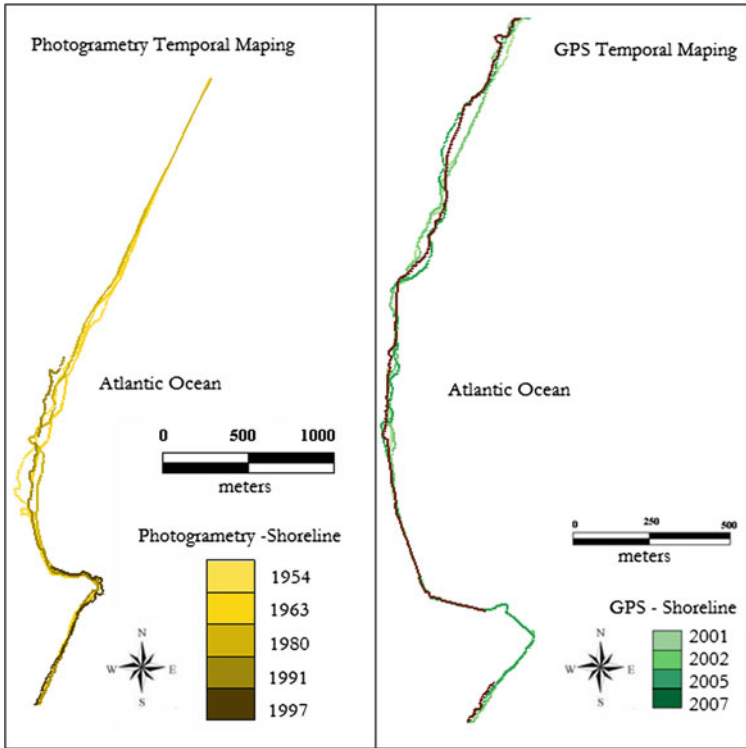


Fig. 24.12 Temporal resolution of the GPS versus photogrammetric mapping. Source Goncalves (2010)

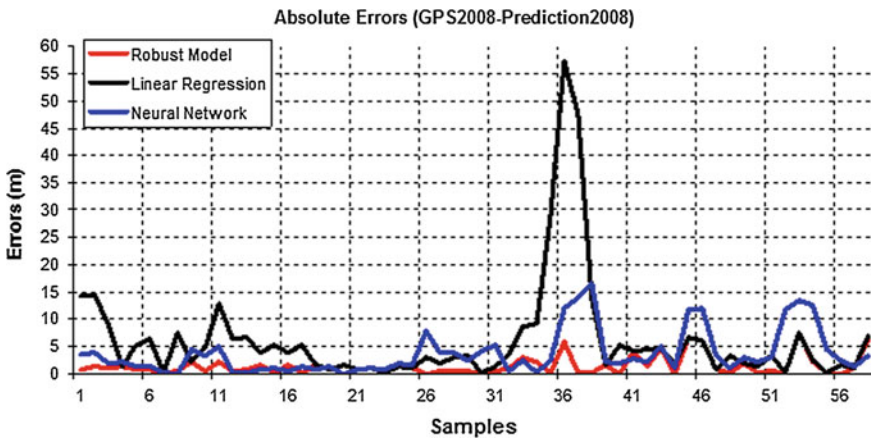


Fig. 24.13 Predicted shoreline using linear regression, neural network and robust estimation models. Source Goncalves (2010)

resources. In particular, remote sensing and GIS are well suited for mapping and inventorying marine habitats. Specifically, optical remote sensing imagery characterized by both high spatial and spectral resolutions as well as microwave imagery offer suitable data. GIS can then be employed to provide a framework for managing marine habitat.

Shorelines are generally unstable and vary over time resulting in either progradation or retrogradation. GNSS could be useful in providing baseline data for shoreline prediction, and also in validating shoreline predicted models. The geoinformatics applications outlined in this chapter are by no means conclusive, but highlight just a few cases where geoinformatics could be used to support marine and coastal habitat monitoring. For example, Ferentinos et al. (2008) propose an inexpensive wireless mobile ocean sensor network (e.g., Sect. 26.3) as an alternative flexible infrastructure for fine-grained ocean monitoring as opposed to the traditional means of observing the ocean, e.g., fixed moorings and radar systems, which are expensive to deploy and provide coarse-grained data measurements of ocean currents and waves. An example of a real-time ocean sensor is presented, e.g., by Pettigrew et al. (2008).

References

- Angulo RJ, Soares CR, Souza MC (2000) Excursion route along the state of Paran (PR). In: 31st international geological congress. Rio de Janeiro, August 6–17, 58–81
- Blasco F, Saenger P, Janodet E (1996) Mangroves as indicators of coastal change. *Catena* 27:167–178
- Boak EH, Turner IL (2005) Shoreline definition and detection: a review. *J Coast Res* 21(4):688–703
- Call KA, Hardy JT, Wallin DO (2003) Coral reef habitat discrimination using multivariate spectral analysis and satellite remote sensing. *International Journal of Remote Sensing* 24:2627–2639
- Crowell M, Douglas BC, Leatherman SP (1997) On forecasting future US shoreline positions: a test of algorithms. *J Coast Res* 13(4):1245–1255
- Demarest JM, Leatherman SP (1985) Mainland influence on coastal transgression: Delmarva Peninsula. *Mar Geol* 63:19–33
- Di K, Ma R, Li R (2003) Geometric processing of IKONOS geostereo imagery for coastal mapping applications. *Photogrammetric Engineering and Remote Sensing* 69:873–879
- Douglas BC, Crowell M (2000) Long-term shoreline position prediction and error propagation. *J Coast Res* 16(1):145–152
- Douglas BC, Crowell M, Leatherman SP (1998) Considerations for shoreline position prediction. *J Coast Res* 14(3):1025–1033
- Fenster MS, Dolan R, Elder JF (1993) New method for predicting shoreline positions from historical data. *J Coast Res* 9(1):147–171
- Fenster MS, Dolan R, Morton RA (2000) Coastal storms and shoreline change: signal or noise? *J Coast Res* 17(3):714–720
- Ferentinos KP, Trigoni N, Nittel S (2008) Impact of drifter deployment on the quality of ocean sensing. In: Nittel S, Labrinidis A, Stefanidis A (eds) *GeoSensor networks*. Lecture notes in computer science 4540. Springer, Berlin, pp 9–24
- Galgano FA, Douglas BC (2000) Shoreline position prediction: methods and errors. *Environ Geosci* 7(1):1–10
- Galgano FA, Douglas BC, Leatherman SP (1998) Trends and variability of shoreline position. *J Coast Res* 26:282–291

- Gibeaut JC, Hepner T, Waldinger R, Andrews J, Gutierrez R, Tremblay TA, Smyth R, Xu L (2001) Changes in gulf shoreline position, Mustang, and North Padre Islands. A report of the Texas coastal coordination council pursuant to National Oceanic and Atmospheric Administration. Bureau of Economic Geology, The University of Texas, Austin Texas, Texas
- Goncalves RM (2010) Short-term trend modeling of the shoreline through geodetic data using linear regression, robust estimation and artificial neural networks. Ph.D. Thesis, Geodetic Sciences Post-graduate Program, Federal University of Parana (UFPR), Curitiba, Brazil, 152p.
- Goncalves RM, Awange JL, Krueger CP (2012) GNSS-based monitoring and mapping of shoreline position in support of planning and management of Matinhos/PR (Brazil). *J Global Positioning Syst* 11(1):156–168. doi:10.5081/jgps.11.2.156
- Gorman L, Morang A, Larson R (1998) Monitoring the coastal environment; Part IV: mapping, shoreline changes, and bathymetric analysis. *J Coast Res* 14:61–92
- Hecky RE, Newbury RW, Bodaly RA, Patalas K, Rosenberg DM (1984) Environmental impact prediction and assessment: the Southern Indian lake experience. *Canadian J Fisheries Aquat Sci* 41(4):720–732
- Held A, Ticehurst C, Lymburner L, Williams N (2003) High resolution mapping of tropical mangrove ecosystems using hyperspectral and radar remote sensing. *Int J Remote Sens* 24:2739–2759
- Karpouzli E, Malthus T, Place C, Chui MA, Garcia MI, Mair J (2003) Underwater light characterization for correction of remotely sensed images. *Int J Remote Sens* 24:2683–2702
- Krueger CP, Centeno JA, Mitishita EA, Veiga LAK, Zocolotti CAJ, Jubanski MJ (2002) Determinacao da linha de costa na regio de Matinhos. *Anais do Simposio Brasileiro de Geomatica, Presidente Prudente - SP*, pp 206–211
- Li R, Di K, Ma R (2001) A comparative study of shoreline mapping techniques. In: The 4th international symposium on computer mapping and GIS for coastal zone management, Nova Scotia
- Ma R, Di K, Li R (2003) 3D shoreline extraction from IKONOS satellite. *J Mar Geodesy* 26:107–115
- Malthus TJ, Mumby PJ (2007) Remote sensing of the coastal zone: an overview and priorities for future research. *Int. J. Remote Sensing* 24:2805–2815
- Metropolitan Borough of Sefton (2002) Shoreline monitoring annual report 2001/2002. http://www.sefton.gov.uk/pdf/TS_cdef_monitor_20012.pdf. Accessed 14 Nov 2008
- Morton RA, Leach MP, Paine JG, Cardoza MA (1993) Monitoring beach changes using gps surveying techniques. *J Coast Res* 9(3):702–720
- Mumby PJ, Green EP, Edwards AJ, Clark CD (1997) Coral reef habitat mapping: how much details can remote sensing provide? *Mar Biol* 130:193–202
- Pettigrew NR, Roesler CS, Neville F, Deese HE (2008) An operational real-time ocean sensor network in the Gulf of Maine. In: Nittel S, Labrinidis A, Stefanidis A (eds) (2008) *GeoSensor networks*. Lecture notes in computer science 4540. Springer, Berlin, pp 213–238
- Pierri N, Angulo RJ, Souza MC, Kim MK (2006). A ocupação e o uso do solo no litoral paranaense: condicionantes, conflitos e tendencias. *Desenvolvimento e meio ambiente. Ocupação e uso do solo costeiro um mosaico de diversidade* (13), editora UFPR, pp 137–167
- Schiff KC, Weisberg SB (2001) Environmental auditing: microbiological monitoring of marine recreational waters in Southern California. *Environ Manage* 27(1):149–157
- Soares CR, Vobel I, Paranhos Filho AC (1995) The marine erosion problem in Matinhos municipality. In: *Land Ocean Interactions on the Coastal Zone, 1995*, São Paulo. *Boletim de Reumos do Land Ocean Interactions on the Coastal Zone*, pp 48–50
- Suguo K (1992). In: Queiroz TA (ed) *Dicionário de geologia marinha*. São Paulo, p171
- White K, Asmar EL (1999) Monitoring changing position of coastlines using thematic mapper imagery, an example from the Nile Delta. *Geomorphology* 29:93–105

Chapter 25

Protection and Conservation of Animals and Vegetation

“During the past 35 years, new technologies have been developed for remotely tracking and studying free ranging animals (Fuller et al. 2005), and advances in technology continue to increase opportunities for incorporating tracking and biotelemetry to study animal behavior and ecology. Perhaps the most revolutionary advance in obtaining animal locations is the use of GNSS.”

Tomkiewicz et al. (2010)

25.1 Introductory Remarks

This chapter presents ways in which geoinformatics could be useful in supporting management and conservation efforts of *animals* and *vegetation*. Ways in which animals and vegetation impact on the environment, and vice versa, i.e., the ways in which the environment impact, through human-induced anthropogenic activities, on the animals and vegetation are considered. Specific emphasis on how geoinformatics could support these efforts through monitoring, thereby enabling remedial measures to be undertaken are presented.

Section 25.2 introduces the concept of GNSS-based animal telemetry, which is an emerging powerful technology for wildlife studies that provides *continuous, high accurate* positional (time-series) data on animal locations, information which when combined with other data, such as very high frequency (VHF) radio tracking and/or remote sensing data (e.g., from MODIS (Moderate-resolution Imaging Spectroradiometer)) in a GIS environment could lead to improved understanding of animal ecology, movement, foraging, and impact on the environment among other benefits. In overall, these benefits will enhance *conservation measures*.

The section starts by presenting the benefits (i.e., usefulness in *conservation* and *monitoring of the endangered species*) and background of animal tracking

in Sect. 25.2.1, which highlights the advantages of GNSS-based animal telemetry approach over the conventional methods (e.g., VHF). Section 25.2.2 then looks at the observation and data management aspects, i.e., how the huge amount of data acquired can be managed using GIS. Finally, Sect. 25.2.3 concludes the section by presenting examples of real application areas where geoinformatics has been used to support animal protection and conservation. The materials presented in this section are largely adopted from the contributions of a theme issue *Challenges and opportunities of using GPS-based location data in animal ecology*, which was held at Edmund Mach Foundation, Viote del Monte Bondone, Trento, Italy, in September 2008, see e.g., (Cagnacci et al. (2010) and the contributions therein).

Section 25.3 then moves away from the animal world, to the plant kingdom and explores means by which geoinformatics could support management and conservation of vegetation. Vegetation itself comprises wide varieties of plant species, some of which are rare species such as those found in Australia. In this section, however, only forests and wetlands are discussed. The geoinformatic methods, nonetheless, are not limited to forests and wetlands, but could be useful to any other species of vegetation being monitored for conservation purposes.

25.2 GNSS Animal Telemetry

25.2.1 Background and Benefits

25.2.1.1 Background

As early as 1960, the Craighead brothers realized the vast potential inherent in locating animals within their natural environment, without physically coming into contact with them, when they radio-collared the first grizzly bears and elk as part of their ground breaking studies in Yellowstone National Park (Craighead 1982; Craighead et al. 1995; Hebblewhite and Haydon 2010). GNSS-based radio telemetry, therefore, could be traced back to the work of these scientists, Hebblewhite and Haydon (2010). Since the pioneering work of the Craigheads, a fully functional GNSS tracking systems for wildlife, which is coupled with data transmission technologies has given birth to a new era of animal tracking as evidenced by recent literature that document numerous examples of successful studies using GNSS positioning, see, e.g., (Tomkiewicz et al. (2010) and the references therein).

Conventional animal location tracking methods include, e.g., manual observation, VHF-based telemetry, camera trapping, landscaping genetics, and Argos among others. GNSS-based telemetry provides systematic, highly accurate and relatively unbiased data compared to these conventional approaches, and enables the correction of bias in the GNSS fix-rate previously ignored in the VHF-based telemetry (Hebblewhite and Haydon 2010). Though GNSS-based telemetry has the above mentioned advantages over the conventional methods, a combination with these methods,

e.g., GNSS-Argos could offer significant improvements as opposed to a stand-alone approach. Hebblewhite and Haydon (2010), for instance, report on the alleviation of substantial amount of time required to manually obtain location-based information brought about by the GPS-Argos combination. The positive outcome of this is the elimination of human bias that could be incurred from manual observation and significant saving of the resources that could have been allocated for such manual observations (Hebblewhite and Haydon 2010). It should also be noted that lessons and experiences learnt from the conventional approaches enhanced the advancement of GNSS-based approach.

This has resulted in a great potential of monitoring the impacts of domestic and wild animals in their habitats. This has come about due to the realization that these animals alter the biological equilibriums of their habitat as they roam about either to graze, look for water, or rest. In Fig. 25.1, for example, the impacts of giraffe on the vegetation of Ruma National park in Kenya can be seen. Such important alteration require an understanding of the impact of animals on their habitat.

One of the main objectives of ethologists and experts in landscape planning is to understand the factors influencing the movements, and therefore the distribution of animals over the land. The *acquisition of this information* is the only way animal

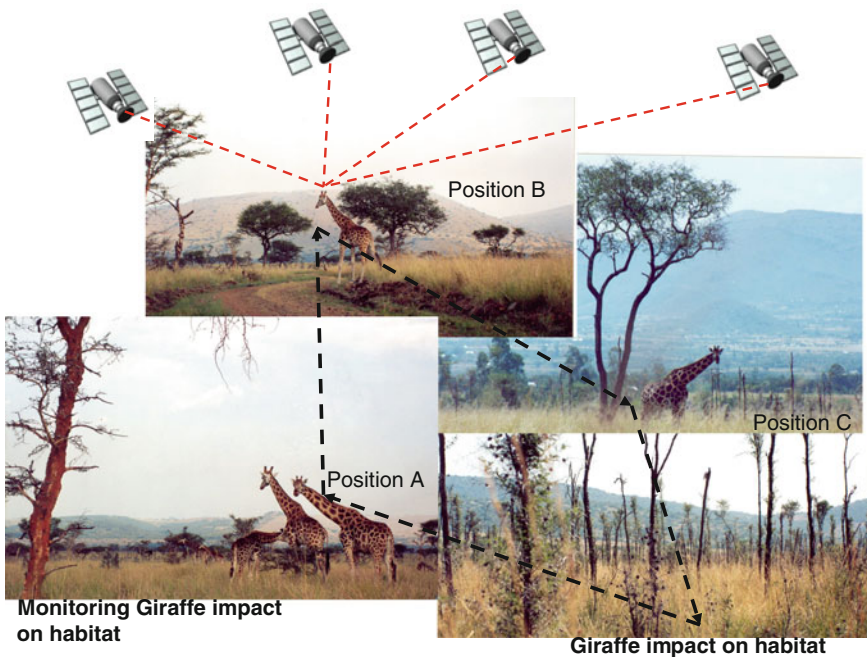


Fig. 25.1 Monitoring the impact of giraffe on habitat at Ruma National Park, Kenya. From the figure, it is noticeable that the giraffes have left the shrub vegetation dilapidated. GNSS could provide the perimeters of such impacted environments, besides providing location-based data for the animal's movement

population, both wild and domestic, will be able to be managed in order to satisfy both the conservationist and the productive aims (Barbari et al. 2006). Geoinformatics is fast becoming the preferred means of gathering information related to animal movement and spatial distribution. For instance, GNSS data can be used to address animal ecology questions (e.g., resource selection, animal movement, and foraging behavior) from a completely new perspective (i.e., closer to the animal point of view (Urbano et al. 2010)).

25.2.1.2 Benefits

Studying animal motion provides ecologists with the necessary location-based data for linking the animals (observed) to their environment (place or location, which they could impact or could inversely impact on them). This link opens the possibility of monitoring and studying how an individual animal interacts with its environment. This could lead to improved knowledge, for instance, on how an animal forages (i.e., what it likes and does not like), and how this impacts on the environment (see the example of giraffe in Fig. 25.1 on p. 417). This knowledge could in turn provide information to policy and decision makers on conservation measures required. Cagnacci et al. (2010) discusses how knowing where animals go can help scientists in their search for understanding key concepts of ecology, e.g., resource use, home range and dispersal, and population dynamics. They postulate that intense sampling of movement, coupled with detailed information on habitat features at a variety of scales could enable the representation of animal's cognitive map of its environment and the intimate relationship between behavior and fitness, data which when used over a long period of time could enhance monitoring of the impacts of climate change on *animal distribution* and *behavior* (Cagnacci et al. 2010; Hebblewhite and Haydon 2010). An interesting example of application of GNSS to monitor the behaviour of animals is given by Janssen (2012) who proposes an indirect, GNSS-based method for tracking drop bears. The method involves tracking the prey rather than the predator in order to map the population of drop bears in a particular area, and can be used to effectively estimate the number of drop bears in the study area (Janssen 2012).

Hebblewhite and Haydon (2010, Table 1) provide a detailed summary of the potential advantages and disadvantages of a combined GNSS and Argos technology for supporting animal ecology and conservation issues such as resource selection and corridor mapping, behaviour, migration, home range, demographic studies (e.g., survival reproduction), movement ecology, human-wildlife conflicts, and climate change. Advantages are listed by Hebblewhite and Haydon (2010, see references therein) as improvements to habitat modelling conservation (e.g., identification of habitat corridors for trans-boundary conservation of Africa elephants see e.g., Steede-Terry (2000, Chap. 8, p. 119), mechanism of migrations (e.g., evidencing the main hypothesis for migration at scales and across system that had previously been unthinkable without GNSS technology), basic ecology and conservation of wide ranging species (e.g., advancement of basic ecology such as where animals forage, movement and distribution), conservation impacts (e.g., GNSS maps of wolf (*Canis lupus*),

telemetry locations that clearly showed a dramatic avoidance of human activities), and projecting impacts of climate change (e.g., the effect of climate change on the predicted distribution of polar bears (*Ursus maritimus*) in the next 50 years).

The shortcoming of a GNSS-based animal telemetry are listed as costs, small sample size and poor population level inferences, overemphasis on the importance of fine-scale data, removing the need of actual human observation, and difficulty in relating fine-scale movements and coarse-scale evaluation of resource and behavior (Hebblewhite and Haydon 2010). It should be pointed out, however, that with the full realization of GNSS satellite constellation, e.g., when most of the satellites discussed in Chap. 4 attain full operational capability, receivers will be manufactured that will integrate the full spectrum and lower the cost. This will have an added advantage for GNSS-based animal telemetry in terms of positional accuracy, which will definitely be an order lower than the 30 m currently achieved (see e.g., Fig. 6.7 on p. 83). Furthermore, the integration of GNSS with other mapping technologies like remote sensing and GIS, when employed in conjunction with communication technologies, is bound to deliver accurate, reliable, complete and timely information that can be applied to support conservation of various animal species.

25.2.2 Observation and Data Management Techniques

As opposed to traditional positioning procedures performed with the privilege of undertaking mission planning (e.g., Sect. 6.3) that enhances the achieved accuracies, animal tracking completely takes the GNSS receiver to the world of uncertainty as it becomes subject to the “animal’s mercy”. The animal dictates where it goes based on factors such as food availability thereby seeing the receiver traverse terrains, some of which may be hostile and others which may illicit blockage of the GNSS signals, especially when the animal moves under trees or inside forests. Two main features of the receiver that immediately come to play are its size, i.e., depending on the animal to be tracked, and the durability of the receiver (i.e., how long is the animal to be observed?).

The positional aspect of GNSS-based telemetry is presented, e.g., by Tomkiewicz et al. (2010) who provide a chronological advancement of the animal based collar receivers. Just like the normal GNSS receivers used for positioning discussed in Chap. 6, a collar-based GNSS receiver also requires a period of initialization also known as initial fix. This is the period, which the receiver obtains its initial position when it is switched on by determining the satellites in view. At the period of infancy of GPS technology, receivers could take more than 30 min to determine their initial positions. Modernization of receiver technology and increased availability of satellites, however, has reduced this period to less than a second. The maturity of the GNSS system will ensure availability of wide range of satellites. Receivers are now also being manufactured that can track multiple satellites from different GNSS constellations.

The basic operational principle involves a collar GNSS receiver that is tied around the animal's neck. The receiver measures positional pseudoranges and satellite ephemeris data (see Sect. 5.3) and stores them, while at the same time transmits the data to the control center. Besides size and durability, power consumption is also a major factor. In order to lower power consumption, the receiver can be set such that it measures only the pseudorange data and later uses precise ephemeris (see Sects. 5.4.1 and 6.4.2), in what is termed as 'rapid fix technology' by Tomkiewicz et al. (2010). Tomkiewicz et al. (2010) present two types of rapid fix (i) the quick fix pseudorange (QFP) and (ii) snapshot depending on whether land animals or marine animals are being monitored. Technological advances have now seen the emergence of smaller low voltage (3.0 Vdc) and low current that allow tracking of smaller mammal species and birds (Tomkiewicz et al. 2010). For animal collar receiver, this initial fix time is of great importance as marine animals, for example, surfaces for a shorter period of time, thus requiring a quick fix. The need to conserve receiver power consumption also dictates the operation as some receivers are turned on and off, thus also calling for quick fix.

In the QFP designed for marine mammals, a standard GNSS receiver that can collect data within 5 s of an animal surfacing is used, where pseudoranges are collected for post-processing and at the same time stored for later downloading if the receiver is recovered (Tomkiewicz et al. 2010). The snapshot receivers are specifically designed to digitize GNSS downlink signals in less than a second and either store the digitized data in raw form thereby incurring huge files and low power consumption, or extracts and calculates the pseudoranges thereby reducing the file sizes that are manageable (comparable to QFP) but using more power (Tomkiewicz et al. 2010).

Due to the fact that GNSS-based radiotelemetry data are integrated with other forms of data (e.g., from remote sensing), a proper data management system is required. For instance, a micro-power data acquisition controller (MDAC) is used to manage the entire operation to achieve a functional system (Tomkiewicz et al. 2010). Urbano et al. (2010) provide an evaluation of the requirement of a good management of GNSS-based animal tracking data and stress the need for a dedicated data management tool and expertise. They propose an example of such a spatial database model and how it operates in Fig. 25.2. In the next two subsections, two examples of application areas; conservation of biodiversity, and migratory/endangered species are presented.

25.2.3 Applications

The use of GNSS-collar receivers to study the position of animals is a common technique for studies on wild animal habitats (such as those of deer, bears, and wolves) (Barbari et al. 2006). Barbari et al. (2006) provides an example on how GNSS is combined with GIS and used to track animal locations in the various grazing areas at the Animal Research Center of the University of Kentucky. In their study, 15 cows were individually equipped with GNSS collar receivers programmed to record positions every 5 min in order to monitor their movements within the grazing area at

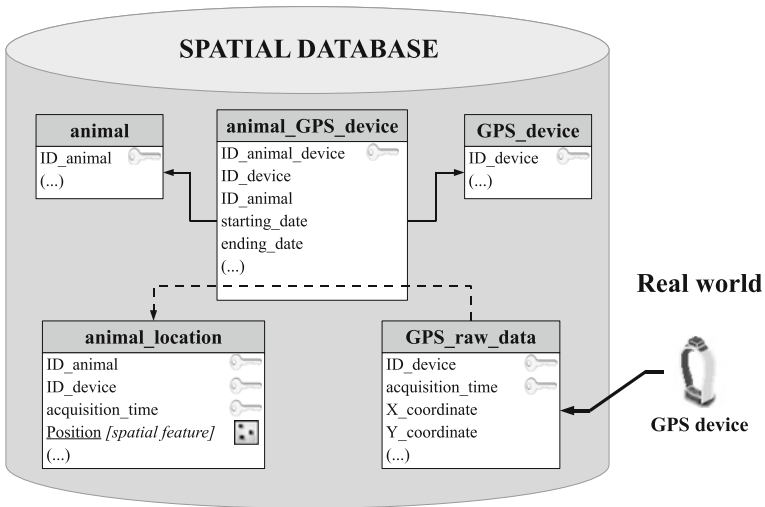


Fig. 25.2 A general representation of a possible standard database data model for core wildlife GNSS (GPS) data by Urbano et al. (2010). When the GNSS device provides coordinates of a location at a specified time, they are uploaded in the database in a table (GPS_raw_data). A device is associated to an animal for a defined time range (table animal_GPS_device, connected to the tables animal and GPS_device with foreign keys, represented by solid arrows in the figure). According to the acquisition time, GNSS-based locations are therefore assigned to a specific animal (i.e. the animal wearing the device in that particular moment) using the information of the table animal_GPS_device. Thus, the spatial table animal_location is filled (dashed arrow) with the identifier of the individual, its position (as a spatial object), the acquisition time and the identifier of the GNSS device. Source Urbano et al. (2010)

regular time lags. The collected data were later downloaded into a GIS and analyzed according to landscape features that were considered. Their results indicated the usefulness of GNSS in gathering location information with increased accuracy.

25.2.3.1 Conservation of Biodiversity

In terms of conservation, Hebblewhite and Haydon (2010) argue that it is the location-based information (i.e., where the animals move) as opposed to the mechanism of motion that have made substantial contribution to conservation. They present an example based on the Canadian Rockies’ wolf that travelled over 100,000 km² area in Alberta, British Columbia, Montana, Idaho, and Washington in 1993 (Hebblewhite and Haydon 2010). Argos collar was used and the results were reported to have given inspiration to the Yellowstone and Yukon conservation initiatives (Chester 2006; Hebblewhite and Haydon 2010). Another example presented in Hebblewhite and Haydon (2010) is the case where GNSS data from a pronghorn antelope in Wyoming revealed the movement corridors that were threatened by oil and gas development in a narrow migration pinch-point (Berger 2004; Hebblewhite and Haydon 2010).

The last example above indicates how GNSS-based animal telemetry supported one of the aims of conservation, i.e., identification of the type, nature, and extent of the main factors affecting the animals in order for intervention measures to be undertaken. Another aim of conservation is that of identifying human impacts on habitats. This, too, could benefit from GNSS-based animal telemetry in that it would yield habitat spatial data, which when combined with external data (e.g., from remote sensing) on the attributes of these habitats, such as human activities, could help identify human impacts on these animals and their environment. Examples are given, e.g., by Hebblewhite and Haydon (2010, see reference therein) on how spatial data contributed to the understanding of the effect of energy development on Mule deer (*Odocoileus hemionus*) and Caribou (*Rangifer tarandus caribou*). Other examples include identification of habitat corridors for trans-boundary conservation of African elephants, see also Steede-Terry (2000, p. 64), and in understanding the impacts of human recreation on wide-ranging carnivores (Hebblewhite and Haydon 2010). Eshiamwata (2012) was recently (2012) able to develop a framework for monitoring bird habitat at key biodiversity sites in Eastern Africa using remote sensing by analyzing land use land cover (LULC) change at Important Bird Areas (IBAs) as summarized in Example 25.1.

The examples above show how humans have impacted on the habitats, yet the reverse can also be said, i.e., the animals' impacts on habitats. As an example, let us consider the Rothschild (*Giraffa camelopardalis rothschildi*) species of giraffes that were relocated from Soi Ranch in the Rift Valley of Kenya to two national parks in the late 1970s and early 1980s in order to conserve the giraffes, which were then threatened by the spread of human settlements (Awange et al. 2004). Twenty-seven (27; five males and 22 females) of these Rothschild giraffes were relocated to Ruma National Park (NP) that was established in 1966 and gazetted as Lambwe Valley Game Reserve in Kenya (Fig. 25.3), and 17 were relocated to Lake Nakuru NP.



Fig. 25.3 In 1983, 27 Rothschild giraffes (*Giraffa camelopardalis rothschildi*) were translocated from Kenya's Rift Valley to Ruma National Park (NP) as a conservation measure

A survey conducted in 2002 at Ruma NP to determine both the giraffe population and the impact of their introduction on the park's other animal species, on park flora, and on human habitat found that the giraffes' population was approximately 75, and their presence had impacted on both the environment and the human communities that surround the park (Awange et al. 2004). Here too, GNSS-based animal telemetry could provide useful information that could be used to study the impacts of giraffes on the environment, and could save resources incurred from undertaking a manual observation as was done in Awange et al. (2004). If these giraffes were collared with GNSS receivers, for example, it would be possible to relate their positions to the habitats as indicated in Fig. 25.1. These spatial information could then be integrated with the attributes of the Park in a GIS to enhance management and the study of the impacts of these giraffes on that habitat that are also home to other species.

Example 25.1 (Land cover change and correlates of change at key biodiversity sites in Eastern Africa. *Source* Eshiamwata (2012))

Human induced land cover change is taking place invariably at different time periods, paces and magnitudes and with diverse biophysical implications on the various land cover types and on biodiversity. This study investigated the extent of land cover change across all major land cover types at a subset of 71 Important Bird Areas (IBAs) in Eastern Africa, including Kenya, Uganda, Tanzania, Rwanda, Burundi and Ethiopia, over a 22-year period using remotely sensed data. At regional level, during the study period, broad land cover and land use trends show a dramatic decline in natural habitats such as forests, shrub lands, herbaceous and flooded vegetation. The decline in natural land cover types and a concomitant increase in the percentage of modified and converted land cover types points to the fact that natural habitats were converted or modified into anthropogenic and intensively managed land cover and land uses types such as agriculture, plantation crops, natural agricultural mosaic and urban areas.

Population density around IBAs was not a significant correlate of extent and rates of land cover change within IBAs for all land cover types except that it slightly contributed to change in shrub land. Agriculture was the most significant correlate of land cover change driving the observed changes in all forests, open forest/woodlands, shrub lands and herbaceous/grasslands. The impact of legal protection and site specific past conservation interventions was assessed. Protection was not a significant factor in reducing land cover type apart from open forest/woodland habitats. Working with Site Support Groups (SSGs) to implement site specific conservation interventions did not translate into reduced land cover change at IBAs across all land cover types apart from shrub land. However, whether this could be attributed to the smaller sample sites of the SSGs used in the study and the shorter period some of the SSGs have been in existence requires further assessment.

End of Example 25.1

25.2.3.2 Monitoring Migratory and Endangered Species

Animals migrate in search of food or mates for reproduction purposes among other reasons. For instance, herbivorous animals will tend to go to areas with green pastures and water, and as they go, so follows the carnivores who hope to benefit. The spectacular annual Wildebeest migration of East Africa, for example, where millions of animals move across the Serengeti and Mara plains (e.g., about 800 km round trip during the migration) in search of food and water, and having to cross the jaws of the waiting crocodiles and other carnivores, has turned out to be one of the world's great wonders. In Lake Victoria in East Africa, fishing birds such as gulls, terns, pelicans, kingfishers and cormorants are abundant in the river mouths of Sondu-Miriu, Kuja-Migori, Yala and Nzoia. Rocky beaches with clear sandy waters host plenty of cormorants, little egrets and African fish eagles. This can be attributed to the fact that the visibility allows the birds to capture prey with little effort.

Studying animal migration provides various examples where a combination of remotely sensed resource availability data together with GNSS movement (location-based data) have yielded definitive ecological insights (Hebblewhite 2009). For instance, Hebblewhite and Haydon (2010) indicate that by combining GNSS data on migratory movements with spatially matched resources available from remote sensing data such as MODIS¹ for terrestrial and aquatic forage resources, clear evidence has been generated for the main hypothesis for migration at scales and across systems that had previously been unthinkable without GNSS technology (Hebblewhite and Haydon 2010, see reference therein).

Besides monitoring of migratory species, GNSS-based animal telemetry could also be useful in monitoring endangered species. Let us consider an example of the roan antelope (*Hippotragus equinus*) at Ruma National Park (NP). The decision to make Ruma a national park was driven by the urgent need to conserve the roan antelope, locally known as “Omoro” (Fig. 25.4).

Roan antelopes are not endangered in the strict classification of endangered species, rather, they are classified as a low-risk, conservation-dependent species by the International Union for the Conservation of Nature and Natural Resources (IUCN) or World Conservation Union (Awange and Ong'ang'a 2006). They range across sub-Saharan Central Africa from Guinea to Ethiopia, and south across Angola to South Africa.

In Kenya, roan antelope are only found in Ruma NP, where habitat factors could potentially enable them to thrive. However, poaching and drought have caused their population to dwindle in recent years. In 1994, research scientists from the Kenya Wildlife Service (KWS)² found only 34, while the census of September 1999 put the number at 25, see e.g., Awange et al. (2004, Table 1).

Figure 25.5 demonstrates how a GNSS-based animal telemetry could be useful in monitoring the roan antelope as it moves from locations A, B, C, D, E, and finally back to A. Assuming these locations have known varying habitat characteristics mapped

¹ Moderate-resolution Imaging Spectroradiometer.

² <http://www.kws.org/>



Fig. 25.4 In Kenya, roan antelope (*Hippotragus equinus*) are found only in Ruma National Park. Their survival, however, is threatened by poaching and drought. GNSS could be used to provide location-based information on areas frequented by the roan antelope to inform conservation and protective measures

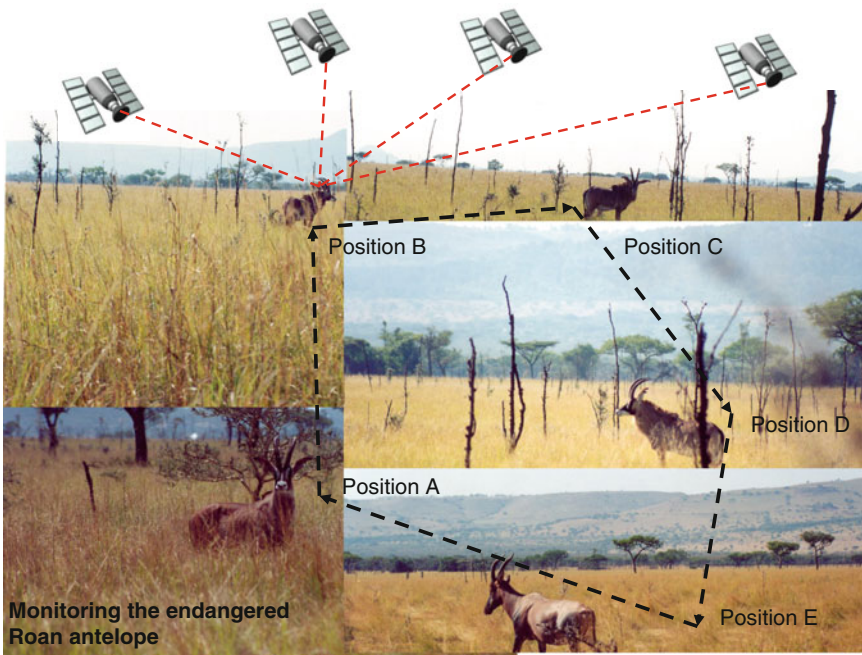


Fig. 25.5 An example of how a GNSS receiver could be used to provide location-based information that could assist in monitoring of the endangered roan species at Ruma National Park, Kenya

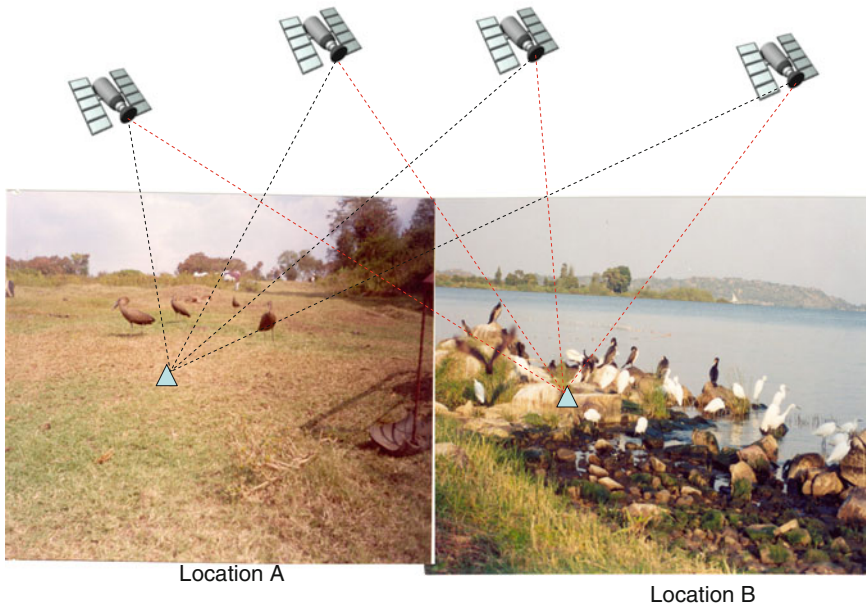


Fig. 25.6 An example of possible use of hand-held GNSS receivers (e.g., Fig. 27.1 on p. 485) to provide location-based information on areas frequented by migratory birds

using remote sensing, if this is integrated with the location-based data captured from GNSS within a GIS environment, conservationists could be able to study the behavior of the roan antelope with regard to these habitats and thus take appropriate conservation measures. Examples of success of GNSS-based animal telemetry in monitoring endangered species are given, e.g., in (Environment Canada 2008), where environmental models for critical habitat identification were developed using data from 250 GNSS-radio collared endangered woodland Caribou (*Rangifer tarandus caribou*) across the entire boreal forest of Canada (Hebblewhite and Haydon 2010).

In Lake Victoria region (Kenya), which is habitat to 34 endemic waterfowl and migratory species, conservation activities have included direct protection of bird types and habitat. The location of these habitats can be mapped using a hand-held GNSS as illustrated in Fig. 25.6. Protected habitats include Important Bird Areas (IBAs) such as Lake Nyamboyo and Usenge. River Yala and Sondu-Miri are home to some of the candidate species for conservation such as the papyrus gonolek (*Luniarus mufumbiri*), the papyrus yellow warbler (*Chloropeta gracilirostris*) and the Madagascar Squacco heron (*Ardea idea*). Plovers, sandpipers and stilts dominate the water edge community on sandy beaches along the Lake shores. Those dependent on emergent vegetation include herons, storks, cranes and passerines (warblers and weavers).

25.3 Vegetation

Environmental monitoring of the *extent* and *quality* of vegetation plays a crucial role of indicating land condition. By monitoring the changes in vegetation color, often as a result of stress, environmental impacts such as those arising from the exposure of plants to pollutants (e.g., air, acid rains, heavy metal contamination of the soil), insect infestation and disease can be deciphered (Holopainen et al. 2006). Besides the stress factors mentioned above, increase in population growth of urban cities lead to vegetation destruction to pave way to settlement or infrastructure. In this scenario, forests are cleared to provide timber for building and fuelwood. As a result, topsoil erosion and sedimentation are enhanced leading to increased suspended solid loads in the rivers that feed the lakes. Monitoring of vegetation, therefore, provides information on the impacts on the environment as a result of both human-induced activities or natural causes.

Remote sensing provides means for detecting vegetation changes through monitoring of the changing vegetation color, which occurs as a result of the stress stated above. Detection of stress with remote sensing in any vegetation type relies on development of methods that highlight properties associated with stress which are discernible from background variation, such as phenological changes (Wessels et al. 2011). Such methods need to distinguish stress response (signal) from changes due to normal leaf aging (noise). Basically, this is achieved through monitoring of vegetation greenness/vigour or the leaf water content in the near infrared region of the electromagnetic spectrum and is usually quantified through the normalized difference vegetation index (NDVI), see e.g., Tucker (1979, 1980). Through integration with of remote sensing satellites, GNSS provides location-based data and controls for vegetation mapping (e.g., Fig. 11.9 on p. 170). GNSS could also find use in monitoring of rangelands, and can also be indirectly used with altimetry satellites such as ICESat-2 to map vegetation.

James et al. (2003) defines rangelands as grasslands, shrublands, and open woodlands managed as natural ecosystems that are traditionally used by grazing animals. Classical land use/land cover studies employing remote sensing data could be used to monitor rangelands. Similarly, GNSS could be used in digital cameras to provide observations on amount and locations of poisonous, invading, or noxious plants; and threatened or endangered species (James et al. 2003). These data could then put in a GIS that would provide a platform for decision support as discussed in Sect. 23.2. The next two subsections examine forests and wetlands as examples of GNSS-based vegetation monitoring.

25.3.1 Forests

The distinct role that forests play towards ensuring global carbon balance through carbon sequestration, discussed in Sect. 21.4 and elaborated in several works (see



Fig. 25.7 Deforestation of the once densely forested Gwasi hills in Kisumu (Kenya) to pave way for farming

e.g., Fearnside and Laurance (2003), Houghton (2005), Malhi and Grace (2000) etc.), is worth mention. Furthermore, the initiative of Reductions in Emissions from Deforestation in Developing (REDD) countries designed to motivate developing countries to voluntarily reduce national deforestation rates and associated carbon emissions through financial incentives (see e.g., Kumi-Boateng (2012), Gibbs et al. (2007) etc.), is equally worth recognition.

Detailed and timely information on forests are required for traditional forest management, forest certification, and in monitoring forest health and biodiversity on the one hand, while on the other hand, there is an increasing need of having the information delivered at a lower cost (Holopainen et al. 2006). Population increase has also put pressure on the available resources, e.g., land leading to increase in deforestation (e.g., Fig. 25.7).

Whereas remote sensing satellites detect damage on trees by monitoring color changes from the leaves, which are indicative of the related stress, Holopainen et al. (2006) discuss the role of GNSS as that of enhancing field work to achieve the required efficiency of acquiring spatial forest resource information at a lower cost.

GNSS applications to forest management span almost two decades. For example, Sirait et al. (1994) pointed out that effective forest management requires balancing conservation and local economic-development objectives and demonstrated the capability of mapping customary land use systems using GNSS and GIS methods among other techniques. The derived maps by Sirait et al. (1994) were then used in *forest protection* and *resource management*, with the limitations being accuracy of the base maps, ability of social scientists and map makers to accurately capture the complex relationships of traditional resource-management systems on maps, and the political will of the parties involved to recognize different forms of land rights (Sirait et al. 1994). Part of the forest protection is in managing forest fires and vegetation

health, an area where GIS has found wide use, thanks to the capability of remote sensing to deliver timely and comprehensive coverage data and GNSS satellites to provide accurate and reliable positioning. For example, GNSS has been in use at the Ventura County Sheriff's Office since the early 1990s to map wildfire perimeters (Steede-Terry 2000). James et al. (2003) point to the use of video cameras with GNSS interface to document occurrences and locations.

Raven Environmental Services (Raven Environmental Services 2008) indicate the possibility of integrating GIS with GPS to produce maps that describe both the property and any underlying inventory data such as timber inventory for forest management units, the location and type of unique plant communities or any other type of special-use zone. From such maps, areas, lengths, distances to other features, and many other useful measures can also be calculated. The resulting underlying data associated with any management unit can then be exported as an Excel file, and used to periodically update a written management plan (Raven Environmental Services 2008).

Integration of GNSS, remote sensing and GIS is exemplified in the work of Brondizio et al. (2005) who produces a georeferenced map of land cover and land use for an area of the Amazon estuary inhabited by three populations of caboclos with distinct patterns of land use. The maps produced by Brondizio et al. (2005) permitted measurements and differentiation of land uses and change detection between small areas of managed floodplain forests and unmanaged forests, and between three distinct age/growth classes of secondary succession following deforestation. Brondizio et al. (2005) suggested means of balancing between use and conservation in Amazonian floodplain and estuarine areas, and the effectiveness of monitoring these types of land cover from space-borne platforms.

ICESat-2 will contribute to mapping of forest productivity by tracking the growth of individual forest stands, observations of tree phenology, forest diseases, and pest outbreaks through associated changes in canopy structures, and the mapping of forest heights and above ground biomass at a scale that approaches one that is appropriate for forest carbon management, which would enable the global ecosystem community to further constrain the sources and sinks of carbon at regional to continental scales (Abdalati et al. 2010). An illustration of ICESat-2's capability to map forest productivity is presented by Harding and Carabajal (2005), e.g., Fig. 25.8 that shows a clear ground return that is spread by the slope of the ground, the top of the canopy, and returns from within the canopy that are indicative of structure within the crown. Abdalati et al. (2010) then provide a global estimate of mean canopy heights derived from ICESat in Fig. 25.9.

25.3.2 *Wetlands*

The Ramsar International Convention on Wetlands of 1971 advocates for the wise use of wetlands by national actions and international co-operation as a means of achieving sustainable development throughout the world. Article 3.1 of the convention states

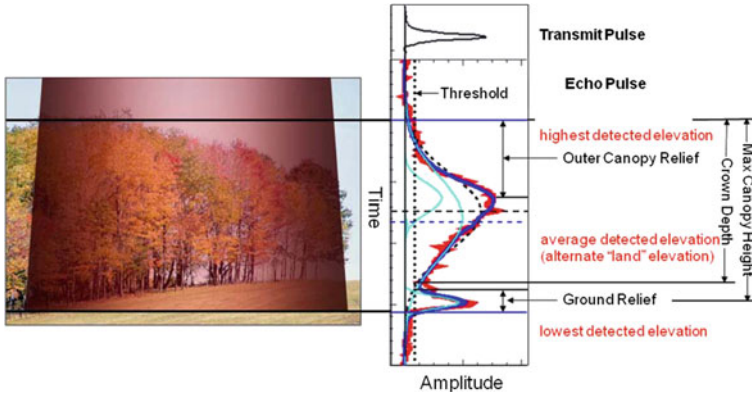


Fig. 25.8 Application of ICESat or ICESat-2 to measure tree heights as presented by Harding and Carabajal (2005)

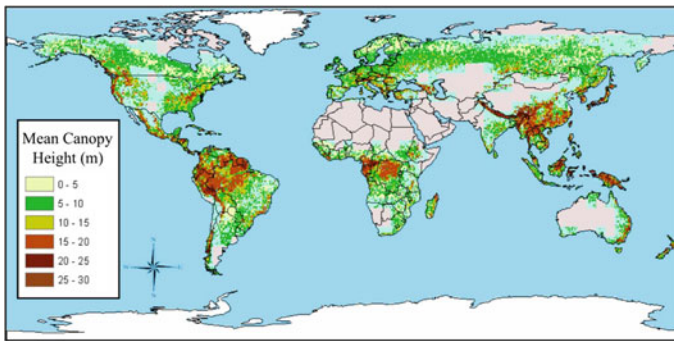


Fig. 25.9 Global estimates of mean canopy heights derived from ICESat as presented by Abdalati et al. (2010). The capability of retrieving tree height with ICESat-2 will contribute to the large-scale biomass assessments

that contracting parties shall formulate and implement their planning so as to promote the conservation of the wetlands, and as far as possible, the wise use of the wetlands in their territory.

Wetlands play a pivotal environmental role of providing sanctuary to biodiversity, store flood water, and improve water quality. It provides habitat for fish and wildlife, supporting a rich biodiversity that include many endangered and threatened species, see e.g., Awange and Ong’ang’a (2006) and Ozesmi and Bauer (2002). Conservation of wetlands is necessary as they have the ability to sequester carbon and also tend to shift to net sources of greenhouse gases when perturbed by land use change such as drainage for agriculture or forestry. In this way, they help in preventing *global warming*, a consequence of *climate change* and its ecological effects on the environment. They have an inherent capacity for storage of carbon. Carbon cycle, conservation,

Table 25.1 Components and products of wetlands theme

Component	Product
I. Global wetland extent and properties	1. Tropical wetland extent and properties
II. Seasonal monitoring of major wetland regions	2. Boreal wetland extent and properties
	3. Seasonal monitoring of major tropical/sub-tropical wetlands
	4. Wetland extent, flood inundation patterns and vegetation change in the Greater Mekong River Basin
	5. Seasonal dynamics of the Pantanal ecosystem
III. Mapping and monitoring of key wetland types	6. Seasonal monitoring of major boreal wetlands
	7. Global mangrove extent and properties
	8. Tropical peat lands extent and properties
	9. Pan-Asian mapping and monitoring of rice paddies
	10. Global lake census

Source Lowry et al. (2009)

and multinational conventions have a range of information requirements relating to wetland inventory, mapping and monitoring as shown in Table 25.1.

Ozesmi and Bauer (2002) suggest the need for inventory and monitoring of wetlands and their adjacent uplands to assist in its conservation and management. Such inventory and monitoring can be achieved using remote sensing techniques, see e.g., Brooks et al. (2006), Emerton and Kekulandala (2003), Jonson and Barson (1993) and Ozesmi and Bauer (2002). Optical sensors that have been applied to wetlands include; Landsat Multi-spectral Scanner (MSS), Landsat Thematic Mapper (TM), SPOT (Système Probatoire d'Observation de la Terre), NOAA AVHRR (Advanced Very High Resolution Radiometer), and radar system (JERS-1, ERS-1, RADARSAT, and ALOS PALSAR). Landsat MSS (bands 4 (0.5–0.6 m), 5 (0.6–0.7 m), 6 (0.7–0.8 m) and 7 (0.8–1.1 m)) provide data that are useful in discriminating large vegetation wetlands (Ozesmi and Bauer 2002). Jensen et al. (1984) indicate its possible use in change detection through multi-temporal analysis. Landsat TM (particularly band 5; 1.55–1.75 m) is useful in identification of wetlands and other land covers types (see, e.g., Han et al. (2007)) and change (Munyati 2000). In practice, a window of 9 pixels would be required to consistently identify an object (Ozesmi and Bauer 2002). Band 5 has the capability to discriminate between vegetation and soil moisture levels. Jensen et al. (1984) add that the separability between wetlands types could be achieved using this band.

For microwave imagery, Lowry et al. (2009) conclude that L-band SAR systems are the single best option for fine spatial-resolution remote sensing of wetland extent and characteristics over large regions because they operate regardless of cloud cover, can distinguish basic vegetation structure, and provide superior canopy penetration and water surface discrimination relative to C-band. Furthermore, a dual-polarization

L-band system such as that provided in the sensor ALOS PALSAR will result in improved accuracy in the discrimination between rough water surfaces and bare ground, and improved mapping of vegetation structural characteristics (Lowry et al. 2009).

SPOT panchromatic (PAN) images have been used to provide reference data for registration and calibration purposes (Ausseil et al. 2007; Welch et al. 1995), while Kasischke and Bourgeau-Chavez (1997) applied ERS-1 to monitor the presence or absence of water in wetlands in south western Florida, USA. Similarly, studies have been done to map zonation of vegetation communities and analyze biophysical properties of aquatic vegetation in the Amazon floodplain using JERS-1 and RADARSAT (Costa 2004; Costa et al. 2002). A combination of optical and radar sensors, where the two complement one another, is presented in the work of Townsend and Walsh (1998) who combine Landsat TM and SAR to detect flooding in a forested wetland on the lower Roanoke River floodplain in North Carolina. Another sensor that has been used for wetland studies is the Indian Remote Sensing (IRS) satellite whose four bands are similar to those of Landsat TM (see, e.g., Chopra et al. (2001)).

Spectral reflections of wetlands provide the possibility of separating various types of wetland vegetation. Classification techniques used for wetlands include visual interpretation, unsupervised or clustering, and supervised (see Chap. 10). The importance of visual analysis in reconnaissance mapping of wetlands is demonstrated by Jonson and Barson (1993) (Costa 2004). Unsupervised classification involve grouping together of pixels of similar spectral values, having the advantage of preserving spatial resolution of the images, see e.g., Jensen et al. (1984). Supervised classification adopts statistical techniques such as the maximum likelihood. A hybrid system adopts a mixture of the two systems.

Vegetation indices find use in highlighting wetlands during classification methods above. Normalized Difference Vegetation Index (NDVI) and Transformed Vegetation Index (TVI) (see Sect. 10.3.3) are some of the techniques used to enhance image identification. In addition, radar information is useful in wetland studies due to its capability to distinguish between flooded and non flooded areas. In all the remote sensing applications above, GNSS could be useful in georeferencing remotely sensed satellite data, providing orientation for aerial photographs, and providing sampled location-based and perimeter/area data.

25.4 Concluding Remarks

The chapter has outlined important functions of geoinformatics in support of animal and vegetation monitoring for conservation purposes. For instance, GNSS has brought with it a new horizon where animal conservation managers can make informed decisions based of simplified presentations (graphics and analysis) at no additional or sophisticated analysis (Hebblewhite and Haydon 2010). Its challenges have also been presented and its role to support forest and wetlands also discussed. As already mentioned in Sect. 25.2.1.2, advantages of obtaining animal positions

using GNSS tracking systems are its capability to record huge amounts of highly accurate animal locations with minimal work by the operators, thus allowing reduced sampling intervals, and increased accuracy and performance when compared with VHF radio-tracking systems (Urbano et al. 2010).

The system also has the capability to position both on the surface of the Earth and in the air, are highly accurate and repeatable compared with ground-based conventional VHF triangulation techniques and VHF tracking from aircraft or Argos satellite Doppler-based positioning, offers the capability of 24-hour coverage with position updates available in rapid succession (one location update per second is typical), the all weather positioning capability when other approaches can be restricted, and the additional accurate time stamping of a position that is delivered besides the actual positions (see Tomkiewicz et al. (2010, and the references therein)). The huge potential of geoinformatics in conservation biology is realised only when all the various independent mapping and ICT technologies e.g., GNSS, remote sensing, GIS are fully integrated to leverage on the strengths of each of them.

References

- Abdalati W, Zwally HJ, Bindschadler B, Csatho B, Farrell SL, Fricker HA, Harding D, Kwok R, Lefsky M, Markus T, Marshak A, Neumann T, Palm S, Schutz B, Smith B, Spinhirne J, Webb C (2010) The ICESat-2 laser altimetry mission. *Proc IEEE* 98(5):735–751. doi:[10.1109/JPROC.2009.2034765](https://doi.org/10.1109/JPROC.2009.2034765)
- Ausseil AE, Dymond JR, Shephard JD (2007) Rapid mapping and prioritisation of wetland sites in the Manawatu–Wanganui region, New Zealand. *Environ Manage* 39:316–325
- Awange JL, Ong’ang’a O (2006) Lake Victoria-ecology, resource of the lake basin and environment. Springer, Berlin
- Awange JL, Aseto O, Ong’ang’a O (2004) A case study on the impact of Giraffes in Ruma National Park in Kenya. *J Wildl Rehabil* 27:16–21
- Barbari M, Conti L, Koostra BK, Masi G, Workman SR (2006) The use of global positioning and geographical information systems in the management of extensive cattle grazing. *Biosyst Eng* 95(2):271–280. doi:[10.1016/j.biosystemseng.2006.06.012](https://doi.org/10.1016/j.biosystemseng.2006.06.012)
- Berger J (2004) The last mile: how to sustain long-distance migration in mammals. *Conserv Biol* 18:320–331. doi:[10.1111/j.1523-1739.2004.00548.x](https://doi.org/10.1111/j.1523-1739.2004.00548.x)
- Brondizio ES, Moran EF, Mausel P, Wu Y (2005) Land use change in the Amazon estuary: patterns of caboclo settlement and landscape management. *Hum Ecol* 22:249–278
- Brooks RP, Wardrop DH, Cole CA (2006) Inventorying and monitoring wetland condition and restoration on a watershed basin with examples from Spring Creek Watershed, Pennsylvania, USA. *Environ Manage* 38:673–687
- Cagnacci F, Boitani L, Powell PA, Boyce MS (2010) Challenges and opportunities of using GPS-based location data in animal ecology. *Philos Trans R Soc B* 365:2155. doi:[10.1098/rstb.2010.0098](https://doi.org/10.1098/rstb.2010.0098)
- Chester CC (2006) Landscape vision and the Yellowstone to Yukon conservation initiative. In: Chester CC (ed) *Conservation across borders: biodiversity in an interdependent world*. Island Press, Washington, pp 134–157
- Chopra R, Verma VK, Sharma PK (2001) Mapping, monitoring and conservation of Harike wetland ecosystem, Punjab India through remote sensing. *Int J Remote Sens* 22:89–98
- Costa M (2004) Use of SAR satellites for mapping zonation of vegetation communities in the Amazon floodplain. *Int J Remote Sens* 25(10):1817–1835

- Costa M, Niemann O, Novo E, Ahern F, Mantovani J (2002) Biophysical properties and mapping of aquatic vegetation during the hydrological cycle of the Amazon floodplain using JERS-1 and RADARSAT. *Int J Remote Sens* 23(7):1260–1401
- Craighead FC (1982) *Track of the grizzly*. Random House, New York
- Craighead JJ, Sumner JS, Mitchell JA (1995) *The grizzly bears of Yellowstone: their ecology in the Yellowstone ecosystem*. Island Press, New York
- Environment Canada (2008) Scientific review for the identification of critical habitat for woodland caribou (*Rangifer tarandus caribou*), boreal population, in Canada, August 2008. Environment Canada, Ottawa, 72 pp. plus 180 pp Appendices
- Emerton L, Kekulandala LDCB (2003) Assessment of the economic value of Muthurajawela wetland. *Occas Pap IUCN Sri Lanka* 4:1–28
- Eshiamwata G (2012) Monitoring habitat at key biodiversity sites in Africa using remote sensing: land cover change at important bird areas in Eastern Africa. PhD, University of Nairobi, Nairobi
- Fearnside PM, Laurance WF (2003) Determination of deforestation rates of the world's humid tropical forests. *Science* 299:10–15
- Fuller MR, Millspaugh JJ, Church KE, Kenward RE (2005) Wildlife radio telemetry. In: Braun CE (ed) *Techniques for wildlife investigations and management*, 6th edn. The Wildlife Society, Bethesda, pp 377–417
- Gibbs HK, Brown S, Niles JO, Foley JA (2007) Monitoring and estimating tropical forest carbon stocks: making REDD a reality. *Environ Res Lett* 2:23–45
- Han M, Sun Y, Xu S (2007) Characteristics and driving factors of marsh changes in Zhalong wetland of China. *Environ Monit Assess* 127:363–381
- Harding DJ, Carabajal CC (2005) ICESat waveform measurements of within-footprint topographic relief and vegetation vertical structure. *Geophys Res Lett* 32:L21S10. doi:10.1029/2005GL023471
- Hebblewhite M, Haydon DT (2010) Distinguishing technology from biology: a critical review of the use of GPS telemetry data in ecology. *Philos Trans R Soc B* 365:2303–2312. doi:10.1098/rstb.2010.0087
- Hebblewhite M (2009) Linking wildlife populations with ecosystem change: state-of-the-art satellite ecology for national-park science. *ParkScience* 26(1). <http://www.nature.nps.gov/ParkScience/index.cfm?ArticleID=280>. Accessed 25 Sept 2011
- Holopainen M, Leino O, Kämäri H, Talvitie M (2006) Drought damage in the park forests of the city of Helsinki. *Urban For Urban Greening* 4:75–83. doi:10.1016/j.ufug.2005.11.002
- Houghton RA (2005) Above ground forest biomass and the global carbon balance. *Glob Change Biol* 11:945–958
- James LF, Young JA, Sanders K (2003) A new approach to monitoring rangelands. *Arid Land Res Manage* 17:319–328. doi:10.1080/15324980390225467
- Janssen V (2012) Indirect tracking of drop bears using GNSS technology. *Australian Geographer* 43:(4) 445–452, doi:10.1080/00049182.2012.731307
- Jensen JR, Christensen EJ, Sharitz R (1984) Nontidal wetland mapping in South Carolina using airborne multi-spectral scanner data. *Remote Sens Environ* 16:1–12
- Jonson RM, Barson MM (1993) Remote sensing of Australian wetlands: an evaluation of landsat TM for inventory and classification. *Aust J Mar Freshw Resour* 44:235–252
- Kasischke ES, Bourgeau-Chavez LL (1997) Monitoring South Florida wetlands using ERS-1 SAR imagery. *Photogram Eng Remote Sens* 63:281–291
- Kumi-Boateng B (2012) A spatio-temporal based estimation of vegetation changes in the Tarkwa mining area of Ghana. Doctor of Philosophy, Dissertation, University of Mines and Technology, Ghana, 165 pp
- Lowry J, Hess L, Rosenqvist A (2009) Mapping and monitoring wetlands around the world using ALOS PALSAR: the ALOS Kyoto and carbon initiative wetlands products. In: Jones S, Reinke K (eds) *Innovations in remote sensing and photogrammetry*. Lecture notes in geoinformation and cartography. Springer, pp 129–144

- Malhi Y, Grace J (2000) Tropical forests and atmospheric carbon dioxide. *Trends Ecol Evol* 15:332–337
- Munyati C (2000) Wetland change detection on the Kafue Flats, Zambia, by classification of a multitemporal remote sensing image dataset. *Int J Remote Sens* 21:1787–1806
- Ozesmi SL, Bauer ME (2002) Satellite remote sensing of wetlands. *Wetlands Ecol Manage* 10:381–402
- Raven Environmental Services (2008) Mapping and GIS/GPS technology services. <http://www.ravenenvironmental.com/mapping.aspx>. Accessed 06 March 2008
- Sirait M, Prasadjo S, Podger N, Flavelle A, Fox J (1994) Mapping customary land in East Kalimantan, Indonesia: a tool for forest management. *Ambio*. Stockholm *AMBIO* 23(7):411–417
- Steede-Terry K (2000) Integrating GIS and the global positioning system. ESRI Press, California
- Tomkiewicz SM, Fuller MR, Kie JG, Bates KK (2010) Global positioning system and associated technologies in animal behaviour and ecological research. *Philos Trans R Soc B* 365:2163–2176. doi:10.1098/rstb.2010.0090
- Townsend PA, Walsh SJ (1998) Modeling floodplain inundation using an integrated GIS with radar and optical remote sensing. *Geomorphology* 21:295–312
- Tucker CJ (1980) Remote sensing of leaf water content in the near infrared. *Remote Sens Environ* 10:23–32
- Tucker CJ (1979) Red and photographic infrared linear combinations for monitoring vegetation. *Remote Sens Environ* 8(2):127–150. doi:10.1016/0034-4257(79)90013-0
- Urbano F, Cagnacci F, Clement C, Dettki H, Cameron A, Neteler M (2010) Wildlife tracking data management: a new vision. *Philos Trans R Soc B* 365:2177–2185. doi:10.1098/rstb.2010.0081
- Welch R, Remillard M, Doran RF (1995) GIS database development for South Florida's National Parks and Preserves. *Photogram Eng Remote Sens* 61:1371–1381
- Wessels K, Steenkamp K, von Maltitz G, Archibald S (2011) Remotely-sensed vegetation phenology for describing and predicting the biomes of South Africa. *Appl Veg Sci* 14:49–66

Chapter 26

Disaster Monitoring and Management

“The greatest exploiter for all of us are floods today, droughts tomorrow, earthquake some times and all of these multiply our trauma of deprivation, pains of poverty and hunger. These disasters take away not only our crops, shelters, lives of our families, friends tattles, but also destroy our hopes and dreams of the future. Is there any event comparable to these, which causes so much human sufferings and injustice?” This is the cry in bewilderment of a common farmer of Koshi River basin, Bihar (India) in the midst of recurrent floods and droughts

Jayaraman et al. (1997)

26.1 Introductory Remarks

Since time immemorial, natural disasters have continued to plague the history of mankind. They have varied in type, frequency, coverage and severity ranging from earthquakes, landslides, droughts, floods, tornadoes, hurricanes, tsunamis, volcanic eruptions etc. Over the last century, the frequency, severity and impact of natural disasters has increased substantially. This has been partly attributable to the destruction of the environment and the concomitant climate change paradigm discussed in Chap. 21. To enhance the sustainability of Earth, and thereby ensure the very survival of humanity, it has become imperative that natural disasters be continually and systematically monitored. This needs to be undertaken for different natural disasters at various levels ranging from local, regional to global monitoring scales.

That space technology has made a significant contribution in disaster monitoring and management over the years is not in dispute. For example, Earth observation remote sensing satellites have continued to provide comprehensive, synoptic and multi-temporal coverage of large areas in real time and at frequent intervals. Data acquired from remote sensing (see Chap. 7) and GNSS (see Chap. 4) have become

valuable for continuous monitoring of atmospheric as well as surface parameters that are critical in disaster monitoring. In general, advancements in remote sensing, GIS, GNSS and communication technologies have assisted in providing a framework for real time monitoring, early warning and quick damage assessment of many natural disasters.

The rest of this chapter is organized as follows; In Sect. 26.2, for purposes of putting this presentation in context and avoiding ambiguity, the definition and scope of natural disasters is outlined. This is followed by Sect. 26.3 which presents geosensor networks employed in disaster monitoring. In Sect. 26.4, floods are addressed, while Sect. 26.5 discusses droughts. Sect. 26.6 discusses vector-borne diseases and outbreak, with Sect. 26.7 focusing on earthquakes. Sect. 26.8 discusses changing sea level, while Sect. 26.9 presents Tsunami early warning systems. The chapter closes with Sect. 26.10 which discusses land subsidence and slides.

26.2 Definition and Scope

A natural disaster is the effect of a natural hazard and may be triggered by natural events such as earthquakes, landslides, droughts, floods, tornadoes, hurricanes, tsunamis, volcanic eruptions etc. Natural disasters are often characterized by substantial financial, environmental, human and/or animal losses. The magnitude of the resulting loss, and ultimately, the impact of the disaster, depends on the *vulnerability* of the affected population to resist the *hazard*. Bankoff et al. (2003) refers to this resistance as the *resilience* of the population/community/nation. This interpretation is premised in the formulation that disasters occur when hazards meet vulnerability as argued in Wisner et al. (2004). Furthermore, a disaster will only be judged to have occurred under these situations if the affected community is unable to cope with the impending hazard. Consequently, what may be interpreted as a disaster in one location may not necessarily be seen as a disaster in another part of the world.

A hazard will therefore never transform and mature into a natural disaster in areas without vulnerability, or in situations where the community can handle the posed hazard challenge. Therefore, a strong earthquake in uninhabited areas may not necessary be flagged as a natural disaster as articulated by Ballesteros (2008). The term *natural* has consequently been disputed because the events simply are not hazards or disasters without human involvement. This has led to the global phenomenon that distinguishes such human induced disasters as *man-made natural disasters*. An example of the division between a natural hazard and a natural disaster is perhaps exemplified by the fact that the 1906 San Francisco earthquake was a disaster, whereas earthquakes are in general hazards (Alexander 2002).

Natural disasters, whether of meteorological origin such as cyclones, floods, tornadoes and droughts, or those having geological nature like earthquakes and volcanoes, are well known to have devastating impacts on human life, economy and environment, and are also formidable physical constraints in our overall efforts to develop and utilize natural resources on a sustainable basis (Jayaraman et al. 1997). Indeed, disasters have been known to hit hard as seen from the floods of

2010–2011 in Pakistan and Australia, the sludge flow in Hungary in 2010, the landslide in Brazil in 2011, and Hurricane Sandy in the US,¹ events which led to environmental catastrophe.

Disaster trends reveal that the most vulnerable and hardest hit are normally the poorest people, most of who live in developing countries. With tropical climate and unstable land forms, coupled with high population density, poverty, illiteracy and lack of infrastructure development, developing countries are more vulnerable to suffer from the damaging potential of such disasters. For example, the year 2004 witnessed one of the greatest tragedies of humankind—the great tsunami that wiped out civilizations in many parts of south-east Asia. Millions were rendered homeless, and hundreds of thousands lost their loved ones.

Though it is almost impossible to completely neutralize the damage due to these disasters, according to Jayaraman et al. (1997) it is, however, possible to;

- (1) minimize the potential risks by developing disaster early warning strategies;
- (2) prepare developmental plans to provide resilience to such disasters;
- (3) mobilize resources including communication and tele-medicinal services; and
- (4) to help in rehabilitation and post-disaster reconstruction.

Disasters such as earthquakes, tsunamis and storm events are of short duration and require a fixed amount of consequence management. Others like outbreak of contagious diseases (e.g., bird flu) and wild fires are more complex and unfold in a non-linear fashion over an extended period necessitating ongoing and adaptive consequence management as argued by Terhorst et al. (2008). Generally speaking, management plans should be put in place comprising three phases, which would address the issues related to

- (a) preparedness;
- (b) response and recovery; and
- (c) mitigation.

The preparedness activities such as prediction and risk zone identification are usually taken up long before the event occurs, whereas the prevention activities such as early warning/forecasting, monitoring and preparation of contingency plans are taken up just before or during the event. Finally, the response/mitigation phase is where activities are undertaken just after the event which include damage assessment and relief management. With regard to response, the concepts documented by Terhorst et al. (2008) are pertinent. These include *level of preparedness*, *response times*, *sustaining the response* and *coordinating the response*. Due to the fact that time is critical, the three primary challenges in the race against time are *uncertainty*, *complexity* and *variability*. As an example, within the context of vegetation fires, Terhorst et al. (2008) propose a *sensor web* (see Sect. 26.3 for discussion on geosensors) that can be used to enhance the tempo of disaster response.

To support these efforts, relevant information needed to undertake risk appraisal including vulnerability analysis of the terrain, prediction, warning, and prevention of

¹ <http://edition.cnn.com/2012/10/29/travel/hurricane-sandy-flight-cancellations/index.html>

a disastrous event need to be identified *a priori*. Disaster management measures also entail examination of the probability of occurrence and the consequences, understanding of the total processes in relation to the cause and effect, identification of preventive measures and implementation of rescue strategies (Jayaraman et al. 1997).

Besides information communication technology (ICT), positioning and mapping technologies play a critical and central role in disaster monitoring and management in general. Consequently, technologies like GNSS, remote sensing and GIS are becoming more and more important, not just in the wake of disaster, when, for instance, relief efforts might call for quicker generated maps of flooded areas, for helicopters to navigate through thick smoke, or for the exact location of people buried alive, but in planning and preparatory phases of emergency management (Steede-Terry 2000). To support disaster management programs, GNSS could be used to provide support in pre-disaster preparedness programs, in disaster response and monitoring activities, and post-disaster reconstruction, specifically in the provision of location-based information. Video cameras fitted with GNSS interface and operating with infra-red sensors, for instance, could help in documenting the occurrences and locations of fire, insects, drought, flood, hail, and frost (James et al. 2003).

Other activities that could also be supported by positioning and mapping technologies include (Jayaraman et al. 1997);

- identification of hazard zones;
- risk assessment;
- creation of awareness at various levels;
- evolving systems for monitoring, prediction and warning;
- designing long-term preventive measures (structural and non-structural) and short-term protective measures and preparedness;
- early intervention measures;
- education, training, public information;
- transfer of technology; and
- research on improved technology and disaster management.

26.3 Geosensor Networks in Disaster Monitoring

A geosensor network is a distributed ad-hoc wireless network of sensor-enabled miniature computing platforms (a sensor network) that monitors phenomena in geographic space (Nittel et al. 2004; Worboys and Duckham 2006), and in which the *geospatial content* of the information collected, aggregated, analyzed and monitored is of fundamental importance (Stefanidis 2006). Similar to the animal telemetry discussed in Sect. 25.2, geosensor networks consist of thousands of sensors (also called nodes, and maybe fixed or mobile) that monitor and process data, and are also capable of communicating to each other, and to transfer data to a central station via wireless communication, hence power consumption becomes a crucial issue (Bill 2011). Since these thousands of sensors are randomly deployed, GNSS plays a crucial role

in providing their locations, to which the monitored environmental parameters (e.g., temperature and humidity) can be related.

Their environmental applications include the monitoring of drinking water quality (Ailamaki et al. 2003), disasters (earthquakes, forest fires, volcanic eruptions, oil spill, movement of glaciers, deformations in wells and bridges, flood detection and prevention) (Bill 2011; Brenner 2011), wildlife habitat monitoring, watershed management, environmental pollution monitoring, deep sea explorations, to monitoring food safety, e.g., in South Africa and precision agriculture for large vineyards (e.g., in Southern Australia) (Nittel et al. 2008). They also offer the advantage of real-time environmental monitoring such as the progress of oil spill as was witnessed in the gulf of Mexico or real-time detection of toxic gas plumes in open public spaces (Nittel et al. 2008).

The advantage of space-based positioning and mapping technologies is that they are unaffected by the actual impact since the sensors are in space and in supporting the emerging geosensor environmental monitoring, particularly in disaster management, they contribute towards a shift from post-event, estimation based, historic data analysis to real-time, sensor-rich event detection and monitoring (Nittel et al. 2008). They are therefore useful in monitoring environmental disasters discussed in the coming sections and compliment ground based geodetic methods. In this regard, the main advantage of RTGPS data discussed in Sect. 6.4.3 would be the improved temporal resolution in observations of natural processes achieved through high-rate information. RTGPS will likely demonstrate an impact similar to that of other high-rate geophysical observations (e.g., from seismological and meteorological networks) for monitoring and understanding earthquakes, seismic wave propagation, volcanic eruptions, magmatic intrusions, movements of ice, landslides, and structure and dynamics of the atmosphere (Hammond et al. 2011).

In the event of a disaster on a large scale, the *International Charter on Space and Major Disasters*² requires its members to provide satellite remote sensing data, free of charge, once an activation of the charter is triggered. The charter aims at providing a unified framework for space data acquisition and delivery to support emergency relief efforts. Each member has devoted resources to support the provisions of the charter and thus help to mitigate the effects of disasters on human life and property. Table 26.1 shows charter members and their diverse space resources. Details on the operation of the charter are outlined in the following example.

Example 26.1 (International Charter on Space and Major Disasters. Source: <http://www.disasterscharter.org>)

The international charter on space and major disasters was signed in October 2000 by the founding members, the European and French space agencies (ESA and CNES), as a follow-up of the UNISPACE III (<http://www.un.org/events/unispace3/>) conference held in Austria in 1999. Since then, the char-

² <http://www.disasterscharter.org/>

ter has grown to a membership of about 20 (see Table 26.1), with the latest member the European Organization for the Exploitation of Meteorological Satellites (EUMETSAT) joining in July 2012. The aim of the charter, underscored by the international agreement among its members, requires members to support relief efforts in the event of emergencies caused by major disasters with space-based data and information. As currently structured, however, the charter provides data to support only in immediate emergency response cases. Consequently, it does not support activities geared towards rehabilitation, reconstruction, prevention, preparedness or scientific research. Moreover, it does not provide maps suitable for use in the field.

Once a request for data support from an authorized user is received the following process is set into motion to activate the charter (<http://www.disasterscharter.org/web/charter/activate>):

- (1) Identification and verification that a disaster has indeed happened and that the charter can help;
 - (2) Operations activity round the clock (24/7) are triggered to respond to the request for support and to quickly task satellites from members;
 - (3) Once the data is acquired, it is quickly processed into images; and
 - (4) The data is further processed and interpreted to extract specific data for the area affected by the disaster which is then delivered to the end user.
- Throughout this exercise a direct link is maintained with the user/response community who will use the information.

Up until now (2012), the charter has covered a total of 314 disasters in approximately 100 countries worldwide. Figure 26.1 illustrates the hazard types for charter activations between 2000 and 2010, while Fig. 26.2 shows the total number of disasters recorded by EM-DAT (<http://www.emdat.net>) over the same duration. From these statistics, out of a total of 292 charter activations made, floods constituted the largest fraction with 46.5%. Similarly, out of 3,638 disasters recorded in the EM-DAT records, floods again were the most dominant contributing about 50.7%.

Evidently, the charter has served as a useful international disaster rapid response instrument (Allenbach et al. 2005; Voigt et al. 2005). However, despite the wonderful work realized by the charter thus far, there are certain critical elements that need to be addressed including; availability of essential datasets, processing time, information extraction and usability of the products by end-users (Buehler and Kellenber 2007). To address some of these issues, the charter intends to in future fully embrace the concept of *universal access*. This means that any national disaster management authority will be able to submit requests for emergency response support, regardless of whether or not they are within the bracket of authorized users or charter members.

End of Example 26.1

Table 26.1 Charter members and their space resources (up to April 2012)

Member	Space resources
European Space Agency (ESA)	ERS, ENVISAT
Centre National dtudes Spatiales (CNES)	
Spotimage—France	SPOT
NSPO—Taiwan	Formosat
Canadian Space Agency (CSA)	RADARSAT
Indian Space Research Organization (ISRO)	IRS
National Oceanic and Atmospheric Administration (NOAA)	POES, GOES
Comisión Nacional de Actividades Espaciales (CONAE)—Argentina	SAC-C
Japan Aerospace Exploration Agency (JAXA)	ALOS
United States Geological Survey (USGS)	Landsat
Digital Globe	Quickbird
GeoEye	GeoEye-1
Disaster Monitoring Constellation International Imaging (DMC):	
Centre National des Techniques Spatiales (Algeria)	ALSAT-1
National Space Research and Development (Nigeria)	NigeriaSat
Tübitak-BILTEN (Turkey)	BILSAT-1
UK Space Agency (UK)	UK-DMC
China National Space Administration (CNSA)	FY, SJ, ZY
	satellite series
German Aerospace Center (DLR)	TerraSAR-X, TanDEM-X
Korea Aerospace Research Institute (KARI)	Kompsat-2
National Institute for Space Research (INPE)—Brazil/China	CBERS
European Organization for the Exploitation of Meteorological Satellites (EUMETSAT)	Meteosat

Source <http://www.disasterscharter.org/web/charter/members>

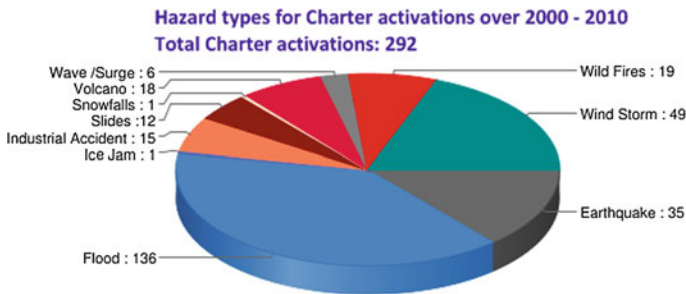


Fig. 26.1 Hazard types for charter activations between 2000 and 2010. (Source <http://www.disasterscharter.org/web/charter/emdat>)

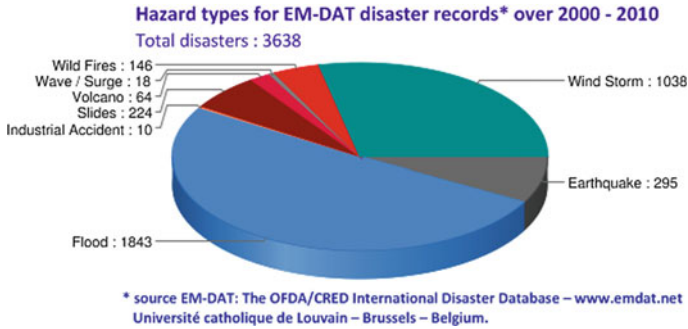


Fig. 26.2 Hazard types for EM-DAT records between 2000 and 2010. (Source <http://www.disasterscharter.org/web/charter/emdat>)

26.4 Floods

In most countries that experience frequent natural disasters, e.g., floods, droughts, earthquakes, forest fires, snow, and typhoons, floods could arguably be defined as among the most devastating natural hazards in the world, claiming more lives and causing more property damage than any other natural phenomena (Jeyaseelan 2004). Moreover, in most cases, floods seem to follow droughts and vice-versa as both disaster types are subject to similar extreme weather and climate conditions. The recurrent nature of these natural disasters is also alarming. For example, almost every year, Pakistan experiences severe floods caused by monsoon rains that often result in considerable economic loss and serious damage to property. Another country that is perennially prone to floods is China, where the frequency of occurrence is higher than the world average, with historical records documenting more than 1000 floods (Zhanga et al. 2002). Similarly, flooding in the City of New Orleans, USA in 2005 that was triggered by Hurricane Katrina causing levee failure set in motion an unanticipated failure of multiple infrastructure systems (Leavitt and Kiefer 2006). Indeed, as articulated in Sect. 21.3.2, floods pose one of the greatest challenges in weather prediction.

A flood can be defined as any relatively high water flow that over-tops a natural or artificial bank in any portion of a river or stream. When such a bank is overrun, water spreads over the flood plain and generally becomes a hazard. In general, floods can be classified into the following types (Jeyaseelan 2004):

- river floods formed from winter and spring rains, coupled with snow melt, and torrential rains from decaying tropical storms and monsoons;
- coastal floods generated by winds from intense off-shore storms and tsunamis;
- urban floods, as urbanization increases runoff two to six times what would occur on natural terrain; and
- flash floods that can occur within minutes or hours of excessive rainfall or a dam or levee failure, or a sudden release of water.

Similar to the discussion advanced in Sect. 26.1, one can distinguish three (3) major phases in flood management namely;

- (1) *Preparedness phase*: This involves activities such as prediction and risk zone identification that are taken up long before the event occurs.
- (2) *Prevention phase*: Where activities such as early warning/forecasting, monitoring and preparation of contingency plans are taken up just before or during the event and
- (3) *Response/mitigation phase*: This encompasses activities taken just after the event and includes damage assessment and relief management.

Evidently, the degree of disaster triggered by floods will vary depending on the type of flood. For instance, in most practical situations, flash floods may pose more disaster risk than river floods. Consequently, they require more urgent response as articulated in Scofield and Achutuni (1996) in their presentation of a satellite-based funnel approach for predicting and forecasting flash floods. In the following sections, we discuss the different phases of flood management as well as present various applications of geoinformatics in flood management.

26.4.1 Flood Risk Zone Mapping

Data, information and experience gathered from previous flood events may help to inform and better understand future flooding events. Active remote sensing sensors can be used to procure time-series data of flood events regardless of the flooding weather conditions. These can be documented, mapped and/or archived within a GIS environment. Besides remote sensing data, LiDAR can also be used at this stage as demonstrated by Webster et al. (2004). Simulations developed using virtual reality models, as well as other animation types, can then be employed to visualize potential flooding scenarios given different hydrological conditions e.g., precipitation.

Ultimately, a flood risk zone map needs to be produced. Two types of these can be distinguished, namely (Jeyaseelan 2004);

- (a) A detailed mapping approach, that is required for the production of hazard assessment for updating (and sometimes creating) risk maps. Such maps contribute to the hazard and vulnerability aspects of flooding.
- (b) A larger scale approach that explores the general flood situation within a river catchment or coastal belt, with the aim of identifying areas that pose the greatest risk.

26.4.2 Flood Monitoring and Forecasting

Flood monitoring can be carried out through remote sensing from global scale to storm scale. However, it is mostly applied at the storm scale using hydrodynamic

models by monitoring the intensity, movement, and propagation of the precipitation system to determine how much, when, and where the heavy precipitation is going to move during the next zero to three hours (Jeyaseelan 2004). Meteorological satellites (such as GOES and POES) help detect various aspects of the hydrological cycle including precipitation (rate and accumulation), moisture transport, and surface/soil wetness (Scofield and Achutuni 1996). Synthetic Aperture Radar (SAR) can achieve regular observation of the earth's surface, even in the presence of thick cloud cover. NOAA AHVRR represents a family of satellites upon which flood monitoring and mapping can almost always be done in near real time. Remote sensing data such as IRS, SAR, SPOT, and to some extent high resolution NOAA images can be used to determine flood extent and areal coverage. Various precipitable water (PW) products have been developed and are available operationally for assessing the state of the atmosphere with respect to the magnitude of the moisture and its transport (Jeyaseelan 2004).

Hydrological models play a major role in assessing and forecasting flood risks. To be successful, however, these models often require several types of input data e.g., land use, soil type, soil moisture, stream/river base flow, rainfall amount/intensity, snow pack characterization, digital elevation model (DEM) data, and static data (e.g., drainage basin size) (Jeyaseelan 2004). Furthermore, they need to be fine-tuned to effectively model a particular drainage basin correctly. Geoinformatic technologies can be employed to deliver most of these data sets and/or their derived products.

Model predictions or simulations of potential flood extent can help emergency managers develop contingency plans well in advance of an actual event to help facilitate a more efficient and effective response (Jeyaseelan 2004). Specifically, flood forecast can be issued over the areas in which remote sensing is complementary to direct precipitation and stream flow measurements, and those areas that are not instrumentally monitored (or the instruments are not working or are in error). Evidently, high temporal resolution remote sensing data is fundamental to effective flood monitoring and forecasting.

26.4.3 Flood Response and Mitigation

During floods, timely and detailed situation reports are required by the authorities to locate and identify the affected areas and to implement appropriate damage mitigation. It is essential that information be accurate and timely, in order to address emergency situations (for example, dealing with diversion of flood water, evacuation, rescue, resettlement, water pollution, health hazards, and handling the interruption of utilities etc.). This represents the most delicate phase of flood management as it involves rescue operations and the safety of people and property.

Jeyaseelan (2004) presents the following lists of information used and analyzed in real time together with the sources for the same (outlined in the brackets): flood extent mapping and real time monitoring (satellite, airborne, and direct survey); damage to buildings (remote sensing and direct inspections); damage to infrastructure

(remote sensing and direct inspection); meteorological (important real-time input from remote sensing data to show intensity/estimates, movement, and expected duration of rainfall for the next 0–3 h); and evaluation of secondary disasters, such as waste pollution, to be detected and assessed during the crisis (remote sensing and others). Adequate communication and logistical support is also important to ensure speedy delivery.

After the flooding, reconstruction of destroyed or damaged infrastructure, facilities and adjustments of the existing infrastructure will occur. At the same time, insurance companies require up-to-date information to settle claims. The time factor is not as critical as in the last stage. Nevertheless, both medium and high-resolution remote sensing images, together with an operational GIS, can help to plan many tasks. The medium resolution data can help establish the extent of the flood damages and can be used to establish new flood boundaries. They can also locate landslides and pollution due to discharge and sediments. On the other hand, high-resolution data employed in conjunction with GNSS are suitable for pinpointing locations and the degree of damages. They can also be used as reference maps to rebuild bridges, washed-out roads, homes and facilities (Jeyaseelan 2004).

26.4.4 Geoinformatics Support of Flood Management

Many examples on the operational use of space-based technology in the detailed monitoring and mapping of floods and post-flood damage assessment have been documented. Remote sensing information delivered from different sensors and platforms (satellite, airplane, and ground etc.) are used for monitoring floods worldwide. To estimate real time flood damages requires that a GIS be used. Besides mapping the flood and damage assessment, high resolution satellite data can be employed for operational management to map post flood river configuration, flood control works, drainage-congested areas, bank erosion and developing flood hazard zone maps.

GNSS could play a useful role of generating DEM (see Fig. 19.3 on p. 262). It could also find use in generating the drainage basin size through a similar approach to that used in obtaining the area of Jack Finney Lake discussed in Sect. 19.3.1.2 on p. 261. For example, GNSS was used to aid development of DEM of a flood prone area in Andhra Pradesh State of India that supported the assessment of spatial inundation at different water levels in the river. When the satellite derived land cover/use and ancillary ground-based socio-economic data was draped over the DEM, flood vulnerability was assessed to provide location specific flood warnings (Jayaraman et al. 1997).

As discussed in Chap. 20, GNSS meteorology promises to be a real boost to atmospheric studies with expected improvements on weather forecasting and climatic change monitoring, which directly impact on our everyday lives. One such area is in the monitoring of flash floods. Flash floods (see Sect. 26.4) are floods that come instantaneously and usually unexpectedly following heavy rains. Factors that lead to flash flood producing rains are summarized in Fig. 26.3. In India for example,

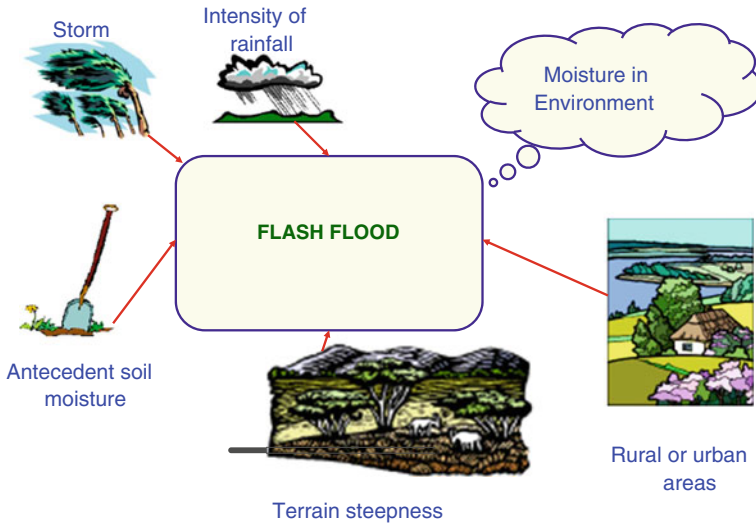


Fig. 26.3 Factors causing flash floods

deforestation, extension of agricultural activities in vulnerable areas, coupled with increased soil erosion and degradation of catchment areas have been cited as factors that have lead to frequent flash floods through reduction in natural storage capacity (Jayaraman et al. 1997).

In Awange and Fukuda (2003), the possible use of IPWV (see Sect.20.2.2) for flash flood prediction is proposed, while Baker et al. (2001) have outlined the potential of water vapor for meteorological forecasting. Let us consider Fig. 26.4³ as an example

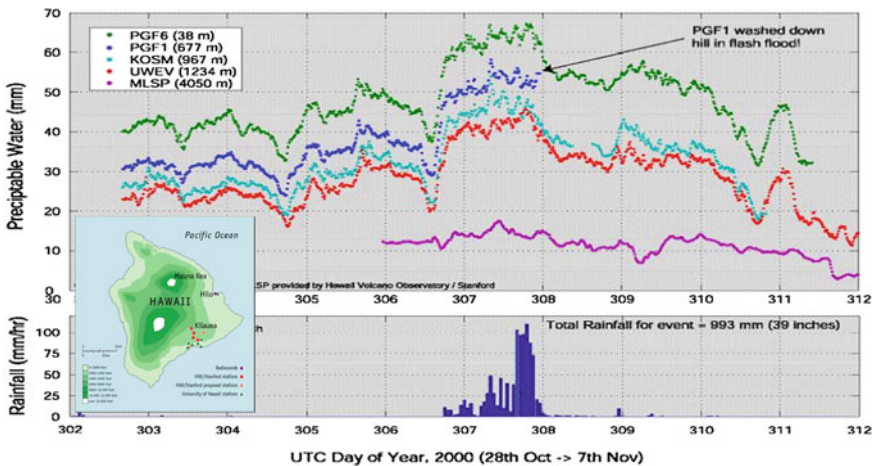


Fig. 26.4 An example of flash flood monitoring using GNSS-derived IPWV

³ Source: Paroscientific Inc., <http://www.paroscientific.com>.

where GNSS-meteorology could have assisted in flash flood forecasting and warning. In the figure, the amount of integrated water vapor in the atmosphere is related to the rainfall and used to monitor flash flood in Hawaii (see the left bottom corner of the figure). One observes that as it was raining, if the Integrated Precipitate Water vapor (IPWV) increased, more rain followed. By monitoring the intensity of water vapor, therefore, one can be able to predict the occurrence of flash flood. Station PGF1 and others were monitored and an increase noted after day 307. Shortly before day 308, the scientist reported the possibility of flash flood and indeed it occurred. Station PGF1 was washed away.⁴

GNSS could be used to map location of features, e.g., water tanks or perimeters of areas of potential danger such as contaminated dams, while in the second case, they could be used in conjunction with remote sensing methods to map inundated areas at large spatial coverage. In mapping flood events and damaged areas, GNSS could also be used to provide both horizontal and vertical controls as exemplified, e.g., in US Army Corps of Engineers (2007), where a constrained adjustment of a static GNSS survey (e.g., Sect. 6.4.2) was performed to set basic horizontal and vertical controls for a flood control project near Guayama on the south coast of Puerto Rico. In this example, precise differential carrier-phase were applied and the end product was to obtain hydrographic and topographic data of project features to generate topographical maps (e.g., Fig. 19.2 on p. 261) for flood control.

In flood mitigation and response situations, location-based data and perimeter/area information could rapidly be provided by remote sensing and GNSS to assist in remedial measures. Furthermore, GNSS in conjunction with remote sensing satellite and GIS could be integrated to provide a unified system of monitoring and evaluating flood disasters. For example, Zhanga et al. (2002) discusses an airplane-satellite-ground system that arose from a research program on flood monitoring promoted by the Chinese government, which integrates remote sensing, GNSS, data transmission, and image processing. Another example is in Brahmaputra river basin in India, where GNSS was used to provide information on flooded areas and damage to croplands, roads and rail-tracks (Jayaraman et al. 1997).

Appropriate remote sensing data applied within a GIS environment could also be useful in identifying flood-prone river basins, assessment of expected risk levels, and selection of suitable land and water management measures to support management of flood plains. These can be employed to produce flood risk zone maps, which are essential in regulating the use of flood plains in a planned manner. For example, this approach was used in India to develop an integrated river basin development plan for major river basins, which was then applied to identify and monitor erosion-prone areas along river banks for the purpose of protecting land and habitat (Jayaraman et al. 1997). Maps prepared from remotely sensed data showing drainage congested areas could also be used effectively to avoid flooding (Jayaraman et al. 1997). In these cases, GNSS could provide location-based information for georeferencing of remote sensing images.

⁴ More on information can be found by visiting <http://www.paroscientific.com>.

As an example, GNSS was used in conjunction with remote sensing satellites in flood management to map flood affected areas as demonstrated in the work of Crétaux et al. (2007) who develop a method of wetland mapping and flood event monitoring based on a satellite multi-sensor data combination. Jayaraman et al. (1997) state that because of the clear difference in the spectral signatures, it is quite possible to map areas under standing water, areas from where flood water had receded, submerged standing crop areas, sand casting of agricultural lands, breaches in the embankments, marooned villages and towns, etc., and that using multi-date satellite imageries enables the extent of damage due to crop loss, and the destruction of infrastructural facilities to be assessed.

Crétaux et al. (2007) employed a series of airborne GNSS measurements to map horizontal areas covered by open water, aquatic vegetation, vegetation on dry land and then detect the limit zone between each type of terrain. This allowed the estimation of threshold values of the surface reflectance in different bands of frequency of the MODIS sensor that was used to characterize the land surface. Besides applying GNSS satellites for mapping purposes, they could be used to calibrate altimetry satellite (e.g., Fig. 20.10 on p. 295). For instance, GNSS data obtained during a field campaign carried out in Summer 2006 was used to calibrate the ICESat (Ice, Cloud, and land Elevation Satellite, e.g., Fig. 20.11 on p. 298)—derived topography on few points of control on the Goyder Lagoon (Crétaux et al. 2007).

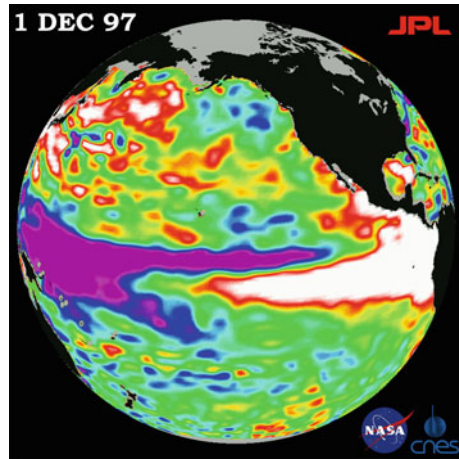
26.4.5 Monitoring of ENSO and IOD

The term “El Niño” originally applied to an annual weak warm ocean current that ran southward along the coast of Peru and Ecuador about Christmas time (hence Niño, Spanish for “the boy Christ-child”) and only subsequently became associated with the unusually large warming that occur every few years and change the local and regional ecology (Trenberth 1997). The coastal warming, however, is often associated with a much more extensive anomalous ocean warming to the International Date Line (IDL), and it is this Pacific basin-wide phenomenon that forms the link with the anomalous global climate patterns (Trenberth 1997). The atmospheric component tied to El Niño is termed the “Southern Oscillation” forming El Niño-Southern Oscillation (ENSO), i.e., the phenomenon where the atmosphere and ocean collaborate together (Trenberth and Guillemot 1996). El Niño then corresponds to the warm phase of ENSO, while the opposite “La Niña” (“the girl” in Spanish) phase consists of a basin-wide cooling of the tropical Pacific and thus the cold phase of ENSO (Trenberth 1997).

Satellite altimetry can play a crucial role in monitoring ENSO by observing the behaviour of the sea surface height (SSH). From the SSH obtained from TOPEX/Poseidon and Jason, Jet Propulsion Laboratory (JPL) use them to calculate the amount of heat stored below the ocean, from which annual and decadal changes in the ocean are used to monitor climate events e.g., ENSO.⁵ Through the

⁵ see e.g., <http://sealevel.jpl.nasa.gov/science/elinopdo/latestdata/>

Fig. 26.5 1997–1998 ENSO monitored using TOPEX/Poseidon satellite. The *white-red* areas indicate unusual pattern of heat storage. *Source* http://en.wikipedia.org/wiki/File:1997_El_Nino_TOPEX.jpg



observation of SSH (see Sect. 20.4), the 1997–1998 ENSO event, which was probably the biggest in recorded history, and whose socio-economic impacts were felt in most places around the world could be monitored. Figure 26.5 shows the image of the Pacific Ocean produced using SSH measurements taken by TOPEX/Poseidon satellite, where the image shows SSH relative to normal ocean conditions on Dec. 1, 1997.⁶ In this image, the white and red areas indicate unusual patterns of heat storage; in the white areas, the sea surface is between 14 and 32 cm (6–13 inches) above normal while in the red areas, it is about 10 cm (4 inches) above normal. The green areas indicate normal conditions, while purple (the western Pacific) means at least 18 cm (7 inches) below normal sea level.⁷

The Indian Ocean Dipole (IOD) is an ocean-atmosphere interaction over the Indian Ocean, with alternative positive and negative sea surface height (Becker et al. 2010). During positive events, anomalous cool (warm) waters appear in the eastern (western) Indian Ocean, associated with large-scale circulation changes that bring anomalous dry conditions to Indonesia and Australia, while East Africa experiences heavy rainfall (Garcia-Garcia et al. 2011). By monitoring changes in stored water using GRACE (Sect. 20.3.3) and computing the correlation between these changes with ENSO-measured southern oscillation index (SOI) and the IOD-measured dipole mode index (DMI) as illustrated in Figs. 22.4, 22.5, 22.6, 22.7 on pp. 353–356, it is possible to relate the effect of climate variability on water resources, see e.g., (Becker et al. 2010; Garcia-Garcia et al. 2011; Ummenhofer et al. 2009).

Garcia et al. (2011) define SOI as being a measure of ENSO, which is based on the pressure difference between Tahiti and Darwin as provided by the Australian Bureau of Meteorology, while the DMI, a measure of IOD is estimated as the difference between the western and South-eastern tropical Indian Ocean sea surface temperature

⁶ http://en.wikipedia.org/wiki/File:1997_El_Nino_TOPEX.jpg

⁷ http://en.wikipedia.org/wiki/File:1997_El_Nino_TOPEX.jpg

(SST) indices. SST data can be obtained from optical remote sensing sensors e.g., NOAA AVHRR and Terra MODIS as well as from microwave radiometer sensors (see Table 9.1 on p. 138).

In conclusion, floods are evidently the most frequent (see Fig. 26.1) and most severe natural disaster occupying the highest rank among other natural disasters (Istomina et al. 2005). They have had a devastating impact in different parts of the world, resulting in the loss of many lives and destruction of numerous livelihoods in their wake. In this section, we have distinguished between different types of floods including; river-, coastal-, urban- and flash floods. Given their spontaneous nature, flash floods are evidently the most difficult type of floods to model. We have also discussed the different phases of flood management namely; flood prone/risk zone identification, flood monitoring and forecasting and lastly, flood response and mitigation. Using typical examples, different applications of geoinformatics in flood management have also been outlined. These range from the predominant use of remote sensing and GIS to the increasing application of GNSS. To wrap up things, the final subsection has focused on monitoring of the ENSO and IOD effects, both of which have a direct consequence on flooding and drought events at a global scale (e.g., Forootan et al. (2012)).

26.5 Droughts

The World Meteorological Organization (WMO)⁸ classifies droughts on the basis of several parameters and considerations including: (i) rainfall, (ii) combinations of rainfall with temperature, humidity and/or evaporation, (iii) soil moisture and crop parameter, (iv) climatic indices and estimates of evapotranspiration, and finally (v) the general definitions and statements. Through such a classification regime, drought can be grouped into *hydrological drought*, *agricultural drought*, and *meteorological drought*, whose sequence of impacts is shown in Fig. 26.6. Its impacts (direct or indirect) include (Jeyaseelan 2004): reduced crop, rangeland, and forest productivity; increased fire hazard; reduced water levels; increased livestock and wildlife mortality rates; and damage to wildlife and fish habitat.

Drought occurrences are subject to extreme weather and climate similar to floods. In contrast to floods, however, drought, which is a slow and progressive extreme climatic event, lasts longer and has been the least anticipated extreme in many regions. Drought is the single most important weather-related natural disaster often aggravated by human action since it affects very large areas for months and years and thus has a serious impact on regional food production, life expectancy for entire populations and economic performance of large regions or several countries (Jeyaseelan 2004). As a result, its impacts are more adverse than, for example, those of floods because of the inadequacy of existing coping mechanisms. Although drought is a natural, recurring phenomenon which cannot be controlled, prediction of its frequency, see

⁸ <http://www.wmo.int/pages/index-en.html>

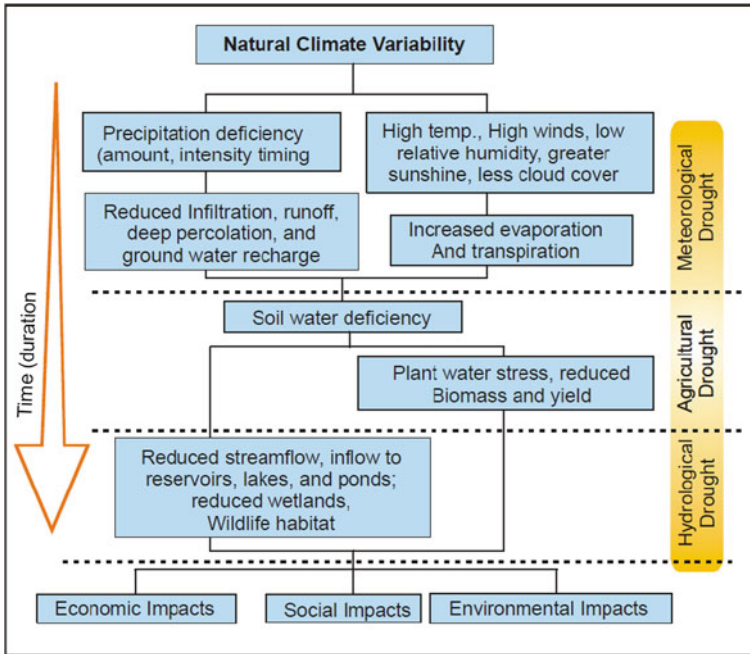


Fig. 26.6 Sequence of hydrological, agricultural, and meteorological drought impacts. (Source Jeyaseelan 2004)

e.g., (Awange et al. (2007), and the references therein), severity and probability is essential for users such as top level policy makers at the national and international organizations, researchers, middle level policy makers at the state, province and local levels consultants, relief agencies and local producers including farmers, suppliers, traders and water managers interested in reliable and accurate drought information for effective planning and management (Jeyaseelan 2004).

In the absence of such information, food security is threatened as exemplified in the 1999–2001 drought that affected most parts of Kenya, including some areas that normally receive high rainfall. At its peak, 4.5 million people in Kenya lost their livelihoods and ability to cope, and were subsequently entirely dependent on relief food provided jointly by the government and donors (DMCN 2002). Evidently, arid and semi-arid regions are more prone to drought. For example, only recently (2011), drought yet again ravished the Horn of Africa affecting countries like Somalia, Ethiopia, and Northern Kenya. Adger et al. (2003) discussed adaptation to climate change related phenomena in developing countries, while Barrett (2002) described food assistance programs. The impacts of such extremes (in the context of climate change) on Lake Victoria Basin (LVB) has been assessed, e.g., in Phoon et al. (2004). On the average, statistics indicate that severe drought occurs once every five years in most of the tropical countries, though often they occur on successive

years causing untold misery to human life and livestock (Jayaraman et al. 1997). For the Lake Victoria basin, Awange et al. (2008, 2007) obtained a cycle of 5–8 years.

To manage the effects of drought, therefore, measures should be taken, which involves both short-term that includes, e.g., early warning, monitoring and assessment of droughts; and long-term strategies aimed at drought mitigation measures through proper irrigation scheduling, soil and water conservation, and cropping pattern optimization (Jayaraman et al. 1997). Jeyaseelan (2004) states that monitoring and assessment of drought using remote sensing and GIS are dependent on the factors that cause drought, and the factors of drought impact.

26.5.1 Early Warning of Drought

The first step in realizing a drought early warning system is to have a preparedness program, where drought-prone areas are identified well in advance, and drought-intensity and cycle predicted, e.g., (Awange et al. 2007). Prediction is based on monitored parameters, e.g., rainfall anomalies, crop conditions, weather, and vegetation. Jayaraman et al. (1997) list factors that can provide early indication of possible droughts as upper air winds, the development of hot low-pressure areas, ENSO phenomena, sea surface temperature (SST), snow cover, cloud patterns, wind velocity and direction, and atmospheric temperature and humidity profiles.

GNSS-meteorology presented in Sect. 20.2 could be useful in providing temperature, pressure, and humidity profiles. Sect. 21.5.3.2 discusses the possibility of using GNSS remote sensing techniques to monitor regional and global warming. Using the Australian example, Khandu et al. (2008) showed how this technique, which has emerged over the past decade could prove to be an important tool for measuring global changes in tropopause's temperatures and heights, a valuable capacity given the tropopause's sensitivity to temperature variations. Similarly, remote sensing sensors like NOAA AVHRR and Terra MODIS could be employed to deliver SST image data and associated anomalies. Remote sensing could also be used to generate vegetation index, data that are useful in providing spatial information on drought-prone areas.

26.5.2 Drought Monitoring and Assessment

Monitoring and assessment of droughts are required for taking corrective measures at appropriate times in order to minimize the reduction in agricultural productivity in drought-prone areas, and also to provide objective information on the prevalence, severity level and persistence of drought conditions in a time-effective manner, which will be helpful to the resource managers in optimally allocating scarce resources to where and when they are most needed (Jayaraman et al. 1997).

Normalized difference vegetation index (NDVI) and its associated derivatives (see Sect. 10.3.3), has traditionally been used for vegetation cover modelling (Privette et al. 1995), and is a good summary overview of the prevailing plant water stress as

a function of the prevailing weather conditions (Hatfield et al. 2004). It measures the amount of radiation absorbed by plants, where this radiation is directly related to evapotranspiration, hence relating NDVI to rainfall. This relationship is already being exploited by the Famine Early Warning Systems Network (FEWS NET)⁹ to monitor crops and range lands in semi arid sub-Saharan Africa. In East Africa, there is a good correlation between NDVI and seasonal rainfall patterns (Nicholson et al. 1990), suggesting its possible use as a drought metric. In a recent study, Omute et al. (2000) indicated that NDVI as a measure of vegetation vigour responded variably to *precipitation* and its *deficiency*. Its sensitivity to vegetation stress enables drought conditions to be continuously monitored on a real-time basis, often helping the decision makers initiate strategies for recovery by changing cropping patterns and practices (Jayaraman et al. 1997).

Remote sensing techniques that provide NDVI could be integrated with GIS and GNSS to effectively forecast and monitor drought, where remote sensing would indicate areas of consistently healthy and vigorous vegetation, as well as stressed vegetation. On the other hand, GNSS would provide location-based information that would enable these vegetation to be located, and play the role of georeferencing these remotely sensed satellite images. Finally, GIS would provide a modeling and decision support framework for analysis. In this regard, the generated NDVI data could be correlated with drought risk areas and integrated with both physical and meteorological data. Physical data could comprise data sets such as topography (slope), soil drainage, ground water resources etc., while meteorological data sets could include annual rainfall, annual frequency rainfall, annual evapotranspiration etc. Within a GIS environment all these different factors could be assigned appropriate weights, derived from expert opinion, and integrated through multi-criteria evaluation methods (see Sect. 17.2.6) to give a realistic drought prognosis for a particular area.

The use of GRACE satellites discussed in Sect. 20.3 could provide spatial and temporal changes in terrestrial water storage, which could be used to monitor hydrological drought. Chen et al. (2009) used GRACE satellites to measure a significant decrease in terrestrial water storage (TWS) in the central Amazon basin in the summer of 2005, relative to the average of the 5 other summer periods in the GRACE era. Their results demonstrated the unique potential of GRACE satellites to remotely sense large-scale severe droughts and flooding events, and in evaluating advanced climate and land surface models.

26.5.3 Combating Drought

Jayaraman et al. (1997) indicate that while the construction of large reservoirs to ensure irrigation and drinking water contributed to a large extent towards mitigation of droughts in different countries, the poor and inefficient management of land and water resources in respective command areas have resulted in massive land

⁹ <http://www.fews.net/Pages/default.aspx>

degradation like salinity/alkalinity, water logging, etc., and thus causing serious concern to the conventional model of drought mitigation. In Chap. 23, ways in which remote sensing, GIS and GNSS could be helpful in land management are presented. Together with remote sensing, GNSS could also be useful in monitoring the large reservoirs.

26.6 Vector-Borne Diseases and Outbreak

Major epidemics of virulent disease have occurred with surprising frequency throughout human history, e.g., the numerous appearance of bubonic plague in Europe in the late Middle Ages, the pandemic spread of influenza in the United States in 1918–1919, and HIV-AIDS in our time (Steede-Terry 2000). Discovering and understanding the life cycle of a disease calls for painstaking research, literally years of trial and error, and for many biologists, geoinformatics could not have come at an opportune time (Steede-Terry 2000). In general, where temporal and spatial information is required, GNSS techniques could be integrated with remote sensing and GIS to enhance optimality and provide useful information applicable, e.g., in monitoring emerging infectious diseases and to studies of global change effects on vector-borne diseases, see e.g., Uriel (1998). For example, an integration of GNSS with GIS, satellite imagery, and spatial statistics tools have been used to analyze and integrate the spatial component in epidemiology of vector-borne disease into research, surveillance, and control programs based on a landscape ecology approach (Uriel 1998).

Defining landscape ecology as dealing with the mosaic structure of landscapes and ecosystems by considering the spatial heterogeneity of biotic and abiotic components as the underlying mechanism which determines the structure of ecosystems, Uriel (1998) describes how the integration of GNSS with the tools above, and the landscape ecology-epidemiology approach could be applicable to vector-borne diseases. He supports his argument by presenting his work on malaria in Israel and tsetse flies in Kenya, and Lyme disease, LaCrosse encephalitis, and eastern equine encephalitis in the north-central United States as examples for application of the tools to research and disease surveillance (Uriel 1998).

On their part, Bonner et al. (2003) consider the combination of GNSS and GIS geocoding in epidemiological research, while Jayaraman et al. (1997) indicate the possible application of remote sensing in the assessment of crop pest/diseases by using the temporal and spatial distribution of desert vegetation and rainfall derived from NOAA data to identify potential locust breeding grounds. Once these locations have been identified, GNSS could help by providing the actual coordinates of these positions.

Environmental determinants such as presence of suitable habitats, temperature and climate, to a large extent, influence the outbreak and spread of vector-borne diseases. Consequently, it is unsurprising that techniques that are routinely used to map these environmental determinants, including remote sensing and GIS, have been employed extensively in public and environmental health to study and control these

diseases, see e.g., (Hay and Lennon 1999; Herbreteau et al. 2007; Lian et al. 2007) etc. Using these techniques, it is possible to identify the spatial patterns of outbreaks through epidemic curves as well as estimate the extent of the risk area through cluster analysis to support in mitigation measures.

The work of Dr. Snow in solving the problem of *cholera* outbreak in London in the 1850s (see Example 26.2) stands out as one of the most famous and earliest cases of maps being applied to understand the spread of a disease. Over the years, remote sensing and GIS have also been extensively employed to map different epidemiological cases including malaria, rift valley fever etc. Furthermore, with a better understanding of the environmental factors that drive the distribution, timing and abundance of pathogen carriers e.g., mosquitoes, tsetse flies etc., it is now possible to develop early warning systems. This can be used to flag regions at high risk of pathogen transmission, and more effectively inform and guide the distribution of surveillance and control measures. For instance, by studying indicators like NDVI it is possible to predict malaria seasons. Today, experts routinely use advanced mapping and computing technologies to understand the diffusion and spread of diseases such as AIDS and cancer. Hence, a map is no longer just an effective tool for finding locations, but it can also be a life saver!

Example 26.2 (Dr. Snow's Cholera analysis using GIS. Source: Snow 2010)

In 1854 a massive cholera outbreak occurred in Soho, London resulting in hundreds of deaths. In trying to diagnose the source of the problem, Dr. John Snow plotted the locations of the deaths on a map and found they clustered around a pump in Broad Street. This provided strong evidence in support of his theory that cholera was a water-borne disease and additionally, that it was spread through dirty water. Specifically, Dr. Snow drew Thiessen polygons around the wells, defining straight-line least-distance service areas for each (see Sect. 17.2.6, p. 229). A large majority of the cholera deaths fell within the Thiessen polygon surrounding the Broad Street pump, and a large portion of the remaining deaths were on the Broad Street side of the polygon surrounding the bad-tasting Carnaby Street well. Then Dr. Snow redrew the service area polygons to reflect shortest paths along streets to wells, and an even larger proportion of the cholera deaths fell within the Broad Street polygon or the Broad Street side of the Carnaby Street well's polygon. He suggested that the Broad Street pump be taken out of service—thus helping end the epidemic.

The above spatial analysis is outstanding as it is often considered to be the first:

- (1) Epidemiological analysis which sought to understand the outbreak of disease by considering environmental factors; and
- (2) Spatial analysis of disease data that involved plotting points on a map and looking for spatial relationships thereof.

End of Example 26.2

Example 26.3 (Leishmaniasis research (Steede-Terry 2000))

Leishmaniasis is one of the infectious diseases causing significant health problems in Asia, Africa, India, North America, Latin America, and Europe, and is caused by a parasitic protozoan, which in turn can infect several hosts (i.e., an organism that harbors a parasite) and vectors (i.e., means of transmission, e.g., mosquitoes for malaria), making it difficult to control (Steede-Terry 2000). Researchers in Texas studied the relationship between the wood rats, which are the mammalian hosts for *Leishmania*, and the sand flies that act as vectors transmitting the disease from one host to another. To assist in their studies, the researchers employed GNSS (DGPS discussed in Sect. 6.4.4.1) to record the locations of the traps used to catch the rats, and also the locations of the Sand fly trapping stations used to catch and monitor the vector. GNSS also plays a subsidiary role of mapping roads and water features that are not found on a map, e.g., Steede-Terry (2000). These information gathered from GNSS are integrated with other information in a GIS system through map overlaying to generate the information (maps) relating the trapping sites and the rats themselves, see e.g., Steede-Terry (2000, p. 478).

End of Example 26.3

26.7 Earthquakes

The outer layer of the Earth is made up of large pieces known as tectonic plates which are in motion. When these plates collide, as indicated in Fig. 26.14 in 468, an earthquake occurs. Other factors that can lead to earthquakes include fault ruptures or forces such as stress and strain. But most causes result from plate collision as they try to move past one another. There is also a tendency of earthquakes to occur in “gaps” that are in places along an earthquake belt where strong earthquake had not previously been observed (Jayaraman et al. 1997). Earthquake risk assessment involves identification of seismic zones through collection of geological/structural, geophysical (primarily seismological) and geomorphological data and mapping of known seismic phenomena in the region (mainly epicenters with magnitudes) (Jayaraman et al. 1997). Kamik and Algermissen (1978) have pointed out that knowledge of trends in time or in space helps in defining the source regions of future shocks, while Jayaraman et al. (1997) point out that accurate mapping of geomorphological features adjoining lineaments reveal active movement or recent tectonic activities along faults.

GNSS satellites are emerging as a powerful geodetic tools for monitoring (geological) changes over time, which is the key for understanding the long-term geodynamical phenomena. They have been particularly useful in measuring the more complex deformation patterns across plate boundaries, where large and regional scale strain

builds up, plate movements, and slips along faults, pre-seismic, co-seismic and post-seismic distortions (Dalton 2007; Hofman-Wellenhof et al. 2001, 2008; Jayaraman et al. 1997). Indeed, GNSS through CORS (see Sect. 6.5) now enable detection of ground motion at the mm to cm-level accuracy before, during and after earthquakes (Jia 2005), and have found use in seismological applications, see e.g., Larson (2009).

Hammond et al. (2011) point out that rapid detection and accurate characterization of earthquake related events can make a crucial difference during the minutes to hours that follow an earthquake event as was the case following the catastrophic 2004 Sumatra and 11th March 2011 Tohoku-oki earthquakes and tsunamis. In both of these events, the initial seismic notification of earthquake magnitude was available in minutes but was more than an order of magnitude smaller than the true event size, an uncertainty that can be addressed by GNSS in the rapid estimation of large earthquake magnitudes (Hammond et al. 2011). A review of the application of GNSS to geodynamics and earthquake studies is presented, e.g., in Segall and Davis (2006).

Since natural disasters don't chose when to take place, prompt response is required, even when they occur at night. Cruz et al. (2007) describe the application of nighttime remote sensors e.g., operational linescan system (OLS), which is a scan radiometer, for rapid detection of affected areas following the Kashmir earthquake of 2005. When nightlights imagery acquired before and after disaster were compared, preliminary observations suggested the reduction of night-lights in the areas worst affected by the earthquake and the increase of ephemeral lights in the nearby areas originated by the concentration of survivors bonfires. This information can be useful in monitoring among other parameters; population movements, location of critical areas, area coordinates for high resolution imagery and dissemination of results to first responders.

Jia (2005) documents three stages upon which measurements for the earthquake can be collected. These are pre-seismic, co-seismic and post-seismic defined as follows (Jia 2005):

Pre-seismic. These are measurements taken before the earthquake and normally serve as an early warning system of potential danger, especially when two plates indicate a possibility of collision (e.g., Fig. 26.14).

Co-seismic. These are measurements that provide direct information on the occurrence during an earthquake and are useful for providing data for estimating the likelihood of future earthquakes through, e.g., further investigations of fault slip models and of other seismic features of the earthquake.

Post-seismic monitoring entails using GNSS receivers to obtain time-series of location and plate movements long after the earthquake has occurred. Such post-seismic deformation information from all available GNSS sites in the earthquake region can help scientists analyze likely elastic, poroelastic and viscoelastic deformation, and plastic flow of the Earth's crust in the earthquake region, giving a better understanding of crustal relocation and redistribution after an earthquake.

By continuously sampling movements of permanent known GNSS locations, e.g., within a CORS network in a seismic area, accurate position differences between the stations (e.g., Fig. 6.12 on p. 94) can be established to an accuracy of a few millimeters in the horizontal and a centimeter in the vertical. These CORS networks

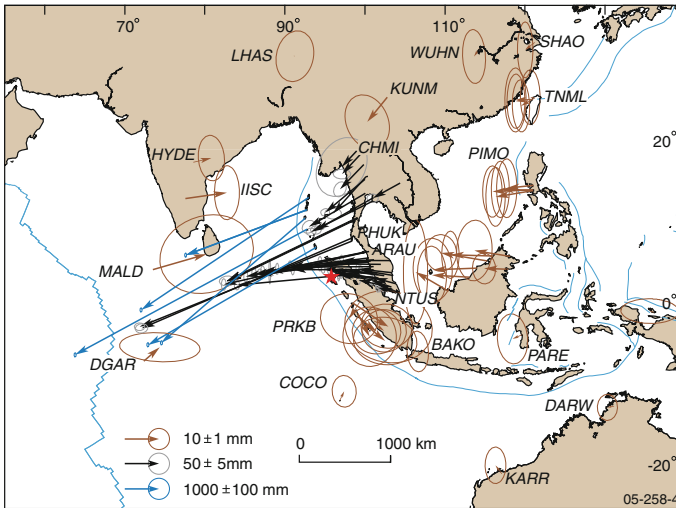


Fig. 26.7 Displacement field for the earthquake region determined by GPS. The *red star* represents the epicentre, and the *blue lines* show plate and fault boundaries. The displacements vary from 3 to 6 m in the Andaman and Nicobar Islands, indicated by the *blue arrows* while the *black arrows* show displacements at sites in Thailand, Malaysia and Sumatra. Almost 28 cm displacement was detected at the GNSS site PHUK (Phuket Island, southern Thailand near northern Malaysia), decreasing gradually towards the north and south. Displacements reduced to 2 cm at the NTUS site (Singapore) and 3 cm at the CHMI site (northern Thailand). Deformation of around 10 mm was detected at large distances, indicated by *brown arrows*. Deformations from these sites, except for sites south-east from the epicentre, were also generally towards the epicentre or the great Sumatra fault, even though they were relatively small compared with their error ellipses. *Source* Jia (2005)

(Sect. 6.5) are normally fitted with telemetry that relays the data to control stations for rapid processing (e.g., Fig. 26.14). The results are analyzed and used as monitoring data for possible future earthquakes. RTGPS presented in Sect. 6.4.3 are suggested by Hammond et al. (2011) to be useful in earthquake monitoring. Its integration with seismic time-series are expected to enhance seismic source monitoring through monitoring earthquake events occurring over very wide range of time scales. Its inclusion to extend measurements beyond typical seismic frequencies is essential to understanding the complete spectrum of fault slip behaviours associated with the earthquake cycle (Hammond et al. 2011). In what follows, two examples on the application of GNSS to monitor earthquakes is presented based on the works of Jia (2005) and GEONET in Japan.

Example 26.4 (Sumatra-Andaman earthquake—Jia (2005))

Jia (2005) assesses the Sumatra-Andaman earthquake by analyzing data from more than 250 GNSS sites distributed through Australia, Malaysia, Thailand, Indonesia, the Philippines, China, India and the Maldives (Fig. 26.7). Co-seismic displacements from two combined seven-days' solutions, one before

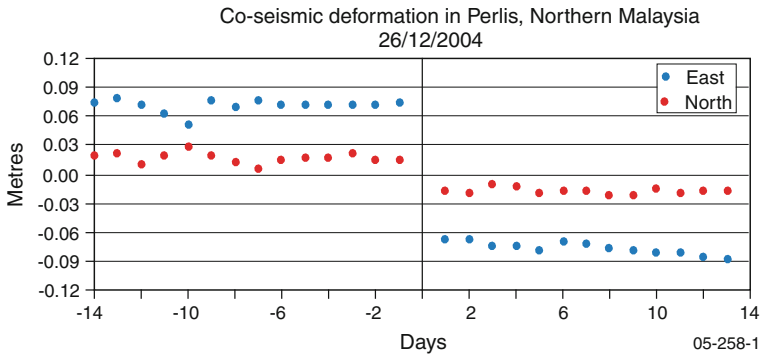


Fig. 26.8 Co-seismic deformation before and after the earthquake at the GNSS site ARAU (Perlis, northern Malaysia). A displacement 15 cm in the east and 3 cm in the north was detected. *Source* Jia (2005)

and one after the earthquake are computed. The displacements of the sites are calculated as the difference between the two solutions and the results presented in Fig. 26.8 for the co-seismic deformation at the GNSS site ARAU (Perlis, northern Malaysia) where a displacements of 15 cm in the east and 3 cm in the north is reported. The results of Jia (2005) indicate that the displacement detected by GNSS varies with location. Looking at the variation in GNSS coordinates computed by Jia (2005) from stations near the earthquake every 30 s over 30-m periods before and after the earthquake (0:59, 26 December 2004) in Fig. 26.9, the progression of the rapture is noticed. Figure 26.9 indicates the deformation of 10 cm at a GNSS site of ARAU. In this particular case, Jia (2005) points out that deformation was detected when the surface waves began to hit the site two minutes after the earthquake; four minutes later, positions at the site were relatively stable again.

Using a long-term GNSS time-series after the earthquake, Jia (2005) then examined the post-seismic deformation process in Fig. 26.10 and showed that the deformation at the GNSS site LGKW (Langkawi Island, Malaysia) declined continuously over time after the earthquake. An eastward deformation of more than 6 cm during the 80-day period after the earthquake is determined.

An example of such long-term GNSS time-series analysis in the work of Jia (2005) shows that the Australian and Indian plates move towards Sumatra-Andaman at a rate of 5 and 4 cm per year, respectively (see Fig. 26.7) (Jia 2005). Jia (2005) concludes that earthquake progressions of co-seismic type enable scientists to better understand the fault rupture process and that such studies could benefit tsunami early warning systems, such as the Australia Tsunami Warning System, <http://www.bom.gov.au/tsunami/about/atws.shtml> by allowing more reliable assessments of the likelihood of tsunami events to be made. For post seismic analysis, Jia (2005) states that deformation information

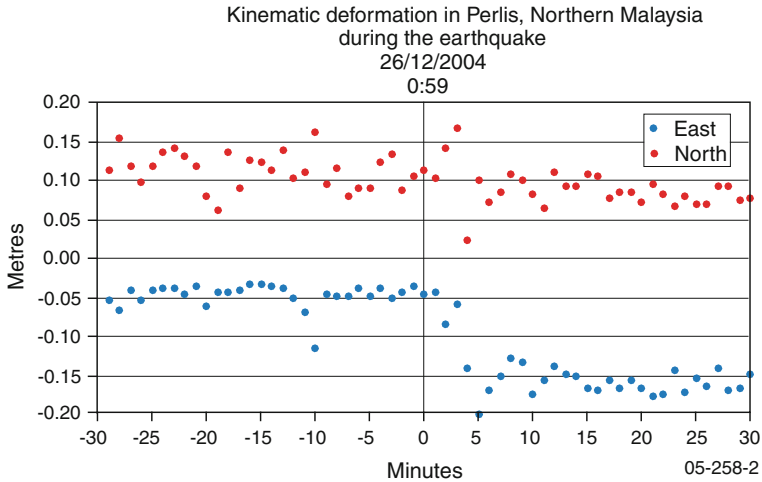


Fig. 26.9 The progression of rapture at a GNSS site ARAU (Perlis, northern Malaysia) during the earthquake, which occurred at about 0:59 on 26 December 2004. Measurements were taken every 30 s for a period of 30 min before and after the earthquake. Two minutes after the earthquake waves hit the site, a deformation of about 10 cm was detected. *Source* Jia (2005)

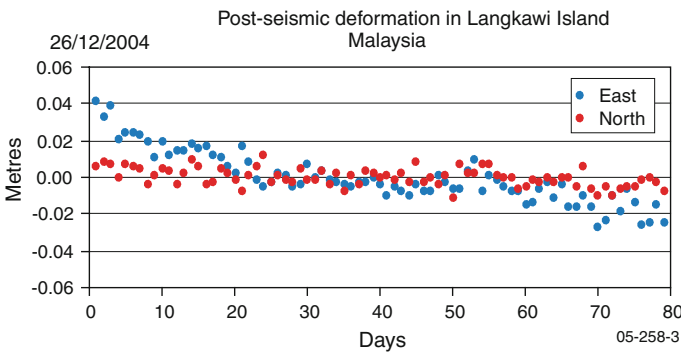


Fig. 26.10 Post-seismic deformation at a GNSS site LGKW (Langkawi Island, northern Malaysia). *Source* Jia (2005)

from all available GNSS sites in the earthquake region can help scientists analyze likely elastic, poroelastic and viscoelastic deformation, and plastic flow of the Earth’s crust in the earthquake region, giving a better understanding of crustal relocation and redistribution after an earthquake.

End of Example 26.4

In post-seismic activities, GNSS are also useful in monitoring deformation in structures such as dams. Other structures that could be monitored for deformation include buildings, bridges, etc. This could be done by installing GNSS equipments at strategic locations on these features and comparing the locations reading before and after the seismic activity. In built environment, Hammond et al. (2010) state that through high-sample rate GNSS data, e.g., from RTGPS discussed in Sect. 6.4.3, the motion of large buildings and bridges in an inertial reference frame can be realized. Remote sensing and terrestrial photogrammetry can be used to document the damage caused immediately after an earthquake, with a view to supporting critical response and recovery operations. Specifically, high resolution satellite imagery (HRSI) (see Sect. 8.3), thermal IR, video etc. are some of the sensors that can be employed at this stage.

Many studies have investigated the viability of HRSI in damage detection and assessment up to the individual building level, see e.g., (Yamazaki et al. 2004, 2005; Kouchi et al. 2004; Al-Khudhairy et al. 2005). Other works have used aerial photographs and stereo aerial photographs, see e.g., (Ogawa and Yamazaki 2000; Turker and Cetinkaya 2005) etc, while very few have even employed unconventional datasets such as aerial television images, see e.g., Hasegawa et al. (2000). The objective has been to classify building damage often using established macroseismic scales like the European Macroseismic Scale (EMS). Increasingly, automated image classification procedures have been employed (see e.g., (Mehdi and Gruen 2007; Bitelli et al. 2004; Turker and Cetinkaya 2005) etc.) away from traditional visual interpretation methods, see e.g., (Ogawa and Yamazaki 2000; Yamazaki et al. 2005). In the post event scenario, GIS can also use building damage data captured from remote sensing to evaluate the structural dynamics for buildings and assess their seismic vulnerability as reported in several works e.g., (Yamaguchi and Yamazaki 2001; Miura and Midorikawa 2006) etc.

Example 26.5 (GNSS monitoring of the Tokai crustal movement)

In Japan, GEONET (see Fig. 6.14, p. 96) has been used to monitor crustal activities by analyzing daily solutions of GNSS stations (e.g., Fig. 6.12 on p. 94) coordinates (Matsuzaka 2006). For example, when an extraordinary data are detected, or a big earthquake or volcanic eruption occurs, emergency analysis is performed to get the solutions every 3 h (Matsuzaka 2006). This enables the determination of displacement rates and strain rates throughout Japan (Sagiya 2005). Matsuzaka (2006) points to the fact that the more than 1200 GEONET CORS stations provide data that are used in various disaster related meetings and geophysical model estimation of crustal activities, and thus reflect the decision making process to cope with disasters, as well as, scientific researches. GEONET is also quite useful in earthquake studies, precisely detecting co-seismic, post-seismic, and inter-seismic deformation signals, with these observations used to infer physical processes at the earthquake sources (Sagiya 2005). GEONET operates by having its stations, which are well dis-

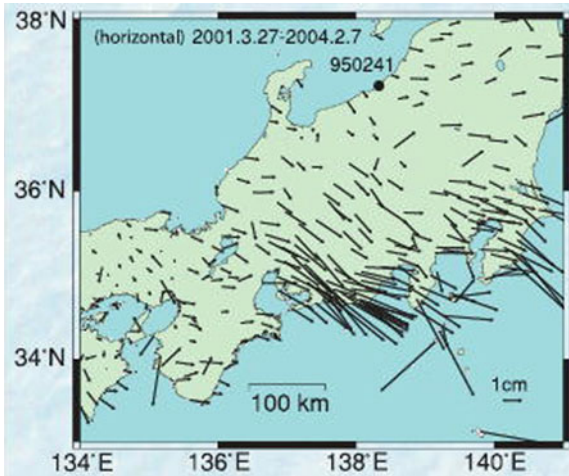


Fig. 26.11 Horizontal displacement observed in the Tokai region due to crustal movements during the period of 27 March 2001–7 February 2004 with reference to the GPS station in Oogata, Niigata Prefecture (950241). Source (http://www.gsi.go.jp/ENGLISH/page_e30068.html)

tributed throughout the country relay real-time data by a dedicated line to the control and analysis center at the Geospatial Information Authority of Japan (GSI) in Tsukuba (Ibaraki Prefecture), thereby enabling a real-time monitoring of crustal movements.

The Tokai crustal movement has been monitored through such analysis (see, e.g., Fig. 26.11). Figure 26.11 shows the data of horizontal displacement observed in the Tokai region due to crustal movements during the period of 27 March 2001–7 February 2004 with reference to the GPS station in Oogata, Niigata Prefecture. (http://www.gsi.go.jp/ENGLISH/page_e30068.html) From the Tokai region to Nagoya, an area of displacement in the southeast direction is identified thus further indicating the possibility of using GNSS as a possible key to understanding a mechanism of the Tokai crustal movement. (http://www.gsi.go.jp/ENGLISH/page_e30068.html)

Slow slip events on plate boundaries as demonstrated above have been found from GNSS data, thus providing an important constraint on the mechanism of faulting (Sagiya 2005). Sagiya (2005), however, pointed to the fact that there had been no success in detecting pre-seismic deformation but highlights the fact that GEONET enabled a good linkage between monitoring and modelling studies, opening a possibility of practical data assimilation. He suggests that for further contribution to earthquake studies, it is necessary to continue GEONET with high traceability on the details in observation and analysis (Sagiya 2005).

End of Example 26.5

Besides the use of GNSS for long term plate motion and plate boundary deformation monitoring as exemplified in the work of Sagiya (2005), other geodetic techniques that may be used are very long baseline interferometry (VLBI, discussed in Sect. 3.4.3) that provides mm-level relative positioning accuracy and laser ranging methods (Sect. 3.4.4).

26.8 Changing Sea Levels

Sea levels have been known to change for a variety of reasons, with the changes varying in temporal and spatial scales, see e.g., Church et al. (2011). In time scales, some changes occur rapidly, e.g., sea level change due to the effects of tsunami, while others take long. Spatially, the changes can be local or global. The average sea level about which these changes occur is generally known as the *mean sea level* (Pugh 2004). Global warming, fueled by the increase in greenhouse effect discussed in Chap. 21 is thought to be having an impact on the sea level rise around the world. This is in part due to the melting of the polar ice on the one hand, and the increase in water temperatures causing expansion on the other hand. Today, one of the highest priorities is to understand and to reliably anticipate changes in the mean sea level and flood risks, particularly those that maybe due to global climate change (Pugh 2004). In order to predict future changes of mean sea level, Pugh (2004) suggests that it is necessary to have a full understanding of all the factors that influence sea levels at the coast and that the first step in realizing this is to measure the sea level over a long period of time to provide baseline data upon which scientific discussions could be made.

Measuring sea level entails the determination of the vertical height between the average surface of the sea and a fixed datum level (see Sect. 6.6.1), where the datum chosen depends on the application (Pugh 2004). Some of the most commonly used datums such as tide gauge benchmark, chart datum, land survey datum (mean sea level), geocentric coordinates and geoid (Fig. 6.18, p. 101) are discussed in Pugh (2004). As was stated in Sect. 20.3.1, the GOCE satellite mission (Fig. 20.8 on p. 291) is anticipated to significantly improve the accuracy of the static geoid, e.g., Hirt et al. (2011), and in so doing contribute to improved monitoring of changes in sea level. Methods of measuring sea levels are listed by Pugh (2004) as:

- (1) Direct measurements by following the moving sea surface, e.g., using tide poles and float gauges. According to Pugh (2004), for offshore, where there are no fixed structures, GNSS receivers have been placed on floating loosely moored buoys that measure sea levels to accuracies of few centimeters after averaging over a long period of time to remove the effect of waves.
- (2) Use of fixed sensors (e.g., acoustic tide gauge and pressure measuring systems).
- (3) Use of satellite altimetry discussed in Sect. 20.4.

Precise measurements from GNSS combined with other methods are crucial in monitoring changing sea levels and provide early warning in case of evacuation. Since

changes in sea level average about 1–3 mm per annum, any vertical motion of the crust must be monitored at this level of accuracy, and within short time spans of 3–5 years (Geoscience Australia 2008). GNSS could also contribute indirectly to monitor changes in sea level through cryospheric measurements as discussed in Sect. 21.5.4 and also through reflected signals discussed in Sect. 20.5.

26.8.1 Impacts of Rise in Sea Level

For sea level changes, climate models used to study the effects of atmospheric greenhouse gases predict an overall increase in the global temperature during the current century to be in the range of 1–3.5 °C (Warrick et al. 1996). Though sea level rise could also be attributed to salinity changes, see e.g., Antonov et al. (2002), increase in magnitude in temperature to the level predicted by Warrick et al. (1996) could easily lead to rapid melting of ice sheets and glaciers that could lead to a sea-level change that departs dramatically from the assumption of a uniform redistribution of meltwater (Mitrovica et al. 2001). For instance, Bamber et al. (2009) reassessed the potential of sea level rise resulting from a collapse of the West Antarctic ice sheet and obtained a value for the global, eustatic (changes due to addition or removal of water mass) sea level rise contribution of about 3.3 m, with important regional variations. The maximum increase was found to be concentrated along the Pacific and Atlantic seaboard of the United States, where the value was about 25 % greater than the global mean, even for the case of a partial collapse (Bamber et al. 2009). Although the eustatic sea-level rise contribution for West Antarctic ice sheet collapse is uncertain (e.g., IPCC estimates 5 m), Mitrovica et al. (2001) show that, whatever the value, sea level changes at some coastal sites will be significantly higher or lower than the predicted eustatic value.

Temperature rise due to global change in climate will have several effects, notably the global rise in sea level, an undesirable scenario given that a large fraction of the Earth's total population resides close to the sea. Catastrophic impacts on agriculture, tourism, industries, etc., of 1 m global rise in sea level have already been pointed out, e.g., by Dickey et al. (1996) who note that low lying regions that slope gently such as Florida and Indonesia with 15 % of the world's coastline or regions lying in the flood plains of large rivers such as Rhine, Nile, etc., are all in great risk, should the sea level rise by the predicted amount.

Titus et al. (1991) estimated that in the United States, a global sea level rise by a similar magnitude would suffice to drown 20–85 % of the coastal wetlands resulting in an encroachment of up to 7,000 square miles (about 18,130 km²), an area the size of Massachusetts. The foregoing discussion therefore clearly indicates the necessity of monitoring of the changes in sea/lake levels in order to provide early warnings and enable formulation of policies that will provide remedial measures.

Although Warrick et al. (1996) report that tide gauge data show the sea level to be already rising at a rate between 1.0 and 2.5 mm/year averaged over the past

century, understanding and characterizing the sources of the rise of sea level remains a problem. The two prominent source of rise in sea level are;

- (1) mass redistribution (from Antarctica, Greenland, and Glaciers and small ice caps), and
- (2) thermal expansion and salinity variation.

In both sources, as already pointed out, global warming contributes to the rise in sea level by melting of the ice and glaciers that find their way into the ocean during mass redistribution. In the latter case, global warming causes the warming and expansion of the water during thermal expansion. Existing methods for determining secular rise in sea level is based on the tide gauge approach, which as already mentioned has its own limitations. For rise in sea level, therefore, it is vital for one to;

- (a) characterize the sources of global rise in order to clearly distinguish between the thermal and mass redistribution contributions, and
- (b) relate the rise in sea level to global warming.

These can be done using remote sensing satellites discussed in Chap. 20, which are specifically designed to provide solutions to problems related to global warming and the changes in sea/lake levels.

26.8.2 Tide Gauge Monitoring

The traditional means of monitoring sea and lake levels has been based on tide gauges, which are normally sensitive to water level changes. Tide gauge records collected over long periods indicate a rise in global sea level of 10–30 cm over the past century (cf. 10–25 cm from Warrick et al. (1996) above), with a large discrepancies in the rates of change of sea level indicated by different tide gauges, or groups of tide gauges spanning particular regions (Geoscience Australia 2008). These differences are considered to be largely caused by vertical land motion resulting from phenomena such as glacial rebound, subsurface fluid withdrawal and sediment consolidation (Geoscience Australia 2008).

In order to decipher the signals observed by a network of tide gauges from vertical crustal movement so that absolute sea level changes could be monitored, it is necessary to establish the absolute positions (heights) of the tide gauges in an accurate, global, geocentric terrestrial reference frame. Currently, the International Terrestrial Reference Frame 2000 (ITRF2000) is used (Geoscience Australia 2008). GNSS are used to georeference these tide gauges.

26.8.3 GNSS Monitoring

GNSS estimation of absolute and relative sea level changes: Due to their capability to provide three-dimensional coordinates $\{\phi, \lambda, h\}$, GNSS satellites play a crucial role in:

- (1) the actual determination of the sea level changes by determining the phase center of the GNSS-equipped buoy receivers, and also through GNSS altimetry, see, e.g., (Lowe et al. (2002), Rius et al. (2002)) discussed in Sect. 20.4, and
- (2) the realization of the reference frame upon which the tide gauges are referred.

For GNSS-equipped buoys capable of measuring dual frequency carrier-phases L1 and L2, their positions $\{\phi, \lambda, h\}$ relative to a fixed reference GNSS receiver can be computed as a function of time. The h component can be used to provide a time-series measurement of sea level. If the buoy is horizontally constrained and measurements are made at appropriate frequency, the mean sea level, the sea level change due to tides, and the wave amplitudes and frequencies can be determined to cm-level accuracy using GNSS (Rocken et al. 1990).

Using kinematic positioning approach (see Sect. 6.42), Kelecy et al. (1994) demonstrated the applicability of GNSS by using two GPS-equipped buoys to collect data at two locations on two different days. Three-dimensional positions of the buoys were then computed using precise carrier-phase measurements relative to a GNSS reference station that was fixed 15 km away. From the derived positions, the height component h corrected for tilt and vertical displacement were then used to compute two mean sea level measurements at the buoy locations to 6 cm-level accuracy when compared to altimetry readings. Kelecy et al. (1994) thus succeeded in demonstrating that accurate GNSS buoy measurements could successfully be used to detect changes in sea levels. They point out that such measurements could find use in complimenting altimetric data, e.g., in calibration of altimetric measurements, see e.g., (Born et al. 1994; Leuliette et al. 2004; Watson et al. 2003), extending altimetric results to smaller scales by using an array of GNSS buoys for local studies, and enhancing the temporal resolution of altimetric data to resolve local uncertainties between satellite passes. Other application areas include measurement of absolute sea level, of temporal variations in sea level, and of sea level gradients (dominantly the geoid), while specific applications would include ocean altimetric calibration, monitoring of sea level in remote regions, and regional experiments requiring spatial and temporal resolution higher than that available from altimetric data (Kelecy et al. 1994).

The variations of vertical crustal velocities at CORS sites (e.g., Fig. 6.12) near tide gauge stations may also be used to determine the “absolute” sea level change with respect to the International Terrestrial Reference Frame, what previously was impossible to conduct before the proliferation of CORS in coastal areas (Snay and Soler 2008). In the realization of the reference frame upon which the tide gauges should be referred, measurements of vertical crustal movement together with tide gauges in a global geocentric reference system has been shown, e.g., by Snay et al. (2007) to have the potential of estimating absolute sea level. Denoting $S(p)$ as the



Fig. 26.12 GNSS absolute sea level monitoring. *Source* Awange (2012)

rate of relative sea level change at a point p measured by a tide gauge and $U(q)$ the vertical velocity at a point q in the ITRF2000 system, Snay et al. (2007) indicate that the absolute sea level is given by

$$S(p) + U(q) = \xi + \epsilon, \quad (26.1)$$

where ξ is the estimated absolute sea level rate for a sample of sites and ϵ the difference between the estimated values and the observations (i.e., the error vector). It is clear from the equation above that GNSS satellites will play a significant role in the determination of each ITRF2000 velocity $U(q)$ for each station using CORS observations (Sect. 6.5). The quantity $S(p) + U(q)$ provides an estimate of the absolute sea level rate at p , denoted $A(p)$, when the distance between p and q (see Fig. 26.12) is small (Snay et al. 2007). In addition to provision of the velocity observations, GNSS contribute to monitoring absolute sea level changes through a regular re-survey of local networks of benchmarks and reference marks (Geoscience Australia 2008).

GNSS remote sensing techniques discussed in Sects. 20.3.3, 20.4, and 20.5 further provide means by which GNSS could be useful in measuring changes in sea level. As an example, Lake Victoria (Sect. 22.4.1.2) water levels for the period 1993–2006 are plotted for both TOPEX/Poseidon derived heights and tide gauge data in Fig. 26.13. The figure indicates a close relationship between the two data sets. Crétaux et al. (2011) compares water levels of Lake Victoria from the Jinja tide gauge and those from Jason-1 altimetry satellite and obtains a coefficient of correlation value of 0.99 with a standard deviation of 2.7 cm for the period 2004–2007. This supports the fact that satellite altimetry provides useful information on changes in sea level, and further shows the significant contribution of GNSS to satellite altimetry used for monitoring changes in water levels. Indeed, by averaging the few-hundred thousand measurements collected by the satellite in the time it takes to cover the global oceans (i.e., 10

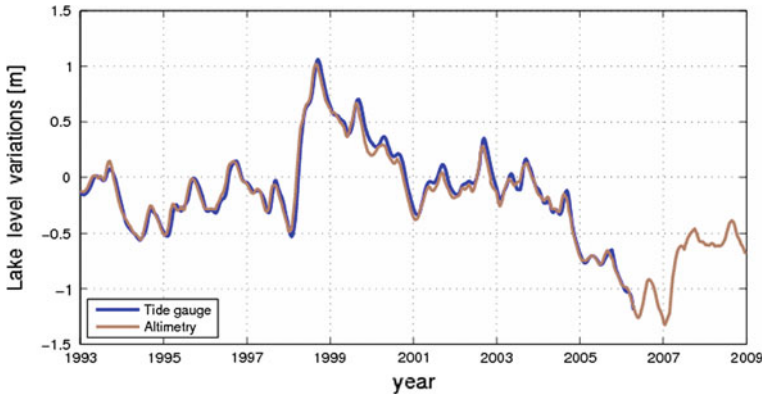


Fig. 26.13 A comparison of water gauge readings at Jinja station in Uganda (near Lake Victoria's outlet, see Fig. 22.8) and water Levels from Topex/Poseidon and Jason-1 altimetry satellites. The figure shows a close match between the tide gauge and satellite altimetry data (cf. Fig. 22.10 on p. 359 obtained from GRACE). *Source* Awange (2012)

days for TOPEX/Poseidon), global mean sea level can be determined with a precision of several millimeters (Pugh 2004). Such information is vital for mitigation of disasters related to sea level changes. Detailed satellite altimetry study on East African lakes (e.g., Fig. 26.13) are given e.g., in Becker et al. (2010), Crétaux et al. (2011).

26.9 Tsunami Early Warning System

Boxing day, the 26th of 2004 will be remembered as the day tsunami caused havoc in Asia and Africa killing more than 280,000 people¹⁰ and destroying property worth millions of dollars. In order to understand the cause of tsunami and how it could possibly be monitored using GNSS, use is made of Fig. 26.14. Tsunami is a series of waves created when a body of water such as ocean is rapidly displaced. Causes often range from land earthquakes, under ocean earthquakes, volcanic eruptions, under water explosions among others. In Fig. 26.14 for example, plate A is seen to move towards the right and as it does, it collides with plate B thereby causing under ocean earthquake with the epicenter at the point of collision as indicated in the figure. The effect of the earthquake immediately displaces the water mass causing rapid moving waves that rises to up to 30 m high (GITEWS 2008). As these approach land, the rapid speed enables the waves to penetrate deep into land causing massive destruction as witnessed by the 11th March 2011 tsunami at Tohoku-Oki in Japan. Monitoring the onset of Tsunami enables early warning system that could at least minimize the loss of lives.

¹⁰ see e.g., <http://www.bom.gov.au/tsunami/about/atws.shtml>

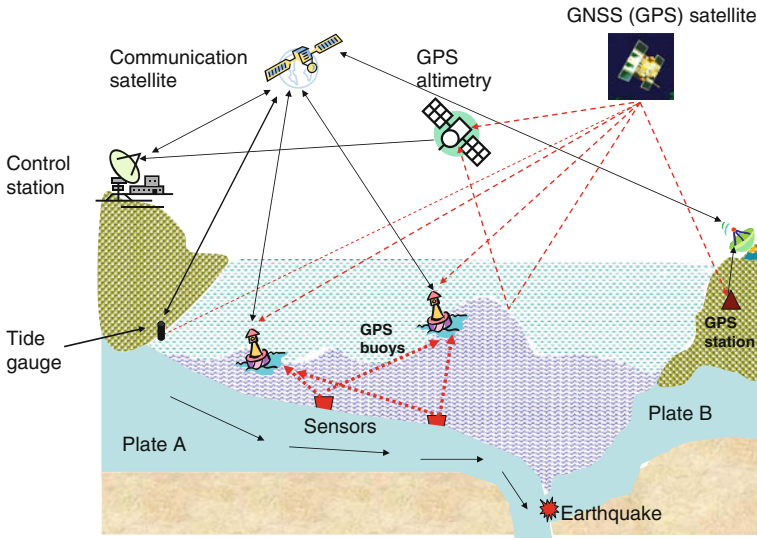


Fig. 26.14 A schematic illustration of the possible application of GNSS to tsunami monitoring. *Source Awange (2012)*

Tsunami warning has particular requirements for calculating accurate earthquake magnitude, propagation direction, and vertical and horizontal motion of the sea-floor, with the goal of rapidly recognizing when a tsunami event is occurring and improving predictions of where the wave will rise on near and distant coasts (Hammond et al. 2011). GNSS satellites are proving to be the key to such early warning systems in light of the fact that displacements at GNSS sites are useful in constraining a fault slip model, which predicts motion of the seafloor (Hammond et al. 2011).

In the German Indonesian Tsunami Early Warning System (GITEWS),¹¹ which went into operation on 11th of November 2008 (GITEWS 2008) with the ownership now in the hands of Indonesia, GNSS plays a leading role in key monitoring areas as demonstrated in Fig. 26.14. The indicators of this system are GNSS instruments, seismometers, tide gauges and GPS-buoys, as well as, ocean bottom pressure sensors. The augmentation of all these sensors ensures a rapid locating and analysis of the tsunami information to inform warning decisions.

Tide gauge sensors: Tide gauges are used to measure changes in sea level and therefore indicate exceptionally rapid rise in sea level, which signals unusual event. To enhance the tide gauges, the GITEWS project has equipped them with GNSS receivers that enable them to measure vertical and horizontal land displacements in addition to sea levels. Measurement of GNSS velocities provide an indication of the direction of horizontal displacement. The actual vertical and horizontal displacement are deduced from the GNSS positional time-series measurements. Any unusual displacement can serve to indicate an oncoming tsunami. During the catastrophic earth-

¹¹ see <http://www.gtz.de/en/21020.htm>

quake of 2004, a horizontal and vertical displacement of several decimeters to meters was evident even at a distance of some hundred kilometers from the earthquake. The direction of this resulting shift gives reference to the mechanism of the earthquake break and thus to the possible tsunami potential and the expected hazard (GITEWS 2008). This information is transmitted towards the communication satellite, which relays it to the control station in Indonesia.

GNSS Buoys: These help to relay information received from the underwater pressure sensors, which detect the effect of the tsunami. Besides relaying the information, the incorporated GNSS antenna can act as a measuring device for sea motion (horizontal motion) and sea level (heights). The buoys therefore provide an independent indicator of the onset of a tsunami. For the GITEWS, the buoys also detect tsunami waves, which with speeds of up to 800 km/h and wavelengths of 200 km in the open sea, and through proper filtering, achieve cm-level accuracy detection of rise in the sea level thus providing also an early detection of a tsunami wave (GITEWS 2008).

Land based GNSS: These are combined with seismometers to provide location-based mapping of the ground motion. Horizontal and vertical displacements together with velocities are delivered by GNSS. All these, plus ground motion from the seismometers are relayed to the communication satellites and further transmitted to the control center in Indonesia where warning decisions are made.

GNSS altimetry: Low flying satellites such as GRACE are able to measure reflected signals from GNSS satellites (see Sect. 20.5). They therefore would measure signals that hit the sea surface and are reflected to the low flying satellites. This helps in determining the sea levels as well as providing more information on tsunami indicators. Besides, the GNSS satellites also help in positioning these low flying satellites in space. Studies have been initiated to test the feasibility of this concept, see e.g., Helm et al. (2007).

An example of a tsunami early warning system that was in test mode during the Tohoku-Oki earthquake and tsunami of 11th March 2011 was the GPS Real-time Earthquake and Tsunami (GREAT) Alert, see e.g., Hammond et al. (2011). The GREAT Alert Project is a NASA-sponsored, multi-agency collaborative effort to develop an advanced Earthquake and Tsunami alert system that uses real-time GNSS (discussed in Sect. 6.43) to enable more accurate and timely assessment of the *magnitude* and *mechanism* of large earthquakes, as well as the *magnitude* and *direction* of resulting tsunamis.¹²

Another example is the Australian Tsunami Warning System (ATWS), which is a national effort involving the Australian Bureau of Meteorology (Bureau), Geoscience Australia (GA) and Emergency Management Australia (EMA) to provide a comprehensive tsunami warning system capable of delivering timely and effective tsunami warnings to the Australian population, and also support international efforts to establish an Indian Ocean tsunami warning system and contribute to the facilitation of tsunami warnings for the South West Pacific.¹³

¹² <http://www.gdgps.net/products/great-alert.html>. Accessed on 21/9/2011.

¹³ <http://www.bom.gov.au/tsunami/about/atws.shtml>

26.10 Land Subsidence and Landslides

The various landslide types and underlying processes are discussed in different works, see e.g., (Cruden and Varnes 1996; Malamud et al. 2004; Wills and McCrink 2002) etc. Land-surface subsidence due to over-extraction of groundwater has long been recognized as a potential problem in many areas that have undergone extensive groundwater development (Motagh et al. 2007). This is particularly significant in expanding metropolitan areas in arid and semi-arid areas as witnessed in most parts of Australia and Iran. Surface subsidence has been observed worldwide in areas where withdrawal exceeds natural recharge thereby depleting the volume of the stored water. This has been evidenced in cities such as Mexico where subsidence of land has reached almost 9 m, Bangkok (Thailand), Shanghai, Tanjin, Xi'an (China), Osaka, Tokyo (Japan), and Las Vegas (USA) (Schenk 2006). Poland (1984) outlines numerous case studies on land subsidence due to groundwater withdrawal. In 1991, the US National Research Council placed the annual costs from flooding and structural damage caused by land subsidence within the United States alone at over \$125 million (Motagh et al. 2007). Another example of anthropogenic subsidence that can lead to property destruction and loss of life is that attributed to mining activities.

Remote sensing and photogrammetric techniques have long been applied in the mapping and monitoring of hazardous slope processes and landforms, see e.g., (Sauchyn and Trench 1978; McKean et al. 1991; Rood 1984). When integrated with height information from DEMs or InSAR¹⁴ data discussed in Sect. 9.5, these methods have yielded relatively higher accuracy capable of monitoring land subsidence evolution (see e.g., Barlow and Franklin 2007; Barlow et al. 2006; Zhang et al. 2007) etc.

Similarly, GNSS and other geodetic techniques, e.g., leveling, gravimetric, and InSAR have been widely used to detect the temporal and spatial pattern of surface deformation due to land subsidence. Of these methods, InSAR (see Sect. 9.5) provides a unique tool for detecting and monitoring deformation over regions of ongoing groundwater development with the advantage of having wide spatial coverage (10,000 km²), fine spatial resolution (100 m²), and high accuracy (~1 cm), and as such, offers new capabilities to measure surface deformation caused by aquifer discharge and recharge at an unprecedented level of detail never before possible with techniques like GNSS and levelling (Motagh et al. 2007). For this reason, Motagh et al. (2007) demonstrate in their study how spatially dense InSAR results complement sparse geodetic measurements from GNSS and levelling, and thereby contributing to a better understanding of land subsidence associated with water extraction in the Mashhad area, northeast Iran (Fig. 26.15). Similarly, Schenk (2006) was able to apply DInSAR¹⁵ to interpret surface displacement in the Tehran / Iran region. He identifies inelastic deformation of the underlying aquifer systems to be the reason for the observed land subsidence affecting an area of 1350 km² and averaging subsidence rates of up 14 mm per month.

¹⁴ Interferometric Synthetic Aperture Radar.

¹⁵ Differential Synthetic Aperture Radar Interferometry.

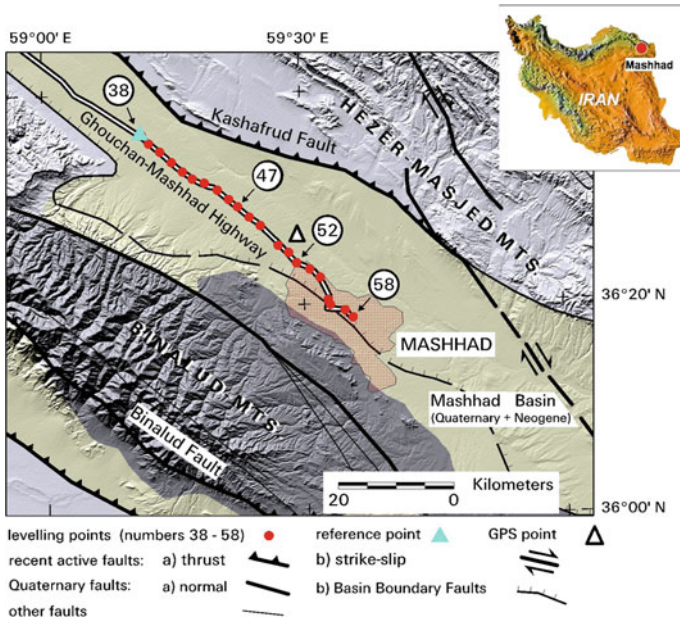


Fig. 26.15 Generalized geologic map of the Mashhad region based on the published 1:2,500,000-scale geological map from National Iranian Oil Company (NIOC), and the map of major active faults in Iran from International Institute of Earthquake Engineering and Seismology (IIEES). The map is draped with a shaded-relief topographic image generated from the 3-arcsecond Shuttle Radar Topography Mission (SRTM) data. The inset shows the location of the figure within Iran. *Source* Motagh et al. (2007)

Example 26.6 (GNSS monitoring of subsidence in Mashhad Motagh et al. (2007)) The Valley of Mashhad is a northwest-southeast (NW-SE) trending valley in northeast Iran and is bounded to the south by the Binalud Mountains and to the north by the Hezar-Masjed Mountains, see Fig. 26.15 (Motagh et al. 2007). The basin encompasses the city of Mashhad, a provincial capital inhabited by over 2 million people and visited annually by millions of tourists (Motagh et al. 2007). Mashhad extends over an area of more than 200 km² across the basin, is the second largest city in Iran, and is one of the fastest growing metropolitan areas in Iran (Motagh et al. 2007). Water supply for the region mainly comes from groundwater, which is used for domestic, industrial and agricultural activities. However, substantial exploitation of this groundwater due to population growth, tourism and development, coupled with deficient natural recharge in recent decades, has resulted in severe depletion of the underground aquifer, leading to regional decline of water-table levels, lack of access to fresh water, and development of earth fissures and local sinking



Fig. 26.16 An example of surface fissures in Mashhad Valley caused probably by excessive groundwater withdrawal and associated aquifer-system compaction. The fissure is located northwest of Mashhad City and to the east of the Tous. A GNSS station is marked by a *triangle* in Fig. 26.15 near the city of Tous. *Source* Motagh et al. (2007)

in many areas of the valley, see Fig. 26.16 (Motagh et al. 2007). From 2005 to 2006, a GNSS CORS station (refer to Sect. 6.5 for CORS) near the city of Tous provided continuous recordings that showed significant subsidence of approximately 22 cm at the station, e.g., Fig. 26.17 (Motagh et al. 2007).

End of Example 26.6

Landslides often occur on steep slopes following heavy rainfall. They often have a devastating effect such as the recent (2011) landslide disaster in Brazil, where more than 1,000 people died and thousands were displaced. Landslide monitoring can be undertaken in two ways (Malet et al. 2002) (i) analyzing and comparing various spatial maps and images, e.g., topographic maps, aerial photographs, remotely sensed imagery, cadastral maps, and digital elevation maps, which represent instantaneous views of an unstable site on different time epochs, and (ii) carrying out in-situ measurements of the surface displacements by combining a space and time resolution adapted to the evolution speeds of the phenomena.

In the context of the first approach, GNSS plays a pivotal role in map production (see, e.g., Figs. 19.2 and 19.3) that would aid in the analysis. With respect to the second approach, for example, GNSS has been applied to the case of monitoring the Vallcebre landslide in the Eastern Pyrenees, Spain (Gili et al. 2000). This landslide had been periodically monitored since 1987 with terrestrial photogrammetry and total stations. The area of movement extended over 0.8 km² and showed displacements as large as 1.6 m during the period 1996–1997. Application of RTK discussed in Sect. 6.11 allowed greater coverage and productivity with similar accuracies (12–

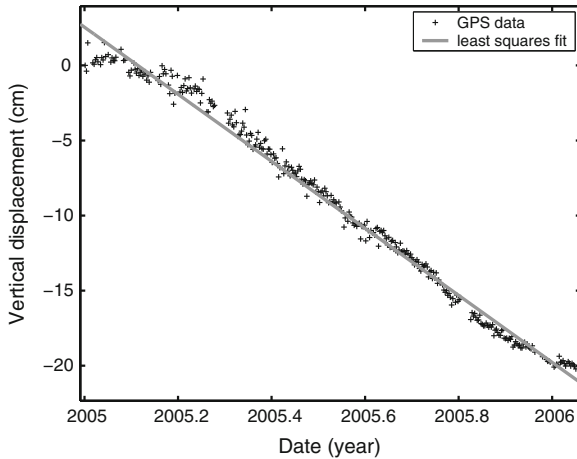


Fig. 26.17 A plot of GNSS vertical components (in cm) for the Tous GPS station (*triangle* in Fig. 26.15) with least-squares linear trend (slope ~ 22 cm year⁻¹) overlain. *Source* Motagh et al. (2007)

16 mm in the horizontal plane, and 18–24 mm in elevation) to classical surveying methods (Gili et al. 2000). A general accuracy of GNSS monitoring of landslide is presented, e.g., in Malet et al. (2002). As elaborated above, GNSS has successfully been applied to monitor landslides. However, in cases where landslide prone areas lie in canyons like in many mountaneous regions GNSS signals are likely to be obscured and hence more innovative deformation monitoring is demanded for Xue et al. (2007). One possible solution is to integrate GNSS observations with height data obtained from remote sensing techniques e.g., InSAR (Motagh et al. 2007).

26.11 Concluding Remarks

The introductory section of this Chapter has defined what constitutes natural disasters. It has gone ahead to point out the semantic controversy in the lexicon “natural”, since disaster events are not hazards or disasters without some form of direct or indirect human involvement. This has led to the paradigm of human induced disasters being referred to as “man-made natural disasters”. The Chapter has distinguished various natural disaster types and described how geoinformatics can contribute to their monitoring and management.

However, it is important to state that what has been presented is by no means exhaustive on areas in which geoinformatics could contribute to monitoring and management of natural disasters. Moreover, it should be emphasized that no single method can provide a full proof monitoring of a disaster. What is discussed in this Chapter are simply ways through which geoinformatics could contribute, albeit marginally, to monitoring and management of disasters, which could lead to early

warning and mitigation measures being taken. Geoinformatics could also contribute towards preparedness measures and also during post-disaster periods as discussed in various sections of the Chapter.

References

- Adger WN, Huq S, Brown K, Conway D, Hulme M (2003) Adaptation to climate change in the developing world. *Prog Dev Stud* 3:179–195. doi:[10.1191/1464993403ps0600a](https://doi.org/10.1191/1464993403ps0600a)
- Ailamaki A, Faloutsos C, Fischbeck P, Small M, VanBriesen J (2003) An environmental sensor network to determine drinking water quality and security. *SIGMOD Rec* 32(4):47–52. doi:[10.1145/959060.959069](https://doi.org/10.1145/959060.959069)
- Alexander D (2002) Principles of emergency planning and management. Terra publishing, Harpenden
- Allenbach B, Andreoli R, Battiston S, Bestault C, Clandillon S, Fellah K, Henry JB, Meyer C, Scius H, Tholey N, Ysou H, de Fraipont P (2005) Rapid EO disaster mapping service: added value, feedback and perspectives after 4 Years of charter actions. In: *IGARSS05 Proceedings*, pp 4373–4378
- Al-Khudhairy DHA, Caravaggi I, Glada S (2005) Structural damage assessments from IKONOS data using change detection, object-oriented segmentation, and classification techniques. *Photogram Eng Remote Sens* 71:825837
- Antonov JI, Levitus S, Boyer TP (2002) Steric sea level variations during 1957–1994: importance of salinity. *J Geophys Res (Oceans)* 107(C12):8013. doi:[10.1029/2001JC000964](https://doi.org/10.1029/2001JC000964)
- Awange JL (2012) Environmental monitoring using GNSS, global navigation satellite system. Springer, Berlin
- Awange JL, Ogallo L, Kwang-Ho B, Were P, Omondi P, Omute P, Omulo M (2008) Falling Lake Victoria water levels: is climate a contribution factor? *J Clim Change* 89:287–297. doi:[10.1007/s10584-008-9409-x](https://doi.org/10.1007/s10584-008-9409-x)
- Awange JL, Aluoch J, Ogallo L, Omulo M, Omondi P (2007) Frequency and severity of drought in the Lake Victoria region (Kenya) and its effects on food security. *Clim Res* 33:135–142. doi:[10.3354/cr033135](https://doi.org/10.3354/cr033135)
- Awange JL, Fukuda Y (2003) On possible use of GPS-LEO satellite for flood forecasting. In: Accepted to the international civil engineering conference on sustainable development in the 21st Century “The Civil Engineer in Development” 12–16 August 2003, Nairobi, Kenya
- Baker HC, Dodson AH, Penna NT, Higgins M, Offiler D (2001) Ground-based GPS water vapour estimation: Potential for meteorological forecasting. *J Atmos Solar Terr Phys* 63(12):1305–1314
- Ballesteros LF (2008) What determines a disaster? 54 Pesos, Sep 2008:54 Pesos 11 Sep 2008. <http://54pesos.org/2008/09/11/what-determines-a-disaster/>. Accessed 12 May 2011
- Bamber JL, Riva REM, Vermeersen BLA, LeBrocq AM (2009) Reassessment of the potential sea-level rise from a collapse of the West Antarctic ice sheet. *Science* 324:901–903. doi:[10.1126/science.1169335](https://doi.org/10.1126/science.1169335)
- Bankoff G, Frerks, G, Hilhorst D (eds) (2003) Mapping vulnerability: disasters, development and people. ISBN 1-85383-964-7
- Barlow J, Franklin SE (2007) Mapping hazardous slope processes using digital data. In: Li J, Zlatanova S, Fabbri A (eds) *Geomatics solutions for disaster management*. Lecture notes in geoinformation and cartography. Springer Verlag, Berlin, pp 74–90
- Barlow J, Franklin S, Martin Y (2006) High spatial resolution satellite imagery. DEM derivatives, and image segmentation for the detection of mass wasting processes. *Photogram Eng Remote Sens* 72(6):687–692
- Barrett CB (2002) Food security and food assistance programs. In: Gardner B, Rausser G (eds) *Handbook of agricultural economics*, vol 2. Elsevier Science, Amsterdam, pp 2103–2190

- Becker M, Llovel W, Cazenave A, Güntner A, Crétaux J-F (2010) Recent hydrological behaviour of the East African Great Lakes region inferred from GRACE, satellite altimetry and rainfall observations. *C R Geosci* 342(3):223–233. doi:10.1016/j.crte.2009.12.010
- Bill R (2011) Precise positioning in ad hoc geosensor networks. http://www.ikg.uni-hannover.de/geosensor/Lecture/Wednesday/Session1/sess1_bill.pdf. Accessed 22 Jan 2011
- Bitelli G, Camassi R, Gusella L, Mognol A (2004) Image change detection on urban areas: the earthquake case. In: Proceedings of the ISPRS XXth congress, Istanbul, vol 35(B7), pp 692–697
- Bonner MR, Han D, Nie J, Rogerson P, Vena JE (2003) Positional accuracy of geocoded addresses in epidemiologic research. *Epidemiology* 14:408–412. doi:10.1097/01.EDE.0000073121.63254.c5
- Born GH, Parke ME, Axelrad P, Gold KL, Johnson J, Key KW, Kubitschek DG, Christensen EJ (1994) Calibration of the TOPEX altimeter using a GPS buoy. *J Geophys Res* 99(C12):24517–24526
- Brenner C (2011) Geo sensor networks—when and how? http://dgk.auf.uni-rostock.de/uploads/media/2_2-Brenner.pdf. Accessed 22 Jan 2011
- Buehler YA, Kellenber TW (2007) Development of processing chains for rapid mapping with satellite data. In: Li J, Zlatanova S, Fabbri A (eds) *Geomatics solutions for disaster management*. Lecture Notes in Geoinformation and Cartography. Springer Verlag, Berlin, pp 16–36
- Chen JL, Wilson CR, Tapley BD, Yang ZL, Niu GY (2009) 2005 drought event in the Amazon River basin as measured by GRACE and estimated by climate models. *J Geophys Res* 114:B05404. doi:10.1029/2008JB006056
- Church JA, Gregory JM, Huybrechts P, Kuhn M, Lambeck K, Nhuan MT, Qin D, Woodworth PL (2001) Changes in Sea Level. In: Houghton JT, Ding Y, Griggs DJ, Noguer M, Van der Linden PJ, Dai X, Maskell K, Johnson CA (eds) *Climate change 2001: the scientific basis: contribution of working group I to the third assessment report of the intergovernmental panel on climate change*. Cambridge University Press, Cambridge, pp 639–694
- Crétaux J-F, Jelinski W, Calmant S, Kouraev A, Vuglinski V, Bergé-Nguyen M, Gennero M-C, Nino F, Cazenave A, Maisongrande P (2011) SOLS: a lake database to monitor in the Near real-time water level and storage variations from remote sensing data. *Adv Space Res* 47:1497–1507. doi:10.1016/j.asr.2011.01.004
- Crétaux J-F, Leblanc M, Tweed S, Calmant S, Ramillien G (2007) Combining of radar and laser altimetry, MODIS remote sensing and GPS for the monitoring of flood events: application to the flood plain of the Diamantina river. *Geophysical Research Abstracts* 9:07496. SRef-ID: 1607-7962/gra/EGU2007-A-07496
- Cruden D, Varnes D (1996) Landslide types and processes. In: Turner K, Schuster R (eds) *Landslides investigation and mitigation, transportation research board special report 247*. National Academy Press, Washington, pp 36–75
- Cruz A, Laneve G, Cerra D, Mielewczyk M, Garcia MJ, Santilli G, Cadau E, Joyanes G (2007) On the application of nighttime sensors for rapid detection of areas impacted by disasters. In: Li J, Zlatanova S, Fabbri A (eds) *Geomatics solutions for disaster management*. Lecture notes in geoinformation and cartography. Springer Verlag, Berlin, pp 16–36
- Dalton R (2007) GPS could offer better fault line mapping. *Nature News*. doi:10.1038/news070521-9. <http://www.nature.com/news/2007/070521/full/news070521-9.html>. Accessed 25 Sept 2011
- Dickey JO, Bentley CR, Bilham R, Carton JA, Eanes RJ, Herring TA, Kaula WM, Lagerloef GSE, Rojstaczer S, Smith WHF, Van Den Dool HM, Wahr JM, Zuber MT (1996) *Satellite gravity and the geosphere*. National Research Council Report. National Academy Press, Washington, 112 pp
- DMCN (Drought Monitoring Centre Nairobi)(2002) *Factoring of weather and climate information and products into disaster management policy. A contribution to strategies for disaster reduction in Kenya*, UNDP, Government of Kenya and WMO, Nairobi
- Forootan E, Awange J, Kusche J, Heck B (2012) Independent patterns of water mass anomalies over Australia from satellite data and models. *Remote Sens Environ* 124:427–443. doi:10.1016/j.rse.2012.05.023

- Garcia-Garcia D, Ummenhofer CC, Zlotnicki V (2011) Australian water mass variations from GRACE data linked to Indo-Pacific climate variability. *Remote Sens Environ* 115:2175–2183. doi:[10.1016/j.rse.2011.04.007](https://doi.org/10.1016/j.rse.2011.04.007)
- Geoscience Australia (2008) Need for the geodetic component for absolute sea level monitoring. <http://www.ga.gov.au/geodesy/slm/spslscmp/>. Accessed 11 Dec 2008
- Gili JA, Corominas J, Rius J (2000) Using global positioning techniques in landslide monitoring. *Eng Geol* 155(3):167–192
- GITEWS (German Indonesian Tsunami Early Warning System) (2008) A new approach in Tsunami—early warning. Press-Information embargo: 11(11), 2008, 10.00 CET. http://www.gitews.de/fileadmin/documents/content/press/GITEWS_operationell_eng_nov-2008.pdf. Accessed 10 Dec 2008
- Hammond WC, Brooks BA, Bürgmann R, Heaton T, Jackson M, Lowry AR, Anandakrishnan S (2010) The scientific value of high-rate, low-latency GPS data, a white paper. http://www.unavco.org/community_science/science_highlights/2010/realtimeGPSWhitePaper2010.pdf [Accessed 06/06/11]
- Hammond WC, Brooks BA, Bürgmann R, Heaton T, Jackson M, Lowry AR, Anandakrishnan S (2011) Scientific value of real-time Global Positioning System data. *Eos* 92(15):125–126. doi:[10.1029/2011EO150001](https://doi.org/10.1029/2011EO150001)
- Hasegawa H, Yamazaki F, Matsuoka M, Seikimoto I (2000) Determination of building damage due to earthquakes using aerial television images. In: Proceedings of the 12th world conference on earthquake engineering, Auckland, CDROM, 8p
- Hatfield JL, Prueger JH, Kustas WP (2004) Remote sensing of dryland crops. In: Ustin S (ed) Remote sensing for natural resources and environmental monitoring: manual of remote sensing, vol 4, 3rd edn. Wiley, New Jersey, pp 531–568
- Hay SI, Lennon JJ (1999) Deriving meteorological variables across Africa for the study and control of vector-borne disease: a comparison of remote sensing and spatial interpolation of climate. *Trop Med Int Health* 4:58–71
- Helm A, Montenbruck O, Ashjaee J, Yudanov S, Beyerle G, Stosius R, Rothacher M (2007) GORS—a GNSS occultation, reflectometry and scatterometry space receiver. In: Proceedings of the 20th international technical meeting of the satellite division of the institute of navigation ION GNSS 2007, Fort Worth, Texas, Sept 25–28, pp 2011–2021
- Herbretau V, Salem G, Souris M (2007) Thirty years of use and improvement of remote sensing applied to epidemiology: from early promises to lasting frustration. *Health Place* 13:400–403
- Hirt C, Gruber T, Featherstone WE (2011) Evaluation of the first GOCE static gravity field models using terrestrial gravity, vertical deflections and EGM2008 quasigeoid heights. *J Geodesy* 85:723–740, doi:[10.1007/s00190-011-0482-y](https://doi.org/10.1007/s00190-011-0482-y)
- Hofman-Wellenhof B, Lichtenegger H, Collins J (2001) Global positioning system: theory and practice, 5th edn. Springer, Wien
- Hofman-Wellenhof B, Lichtenegger H, Wasle E (2008) GNSS global navigation satellite system: GPS, GLONASS, Galileo and more. Springer, Wien
- Istomina MN, Kocharyan AG, Lebedeva IP (2005) Floods: genesis, socioeconomic and environmental impacts. *J Water Resour* 32(4):349–358
- James LF, Young JA, Sanders K (2003) A New approach to monitoring rangelands. *Arid Land Res Manag* 17:319–328. doi:[10.1080/15324980390225467](https://doi.org/10.1080/15324980390225467)
- Jayaraman V, Chandrasekhar MG, Rao UR (1997) Managing the natural disasters from space technology inputs. Elsevier Science Ltd, Great Britain
- Jeyaseelan AT (2004) Droughts and floods assessment and monitoring using remote sensing and GIS. In: Satellite remote sensing and GIS applications in agricultural meteorology, pp 291–313
- Jia M (2005) Crustal deformation from the Sumatra-Andaman Earthquake. Geoscience Australia's analysis of the largest earthquake since the beginning of modern space geodesy. *Ausgeo news*, issue 80
- Kamik V, Algermissen ST (1978) Seismic Zoning—chapter in the assessment and mitigation of earthquake risk. UNESCO, Paris, pp 1–47

- Kelecy TM, Born GH, Parke ME, Rocken C (1994) Precise mean sea level measuring using global positioning system. *J Geophys Res* 99(c4):7951–7959
- Khandu J (2008) GPS remote sensing of the Australian tropopause. Honours dissertation, Curtin University of Technology
- Kouchi K, Yamazaki F, Kohiyama M, Matsuoka M, Muraoka N (2004) Damage detection from Quickbird high-resolution Satellite images for the 2003 Boumerdes, Algeria Earthquake. In: *Proceeding of the Asian conference on earthquake engineering, Manila, Philippines, CD-ROM*, pp 215–226
- Larson KM (2009) GPS seismology. *J Geodesy* 83:227–233. doi:[10.1007/s00190-008-0233-x](https://doi.org/10.1007/s00190-008-0233-x)
- Leavitt WM, Kiefer JJ (2006) Infrastructure interdependency and the creation of a normal disaster: the case of Hurricane Katrina and the City of New Orleans. *J Public Works Manag Policy* 10(4):306–314
- Leuliette EW, Nerem RS, Mitchum GT (2004) Calibration of TOPEX/Poseidon and Jason altimeter data to construct a continuous record of mean sea level change. *Mar Geodesy* 27(1):79–94. doi:[10.1080/01490410490465193](https://doi.org/10.1080/01490410490465193)
- Lian M, Warner RD, Alexander JL, Dixon KR (2007) Using geographic information systems and spatial and space-time scan statistics for a populationbased risk analysis of the 2002 equine West Nile epidemic in six contiguous regions of Texas. *Int J Health Geogr* 6:42. www.ij-healthgeographics.com/content/6/1/42
- Lowe ST, LaBrecque JL, Zuffada C, Romans LJ, Young L, Hajj GA (2002) First spaceborne observation of an earth-reflected GPS signal. *Radio Science* 37(1):1007. doi:[10.1029/2000RS002539](https://doi.org/10.1029/2000RS002539)
- Malamud B, Turcotte D, Guzzetti F, Reichenbach P (2004) Landslide inventories and their statistical properties. *Earth Surf Proc Land* 29:687–711
- Malet JP, Maquaire O, Calais E (2002) The use of global positioning system techniques for the continuous monitoring of landslides: application to the Super-Sauze earthflow (Alpes-de-Haute-Provence, France). *Geomorphology* 43(1–2):33–54. doi:[10.1016/S0169-555X\(01\)00098-8](https://doi.org/10.1016/S0169-555X(01)00098-8)
- Matsuzaka S (2006) GPS network experience in japan and its usefulness. In: *Seventeenth United Nations regional cartographic conference, Geographical Survey Institute, Bangkok*
- McKean J, Buechel S, Gaydos L (1991) Remote sensing and landslide hazard assessment. *Photogram Eng Remote Sens* 57(9):1185–1193
- Mehdi R, Gruen A (2007) Automatic classification of collapsed buildings using object and image space features. In: *Li J, Zlatanova S, Fabbri A (eds) Geomatics solutions for disaster management. Lecture notes in geoinformation and cartography. Springer Verlag, Berlin*, pp 135–148
- Mitrovica JX, Tamisiea ME, Davis JL, Milne GA (2001) Recent mass balance of polar ice sheets inferred from patterns of global sea-level change. *Nature* 409:1026–1029. doi:[10.1038/35059054](https://doi.org/10.1038/35059054)
- Miura H, Midorikawa S (2006) Updating GIS building inventory data using high-resolution satellite images for earthquake damage assessment: application to metro Manila, Philippines. *Earthq Spectra* 22:151–168
- Motagh M, Djamour Y, Walter TR, Wetze H, Zschau J, Arabi S (2007) Land subsidence in Mashhad Valley, northeast Iran: results from InSAR, levelling and GPS. *Geophys J Int* 168:518–526. doi:[10.1111/j.1365-246X.2006.03246.x](https://doi.org/10.1111/j.1365-246X.2006.03246.x)
- Nicholson SE, Davenport ML, Malo AR (1990) A comparison of the vegetation response to rainfall in the Sahel and East Africa, using normalized difference vegetation index from NOAA AVHRR. *Clim Change* 17(2–3):209–241. doi:[10.1007/BF00138369](https://doi.org/10.1007/BF00138369)
- Nittel S, Labrinidis A, Stefanidis A (eds) (2008) *GeoSensor networks. Lecture notes in computer science 4540. Springer, Berlin*, pp 1–6
- Nittel S, Stefanidis A, Cruz I, Egenhofer M, Goldin D, Howard A, Labrinidis A, Madden S, Voisard A, Worboys M (2004) Report from the first workshop on Geo Sensor Networks. *ACM SIGMOD Rec* 33(1):141–144
- Ogawa N, Yamazaki F (2000) Photo-interpretation of buildings damage due to earthquakes using aerial photographs. In: *Proceedings of the 12th world conference on earthquake engineering, Auckland, CD-ROM*, 8p

- Omute P, Corner R, Awange JL (submitted) NDVI monitoring of Lake Victoria water level and drought. Water Resource Management
- Phoon SY, Shamseldin AY, Vairavamoorthy K (2004) Assessing impacts of climate change on Lake Victoria Basin, Africa: people-centred approaches to water and environmental sanitation. In: International Conference on 30th water engineering and development centre (WEDC), Vientiane, Lao PDR, pp 392–397
- Poland JF (1984) Guidebook to studies of land subsidence due to water withdrawal. UNESCO, Technical report
- Privette JL, Fowler C, Wick GA, Baldwin D, Emery WJ (1995) Effects of orbital drift on advanced very high resolution radiometer products: normalized difference vegetation index and sea surface temperature. *Remote Sens Environ* 53(3):164–171. doi:10.1016/0034-4257(95)00083-D
- Pugh D (2004) Changing sea levels. Effect of tides, weather and climate. Cambridge University Press, Cambridge
- Rius A, Aparicio JM, Cardellach E, Martín-Neira M, Chapron B (2002) Sea surface state measured using GPS reflected signals. *Geophys Res Lett* 29(23):21–22. doi:10.1029/2002GL015524
- Rocken C, Kelecy TM, Born GH, Young LE, Purcell GH, Wolf SK (1990) Measuring precise sea level from a buoy using the global positioning system. *Geophys Res Lett* 17(12):2145–2148
- Rood K (1984) An aerial photograph inventory of the frequency and yield of mass wasting on the Queen Charlotte Islands. British Columbia, BC Ministry of Forests, Land Management Report 34
- Sagiya T (2005) A decade of GEONET: 1994–2003 the continuous GPS observation in Japan and its impact on earthquake studies. *Earth Planets Space* 56:xxix–xli
- Sauchyn D, Trench N (1978) Landsat applied to landslide mapping. *Photogram Eng Remote Sens* 44:735–741
- Schenk A (2006) Interpreting surface displacement in Tehran/Iran region observed by differential synthetic aperture radar interferometry (DINSAR). Diplomarbeit, Technische Universität Berlin, Institut für Angewandte Geowissenschaften Fachgebiet Angewandte Geophysik
- Scofield RA, Achutuni R (1996) The satellite forecasting funnel approach for predicting flash floods. *Remote Sens Rev* 14:251–282
- Seidel DJ, Randel WJ (2006) Variability and trends in the global tropopause estimated from radiosonde data. *J Geophys Res* 111. doi:10.1029/2006JD007363
- Snay R, Cline M, Dillinger W, Foote R, Hilla S, Kass W, Ray J, Rohde J, Sella G, Soler T (2007) Using global positioning system-derived crustal velocities to estimate rates of absolute sea level change from North American tide gauge records. *J Geophys Res* 112:B04409. doi:10.1029/2006JB004606
- Snay R, Soler T (2008) Continuously operating reference station (CORS): history, applications, and future enhancements. *J Surv Eng* 134(4):95–104. doi:10.1061/(ASCE)0733-9453(2008)134:4(95)
- Snow J (2010) GIS analyses of Dr. Snow's Map. <http://www.udel.edu/johnmack/frec480/cholera/cholera2.html>. Accessed on 02 April 2010
- Steede-Terry K (2000) Integrating GIS and the global positioning system. ESRI Press, California
- Stefanidis A (2006) The emergence of geoSensor networks. *Directions Magazine*. <http://www.directionsmag.com/articles/the-emergence-of-geosensor-networks/123208>. Accessed 22 Jan 2011
- Terhorst A, Moodley D, ISimonis I, Frost P, McFerren G, Roos S, van den Bergh F (2008) Using the sensor web to detect and monitor the spread of vegetation fires in southern Africa. In: Nittel S, Labrinidis A, Stefanidis A (eds) *GeoSensor networks*. Lecture notes in computer science 4540. Springer, Berlin, pp 239–251
- Titus JG, Park RA, Leatherman S, Weggel R, Greene MS, Treehan M, Brown S, Gaunt C, Yohe G (1991) Greenhouse effect and sea level rise: the cost of holding back the sea. *Coast Manag* 19:171–204
- Trenberth K, Guillemot C (1996) Evaluation of the atmospheric moisture and hydrological cycle in the NCEP Reanalyses. NCAR Technical Note TN-430

- Trenberth KE (1997) The definition of El Niño. *Bull Am Meteorol Soc* 78:2771–2777
- Turker M, Cetinkaya B (2005) Automatic detection of earthquake-damaged buildings using DEMs created from pre- and post-earthquake stereo aerial photographs. *Int J Remote Sens* 26(4):823–832
- Ummerhofer C, England M, McIntosh P, Meyers G, Pook M, Risbey J, Gupta A, Taschetto A (2009) What causes southeast Australia's worst droughts? *Geophys Res Lett* 36:L04706. doi:[10.1029/2008GL036801](https://doi.org/10.1029/2008GL036801)
- Uriel K (1998) Landscape ecology and epidemiology of vector-borne diseases: tools for spatial analysis. *J Med Entomol* 35(4):435–445
- US Army Corps of Engineers (2007) NAVSTAR global positioning system surveying. Engineering and Design Manual, EM 1110-1-1003
- Voigt S, Riedlinger T, Reinartz P, Knzer C, Kiefl R, Kemper T, Mehl H (2005) Experience and perspective of providing satellite based crisis information, emergency mapping & disaster monitoring information to decision makers and relief workers. In: Zlatanova S, Fendel E, van Oosterom P (eds) *Geoinformation for disaster management*. Springer, Berlin, pp 519–531
- Warrick RA, Le Provost C, Meier MF, Oerlemans J, Woodworth PL (1996) Changes in sea level. In: Houghton JT, Meira Filho LG, Callander BA, Harris N, Klattenberg A, Maskell K (eds) *Climate change 1995. The science of climate change*. Cambridge University Press, Cambridge, pp 359–405
- Watson C, Coleman R, White N, Church J, Govind R (2003) Absolute calibration of TOPEX/Poseidon and Jason-1 Using GPS Buoys in Bass Strait, Australia. *Mar Geodesy* 26(3–4):285–304. doi:[10.1080/01490410390256745](https://doi.org/10.1080/01490410390256745)
- Webster TL, Forbes DL, Dickie S, Shreenan R (2004) Using topographic LiDAR to map flood risk from storm-surge events for Charlottetown, Prince Edward Island, Canada. *Can J Remote Sens* 30:64–76
- Wills C, McCrink T (2002) Comparing landslide inventories: the map depends on the method. *Environ Eng Geosci* VIII 4:279–293
- Wisner B, Blaikie P, Cannon T, Davis I (2004) *At risk—natural hazards, people's vulnerability and disasters*. Routledge, Wiltshire
- Worboys M, Duckham M (2006) Monitoring qualitative spatiotemporal change for geosensor networks. *Int J Geogr Inf Sci* 20(10):1087–1108. doi:[10.1080/13658810600852180](https://doi.org/10.1080/13658810600852180)
- Xue Z, Li G, Li Z, Wu X, Wei J (2007) Monitoring Xian land subsidence evolution by differential SAR interferometry. In: Li J, Zlatanova S, Fabbri A (eds) *Geomatics solutions for disaster management. Lecture notes in geoinformation and cartography*. Springer Verlag, Berlin, pp 427–437
- Yamaguchi N, Yamazaki F (2001) Estimation of strong motion distribution in the 1995 Kobe earthquake based on building damage data. *Earthq Eng Struct Dynam* 30(6):787–801
- Yamazaki F, Kouchi K, Kohiyama M, Muraoka N, Matsuoka M (2004) Earthquake damage detection using high-resolution satellite images. In: *Proceedings of IEEE 200 international geoscience and remote sensing symposium, IEEE, CD-ROM*, 4p
- Yamazaki F, Yano Y, Matsuoka M (2005) Visual damage interpretation of buildings in Bam City using QuickBird images. *Earthq Spectra* 21(1):329–336
- Zhang Q, Zhao C, Ding X, Peng J (2007) Monitoring Xian land subsidence evolution by differential SAR interferometry. In: Li J, Zlatanova S, Fabbri A (eds) *Geomatics solutions for disaster management. Lecture notes in geoinformation and cartography*. Springer Verlag, Berlin, pp 91–102
- Zhang J, Zhou C, Xua K, Watanabe M (2002) Flood disaster monitoring and evaluation in China. *Environ Hazards* 4:33–43. doi:[10.1016/S1464-2867\(03\)00002-0](https://doi.org/10.1016/S1464-2867(03)00002-0)

Chapter 27

Environmental Pollution

“People blame their environment. There is only one person to blame—and only one—themselves.”

Robert Collier

27.1 Concept of Pollution and Role of Geoinformatics

There exist various definitions to the word *pollution* depending on one’s jurisdiction and the laws of a particular country. Springer (1977, see references therein) looks at the meaningful concept of defining pollution in international law by posing the questions: “What are you talking about when you are talking about pollution? What is pollution? How would you define it if you are going to remove the concept of damage from it?” These questions are not easily answerable and as Springer (1977) acknowledges, the term pollution is a word whose precise meaning in law, particularly international law, is not easily discerned (Springer 1977). It has been used in a wide variety of contexts, from international conventions to pessimistic speeches about the state of the environment, to describe different levels and kinds of man-induced changes in the natural world Springer (1977).

Within a particular context, pollution assumes a meaning, either explicitly stated or implicitly developed, which may bear little resemblance to its usage elsewhere. Springer (1977) discusses the basic conceptual categories within which pollution has been approached in the past such as; pollution as an alteration of existing environment, pollution as a right to territorial sovereignty, pollution as a damage (to man and his property, and the environment), pollution as interference with other uses of environment, and pollution as exceeding assimilative capacity of environment.

Within this concept of environmental pollution, whether on land, water, or air, geoinformatics plays an important role in a number of ways:

- (a) providing maps indicating the precise *locations of the point and non-point sources of the pollutants*. GNSS could be very useful in mapping point sources, while non-point sources could be mapped using remote sensing.
- (b) mapping the *spatial coverage* of areas that are already affected as well as those likely to be affected by the pollution. Remote sensing and GIS could be very useful in this endeavor. GNSS could also be useful in providing boundaries for sampling data for the purpose of pollution monitoring, e.g., air pollution monitoring that is irregular and cannot be represented by regular grids, see e.g., Gibson and MacKenzie (2007).
- (c) *documenting and visualizing the changes* in areas affected by the pollution. High resolution, multispectral and multi-temporal satellite imagery could be very useful in this.
- (d) *modeling* various possible impact scenarios for the pollution to develop strategies for curtailing or minimizing human exposure to pollution. This is the strength of GIS.

27.2 Water Pollution

That fresh water has played a key role in agriculture, industries, and municipalities, among others is highlighted for instance by Mackenzie (2003, p. 314). Whereas most of the world's fresh water lakes carry natural substances and nutrients, today, in addition to these natural materials, pollutants, e.g., chemicals and excess eroded soil also find their way into the lakes, e.g., Awange and Ong'ang'a (2006).

Oceans, home to salt water marine, also face pollution from human-induced activities as witnessed by the BP oil leak at the Gulf of Mexico in 2010. There is need, therefore, to ensure that this vital source of life suffers minimum pollution as possible. Mackenzie (2003, p. 314) defines water pollution as any physical or chemical change in water from both natural and anthropogenic sources that adversely affects the organisms living in it. Water resources undergoes pollution from both *point* and *non-point* sources discussed next.

27.2.1 Point and Non-point Sources

Points sources are, e.g., factory outlet pipes and sewage treatment plant outlets whose positions can be accurately mapped using GNSS receivers. *Surface pollutants* include those produced from factories and industries, and agricultural activities. During rainy seasons, storm water carries with it chemicals from fertilizers and pesticides from farms, together with other nutrients from the neighboring towns. These materials are either swept into water bodies (rivers, dams, boreholes, etc.) through surface runoffs or percolate into the ground to reach groundwater flows, and finally into the rivers. The rivers eventually pour their contents into the lakes and oceans. The consequence

Fig. 27.1 Mobile hand-held GNSS. Source ©1995–2010 ESRI. <http://www.esri.com/technology-topics/mobile-gis/graphics/geoxt-web-1g.jpg>



of sewage contamination of water quality include outbreak of human diseases and eutrophication problem, which result in the proliferation of algal blooms and undesirable aquatic macrophytes, e.g., water hyacinth, see e.g., Awange and Ong'ang'a (2006). In some developing countries, where the compliance and enforcement of environmental laws is generally weak, such as Kenya, raw sewage and other industrial effluent are emptied untreated directly into the rivers or lakes. GNSS could be useful in mapping the locations and perimeters of these sources of sewage pollution, what could simply be achieved using a low cost hand-held GNSS receiver (Fig. 27.1) in autonomous mode (see Sect. 6.4.1). This data can then be integrated into a GIS system to inform decisions by the stakeholders.

An example of the effect of toxic chemical poisoning of water and its subsequent repercussion on human health was illustrated by the mercury poisoning of Minamata Bay in Japan Mackenzie (2003, p. 324). Around 1950s, mercury was discharged from a chemical plant located on a river flowing into the bay. The traces of this mercury found themselves in fish and were eventually consumed by people leading to the Mad Hatter's disease, a disease that affects the nervous system. Mackenzie (2003, p. 324) report that older Japanese living around the bay today still exhibit evidence of the disease that has killed a number of people.

Another example of water pollution is presented by the case of Kisumu (Kenya) where pit latrines (Fig. 27.2) are in the same locality with boreholes supplying groundwater (Fig. 27.3) thus contaminating the water. GNSS could be useful in providing the locations and perimeters/areas data of these features (pit latrines and boreholes), which could be mapped in a GIS system to support waste management and policy formulations.

Non-point sources are those that are difficult to identify, e.g., pollution from transportation sector and waste from mining operations, agricultural activities, and waste carried by street runoffs and drainage. From the atmosphere, precipitation containing chemical such as *sulfur* and *nitrogen* oxides also contaminate water sources. Owing

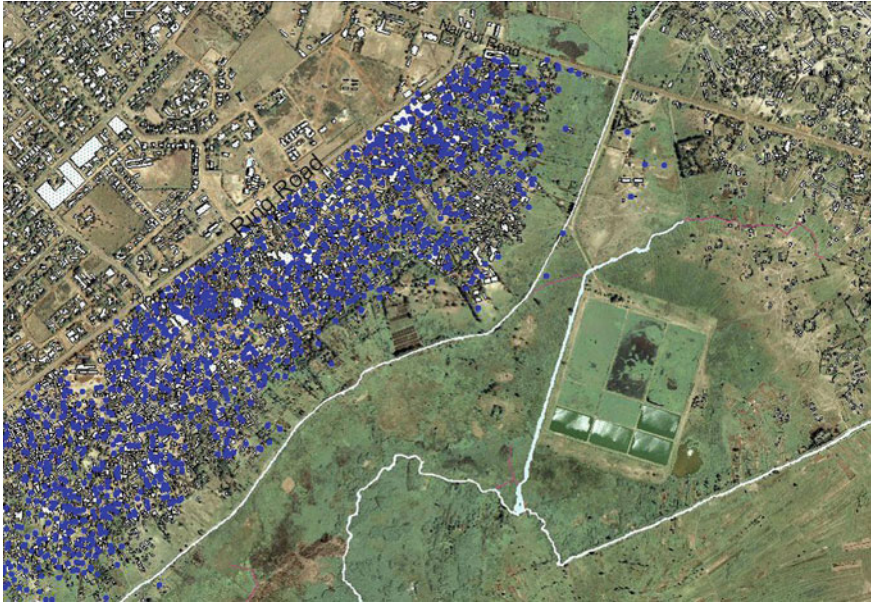


Fig. 27.2 Pit latrine (*dotted blue*) plotted on a Map of Nyalenda (Kisumu, Kenya). GNSS could be useful in providing the perimeter/area covered by these pit latrines in addition to their actual locations. This could be mapped into a GIS system to support management issues. *Source* Department of Planning, MCK (Municipality of Kisumu, Kenya) and Regional Center for Mapping of Resources for Development (2006) in Opande (2008)

to their dispersive nature, non-point sources are difficult to control and can only be mapped using remote sensing techniques.

For Lake Victoria, studies indicate that the high *phosphorous* and *nitrogen* loans choking it are attributed to several non-point sources. The most important of these are *agriculture*, *livestock*, *domestic* and *industrial effluents*. Most of these activities use large amounts of synthetic compounds including fertilizers and pesticides, see e.g., Kairu (2001). Although animal manure and domestic wastes contribute about 3000 tons and 132 tons of the total, respectively, their nitrogen inputs are estimated at over 40,000 tons per year Aseto and Ong'ang'a (2003, p. 106). This represents more than three times the amount contributed by synthetic fertilizers. GNSS could be useful in providing sampling boundaries for measuring the contributions of these pollutants, see e.g., Gibson and MacKenzie (2007).

27.2.2 Eutrophication of Lakes

Mackenzie (2003, p. 318) defines eutrophication as the process of being fed too well. Eutrophication leads to water quality deterioration, taste and odour problems,

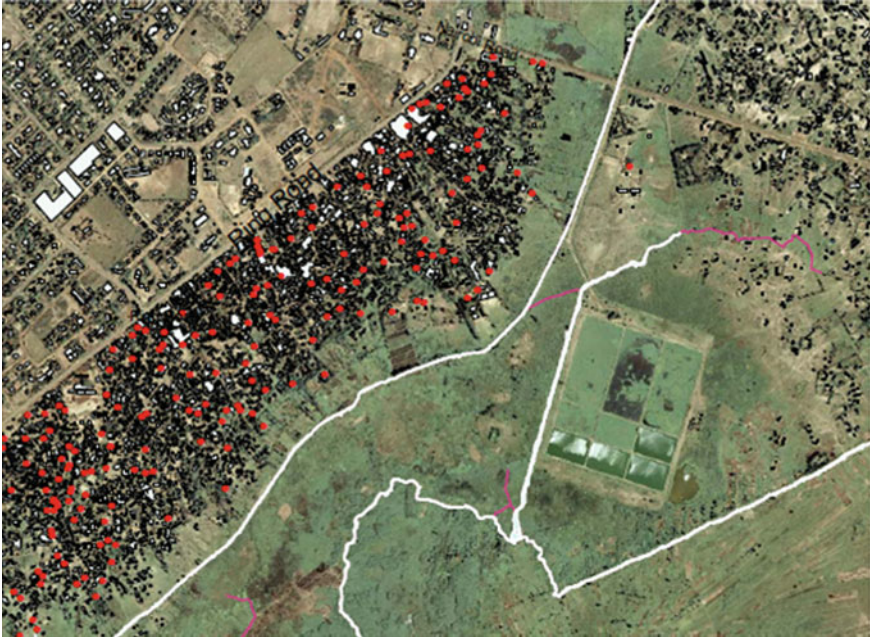


Fig. 27.3 Well-water point locations (*dotted red*) plotted on a Map of Nyalenda (Kisumu, Kenya). GNSS could be useful in providing the positions of these wells, which could be mapped into a GIS system to support management issues. *Source* Department of Planning, MCK and Regional Center for Mapping of Resources for Development (2006) in Opande (2008)

oxygen depletion, increased turbidity, decline of fisheries, possible fish kills, clogging of waterways and toxic effects on animals and human beings. The phenomenon is a typical result of nutrient imbalances at several levels. The source of nutrients include agricultural activities, which produce a nutrient rich runoff resulting from the leaching of fertilizers and manure, garbage dumps, sewage, and industrial effluent. Odada et al. (2004) listed three causes of eutrophication as:

- (a) Enhanced effluent discharge.
- (b) Runoff and storm water.
- (c) Enhanced discharge of solids.

The first two are the most important causes of eutrophication. Sources of effluent discharge could be mapped using hand-held GNSS receivers (Fig. 27.1), while remote sensing and GIS could be applied to monitor effluent discharge. In the US, the *Clean Water Act* 1972 focused on eliminating point source pollutants through regulating discharges from such point-sources. This was achieved by setting effluent limits which businesses were required to adhere to. By the 1980s, better control point-source posed a minor threat to public waters and focus shifted to storm water management. The San Francisco Public Utilities Commission (SFPUC) in its attempt to reduce storm water pollution mapped the city's storm drain using a hand-held GNSS-based

data collection device (e.g., Fig. 27.1) that captured the drain's precise locations and recorded digital notes on their conditions creating a GIS database Corbley and Stauffer (2006).

27.3 Air Pollution

27.3.1 Background

As stated in Chap. 1, environmental monitoring is concerned with monitoring the Earth's surface as well as the atmosphere. The Earth's atmosphere is known to be sensitive to *global warming*, *ozone layer depletion*, and *air pollution*. Air pollution is the emitting of harmful substances into the air that are detrimental to the environment. These substances could include, e.g., harmful poisonous gases, volcanic eruptions, e.g., the Indonesian eruption of 2010, greenhouse gases such as CO₂ that contribute to global warming, just to list but a few. Perhaps, the mostly crucial, is the emission of greenhouse gases from transport sector.

In both developed and developing nations, urban air pollution is increasingly being recognized as a major public health and environmental concern. In most developing countries, however, air quality monitoring is not routinely conducted and in some urban areas, such information does not even exist, though signs of deteriorating air quality and health problems related to air pollution are visible (Odhiambo et al. 2010). In Chap. 21, the role and possible contribution of geoinformatics to global warming monitoring is discussed. In the next section, the role and possible contributions of geoinformatics in monitoring local pollution are presented. The benefits of local monitoring is that it supports environmental quality conservation.

Remote sensing and GIS have been proven to be most appropriate and effective techniques for handling spatial data that describe urban air pollution, urban thermal environment, and land use and land cover (LULC) patterns Weng (2010). For example, by making use of remote sensing techniques it is possible to obtain reasonably high-quality land surface temperature (LST) estimates Voogt and Oke (2003); Nichol (2005); Oke (1988). Satellite data has been extensively used in air pollution mapping and monitoring in many urban environments, see e.g., Sifakis et al. (1998); Ung et al. (2001); Wald and Baleynaud (1999) etc. On the other hand, as a decision support tool, GIS is effective in mapping the spatio-temporal pattern of air pollution and examining its association with diverse land use activities Weng (2010); Mulaku and Kariuki (2002). GIS has also been employed to model air pollution variation through various statistical interpolation methods, see e.g., Carletti et al. (2000); Collins et al. (1995); Denby et al. (2005); Tayanc (2000) etc. Furthermore, GIS offers the potential for exposure assessment in support of not only air pollution epidemiology, but also air quality policy and environmental justice Briggs (2005); Maantay (2005); Jerrett et al. (2001).

GNSS is useful in providing location data. It is advantageous that an integrated approach drawing from remote sensing, GIS, and GNSS be developed and applied when examining the fairly complex relationships among spatial variables such as urban land use, pollution, and thermal variation, especially within an urban context. At a local level, one major air pollutant is the transport sector that emits CO₂ gases to the atmosphere. Example of possible use of GNSS to monitor transport related pollution is presented in Sect. 27.3.2. Other source include industrial pollutants whose exact locations can readily be mapped using a hand-held GNSS receivers. These GNSS-based location data could then be integrated with other information such as the emission level per location in a GIS system to give a real-time air pollution monitoring capability.

For non-point sources, GNSS could play a role of mapping atmospheric quality parameters by being integrated with other devices in a geosensor network (e.g., Sect. 26.3), e.g., gas sensors, remote sensors, cell phones, and laptops in a mobile device such as that discussed, e.g., in Schreiner et al. (2006). In the work of Schreiner et al. (2006), GNSS provided location-based data in terms of longitude, latitude, and altitude at points where the sensor recorded the pollution level. Both the sensor and GNSS transmitted their measured data to a laptop, which processed the information and relayed it to a mobile phone for remedial actions to be taken.

27.3.2 Pollution from Transportation Sector

Increased traffic volumes (see e.g., Fig. 27.4, right) in major towns such as Beijing, New York, etc., has potential for affecting ambient air. In most developing nations, such as Kenya, most of the vehicles are of the older generation (e.g., Fig. 27.4, left) and cannot sustainably run on unleaded fuel, as the conditions generated during combustion contribute to a rapid erosion of the valve seats, resulting in loss of engine performance through poor valve sealing.

The high lead content combined with the low combustion efficiency of the older type of engines lead to the emission of high volumes of exhaust gases, which contain semi-combusted fuels combined with worn out engine parts and waste oils [?], hence high concentration of particulate matter in the air. From their study of air pollution in Beijing, Yang et al. (2000) found that the relative particulate mass and the elemental concentrations of crustal and pollutant elements in the air particulate matter collected over the urban area was higher than in rural areas.

The possible role that could be played by geoinformatics in supporting monitoring of transportation related emission and noise pollution is exemplified in the study of Taylor et al. (2000) who discuss the Transportation System Center (TSC) developed at the University of South Australia based on the integration of GIS and GNSS systems. In this system, GIS played the role of data management, i.e., data entry and integration, data analysis and display, while GNSS had the role of determining the locations of both static observations and dynamic recordings of the vehicle positions over time. The GIS-GNSS system is further integrated with an engine

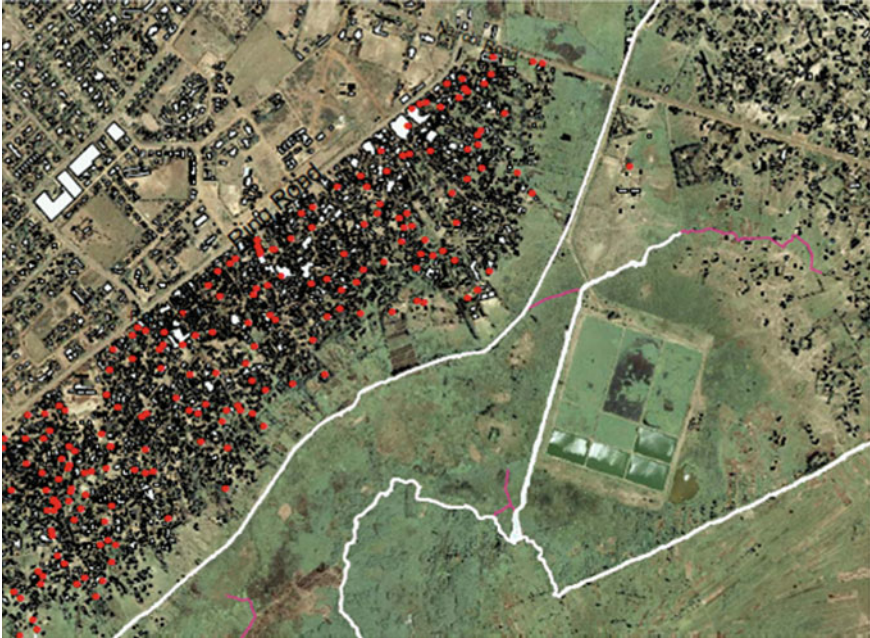


Fig. 27.4 Exhaust pollution and vehicle congestion

management system of the vehicle to provide time-tagged data on GNSS position and speed, distance traveled, acceleration, fuel consumption, engine performance, and air pollution on a second-by-second basis Taylor et al. (2000).

Such data is vital not only for air pollution monitoring but also for *energy conservation* through monitoring of engine performance and fuel consumption. Acceleration data are useful in monitoring *noise pollution* level coming from the engine. An essential component of transportation that contributes to large fuel consumption and higher emission of greenhouse CO₂ gases is *traffic congestion*. In this GIS-GNSS system of Taylor et al. (2000), GNSS played a role of monitoring traffic congestion by measuring some component of total delay time, e.g., stopped time and acceleration noise (indicated by speed variation depending on the road condition). GNSS could also be useful in providing speed data, see e.g., Zito et al. (1995); Zito and Taylor (1994). Further, congestion can be identified by the presence of queues, and as such, the knowledge of the incidence of queuing in any congestion monitoring system is essential Taylor et al. (2000). As already stated, GNSS could help in measuring the proportion of stopped time (PST), which indicate the amount of time spent in queues during a journey Taylor et al. (2000).

Example 27.1 (Air pollution in Guangzhou, China. Source: Weng (2010))

This study investigated the air pollution pattern in this fast growing political, economic, and cultural center in South China using geoinformatics. Findings from the study indicate that high-quality data and reliable information regarding Land use and land cover (LULC) patterns and Land surface temperature (LST) can be derived with satellite remote sensing and GIS technologies and that the data so derived closely correspond to ambient air-quality measurements. Furthermore, the spatial patterns of air pollution depend on many factors tied to land-use activities e.g., division of functional districts, distribution of land-use types, water bodies and parks, building and population densities, layout of the transportation network, and air flushing rates.

In Guangzhou, ambient air quality was monitored between 1980 and 2000 and concentrations of sulfur dioxide (SO₂), nitrogen oxides (NO_x), carbon monoxide (CO), and total suspended particles (TSPs), as well as dust level spatially documented using geographic distribution maps. These maps were digitized and converted into GIS data layers for interpretation of the spatial patterns of air pollution. Results indicate that the impact of various factors varied with different pollutants, and the street canyon effect was particularly evident owing to Guangzhou's closely spaced highrise buildings and low-wind environment. Because of the locations of industrial plants, high population density, clustering of the catering industry, and low air-flushing rates, two urban localities (namely the Liwan and Yuanchun Districts) became the pollution hubs for SO₂, dust, and other pollutants Weng (2010). Positive correlation identified between the concentrations of the pollutants probed and satellite-derived LST values confirms that both ambient air quality and LSTs were related to land use activities. The study demonstrates that GIS is effective in examining the spatial pattern of air pollution and its association with urban built-up density.

End of Example 27.1

27.4 Land Pollution

27.4.1 *Solid Waste Collection and Management*

Natural resources on the fringes of urban areas always suffer severe depletion and degradation as urban centers create demand for goods and services thus exerting tremendous pressure on fragile ecosystems. The high rate of urbanization therefore rapidly increases the pressure on these ecosystems. The increasing population and

economic growth of cities associated with urbanization create externalities due to the demand for resources and waste disposal Leitman (2000).

Solid waste includes refuse from households, non-hazardous solid waste from industrial, commercial and institutional establishments (including hospitals and other health care facilities), market waste, yard waste and street sweepings. Solid Waste Management (SWM) encompasses the functions of storage, collection, transfer, treatment, recycling, resource recovery and disposal. Its first goal is to protect the health of the population. Other goals include promotion of *environmental quality* and *sustainability*, support of economic productivity and employment generation. Achievement of SWM goals requires sustainable systems, which are adapted to and carried out by the municipalities and their local partners including the communities within their jurisdictions.

In many cities of developing countries, private or public systems of SWM are inadequate, only able to achieve collection rates of between 30 and 50%. The uncollected wastes are often disposed off in ways detrimental to the environment such as open burning, burying, or dumping in rivers Hoornweg and Thomas (1999). This problem is further compounded in low income areas where the authorities normally prioritize SWM lowly as compared to water supply, electricity, roads, drains, and sanitary services Schubeler et al. (1996). SWM is a major responsibility of local governments in developing countries consuming between 20 and 50% of their total budgets Van Beukering et al. (1999). It is a complex supply driven task, which depends as much upon organization and cooperation between households, communities, private enterprises, and government authorities, as it does upon the selection and application of appropriate technical solutions for collection, transfer, recycling and disposal (United Nations Centre for Human Settlement (UNCHS) and United Nations Environmental Programme (UNEP) 1996). It should therefore, be approached from the perspective of the entire cycle of material use with a broad scope encompassing planning and management, *waste generation* and waste handling processes Schubeler et al. (1996).

27.4.2 Role of Geoinformatics in Solid Waste Management

The functioning of solid waste management systems is influenced by the waste handling patterns and underlying attitudes of the urban population who are the waste generators; these factors are themselves, conditioned by the people's social and cultural context Schubeler et al. (1996). Fast growing low-income residential communities often comprise of a considerable social, religious and ethnic diversity, which strongly influences the waste characteristics and socio-economic patterns thereby influencing the choice of SWM techniques to be applied (Fig. 27.5).

In urban areas, the physical characteristics of a settlement such as the road conditions, topography, waste characteristics, etc., need to be considered when selecting and/or designing waste collection and transportation procedures and equipment. Use of GNSS and GIS technology could be valuable in visualizing this physical character-



Fig. 27.5 Informal waste dumping locations (*dotted red*) plotted on Map of Nyalenda (Kisumu, Kenya). GNSS could be useful in providing these locations. *Source* Opande (2008)

istic to improve on collection efficiency. More importantly, GNSS and GIS could be vital tools for urban planners in that they could enable them harmonize solid waste management and other services such as water, electricity, access roads, physical planning, and sanitation, all of which are associated with inadequate service delivery within a municipality. This technology would help in getting the exact location and properties of the containers, understanding the attributes of the infrastructure, and routing of the secondary collection vehicles.

At the level of natural systems, the interaction between waste handling procedures and public health conditions is influenced by climatic conditions such as seasonal weather variations and other ecological factors, e.g., the nature of animals reared within the homestead. In practical terms, climate determines the frequency by which waste collection points must be serviced in order to limit negative environmental consequences. The contribution of geoinformatics to weather and climate monitoring are presented in Chaps. 20 and 21.

The management methods and techniques employed in SWM should pay more attention to integrated approaches based on adequate information systems, e.g., GIS among other tools. With regard to operational planning and appropriate management methods, the approach should include among others, data collection techniques, analysis of waste composition, projecting waste amounts, scenario techniques and formulation of equipment specifications Senkwe and Mwale (2001), all of which could be supported by geoinformatics as discussed above.

Waste disposal in drains



Waste gets into main drain



package waste at Lake Shore



Fig. 27.6 Waste accumulation at bus termini in Kisumu (Kenya)

Old and broken brake pads



Bearings, air and oil filters



scrapped paint and scrap metals



Fig. 27.7 Wastes from vehicle repair known as Jua Kali in Kisumu (Kenya)

27.4.3 Solid Waste from Transportation Sector

Although pollution from industry, agrochemical factories and farmlands have been well documented (see, e.g., Sect. 27.2), the contribution of the transportation sector to the pollution of environment in terms of solid waste also deserve to be mentioned. Contribution of pollution from the vehicles takes the form of;

- litter generated at the termini and along the roads (e.g., Fig. 27.6),
- vehicle repair, service and maintenance yards and garages commonly known in Kenya as “Jua Kali” (i.e., open garages indicated by Figs. 27.7 and 27.8),
- exhaust fumes and oil spills on to the roads, which are washed into the water sources (Figs. 27.9 and 27.10).

A hand-held GNSS receiver (e.g., Fig. 27.1) could be useful in providing locations of these sources, which could then be mapped and integrated with other data in a GIS to develop a real-time monitoring of system for decision makers in municipalities.

Car Washing: In East Africa, an increasingly popular practice at the beaches today is the car washing (Fig. 27.11) whose history stretches back to the late 1950s. The beach records very high turn over of vehicles of different classes that are washed at the Lake every day, see e.g., Awange and Obera (2007); Awange and Ong’ang’a (2006). Casual observations reveal that the shore waters are now dirtier and greasier. The waste oils from these vehicles, and dirt accumulated in transit are all washed into the Lake. Some of the vehicles have leaking systems hence the oils or the fuels drip into the Lake while they are being washed, further compounding the problem.

As can be seen in Fig. 27.12, the shores are no longer supporting the original vegetation or other aquatic life forms, due to the conscious removal by the car washers



Fig. 27.8 The spray painting process and wastes in Kisumu (Kenya)

Oil spills on tarmac roads



Oil spills on earthen roads



Fig. 27.9 Oil spills in Kisumu (Kenya)

The waste water drainage



Car washing



The Lake side Caltex depot



Fig. 27.10 Petrol station operations and the caltex petrol depot at the Lake side in Kisumu (Kenya)

or possibly due to the decrease in the oxygen levels in the water occasioned by the oil covering the water surface. In Fig. 27.12, the floral and faunal composition has also changed as can be detected by the lack of shells at the car washing area. There has been a change in the trophic relations at the car washing area, which affects the entire Lake. It should be pointed out that Kichinjio beach in Kisumu (Kenya) is one of the breeding sites for some fish species and other aquatic life forms within the



Fig. 27.11 Washing of heavy petroleum vehicle in Lake Victoria in Kisumu (Kenya)

Ground at car wash



Snail shells at undisturbed site



Birds on undisturbed beach



Fig. 27.12 Environmental impacts of washing of heavy petroleum vehicles in Lake Victoria in Kisumu (Kenya). A hand-held GNSS could provide the location, perimeter, and area information of such impacted areas. This information could then be incorporated into a GIS system to support habitat conservation and management

lake, a characteristic that is fast disappearing. The disturbance accompanied by oils in the water could have adversely affected them. A hand-held GNSS receiver as well as high resolution satellite imagery could play a vital role in providing locations, perimeters, and areas of such car washing impacted areas for the purposes of habitat conservation and management.

27.4.4 Acid Mine Deposit Sites

Sulfide minerals occurring naturally are common minor constituents of the Earth's crust but occur in large quantities in some metallic ore deposits (e.g., Cu, Pb, Zn, Ni, U, Fe), phosphate ores, coal seams, oil shales and mineral sands Lottermoser (2003, p. 29). When not exposed to oxygen, sulphide are harmless. However, when exposed to oxygen through, e.g., mining, excavation, waste rock dams, etc., they become oxidized to produce sulphuric acid and high concentration of heavy metals such as Cu and Zn, see e.g., (Laboratory Manual 2008, p. 33). Lottermoser (2003, p. 29) point to the fact that the mineral pyrite (FeS_2) tend to be the most common sulphide mineral present whose weathering at mine sites cause the largest, and most testing, environmental problem facing the industry today—the acid mine drainage (AMD).

AMD generation can lead to the contamination of surface and ground water resulting in expensive treatment. Johnson and Wichern (2007) indicate that the cost of remediating impacts of AMD in Canada for example was in excess of \$3 billion. In Australia, the environmental impact of AMD is most significant in the abandoned mines, e.g., Rum Jungle (NT), Mt. Lyell (Tas) and Mt. Morgan (Qld) (Laboratory Manual 2008, p. 34). The problem with AMD is that where it enters streams, there is a drop in pH leading to the disappearance of *aquatic ecosystems* and backside *plant communities*, soil contamination, the degradation of the food chain and contaminated groundwater Lottermoser (2003, p. 69) and (US-EPA (U.S. Environmental Protection Agency) 1994). According to Lottermoser (2003, p. 29), long-term exposure to contaminants in farmed food products may have the possibility of increasing health problems for humans. The extent to which extreme conditions of AMD develop depends on (Laboratory Manual 2008):

- Water availability for oxidation and transportation.
- Oxygen availability.
- Physical characteristic of materials.
- Temperature, ferrous/ferric iron equilibrium, and microbial activity.

An effective approach for handling AMD entails managing of one of the factors above. Encapsulations of acid generating materials to prevent water leaching through the sulfidic materials and to limit oxygen contact with it are the two most important principles to apply (Laboratory Manual 2008). The two steps above can only be applied once the materials on the mine sites, which have acid generating potential, have been identified (Laboratory Manual 2008).

GNSS could be useful in providing the locations of the materials once they have been identified and also in mapping sample sites for which tests such as net acid generation (NAG) are to be undertaken. When integrated in a GIS, these location-based data could support management measures by showing decision makers the exact places where the factors listed above have been implemented.

27.5 Concluding Remarks

This chapter has outlined some examples of areas where geoinformatics could be employed to support in the monitoring and management of pollution. The materials presented in the chapter are by no means exhaustive, but are intended to provide an impetus and motivation for further research on how the application of an integrated geosensor framework (see e.g., Sect. 26.3) could be developed to enhance comprehensive pollution monitoring and management. This is demonstrated, e.g., in the case of monitoring air pollution and storm water pollution, wherein GNSS is integrated with gas sensors, remote sensors and GIS respectively. It is also shown that GNSS will play a crucial role in transport pollution related monitoring through measurements, e.g., of stoppage time, and provision of location-based data. On the other end of the divide, away from technical matters, it is imperative to educate people on the need for citizens to take responsibility for their own environment, while at the same time enforcing full compliance of environmental rules and legislation. Such education could be enhanced by the use of GIS, which could be used to provide visual maps that are simple enough to be understood by the local community.

References

- Aseto O, Ong'ang'a O (2003) Lake Victoria (Kenya) and its environs: resource opportunities and challenges. Africa Herald Publishing House, Kendu Bay
- Awange JL, Obera B (2007) Motor vehicles: are they emerging threats to Lake Victoria and its environment? *Water Air Soil Pollut* 182(1–4):43–56. doi:10.1007/s11270-006-9319-3
- Awange JL, Ong'ang'a O (2006) Lake Victoria—ecology, resource of the Lake Basin and environment. Springer, Berlin
- Briggs D (2005) The role of GIS: coping with space (and time) in air pollution exposure assessment. *J Toxicol Environ Health* 68(13–14):1243–1261. doi:10.1080/15287390590936094
- Carletti R, Picci M, Romano D (2000) Kriging and bilinear methods for estimating spatial pattern of atmospheric pollutants. *Environ Monit Assess* 63:341–359
- Collins S, Smallbone K, Briggs D (1995) A GIS approach to modelling small area variations in air pollution within a complex urban environment. In: Fisher P (ed) *Innovations in GIS 2*. Taylor and Francis, London, pp 245–253
- Corbley KP, Stauffer R (2006) Curbing water pollution with mobile GIS: mobile data collection with handheld GPS units facilitates a San Francisco utility's quest for cleaner water, enabling a two-pronged effort to build a storm drain GIS layer and educate citizens about pollution. *Geospatial Solutions*. <http://www.gpsworld.com/gis/local-government/curbing-water-pollution-with-mobile-gis-5361>. Accessed on 20 Jan 2011
- Denby B, Walker SE, Horálek OJ, Eben K, Fiala J (2005) Interpolation and assimilation methods for European scale air quality assessment and mapping. Review and recommendations. European topic centre on air and climate change technical paper, vol 7
- Gibson J, MacKenzie D (2007) Using global positioning systems in household surveys for better economics and better policy. *World Bank Res Obs* 22(2):217–241. doi:10.1093/wbro/lkm009
- Hoornweg D, Thomas L (1999) What a waste: solid waste management in Asia. Urban development sector unit East Asia and Pacific region. The international bank for reconstruction and development/THE WORLD BANK, Washington

- Jerrett M, Burnett RT, Kanaroglou P, Eyles J, Finkelstein N, Giovis C, Brook JR (2001) A GIS: environmental justice analysis of particulate air pollution in Hamilton, Canada. *Environ Plann* 33(6):955–973
- Johnson R, Wichern D (2007) *Applied multivariate statistical analysis*, 6th edn. Prentice Hall, Upper Saddle River
- Kairu JK (2001) Wetland-use and impact on Lake Victoria. *Lakes Reserv Resour Manage* 6(2):117–125. doi:10.1046/j.1440-1770.2001.00135.x
- Laboratory Manual (2008) ENV 310 land management practical manual. Learning materials: school of environmental science. Murdoch University, Murdoch
- Leitman J (2000) Rapid environmental assessment: lessons from cities in the developing world, vol 1. Methodology and preliminary findings. Urban management programme, UNHCS, UNDP and the World Bank
- Lottermoser B (2003) *Mine wastes. Characterization, treatment and environmental impacts*. Springer, Berlin
- Mackenzie FT (2003) *Our changing planet; an introduction to earth system science and global environmental change*, 3rd edn. Prentice Hall, New Jersey
- Maantay J (2005) Asthma and airpollution in the bronx: methodological and data considerations in using GIS for environmental justice and health research, health and place: environmental justice, population health, critical theory and GIS, vol 13, issue no.1. Elsevier, pp 32–56
- Mulaku GC, Kariuki LW (2002) Mapping air pollution in Nairobi, Kenya. *African. J Environ Assess Manag* 4(1):29–37
- Nichol JE (2005) Remote sensing of urban heat islands by day and night. *Photogramm Eng Remote Sens* 71:613–623
- Odada EO, Olago DO, Kulindwa K, Ntiba M, Wandiga S (2004) Mitigation of environmental problems in Lake Victoria, East Africa: causal chain and policy options analyzes. *Royal Swed Acad Sci* 33(1):13–17
- Odhiambo GO, Kinyua AM, Gatebe CK, Awange JL (2010) Motor vehicles air pollution in Nairobi, Kenya. *Res J Environ Earth Sci* 2(4):178–187
- Oke TR (1988) The urban energy balance. *Prog Phys Geogr* 12:471–508
- Opande T (2008) Planning solid waste collection in low income settlements of Nyalenda and Ondiek in Kisumu town, Kenya. MSc Thesis, Maseno University, Kenya
- Schreiner C, Branzila M, Trandabat A, Ciobanu RC (2006) Air quality and pollution mapping system, using remote measurements and gps technology. *Global NEST J* 8(3):315–323
- Schubeler P, Wehrle K, Christen J (1996) Conceptual framework for municipal solid waste management in low income countries. UMP working papers series no.9, UNDP/SDC/UNCHS/World Bank, UMP/SKAT
- Senkwe B, Mwale A (2001) Solid waste in Kitwe, Zambia. A solid waste characterization study for the city of Kitwe, Zambia. Phase I. A consultancy report for SINPA, Zambia; institute for housing and urban development studies, Netherlands; and the Copper Belt University, Kitwe, Zambia
- Sifakis NL, Soulakellis NA, Paronis DK (1998) Quantitative mapping of air pollution density using earth observations: a new processing method and application to an urban area. *Int J Remote Sens* 19(17):3289–3300
- Springer AL (1977) Towards a meaningful concept of pollution in international law. *Int Comp Law Quarte* 26:531–557
- Taylor MAP, Woolley JE, Zito R (2000) Integration of the global positioning system and geographical information systems for traffic congestion studies. *Transp Res Part C* 8(1–6):257–285. doi:10.1016/S0968-090X(00)00015-2
- Tayanc M (2000) An assessment of spatial and temporal variation of sulphur dioxide levels over Istanbul, Turkey. *Environ Pollut* 107(1):61–69
- United Nations Centre for Human Settlement (UNCHS) and United Nations Environmental Programme (UNEP) (1996) *International source book on environmentally sound technologies for municipal solid waste management*. IECT technical publication series, New York

- Ung A, Wald L, Ranchin T, Weber C, Hirsch J, Perron G, Kleinpeter J (2001) Satellite data for air pollution mapping over a city—virtual stations, Proceeding of the 21st EARSeL symposium. New solutions for a New Millenium, Paris, France, Observing our environment from space, pp 14–16
- US-EPA (U.S. Environmental Protection Agency) (1994) Technical document. Acid mine drainage prediction. EPA 530-R-94-036; NTIS PB94-201829
- Van Beukering P, Sekher M, Gerlagh R, Kumar V, (1999) Analyzing urban solid waste in developing countries; a perspective on Bangalore, India. International Institute for Environment and Development (IIED), Working paper No.24. CREED, London
- Voogt JA, Oke TR (2003) Thermal remote sensing of urban climate. *Remote Sens Environ* 86:370–384
- Wald L, Baleynaud J-M (1999) Observing air quality over the city of Nantes by means of LANDSAT thermal infrared data. *Int J Remote Sens* 20(5):947–959
- Weng Q (2010) Remote sensing and GIS integration: theories, methods, and applications. McGraw-Hill, New York, p 416
- Yang S, Dong J, Cheng B (2000) Characteristics of air particulate matter and their sources in urban and rural area of Beijing. *Ch J Environ Sci* 12:402–409
- Zito R, D’Este GM, Taylor MAP (1995) Global positioning systems in the time domain: how useful a tool for intelligent vehicle-highway systems. *Transp Res C*3(4):193–209
- Zito R, Taylor MAP (1994) The use of GPS in travel time surveys. *Traffic Eng Control* 35(12):685–690

Chapter 28

Environmental Impact Assessment

“Distances and locations are the important determinants of many choices that economists study. Economists often rely on information about these variables that are self-reported by respondents in surveys, although information can sometimes be obtained from secondary sources. Self-reports are typically used for information on distances from households or community centers to roads, markets, schools, clinics, and other public services. There is growing evidence that self-reported distances are measured with errors and that these errors are correlated with the outcomes of interest. In contrast to self-reports, global positioning systems (GPS) can determine locations to within 15 m in most cases. The falling cost of GNSS receivers makes it increasingly feasible for field surveys to use GNSS to more accurately measure locations and distances.”

J. Gibson and D. MacKenzie (2007)

28.1 Role of Geoinformatics in EIA, SEA, and SA

28.1.1 Impact Assessments and the Need for Monitoring

Environmental Impact Assessment (EIA) is defined by Munn (1979) as the need to *identify* and *predict* the impact on the environment and on man’s health and well-being of legislative proposals, policies, programs, projects, and operational procedures, and to interpret and communicate information about the impact. EIA is thus a process, a systematic process that examines the environmental consequence of development actions in advance (Glasson et al. 2005, p. 4). Glasson et al. (2005) have defined the purpose of EIA as an *aid to decision making*, an *aid to the formulation of the development actions*, and an *instrument to sustainable development*. In order to achieve these goals, EIA requires monitoring data that can be used to

identify and predict impacts, and also to evaluate the impacts of a given project once approved. Whereas EIA has been traditionally restricted to projects that are deemed to have significant impacts on the environment, it has recently expanded to include *strategic environmental assessment* (SEA) discussed in Sect. 28.4 and *sustainability assessment* (SA) presented in Sect. 28.5.

Monitoring involves the measuring and recording of physical, social and economic variables associated with development impacts (see Chap. 1). The activities seek to provide information on the characteristics and functioning of variables in *time*, *space*, and *scale* (discussed in Sect. 2.1), and in particular in the occurrence and magnitude of impacts (Glasson et al. 2005, p. 185). It offers the possibility of determining or assessing the extent of human impacts on the environment and also compares human impacts with natural variation in the environment. The advantages of monitoring following project implementations are that it can improve project management, it can be used as an early warning system to identify harmful trends in a locality before it is too late to take remedial action, it can help to identify and correct for unanticipated impacts, and it can also be used to provide acceptable data and information, which can be used in mediation between interested parties (Glasson et al. 2005, p. 185). Glasson et al. (2005, p. 186) defines environmental impact auditing as the comparison between the impacts predicted in *environmental impact statements* (EIS) and those occurring after implementation in order to assess whether the impact prediction performs satisfactorily. EIS is the document that contains the information and estimates of impacts derived from the various steps of the EIA process.

28.1.2 Applications of Geoinformatics

GNSS satellites could be used to support the processes of project-based EIA, SEA and SA in provision of location-based data that support *monitoring* and *auditing*. As an example, in March of 2009, Kelly Core Salmon (KCS) Ltd filed an application with the Nova Scotia Department of Fisheries and Aquaculture (NSDFA) to relocate and expand the boundaries of the existing three aquaculture sites (Sand Point, Boston Rock, and Hartz Point) located in Shelburne Harbour, Nova Scotia (Sweeney International Management Corp 2009). The desire to relocate and expand was motivated by the need to improve the environmental performance of the three sites by allowing a greater flow and depth on the sites, easier access to the sites, and increased production, ensuring greater economic stability for KCS production in Nova Scotia (Sweeney International Management Corp 2009).

For the relocations and expansion to take place, EIA was undertaken in order to satisfy the criteria of the New Brunswick Department of Agriculture and Aquaculture (NBDAA), Nova Scotia Department of Agriculture and Aquaculture (NSDAA), and Fisheries & Oceans Canada (DFO) (Sweeney International Management Corp 2009). In support of provision of location-based data, GNSS-DGPS (see Sect. 6.4.4.1) was employed to provide the relocated boundary co-ordinates.

GNSS could also be useful in supporting impact assessments in the following ways:

- (a) Provide location-based data useful in identification of features of interest, which could be impacted during the undertaking of the project-based EIA. For example, GNSS could be used to provide the locations of boreholes in a given region where a project that has the potential of contaminating groundwater has been proposed.
- (b) Providing distance information that is useful in measuring access to infrastructure and social services such as health care. Gibson and MacKenzie (2007) discuss how GNSS-based information on spatial distribution of population and services can lead to improved understanding of access to services. Understanding access to services is essential in spatial multi-criteria selection (e.g., Sect. 28.3.2), where a decision to choose an option from various alternatives is to be made. For instance, Perry and Gessler (2000) applied GNSS to measure access from communities to health-care facilities in Andean Bolivia, and used the results to propose an alternative model of health distribution in the study area.
- (c) Its distance and travel time data can be useful in identifying barriers to the use of services (Gibson and MacKenzie 2007). Often, such hidden barriers can lead to poor decision leading to the selection of a given alternative at the expense of the other methods, which might be optional. Knowledge of these hidden barriers could thus enable policy and decision makers to make informed decisions.
- (d) A combination of GNSS-based location data and GIS would be very effective in illustrating access to services in a form that would be easily understood by the community during participatory stage of discussing environmental impact statement (EIS), and also for policy and decision makers during the selection of an option from given alternatives.
- (e) In support of collection of socio-economic data, e.g., household surveys. Here, GNSS could be useful in improving the quality and cost-effectiveness of the survey data. GNSS locations could for instance be used to provide sampling boundaries as opposed to cases where such boundaries are arbitrarily selected or regular grids used where they are not useful (e.g., in monitoring variable features irregularly distributed over space such as air pollution). For example, Kumar (2007) show how a combination of GNSS and remote sensing was useful in drawing samples in a survey of 1,600 households spread across different air pollution zones in Delhi (India).
- (f) For SEA and SA, GNSS can be of use in providing data for econometric modeling of casual impacts of policies (Gibson and MacKenzie 2007). In this regard, it could provide data that could enable practitioners to better control the geographical and regressional characteristic of their models, e.g., by comparing individuals who are subjected to a given policy and those who are not.
- (g) Further, for SEA and SA, its integration with GIS can prove particularly useful in supporting the evaluation of cumulative impacts (see e.g., Sect. 28.4.1). This is achieved through the ability of GIS-GNSS to consider spatial component and allow the analysis of the temporal evolution, see, e.g., Smit and Spalding (1995).

28.2 Impact Monitoring to Detect Change

In defining monitoring in Sect. 1.1, *impact monitoring* was noted to focus on identifying possible impacts of human activities on environment and to distinguish them from the non-human environmental processes, while *compliance monitoring* had the objective of supporting stipulated legislations that aim at protecting and conserving the environment. According to Downes et al. (2002), both compliance and impact assessments have a key objective of detecting change in selected variables, with impact assessment relying on comparisons within the collected data to assess whether an impact has occurred and the magnitude of such impact. Because impact assessment monitoring tend to be defined relative to natural conditions rather than being pegged to external criteria, Downes et al. (2002) propose a monitoring design model, which if properly implemented, could support *change detection*.

The model is location-based taking into consideration the fact that in most cases, variables are measured at a specific impact location or locations, i.e., the *impact location(s)*. They then argue that a change being monitored in a variable should be seen to have occurred by comparing the variable's status prior to the activity (baseline data) which they call "*Before*" and after or during the activity (operational data) which they call "*After*". This Before-After model takes place at the impact location. In order to distinguish between natural and impact induced changes, a location outside the activity (impact area) is suggested, i.e., the "*control*" upon which data is to be simultaneously sampled together with the impact location "before" and "after". This before and after, control and impact locations form the BACI (Before-After-Control-Impact) model. The model proceeds as follows (Downes et al. 2002):

- Data are collected at some *impact locations* over some period *before* the activity starts.
- Data are collected at some *impact locations* over some period *after* the activity starts.
- Data are collected at some *control locations* over the same period *before* the activity starts.
- Data are collected at some *control locations* over the same period *after* the activity starts.

In the BACI model above, the control location provides proxy data that are used to remotely sense the impact locations in the absence of a triggering activity. The assumption of the model is that if similar changes occur at both the control and impact locations, then the trigger for this changes would be natural causes since the control location does not have the activity. On the contrary, if the changes are only noticeable at the impact's location and not at the control location, then the activity at the impact location would be the most likely suspect. Because of the varying dynamics of the impacts and control locations, Downes et al. (2002) suggest that several control locations and possibly impact locations be used, thus extending the BACI model to MBACI model, where multiple locations are considered.

Within these BACI and MBACI models, GNSS could be useful in providing the positions of control and impact locations upon which environmental impact

assessment monitoring could be collected simultaneously before and after the activity. Remote sensing could be employed to collect variable spatio-temporal data, with GIS being used to manage the various datasets, in addition to providing the platform for detecting the change being monitored.

Example 28.1 (Illustration of tourism impact on groundwater) Consider that a particular hotel utilizes groundwater and due to increased number of tourists, plenty of water is used, and that the impact of groundwater abstraction on the hotel is to be monitored to avert the potential danger of the building collapsing. Using relative positioning technique discussed in Sect. 6.4.2, coordinates of the hotel being monitored could be measured *before* it started operating to provide base data. During the operational phase, GNSS could be used to provide continuous coordinates of the building *after* the groundwater abstraction started. These observations are simultaneously observed to an established GNSS control points on stable locations some distance far away from the hotel both before, and after the groundwater abstraction started. The *relative positions* obtained will indicate the spatial variation of the hotel's position relative to the GNSS control (reference) before-and-after-the-impact. If no variation is noticed at the control location, but visible at the hotel (impact) location, then the variation could be attributed to groundwater abstraction. In such case, GNSS would have played a double role of providing locations of both impact (hotel) area and the control area, and also provision of time-variable data useful in generating relative motion (both horizontal and vertical) of the hotel useful in assessing the impact of groundwater abstraction.

End of Example 28.1

28.3 Project EIA

28.3.1 Geoinformatics in Support of EIA Process

EIA generally goes through various stages, see e.g., Glasson et al. (2005, pp. 88–184) and Munier (2004, p. 8). Some of these stages, and possible areas in which geoinformatics could be useful are discussed. The first of these stages is *screening*, where a project is assessed as to whether it requires EIA or not. GIS is the basic tool that could be employed to support screening in EIA. For example, in the work of Geneletti (2007), GIS was combined with a decision aiding tool known as Multi-criteria analysis (MCA) to produce thematic nature conservation layer maps used to support decisions on whether to undertake EIA for a proposed project and also to choose the most suitable locations for new projects in the alpine area located in Trentino (northern Italy). Antunes et al. (2001) propose a GIS approach for computing

scores for criteria for use in MCA. Since GIS brings visual capability, its combination with MCA analytical tools will play a significant role in screening EIA projects as discussed in the next section. As a matter of fact, virtually all commercial GIS software in operation today have built and integrated MCA functionality into their systems.

The next stage of EIA after screening is the *scoping* stage, where the impacts and issues to be considered are identified. The process of scoping is that of deciding, from all of a projects possible impacts, and from all the alternatives that could be addressed, which ones are the most significant (Glasson et al. 2005, p. 91). Identification of significant alternatives requires comparison to be made at the scoping phase. Usually, at the initial phase of scoping, a small number of alternatives will be selected for further analysis from many potential alternatives, and in the final evaluation, these alternatives are subjected to more detailed evaluation. An example is presented in the rare earth case where 15 sites were selected in the initial case from which 6 sites were chosen for further analysis (Ashton Mining Ltd 1991).

In evaluating possible alternatives, GIS is an attractive proposition given its ability to consider different factors within an integrated framework. In this respect, remote sensing could be employed to develop various factor maps. GNSS satellites could also play a vital role of not only providing the coordinates (i.e., positions) of alternative locations, but could be used to provide rapid field measurements of factors such as distances to environmental sensitive locations (e.g., groundwater or conservation parks), and the actual spatial coverage of areas of each alternative.

Example 28.2 (GNSS in support of choosing from alternative locations) Consider Fig. 28.1 where three alternative perimeter locations are to be considered for the purpose of setting out a project such as sugar processing factory. *First*, the areas of these locations are to be established so that the smallest parcel of land is chosen to accommodate the factory and at the same time minimize on the land purchasing cost. *Second*, the distances of the sites to the nearest water source is required so as to assess the potential of the sugar factory contaminating the groundwater source. GNSS could be used to establish the corner positions of the various sites A, B, and C from which the perimeter and area of each parcel of the land could be rapidly calculated. Further, distances from each site to the nearest water source can rapidly be obtained in the field by measuring baselines of two receivers, one stationed at a given site and the other stationed at the water source as illustrated in Fig. 28.1. Another possibility would be to use a hand-held GNSS (e.g., Fig. 27.1 on p. 485) to obtain the direct distance measurements from each site to the water source using the navigation functions of these receivers by simply walking from the water source to the proposed sites. It is worth mentioning that these analyzes could be best undertaken within a GIS environment.

End of Example 28.2

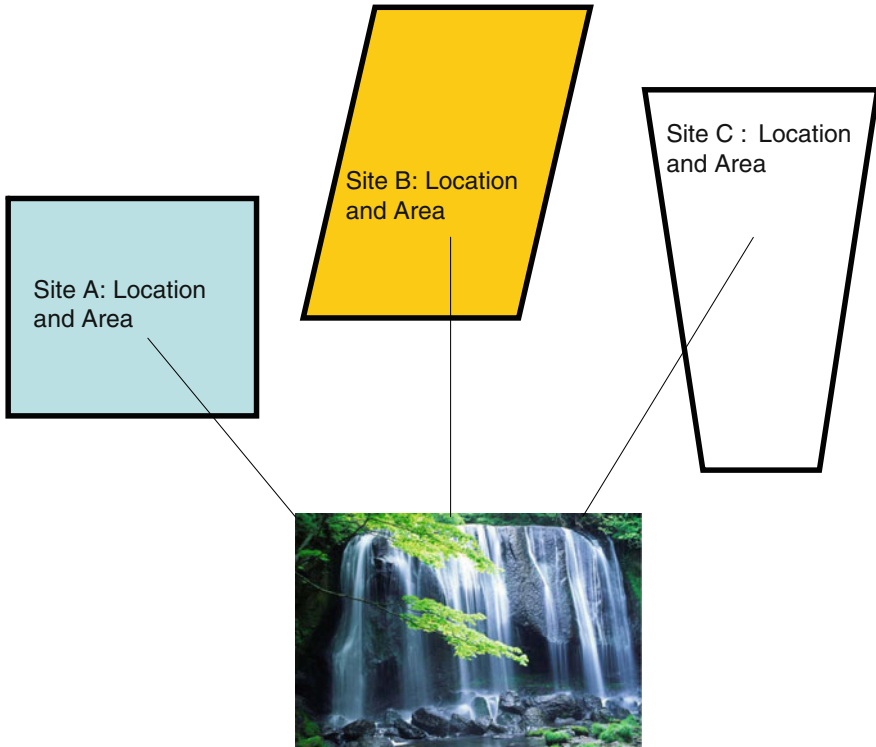


Fig. 28.1 GNSS support of site selection from three different alternatives. GNSS could be useful in providing positions, distances, perimeters and areas of each site, information that could inform decision makers choice of the correct site

Analysis stage of EIA consists of *identification*, *prediction* and *evaluation* (Al-Rashdan et al. 1999). Impact identification brings together project characteristics and baseline environmental characteristics with the aim of ensuring that all the potential significant environmental impacts (adverse or favorable) are identified and taken into account during EIA process (Glasson et al. 2005, p. 107). Remote sensing, photogrammetry and GNSS could help in provision of environmental baseline data before the project is established. This could then be used in impact prediction which requires that it be based on available environmental baseline data and proper use of technology to identify environmental modification, forecast the quantity and/or *spatial dimension of change* in the environment, and estimation of the probability that the impact will occur (Al-Rashdan et al. 1999).

Techniques for impact identification and prediction are discussed, e.g., in Glasson et al. (2005, pp. 88–184). Several methods of impact identification exist and are generally divided into the following categories (Glasson et al. 2005, p. 108); *checklist*, *matrices*, *quantitative methods*, *networks* and *overlay maps*. These methods have been discussed in detail, e.g., by Shopley and Fuggle (1984) and Westman (1985).

Incidentally, the last impact identification method i.e., overlay of maps provides spatial visualization and is best carried out within a GIS environment as discussed in Chap. 17. Evaluation in EIA looks mostly at the cost and benefits of a proposed projects to the users, assesses the impact on environment and compares various alternatives that will yield benefit of the project with minimum environmental and social impacts. Such alternatives could be evaluated through methods such as multi-criteria analysis (see Sect. 28.3.2). Remote sensing and GNSS satellites can play a vital role in this aspect of EIA with regard to documenting and identifying impacts associated with spatial changes. As illustrated in Fig. 28.1, GNSS could also assist in the determination of positions, distances, perimeters, and areas needed by decision makers to make informed choices.

28.3.2 *Geoinformatics and Multi-Criteria Analysis (MCA)*

28.3.2.1 Spatial Multi-Criteria Analysis

The vast majority of environmental management decisions are guided by multiple stakeholders' interests. These decisions are often characterized by *multiple objectives*, *multiple alternatives* and *considerable uncertainties* (Gough and Ward 1996). Alternatives are means for accomplishing particular goals (Therivel 2004, pp. 109–110) and their evaluation is a requirement in EIA of some countries. For example, the *National Environmental Policy Act* (NEPA) 1969 (US) requires that alternatives be considered while undertaking EIA. When multiple stakeholders with varied interests are involved, and multiple objectives and alternatives have to be considered, the situation often turns out to be very complex. In such cases, *multi-criteria analysis* (MCA) (see Chap. 17), a framework for evaluating decision alternatives against multiple objectives comes in handy. MCA is currently emerging as a popular approach for supporting multi-stakeholder environmental decisions as reported, e.g., in Regan et al. (2006).

MCA are methods that seek to allow for a pluralist view of society, composed of diverse stakeholders with diverse goals and with differing values concerning environmental changes (Glasson et al. 2005). According to Munier (2004, p. 132), MCA are tools that are used for the analysis of projects, plans, programmes and options either with single objective or with several objectives with many different attributes or criteria. Besides being a tool for aiding the selection of the best preferred alternative, Marttunen and Haimailainen (1995) suggests that it could also be used to increase the understanding of the problem by value structuring (i.e., identification of the objective and the analysis of values). The components of MCA are listed by Annandale and Lantzke (2000) as;

- a given set of alternatives,
- a set of criteria for comparing the alternatives, and
- a method for ranking the alternatives based on how well they satisfy the criteria.

Spatial multi-criteria decision problems typically involve a set of geographically-defined alternatives (events) from which a choice of one or more alternatives is made with respect to a given set of evaluation criteria (Jankowski 1995; Malczewski 2006). For spatial multi-criteria decision analysis, two considerations that are of utmost importance are (Jankowski 1995; Carver 1991):

- (1) A GIS component such as data acquisition, storage, retrieval, manipulation, and analysis capability.
- (2) Spatial analysis component such as aggregation of spatial data and decision maker's preferences into discrete decision alternatives.

MCA can help decision makers to choose between several alternatives by comparing the advantages and disadvantages of each alternative, one against the other, see e.g., Janssen (2001). The significant advantage of most MCA methods as stated by Annandale and Lantze (2000) is the capability to allow the evaluation criteria to be measured in either quantitative and/or qualitative terms, thus providing flexibility compared with other techniques such as cost-benefit analysis that require quantification of all values. Cost benefit analysis techniques are used, e.g., in economics to evaluate different alternatives, see e.g., Munier (2004, pp. 106–114).

There are several MCA techniques in operation in various countries, see e.g., Lahdelma et al. (2000) and Munier (2004). Examples of these techniques include Analytical Hierarchy Process (AHP), Mathematical Programming (MP), Additive Weighting and Concordance Analysis presented, e.g., in Annandale and Lantze (2000), Munier (2004) and Ministry of Environment and Energy, Government of Ontario (1990). Malczewski (2006) conducts a survey of GIS-based multi-criteria decision analysis. A principled problem in choosing a decision aid method for a real-life problem is that, for the same data, different methods may produce different results (Lahdelma et al. 2000). This problem is further compounded by the difficulty of objectively identifying the best alternative or method in view of these differing results. In realization of this shortcoming, Lahdelma et al. (2000) lists the requirements of MCA methods for use in environmental problems as:

1. Being well defined and easy to understand, particularly regarding the essential tasks such as setting of criteria and definition of weights.
2. Being able to support the necessary number of decision makers.
3. Being able to manage the necessary number of alternatives and criteria.
4. Being able to handle the inaccurate or uncertain criteria information.
5. Due to time and money constraints, the need of preference information from the decision makers should be as small as possible.

Clearly, it is difficult to have a method that satisfies all these requirements. All MCA methods have their strengths and weaknesses. The Additive weighting and Concordance analysis presented in the Example of Sect. 28.3.2.3 fulfil requirements 1, 2 and 3.

MCA does not actually provide an absolute answer by specifying a particular alternative, instead, it provides a process that ranks various alternatives and leaves the final decision to the policy makers. On the one hand, several studies indicate

the success of MCA in ranking alternatives and therefore aiding in decision making, see e.g., Regan et al. (2006). On the other hand, researchers are still learning how it impacts on what could otherwise be an intuitive or ad-hoc group decision-making process (Hajikowicz 2007). As an example, Bojorquez-tapia et al. (2005) report that some researchers have found out that MCA can alienate decision makers or experts in multi-stakeholder problems due to its complexity and ‘black box’ nature.

To address the shortcoming of alienating stakeholders, who most often comprise of the community (e.g., conservation groups and people likely to be directly affected by the project), CWP (community weighting process) in MCA is currently gaining momentum as a possible solution that attempts to cater for the community’s interests. The increasing role played by CWP in environmental decision making with MCA as a processing tool is captured, e.g., by Hajikowicz (2007) who states that the common reasons for applying MCA in multi-stakeholder decisions are to provide a transparent, structured, rigorous and objective evaluation of options.

Some examples of applications of MCA in EIA:

As already discussed, EIA processes involve several stages, see, e.g., in Glasson et al. (2005, pp. 88–184), and Munier (2004, p. 8) many of which may utilize MCA. At the screening stage, for example, where a project is assessed whether or not it requires EIA, MCA could be used, e.g., where one alternative location is to be chosen from several, see, e.g., Kiker et al. (2005). The scoping stage of EIA is that of deciding, from all of a project’s possible impacts, and from all the alternatives that could be addressed, which are the significant ones (Glasson et al. 2005, p. 91). Identification of significant alternatives requires comparison to be made at the scoping phase. Usually, at the initial phase of scoping, a number of alternatives are selected for further analysis, and in the final stage, a small number of alternatives are chosen and subjected to more thorough evaluation. An example is provided by the EIA performed for Ashton Mining Ltd, which required a selection of the best location for iron ore processing from six possible locations (Ashton Mining Ltd 1991). MCA could be used in such scenario during scoping stage. This example is discussed further in Sect. 28.3.2.3.

Evaluation in EIA looks mostly at the cost and benefits of a proposed project to users, assesses the impacts on environment, and compares various alternatives that will yield benefits to the project, while at the same time minimizes environmental and social impacts. MCA plays a vital role in evaluation in EIA as exemplified in the work of Janssen (2001).

28.3.2.2 Decision Making and Alternatives

Steinemann (2001) considers alternatives as means to accomplish ends, and that from the perspective of EIA; these ends include not just a particular agency’s goals, but also broader societal goals such as the *protection* and *promotion* of environmental quality. Steinemann (2001) further opines that developing the set of alternatives that become the choice set and the center of analyzes is the most important part of the EIA process. Decision makers can then chose from these choice sets rather than

simply having to rubber stamp a proposal. However, two problems that confront the development of alternatives are cited by Steinemann (2001). *First*, the public involvement often occurs too late to influence the development of the alternatives, and *second*, the alternatives are frequently eliminated from further consideration based on weak evaluations, which are not well-documented in the environmental impact statements (EISs). The first problem is associated with the very nature of project based EIA where the outcomes are almost always predetermined. In contrast to the project based EIA, SEA (Sect. 28.4) and SA (Sect. 28.5) enable earlier participation of the public. In evaluating alternatives, decision making is often based on some selected *criteria* and the desired objectives. Criteria are aggregate values computed from a much larger amount of so-called primary factors, which form the lowest level of information, also known as the assessment level (Lahdelma et al. 2000).

The problems with environmental decision making, however, are that they are intrinsically complex because they almost always involve many alternatives and multiple attributes (e.g., biological, economical, and social), the relative importance of which has to be determined by subjective evaluations (Marttunen and Haimailainen 1995). In an effective EIA process, alternatives will be sought that attempt to balance the data set with multiple attributes. The balancing act becomes even more crucial in SEA or SA where the desire is to balance the diverse ecological, social, and economic values over space, time and scale. These values are usually represented in the form of multiple criteria and *indicators* that sometimes express conflicting management objectives (Varma et al. 2000).

In SEA or SA, complex projects are often involved, which present many alternatives to choose from, necessitating the need for MCA for comparison. The situation is worsened when many stakeholders are involved and they conflict over the relative importance of the different comparison criteria. Annandale and Lantzke (2000) state that “when decisions become this complex, there is a need for special tools or techniques to help in making sense of what can be a large amount of information”. In addition, complex environmental planning problems will almost always include value judgements, public opinion, and controversies. So, the techniques need to deal with more than just technical information (Annandale and Lantzke 2000).

In such complex situations, MCA provides the means for comparing the advantages and disadvantages of each alternative, one against the other. By doing this, decision makers are provided with the means of choosing between several alternatives (Janssen 2001). One of its advantages is that it permits public involvement in the process by allowing their voices to be heard through weighting of the criteria according to their preferences. Community weighting process (CWP) in MCA therefore leads to the community participating in decision making as already stated, and enhances public confidence in the final decision as opposed to where decisions are made using weak evaluation tools as already pointed out by Steinemann (2001). Its vital role is captured by Sheppard and Meitner (2005) who state that “public involvement needs more effective, defensible techniques usable by managers at the sharp end of decision making, rather than just in the scoping of public concerns and in setting broad strategies”.

Specification of alternatives: Alternatives are different ways of achieving an objective. For example, if the objective is to find a suitable waste dumping site, the alternatives would be the various possible locations that can serve as dumping sites at a minimal cost and minimize environmental and social impacts. In real life, there will be, almost always, people with vested interest(s) in these locations, thereby complicating the task of objectively identifying a suitable site. Specification of alternatives is helpful in such situations as they account for as many of the stakeholder opinions as possible. Annandale and Lantzke (2000) suggest that the best approach in determining alternatives for a decision aiding exercise is the involvement of stakeholders and allowing them to offer as many alternatives as possible.

Specification of comparison criteria: In comparing alternatives, decision makers look for those alternatives that would be less costly in implementing but at the same time satisfy the environmental and social benefits. Criterion offers a possibility of comparing alternatives. Munier (2004, p. 48) defines criteria as parameters used to evaluate the contribution of a project to meet the required objectives. Desirable properties for criteria are presented, e.g., in Annandale and Lantzke (2000).

Scoring the alternatives: Annandale and Lantzke (2000) discuss the three types of measurement scales; *ordinal*, *interval* and *ratio*. According to Annandale and Lantzke (2000) ordinal scales provide information on order only and are unsuitable for mathematical manipulations (addition, subtraction, multiplication and division). It can only indicate that one alternative scores higher than another alternative, but does not indicate by how much (i.e., magnitude). Ordinal scales favour qualitative attributes and are often used interchangeably with quantitative reserved for ratio or interval scales (Annandale and Lantzke 2000). The interval scale indicates the difference between two alternatives without giving the actual magnitude. Its advantage over the ordinal scale is that it permits addition and subtraction only. The ratio scale has a natural origin (zero value) and provides a measure of both difference and magnitude (Annandale and Lantzke 2000). It permits the mathematical operations and as such, favours scores obtained when the attributes are directly measured. Glasson et al. (2005) suggests that scoring may use qualitative or quantitative scales according to the availability of information. Both qualitative and quantitative scales could be used simultaneously as demonstrated in Annandale and Lantzke (2000).

Weighting the criteria: Commonly, in MCA methods, a number is assigned to each criterion describing its importance relative to other criteria. These numbers are called weights, and they model the decision maker's subjective preferences (Lahdelma et al. 2000). The interpretation of weights depends completely on the decision model used. Therefore, it is essential that the decision model be chosen prior to collecting weights, see e.g., Vincke (1992). The primary purpose of weighting the criteria is to develop a set of values which indicate the relative importance of each criterion as valued by the community. These values are then used in ranking algorithms to determine the relative value of each alternative (Hajikowicz et al. 2000).

There are several ways of assigning weights. For example, weights could be assigned directly by the individuals undertaking the analysis to represent hypothetical point of view, or they could be based on the data collected from opinion polls, focus groups, public meetings or workshops, or other direct forms of sampling public or

expert opinion (Annandale and Lantzke 2000; Lantzke 2006). Weights can also be assigned using some mathematical functions as indicated, e.g., in Munier (2004, p. 53). This is therefore the part of MCA, which takes into consideration divergent views of stakeholders on a project.

This is captured by Glasson et al. (2005, p. 145) who states that MCA seeks to recognize plurality of views and their weights. Weights thus allow different views and their impacts on the final outcome to be expressed explicitly (Annandale and Lantzke 2000). Several techniques for weighting are presented in literatures, e.g., direct assessment and pair-wise comparison methods such as AHP, see e.g., Saaty (1980, 1987). In general, there exist no right weights that would allow comparisons between different alternatives. The weights obtained depend on the technique used (Lahdelma et al. 2000).

28.3.2.3 Application of Geoinformatics in Support of MCA

The following example illustrates how geoinformatics could be used together with MCA to assist in the selection of alternatives for siting of the secondary processing plant of a high-grade rare earth's deposit at Mt. Weld reported in Ashton Mining Ltd (1991, 1992). This example uses both ratio and ordinal scales to score the alternatives relative to the criteria.

Background of the Mt. Weld project: In 1991, a two-year study program was undertaken by Ashton Mining Ltd (1991) to determine the feasibility of commercial development of a high-grade rare earth's deposit at Mt. Weld, near Laverton in the Eastern Goldfields in Western Australia. The project was to involve the mining and beneficiation of ores at Mt. Weld and the secondary processing of rare earth concentrates to produce rare earth chemicals at a site that was to be determined (Ashton Mining Ltd 1991). The evaluation of the sites was undertaken in two stages. In the first stage, 15 sites assessed to have the potential for the siting of the secondary processing plant were evaluated. These were (Ashton Mining Ltd 1991): Collie, East Rockingham, Esperance, Kalgoorlie, Karratha, Kemerton, Koolyanobing, Kwinana, Moore River, Mt. Weld, Muchea, Geraldton, Picton, Pinjarra and Northam in Western Australia.

Ashton Mining Ltd (1991) adopted *qualitative* and *semi-quantitative* approaches to compare each of the sites. The *semi-quantitative* method focused on the economic considerations, i.e., capital and operating costs, while the qualitative assessments included environmental considerations namely; public health, town planning, flora and fauna, and groundwater. It also included social considerations such as community infrastructure, availability of skilled labor, road and road-rail transport, and social acceptance.

Five appraisal categories adopted for each of the factors were; little or no constraint; manageable constraint, significant constraint, requiring detailed evaluation, and overriding constraint with the potential to preclude development. Out of the 15 sites, 6 (East Rockingham, Collie, Kalgoorlie, Kemerton, Geraldton and Northam) were selected and subjected to further evaluation (Ashton Mining Ltd 1991).

The results of the second evaluation stage indicated *Northam* as the preferred site. Five alternative sites in the Northam region were then evaluated, and the proposed Meenaar Industrial Park was assessed as being the site with the greatest potential (Ashton Mining Ltd 1992). Between road only and road-rail options considered for transporting the ore concentration, residues and chemicals, the road option was preferred. The proposal was then submitted for environmental impact assessment (EIA) and was subjected to a public environmental review (PER) in 1992, see Ashton Mining Ltd (1991).

Now, let us apply two multi-criteria analysis (MCA) methods (*Additive weighting* and *Concordance analysis*) together with geoinformatics to assist in the selection of alternatives and show that the same results, i.e., Northam could have been reached. Six alternative sites for the Mt. Weld EIA case study are evaluated using these MCA methods. For each of the 6 alternatives, 11 criteria were compared and scored using ratio and ordinal scales and processed.

Application of MCA:

Site Evaluation Criteria: In the site evaluation by Ashton Mining Ltd, a number of general and specific site requirements were identified and used to develop appropriate criteria, which were applied to each site, see e.g., Ashton Mining Ltd (1991, pp. 24–25). The site evaluation criteria considered were those most suitable for the establishment of the secondary processing plant. Ashton Mining Ltd (1991) adopted *economic, environmental* and *social* criteria to evaluate the sites. In these criteria, which we discuss below, GNSS could play the role of providing site locations and the distances of various environmental features, e.g., groundwater source or community infrastructure from a given site.

The main economic criteria considered were to minimize the capital and operating cost to establish and operate the plant. Capital cost was needed for the construction of the secondary processing plant and to establish infrastructure (i.e., supplying power, water, natural gas and housing). Operating cost was to cover the cost of power, water, natural gas, land rates, transport of concentrates, residues, chemicals and products. All the assumptions made in calculating capital and operating costs are presented in Ashton Mining Ltd (1991, p. 52).

The environmental and social criteria adopted were those which minimized a site's potential for (Ashton Mining Ltd 1991, p. 24): Off-site effects on the public and to public health; conflict with surrounding (and future) land use, impact on the existing flora and fauna, impact on high-quality groundwater resources or other significant components of the physical environment, and inefficient utilization of land.

Social criteria were those which would ensure a site (Ashton Mining Ltd 1991, p. 25); is close to established and well developed community infrastructure, is near a suitably sized labor force with appropriate skills, minimizes the disruption and risks to the public from the transportation of materials, and is likely to be acceptable to the public. The assumptions made in deriving the environmental and social criteria are presented in Ashton Mining Ltd (1991, p. 25). Both the environmental and social factors can be modeled in a GIS environment with appropriate cost layers developed for the different factors.

The results of the example when MCA was applied indicated both additive and concordance methods ranked Northam as the top site followed by East Rockingham, and demonstrated the suitability of Concordance analysis for evaluating alternatives when the criteria are scored using mixed ratio and ordinal scales, thus underscoring the usefulness of MCA in assisting decision makers to choose between alternatives during the evaluation process of environmental impact assessment (EIA). Care should however be taken to know the limitations of each method (e.g., Additive weighting), use proper weights, and agreeable threshold.

28.3.3 Example of Gnangara Mound Groundwater Resources

During 1992–1995, a review was undertaken in Western Australia on the proposed changes to environmental conditions of Gnangara Mound groundwater resources under Section 46 of the *Environmental Protection Act (EPA) 1986 (WA)*. Using it as an example, a theoretical examination of the possible areas of EIA process that could have benefited from using geoinformatics is presented.

28.3.3.1 Background

The Gnangara Mound is Western Australia's largest source of groundwater, supplying up to 60 % of Perth's drinking (Australian Water Resource 2005; Department of Water 2008). Its area is estimated to be 2,356 km² and comprises Gnangara, Yanchep, Wanneroo, Mirrabooka, Gwelup, Perth and Swan Groundwater Management Units (GMUs). Gnangara Mound supports local wetlands and lake ecosystems and supplies irrigation for horticulture and agriculture (Australian Water Resource 2005). It is also a major water source supporting a number of groundwater abstraction schemes operated by the Water Authority of WA (1995). It is bounded to the north by Gingin Brook and Moore river, to the East by Ellen Brook, to the south by Swan River, and Indian Ocean to the West.¹

Physical environment: Gnangara Mound is characterized by hot dry summers and mild wet winters with an average annual rainfall of about 800 mm (Water Authority of WA 1995). Department of Water (2007) gives an average annual value of 814 mm. The hottest month of the year is reported as February with an average maximum temperature of 34°, while August is the coldest month with an average maximum of 18° (Water Authority of WA 1995). Water Authority of WA (1995) state that the area does not have natural surface runoff due to the porous nature of soil in the area. Most of the water that falls as rainfall recharges the groundwater and that any surface water is due to discharge from groundwater. Recharge of groundwater depends largely on rainfall pattern, vegetation cover, and the water table.

Groundwater flows westerly from the top of the Mound following the terrain slope. Wetlands are generally found in the low areas where the water table reaches

¹ See, e.g., <http://www.water.wa.gov.au/sites/gss/ggs.html>

above the ground surface much of the year. Due to the presence and absence of water above the ground in these wetlands, soil and vegetation have adapted to the pattern of groundwater. In general, groundwater quality is reported to be excellent (Water Authority of WA 1995). It is however widely recognized that sustainability of the Mound as a water resource is under threat due to *climate change* and excessive drawing of water.

Biological environment: Water Authority of WA (1995) reported the dominant terrestrial vegetation as the candle Banksia (*Banksia attenuate*) and firewood Banksia (*B. Menziesii*). Vegetation of high significant conservation value was also reported in the area (Water Authority of WA 1995). Vegetation, soils and land forms of Gngangara have been mapped, e.g., in Macarthur (2004). Fauna survey of 1977 and 1978 recorded 12 native mammals, 70 reptiles and amphibians and 223 bird species. Five caves out of the 273 documented caves in the Yanchep National Park were reported to be the most species rich subterranean ecosystem ever recorded, supporting 30 and 40 species compared to caves elsewhere in the world, which rarely have five animal species (Water Authority of WA 1995). GNSS could be useful in providing the locations of these five caves.

Social environment: Water Authority of WA (1995) reported a general increase in urbanization in the Gngangara Mound area that led to incremental approach to planning, subsequently having significant implications for the future of the area. Increase in urbanization comes along with changes in land use, which in turn impacts on the groundwater level. In the rural areas, common land uses reported at the time included market gardening and poultry farming. Specialized activities included flower, mushroom, and strawberry growing, and gourmet pheasant production, all of which required groundwater. Large areas of Gngangara Mound are State Forest under the management of Conservation and Land Management (CALM). Approximately 20,000 ha of this land was Pine plantation with the remainder of the State Forest being natural bushland (Water Authority of WA 1995).

Water Authority of WA (ibid) further reported 14 archaeological sites registered with the Western Australian Museum. Specifically, McNess, Lake Mariginiup, Lake Joondalup, Lake Goollelal, and Lake Gngangara among others were said to be sites of Aboriginal mythology and/or historical Aboriginal use. According to Water Authority of WA (1995), it was also likely that most of the wetlands in the western linear wetland chain are potential areas of Aboriginal significance.

28.3.3.2 Review of Allocation and Management of Groundwater Resource

Under the guidance of the Environmental Protection Authority (EPA), Water Authority of WA manages groundwater resources of the Mound. Private groundwater abstraction is managed through area allocation and licensing of users (Water Authority of WA 1995). Water Resource Authority, therefore, has the task of ensuring that the environmental impacts from users and its own activities are minimized. This is achieved, e.g., through assessing the impacts of proposed land use changes on groundwater levels and in providing advice to land management and planning orga-

nizations. In 1986, Water Authority of WA submitted the Gngangara Mound Water Resources Environmental Review and Management Program (ERMP) to Environmental Protection Authority (EPA) for;

- (1) approval to develop the Pinjar Groundwater Scheme, and
- (2) approval for changes to private groundwater allocations.

In 1988, the Minister of Environment approved development of Pinjar Stage 1 Groundwater Scheme and the changed private groundwater allocation quotas, subject to a number of environmental conditions (Water Authority of WA 1995). The approval allowed for increased abstraction of groundwater by the Water Authority of WA and other users. The conditions to be met included measures to protect the environment through; *Maintenance of water level in the wetlands, limits on private groundwater allocations, establishment of a management and monitoring program, and setting in place a range of administrative mechanism regarding inter agency interaction on groundwater management* (Water Authority of WA 1995). In 1992, Water Authority of WA identified the need to review the management of the southern portion of the Mound. Factors which necessitated the requirement for the review were (Water Authority of WA 1995):

- Identification of other ecosystems, which had been, or had the potential of being affected by groundwater abstraction. These included shallow cave streams and phreatophytic vegetation.
- Rapid increase in knowledge of Environmental Water Requirements (EWR), which suggested that water levels set by EPA in 1988 should be reviewed.
- Increase in demand of groundwater by private users called for an assessment of the potential impacts that would result from further groundwater allocation.
- There was a need by Water Authority of WA to further develop groundwater schemes (e.g., Pinjar Stages 2 and 3) on the Gngangara Mound and as such, a review of allocation and management was essential before development of the schemes could commence.
- The recognition that land use on the Mound could significantly affect groundwater availability required that the impacts of likely future land use scenarios be considered in allocating and managing groundwater.
- Since the outcome of the review was likely to involve changes in some of the environmental conditions which applied to the management of Gngangara Mound, notably wetland water levels, allocation quotas and land use issues, consideration of any changes required the review to take the form of Environmental Impact Assessment (EIA).

A formal referral was submitted by Water Authority of WA to the EPA² in late 1992, and it was decided that the conditions should be reviewed under Section 46 of the *Environmental Protection Act (EPA) 1986* (WA). This then led to the review of allocation and management of groundwater resource by Water Authority of WA.

² Environmental Protection Authority.

EPA guidelines for this review are presented in Water Authority of WA (1995, Appendix 2).

Focus of the environmental review: Environmental conditions reviewed focused on three main areas; *wetland water level, allocation quotas* and *land use issues*. EPA acknowledged that little information was available to determine EWR³ for the wetlands and that there maybe changes to the set levels in future and required the initiation of research to provide an improved understanding of wetland ecology, which could then be used as a basis to review the wetland water level criteria.

With the continuing urban development in the Wanneroo region, evolving patterns of land use led to considerable changes in the pattern for demand for private water. Water demand in some areas, e.g., Flynn Drive could not be met. There was need to review groundwater availability with the view of allocating further resources to high demand areas. This could be achieved through further development of groundwater schemes within Gngangara Mound comprising Pinjar Stage 2 Part 1 groundwater scheme, which was scheduled for December 1996 and had been approved by EPA subject to the outcome of the allocation and management review.

Since also allocation of Pinjar Stage 2 Part 2 and Stage 3 groundwater schemes were being sought at the time, Water Authority of WA believed in reviewing the allocation and management of water resource before further development of groundwater schemes so as to ensure equitable distribution between the public water supply and private use while minimizing environmental impacts.

28.3.3.3 Possible Areas of Geoinformatics Support to the Gngangara EIA

Impacts identification: Water Authority of WA adopted the checklist method in identifying the impacts. This is the common procedure used in Western Australia where the proponent is required to complete a referral form (Department of Water 2007). In what follows, a network approach based on Sorensen (1971) and a GIS method are compared in order to demonstrate how geoinformatics could have been useful in enhancing impact identification.

The Sorensen Network Approach: Recreating the impacts in Water Authority of WA (1995), first the activities to be undertaken in the Gngangara Mound review are specified. In this case, three major activities are identified from Water Authority of WA (1995) as; *groundwater allocation, land use, and artificial maintenance of wetland's water levels*. Let us add rainfall to this list as a climate variable that has the potential of impacting on the water level. The causes of environmental changes associated with the activities above are then identified and a matrix format applied to trace its impact. In Fig. 28.2, use is made of the Sorensen (1971) principles to identify the impacts.

For instance, land use activity potentially results in clearing of vegetation, water abstraction, increase and decrease in density of pine plants, and climate change. These environmental changes, in turn, results in increased water level (e.g., when

³ Environmental water requirement.

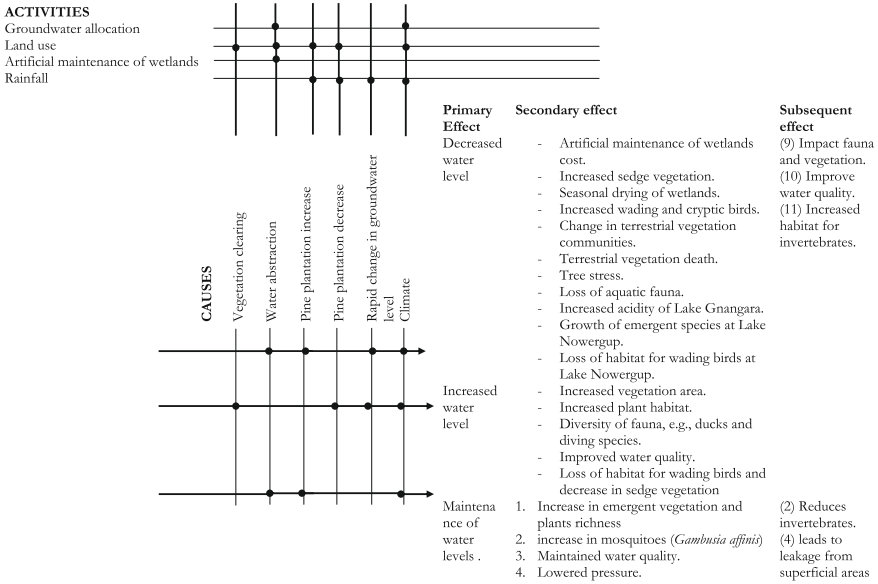


Fig. 28.2 Sorensen Network for Gngagara Mound impact identification

vegetation is cleared) as the primary effect. Increase in water level in turn leads to increased wetland vegetation areas and plant habitats, diversity of fauna, e.g., ducks and diving species, and improved water quality all of which are positive secondary impacts. A negative secondary impact is the loss of habitat for wading bird species and sedge vegetation that rely on seasonal drying of the wetlands.

Water abstraction will occur when land use activities involve irrigation of farms, maintenance of golf course, and other uses which require water. This in turn leads to low wetland water levels as primary effects. Secondary effects as a result of the primary impact are presented in Fig. 28.2. All the potential impacts of land use can be traced in a similar way as demonstrated in Fig. 28.2. As demonstrated for the case of land use activity, the Sorensen network is used to identify the primary, secondary and subsequent impacts associated with the allocation of groundwater, artificial maintenance of wetlands and rainfall. Figure 28.2 summarizes the identified impacts using this method. It is evident that the identified impacts compare well with those reported in Water Authority of WA (1995).

GIS Approach: For identification of environmental impacts having spatial distribution in nature, GIS with the assistance of GNSS satellites is an ideal tool. The potential of GIS in environmental impact assessments has been demonstrated, e.g., by Antunes et al. (2001) who applied it to evaluate the impacts of a proposed highway in Central Portugal. Antunes et al. (2001) suggested identification of environmental components (e.g., ecosystem) and receptors (e.g., a particular species likely to be affected by the component) using GIS. Another example of application of GIS to

EIA is presented by Haklay et al. (1998) who advances a GIS-based scoping method and discusses the conditions necessary for its utilization.

For the Gngangara Mound example, the environmental components that were likely to be affected by groundwater allocation and management were *pine trees, vegetation* and *wetlands*. Using Gngangara Mound Map of 1987 as a base for example, annual map layers of pine trees, vegetation, wetlands and urbanization can be overlaid on the base map in a GIS environment to produce a composite map, which can be used to identify hot spots (areas where land use are clearly identified to impact on wetland water levels and wetland vegetation). In this example, 1987 is selected as a base since environmental conditions issued by the Minister became operational in 1988. Annual groundwater level for specific wetlands are entered as attributes or produced in maps as contours. From the hot spots, areas and contours indicating water level changes and potential impacts can be identified. Where there is intense land use and sharp reduction in wetlands vegetation area, that specific land use could be said to impact on wetland water level, and subsequently vegetation. Linear trends can also be obtained on, e.g., the rate of pine growth/decline, vegetation clearing and urbanization by comparing annual values from 1997 to 1995. These could then be correlated with the groundwater levels to further identify the impacts. Negative linear trends will indicate adverse impact, while positive trend will indicate positive impact. Besides the trend analysis, visual examination of the layers could also indicate the spatial distribution. In this method, GNSS satellites provide location-based data to which the attributes, such as impacts on wetlands, are related.

Compared to the Sorensen method, the GIS approach has the advantage of being able to identify pertinent environmental effects on the basis of readily available information under stringent time and budget constraints (Haklay et al. 1998). Since it is best suited for *spatially distributed impacts*, it can analyze cumulative impacts better than the checklist or Sorensen network approach. It also provides friendly visual presentations, which are easily understandable by non-experts. Its drawbacks, however, are that it does not consider the likelihood of an impact, secondary impacts of the difference between reversible and irreversible effects (Glasson et al. 2005), and that it may require initial capital to establish.

Impacts prediction: Impact prediction requires that it be based on available environmental baseline data. In this example, the baseline data were readily available since regular water level monitoring had been taking place as part of the initial Ministerial conditions set out in 1988. Geoinformatics could have supported impact prediction of this EIA in several ways namely:

1. Provision of baseline data, and
2. Using the technique discussed in Chap. 19 to map boundaries of changing spatial features, e.g., wetland boundary changes as illustrated in Fig. 28.3.
3. Visualization of various “what if scenarios” that are likely to result from some prior conditions being fulfilled, e.g., understanding impact of drought. This can be implemented using GIS modeling techniques.

By having permanent reference marks set around the wells, GNSS satellite could be used to provide continuous measurements of positions and elevations of these ref-

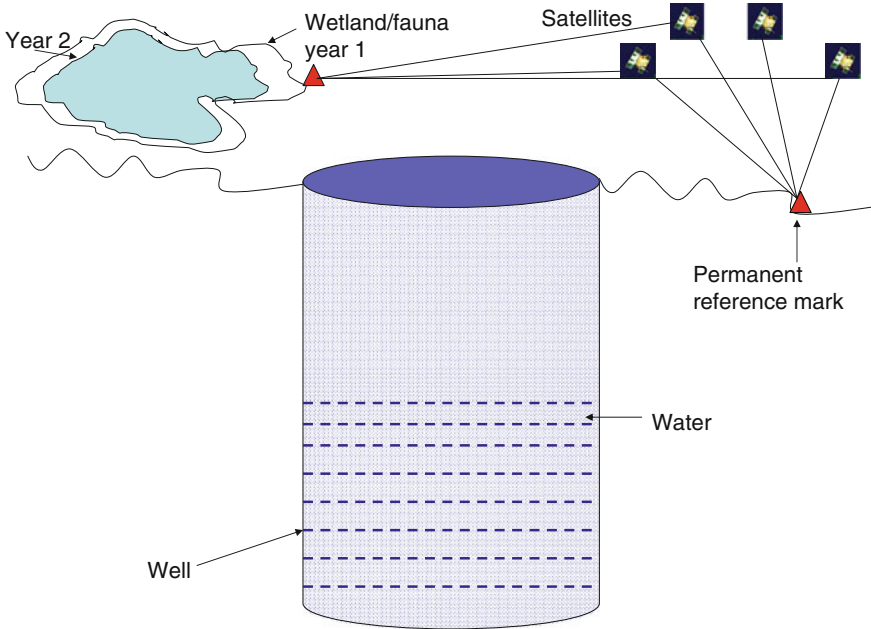


Fig. 28.3 GNSS monitoring of the impacts of well water abstraction using, e.g., techniques discussed in Sect. 19.3.1.2 spatial changes maps of wetlands from years 1 to 2 (see e.g., Fig. 19.5) on p. 264. Also, GNSS provides reference points upon which measured groundwater levels can be referenced

reference marks. The measured depths of the wells could then be referred to these reference marks and thus help in monitoring the state of the groundwater levels (Fig. 28.3). This can be related to the state of vegetation and fauna. To predict the impacts of groundwater abstraction on wetlands and other vegetation, similar techniques to those discussed in Sect. 19.3.1.2 (where GNSS is used to monitor Lake Finnelly) could be used to document changes in the wetlands' boundaries (i.e., perimeters and areas), as illustrated in Fig. 28.3 for years 1 and 2). By analyzing annual trend of these boundary changes, it is possible to predict the impacts of groundwater abstraction on e.g., wetlands, assuming that the changes are unrelated, e.g., to evaporation. This will require some control location (see e.g., discussions on BACI model in Sect. 28.2).

Impacts of groundwater variation on terrestrial vegetation were reported by Mattiske (1994) as ranging from small change in community structure in favour of more drought tolerant species, through to deaths of Banksia woodland vegetation. Indeed, that the death of Banksia vegetation were triggered by groundwater variation was supported by the findings of Water Authority of WA (1992), which suggested that Banksia trees that occurred where depth to groundwater was less than 6 m were most vulnerable to groundwater reduction. The study further suggested a general stress on vegetation due to reduced groundwater level.

Groom et al. (2000) deduced that a lowering of groundwater level by 2.2 m at a station P50 between the summers of 1990 and 1991, resulting from the cumulative effects of abstraction and below average annual rainfall (low groundwater recharge), coincided with a loss of between 20 and 80 % of mature *Banksia* species within 200 m of the bore. Over a similar time period, no significant decreases in the abundance of species were recorded in the monitored site to have been influenced by groundwater abstraction. They concluded that negative impact of groundwater draw-down on *Banksia* populations made it an important indicator of decreasing groundwater levels on the Gngarara groundwater Mound. GNSS monitoring of groundwater abstraction (Fig. 28.3) therefore could be useful in predicting impact on *Banksia* trees if the proposed changes in environmental condition would impact on groundwater by similar level, i.e., lowering of groundwater level by more than 2.2 m.

Geneletti (2007) demonstrates the capability of using GIS method to compute spatial indicators to predict and quantify critical impacts, such as ecosystem loss and fragmentation, soil erosion, geomorphologic hazards, interference with flora and fauna, and visibility. Since GIS has successfully been used by Geneletti (2007), it could be applied together with GNSS to predict variation in spatial distribution of environmental components caused by groundwater level variation.

Once groundwater changes have been obtained using, e.g., piezometric readings, and boundaries of impacted features (e.g., wetland in Fig. 28.3) mapped using GNSS, overlaying the land use and vegetation cover maps could then be performed using GIS for the same time period. Correlation between the land use, terrestrial vegetation and groundwater level could then be developed and predictions made on the impact of land use and terrestrial vegetation on groundwater level, and impacts of groundwater level on wetland vegetation. Linear and cyclic trends analysis could then be developed to give predictions at various temporal resolutions.

To support the prediction of impact of groundwater abstraction on fauna in caves, hand-held GNSS receivers can be used to provide locations of these caves, which can be related to groundwater level. Jasinska and Knott (1991) listed about 100 caves in Yanchep National Park and reported that little information was known about the biology of the aquatic fauna within these caves. They found aquatic species of high conservation value and concluded that one of the greatest threats to these species would be the permanent or temporary drying of the caves streams in which they occur. Since these aquatic fauna are of high conservation value, they could be seriously affected by drying of the streams within the cave to a point of extinction. GNSS could be useful in the prediction of the effect of regional warming on groundwater through the analysis of the GNSS derived tropopause heights as discussed in Chap. 21.

Comparison of the prediction methods: The model based approach adopted by the Water Authority of WA (1995) is the most commonly used method in most EIA of groundwater impacts. Models rely on the input data and the assumptions that are taken into consideration. The more they fit in the model, the more reliable are the output. The disadvantage of using models, however, is that they require some expert knowledge during their development and operation stages. Any wrong assumptions, input data, and usage can lead to false information and interpretation.

The Field experiment using GNSS and GIS has the advantage of using real data in their predictions as opposed to simulated values as is the case of models. They also provide easy visual interpretation of the results. The disadvantage is that it comes at a cost. The initial cost of installing a GIS may be high. Besides, there is the cost of validating the data using GNSS. Another disadvantage is the incapability to predict higher order impacts. In the Gngangara Mound example, it was difficult to use GNSS and GIS to predict the impacts of variation of wetland vegetation to fauna which may require other methods for enhancement.

In summarizing this example, in identifying and predicting the impacts for Gngangara Mound using alternative GIS-based methods to those adopted in the Water Authority of WA (1995), it has been pointed out that identification and prediction models are labor intensive and require knowledge of the system. More often, they are based on assumptions which may not fit the model leading to delivery of meaningless results. Field experiments, though straight forward, requires some validation which may increase the cost of EIA. Finally, baseline environmental parameters should be established upon which judgment of an impact can be made. Identification method should be a combination of methods that are simple to use, but which are capable of identifying higher order impacts and their inter-relations. Where models are adopted, they should be well understood by the analyst and assumptions must be clear and meaningful.

In particular, when used in conjunction with GIS and field data from the GNSS, a suitable approach for identifying and predicting impacts, which are spatially distributed could be obtained. This example indicates the possibilities of geoinformatics techniques to support identification and prediction of environmental impacts associated with the proposed change in environmental conditions of Gngangara Mound and highlight the limitations of the methods.

28.4 Strategic Environmental Assessment

Strategic Environmental Assessment (SEA) is the process that aims at integrating environmental and sustainability considerations in strategic decision-making (Therivel 2004). In so doing, the goal is to protect the environment and promote sustainability. Sadler and Verheem (1996) define SEA as a systematic process for evaluating the environmental consequences of a proposed policy, plan or program initiative in order to ensure that they are fully included and appropriately addressed at the earliest appropriate stage of decision making at par with economic and social considerations. Wood and Djeddour (1991) define a policy as inspirational and guidance for action, a plan as a set of coordinated and timed objectives for the implementation of the policy, and a programme as a set of projects in a given area, see also Therivel (2004, p. 12).

The basic principles of SEA have been presented, e.g., by Therivel (2004) as being a tool for improving the strategic actions, promoting participation of stakeholders in decision making process, focusing on key environmental/sustainability constraints,

identifying the best option; minimizing negative impacts, optimizing positive ones, and compensating for the loss of valuable features and benefits; and ensuring that strategic actions do not exceed limits beyond which irreversible damage from impacts may occur. Its advantages include (Therivel 2004):

- (1) Being able to shape the projects at an earlier stage through the appraisal of strategic action. This offers the chance to influence the kinds of projects that are going to happen, not just the details after the projects are already being considered.
- (2) SEA deals with impacts that are difficult to consider at project level. It deals with *cumulative* and *synergistic* impacts of multiple projects, e.g., cumulative impacts of various mining sites on the development of an entire area.
- (3) SEA can deal with large-scale environmental impact such as those of biodiversity or global warming more effectively than individual EIA.
- (4) Unlike project based EIA, which formulate goals around an already selected approach, SEA promotes better consideration of alternatives, thereby ensuring a strategic approach to action.
- (5) It incorporates environmental and sustainability consideration in decision making thus adding an additional dimension to decision making.
- (6) It enables public participation in decision making thus making the whole process inclusive and transparent.
- (7) It has the potential to promote streamlined decision making.

SEA has also benefited from MCA as illustrated by Noble (2002) who presents five scenarios that were evaluated within SEA to determine the most suitable option for power generation to be developed to cover the Canadian need up to the year 2050. The role and contribution of geoinformatics in supporting global warming monitoring is treated in Chap. 21. In what follows, the cumulative impact aspect of SEA and the possible role and contribution of geoinformatics is discussed.

28.4.1 Geoinformatics and Cumulative Impacts Assessments

Cumulative effects refer to the phenomenon of *temporal* and *spatial* accumulation of change in environmental systems in an additive or interactive manner and may originate from either an individual activity that recurs with time and is spatially dispersed, or *multiple activities* (independent or related) with sufficient spatial and temporal linkage for accumulation to result (Spaling and Smit 1993). The attributes of cumulative effects are classified by Spaling and Smit (1993) into three categories; temporal accumulation, which occurs if the interval between perturbation is less than the time required for an environmental system to recover from each perturbation, *spatial accumulation, which results where spatial proximity between perturbation is smaller than the distance required to remove or disperse each perturbation*, and the nature of human induced activities or perturbations, which also affect accumulation of environmental change provided the perturbations are sufficiently linked in time, space and scale.

Cumulative impact assessment is thus defined by the Commonwealth Environmental Protection Agency (1994) as predicting and assessing all other likely existing, past and reasonable foreseeable future effects on the environment arising from perturbations. In some legislations, e.g., in Canada, EIA regime has made it specific and mandatory, where consideration of cumulative effects assessment has been made explicit and mandatory both federally and in several provinces (Glasson et al. 2005). In USA, *National Environmental Policy Act* (1967) requires the assessment of cumulative impacts, while in Australia, assessments have largely been carried out by regulatory authorities, rather than project proponents. In Western Australia for example, the EIA process does not come out forcefully on cumulative impacts assessment.

Spaling and Smit (1993) provide an in-depth look at the contributions and shortcomings of EIA to assessing cumulative impacts. Three key factors in favor of EIA are theoretical understanding of environmental change through empirical analysis and modeling of responses of environmental systems through human induced perturbations, the development of various analysis methods for projecting and assessing the various environmental changes associated with the proposed human activities, and regulatory and administrative mechanism contributed by EIA in the integration of environmental consideration in decision making. In EIA, cumulative impacts can be identified at the *scoping stage* where issues to be examined are pruned. It is at this stage where the spatial and temporal effects of cumulative impacts can be considered (Scace 2000).

Geoinformatics could be useful in *providing the locations of multiple activities, mapping the changes in spatial coverage* (see e.g., Fig. 19.5 on p. 264), and *monitoring variation in groundwater* as a result of cumulative impacts.

28.4.2 Example of Marillana Creek (Yandi) Mine

Background: Marillana Creek (Yandi) Mine operated by BHP Billiton Ore Pty Ltd (BHPBIO) is located approximately 90 km north-west of Newman in the Pilbara region of Western Australia (BHPBIO 2005). The mine is situated within lease ML 270SA, and is operated under the Iron Ore (Marilliana Creek) Agreement Act 1991 (BHPBIO 2005). BHPBIO also has a smaller lease (M 47/292) located to the immediate north of ML 270SA. The Yandi ore body occurs within an ancient channel iron deposit (CID). This deposit is subdivided into a series of mine areas, i.e., central pits (C1 to C5), eastern pits (E1 to E8), and the western mesa pits (W1 to W6) (BHPBIO 2005). The CID is about 80 m thick and the majority of mining is within the upper 60 m. BHPBIO (referred to as proponent in this example) operates dewatering bores that lower the water table in the vicinity of each pit by approximately 30 m (BHPBIO 2005).

In May 1988, an approval was granted by the Minister for Environment to mine E2 and C5 at a rate of 5 million tonnes per annum (EPA 1988) and in 1991, mining commenced. In 1992, 1994 and 1995, EPA assessed modifications to the original proposal, which involved increased rates of production and mining of additional pits (EPA 1992, 1994, 1995). At the time of application for approval by the propo-

nents, mining was taking place in the E2, C1/C2 and C5 areas. In 2004, the proponent sought approval under Part IV of the *Environmental Protection Act (WA) 1986* to concurrently mine from pits across the leases (ML 270SA and M 47/292), and in addition update, assess, and agree on closure concepts for the whole of the deposit. During the mining of individual pits, the proponents proposed to partially fill the voids with overburden (waste) material from other pits, and to use the same open cut mining techniques and ore processing methods over the remaining life of the mine (BHPBIO 2005). The agreed concepts were to be documented through closure specific conditions that were issued by the Minister of Environment. The project was called the Marillana Creek (Yandi) Life of Mine and was expected to deliver 40 million tonnes per annum with a lifespan of 30 years (BHPBIO 2005).

The expansion of delivery capacity from an initial 5 million tonnes per annum to 40 million tonnes per annum resulting from concurrent pit mining had the potential to *significantly impact* on the environment. Besides, Hamersley Iron also holds a mining lease (274SA) over the CID, east of BHPBIO's lease, and was mining up to 34 million tonnes per annum at the same time. The potential impact on environment, therefore, was not only likely to come from the proposed project but also *cumulative* taking Hamersley into consideration. Thus, there existed a need for EIA under Part IV of the *Environmental Protection Act (EPA) 1986 (WA)*.

BHPBIO (2005) produced an EIS⁴ that documented the environmental objectives, potential impacts, proposed environmental management measures and predicted outcomes. Environmental Management Plan and Decommissioning and Final Rehabilitation Plan were also presented as key supportive documents to the Environmental Protection Statement (EPS). EPA was advised of the proposal in January 2004 and based on the information provided, considered that the proposal had the potential to impact on the environment, but could be managed to meet the EPA's environmental objectives (EPA 2005). Consequently, EPA determined, under Section 40(1) of the *EPA 1986 (WA)*, that the level of assessment for the proposal was EPS.⁵ EPA's advice and recommendations were then forwarded to the Minister of Environment in accordance with Section 44(1) of *EPA 1986 (WA)* (EPA 2005). The Minister of Environment granted approval with a set of conditions on 6th of July 2005.

Cumulative impacts: Since the EPS proposed to concurrently mine the pits within the leases as opposed to the previous pit by pit mining, there existed a potential to lead to *cumulative impacts* as discussed in Spaling and Smit (1993). Cumulative impacts were likely to be felt on the surface and groundwater. As part of the effort to manage cumulative effects accrued from surface water, the proponent proposed to integrate the surface water monitoring program to a wider monitoring initiative in the Marillana Creek catchment. This was to be achieved by adding flow gauge stations on the Marillana Creek and its tributaries within, upstream, and downstream of ML 270SA and 47/292 (BHPBIO 2005).

On groundwater resource, BHPBIO (2005) identified the potential of cumulative impacts given the presence of Hamersley Iron operation in the neighborhood. The

⁴ Environmental impact statements (EIA).

⁵ Environmental protection statement.

proponents took into account the impacts in their regional groundwater model and de-watering license. Both surface and groundwater monitoring to be undertaken by the proponents during mining was expected to provide a mechanism for monitoring cumulative impacts (BHPBIO 2005). GNSS could play a role in providing location-based information on test sites (flow gauge station) and also provide perimeter/area information that could help in monitoring of the cumulative impacts in the entire mining region (e.g., Fig. 28.3). This information could be integrated with a GIS to support management decisions.

28.5 Sustainability Assessment

Sustainability has been defined as meeting the needs of current and future generations through integration of environmental protection, social advancement and economic prosperity (Government of Western Australia 2003). Sustainability assessment (SA) can be performed when a proponent requests a regulator to do so (external) for the purpose of approval or internally as a mechanism for improving internal decision-making and the overall sustainability of the final proposal, see e.g., Pope (2006) and Pope and Grace (2006).

Pope et al. (2004, 2005) classify SA into objective-led (strategic) and EIA based (narrow) approaches. Morrison-Saunders and Therivel (2006) rank the various SA approaches with the EIA-led approach on bottom and the integrated (objective-led) approach at the top, see also Hacking and Guthrie (2008). Between them are various approaches, e.g., the win-win-win. Citing the dangers inherent in using the separate findings of the three sustainability pillars (environment, social, and economics) at the decision stage, Gibson (2006) proposes adoption of an integrated approach. Caution should, however, be observed when using the term “integration” as it is used variedly by different authors, see e.g., Lee (2006) and Morrison-Saunders and Therivel (2006).

SA involves (i) *Sustainable decision making protocol*. A sustainable decision making protocol is a process of setting objectives, criteria and targets that underpin SA. Hacking and Guthrie (2006) present several sources of sustainability development objectives and propose the use of threshold as one of the means, (ii) *alternative approaches*, which are options, choices, or courses of action. They are means to accomplish particular goals (Steinemann 2001). Alternatives have been shown to be affected by the formulation of the decision question. SA, similar to SEA, has also benefited from MCA. In the province of Reggio Emilia (Northern Italy), Ferrarini et al. (2001) used MCA to rank 45 municipalities based on 25 state of the environment indicators. Their results provided information on the state of sustainability in the province as a whole. GIS could support SA in choosing the best alternative as already discussed in Sect. 28.3.2.2.

28.6 Concluding Remarks

The use of GIS to support impacts' assessment is still developing and certainly that of GNSS is a new concept. This chapter attempted to motivate EIA, SEA and SA experts dealing with impact assessments to exploit the full potential of GNSS, especially with regard to its superb provision of location-based information and measurement of spatial variations. GNSS satellites could for example be used to provide information related to distances, e.g., distances of the alternative sites from established and well developed community infrastructures. The distances can readily be computed and incorporated into the MCA criteria and used to compute the desirable alternative that will inform decision making. GNSS could also be useful in providing information on spatial coverage of the proposed sites and also in environmental audit to evaluate compliance where location and spatial variation data are required (see e.g., Fig. 19.5 on p. 264). GNSS data together with remote sensing data can then be integrated in GIS to support the EIA process as discussed in the chapter.

References

- Al-Rashdan D, Al-Kloub B, Dean A, Al-Shemmeri T (1999) Environmental impact assessment and ranking the environmental projects in Jordan. *Eur J Oper Res* 118:30–45. doi:[10.1016/S0377-2217\(97\)00079-9](https://doi.org/10.1016/S0377-2217(97)00079-9)
- Anandale D, Lantze R (2000) Making good decisions: a guide to using decision-aiding techniques in waste facility siting. Institute for Environmental Science, Murdoch University, Perth, Australia
- Antunes P, Santos R, Jorda OL (2001) The application of geographical information Systems to determine environmental impact significance. *Environ Impact Assess Rev* 21:511–535
- Ashton Mining Ltd (1991) Mt Weld rare earths project: sites evaluation study for a rare earths Secondary Processing Plant, report prepared by Kinhill Engineers
- Ashton Mining Ltd (1992) Mt Weld rare earths project: public environmental review, report prepared by Kinhill Engineers
- Australian Water Resource (2005) Combined water management area: Gngangara Mound. http://www.water.gov.au/RegionalWaterResourcesAssessments/SpecificGeographicRegion/TabbedReports.aspx?PID=WA_GW_51x. Accessed 08 March 2008
- BHPBIO (BHP Billiton Iron Ore Pty Ltd) (2005) Marillana Creek (Yandi) Mine—environmental management plan, revision 3
- Bojorquez-tapia LA, Sanchez-colon S, Martinez AF (2005) Building consensus in environmental impact assessment through multicriteria modeling and sensitivity analysis. *Environ Manag* 36:469–481
- Carver SJ (1991) Integrating multi-criteria evaluation with geographical information systems. *Int J Geogr Inf Syst* 5(3):321–339. doi:[10.1080/02693799108927858](https://doi.org/10.1080/02693799108927858)
- Commonwealth Environmental Protection Agency (1994) Review of Commonwealth environmental impact assessment. In: CEPA 10, Canberra
- Downes BJ, Barmuta LA, Fairweather PG, Faith DP, Keough MJ, Lake PS, Mapstone BD, Quinn GP (2002) Monitoring ecological impacts: concepts and practise in flowing waters. Cambridge University Press, Cambridge
- Department of Water (2008) Gngangara Mound—a unique water resource. <http://portal.water.wa.gov.au/portal/page/portal/WaterManagement/Groundwater/Gngangara/>. As of 14 March 2008

- Department of Water (2007) Environmental Management of Groundwater Abstraction from the Gngangara groundwater Mound 2004–05. Annual compliance report to the Environmental Protection Authority, July 2004–June 2005
- EPA (Environmental Protection Authority) (2005) Marillana Creek (Yandi) Mine life of Mine proposal, mining leases 270SA and 47/292, 90 km north-west of Newman. Report and recommendation of the EPA, assessment no 1555, Bulletin 1166. Perth, WA
- EPA (1992) Yandicoogina (Marillana) iron ore project—change of ministerial condition due to increase in rate of production. Report and Recommendations of the Environmental Protection Authority, Bulletin 622, Environmental Protection Authority, Perth, WA
- EPA (1994) Yandicoogina (Marillana) iron ore project—change of environmental conditions due to increase in rate of production. Report and Recommendations of the Environmental Protection Authority, Bulletin 738, Environmental Protection Authority, Perth, WA
- EPA (1995) Duplication of iron ore mining operation, Yandi mine ML 270SA, Hamersley Range, 90 km north west of Newman, Report and Recommendations of the Environmental Protection Authority, Bulletin 802, Environmental Protection Authority, Perth, WA
- EPA (1988) Yandicoogina (Marillana) iron ore project, Report and Recommendations of the Environmental Protection Authority, Bulletin 323, Environmental Protection Authority, Perth, WA
- Ferrarini A, Bodini A, Becchi M (2001) Environmental quality and sustainability in the province of Reggio Emilia (Italy): using multi-criteria analysis to assess and compare municipal performance. *J Environ Manag* 63:117–131. doi:10.1006/jema.2001.0465
- Geneletti D (2007) An approach based on spatial multicriteria analysis to map the nature conservation value of agricultural land. *J Environ Manag* 83:228–235
- Gibson J, MacKenzie D (2007) Using global positioning systems in household surveys for better economics and better policy. *World Bank Res Obs* 22(2):217–241. doi:10.1093/wbro/lkm009
- Gibson R (2006) Beyond the pillars: sustainability assessment as a framework for effective integration of social, economic and ecological considerations in significant decision-making. *J Environ Assess Policy Manag* 8(3):259–280. doi:10.1142/S1464333206002517
- Glasson J, Therivel R, Chadwick A (2005) Introduction to environmental impact assessment, 3rd edn. Routledge, New York
- Gough JD, Ward JC (1996) Environmental decision making and land management. *J Environ Manag* 48(1):1–15
- Government of Western Australia (2003), Hope for the future: the Western Australian State sustainability strategy. Department of the Premier and Cabinet, Perth, WA. <http://www.sustainability.dpc.wa.gov.au/docs/Final/%20strategy/SSSFinal.pdf>. Accessed 02 March 2008
- Groom BPK, Froend RH, Mattiske EM (2000) Impact of groundwater abstraction on woodland, Swan Coastal Plain, WA. *Ecol Manag Restor* 1:117–124
- Hacking T, Guthrie P (2006) Sustainable development objectives in impact assessment: why are they needed and where do they come from? *J Environ Assess Policy Manag* 8(3):341–371. doi:10.1142/S1464333206002554
- Hacking T, Guthrie P (2008) A framework for clarifying the meaning of triple bottom-line, integrated, and sustainability assessment. *Environ Impact Assess Rev* 28(2–3):73–89. doi:10.1016/j.eiar.2007.03.002
- Hajikowicz SA (2007) Supporting multi-stakeholder environmental decisions. *J Environ Manag*. doi:10.1016/j.jenvman.2007.03.020
- Hajikowicz SA, McDonald GT, Smith PN (2000) An evaluation of multiple objective decision support weighting technique in natural resource management. *J Environ Plan Manag* 43(4):505–518
- Haklay M, Feitelson E, Doytsher Y (1998) The potential of a GIS-based scoping system: an Israeli proposal and case study. *Environ Impact Assess Rev* 18:439–459
- Jankowski P (1995) Integrating geographical information systems and multiple criteria decision making methods. *Int J Geogr Inf Syst* 9(3):251–273
- Janssen R (2001) On the use of multi-criteria analysis in environmental impact assessment in The Netherlands. *J Multi-Crit Decis Anal* 10:101–109

- Jasinska EJ, Knott B (1991) Stability of root mat ecosystem in groundwater stream: Cabaret cave, Yanche National Park, WA, University of Western Australia
- Kiker GA, Bridges TS, Varghese A, Seager TP, Linkov I (2005) Application of multicriteria decision analysis in environmental decision making. *Integr Environ Assess Manag* 1(2):95–108. doi:10.1897/IEAM_2004a-015.1
- Kumar N (2007) Spatial sampling for collecting demographic data. Paper presented at the annual meeting of the population association of America, New York, 29–31 March 2007
- Lahdelma R, Salminen P, Hokkanen J (2000) Using multicriteria methods in environmental planning and management. *Environ Manag* 26:595–605
- Lantze R (2006) MCA: the weighting process and overall comments on a weighting process. Environmental Science, Murdoch University. Unpublished. <http://lms.murdoch.edu.au/webct/urw/lc152224987001.tp152225013001/RelativeResourceManager/Template/content/1013evaluation/three-mca-wt-mthds.pdf>. Accessed 15 April 2008
- Lee M (2006) Bridging the gap between theory and practise in integrated assessment. *Environ Impact Assess Rev* 28:57–78. doi:10.1016/j.eiar.2005.01.001
- Macarthur R (2004) Geographical information systems and their use for environmental monitoring. In: Artiola J, Pepper IL, Brusseau ML (eds) *Environmental monitoring and characterization*. Elsevier Academic Press, New York
- Malczewski J (2006) GIS-based multicriteria decision analysis: a survey of the literature. *Int J Geogr Inf Sci* 20(7):249–268
- Marttunen M, Haimailainen RP (1995) Decision analysis interviews in environmental impact assessment. *Eur J Oper Res* 87:551–563
- Mattiske EM (1994) Monitoring the effects of groundwater extraction on native vegetation on the Northern Swan Coastal Plain. EM Mattiske and associates
- Ministry of Environment and Energy, Government of Ontario (1990) Evaluation methods in environmental assessment, pp 3–12, 33–51, 112–137
- Morrison-Saunders A, Therivel R (2006) Sustainability integration and assessment. *J Environ Assess Policy Manag* 8(3):281–298. doi:10.1142/S1464333206002529
- Munier N (2004) *Multicriteria environmental assessment. A practical guide*. Kluwer Academic, Dordrecht
- Munn RE (1979) *Environmental impact assessment: principles and procedures*, 2nd edn. Wiley, New York
- Noble B (2002) Strategic environmental assessment of Canadian energy policy. *Impact Assess Project Apprais* 20(3):177–188. doi:10.3152/147154602781766681
- Perry B, Gessler W (2000) Physical access to primary health care in Andean Bolivia. *Social Sci Med* 50(9):1177–1188. doi:10.1016/S0277-9536(99)00364-0
- Pope J (2006) What's so special about sustainability assessment? *J Environ Assess Policy Manag* 8:v–x. doi:10.1142/S1464333206002505
- Pope J, Grace W (2006) Sustainability assessment in context: issues of process, policy, and governance. *J Environ Assess Policy Manag* 8:373–398. doi:10.1142/S1464333206002566
- Pope J, Annandale D, Morrison-Saunders A (2004) Conceptualizing sustainability assessment. *Environ Impact Assess Rev* 24:595–616. doi:10.1016/j.eiar.2004.03.001
- Pope J, Annandale D, Morrison-Saunders A (2005) Applying sustainability assessment models. *Impact Assess Project Apprais* 23(4):293–302. doi:10.3152/147154605781765436
- Regan HM, Colyvan M, Markovchick-Nicholls L (2006) A formal model for consensus and negotiation in environmental management. *J Environ Manag* 80(2):167–176
- Saaty TL (1980) *The analytic hierarchy process*. McGraw-Hill, New York
- Saaty TL (1987) Analytical hierarchy process what it is and how it is used. *Math Model* 9(3):161–176
- Sadler B, Verheem R (1996) SEA: status, challenges and future directions. Report 53, Ministry of Housing, Spatial Planning and the Environment, The Hague, The Netherlands

- Scace R (2000) Vital relationship: complementary responsibilities of Government and proponents in scoping. In: Kennedy A (ed) *Cumulative environmental effects management: tools and approaches*. Alberta Association of Professional Biologists, Edmonton, pp 31–41
- Sheppard SRJ, Meitner M (2005) Using multi-criteria analysis and visualisation for sustainable forest management planning with stakeholder groups. *Forest Ecol Manag* 207:171–187
- Shopley J, Fuggle R (1984) A comprehensive review of current EIA methods and techniques. *J Environ Manag* 18:25–47
- Sweeney International Management Corp (2009) Environmental impact assessment for Kelly Cove Salmon Ltd. proposed aquaculture site relocation for Sand Point, Boston Rock, and Hartz Point. Submitted to NS Department of Fisheries & Aquaculture. SIMCorp. File #SW2008-016, 017 & 018
- Smit B, Spalding H (1995) Methods for cumulative effects assessment. *Environ Impact Assess Rev* 15(1):81–106. doi:[10.1016/0195-9255\(94\)00027-X](https://doi.org/10.1016/0195-9255(94)00027-X)
- Sorensen JC (1971) A framework for the identification and control of resource degradation and conflict in multiple use of the coastal zone. Department of Landscape Architecture, University of California, Berkeley
- Spaling H, Smit B (1993) Cumulative environmental change: conceptual frameworks, evaluation approaches, and institutional perspectives. *Environ Manag* 17(5):587–600. doi:[10.1007/BF02393721](https://doi.org/10.1007/BF02393721)
- Steinemann A (2001) Improving alternatives for environmental impact assessment. *Environ Impact Assess* 21:3–21
- Therivel R (2004) *Strategic environmental assessment in action*. Earthscan, Sterling
- Varma VK, Ferguson I, Wild I (2000) Decision support system for the sustainable forest management. *Forest Ecol Manag* 128:49–55
- Vincke P (1992) *Multicriteria decision-aid*. Wiley, Chichester
- Water Authority of WA (1992) Gnangara Mound vegetation stress study results of investigation. Report No WG 127, Water Authority of WA
- Water Authority of WA (1995) Review of proposed changes to environmental conditions—Gnangara Mound groundwater resources (Section 46), Water Authority of WA
- Westman WE (1985) *Ecology, impact assessment, and environmental planning*. Wiley, New York
- Wood C, Djeddour M (1991) Strategic environment assessment of policies, plans and programmes. *Impact Assess Bull* 10(1):3–22

Index

A

Abel's inversion, 282
Absolute orientation, 171
Absolute point positioning, 81
Absorption, 115, 116
Acid mine drainage (AMD), 497
Adaptive management, 5
Additive weighting, 515
Aerial photographs, 207
Aerial triangulation, 171, 173
Aerosol, 9, 297, 321
Afforestation, 330, 331
Agriculture, 344, 385, 465, 515
Air pollution, 488
Alternatives, 508, 510, 511
Analysis cycle, 313
Animal behaviour, 418
Animal distribution, 418
Animal ecology, 415, 418
Animals, 306, 415
Antarctica, 327
Antenna, 81
Anthropogenic forcing, 321
Antispoofing, 60
Aquaculture, 332
Aquatic, 485, 495
Aquatic ecosystems, 497
Aquatic vegetation, 450
Aquifer-storage, 347
Archaeological sites, 516
Area-based matching, 179
Association, 147
Atmosphere, 270, 272, 280, 306
Atmospheric
 hydrostatic part, 68
Atmospheric circulation, 310
Atmospheric errors, 66

 wet part, 68

Atoms, 66
Attenuation, 136
Automated feature extraction, 185
Automated terrain extraction, 184
Automatic scanning, 211
Autonomous positioning, 81

B

BACI model, 5, 504
Baseline survey, 74
Beach erosion, 403
Bending angles, 273
Best estimate, 313
Bilinear, 151
Biodiversity, 341, 345, 366, 385, 389, 420, 428, 430
Biological variables, 73
Bird species, 516, 518
Blue Nile, 349
Broadcast ephemeris, 65
Bundle adjustment, 172
Bushfire, 325

C

C/A-code, 59, 280
Camera calibration, 168
Carbon dioxide, 306, 321
Carrier-phase, 280
Catchment management, 379
Central perspective projection, 159
CHAMP, 270, 285
Change and updating, 216
Change detection, 429, 504
Chemical variables, 73

- Climate, 272, 305, 307, 318, 324, 344, 452
 - Climate change, 5, 6, 11, 270, 272, 299, 305, 306, 309, 311, 318, 319, 321, 323–325, 357, 368, 418, 430, 447, 453, 464, 515
 - Climate indicators, 309
 - Climate models, 297
 - Climate variability, 305, 311, 318, 352
 - Climatic changes, 7
 - Climatic conditions, 365
 - Climatic predictions, 8
 - Climatology, 312
 - Clock errors, 65
 - Cloud GIS, 197, 247
 - Clouds, 297, 310, 312
 - Coal, 306
 - Coastal terrestrial, 397
 - Code pseudoranges, 62, 81, 85
 - Cold point, 321
 - Collinearity condition equations, 159
 - Compass, 51
 - Compliance monitoring, 4
 - Conceptual modeling, 221
 - Concordance analysis, 513
 - Conjugate point measurement, 182
 - Connectivity analysis, 229
 - Conservation, 13, 415, 418, 421, 426, 428–430, 506, 522
 - Conservation impacts, 418
 - Contrast enhancement, 151
 - Control segment, 57
 - Conventional terrestrial reference system (CTRS), 102
 - Coordinate, 101
 - Coordinate system, 71, 98, 101, 102
 - Coordinate transformation, 103
 - Coordination, 212
 - Coral reef, 399
 - CORS, 93, 458
 - GEONET, 288
 - stations, 97
 - uses, 95
 - COSMIC, 270
 - COSMIC mission, 285
 - Coverage rebuilding, 227
 - Criteria, 510, 512
 - Crop conditions, 454
 - Cross sections, 173
 - Crustal deformation, 320
 - Crustal motion, 96
 - Cubic convolution, 151
 - Cumulative impacts, 520, 523, 524
 - Cyclones, 438
 - Cyrosphere, 326
- D**
- Data, 21
 - Data assimilation, 312, 313
 - Database management system, 216
 - Data capture, 208
 - Data collection, 74
 - Data link, 86
 - Data management, 215
 - Data mining, 225
 - Datum, 98
 - Decision making, 510, 524
 - Decision support system, 118
 - Deforestation, 315, 428
 - Deformation, 83, 97
 - Deformation monitoring, 317
 - DEM/DTM, 173
 - Density, 285
 - Desertification, 7
 - DGPS, 392
 - Differential positioning, 81
 - Differential rectification, 172, 184
 - Digital earth, 22
 - Digital image analysis, 145
 - Digital rectification, 151
 - Digitization, 209
 - Dipole moment, 276
 - Disaster management, 441
 - Disasters, 96, 439, 452
 - Discharge, 389
 - DOP, 70
 - Doppler effect, 139
 - Doppler shift, 281
 - Drought, 307, 308, 344, 424, 438, 444, 452, 455
 - cycle, 309
 - intensity, 454
 - severity, 455
 - Dry delay, 68
 - Dryland salinisation, 387
 - Dunes, 406
- E**
- Early warning system, 270, 454, 470, 502
 - Earth observation satellites (EOS), 9
 - Earthquake, 13, 96, 271, 289, 293, 438, 441, 444, 458, 469
 - ECMWF, 306
 - Ecological system, 344
 - Ecology, 365, 418
 - Ecosystem, 8, 317, 368, 385, 389, 516, 517, 521
 - EGNOS, 87, 44

- EIA
 program, 523
 public participation, 524
 scoping, 506, 519, 525
 screening, 505
- El’Nino southern oscillation (ENSO), 309, 450
- Electromagnetic radiation, 111
- Electromagnetic spectrum, 114
- Electrons, 66, 276
- Elevation angle, 68
- Emitted or thermal IR, 114
- Endangered species, 13, 415, 420, 423, 424, 427, 430
- Energy conservation, 490
- Energy transport, 334
- Environmental
 audit, 255
 change, 508, 518, 524
 conditions, 517
 conservation, 343, 345, 366, 391
 decision making, 508, 511
 degradation, 351, 405, 406
 impacts, 392, 394, 511, 516, 518
 management, 383, 402, 404, 526
 monitoring, 299
 promotion, 510
 protection, 345, 366, 391, 510, 517, 526
 quality, 510
 regulation, 381
- Environmental audit, 8
- Environmental changes, 6, 9
- Environmental impact assessment (EIA), 255, 404, 501, 505, 508, 519
- Environmental impacts, 415
 predictions, 5
- Environmental impact statements (EIS), 502, 510, 526
- Environmental management, 5, 11, 12
- Environmental management plan (EMP), 526
- Environmental planning, 5
- Ephemeris errors, 65
- Erosion, 385, 406, 427
- Ethiopian highlands, 349
- Euclidean geometry, 18
- Eustatic, 465
- Eutrophication, 381, 385
- Evaporation, 310
- Evapotranspiration, 347, 454
- Evidence, 21
- Excess Doppler shift, 281
- Excess path length, 273
- Exhaust gases, 489
- Exterior orientation, 159
- External modeling, 221
- F**
- Farming, 308
- Fast static, 87, 88
- Fauna, 513, 514, 518, 520, 522
- Fauna monitoring, 522
- Feature-based matching, 180
- Feature extraction, 152
- Fermat’s principle, 281
- Fish breeding sites, 495
- Flash flood monitoring, 448
- Flash floods, 311
- Flooding, 7
- Floods, 13, 307, 438, 444, 452, 455
 control maps, 255
 detection, 441
 prevention, 441
- Flora, 513, 514, 522
- Floriculture, 363–365
- Food
 availability, 419
 production, 307, 452
 safety, 441
 security, 307, 453
 supply, 379
- Foraging behavior, 418
- Foreshortening, 139
- Forests, 427
 diseases, 429
 management, 428, 429
 protection, 428
- Forests fires, 444
- Fossil fuels, 306
- Frequency, 274
- Fuel consumption, 490
- Fuelwood, 427
- G**
- Galileo, 47
- Gauss elimination, 64
- GDOP, 75
- Generalization, 227
- General purpose maps, 255
- Geo-referencing, 150
- Geocoding, 246
- Geodata, 21
- Geographic information science
 and technology, 191
- Geographic information system, 118, 191
- Geoid, 100, 346
- Geolocating, 246
- Geometrical delay, 273
- Geometric distortion, 150
- GEONET, 97

- Geopotential heights, 273, 319
 - Geosensor networks, 440
 - Geospatial, 21
 - Geothermal power, 366
 - Giraffe, 365
 - GIS, 10
 - Glacial ice, 342
 - Glaciers, 293, 306, 465
 - Global circulation models (GCM), 312
 - Global differential GPS (GDGPS), 85
 - Global system for mobile communication, 118
 - Global warming, 5, 6, 10, 13, 269, 306, 309, 310, 317, 319, 320, 324, 430, 464, 466, 523
 - related diseases, 306
 - GLONASS, 47, 49, 51
 - GNSS, 47, 93, 118
 - GNSS-meteorology, 8, 271, 272
 - EUMETSAT, 272
 - GRAS, 272
 - IPWV, 272
 - NOAA, 323
 - NWP models, 7
 - GNSS positioning method, 75
 - GNSS-reflection (GNSS-R), 298
 - GNSS-reflectometry, 298
 - Google Earth, 22
 - GPS, 47, 55
 - application to conflict resolution, 361
 - atmospheric errors, 66
 - carrier-phase pseudorange, 62
 - clock errors, 65
 - ephemeris errors, 65
 - GDOP, 74
 - measurement errors, 64
 - measuring principle, 61
 - receivers, 270
 - GPS meteorology
 - ECMWF, 68
 - NCEP, 68
 - GPS meteorology METEOSAT, 9
 - GPS meteorology NOAA, 9
 - GPS observation principle, 59
 - GPS remote sensing, 270
 - GRACE, 269, 270, 298, 299
 - GRACE satellites, 292
 - uses of GNSS, 292
 - Gravitational attraction, 65
 - Gravity, 269, 346, 347
 - Gravity field, 43, 289, 293, 346
 - Greenhouse gas, 6, 306, 310, 319, 321, 322, 464, 465
 - Greenland, 327
 - Ground based augmented systems (GBAS), 87
 - Ground control points, 151
 - Ground survey, 208
 - Ground truth, 152
 - Groundwater, 6, 293, 294, 341, 342, 346, 441, 454, 506, 513, 515, 517, 518, 520
 - abstraction, 516
 - allocation, 518
 - aquifer, 387
 - level, 516
- ## H
- Habitat, 306, 397, 399, 400, 402, 417, 418, 421, 423, 430, 449, 518
 - conservation, 495
 - management, 495
 - Habitat mapping, 90
 - Hazard predictions, 270
 - Hazards, 444, 522
 - Heights, 322
 - High spatial resolution image, 208
 - Histogram equalization, 151
 - Horizon, 76
 - Horticulture, 363, 515
 - Humidity, 68, 311, 441, 454
 - Hurricanes, 308, 310, 401
 - Hydrological cycle, 310, 317, 345, 346
 - Hydrology, 256, 318
 - Hydrostatic, 277
 - Hydrostatic delay, 68
 - Hydrostatic refractivity, 276
- ## I
- Ice, 293, 294, 309
 - Ice cover, 348
 - Ice-layer, 298
 - Ice sheet, 293, 296, 465
 - Image classification, 152
 - Image correlation, 176, 179
 - Image enhancement, 151
 - Image matching, 176, 179
 - Image pre-processing, 149
 - Imaging, 75
 - Impact monitoring, 4
 - Impacts, 502
 - identification, 518
 - location, 504
 - monitoring, 504
 - parameter, 281
 - prediction, 520, 523
 - Index of refraction, 273

- Indicators, 511
- Industries, 464
- Inertial mapping units, 118
- Information, 21
- Information classes, 152
- Information system, 21
- Infrared, 114
- Input of GIS data, 207
- Integer ambiguity, 63, 91
- Integrated monitoring, 4
- Integrated precipitate water vapor (IPWV), 448
- Integrated water vapour, 311
- Integrity, 50
- Interferogram, 142
- Interferometric SAR, 141
- Interior orientation, 168
- International terrestrial reference frame (ITRF), 103
- Internet, 118
- Interpretation and analysis, 145
- Interpretation keys, 147
- Intersection, 160
- Ionosphere, 66, 270, 280
- Ionosphere-free, 67
- Ionospheric delays, 50
- Ionospheric errors, 61, 67
- Ions, 66

- K**
- Kepler's laws, 120
- Kinematic survey, 87
- Kinematic surveying, 90
- Knowledge, 21
- Kyoto protocol, 329

- L**
- L2C-code, 61
- L5-code, 61
- Lake level, 466
- Lakes, 383
- Land
 - degradation, 383
 - evaluation, 379
 - management, 379, 455
 - resource, 383
 - subsidence, 344
- Land submergence, 93
- Land subsidence, 83, 100
- Land use, 386, 389, 429, 514, 516, 518
 - change, 331
 - patterns, 352
 - planning, 379
- Land-use/cover change, 330
- Landforms, 256
- Landsat, 331
- Landscape ecology, 456
- Landslides, 441
- Lapse-rate, 321
- Laser scanner remote sensing, 117
- Latent heat, 310
- Latitude, 47
- Layover, 139
- LiDAR, 117
- Location, 343
- Logical modeling, 221
- Long term monitoring, 4
- Longitude, 47

- M**
- M-code, 61
- Man-made objects, 153
- Management plans, 8, 367
- Management policies, 344
- Manual digitizing, 210
- Map projection, 98, 104
- Marine habitats, 398
- MBACI model, 504
- Mean sea level, 100, 464
- Measurements, 226
- Medium range forecasts, 312
- Microwave regions, 115
- Microwave remote sensing, 117, 134
- Microwave sounding units (MSU), 319, 323
- Microwave soundings unit, 321
- Mie scattering, 116
- Migratory species, 420, 423
- Mining, 308
- Mission planning, 76
- Modeling climatic change, 310
- Modulation transfer function, 121, 168
- Moisture, 310
- Molecules, 66
- Monitoring, 3, 502
 - pest and diseases, 5
- Monitoring parameters, 73
- Monitoring techniques, 74
- Monsoon rains, 325
- Multi-criteria analysis, 323, 508
- Multi-sensor, 148
- Multi-spectral, 148
- Multi-temporal, 148
- Multipath, 69, 75, 105

N

Nadir-viewing microwave, 320
 Native vegetation, 387
 Natural forcing, 321
 NDVI, 151
 Nearest neighbor, 151
 Network analysis, 323
 Newtonian time, 19
 Noise pollution, 487
 Non-Euclidean geometry, 18
 Non-selective scattering, 116
 Normalized difference vegetation index (NDVI), 454
 Normalized height model, 128
 Numerical weather prediction (NWP), 307, 311, 312

O

Ocean
 bottom, 397
 monitoring, 410
 Ocean circulation, 289
 Oil, 306
 Oil leak, 484
 On-the-fly, 88
 Optical delay, 273
 Orthoimage, 172
 Orthophoto maps, 172
 Ozone, 319, 321

P

P-code, 59, 280
 Parallax, 147
 Partition of data, 216
 Passive and active remote sensing, 117
 PDOP, 70, 75, 88
 Photogrammetric restitution, 167
 Photogrammetry, 117, 157
 Photographic interpretation, 146
 Physical modeling, 222
 Physical variables, 73
 Plan, 523
 Plant communities, 497
 Plants, 306
 Plate tectonic motion, 93
 Plate tectonics, 43
 Platform, 120
 Poisonous gases, 488
 Polar ice cap, 308
 Policy, 523
 Pollution

 distribution, 325
 monitoring, 441
 non-point sources, 485
 nutrients, 484
 point sources, 484
 transportation sector, 493
 Positioning modes and accuracies, 106
 Positions, 73
 Poverty, 307
 Precipitable water, 288, 310
 Precipitation, 309, 310, 312, 313, 322, 324, 347, 368
 Precipitation forecast, 316
 Precise ephemeris, 65, 84
 Precision farming, 257, 258, 389, 439
 Prediction of weather, 310
 Pressure, 68, 269, 271, 273, 280, 285, 286, 319, 321, 324
 Principal atmospheric windows, 114
 Process of remote sensing, 111
 Profiles, 173
 Proximity analysis, 229
 Pseudo random noise (PRN), 60
 Pseudoranges, 62

Q

Quality control, 4
 Query, 226

R

Radiation, 321
 Radio waves, 280
 Radiometers, 320
 Radiometric distortion, 149
 Radiometric resolution, 123
 Radiosondes, 7, 306, 311, 312, 321, 322
 Rainfall, 346, 387
 Rainfall anomalies, 454
 Rainfall pattern, 515
 Range corrections, 86
 Ranking, 227
 Ranking method, 229
 Rapid static, 87, 88
 Rasterization, 212
 Rayleigh scattering, 116
 Re-selection, 227
 Real-time GNSS, 85
 Real-time kinematic (RTK), 90, 92, 392
 Reanalyses, 324
 Recharge, 389
 Reclassification, 227

- REDD, 196, 315, 427
- Reference ellipsoid, 100
- Reference frame, 102
- Reference site monitoring, 4
- Reference stations, 74, 77, 83, 86
- Reference system, 102
- Reflected IR, 114
- Reflected signals, 269
- Reflection, 116
- Reforestation, 330, 331
- Refraction angle, 280
- Refractive index, 282
- Refractivity, 269, 273, 274, 277
- Regional warming, 325
- Relative orientation, 170
- Relative positioning, 81, 82
- Relativity, 18
- Remnant vegetation, 380, 385
- Remote sensing, 9, 111
- Reptiles, 516
- Resource management, 428
- Resources, 12, 366
- Rise in sea level, 100, 447
- Risk zone maps, 449
- River Nile, 466
- Rotation sensors, 118
- Roving receiver, 86

- S**
- Salinity, 6, 298, 344, 345, 379, 385, 386, 389, 397, 455, 465, 466
 - impacts, 387
 - irrigation, 387
 - primary, 386
 - secondary, 386
- Sanitation, 492
- SAR, 139
- Satellite altimetry, 294
- Satellite based augmented systems (SBAS), 87
- Satellite geometry, 105
- Satellite imagery, 207
- Satellite laser ranging, 93
- Satellite remote sensing, 117
- Satellites
 - CHAMP, 272
 - COSMIC, 272
 - geostationary, 9
 - GPS, 8
 - GRACE, 272
 - LEO, 280
 - remote sensing, 9
 - velocities, 281
- Satellites polar, 9
- Scattering, 115
- Scheduling, 216
- Sea level, 13, 309, 466
- Sea level change, 289, 293, 296, 401, 405, 464
- Sea-wind, 298
- Seawater salinity, 298
- Secondary salinity, 6, 387
- Security, 216
- Sensor-platform, 119
- Sewage, 484
- Shadow, 139, 147
- Shape, 147
- Shoreline, 400, 402, 406
 - progradation, 400
 - retrogradation, 400
- Shorelines, 400
- Short range forecasts, 312
- Signal delay, 270
- Signals, 59, 75
- Siltation, 100, 385
- Simple monitoring, 4
- Size, 146
- Skeletonization, 212
- SLAR, 139
- Snell's law, 281
- Snow, 293, 342, 347, 348, 444
- Social impacts, 510, 511
- Socio-cultural activities, 379
- Soil, 257
 - erosion, 257, 386, 392, 401, 522
 - landscape, 383
 - maps, 255, 383
 - moisture, 293, 294, 299, 348
 - quality, 379
 - types, 255
- Soil analysis, 81
- Soil landscape mapping, 383
- Solar radiation, 310
- Solid waste management, 492
- Space resection, 160
- Space segment, 56
- Space utility vehicles, 121
- Space-time, 19
- Spatial, 74
- Spatial analysis, 225
- Spatial data infrastructure, 22, 186, 197, 198, 209, 213, 223
- Spatial database, 215
- Spatial enhancement, 151
- Spatial environmental changes, 8
- Spatial resolution, 121
- Spatial variations, 83
- Spatially distributed impacts, 520
- Special purpose maps, 255

- Speckle, 140
 - Spectral classes, 152
 - Spectral reflectance curves, 116
 - Spectral resolution, 123
 - Spectral signatures, 116
 - Spectral transformation, 151
 - SQL, 226
 - Standards, 216
 - Stereo-model, 147, 170
 - Stereopairs, 160
 - Stereoscopes, 147
 - Stereoscopic information, 147
 - Stereoscopic parallax, 160
 - Stereoscopic vision, 147
 - Stop-and-go, 88
 - Stop-and-go survey, 87
 - Storage media, 216
 - Storms, 308, 325, 401
 - Strategic environmental assessment (SEA), 502
 - Stratosphere, 9, 301, 320, 321, 323
 - Subsidence, 256, 265
 - Supervised classification, 152
 - Surface pollutants, 484
 - Surface scattering, 135
 - Surface temperature, 324
 - Surface water, 293, 294
 - Surrogate monitoring, 4
 - Surveillance, 3, 93
 - Survey monitoring, 4
 - Surveying, 3
 - Sustainability, 12, 523, 524, 515, 517–520
 - Sustainability assessment, 502, 526
 - Sustainable agriculture, 391
 - Sustainable development, 501
 - Synthetic aperture radar (SAR), 317
- T**
- TEC, 66
 - Temperature, 9, 68, 269, 271, 273, 280, 285, 286, 299, 306, 309, 313, 316, 319, 321–324, 397, 441, 454, 465
 - Temporal, 74
 - Temporal resolution, 74, 123
 - Terrestrial water storage, 290
 - Texture, 147
 - Thematic maps, 255
 - Thermal expansion, 309, 466
 - Thermal remote sensing, 117
 - Thunderstorm, 322
 - Tide gauge, 466, 467
 - Tone, 146
 - Topographic maps, 255, 259
 - Topology reconstruction, 213
 - Tornadoes, 438
 - Total electronic contents (TEC), 271, 272
 - Tourism, 458, 469
 - Traffic congestion, 490
 - Transformations, 227
 - Transmission, 116
 - Tropical Rainfall Measuring Mission, 136
 - Tropopause, 299, 306, 320, 321
 - heights, 269, 321
 - parameters, 324
 - variability, 321
 - Troposphere, 67, 306, 320, 321, 323
 - Tropospheric, 270
 - Tropospheric error, 67
 - Tsunami, 13, 96, 271
 - Typhoon, 308, 310, 444
- U**
- Ultraviolet, 114
 - Universal access, 444
 - Unsupervised classification, 152
 - User segment, 58
- V**
- Variation in sea levels, 93
 - Vector and raster models, 201
 - Vector-borne disease, 456
 - Vectorization, 212, 454, 455, 515, 517–520
 - Vegetation, 6, 75, 256, 379, 415, 426
 - biomass, 296
 - canopy, 328
 - index, 454
 - maps, 255
 - Vegetation fires, 439
 - Vertical datum, 100
 - Very Long Baseline Interferometry, 93
 - Visual image interpretation, 145
 - Volcanic eruption, 441, 469
 - Volcanoes, 289, 438
 - Volume scattering, 135
 - von Gruber locations, 170
- W**
- Waste disposal, 491
 - Waste generation, 492
 - Water, 308, 341, 344, 450
 - pollution, 484
 - quality, 363, 518
 - quantity, 368, 430
 - recharge, 383

- resource, 289, 293, 308, 309, 343, 344, 349, 364
 - scarcity, 363
 - security, 363
 - supply, 351
 - table, 515
 - availability, 363
 - balance, 379
 - conservation, 257, 344
 - discharge, 385
 - hyacinth, 485
 - level, 343, 518, 519
 - management, 343, 344, 449
 - protection, 343
 - quantity, 309
 - reservoir, 299
 - storage, 348
 - supply, 309
 - Water logging, 455
 - Water vapour, 9, 66, 68, 271, 273, 274, 276, 280, 286, 293, 299, 306, 310, 316, 317, 319, 321, 346
 - roles, 310
 - Water vapour radiometers, 69
 - Water-logging, 385, 393
 - Watershed management, 441
 - Weather, 272, 305, 307, 318, 452, 454
 - prediction, 444
 - satellites, 312
 - balloons, 306
 - forecast, 270, 307, 310, 311, 317, 447
 - Weather forecast, 307, 318
 - Weather forecasting, 4
 - Weather fronts, 68
 - Weather impacts, 307
 - Weather monitoring, 316
 - Weighting point method, 228
 - Weights, 512
 - Wet delay, 288
 - Wetlands, 345, 406, 466, 517–520
 - ecosystem, 344
 - conservation, 430
 - ecology, 517
 - mapping, 449
 - Ramsar Convention, 430
 - White Nile, 349
 - Wide area differential GPS (WADGPS), 87
 - Wildlife, 430
 - Wind erosion, 385
 - Wind speed, 313
 - Wireless sensor networks, 118
 - Wisdom, 21
 - World geodetic system (WGS-84), 103
- Z**
- Zenith wet delay, 69